Caractérisation des environnements sédimentaires hybrides (houle-marée) dans des systèmes anciens et actuels

Romain Vaucher

N°d'ordre NNT : xxx

THESE de DOCTORAT DE L'UNIVERSITE DE LYON
opérée au sein de
l'Université Claude Bernard Lyon 1

Ecole Doctorale N°ED 341
Évolution Écosystèmes Microbiologie Modélisation

Spécialité de doctorat : Sciences de la Terre
Discipline : Sédimentologie

Soutenue publiquement le 10/03/2017, par :

Romain Vaucher

Caractérisation des environnements sédimentaires hybrides (houle-marée) dans des systèmes anciens et actuels

Devant le jury composé de :

TESSIER, Bernadette	Directrice de recherche	UniCaen/CNRS	Rapporteur
GHIENNE, Jean-François	Chargé de recherche	UniStra/CNRS	Rapporteur
VENNIN, Emmanuelle	Professeur	UniBourgogne	Examinatrice
QUANTIN, Cathy	Professeur	UCBL	Examinatrice
PITTET, Bernard	Maître de conférence	UCBL	Directeur de thèse
LEFEBVRE, Bertrand	Chargé de recherche	UCBL/CNRS	Co-directeur de thèse

Remerciements

La thèse… et bien c'est une expérience incroyable avec des hauts et débats (celle là elle est pour vous Bernard et Bertrand). La majeure partie des personnes qui liront cette partie sera des thésards donc dans les moments de doutes associés à votre travail, dîtes vous que vous avec la chance de faire un travail où l'objectif est de satisfaire votre curiosité et ça c'est comme même pas rien! Enjoy!

Bernard, la première fois qu'on s'est rencontré, dans un entre-deux clopes, j'ai confondu des *herring bones* avec des *HCS* mais tu m'as quand même donné l'opportunité de faire cette thèse. Pour toute la connaissance et la culture scientifique que tu m'as transmises, pour la patience dont tu as fait preuve quand je ne comprenais pas, ainsi que pour la qualité de l'encadrement dont tu as fait preuve à mon égard, je te remercie! **Bertrand** (krkrkrkrkr seul les initiés comprendront) je tiens à te remercier de m'avoir fait découvrir l'univers incroyable du monde animal paléozoïque à travers, entre autres, des tâches rouges que j'aurais pu nonchalamment jeter dans les déblais. Merci pour ta bonne humeur, ton énergie et surtout … tes calembours, qui associés à ceux de Bernard, deviennent interminables!

Je tiens à remercier les membres du jury qui m'ont fait l'honneur de prendre du temps afin d'évaluer mon travail, **Bernadette Tessier**, **Emmanuelle Vennin**, **Cathy Quantin** et **Jean-François Ghienne**, je vous remercie.

Mon comité de suivi de thèse, qui fût constitué de **Jean Vannier**, **Gilles Escarguel**, **Philippe Sorrel** et **Pascal Kindler**, est chaleureusement remercié pour toutes les discussions, conseils et soutiens dont il a pu faire preuve.

Merci aux différents collaborateurs avec qui j'ai eu l'opportunité de travailler, c'est à dire, **Pascal Allemand**, **Sophie Passot**, **Philippe Grandjean**, **Thomas Humbert** (mec quand on s'est connu en CM1 j'aurais pas imaginé un tel chemin), **Elise Nardin**, **Daniel Viscaïno**, **Hendrik Nowak**, **Khadija El Hariri**, **Hélène Hormière** et **Ninon Allaire**. Je tiens également à remercier **Samuel Mailliot** pour la qualité et l'efficacité de son travail. Même si je n'ai pas collaboré avec toi, **Emanuela Mattioli**, je te remercie pour tes qualités humaines de directrice de laboratoire, ce fût un plaisir de t'avoir comme big boss!

Certaines personnes n'ont pas de lien direct avec ma thèse mais ont tout de même eu une grande importance, je remercie donc **Alexandra Elbakyan** (pour ceux qui se demandent qui est cette personne, et bien il s'agit de la fondatrice de Sci-Hub), **Ian Malcolm** & **Alan Grant** (faut-il vraiment les présenter?), le **Garage Sahara Zagora** pour avoir réparé à de nombreuse reprises le 4x4 un peu abîmé … et surtout le personnel de l'**Hôtel la Palmeraie** de Zagora pour l'accueil et la convivialité lors de nos missions de terrains … 'ti whisky berbère?

Avant de débarquer à Lyon pour commencer cette thèse j'étais à Genève et je tiens à remercier **Claude-Alain Hasler**, **Grégory Frébourg**, **Elias Samankassou**, **Rosana Martini**, **Daniel Ariztegui**, **Pascal Kindler**, **Eric Davaud** et **Georges Gorin** qui par leur passion et leur qualité d'enseignants m'ont donné goût à la sédimentologie!

Corentin Gibert et **Emmanuel Martin**, deux créatures adorablement paedomorphosées (alors c'est qui le paleu?) avec qui j'ai eu le bonheur de partager le bureau le plus rock'n'roll de tout le bâtiment où pas une journée ne se soit écoulée sans que je sois content de les retrouver pour faire des batailles de NERF©. Merci les

potos! C'est deux derniers énergumènes ne sont que la partie émergée de l'iceberg de personnes formidables que j'ai pu côtoyer pendant ces années, dans les copains cailloux j'ai nommé **Guillaume Suan** & **Peggy Vincent** (Corentine et Romain c'est bien comme prénoms n'oubliez pas!), **Vincent Perrier** (le plus … de Lyon 1, toi même tu sais), **Jérémy Martin** (cap'tain moutarde aux petits plats préparés par mÔman), **Claire Duchet** (Oohhh noooon!), **Arnauld Vinçon-Laugier** (t'as pas de gel aujourd'hui?), **David Sala** (50 nuances de blancs), **Emmanuel Guillerm** (le poirier breton), **Vincent Grossi** (oublie pas t'as une conférence à suivre le 6 février 2017), **Alex Lena** (elle aussi???), **Gilles Escarguel** (biologiiissstteee ooouuuuuuh!), **Véronique Gardien** (une véritable mère… bosse un peu Véro sérieux!), **Jean-Emmanuel Martelat** (racketteur mensuel pour approvisionnement en liquide caféiné!!!), **Alexandre Aubray** (mais qu'est ce que tu es beau ce matin), **Baptiste Suchéras-Marx** (bah alors m'a p'tite ratatouille?), **Anne-Sabine Grosjean** (grande sœur aux précieux conseils), **Axelle Zacaï** (modeste et efficace, *best paper of 2016*, sccuuusssee), **Jean-Michel Brazier** (iiicccciii c'est pompeï!!! pas l'time gros!) et finalement tous les locataires du **R4 de Géode** et ces millionnaires, qui ont supportés nos diverses actions puériles pendant plus de 3 ans! Le fric **Renauld**, le fric!!!

Méééééé mmmmeeeekkk, est l'expression par laquelle commence une conversation avec la **Awesometeam** formée à la fac pendant le bachelor composée de **Gabriel Hunger**, **Elme Rusillon**, **Aymeric Le Cotonnec** et **Vincent Martinuzi**, merci les animaux pour toutes ces années!

Un énorme merci à mes amis non cailloux de longue date plus communément appelés la *Bonne Franquette*! Merci à **Armel** (moussaillon polisson éleveur d'*Arenicola marina*), **Pauline** (Belle Lille en Mars), **Yvan** (un homme, un vrai), **Yuu** (tellement fier du vocabulaire que Yvan peut t'apprendre au quotidien), **David** (à quand notre airbnb dans le parc d'Ojców? fritki?), **Agathe** (sombre histoire de flotteur), **Jérémy** (copains, câlins, copinou, bisous), **Nawal** (molo molo sur les baskets hein), **Laurie** (t'as fais l'école du rire?), **Julien** (coq spirit), **Pierre-François** (j'ai eu Amazon, ils s'excusent pour le retard), **Tom** (la force tranquille), **Gaëtan** (twerkeur en chef à domicile), **Raphaël** (pas de cartier!), **Antoine** (mec t'as la start-up!), **Kevin** (j'y vais au culot!), **Fanny** (tiens c'est la gnôle à papy!), et **Emmanuelle** (pas très COP21 tout ça). Un énorme merci à *La soirée Jeudi chez Nini*, **Alice** (bouli bouli bouli), **Amaury** (vivifiant à souhait), **Adrien** (hbarkak vé jo?), **Romain** (licchhaaa), **Serge** (comment va Sinatra?), **Mélissandre** (le pouvoir…), **Alexandre** (RMY) et **Emmanuel** (el pistoleto).

Un immense merci à ma **maman**, mon **papa** et mon **frère**… et oui, il en fallait bien un sur les quatre qui ne finisse pas infirmier! Merci pour votre présence et votre soutien tout au long de ces années. Je tiens à remercier particulièrement mes parents qui m'ont transmis leur curiosité ainsi que leur passion de la nature à travers les voyages, les documentaires, les cartes dinosaures à collectionner, etc. Un grand merci du fond du cœur pour tout!

Je terminerai en remerciant **Samantha**, celle qui depuis des années me supporte contre vents et marées. Ta présence à mes côtés et plus particulièrement sur la fin de la thèse furent indispensable à l'aboutissement de ce travail. Pour toutes ces choses et avec tout mon amour je te dis merci.

شكرا

Résumé

Caractérisation des environnements sédimentaires hybrides (houle-marée) dans des systèmes anciens et actuels

La reconnaissance de systèmes sédimentaires hybrides (houle-marée) dans l'enregistrement sédimentaire n'est pas triviale lorsque l'un des processus (ici la marée) ne laisse pas de traces sédimentaires directes permettant de l'identifier. La succession sédimentaire de l'Ordovicien inférieur (formations des Fezouata et du Zini) de la région de Zagora (Anti-Atlas ; Maroc) enregistre une dominance de la houle. Cependant, de nombreuses structures et géométries de dépôts sédimentaires sont atypiques de l'action de la houle. L'explication proposée dans ce travail est la modulation de l'action de la houle par la marée qui va s'exprimer de différentes façons en fonction de la bathymétrie. Un modèle sédimentaire de dépôt est proposé pour ce système hybride. Les Fezouata ont non seulement un intérêt sédimentologique mais aussi un grand intérêt paléontologique par la présence de gisements à préservation exceptionnelle qui enregistrent les débuts de la Grande Biodiversification Ordovicienne. L'élaboration du modèle sédimentaire de dépôt a permis de contraindre les faciès sédimentaires associés aux fossiles retrouvés, permettant ainsi de définir un contexte paléoenvironnemental de vie de ces communautés primitives. Afin de mieux caractériser les différentes structures sédimentaires ainsi que leurs distributions au sein de la zone intertidale d'un environnement mixte, deux analogues, un méga- et un macro-tidal tout deux dominés par la houle, ont été choisis : Berck-Plage (Pas-de-Calais ; France) et la pointe du Cap-Ferret (Gironde ; France). La zone intertidale de Berck-Plage a permis de montrer que la quasi majorité des structures sédimentaires est formée par un courant oscillatoire et que la géomorphologie côtière (barres-et-bâches), induisant la réfraction des fronts d'ondes (houle) incidentes, joue un rôle majeur dans la distribution et la formation des structures sédimentaires. Des morphologies particulières en mamelons ont été observées à Berck-Plage mais l'homogénéité granulométrique de la zone d'étude n'a pas permis l'observation de leurs structures internes. Des morphologies similaires ont ainsi été étudiées à la pointe du Cap-Ferret. Cette dernière étude met en avant la formation de structures sédimentaires en mamelons comme étant le résultat de flux supercritiques initiés par le reflux de la houle préalablement réfractée par la géomorphologie non linéaire de la côte.

Mots-clefs : houle, marée, Ordovicien inférieur, Fezouata, analogues actuels

Abstract

Characterization of hybrid sedimentary environments (wave-tide) in ancient and modern systems

Recognition of hybrid sedimentary systems (wave-tide) in the sedimentary record is not trivial when one of the processes (here, the tide) does not leave direct sedimentary traces allowing its identification. The Lower Ordovician sedimentary succession (Fezouata and Zini formations) of the Zagora region (Anti-Atlas, Morocco) records a dominance of wave action. However, many sedimentary structures and depositional geometries are atypical of a wave dominated sedimentary system. The explanation proposed in this work is a modulation of the wave action by tides, which is expressed in different manners depending to the bathymetry. A model of deposition is then proposed for this hybrid sedimentary system. The Fezouata not only have a sedimentological interest but also a great paleontological interest due to the presence of exceptionally well-preserved fossils dating from the initial steps of the Great Ordovician Biodiversification Event. The development of the model deposition allowed to constrain the sedimentary facies associated with the fossils discovered, thus allowing to provide a paleoenvironmental life context for these primitive communities. In order to better characterize the different sedimentary structures and their distribution through the intertidal zone of hybrid environments, two analogues, one mega- and the other macro-tidal, both dominated by wave action were chosen: Berck-Plage (Pas-de-Calais; France) and the tip of Cap-Ferret (Gironde; France). The analysis of the intertidal zone of Berck-Plage has shown that the majority of the sedimentary structures are formed under oscillatory flows and that the coastal geomorphology (in ridges-and-runnels), inducing refraction of the incident wave fronts, plays a major role in the distribution and formation of the sedimentary structures. Peculiar dome-like morphologies were observed at Berck-Plage but the grain size homogeneity in this area did not allow the observation of their internal structures. Similar morphologies have been studied at the tip of Cap-Ferret. This last study highlights that the formation of dome-like bedforms is the result of supercritical flows initiated by the backwash of waves previously refracted by the non linear coastal geomorphology.

Keywords: wave, tide, Lower Ordovician, Fezouata, modern analogues

TABLE DES MATIÈRES

CHAPITRE I :

INTRODUCTION ET CONTEXTE GÉNÉRAL DE CE TRAVAIL

I) Origines de ce travail

L'idée de ce travail de thèse de doctorat en sédimentologie a été initié par une problématique paléontologique : la Grande Biodiversification Ordovicienne (GBO). Cet événement biologique majeur représente la radiation animale la plus importante du Phanérozoïque. Elle est le prolongement de l'Explosion Cambrienne. Les gisements fossilifères (*Lagerstätten*) à préservation exceptionnelle du Cambrien sont beaucoup plus nombreux que ceux que l'on peut retrouver dans l'Ordovicien. Néanmoins, le *Lagerstätte* des Fezouata dans l'Anti-Atlas marocain (région de Zagora) est le seul à avoir fourni un assemblage faunistique très diversifié et qui enregistre le début de la GBO. Il est donc d'une importance capitale pour la compréhension de l'avènement du règne animal ainsi que de la mise en place des écosystèmes au Paléozoïque. Depuis les années 2000, ces gisements ont fait l'objet d'un grand nombre de fouilles paléontologiques. En 2009, le projet : *Les faunes à conservation exceptionnelle de l'Ordovicien de l'Anti-Atlas (Maroc): implications évolutives et écologiques,* entre le CNRS (Dr. Bertrand Lefebvre ; Lyon, France) et le CNRST (Dr. Khadija El Hariri ; Marrakech, Maroc) est mis en place pour les années 2009 à 2012. En 2011, le projet RALI (***R****ise of* ***A****nimal* ***Li****fe (Cambrian-Ordovician) - organisation and tempo: evidence from exceptionnaly well preserved biotas* - ANR-11-BS56-0025) voit le jour, créant une collaboration scientifique internationale à l'initiative de chercheurs lyonnais (Dr. Jean Vannier et Dr. Bertrand Lefebvre) et lillois (Dr. Thomas Servais). Quelques années plus tard, le projet de collaboration (faisant suite à celui initié en 2009) VALORIZ : *Protection et* ***Val****orisation des gisements fossilifères à préservation exceptionnelle de l'****Or****dovicien Inférieur (480 ma) de la région de* ***Z****agora (Anti Atlas central, Maroc)* entre le CNRS et le CNRST est mis en place pour les années 2013 et 2014. Les missions de terrain se succédant, de plus en plus de fossiles sont découverts et les études paléontologiques avancent à grand pas. Les dernières découvertes ont fait l'objet d'un volume spécial dans la revue *Palaeogeography, Palaeoclimatology, Palaeoecology*, édité par Bertrand Lefebvre, Thomas Servais, Rudy Lerosey-Aubril et Peter Van Roy. Le contexte stratigraphique de la région a été étudié dans les années 1950. En revanche, le contexte paléoenvironnemental associé à la GBO dans la région de Zagora n'avait encore jamais été analysé. C'est ainsi que la problématique sédimentologique prend place dans cette thématique paléontologique afin d'identifier les environnements sédimentaires de l'Ordovicien inférieur dans lesquels sont préservés les fossiles.

Bien que l'aspect paléontologique de cette étude fût l'initiatrice de ce sujet, des questions propres à la sédimentologie sont rapidement apparues. Les dépôts sédimentaires de l'Ordovicien inférieur (formations des Fezouata et du Zini) enregistrent une dominance de l'action de la houle (de beau temps et de tempête). Cependant, la succession sédimentaire présente des structures sédimentaires ainsi que des géométries de dépôts atypiques pour un système de dépôt dominé par l'action de la houle. Une influence tidale est alors mise en avant. Afin de mieux contraindre ces dépôts sédimentaires, l'analyse

d'environnements analogues actuels (où les actions de la houle et de la marée coexistent) a été entreprise dans deux localités du littoral français (Cap-Ferret, Département de la Gironde et Berck-Plage, Département du Pas-de-Calais).

II) Objectifs et structure de ce travail

Les objectifs de ce travail de thèse sont les suivants :

- ► Analyser la succession sédimentaire à double influence (houle - marée) de l'Ordovicien inférieur de la région de Zagora afin de proposer un modèle sédimentaire de dépôt.

- ► Caractériser les processus sédimentaires responsables de la formation des gisements à préservation exceptionnelle de la GBO et replacer les fossiles dans leur contexte paléoenvironnemental.

- ► Analyser des environnements sédimentaires modernes potentiellement analogues à ceux de l'Ordovicien inférieur afin de mieux contraindre les successions sédimentaires anciennes à double influence houle - marée.

Les études sédimentologiques des dépôts sédimentaires de l'Ordovicien inférieur de l'Anti-Atlas et des environnements actuels vont s'articuler de la façon suivante :

Chapitre I : Ce premier chapitre introductif a pour but de préciser au lecteur le cadre général des Chapitres II, III et IV. Ces trois chapitres sont des articles scientifiques rédigés en anglais, publiés, soumis ou en préparation pour publication dans des revues scientifiques à comité de lecture. Chacun de ces chapitres contient en première partie un résumé étendu en français.

Chapitre II : Dans un premier temps il a fallu définir un modèle sédimentaire de dépôt pour l'Ordovicien inferieur de l'Anti-Atlas, intégrant une dominance de la houle et une influence tidale. Ces dépôts sédimentaires enregistrent des environnements allant de la plage à l'offshore proximal et la double influence (houle - marée) s'exprime de différentes façons en fonction de la bathymétrie. Les résultats obtenus dans ce premier chapitre nous ont permis de placer les fossiles découverts dans le modèle sédimentaire de dépôt (Chapitre II) et d'identifier de possibles analogues dans des environnements modernes (Chapitre IV). A la fin de ce chapitre, une discussion des corrélations effectuées entre les différentes coupes stratigraphiques analysées est proposée. Ces corrélations ne sont à ce jour pas publiées, mais pourraient faire l'objet d'un manuscript, car les corrélations ont des implications fortes sur la géométrie des réservoirs dans les contextes à dominance de houle influencés par la marée.

Chapitre III : Le modèle sédimentaire de dépôt étant établi, ce chapitre vise à caractériser les processus sédimentaires à l'origine de la préservation des fossiles dans les gisements fossilifères de la Formation des Fezouata et à replacer les organismes fossilisés dans leur contexte paléoenvironnemental.

Chapitre IV : Le modèle sédimentaire de dépôt préalablement établi dans le chapitre II concerne une succession sédimentaire paléozoïque. La reconnaissance de ce type d'environnement hybride (houle et marée) dans l'ancien reste une tâche compliquée. Afin de fournir de nouvelles clefs de reconnaissance de tels systèmes, une étude d'environnements analogues actuels (Berck-Plage, Cap Ferret) a été réalisée afin de mieux contraindre les processus physiques à l'origine des structures et géométries sédimentaires de houles atypiques observées dans l'Ordovicien du Maroc.

Chapitre V : Ce dernier chapitre contient les informations non traitées dans les articles des chapitres précédents et propose des perspectives en lien avec les Chapitres II, III et IV. Ce chapitre se conclura par des perspectives plus larges concernant les systèmes hybrides houle-marée.

Annexes : Au cours de mon travail de thèse, j'ai eu l'opportunité de collaborer en tant que co-auteur à différentes études majoritairement axées sur des problématiques paléontologiques en lien avec l'Ordovicien inférieur de la région de Zagora. Ces études seront présentées dans cette partie.

III) Les processus côtiers

L'orientation principale de ce travail fût de caractériser l'impact de la houle lorsqu'elle est modulée par l'action de la marée. Les questions principales concernant les environnements passés ou actuels furent :

- ► Comment l'architecture de dépôts sédimentaires est-elle influencée par ces deux mécanismes ?

- ► Quels critères de reconnaissance permettent d'identifier cette double influence ?

Les sédiments (marins, éoliens, fluviatiles, etc.) présentent un très large éventail de structures sédimentaires associées. Ces structures sont l'expression des paramètres hydrodynamiques du fluide ambiant qui sont contraints par différents processus agissant sur l'environnement. Dans le cas d'un environnent marin peu profond, les trois principaux acteurs sont : la houle, les marées et les rivières. Si l'on considère l'action de l'un des trois processus sans action subordonnée de l'un des deux autres, on obtient une classification

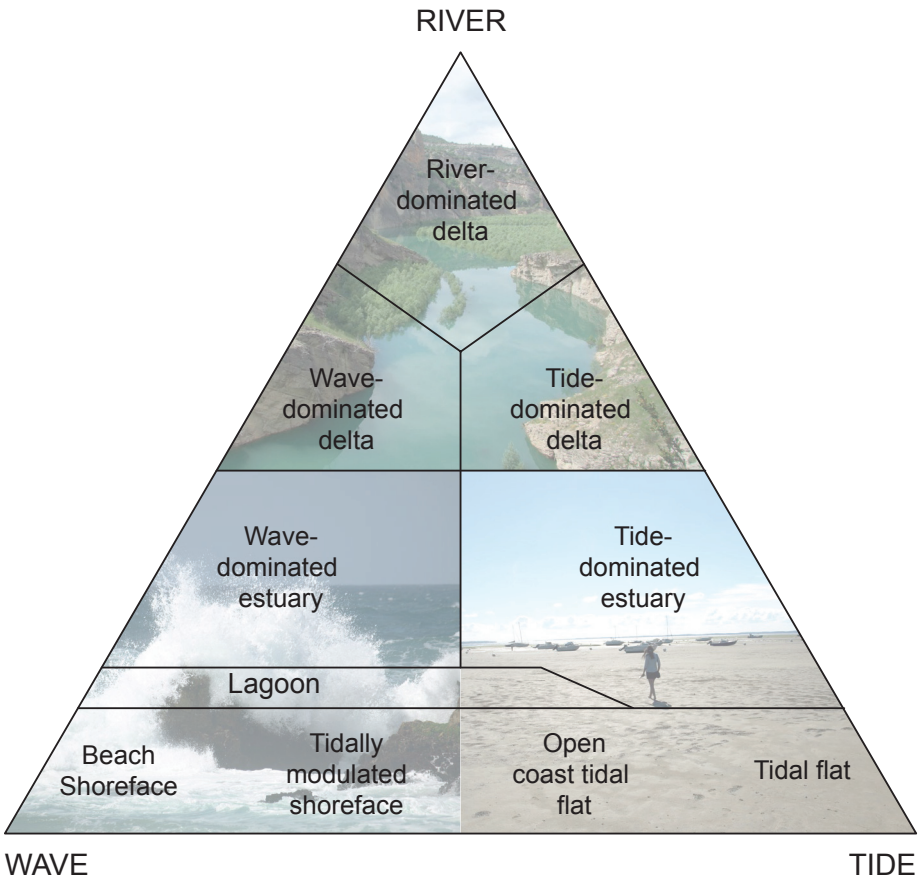

Fig. 1.1. *Classification des environnements côtiers en fonction de la houle, des marées et des rivières. Les sous-environnements créés résultent de l'interaction d'au moins deux processus. Figure modifiée d'après Dashtgard et al. (2009).*

ternaire des environnements (Fig. 1.1). Dans la nature il y a rarement dominance absolue d'un de ces trois processus, mais presque toujours une influence d'au moins deux d'entre eux. Il en résulte l'existence de sous-environnements dont la nomenclature dépend des processus en jeu (Fig. 1.1). Les modèles sédimentaires de dépôts, dominés par la houle (e.g. Clifton et al., 1971 ; Davis Jr & Hayes, 1984 ; Davis Jr, 1985 ; McLane, 1995 ; Allen, 1997 ; Clifton, 2006 ; Plint, 2010) ou par les marées (e.g. Dalrymple, 1992, 2003 ; Davis & Dalrymple, 2012), sont déjà bien contraints dans la littérature. Cependant, les modèles sédimentaires de faciès pour les sous-environnements à doubles ou triples influences (Fig. 1.1) ne sont pas toujours bien contraints. Dans les études réalisées (sur des environnements anciens et actuels) au cours de ce travail, la houle est le processus principal qui régit la sédimentation mais une action subordonnée de la marée est également présente. Avant d'aller plus loin dans la caractérisation des environnements hybrides (houle-marée) un petit rappel sur ces deux processus et leur action sur la sédimentation est proposé ci-dessous.

a. La houle

Une vague est une perturbation qui se propage à la surface de l'eau. Elle n'entraine pas de transport de matière, mais crée un mouvement oscillatoire à la surface de l'eau. Cette onde (la vague) peut être initiée par différents mécanismes (vent, tremblements de terre, glissement de terrains, etc.) dans différents milieux (mer, lac, etc.). Dans le cas où cette vague est formée en mer par le vent, on parle de houle.

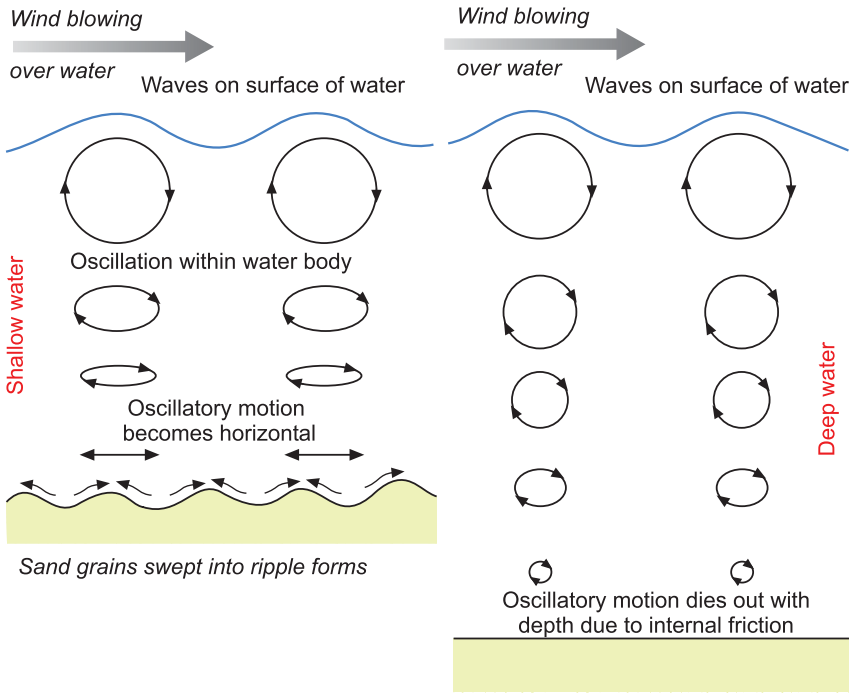

Fig. 1.2. *Formation de rides symétriques de houle résultant du courant oscillatoire horizontal généré à l'interface eau-sédiment. On remarque que ces rides ne se forment pas à toutes profondeurs. Dans le cas de droite la colonne d'eau est trop importante et la friction interne de la masse d'eau tend à stopper le mouvement oscillatoire. Ainsi la limite d'action de la houle est mise en avant. Figure modifiée d'après Nichols (2009).*

Le mouvement oscillatoire généré à la surface de l'eau est lié aux mouvements circulaires des molécules d'eaux générés par la houle. Ce mouvement circulaire (orbital) se propage verticalement dans la colonne d'eau. L'augmentation de la profondeur entraine une augmentation de la friction interne et ce mouvement circulaire tend à s'amortir puis à disparaître avec la profondeur (Fig. 1.2). Pour un mouvement circulaire généré par une houle de beau temps, la profondeur à laquelle il n'y a plus de mouvement induit par la houle correspond à la limite d'action des vagues de beau temps. Dans des environnements peu profonds (i.e. au-dessus de la limite d'action des vagues de beaux temps), les orbitales vont s'aplanir, adoptant une morphologie elliptique jusqu'à se transformer en courant oscillatoire horizontal (Fig. 1.2). Ce dernier va être à l'origine des structures sédimentaires symétriques appelées rides de houle. La longueur d'onde des rides de houle (λ) est donnée par la relation :

$$\lambda = 0.65 d_o \quad (1)$$

où d_o correspond au diamètre du l'orbitale à la limite eau-sédiment qui est principalement fonction de la hauteur (H) de la houle et de la profondeur (D) (Komar, 1974 ; Clifton, 1976). Le coefficient 0.65 est généralement utilisé pour des courants oscillatoires mais cette valeur peut varier de 0.7 (Yang et al., 2006) à 0.82 (dans le cas d'un courant combiné; Perillo et al., 2014). Par ailleurs la vitesse oscillatoire de fond (U_o) à l'origine de la formation de structures sédimentaires oscillatoires va dépendre de la célérité (c) de l'onde (ici, la houle):

$$c = \sqrt{\frac{g.L}{2\pi}.\tanh\left(\frac{2\pi.D}{L}\right)} \quad (2)$$

L'onde est principalement caractérisée par sa longueur d'onde (L), sa hauteur (H), sa période (T), et de sa célérité (c) qui sont fonction de la profondeur (D) pour une longueur d'onde (L).

b. La marée

La marée est un phénomène physique dont le résultat observable est une variation verticale du niveau de l'hydrosphère. Cet effet a pour cause l'action combinée de la gravitation de la Lune et du Soleil sur la Terre (Fig. 1.3). L'hydrosphère subit une attraction gravitaire par la Terre mais quand elle est au plus proche de la Lune l'attraction du satellite s'exprime et un gonflement de marée prend place. Lorsque les astres sont alignés (syzygie), leurs influences respectives se combinent et donnent lieu aux marées de vives-eaux. Dans le cas où la Lune est à l'orthogonale de l'axe Soleil-Terre (quadrature) les marées sont dites de mortes-eaux.

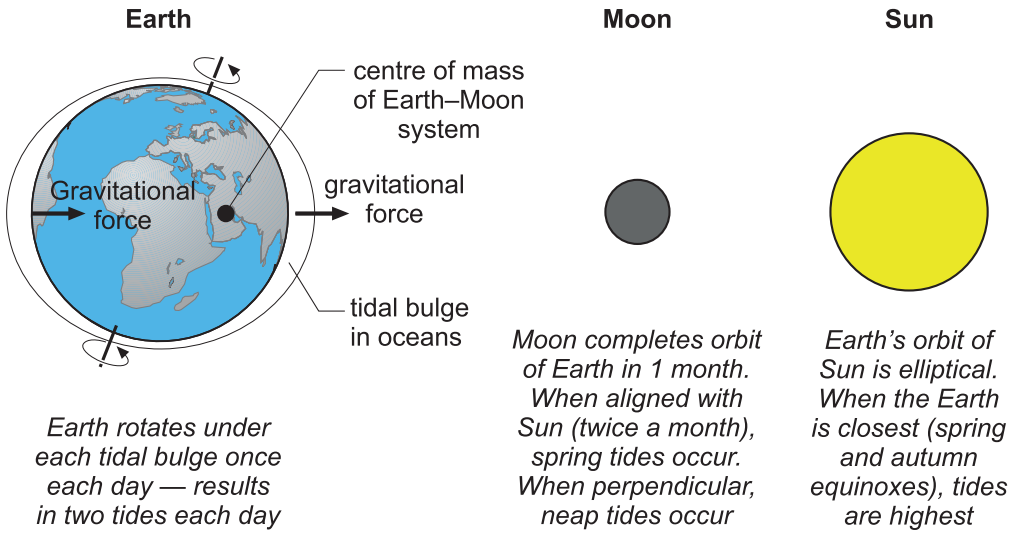

Fig. 1.3. *Les forces gravitationnelles de la Terre, de la Lune et du Soleil ainsi que la force centrifuge de la Terre, sont à l'origine du phénomène de marée. Dans la position des astres ci-dessus (aligné sur le même axe) on parle de syzygie. Dans cette alignement des marées de vives-eaux sont alors générées (figure modifiée d'après Nichols, 2009).*

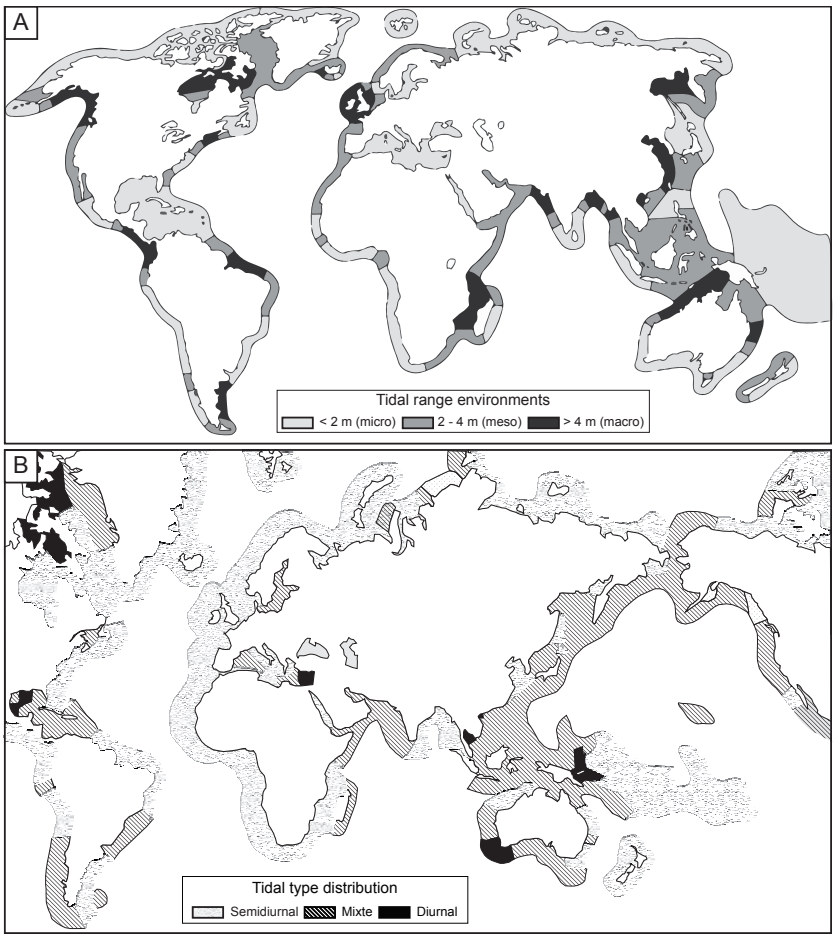

Fig. 1.4. *Répartitions des différents catégories de marnage (A) et de type de marée (B) sur Terre. Modifié d'après Davies (1964, 1972).*

Le marnage correspond à la variation d'altitude entre les niveaux de marée basse et marée haute. Ce marnage va donc varier entre les périodes de vives-eaux et de mortes-eaux. Lorsque le marnage est inférieur à 2 m, c'est un marnage microtidal, quand il est compris entre 2 et 4 m il s'agit d'un marnage mésotidal et lorsqu'il est supérieur à 4 m, le marnage est macrotidal (Fig. 1.4A) (Davies, 1964, 1972). Lorsque le marnage dépasse les 8 m, comme dans la baie du Mont Saint-Michel par exemple, ce dernier est qualifié de mégatidal (Levoy et al., 2000).

Les marées ne sont pas égales de partout à travers le globe (Fig. 1.4B). En effet, sur les côtes françaises qui nous sont les plus familières, on peut observer deux marées hautes et deux marées basses par jour : il s'agit ici de marées semi-diurnes. Lorsqu'une seule pleine mer et une seule basse mer sont observées au cours d'une journée, on parle de marée diurne. Dans le cas intermédiaire il s'agit de marée mixte. Ce type de marée se caractérise par une alternance entre des phases de marée diurne et semi-diurne.

Contrairement à la houle qui génère un courant oscillatoire, la marée produit un courant unidirectionnel, tantôt dans un sens et tantôt dans l'autre : il s'agit d'un courant bimodal. Lorsque que la marée est montante, le courant associé s'appelle le flot ou flux et quand elle est descendante c'est le jusant ou le reflux. Lors d'un cycle de marée, quand le niveau d'eau est au plus haut ou au plus bas on parle d'étale. Les courants générés par

la force de marée vont avoir un impact sur les sédiments et des signatures classiques de marée, comme les *flaser*-, *wavy*-, *lenticular-beddings*, des rides et dunes asymétriques de courants (Fig. 1.5) seront alors formées principalement en fonction du marnage et de la position proximale-distale au sein de la zone intertidale.

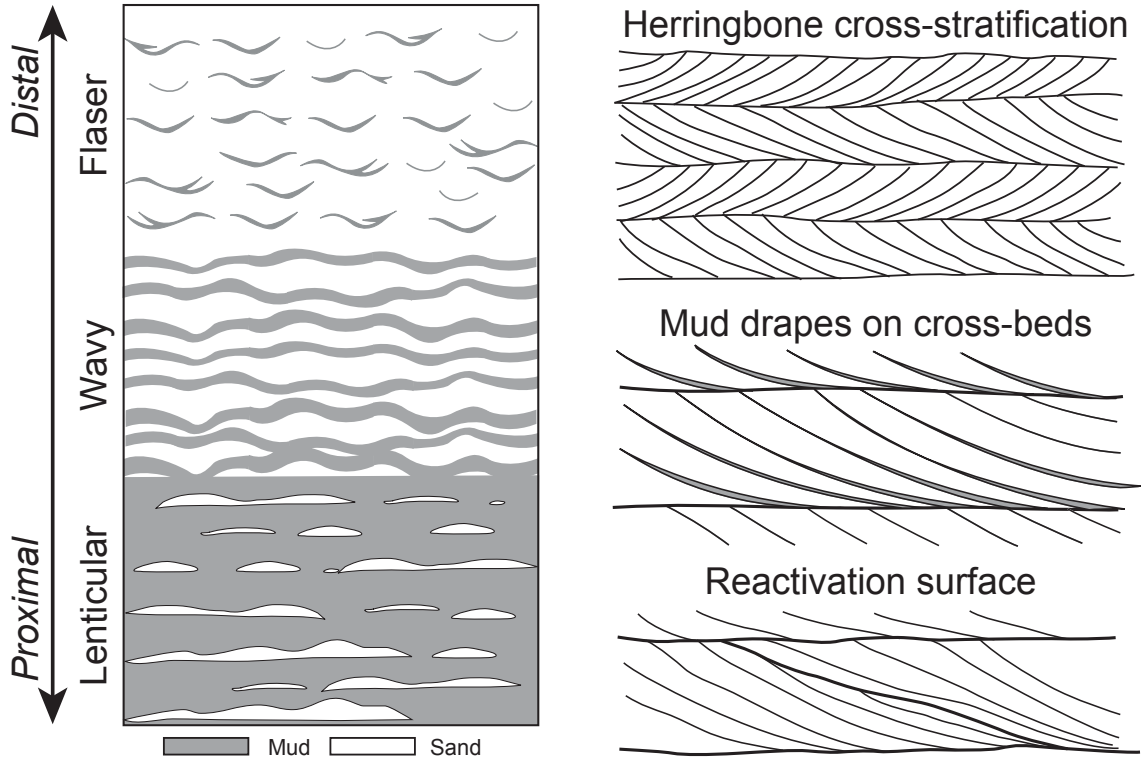

Fig. 1.5. *Structures sédimentaires pointant une influence tidale dans l'enregistrement sédimentaire. Les Lenticular- Wavy- et Flaser-beddings sont des alternances de sable et de boue en différentes proportions. Leurs reconnaissances dans une succession sédimentaire permet d'approximer une position à travers l'estran. Les Herrigbone cross-stratifications témoignent de la bimodalité du courant. Les Mud drapes se forment durant l'étale de la marée lors d'absence de courant. Les Reactivation surfaces sont formées lors de l'inversion de sens du courant de la marée. Figure modifiée d'après Nichols (2009).*

IV) Contexte général en lien avec les Chapitres II et III : environnements anciens (Ordovicien inférieur)

Les Chapitres II et III se focalisent sur une succession sédimentaire datant de l'Ordovicien inférieur (Trémadocien - Floien) de l'Anti-Atlas marocain dans la région de Zagora. L'Ordovicien inférieur de cette région est subdivisé en deux formations : Fezouata et Zini. L'intérêt porté à cette région est lié principalement à la présence de gisements fossilifères à préservation exceptionnelle (*Lagerstätten*). Ces intervalles stratigraphiques sont d'un grand intérêt pour les paléontologues car ils correspondent au début de la Grande Biodiversification Ordovicienne. Afin de pouvoir placer ces fossiles dans un contexte paléoenvironnemental, un modèle sédimentaire de dépôt a dû être créé pour cette succession sédimentaire à double influence (houle-marée). Afin de mener à bien ces deux études, 7 semaines de travail de terrain dans la région de Zagora ont été nécessaires.

a. La Grande Biodiversification Ordovicienne

La Grande Biodiversification Ordovicienne représente classiquement la deuxième grande étape de la diversification des métazoaires lors du Phanérozoïque. Elle fait suite à l'Explosion Cambrienne (Fig. 1.6). Initialement, ces deux évènements étaient considérés comme distincts l'un de l'autre mais à mesure que les résultats des découvertes paléontologiques arrivent, ils semblent être le continuum d'un seul et même événement (Martin, 2016). La GBO est l'une des radiations les plus importantes du Phanérozoïque. Cet événement biologique majeur débute durant l'Ordovicien inférieur (Trémadocien) soit environ 35 millions d'années après l'Explosion Cambrienne (ca. 485.4 – 470 Ma ; e.g. Sepkoski Jr, 1979 ; Bambach et al., 2004 ; Servais et al., 2008 ; 2010). La GBO est caractérisée par une diversification exponentielle des classes au sein des différents phylums apparus au cours du Cambrien (e.g. Harper, 2006 ; Servais et al., 2008 ; 2010). Cependant, l'enregistrement des faunes à corps mous n'est pas continu au cours du temps : ainsi très peu de gisements à préservation exceptionnelle (*Lagerstätten*) ont été découverts au cours de l'intervalle Cambrien supérieur (Furongien) - Ordovicien moyen (Darriwilien moyen) (Fig. 1.7). Les gisements à préservation exceptionnelle de l'Ordovicien moyen à supérieur sont rares et postdatent les étapes initiales de la GBO (e.g. Briggs et al., 1991 ; Aldridge et al., 1994 ; Liu et al., 2006 ; Young et al., 2007 ; Botting et al., 2011). La première publication reportant un assemblage faunique diversifié de l'Ordovicien inférieur fut réalisée par Van Roy et al. (2010). Ces derniers mettent pour la première fois en avant que la majeure partie des taxons trouvés dans les Fezouata ont une affinité cambrienne. Les plus récentes découvertes paléontologiques, principalement d'âge trémadocien

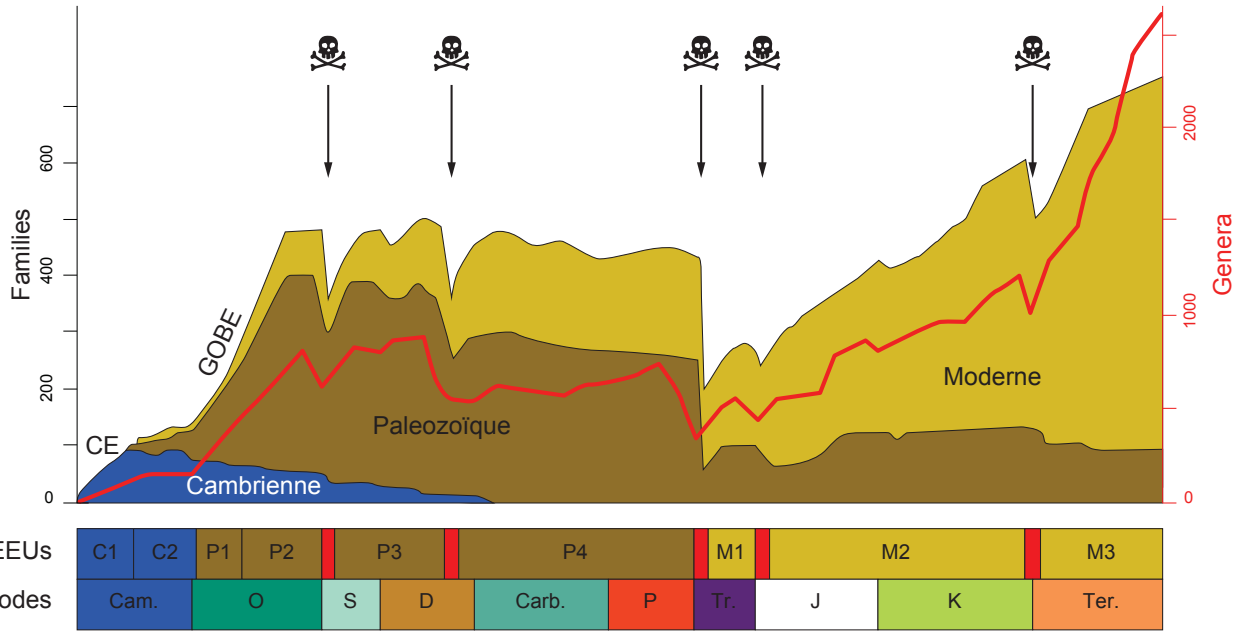

Fig. 1.6. *Courbe de biodiversité des invertébrés marins au cours du Phanérozoïque. La courbe des Familles provient de Sepkoski (1977) alors que la courbe des Genres provient de Alroy et al. (2008). EEUs : Ecological-Evolutionnary Units d'après Sheehan (1996); CE : Explosion Cambrienne ; GOBE : Grande Biodiversification Ordovicienne; C1-2: Faune Cambrienne; P1-4 : Faune Paléozoïque; M1-3 : Faune Moderne. Les 5 grandes extinctions de masse sont indiquées par des têtes de morts; Cam : Cambrien; O : Ordovicien; S : Silurien; D : Dévonien; Carb : Carbonifère; P : Permien; Tr : Trias; J : Jurassique; K : Crétacé; Ter : Tertiaire.*

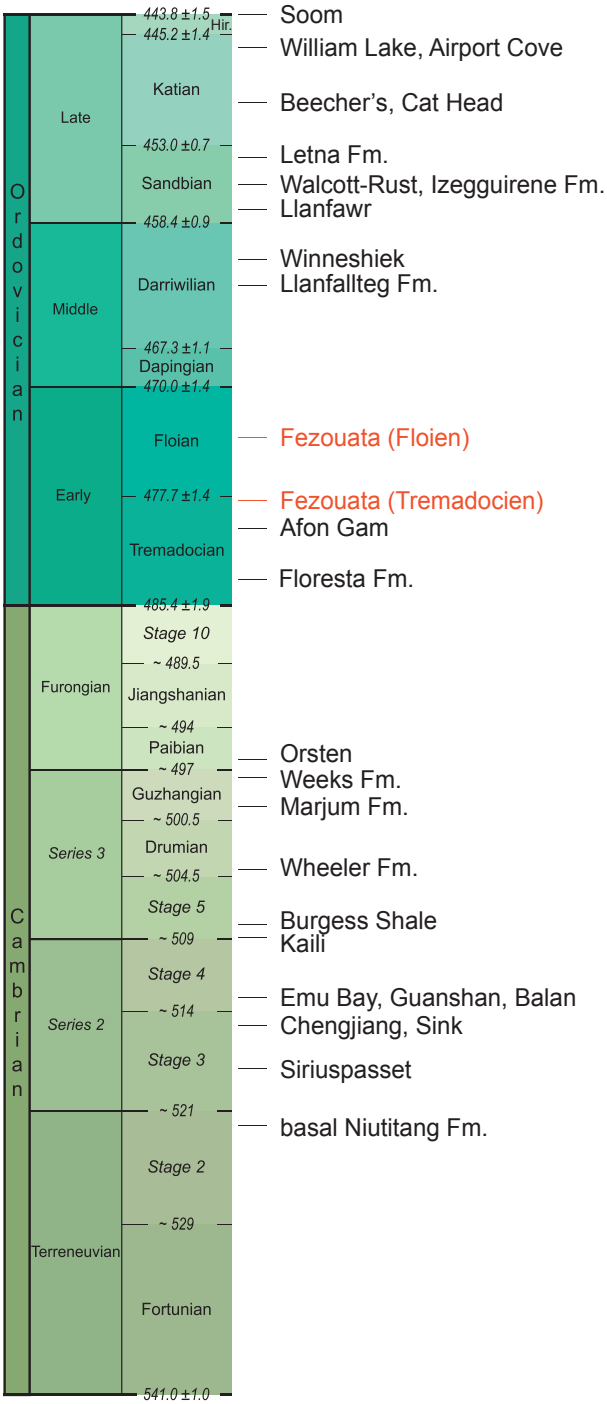

Fig. 1.7. *Les principaux gisements fossilifères à préservation exceptionnelle pour la période Cambro-Ordovicienne à travers le monde. Hir. : Hirnatian. Modifié d'après Van Roy et al. (2015).*

(Ordovicien inférieur) de la région de Zagora, dans la partie inférieure de la Formation des Fezouata ont permis de contraindre les affinités écologiques de différents groupes tels que les échinodermes (Lefebvre et al., 2016c), les graptolites (Gutiérrez-Marco & Martin, 2016), les conodontes (Lehnert et al., 2016), les palynomorphes (Nowak et al., 2016), les éponges (Botting, 2016), les gastéropodes (Ebbestad, 2016), les bivalves (Polechová, 2016), les paléoscolécides (Martin et al., 2016a), les trilobites (Martin et al., 2016c), les hyolithes (Martí Mus, 2016) et les cnidaires (Van Iten et al., 2016). Cependant, certains assemblages fauniques exceptionnellement bien préservés ont été aussi retrouvés dans des niveaux sédimentaires d'âge floien (Lefebvre et al., 2016c). Ces découvertes sont d'une importance capitale et permettent de compléter partiellement le grand puzzle de l'avènement du règne animal (projet RALI), ainsi que de la mise en place des écosystèmes au Paléozoïque (Fig. 1.8).

b. Lagerstätte

Lagerstätte ou *Lagerstätten* au pluriel, est un terme d'origine allemande qui sera fréquemment utilisé dans ce travail. A l'origine, ce mot désigne dans l'industrie minière une roche présentant un intérêt économique (Seilacher, 1970 ; 1990). Appliqué à la paléontologie, ce terme est employé pour des dépôts sédimentaires contenant des fossiles exceptionnellement bien préservés ou particulièrement abondants (e.g. Seilacher, 1970 ; Allison, 1988 ; Seilacher, 1990). Classiquement, deux types de *Largerstätten* sont reconnus : (1) l'un associé à la préservation exceptionnelle des fossiles (parties molles préservées) et (2) l'autre en rapport avec une concentration très importante de fossiles dans une couche sédimentaire. Ils sont qualifiés respectivement de *Konservat-Lagerstätten* et de *Konzentrat-Lagerstätten*.

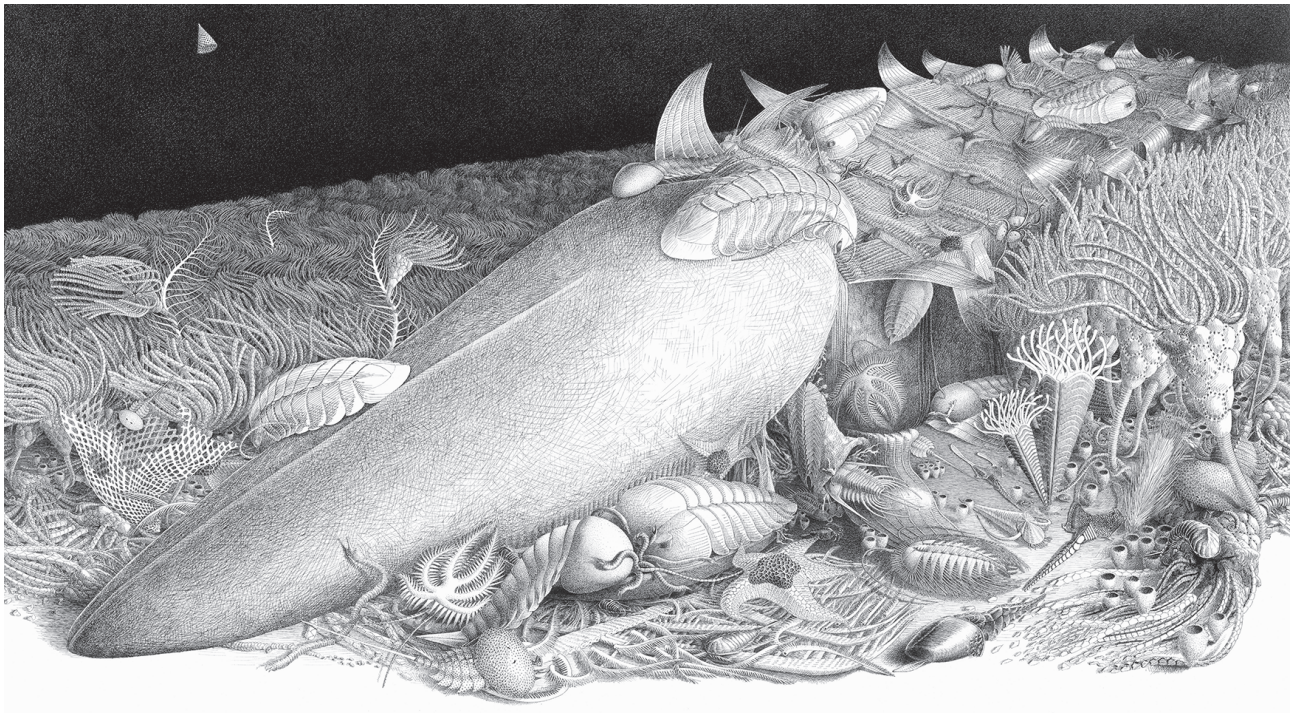

Fig. 1.8. *Reconstitution des communautés animales des Fezouata par Madmeg (Lefebvre et al. 2016a).*

c. Contexte géographique

Les dépôts sédimentaires de l'Ordovicien inférieur (Trémadocien-Floien) appartiennent à deux unités lithostratigraphiques (formations des Fezouata et du Zini), qui affleurent dans la majeure partie de l'Anti-Atlas marocain. Ce dernier est une chaine de montagne qui fait partie de la grande chaine montagneuse de l'Atlas (Fig. 1.9). La chaine de l'Atlas s'étend sur plus de 2500 km de long à travers le Maroc, l'Algérie et la Tunisie et résulte de la convergence lithosphérique entre l'Afrique et l'Europe durant le

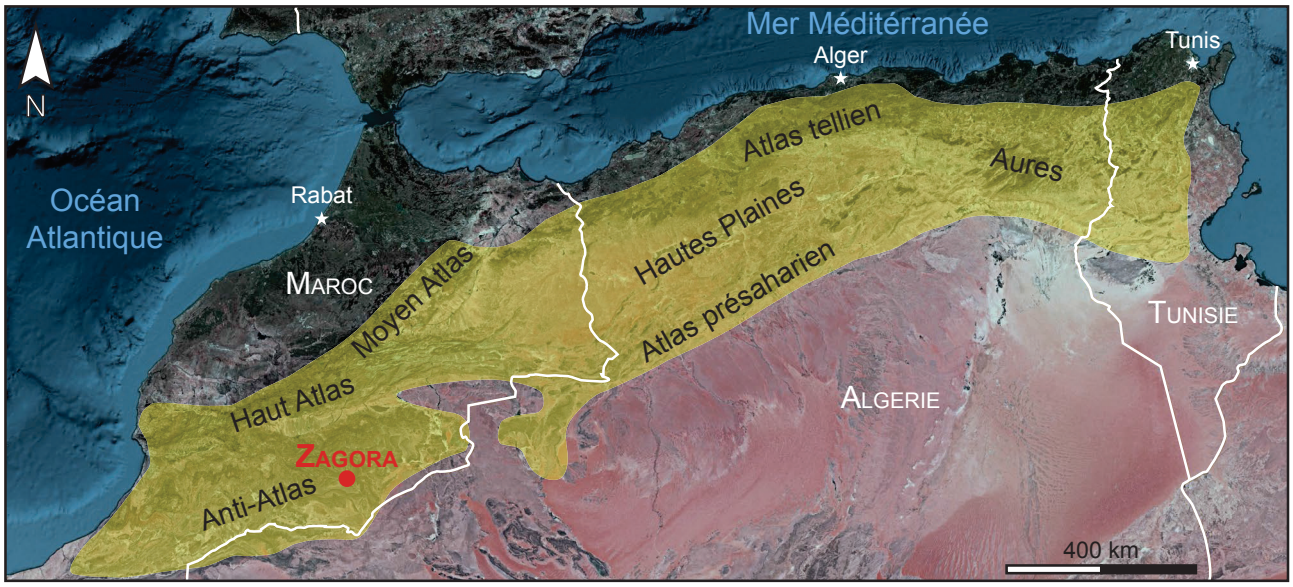

Fig. 1.9. *La chaine de l'Atlas recoupant les trois pays du Maghreb (Maroc; Algérie; Tunisie) en jaune. Les sous domaines atlasiques sont montrés ainsi que la position géographique de la ville de Zagora. Image Google Earth.*

Cénozoïque (e.g. Frizon de Lamotte et al., 2000). L'Atlas marocain est divisé en trois parties. La partie la plus septentrionale est le Moyen-Atlas, la partie centrale est le Haut-Atlas et la plus méridionale, qui est l'une des zones d'étude de ce travail, est l'Anti-Atlas. Les analyses sédimentologiques en lien avec les formations sédimentaires ordoviciennes ont été réalisées dans la région de Zagora, là où les principaux gisements fossilifères à préservation exceptionnelle ont été découverts.

d. Cadre géologique et biostratigraphique

Les premières explorations géologiques dans l'Anti-Atlas remontent à la fin du XIX^{ème}. Parmi les différents scientifiques de l'époque, on retiendra Thomson (1888) qui proposa la première interprétation géologique de l'Anti-Atlas sans se rendre sur place mais sur la base de ce qu'il a pu observer depuis le Haut-Atlas. Thomson attribua un âge crétacé inférieur à toute la succession sédimentaire de l'Ordovicien anti-atlasique. Cette anecdote historique n'est qu'une parmi toutes celles résumées dans la synthèse réalisée par Lefebvre et al. (2016b) sur l'historique des découvertes et des avancées scientifiques sur la Formation des Fezouata. Il faudra attendre les années 1940 pour que le géologue français Georges Choubert définisse 4 principales subdivisions lithostratigraphiques (Fig. 1.10) pour la succession ordovicienne (Choubert, 1942) : le Groupe des Feijas externes, le Groupe du 1er Bani, le Groupe du Ktaoua et le Groupe du 2ème Bani. Choubert (1956) propose la première carte géologique détaillée du Maroc (Fig. 1.11A) et la partie concernant l'Anti-Atlas sera mise à jour une trentaine d'années plus tard par Hollard et Choubert (1985) (Fig. 1.11B). Quelques années après le découpage lithostratigraphique fait par Choubert, un autre géologue français, Jacques Destombes (1962), subdivise à son tour les groupes en formations (Fig. 1.10 et 1.12). Le Groupe des Feijas externes est alors composé des formations inférieure et supérieure des Fezouata, du Zini et du Tachilla. Le

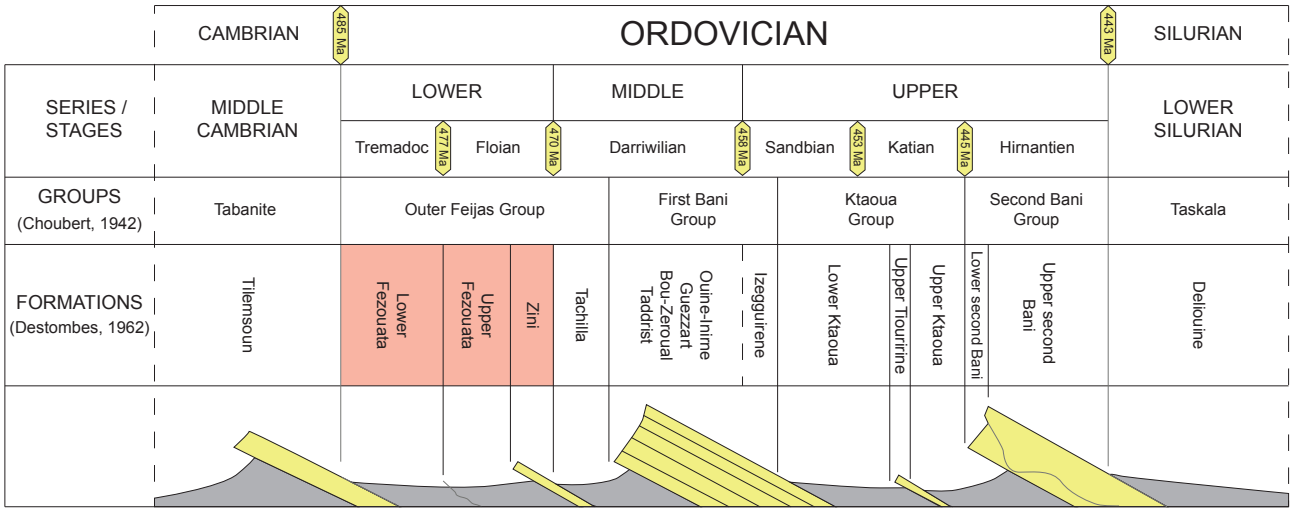

Fig. 1.10. *Découpage lithostratigraphique de l'Odovicien dans la région de Zagora. Les Groupes sont définis d'après Choubert (1942) et les formations d'après Destombes (1962). La zone en rose correspond aux formations sédimentaires qui font l'objet d'étude d'une partie de ce travail. Figure modifiée d'après Marante (2008).*

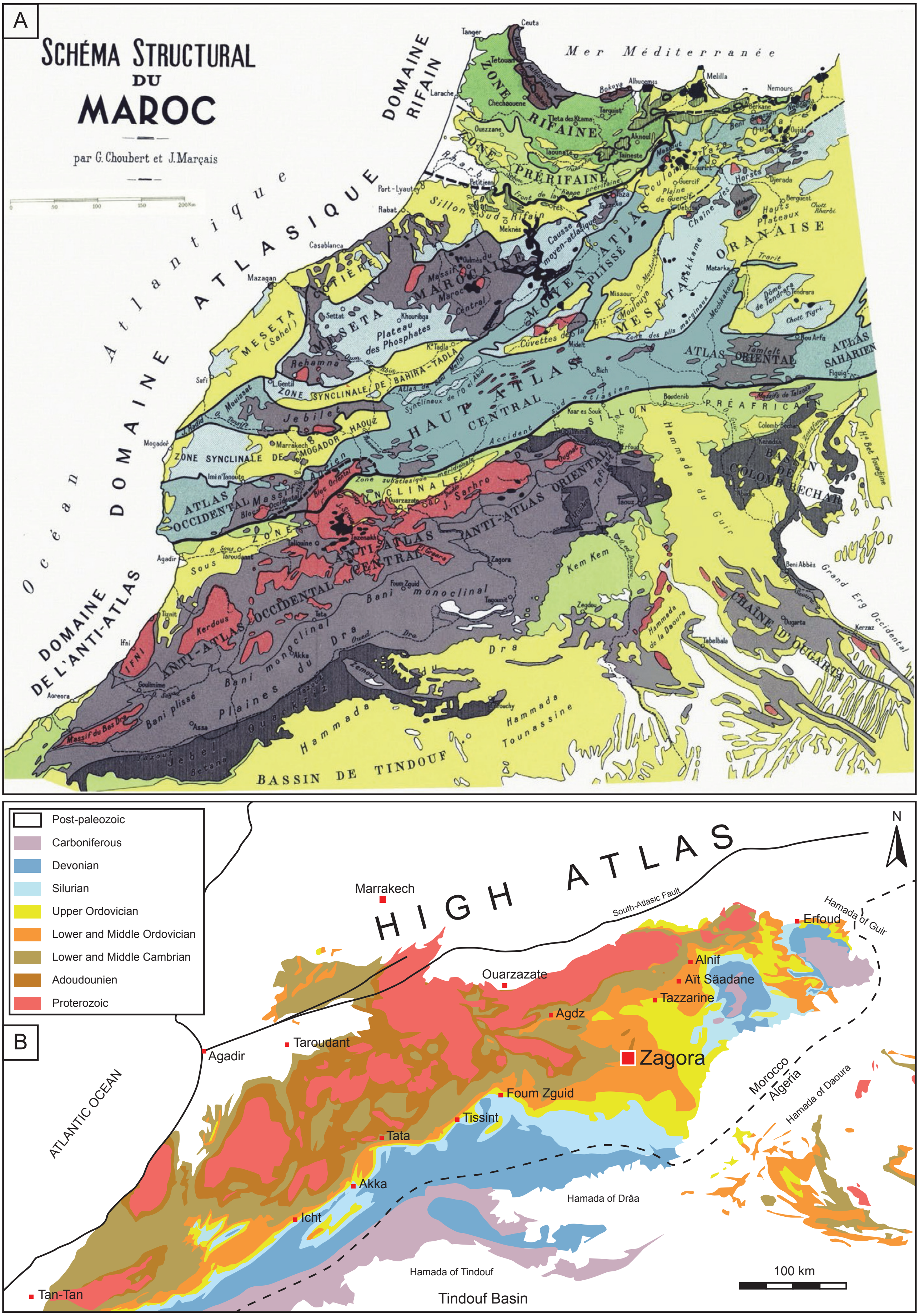

Fig. 1.11. *(A) Carte géologique du Maroc réalisé par Choubert (1956); (B) Carte géologique de l'Anti-Atlas marocain modifié d'après Hollard & Choubert (1985).*

Groupe des Feijas externes fera l'objet d'une partie de ce travail de thèse (à l'exception de la Formation du Tachilla). L'affinage de la nomenclature ordovicienne réalisé par Destombes est principalement basé sur des données lithologiques et paléontologiques. Il caractérisa la Formation inférieure des Fezouata (≈ 400 m d'épaisseur dans la région de Zagora) comme des schistes argileux, vert-bleus, présentant des graptolites (*Dictyonema, Bryograptus, Anisograptus, Clonograptus*) et des trilobites (*Parapilekia, Asaphopsis, Platypeltoides, Asaphellus*). Elle repose sur les Grès de Tabanite du Cambrien moyen (Fig. 1.10) et son sommet est défini par un niveau de minerai de fer oolithique ou de glauconite. La Formation supérieure des Fezouata (≈ 600 m d'épaisseur dans la région de Zagora) est constituée de schistes verts argilo-sableux et contient des graptolites (*Didymograptus, Temnograptus, Schizograptus, Isograptus, Hermanograptus, Tetragraptus*) et des trilobites (*Calymenidae, Asaphidae*). Elle est localement surmontée par les quartzites du Zini ou par un niveau de minerai de fer oolithique. La Formation du Zini (≈ 8 m d'épaisseur dans la région de Zagora) est principalement constituée de grès et très peu de fossiles ont été retrouvés. Cependant, Lefebvre et al. (2016c) y ont noté la présence ponctuelle de moulages externes de thèques de diploporites (échinodermes). Dans la région de Zagora, la Formation du Zini présente une faible épaisseur par rapport à son équivalent au Sud-Ouest dans la région de Tilesoun (Fig. 1.12) où elle peut atteindre 350 m d'épaisseur. Les travaux de sédimentologie les plus récents dans la région de Zagora (Vaucher et al., 2016 ; sous presse) ont permis de mettre en évidence que l'intervalle stratigraphique correspondant à l'Ordovicien inférieur (formations inférieure et

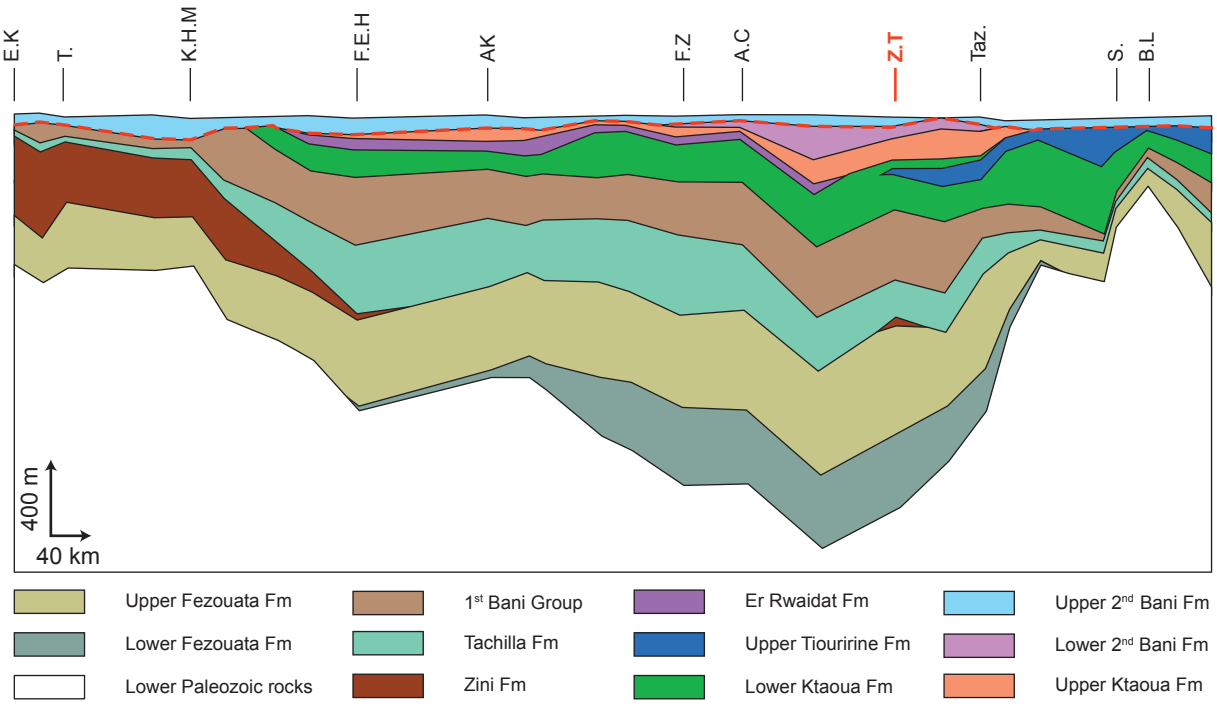

Fig. 1.12. *Variations d'épaisseurs des séries Ordoviciennes dans l'Anti-Atlas selon un profil sud-ouest nord-est. La ligne rouge en pointillé correspond à la discontinuité associée à la glaciation hirnentienne. E.K : El Khannfra; T. : Tilesoun; K.H.M : Kheneg-M'Karz; F.E.H : Foum El-Hassane; AK. : Akka; F.Z : Foum-Zguid; A.C : Azib-Cebbi; Z.T : Zagora Tagounite (zone d'étude en rouge); Taz. : Tazzarine; S. : Siguente; B.L : Bou-Legroun. Modifié d'après Destombes et al. (1985).*

supérieure des Fezouata et du Zini) a une épaisseur plus faible (≈ 870 m) que celle estimée par Destombes (1962). Le niveau ferrugineux et glauconieux servant de limite entre les formations inférieure et supérieure des Fezouata (Destombes, 1962) n'est pas présent dans la région de Zagora. Martin et al. (2016b) proposent de les regrouper en une seule et même unité lithostratigraphique: les Schistes des Fezouata. Récemment, plusieurs études biostratigraphiques ont été menées dans les Schistes des Fezouata. Le contrôle temporel de la distribution sédimentaire des séries de l'Ordovicien inférieur a principalement été réalisé à l'aide des graptolites et de leurs biozones associées (Gutiérrez-Marco & Martin, 2016). Concernant l'intervalle sédimentaire livrant les gisements à préservation exceptionnelle, les fossiles marqueurs utilisés furent : les graptolites (Martin et al., 2016b), les conodontes (Lehnert et al., 2016), les chitinozoaires et les acritarches (Nowak et al., 2016). Les reconstitutions paléogéographiques suggèrent que les séries sédimentaires de l'Ordovicien inférieur se sont déposées dans une mer épicontinale proche du pôle Sud (Fig. 1.13) en contexte extensif post-rifting lié à la migration d'Avalonia vers le Nord qui initie l'ouverture de l'Océan Rhéique (e.g. Torsvik, 2009 ; Torsvik & Cocks, 2013).

Fig. 1.13. *Reconstitution paléogéographique de l'Ordovicien inférieur (ca. 480 Ma). L'étoile rouge montre la position paléogéographique de la région de Zagora à cette époque. Modifié d'après Torsvik (2009).*

e. Vulgarisation

Lors de ma thèse, j'ai participé à un atelier de vulgarisation BARCamp (Bienvenue A la Recherche) qui s'est tenu à la Bibliothèque Universitaire de Lyon 1. Cet exercice avait pour but de permettre aux doctorants de présenter leurs activités de recherches à un public non averti. Pour les néophytes en géologie ou pour les plus paresseux, vous pouvez regarder la vidéo ci-après. Elle dure une dizaine de minutes et vulgarise les résultats présentés dans les Chapitres II et III de ce travail. La vidéo est uniquement accessible sur la version pdf de ce travail.

Si il y a un espace vide au-dessus, c'est que vous lisez actuellement la version papier de cette thèse. Sur la version électronique : clic droit et activer le contenu. Pensez à allumer vos hauts parleurs!

IV) Contexte général en lien avec le Chapitre IV : environnements actuels

Le Chapitre IV contient deux études qui tendent à caractériser les différentes structures sédimentaires observées dans deux localités du littoral français à dominance de houle mais influencées par la marée :

- Berck-Plage, département du Pas-de-Calais (France)
- Cap-Ferret, département de la Gironde (France)

La première étude concerne la zone intertidale de Berck-Plage. Nous nous sommes rendus sur place lors de la marée du siècle en mars 2015, afin d'inventorier et de caractériser les différentes structures sédimentaires formées ainsi que leur distribution au sein de la zone intertidale. Cette mission a été initiée par les observations et conclusions tirées du Chapitre II. En effet, nous avons interprété la Formation ordovicienne du Zini comme un système mégatidal en barres-et-bâches (*ridges-and-runnels*) ayant, par exemple, pour analogue moderne la Côte d'Opale dans le Nord de la France. A Berck-Plage comme dans l'Ordovicien inférieur, une dominance de houle (de beau temps ou de tempête) influencée par l'action de la marée est présente. Cette dernière va jouer un rôle majeur dans la distribution ainsi que dans la formation des structures sédimentaires au sein de la zone intertidale.

La deuxième étude concerne la pointe du Cap-Ferret. Cette étude est encore en cours. Le choix de cette zone est lié à la présence de structures sédimentaires ayant des morphologies externes en dômes (Fig. 1.14A). Une variabilité morphologique intrinsèque est toutefois observée, donnant lieu à des géométries tantôt en croissant ou tantôt allongée bien que la morphologie en dôme prédomine. Ces structures sédimentaires mamelonnées

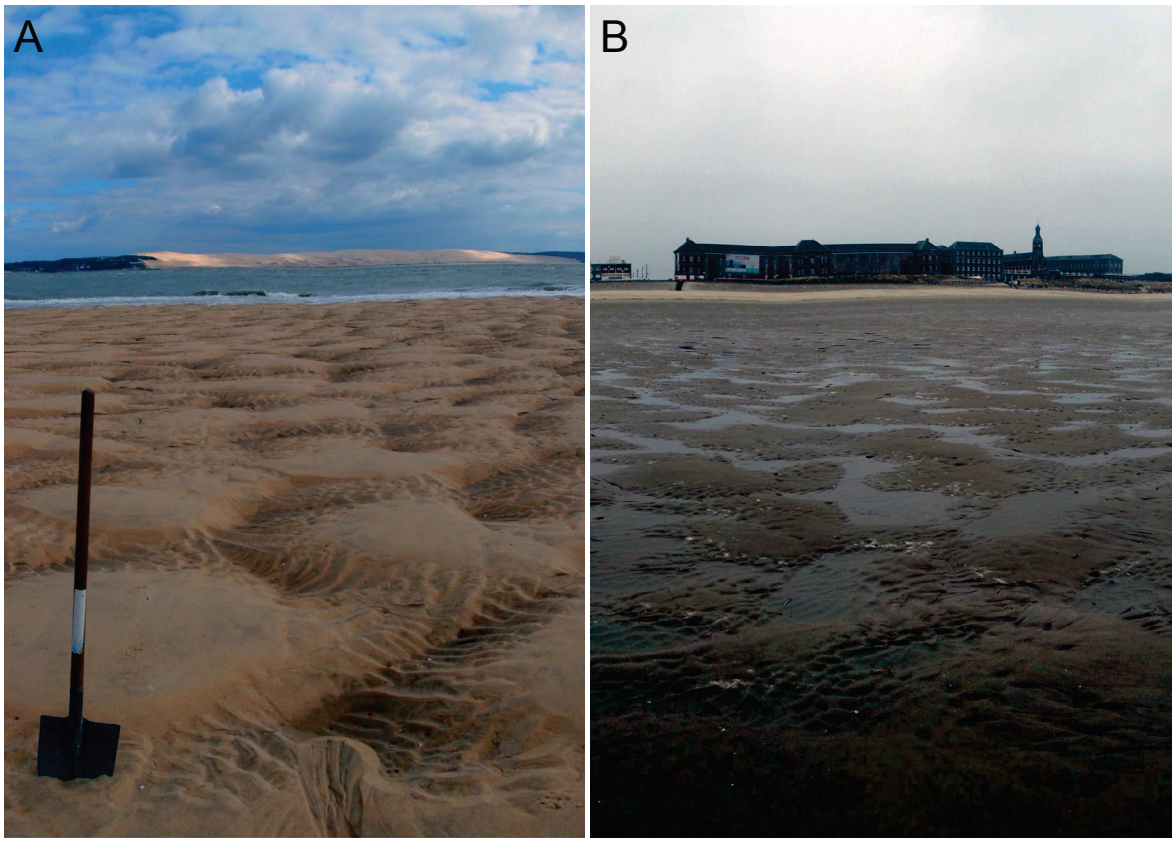

Fig. 1.14. *Structures sédimentaires en mamelons observées dans la zone intertidale à marée basse à la pointe du Cap-Ferret (A) et à Berck-Plage (B). Ces morphologies en dômes miment d'un point de vu externe celles des Hummocky cross-stratifications. La longueur d'onde de ces structures est d'environ de 1,5 m (A) et de 1,2 m (B).*

sont séparées les unes des autres par des creux. Elles ont une longueur d'onde d'environ 1 - 1,5 m pour une élévation (du creux au sommet des mamelons) d'environ 30 cm. D'un point de vue de leur morphologie externe, ces structures peuvent être considérées comme étant des dunes hydrauliques ou des mégarides (e.g. Clifton et al., 1971 ; Harms, 1979 ; Chauhan, 2000 ; Gallagher, 2003 ; Dumas et al., 2005 ; Perillo et al., 2014 ; Larsen et al., 2015). Néanmoins, la morphologie en dôme rappelle les fameuses *Hummocky cross-stratifications* (HCS ou stratifications entrecroisées en mamelons ; Fig. 1.15) décrites pour la première fois par Harms et al. (1975). L'analogie entre ces mégarides et les HCS a été mentionnée dans la thèse de Thiry-Bastien (2002) et par Ferry (2015) qui suggèrent, de par leurs structures internes, une affinité entre ces structures et celles des HCS. Ils en conclurent que la houle (de beau temps) est responsable de ces structures. Au sein de cette étude préliminaire, nous montrons que le mécanisme initiant la formation de ces mamelons résulterait d'une interférence de fronts de houle générée par la géomorphologie

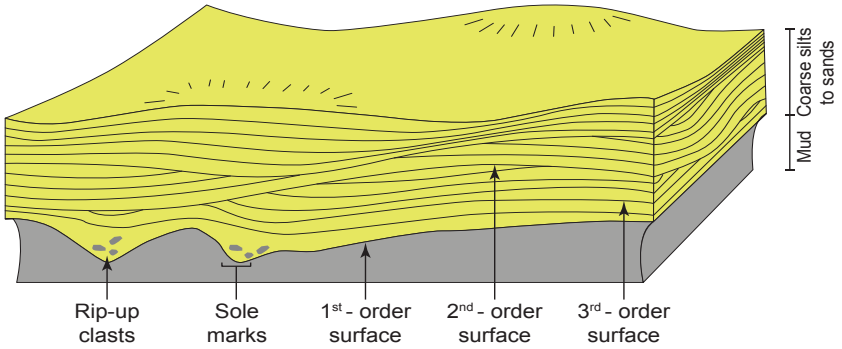

Fig. 1.15. *Hummocky cross-stratifications (HCS ou stratifications entrecroisées en mamelons) et ses différents ordres de surfaces (Modifié d'après Harms et al., 1975 et Cheel, 2003).*

côtière. Cependant, l'interférence de houle est peut être responsable d'une partie de ces structures mais comme nous le verrons dans ce Chapitre IV, ces structures présentent une grande affinité avec des structures sédimentaire formées par des flux supercritiques (e.g. Alexander et al., 2001 ; Lang & Winsemann, 2013 ; Cartigny et al., 2014) qui seront dans le cas présent liés au reflux des vagues ayant déferlé (Brocchini & Baldock, 2008). Ces mamelons ont aussi été observés à Berck-Plage (Fig. 1.14A), mais l'homogénéité granulométrique de Berck-Plage n'a pas permis l'identification de structures internes. La palette granulométrique plus large des sédiments du Cap-Ferret permet l'observation des laminations internes qui constituent l'architecture interne de ces morphologies en dômes.

a. Berck-Plage

i. Situation géographique

La zone d'étude de Berck-Plage se situe dans le département du Pas-de-Calais dans le Nord de la France. Allongé selon un axe nord-sud, cet environnement fait partie de la Côte d'Opale de la Manche (Fig. 1.16). La zone intertidale de Berck-Plage est bornée au nord par la Baie de Canche et au sud par la Baie d'Authie.

ii. Caractéristiques de la zone d'étude

La zone intertidale de Berck-Plage est caractérisée par plusieurs barres de sable parallèles à la côte. Ces barres ont une élévation d'environ 1 m et sont espacées les unes des autres de 50 à 150 m. Chacune des barres est régulièrement fractionnée tous les 100 - 150 m par des chenaux (Masselink et al., 2006). Les creux séparant les barres sont appelés bâches. Ce système de barres-et-bâches (*ridges-and-runnels*) a été décrit la première fois par King et Williams (1949). Les grains sédimentaires composant la zone intertidale sont des grains fins à moyens de quartz, ainsi que quelques débris coquilliers.

iii. Paramètres océaniques

La côte de Berck-Plage est soumise à un marnage mégatidal semi-diurne pouvant atteindre 10,5 m durant les marées de vives-eaux (Anthony et al., 2004). Lors de notre mission du 17 au 21 mars 2015, les coefficients de marées de vives-eaux étaient de 71 à 118 donnant lieu à un marnage allant de 6,5 à 10,5 m. Les vents soufflant sur la Manche soumettent la zone intertidale à des vagues de beau temps (< 1.5 m) et occasionnellement à des vagues de tempêtes (2 à 4 m) (Augris et al., 2004) majoritairement en provenance de l'ouest / sud-ouest. Cette houle permet la mise en place d'une dérive littorale vers le nord. Durant la mission de terrain, la houle incidente avait des hauteurs inférieures à 2 m pour une périodicité entre 8 et 10 s.

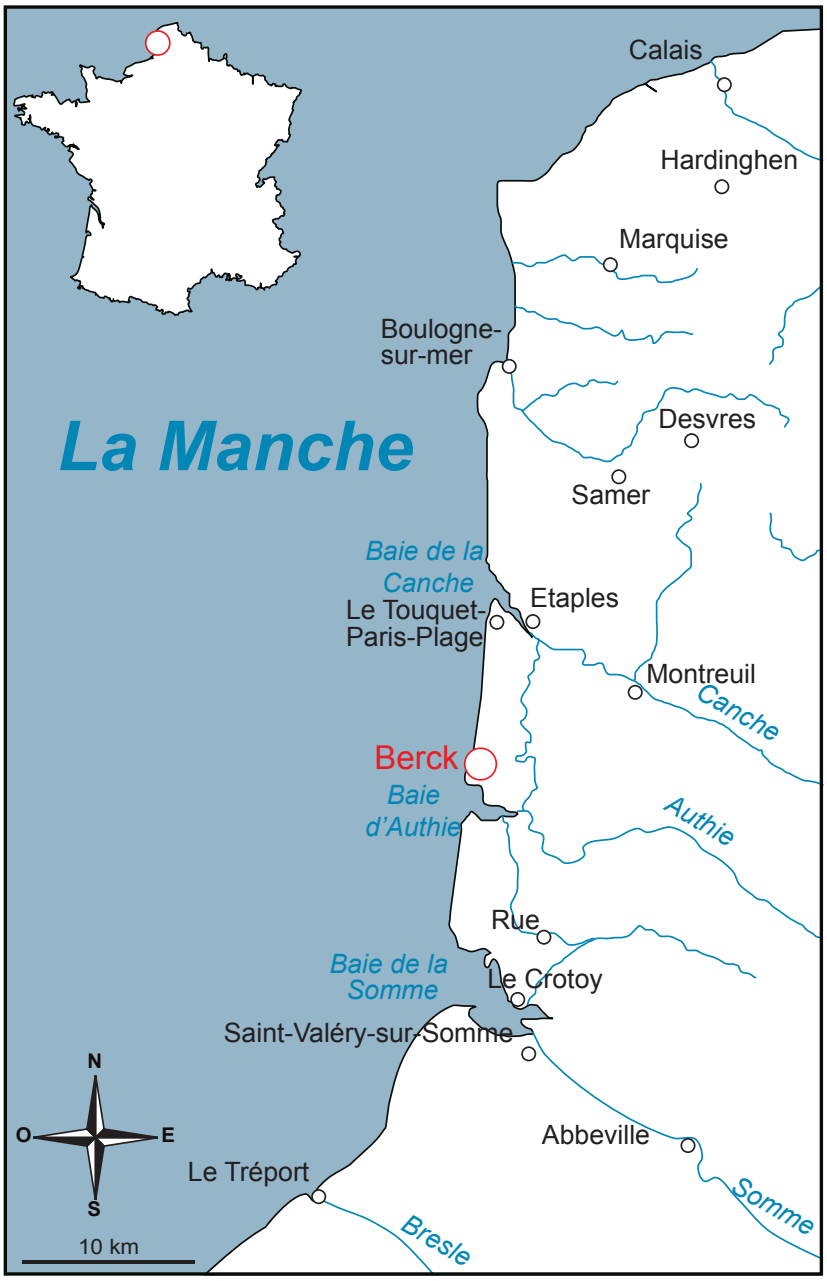

Fig. 1.16. *Carte géographique de la Côte d'Opale. Ce littoral allongé nord-sud est situé au Nord de la France sur la façade de la Manche. La première étude du Chapitre IV se focalise sur la zone intertidale de Berck. Carte modifiée d'après Bourichon (2009)*

b. Cap-Ferret

i. Situation géographique

La pointe du Cap-Ferret fait partie de la commune de Lège-Cap-Ferret. Elle se situe dans le département de la Gironde dans le Sud-Ouest de la France, sur la façade atlantique (Fig. 1.17). La pointe du Cap-Ferret est le point le plus méridional de la flèche sableuse du Cap-Ferret. Cette flèche s'étend sur 18 km de long et sur 5,5 km de large au maximum. Elle est principalement constituée de dunes éoliennes holocènes. Elle ceinture l'ouest du Bassin d'Arcachon.

ii. Caractéristiques de la zone d'étude

Cette pointe du Cap-Ferret est une flèche sableuse associée à de nombreux systèmes de baïnes. La flèche ainsi que les baïnes associées progradant vers le sud sont initiées par une houle provenant principalement du nord-ouest, créant ainsi une dérive littorale en direction du sud (e.g. Thauront, 1994 ; Cayocca, 1996). La granulométrie de la pointe du Cap-Ferret va du sable fin à grossier. La fraction sédimentaire la plus fine provient du Bassin d'Arcachon, principalement alimenté par le fleuve l'Eyre (ou Leyre), qui prend sa source plus au sud dans les Landes.

iii. Paramètres océaniques

Au niveau du Cap-Ferret, la marée semi-diurne présente un marnage macrotidal. Lors des marées de mortes-eaux le marnage est d'environ 0,8 m, alors qu'il peut atteindre 4,6 m lors des marées de vives-eaux. La houle incidente présente la majeure partie de l'année des hauteurs inférieures à 2 m bien qu'elle puisse occasionnellement atteindre les 4 m (e.g. Thauront, 1994 ; Cayocca, 1996). Lors de la mission effectuée entre le 8 et le 11 mars 2016, les coefficients de marée de vives-eaux étaient compris entre 101 et 116 donnant lieu à un marnage variant respectivement de 3,72 à 4,31 m. La houle incidente avait des hauteurs inférieures à 2 m pour une périodicité entre 8 et 10 s.

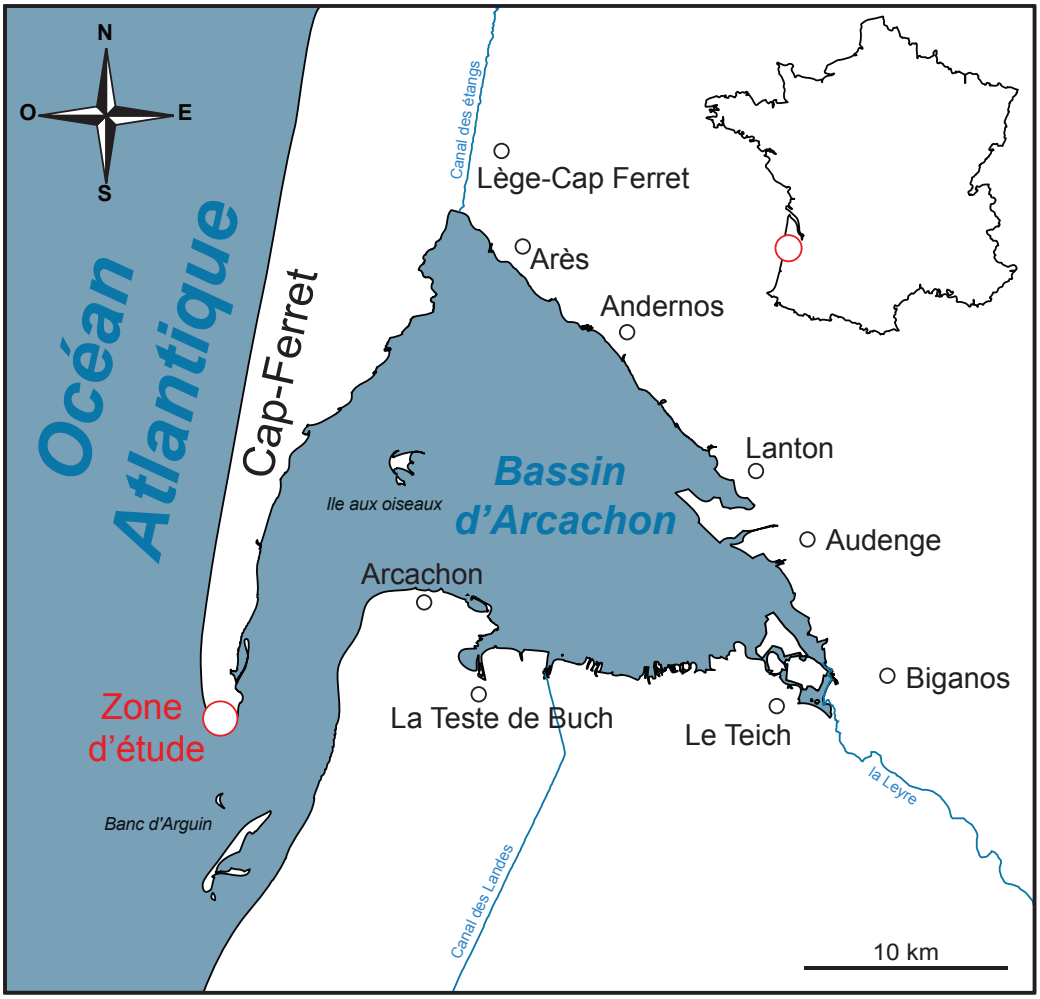

Fig. 1.17. *Carte géographique du Bassin d'Arcachon. Ce bassin est ceinturé à l'ouest par la flèche du Cap-Ferret. La deuxième partie du Chapitre IV se focalise sur la zone intertidale de la pointe du Cap-Ferret. Source SHOM.*

V) Références

Aldridge, R.J., Theron, J.N., Gabbott, S.E., 1994. The Soom Shale: a unique Ordovician fossil horizon in South Africa. Geology Today, 10(6): 218-221.

Alexander, J., Bridge, J.S., Cheel, R.J., Leclair, S.F., 2001. Bedforms and associated sedimentary structures formed under supercritical water flows over aggrading sand beds. Sedimentology, 48(1): 133-152.

Allen, P.A., 1997. Earth Surface Processes. Blackwell Science, London, UK, 404 pp.

Allison, P.A., 1988. Konservat-Lagerstatten: cause and classification. Paleobiology: 331-344.

Alroy, J., Aberhan, M., Bottjer, D.J., Foote, M., Fürsich, F.T., Harries, P.J., Hendy, A.J.W., Holland, S.M., Ivany, L.C., Kiessling, W., Kosnik, M.A., Marshall, C.R., McGowan, A.J., Miller, A.I., Olszewski, T.D., Patzkowsky, M.E., Peters, S.E., Villier, L., Wagner, P.J., Bonuso, N., Borkow, P.S., Brenneis, B., Clapham, M.E., Fall, L.M., Ferguson, C.A., Hanson, V.L., Krug, A.Z., Layou, K.M., Leckey, E.H., Nürnberg, S., Powers, C.M., Sessa, J.A., Simpson, C., Tomašových, A., Visaggi, C.C., 2008. Phanerozoic Trends in the Global Diversity of Marine Invertebrates. Science, 321(5885): 97-100.

Anthony, E.J., Levoy, F., Monfort, O., 2004. Morphodynamics of intertidal bars on a megatidal beach, Merlimont, Northern France. Marine Geology, 208(1): 73-100.

Augris, C., Clabaut, P., Costa, S., Gourmelon, F., Latteux, B., 2004. Evolution morpho-sédimentaire du domaine littoral et marin de la Seine-Maritime. Conseil Général de la Seine-Maritime, EDF, 2d. Ifremer, Bilans et Perspectives, Ifremer, 159 p.

Bambach, R.K., Knoll, A.H., Wang, S.C., 2004. Origination, extinction, and mass depletions of marine diversity. Paleobiology, 30(4): 522-542.

Botting, J.P., 2016. Diversity and ecology of sponges in the Early Ordovician Fezouata Biota, Morocco. Palaeogeography, Palaeoclimatology, Palaeoecology, 460: 75-86.

Botting, J.P., Muir, L.A., Sutton, M.D., Barnie, T., 2011. Welsh gold: A new exceptionally preserved pyritized Ordovician biota. Geology, 39(9): 879-882.

Bourichon, 2009. https://commons.wikimedia.org/wiki/File%3AC%C3%B4te_d'Opale_topographic_map-fr.svg.

Briggs, D.E.G., Bottrell, S.H., Raiswell, R., 1991. Pyritization of soft-bodied fossils: Beecher's trilobite bed, Upper Ordovician, New York State. Geology, 19(12): 1221-1224.

Brocchini, M., Baldock, T.E., 2008. Recent advances in modeling swash zone dynamics: Influence of surf-swash interaction on nearshore hydrodynamics and morphodynamics. Reviews of Geophysics, 46(3).

Cartigny, M.J.B., Ventra, D., Postma, G., van Den Berg, J.H., 2014. Morphodynamics and sedimentary structures of bedforms under supercritical-flow conditions: New insights from flume experiments. Sedimentology, 61(3): 712-748.

Cayocca, F., 1996. Modélisation morphodynamique d'une embouchure tidale : application aux passes d'entrée du Bassin d'Arcachon, Unpublished PhD thesis, University Bordeaux 1, Bordeaux, France, 426 pp.

Chauhan, P.P.S., 2000. Bedform Association on a Ridge and Runnel Foreshore: Implications for the Hydrography of a Macrotidal Estuarine Beach. Journal of Coastal Research, 16(4): 1011-1021.

Cheel, R.J., 2003. Hummocky and swaley cross-stratification. In: G.V. Middleton (Ed.), Encyclopedia of Sediments and Sedimentary Rocks. Kluwer Academic Publisher, Dordrecht, The Netherlands, pp. 362–364.

Choubert, G., 1942. Constitution et puissance de la série primaire de l'Anti-Atlas. CR Acad. Sci. Paris, 215: 445-447.

Choubert, G., 1956. Lexique stratigraphique du Maroc. NotesMém. Serv. Géol.Maroc. 134, 39–165.

Clifton, H.E., 1976. Wave-generated structures: a conceptual model. in Davis, J.R.A., and Ethrington, R.L., eds., Beach and Nearshore Processes: Society of Economic Paleontologists and Mineralogists, Special Publication(24): 126-148.

Clifton, H.E., 2006. A re-examination of facies models for clastic shorelines. In: H.W. Posamentier, R.G. Walker (Eds.), Facies Model Revisited. SEPM, Special Publication, vol. 84, pp. 293-337.

Clifton, H.E., Hunter, R.E., Phillips, R.L., 1971. Depositional structures and processes in the non-barred high-energy nearshore. Journal of Sedimentary Research, 41(3).

Dalrymple, R.W., 1992. Tidal depositional systems. Facies models: Response to sea level change: 195-218.

Dalrymple, R.W., 2003. Sedimentology and stratigraphy of a tide-dominated, foreland-basin delta (Fly River, Papua New Guinea).

Davies, J.L., 1964. A morphogenic approach to world shorelines. Zeitschrift fur

Geomorphologie, 8, 127-142.

Davies, J.L., 1972. Geographical Variation in Coastal Development. Oliver and Boyd, Edinburgh, 204 pp.

Davis Jr, R.A., 1985. Beach and nearshore zone, Coastal sedimentary environments. Springer, pp. 379-444.

Davis Jr, R.A., Hayes, M.O., 1984. What is a wave-dominated coast? Marine Geology, 60(1–4): 313-329.

Davis, R.A.J., Dalrymple, R.W., 2012. Principles of tidal sedimentology. Springer.

Destombes, J., 1962. Stratigraphie et paléogéographie de l'Ordovicien de l'Anti-Atlas (Maroc). Un essai de synthèse. Bull. Soc.Géol. Fr., 7: 453-460.

Dumas, S., Arnott, R.W.C., Southard, J.B., 2005. Experiments on Oscillatory-Flow and Combined-Flow Bed Forms: Implications for Interpreting Parts of the Shallow-Marine Sedimentary Record. Journal of Sedimentary Research, 75(3): 501-513.

Ebbestad, J.O.R., 2016. Gastropoda, Tergomya and Paragastropoda (Mollusca) from the Lower Ordovician Fezouata Formation, Morocco. Palaeogeography, Palaeoclimatology, Palaeoecology, 460: 87-96.

Ferry, S., 2015. Influence du cycle de marée sur les HCS littoraux. Données comparées de plages actuelles et de séquences côtières anciennes., 15ème Congrès Français de Sédimentologie, Chambery, France.

Frizon de Lamotte, D., Saint Bezar, B., Bracène, R., Mercier, E., 2000. The two main steps of the Atlas building and geodynamics of the western Mediterranean. Tectonics, 19(4): 740-761.

Gallagher, E.L., 2003. A note on megaripples in the surf zone: evidence for their relation to steady flow dunes. Marine Geology, 193(3–4): 171-176.

Gutiérrez-Marco, J.C., Martin, E.L.O., 2016. Biostratigraphy and palaeoecology of Lower Ordovician graptolites from the Fezouata Shale (Moroccan Anti-Atlas). Palaeogeography, Palaeoclimatology, Palaeoecology, 460: 35-49.

Harms, J., 1979. Primary sedimentary structures. Annual Review of Earth and Planetary Sciences, 7: 227.

Harms, J.C., Southard, J.B., Spearing, D.R., Walker, R.G., 1975. Depositional environments as interpreted from pri- mary sedimentary structures and stratification sequences. SEPM Short Course, 2.

Harper, D.A.T., 2006. The Ordovician biodiversification: setting an agenda for marine life. Palaeogeography, Palaeoclimatology, Palaeoecology, 232(2): 148-166.

Hollard, H., Choubert, G., 1985. Carte geologique du Maroc, 1/1000000. Ministère de l'Energie et des Mines, Direction de la Géologie, Editions du Service Géologique du Maroc.

King, C.A.M., Williams, W.W., 1949. The Formation and Movement of Sand Bars by Wave Action. The Geographical Journal, 113: 70-85.

Komar, P.D., 1974. Oscillatory ripple marks and the evaluation of ancient wave conditions and environments. Journal of Sedimentary Research, 44(1): 169-180.

Lang, J., Winsemann, J., 2013. Lateral and vertical facies relationships of bedforms deposited by aggrading supercritical flows: From cyclic steps to humpback dunes. Sedimentary Geology, 296: 36-54.

Larsen, S.M., Greenwood, B., Aagaard, T., 2015. Observations of megaripples in the surf zone. Marine Geology, 364: 1-11.

Lefebvre, B., Lerosey-Aubril, R., Servais, T., Van Roy, P., 2016a. The Fezouata Biota: An exceptional window on the Cambro-Ordovician faunal transition. Palaeogeography, Palaeoclimatology, Palaeoecology, 460: 1-6.

Lefebvre, B., El Hariri, K., Lerosey-Aubril, R., Servais, T., Van Roy, P., 2016b. The Fezouata Shale (Lower Ordovician, Anti-Atlas, Morocco): A historical review. Palaeogeography, Palaeoclimatology, Palaeoecology, 460: 7-23.

Lefebvre, B., Allaire, N., Guensburg, T.E., Hunter, A.W., Kouraïss, K., Martin, E.L.O., Nardin, E., Noailles, F., Pittet, B., Sumrall, C.D., Zamora, S., 2016c. Palaeoecological aspects of the diversification of echinoderms in the Lower Ordovician of central Anti-Atlas, Morocco. Palaeogeography, Palaeoclimatology, Palaeoecology, 460: 97-121.

Lehnert, O., Nowak, H., Sarmiento, G.N., Gutiérrez-Marco, J.C., Akodad, M., Servais, T., 2016. Conodonts from the Lower Ordovician of Morocco — Contributions to age and faunal diversity of the Fezouata Lagerstätte and peri-Gondwana biogeography. Palaeogeography, Palaeoclimatology, Palaeoecology, 460: 50-61.

Levoy, F., Anthony, E.J., Monfort, O., Larsonneur, C., 2000. The morphodynamics of megatidal beaches in Normandy, France. Marine Geology, 171(1–4): 39-59.

Liu, H.P., McKay, R.M., Young, J.N., Witzke, B.J., McVey, K.J., Liu, X., 2006. A new Lagerstätte from the Middle Ordovician St. Peter formation in northeast Iowa, USA. Geology, 34(11): 969-972.

Marante, A., 2008. Architecture et dynamique des systèmes sédimentaires silico-clastiques sur «la plate-forme géante» nord-gondwanienne. L'Ordovicien moyen de l'Anti-Atlas marocain, Unpublished PhD Thesis, Université Michel Montaigne Bordeaux 3, Bordeaux, France, 229 pp.

Martí Mus, M., 2016. A hyolithid with preserved soft parts from the Ordovician Fezouata Konservat-Lagerstätte of Morocco. Palaeogeography, Palaeoclimatology, Palaeoecology, 460: 122-129.

Martin, E., 2016. Communautés animales du début de l'Ordovicien (~ 480 Ma) : études qualitatives et quantitatives a partir des sites a préservation exceptionnelle des Fezouata, Maroc., Unpublished PhD thesis. University Claude Bernard Lyon 1, 496 pp.

Martin, E.L.O., Lerosey-Aubril, R., Vannier, J., 2016a. Palaeoscolecid worms from the Lower Ordovician Fezouata Lagerstätte, Morocco: Palaeoecological and palaeogeographical implications. Palaeogeography, Palaeoclimatology, Palaeoecology, 460: 130-141.

Martin, E.L.O., Pittet, B., Gutiérrez-Marco, J.-C., Vannier, J., El Hariri, K., Lerosey-Aubril, R., Masrour, M., Nowak, H., Servais, T., Vandenbroucke, T.R.A., Van Roy, P., Vaucher, R., Lefebvre, B., 2016b. The Lower Ordovician Fezouata Konservat-Lagerstätte from Morocco: Age, environment and evolutionary perspectives. Gondwana Research, 34: 274-283.

Martin, E.L.O., Vidal, M., Vizcaïno, D., Vaucher, R., Sansjofre, P., Lefebvre, B., Destombes, J., 2016c. Biostratigraphic and palaeoenvironmental controls on the trilobite associations from the Lower Ordovician Fezouata Shale of the central Anti-Atlas, Morocco. Palaeogeography, Palaeoclimatology, Palaeoecology, 460: 142-154.

Masselink, G., Kroon, A., Davidson-Arnott, R.G.D., 2006. Morphodynamics of intertidal bars in wave-dominated coastal settings — A review. Geomorphology, 73(1–2): 33-49.

McLane, M., 1995. Sedimentology. Oxford university press, New York; Oxford, 423 pp.

Morsilli, M., Pomar, L., 2012. Internal waves vs. surface storm waves: a review on the origin of hummocky cross-stratification. Terra Nova, 24(4): 273-282.

Nowak, H., Servais, T., Pittet, B., Vaucher, R., Akodad, M., Gaines, R.R., Vandenbroucke, T.R.A., 2016. Palynomorphs of the Fezouata Shale (Lower Ordovician, Morocco): Age and environmental constraints of the Fezouata Biota. Palaeogeography, Palaeoclimatology, Palaeoecology, 460: 62-74.

Perillo, M.M., Best, J., Garcia, M.H., 2014. A New Phase Diagram for Combined-Flow Bedforms. Journal of Sedimentary Research, 84(4): 301-313.

Plint, A.G., 2010. Wave-and storm-dominated shoreline and shallow-marine systems. In: R.W. Dalrymple, N.P. James (Eds.), Facies models. Geol. Assoc. Canada, St John's, pp. 167-200.

Polechová, M., 2016. The bivalve fauna from the Fezouata Formation (Lower Ordovician) of Morocco and its significance for palaeobiogeography, palaeoecology and early diversification of bivalves. Palaeogeography, Palaeoclimatology, Palaeoecology, 460: 155-169.

Seilacher, A., 1970. Begriff und bedeutung der Fossil-Lagerstätten. Neues Jahrbuch für Geologie und Paläontologie, Monatshefte, 1970(1): 34-39.

Seilacher, A., 1990. Taphonomy of fossil-lagerstätten: overview. Palaeobiology: a synthesis: 266-270.

Sepkoski Jr, J.J., 1979. A kinetic model of Phanerozoic taxonomic diversity II. Early Phanerozoic families and multiple equilibria. Paleobiology: 222-251.

Servais, T., Lehnert, O., Li, J., Mullins, G.L., Munnecke, A., Nuetzel, A., Vecoli, M., 2008. The Ordovician Biodiversification: revolution in the oceanic trophic chain. Lethaia, 41(2): 99-109.

Servais, T., Owen, A.W., Harper, D.A.T., Kröger, B., Munnecke, A., 2010. The great ordovician biodiversification event (GOBE): the palaeoecological dimension. Palaeogeography, Palaeoclimatology, Palaeoecology, 294(3): 99-119.

Sheehan, P.M., 1996. A new look at Ecologic Evolutionary Units (EEUs). Palaeogeography Palaeoclimatology Palaeoecology, 127: 21-32.

Thauront, F., 1994. Les transits sédimentaires subtidaux dans les passes internes du Bassin d'Arcachon, Unpublished PhD thesis, Unversity Bordeaux 1, Bordeaux, France, 304 pp.

Thiry-Bastien, P., 2002. Stratigraphie séquentielle des calcaires bajociens de l'Est de la France (Jura - Bassin de Paris), Unpublished PhD Thesis, Université Claude Bernard Lyon 1, 411 pp.

Thomson, J., 1888. Map of Southwestern Morocco. Philip, London and Liverpool.

Torsvik, T.H., 2009. BugPlates: linking biogeography and palaeogeography [WWW Document]. URL http://www.geodynamics.no/bugs/SoftwareManual.pdf (accessed 1 September 2014).

Torsvik, T.H., Cocks, L.R.M., 2013. Gondwana from top to base in space and time. Gondwana

Research, 24(3): 999-1030.

Van Iten, H., Muir, L., Simões, M.G., Leme, J.M., Marques, A.C., Yoder, N., 2016. Palaeobiogeography, palaeoecology and evolution of Lower Ordovician conulariids and Sphenothallus (Medusozoa, Cnidaria), with emphasis on the Fezouata Shale of southeastern Morocco. Palaeogeography, Palaeoclimatology, Palaeoecology, 460: 170-178.

Van Roy, P., Orr, P.J., Botting, J.P., Muir, L.A., Vinther, J., Lefebvre, B., el Hariri, K., Briggs, D.E., 2010. Ordovician faunas of Burgess Shale type. Nature, 465(7295): 215-218.

Vaucher, R., Martin, E.L.O., Hormière, H., Pittet, B., 2016. A genetic link between Konzentrat- and Konservat-Lagerstätten in the Fezouata Shale (Lower Ordovician, Morocco). Palaeogeography, Palaeoclimatology, Palaeoecology, 460: 24-34.

Vaucher, R., Pittet, B., Hormière, H., Martin, E.L.O., Lefebvre, B., sous presse. A wave-dominated, tide-modulated model for the Lower Ordovician of the Anti-Atlas, Morocco. Sedimentology.

Yang, B., Dalrymple, R.W., Chun, S., 2006. The significance of hummocky cross-stratification (HCS) wavelengths: Evidence from an open-coast tidal flat, South Korea. Journal of Sedimentary Research, 76(1-2): 2-8.

Young, G.A., Rudkin, D.M., Dobrzanski, E.P., Robson, S.P., Nowlan, G.S., 2007. Exceptionally preserved Late Ordovician biotas from Manitoba, Canada. Geology, 35(10): 883-886.

CHAPITRE II :

UN MODÈLE SÉDIMENTAIRE DE DÉPÔT DOMINÉ PAR LA HOULE ET MODULÉ PAR LA MARÉE

«Vous arrivez devant la nature avec des théories, la nature flanque tout par terre»

Auguste Renoir

I) Résumé :

Les systèmes sédimentaires hybrides résultent de l'interaction de deux ou plusieurs processus hydrodynamiques. Ces derniers contrôlent la distribution des faciès sédimentaires ainsi que leurs structures sédimentaires et géométries de dépôts. L'identification de l'interaction houle-marée dans des successions sédimentaires anciennes ou dans des environnements modernes est peu décrite dans la littérature. Les environnements marins mixtes (houle et marée) sont identifiés par la présence de structures formées par l'action de la houle et/ou de la marée. Ces structures sédimentaires sont facilement identifiables dans les environnements actuels les plus côtiers, ce qui n'est pas le cas dans les environnements marins plus distaux (ex : avant-plage inférieure/ offshore). L'analyse détaillée de 10 coupes stratigraphiques de la succession sédimentaire de l'Ordovicien inférieur dans la région de Zagora (formations des Fezouata et du Zini; Anti-Atlas, Maroc) a permis de définir 14 faciès sédimentaires, tous regroupés en 4 zones de faciès sédimentaires (plage; avant-plage supérieure; avant-plage inférieure; offshore). Ces différents faciès sédimentaires appartiennent à un système silicoclastique caractérisé par des rides symétriques de taille variable (ex : rides de houle; stratifications entrecroisées en mamelons) soulignant la dominance de la houle (de beau temps et de tempête) sur le système de dépôt analysé.

L'organisation ainsi que l'architecture interne des structures sédimentaires présentent cependant certaines particularités que l'action de la houle n'explique pas : (A) les structures sédimentaires de houle (beau temps et tempête) montrent une variation cyclique de leur longueur d'onde; (B) des gouttières d'érosion (profondes d'une dizaine de centimètres) sont enregistrées dans les swaley cross-stratifications; (C) les dépôts de tempête enregistrent des surfaces d'érosion interne décimétriques; (D) des niveaux gréseux discontinus dans la plupart des environnements de dépôt, ainsi que des couches lenticulaires gréseuses ayant une extension latérale limitée montrent que les dépôts sédimentaires à toute échelle (métrique à kilométrique) sont discontinus; (E) des rides d'oscillation combinées aggradantes-progradantes alternent avec des rides d'oscillation purement aggradantes; et (F) des environnements proximaux (plage) caractérisés par des stratifications parallèles et des surfaces de réactivation d'une dizaine de mètres de large alternent avec des structures oscillatoires de petite (décimétrique) et grande (pluridécimétrique à métrique) longueur d'onde.

Toutes ces caractéristiques de dépôt suggèrent que l'intensité de la houle, que ce soit en condition de beau temps ou de tempête, a été continuellement modulée par un autre facteur : la marée. Cependant, aucune structure de marée n'a été identifiée : elles n'ont probablement pas été préservées en raison de l'action dominante de la houle (de tempête et de beau temps). Un modèle de dépôt sédimentaire est alors proposé pour ce système marin dominé par la houle et modulé par la marée pour des environnements allant de l'offshore jusqu'à la zone intertidale et la plage.

II) Article :

A wave dominated tide modulated model for the Lower Ordovician of the Anti-Atlas, Morocco

Auteurs : **Romain Vaucher**, Bernard Pittet, Hélène Hormière, Emmanuel L.O. Martin, Bertrand Lefebvre

Article publié dans *Sedimentology*

Année : sous presse

DOI : http://dx.doi.org/10.1111/sed.12327

SEDIMENTOLOGY the journal of the International Association of Sedimentologists

Sedimentology (2016) doi: 10.1111/sed.12327

A wave-dominated, tide-modulated model for the Lower Ordovician of the Anti-Atlas, Morocco

ROMAIN VAUCHER, BERNARD PITTET, HÉLÈNE HORMIÈRE, EMMANUEL L. O. MARTIN and BERTRAND LEFEBVRE
Univ Lyon, Université Claude Bernard Lyon 1, ENS de Lyon, CNRS, UMR 5276 LGL-TPE, F-69622 Villeurbanne, France (E-mail: romain.vaucher@univ-lyon1.fr)

Associate Editor – Mariano Marzo

ABSTRACT

Hybrid depositional systems are created by the interaction of two or more hydrodynamic processes that control facies distribution and their characteristics in terms of sedimentary structures and depositional geometry. The interaction of wave and tide both in the geological sedimentary record and modern environments has been rarely described in the literature. Mixed coastal environments are identified by the evidence of wave and tidal structures and are well identified in nearshore environments, while their recognition in lower shoreface–offshore environments lacks direct information from modern settings. Detailed field analyses of 10 stratigraphic sections of the Lower Ordovician succession (Fezouata and Zini formations; Anti-Atlas, Morocco) have allowed the definition of 14 facies, all grouped in four facies zones belonging to a storm-dominated, wave-dominated sedimentary siliciclastic system characterized by symmetrical ripples of various scales. Peculiar sedimentary organization and sedimentary structures are observed: (i) cyclical changes in size of sedimentary structures under fair-weather or storm-weather conditions; (ii) decimetre-deep erosional surfaces in swaley cross-stratifications; (iii) deep internal erosion within storm deposits; (iv) discontinuous sandstone layers in most depositional environments, and common deposition of sandstones with a limited lateral extension, interpreted to indicate that deposition at all scales (metric to kilometric) is discontinuous; (v) combined flow–oscillation ripples showing aggrading–prograding internal structures alternating with purely aggrading wave ripples; and (vi) foreshore environments characterized by alternating phases of deposition of parallel stratifications, small-scale and large-scale ripples and tens of metres-wide reactivation surfaces. These characteristics of deposition suggest that wave intensity during storm-weather or fair-weather conditions was continuously modulated by another controlling factor of the sedimentation: the tide. However, tidal structures are not recognized, because they were probably not preserved due to dominant action of storms and waves. A model of deposition is provided for this wave-dominated, tide-modulated sedimentary system recording proximal offshore to intertidal–foreshore environments, but lacking diagnostic tidal structures.

Keywords GOBE, Lower Ordovician, palaeoenvironments, siliciclastic platform, storm deposits, tides.

INTRODUCTION

The facies model for wave-dominated and storm-dominated depositional environments is well-established in the literature for both the modern and the fossil records (e.g. Davies & Moses, 1964; Bluck, 1967; Goldring & Bridges, 1973; Harms, 1979; Heward, 1981; Brenchley & Newall, 1982; Dott & Bourgeois, 1982; Davis & Hayes, 1984; Davis Jr, 1985; Brenchley *et al.*, 1986; Boyd *et al.*, 1992; Dumas & Arnott, 2006; Plint, 2010), providing a predictable zonation of the sedimentary structures created by the collapse of wave orbitals on the sea floor (Allen, 1997). However, wave-dominated and storm-dominated environments represent one end member of the three processes (rivers, tides and waves) that influence coastal environments. A mixed coastal depositional system is generated when the dominant controlling process is overlapped by one of the two others (Boyd *et al.*, 1992; Dalrymple, 1992). Recent studies have discussed the sedimentary organization of modern coastal systems under the influence of waves and tides (e.g. Li *et al.*, 2000; Yang & Chun, 2001; Dalrymple *et al.*, 2003; Yang *et al.*, 2005, 2006; Dashtgard *et al.*, 2009, 2012). Similar systems certainly existed in the past but only few of them have been described so far in ancient sedimentary successions (e.g. Plink-Björklund, 2008; Billeaud *et al.*, 2009; Basilici *et al.*, 2011, 2012; Vakarelov *et al.*, 2012; Rossi & Steel, 2016). The studies on modern and ancient coastal environments focused on the shallowest parts of these mixed systems, namely on the intertidal and shallow subtidal zones. The continuation of these systems towards the offshore is not constrained, and very few models that integrate such a sedimentary context from the coastline to the offshore have been proposed (e.g. Vakarelov *et al.*, 2012).

In sedimentary systems dominated by waves and storms, tidal influence is generally obliterated, and tide-related sedimentary structures have a much lower preservation potential than wave-related structures (Li *et al.*, 2000). Consequently, evidencing the influence of tides in a wave-dominated sedimentary environment by the identification of unambiguous tidal structures can be difficult or unfeasible. This difficulty probably explains why these types of environments have not been widely recognized in ancient a sedimentary successions (Fan *et al.*, 2004; Yang *et al.*, 2005). However, Vakarelov *et al.* (2012) identified one example of a hybrid system in the Campanian strata with both wave and tide influence on the sedimentation. This identification was based on the observation of sedimentary features generated by both waves and tides (Vakarelov *et al.*, 2012). An alternative approach for recognizing tide influence (when no tide-generated structures are present) is to understand how changes in sea-level during tide cycles can modify both the sedimentary structures formed by waves and storms and the general sedimentary architecture of these peculiar wave-dominated systems (e.g. Dashtgard *et al.*, 2012).

The Lower Ordovician succession of Morocco (Fezouata and Zini formations; central Anti-Atlas; Zagora area; Fig. 1A) was deposited in a wave-dominated sedimentary system (Martin *et al.*, 2016) that, however, exhibits uncommon sedimentary features and geometrical organization when compared with the well-established facies model for wave-dominated coastal environments. This study showed that tide modulation strongly impacts the organization of wave-dominated deposits and explains the uncommon sedimentary features and architecture observed in the Lower Ordovician succession of the central Anti-Atlas. A facies model for this type of mixed system is proposed by giving new keys for its recognition.

The Lower Ordovician of the Anti-Atlas is also of prime importance for the understanding of the rise of animal life (e.g. Van Roy *et al.*, 2010, 2015; Martin *et al.*, 2014, 2016) because the Fezouata Formation contains one of the few *Lagerstätten* (Fig. 1B) recording the initial stages of the Great Ordovician Biodiversification Event (e.g. Bambach *et al.*, 2004; Servais *et al.*, 2008, 2010). A better constrain of the sedimentary dynamics involved in the exceptional preservation of soft tissues is also briefly discussed in this work.

GEOLOGICAL SETTING

At the end of the Precambrian, the Pan-African tectonic event formed the super-continent Gondwana. This super-continent extended from the Equator to the South Pole (Fig. 2A). During the Cambrian Period, the mean sea-level rose related to the oceanic expansion and resulted in the development of shallow epicontinental seas (Destombes *et al.*, 1985; Fabre, 1988; Boote *et al.*, 1998; Carr, 2002; Coward & Ries, 2003). At beginning of the Ordovician, a long-term transgression took place (e.g. Meyers & Peters, 2011). During the Early Ordovician, a rifting

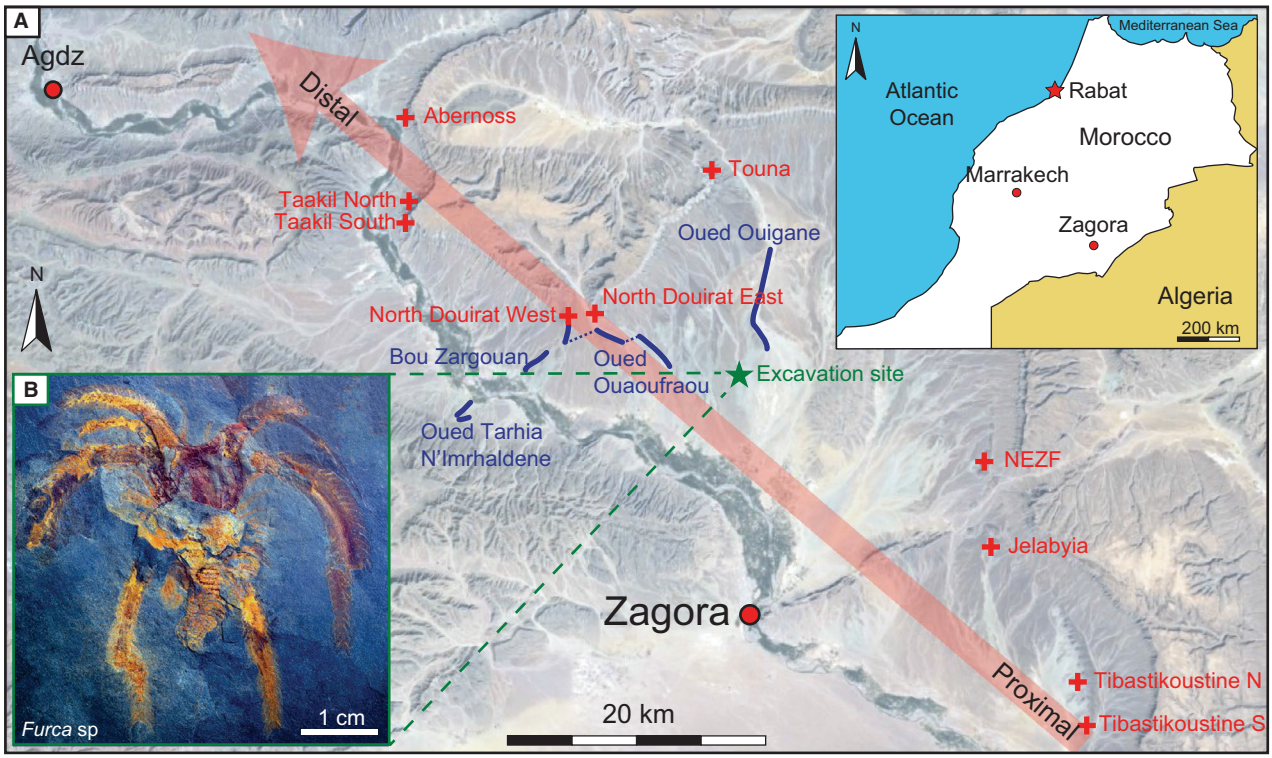

Fig. 1. (A) Satellite image from Google Earth showing the location of the study area in the central part of the Anti-Atlas (Zagora area, Morocco). The blue lines represent the location of the sections logged to reconstruct the stratigraphy of the entire Fezouata Formation; red crosses indicate the location of the sections logged in the upper part of the Fezouata and the Zini formations (NEZF = north-east Zagora fault). The green star shows the location of the excavation site. (B) Marrellomorph arthropod specimen (AA-BIZ31-OI-39, collections of the Cadi Ayyad University, Marrakech), probably belonging to the genus *Furca,* typical of the middle Cambrian, but discovered in the Lower Ordovician excavation site (Martin *et al.*, 2016).

phase took place resulting in the separation of Avalonia from Gondwana (Fig. 2A). The entire Lower Ordovician sedimentary succession of Morocco (Anti-Atlas; Fig. 2B) was deposited on a passive margin (Cocks & Torsvik, 2004).

This study focuses on the Fezouata and Zini formations in the central-eastern part of the Anti-Atlas, in the area of Zagora, south-eastern Morocco (Fig. 1A). In this area, the Lower Ordovician (Tremadocian and Floian) deposits are laying unconformably on the Guzhangian sandstones (Cambrian series 3; middle Cambrian; Fig. 2C) of the Tabanite Group (Geyer & Landing, 2006). The two studied formations (Fezouata and Zini) belong to the Outer Feijas Group (Fig. 2C) (Choubert, 1942), which is composed of the Lower Ordovician Fezouata and Zini formations and of the early Middle Ordovician Tachilla Formation.

Destombes (1962) was the first to describe the stratigraphic units of the Ordovician series in the central Anti-Atlas. The lower part of the Fezouata Formation (Tremadocian in age; Figs 2C and 3) consists of quartz-rich siltstones. Glauconite is an important component of the sediment. The upper part of the Fezouata Formation (Floian in age) is locally based by a horizon rich in ferruginous ooids or glauconite and is composed of siltstones that gradually alternate with more frequent sandstones in the uppermost part of the Fezouata Formation below the Zini Formation (Figs 2C and 3). The Fezouata Formation is locally overlain by massive black sandy beds characteristic of the Zini Formation (late Floian). In some localities, a layer containing ferruginous ooids is present in the uppermost sandstone bed constituting the Zini Formation (Destombes, 1962). In the Zagora area, the thickness of the Zini Formation does not exceed 10 m. Both the Fezouata and the Zini formations were deposited in an epicontinental sea (Fig. 2A) at a high palaeolatitude (*ca* 60°S) at the periphery of Gondwana (Smith, 1997; Cocks & Torsvik, 2004; Veevers,

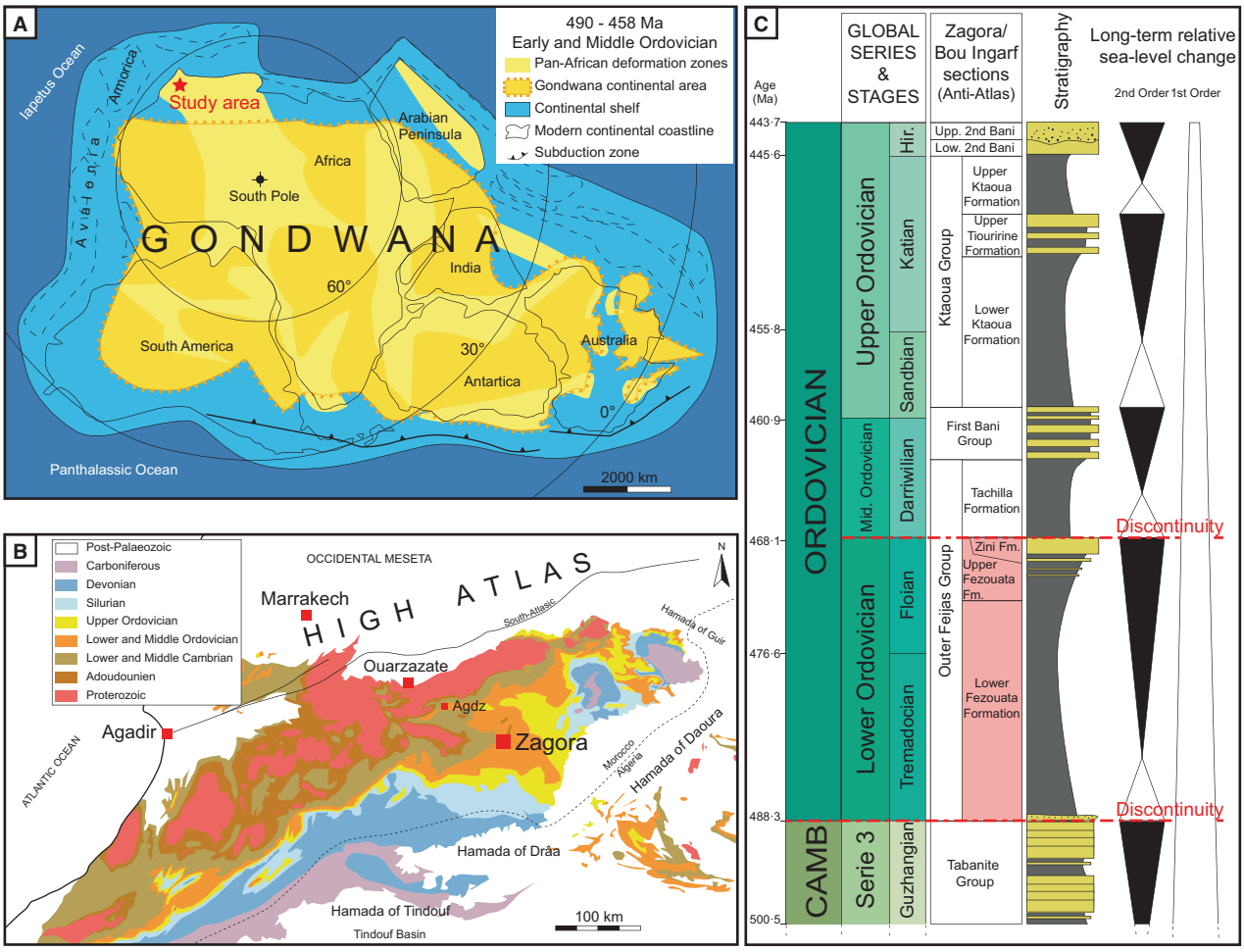

Fig. 2. Geological context. (A) Palaeogeography of Gondwana during the Early to Middle Ordovician modified after Veevers (2005). Note that the study area (red star) was located in an epicontinental sea. (B) Simplified geological map of the Anti-Atlas, after Hollard & Choubert (1985). (C) Lithostratigraphic column of the Cambro-Ordovician succession in the Zagora area, modified after Destombes *et al.* (1985); Ordovician sequences of Gasquet *et al.* (2001) are also shown; the studied interval (in pink) is bounded by two major second-order discontinuities.

2005; Torsvik & Cocks, 2013). Sediments are mainly composed of quartz and muscovite. Pyrite and iron oxides are also present. Uranium–lead (U-Pb) analyses of detrital zircons from the Cambro–Ordovician successions of Algeria and Israel (Williams *et al.*, 2002; Avigad *et al.*, 2003) indicate a Neoproterozoic age for the source of the sediments, thus pointing to Pan-African terranes.

MATERIALS AND METHODS

All of the accessible and well-outcropping Lower Ordovician sections in the surroundings of Zagora were analysed. Ten stratigraphic sections (red crosses, Fig. 1A), *ca* 50 to 200 m thick, of the upper part of the Fezouata and the Zini formations were logged at decimetre-scale and analysed for their facies. This part of the Lower Ordovician succession exhibits the highest facies variability, from facies typical of the Fezouata Formation (argillites and siltstones) to sandstone facies, more typical of the Zini Formation. One longer (*ca* 900 m thick) stratigraphic log, less detailed, was built from composite sections representing the complete Lower Ordovician sedimentary succession (Fig. 3). The combined analysis of lithology, grain size, sedimentary structures (and their wavelength; Fig. 4) and depositional geometries made it possible to describe 14 different facies (Table 1; Figs 5, 6, 7 and 8).

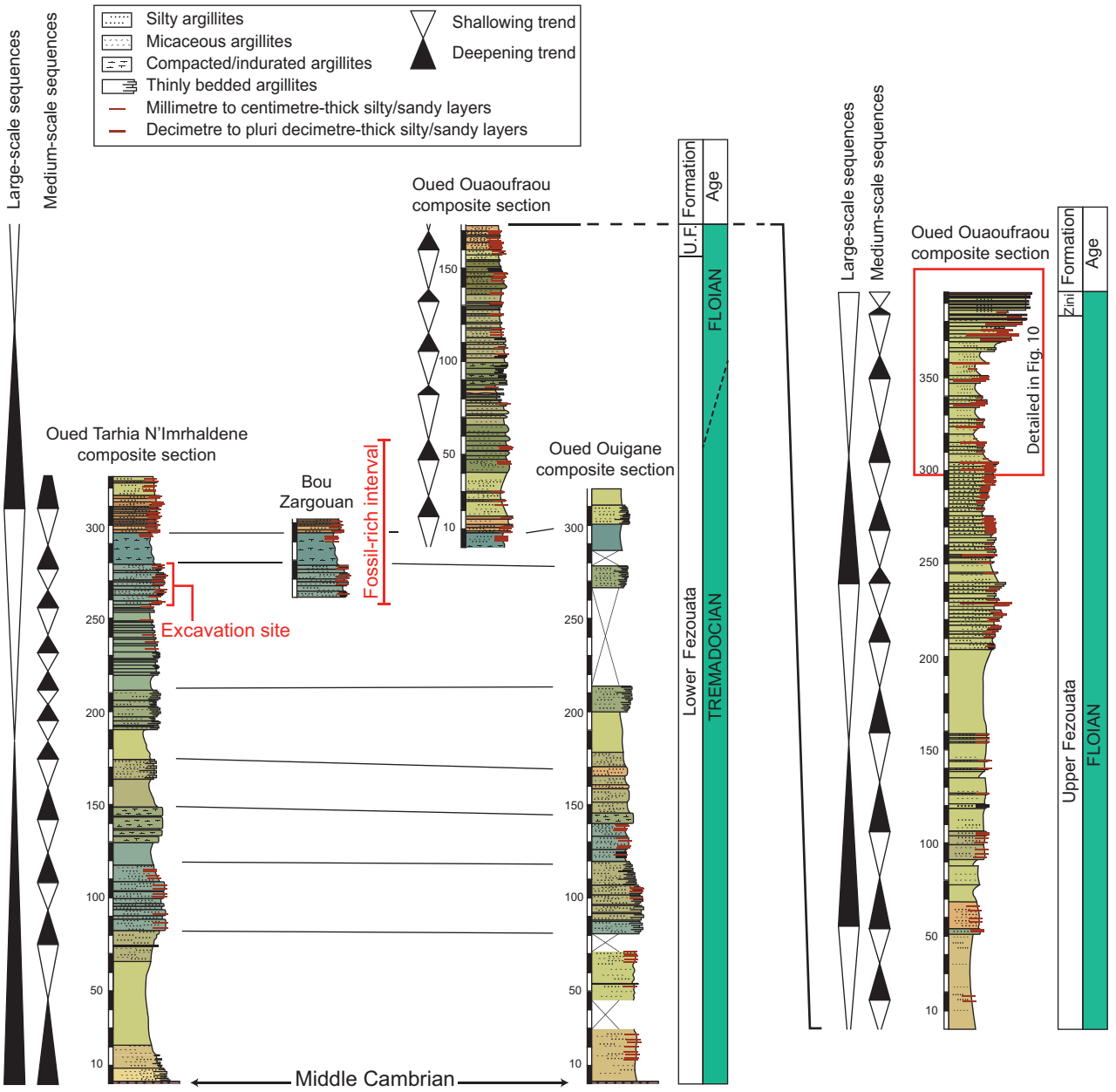

Fig. 3. Sections showing the lithostratigraphic succession of the Fezouata and Zini formations in the Zagora area. Location in Fig. 1. The stratigraphic interval containing the fossiliferous levels of the excavation site is shown. The colours used on the logged section approximate the colours of the rocks observed in the field.

These facies were then grouped into four facies zones corresponding to distinct depositional sub-environments. A facies model for the deposition of the Lower Ordovician sedimentary succession is then proposed that takes into account the facies succession in the studied sections in application of Walther's law (1894), and the geographical distribution of facies in the *ca* 1500 km^2 wide study area (Fig. 1A).

SEDIMENTARY FACIES AND FACIES ZONES

In the Zagora area, the Lower Ordovician sedimentary succession is upward coarsening (Figs 2C, 3 and 4A) and shows no or limited lateral continuity of the sandstone deposits in both the Fezouata (Fig. 4B) and the Zini formations (Fig. 4C). Symmetrical (oscillation) and slightly

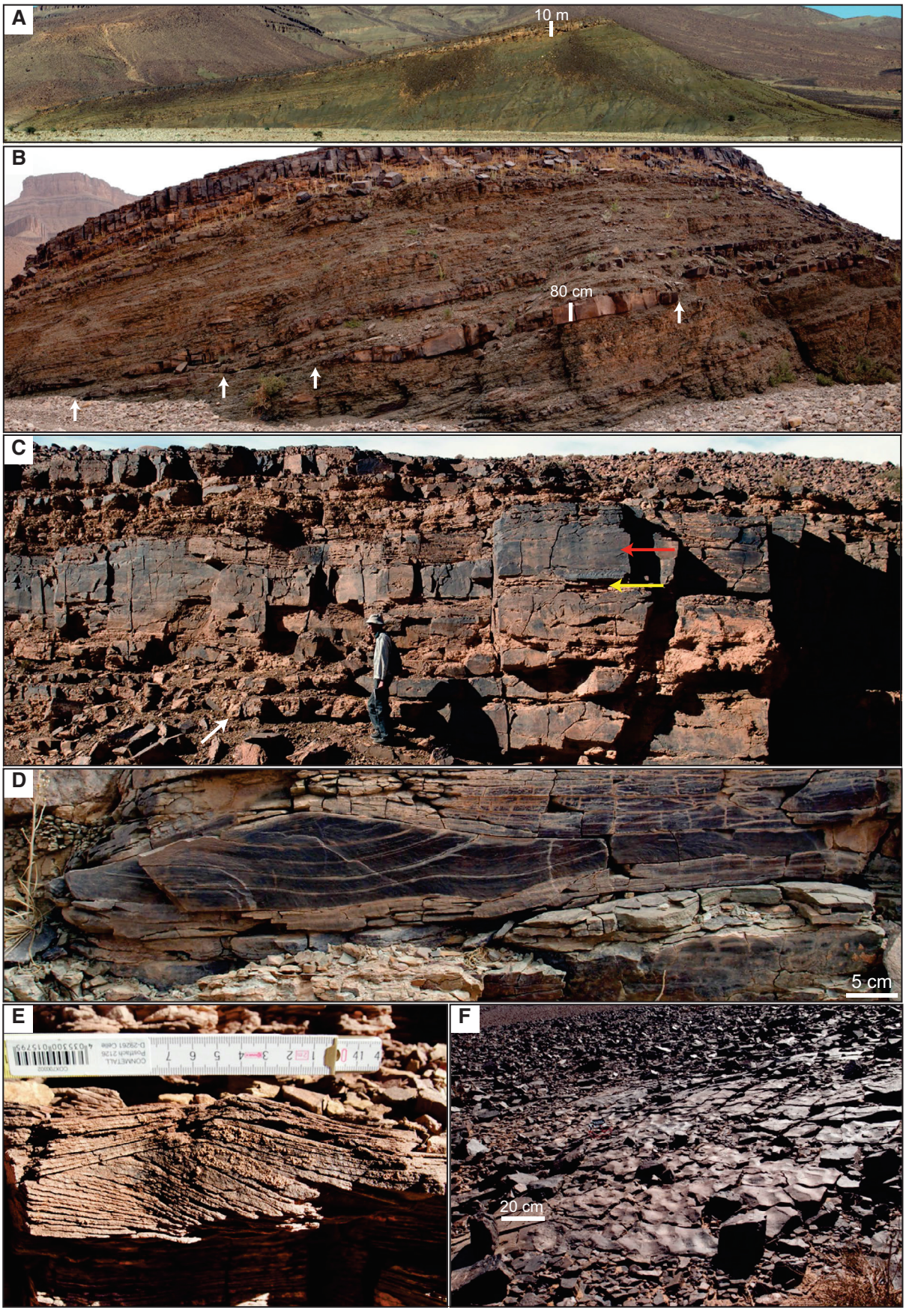

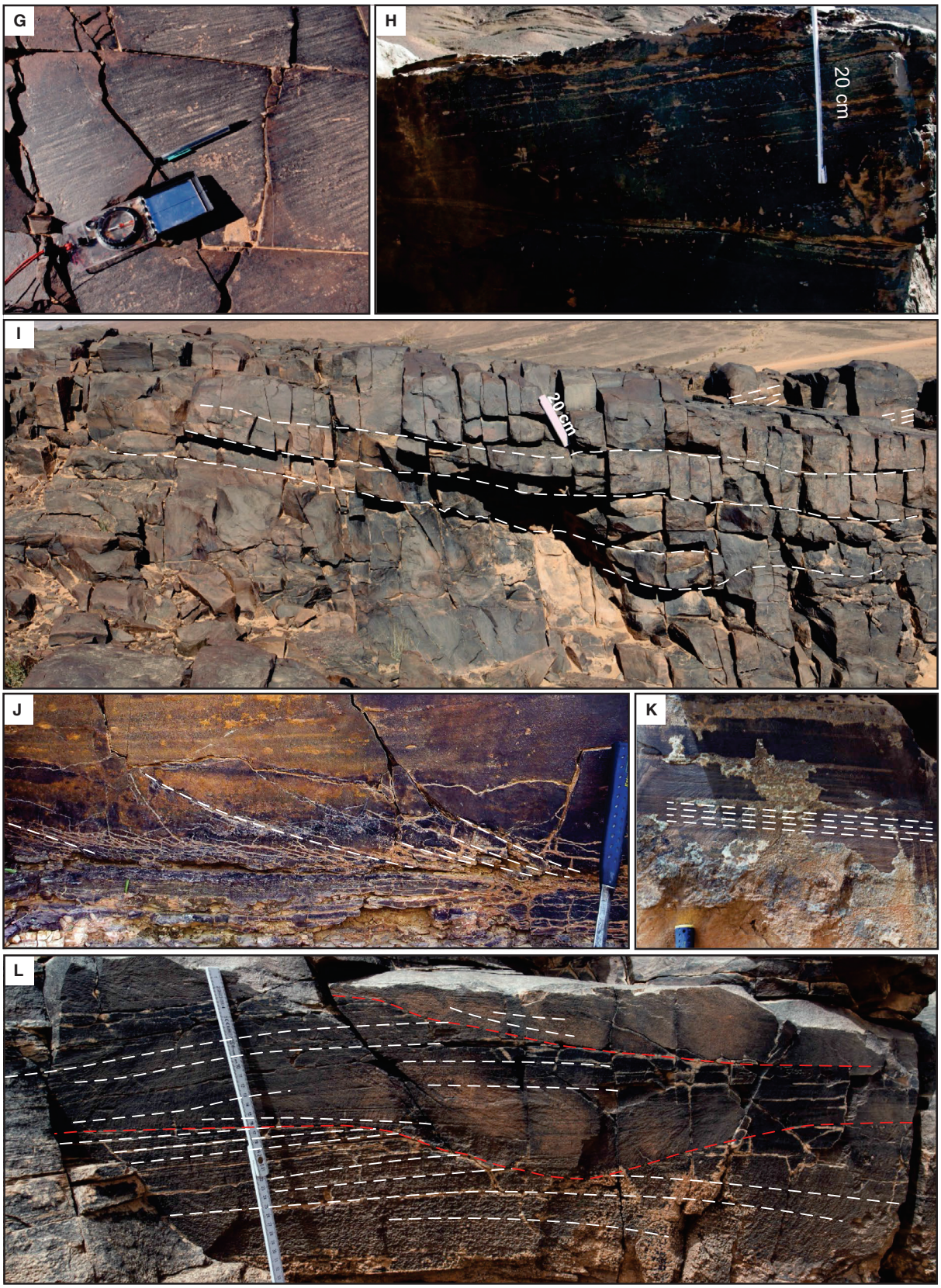

Fig. 4. (Continued)

Fig. 4. (A) Outcrop of North Douirat West (30°31′18·98″N 5°59′29·44″O) showing the studied stratigraphic succession; the greenish part corresponds to the upper part of the Fezouata Formation and the uppermost brown part at the top of the hill is the Zini Formation. (B) Outcrop of North Douirat, showing the transition between the upper part of the Fezouata Formation and the Zini Formation. Note that the beds are generally discontinuous as indicated by arrows. (C) Overview of the Zini Formation showing alternating Facies 10 (red arrow) and Facies 11 (yellow arrow). Note that the beds are generally discontinuous as indicated by the white arrow. Person for scale is *ca* 170 cm. (D) Discrete scour and drape hummocky cross-stratifications (Facies 6). (E) Typical symmetrical wave ripples (here in Facies 6). (F) Three-dimensional wave ripples in the Zini Formation (Facies 11). (G) Horizontal lineation on the top of a bed characterized by plane-parallel stratifications in the Zini Formation (Facies 10). The compass is 21 cm long. (H) Cross-bedded tabular stratifications in the Zini Formation (Facies 10). (I) Erosional surface interpreted as large beach cusps in the Zini Formation (Facies 10). (J) Tangential cross-stratifications in the Zini Formation (Facies 10). Hammer handle is 15 cm long. (K) Plane-parallel stratifications in the Zini Formation (Facies 10). (L) Large amalgamated oscillatory structures (white lines) are commonly observed in the topmost Fezouata and Zini formations (Facies 10) (red lines are reactivation surfaces). Measuring stick is marked in centimetres.

asymmetrical (combined flow–oscillation) ripples, with two-dimensional and three-dimensional morphologies, and hummocky cross-stratification (HCS; 'scour and drape' and accretionary) (Fig. 4D to F), are the main sedimentary features observed in the silty to fine-sandy parts of the sections (upper part of the Fezouata Formation). Horizontal lineation on bed surfaces (Fig. 4G), tabular cross-beds (Fig. 4H), metre-scale to tens of metre-scale wide erosional surfaces (Fig. 4I), tangential cross-stratification (Fig. 4J), plane-parallel stratification (Fig. 4K) and large amalgamated oscillation (symmetrical megaripple) structures (Fig. 4L) are commonly observed in the sandstones of the Zini Formation. Based on lithology, grain size, sedimentary structures and their size, as well as the stratinomy, 11 facies (F1 to F11) are defined (Fig. 5; Table 1). Three distinct, additional facies (SL 1 to SL 3) associated with sandstone to siltstone lenses were also observed in the sedimentary succession and are described here (Figs 6, 7 and 8). All facies were grouped into four Facies Zones (FZ). Facies description is shown in Table 1.

Facies zone 1 (FZ1): Proximal offshore

Description

This facies zone (FZ1) consists of three main facies (F1–F3–F4; see Table 1). Facies F1 is the most common facies in FZ1 and is composed of siltstones (Fig. 5A) and rare very fine-sandy layers displaying centimetre-scale wave ripples. Thin, millimetre-scale, argillaceous intercalations devoid of structures frequently occur. Facies F3 are convex sedimentary bodies that are few hundreds of metres wide and few metres thick, and are constituted of coarse siltstones to very fine sandstones. The thickness of F3 decreases laterally, passing from 8 m to several decimetres thick some hundreds of metres further to finally be blended with the host sediments of F1 (Fig. 5C). These convex sedimentary bodies of F3 conformably lay on siltstones of F1 (no erosion at their base). From base to top of F3, a thickening upward of the beds is observed as well as a decrease in the thickness and abundance of muddy intercalations between the beds (Fig. 5D). Plane-parallel laminations and few current ripples (Fig. 5F) occur in F3; oscillatory structures are absent. Locally, more massive (absence of muddy intercalations) sandy intervals lay on erosional surfaces, thus cutting the beds formed of coarse siltstones to very fine sandstones, and are observed within F3 (Fig. 5E). The erosional surfaces are few metres wide and rarely more than 1 m deep. Facies F3 is intercalated within thick (up to 10 m) siltstones or argillaceous siltstones of F1. Facies F4 consists of very fine sandstones displaying centimetre-scale to decimetre-scale wave ripples (Fig. 5G); the laminations are underlain by thin layers of coarser quartz grains (Fig. 5H).

Interpretation

Facies zone 1 is interpreted as being deposited in the proximal offshore, close to the limit of the storm-weather wave base (SWWB). Host sediments expressed by F1 would represent the background sedimentation, which derived from terrestrial input in the basin. The argillaceous fraction in F1 would result from gravitational settling or from gravity flows (fluid muds; e.g. Ichaso & Dalrymple, 2009, and references herein). Here, the slightly coarser sediments displaying centimetre to centimetre wave ripples (F4) deposited during storm events (e.g. Myrow & Southard, 1996) suggest a strongly attenuated influence of storm current and oscillation, and are interstratified with the background muddy to

Table 1. Summary of facies characteristics.

Facies	Dominant lithology	Grain size	Bed thickness	Sedimentary structures	Associated structures	Bed organization	General organization	Remarks	Figures
F1	Siltstone	Silt/mud	1–3 cm	Centimetre-scale wave ripples	Few vertical burrows	Wavy shaped	Mostly continuous	This facies forms the background sedimentation in distal environments probably deriving from terrestrial input in the basin. It is dominated by siltstones but thin, millimetre-scaled mud intercalations frequently occur	5A
F2	Sandstone	Coarse silt to very fine sand	3–8 cm	Decimetre-scale wave ripples	Few vertical burrows at the top	Wavy shaped	Mostly continuous	This facies corresponds to the background sedimentation in proximal environments probably deriving from terrestrial input in the basin	5B
F3	Sandstone	Coarse silt to very fine sand	10–90 cm	Generally plane-parallel stratifications, few current ripples, festoons and rare centimetre-scale to decimetre-scale wave ripples	Channel infills, metre-scale lobes	Mostly tabular, alternations of beds formed of coarse siltstones and fine sandstones	Tens to hundreds of metre-long lobes, up to 8 m thick	This facies is intercalated within thick (up to 10 m) siltstones or argillaceous siltstones of F1	5C/D/E/F
F4	Sandstone	Very fine sand	1–5 cm	Centimetre-scale to decimetre-scale wave ripples, the laminations are underlined by thin layers of coarser quartz grains	Few vertical burrows at the top	–	Discontinuous at metre to tens of metre-scale	This facies is intercalated within the distal background sedimentation (F1)	5G/H
F5	Sandstone	Fine sand	5–15 cm	Decimetre-scale wave ripples, few aggrading–prograding combined wave–flow ripples	Sometimes displaying an erosional base	Wavy shaped	Discontinuous at metre to tens of metre-scale	This facies is intercalated within the proximal background sedimentation (F2)	5I
F6	Sandstone	Fine sand	15–30 cm	Decimetre-scale discrete scour and drape hummocky cross-stratifications (HCS), few aggrading–prograding combined wave–flow ripples	Sometimes with an erosional base, and centimetre-scale to decimetre-scale wave ripples at the top of the HCS	Bioclastic lags are common at the base of the beds	Discontinuous at tens to hundreds of metre-scale	This facies is intercalated within the proximal background sedimentation (F2)	5J
F7	Sandstone	Fine sand	30–80 cm	Metre-scale discrete (few accretionary) scour and drape HCS	Sometimes with an erosional base, and centimetre-scale to decimetre-scale wave	Bioclastic lags are common at the base of the beds	Discontinuous at tens to hundreds of metre-scale	This facies is intercalated within the proximal background sedimentation (F2)	5K

Table 1. (continued)

Facies	Dominant lithology	Grain size	Bed thickness	Sedimentary structures	Associated structures	Bed organization	General organization	Remarks	Figures
					ripples at the top of the HCS				
F8	Sandstone	Fine sand	60–80 cm	Metre-scale amalgamated, scour and drape HCS	Sometimes with an erosional base, and centimetre-scale to decimetre-scale wave ripples at the top of the HCS	–	Discontinuous at tens to hundreds of metre-scale	This facies is intercalated within the proximal background sedimentation (F2)	5L
F9	Sandstone	Fine to medium sand	20–40 cm	Swaley cross-stratifications	Up to 15 cm deep erosional gutters sometimes occur	–	Discontinuous at tens to hundreds of metre-scale	This facies is rarely observed, and is intercalated with silts and mud of F1 and fine sandstones of F2	5M
F10	Sandstone	Fine to medium sand	Up to 2 m	Plane-parallel stratifications, tens of decimetre-scale to metre-scale oscillatory structures	Rare tens of metre-large erosional surfaces (beach cusps), cross-stratifications of tabular stratifications (berms), keystone vugs	Mostly tabular with a light wavy shape	Mostly continuous	This facies, with F11, constitutes the Zini Formation	4C/G/H/I 4J/K/L 5N
F11	Sandstone	Fine to medium sand	1–10 cm	Centimetre-scale to decimetre-scale wave ripples	Commonly sharp-crested ripples, few double-crested ripples	–	Discontinuous at tens to hundreds of metre-scale	This facies exclusively alternates with F10	5O
SL1	Sandstone	Coarse silt to fine sand, centimetre-scale bioclast	5–10 cm	Decimetre-scale to metre-scale HCS	Bioclastic layers (up to 30 cm thick)	Alternation of four to eight beds showing decreasing wavelength size in each bed, upward and laterally	Lenticular shape, average size: 280 cm long 35 cm thick	This lenses are isolated or connected to other similar lenses in the stratigraphic plane intercalated in F2	7A/B/C/D 8B 13A/B
SL2	Sandstone	Coarse silt to fine sand, centimetre-scale bioclast	5–10 cm	Decimetre-scale to metre-scale HCS	Disconnected bioclastic lags (few centimetres thick)	Alternation of three to six beds showing decreasing wavelength size in each bed, upward and laterally	Lenticular shape, average size: 175 cm long 40 cm thick	These lenses are isolated or connected to other similar lenses in the stratigraphic plane intercalated in F2	7E/F/G 8A/C
SL3	Sandstone	Coarse silt to fine sand	5–10 cm	Centimetre-scale to decimetre-scale HCS	Isolated bioclasts	Alternation of two to four beds showing decreasing wavelength size in each bed, upward and laterally	Lenticular to spherical shape, average size: 100 cm long 35 cm thick	These lenses are mostly isolated, or aligned with other similar lenses and intercalated in F2 (few in F1)	8D/E

silty sediments of F1. Locally, F3 is interstratified with the background fine-grained sediments (F1). The lack of unequivocal oscillation ripples in F3 suggests that this facies was deposited below the SWWB, deeper than F4. The overall morphology of F3 (conformable basal surface, important thickness variations due to the lobate shape) associated with current ripples, plane-parallel stratifications and internal large erosional surfaces suggests lobe deposition. The localized, metre-scaled erosive sedimentary bodies in F3 are interpreted as channels, possibly the channels feeding the lobes (e.g. Fildani & Normark, 2004; Gervais *et al.*, 2006). The process responsible for the lobe formation is not yet clearly understood, and these distal lobes are either formed by turbidity currents, storm backcurrents or storm-initiated currents.

Facies zone 2 (FZ2): Lower shoreface

Description

The facies zone 2 (FZ2) is formed by five main facies (F2 – F4 – F5 – F6 – F7; see Table 1). Facies F2 is the most common facies in FZ2 and is constituted by coarse siltstones to very fine sandstones displaying decimetre-scale wave ripples (Fig. 5B). Facies F4 to F7 are all fine-grained to medium-grained sandstones interstratified in F2. Facies F5 displays decimetre-scale wave ripples (Fig. 5I) and combined lateral and vertical accretionary wave ripples. Facies F6 exhibits decimetre-scale wavelength scour and drape HCS (Fig. 5J), and few combined lateral and vertical accretionary wave ripples. Facies F7 is characterized by metre-scale wavelength scour and drape and rare accretionary HCS (Fig. 5K).

Interpretation

Facies zone 2 is interpreted as the lower shoreface, here defined as being comprised between the SWWB and the fair-weather wave base (FWWB). Facies F2 would correspond to the continuous terrestrial input of sediment in the basin. From F4 to F7, a gradual increase in the size of the oscillatory structures (HCS) is associated with a coarsening and thickening upward of the storm layers (Fig. 5G, I, J and K), thus suggesting that F4 to F7 were, respectively, deposited in distal to proximal settings within the lower shoreface (Heward, 1981; Davis & Hayes, 1984; Boyd *et al.*, 1992; Yang *et al.*, 2006). Facies zone FZ2 can therefore be subdivided in two subzones: FZ2-a for the distal lower shoreface with F4 and F5 as characteristic facies and FZ2-b for the proximal lower shoreface indentified by F6 and F7. Commonly, F2 is several metres thick and laterally continuous. However, a peculiar organization between F1 and F2 can be observed close to the SWWB. A repeated, regular alternation of F1 and F2 at decimetre-scale suggests that a cyclical process of deposition (such as tides) is responsible for this pattern.

Facies zone 3 (FZ3): Upper shoreface

Description

Facies zone 3 consists of three facies (F2 – F8 – F9; see Table 1). Fine-grained to medium-grained sandstones displaying amalgamated HCS (F8; Fig. 5L) and rare sandstones displaying cross-cutting sets of gently dipping, concave-up laminations, considered as SCS with rare localized internal erosion (F9; Fig. 5M), are intercalated with F2. These sandstone beds commonly have an erosional base.

Interpretation

Amalgamated HCS and SCS are formed above the FWWB. They are the result of storm and wave activity in proximal environment, where the waves constantly rework the sediment during both fair-weather and storm-weather conditions, thus vertically stacking HCS to form amalgamated HCS or truncating the hummocks of HCS to create SCS. The rare local decimetre-deep local erosion that occurs in the swaley cross-stratified sandstone is interpreted as gutter. This facies zone indicates constant high-energy conditions in the upper shoreface (e.g. Hampson & Storms, 2003).

Facies zone 4 (FZ4): Foreshore

Description

This facies zone (FZ4) is composed of two facies (F10 and F11; see Table 1). Facies 10 (Fig. 5N) is composed of fine-grained to medium-grained sandstones and displays cross-bedded tabular stratifications (Fig. 4H), rare tens of metre-wide erosional surfaces (Fig. 4I), very rare tangential cross-beds (Fig. 4J), plane-parallel stratifications (Fig. 4K), tens of decimetre-scale to metre-scale oscillatory structures (Fig. 4L). Few sandstone levels display aligned pores (millimetre-scale of diameter on outcrops). Facies F11 (Fig. 5N) composed of fine to medium sandstone is characterized by decimetre to multi-decimetre oscillation structures and frequent bioturbations (white arrows in Fig. 5O), probably resulting from the activity of annelids, trilobites or other arthropods

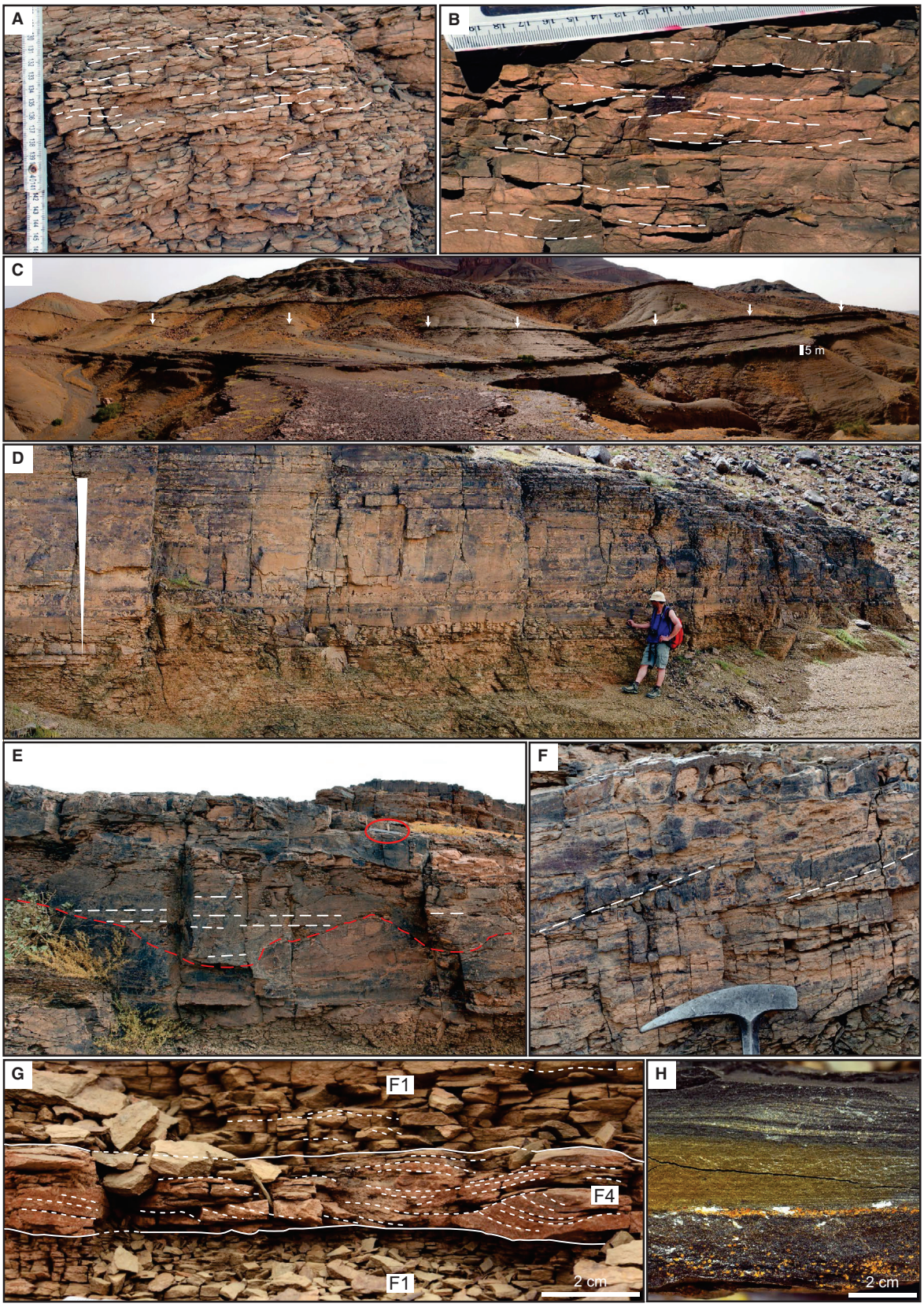

Fig. 5. Overview of facies characterizing both the Fezouata and Zini formations. (A) to (L) are present in the Fezouata Formation, (M) and (N) in the Zini Formation. (A) Facies F1 forming the background sedimentation in distal environment (proximal offshore to distal lower shoreface). This facies is dominated by siltstones with thin intercalated muddy layers. (B) F2 represents the background sedimentation in more proximal environments than F1 (distal lower shoreface to upper shoreface). This facies is constituted by coarse siltstones to very fine sandstones and displays decimetre-scale wave ripples. (C) Facies F3 are convex sedimentary bodies that are few hundreds metres wide and few metres thick, are constituted of coarse siltstones to very fine sandstones, which correspond to distal storm-derived sedimentary lobes. F3 conformably lay on siltstones of F1 (no erosion at their base). Note that this facies is observed in discontinuous beds (arrows). (D) F3 displaying a thickening-upward and coarsening-upward trend and an upward decrease in muddy intercalations between the beds. Person for scale is *ca* 1·8 m tall. (E) Individual beds of F3 commonly display internal erosional surfaces interpreted as the base of channels that fed the lobes (white bar in the red circle is 20 cm). (F) At the top of beds of F3, currents ripples are common. The hammer head is 15 cm. (G) Facies F4 are sandstones corresponding to distal tempestites displaying centimetre-scale to decimetre-scale wave ripples. (H) Section of F4 showing a coarser base, then parallel laminations underlined by coarser quartz and finally the waning flow-related ripples at the top. (I) F5 is constituted of fine sandstones with discontinuous layers (5 to 15 cm thick) showing decimetre-scale wave ripples, and a few aggrading–prograding combined wave–flow ripples. (J) Facies F6 is formed of fine sandstone beds (15 to 30 cm thick) that display discrete scour and drape HCS that commonly have an erosional base. (K) F7 is constituted of thick continuous dark grey beds (30 to 80 cm). Beds show metre-scale discrete accretionary HCS. Hammer is 28 cm. (L) F8 is constituted of sandstones displaying metre-scale amalgamated scour and drape HCS. (M) Facies F9 is formed by sandstones displaying swaley cross-stratifications (SCS); the arrow point out a local overdigging. Pen is 14 cm long. (N) Alternations of F10 (yellow line) and F11 (red line); F10 forms sandy black massive beds (<80 cm). (O) F11 is formed of sandstones with decimetric oscillatory structures and common bioturbation; vertical burrows are observed (white arrow). Stick is 16 cm long.

on the sediment surface. Facies F11 forms fine-grained to medium-grained sandstone layers discontinuous at metre-scale, always intercalated in F10 (Fig. 5N).

Interpretation

The most frequently observed sedimentary structures in the Zini Formation are low-angle parallel stratifications with few levels of probable keystone vugs (aligned pores). Large erosional surfaces interpreted as beach cusps due to the storm swash (e.g. Inman & Guza, 1982), mega-ripples and tabular cross-beds corresponding to berms (e.g. Hine, 1979) are also observed in the sandstones of the Zini Formation (FZ4). These observations strongly suggest that FZ4 records the most proximal deposits (foreshore). Facies F11 with decimetre-scale wave ripples, vertical and horizontal burrows intercalated between F10 is interpreted as an intertidal zone in an open-coast environment, whereas F10 would represent foreshore environments or surf bars developing between the high-tide beach and the low-tide beach (Masselink & Short, 1993; Davis Jr & Dalrymple, 2012). Facies F10 rarely exceeded 2 m in thickness and is discontinuous over tens to hundreds of metres. Each bed of F10 is separated by thin levels with decimetre-scale wave ripples, vertical and horizontal burrows of F11. Such a pattern is not likely to correspond to a classic foreshore (wave/storm-dominated) but could correspond to a ridge and runnel, or multi-bar foreshore environment occurring in wave/storm-dominated, tide-influenced coastal context (Masselink & Short, 1993; Davis Jr & Dalrymple, 2012). This kind of foreshore displays several shore-parallel sand banks (ridges) separated from one another by troughs (runnel). In modern environments, the ridges function as surf bars when submerged and as swash-bars when exposed (e.g. Masselink & Anthony, 2001) and the ridges are dissected regularly (each hundred metres) by rip channels (e.g. Masselink *et al.*, 2006). Facies characteristics in F10 probably correspond to ridges, while facies characteristics in F11 to runnels (e.g. Chauhan, 2000). The rarely observed tangential cross-beds possibly correspond to current structures formed by the tides.

Sandstone to siltstone lenses

Descriptions

Sandstone to siltstone lenses (SL; see Table 1) are metre-scale sedimentary features composed of several beds (two to eight) and are a few metres long (idealized SL in Fig. 6); SL can be easily identified in the field, based on both their colour (yellowish/orange) and their cementation (Figs 7 and 8). In cross-section, the centre of each bed consists of fine-grained sandstones (locally coarse bioclastic discontinuous layers occur), which gradually pass laterally into siltstones (Figs 6 and 7). The first bed at the bottom

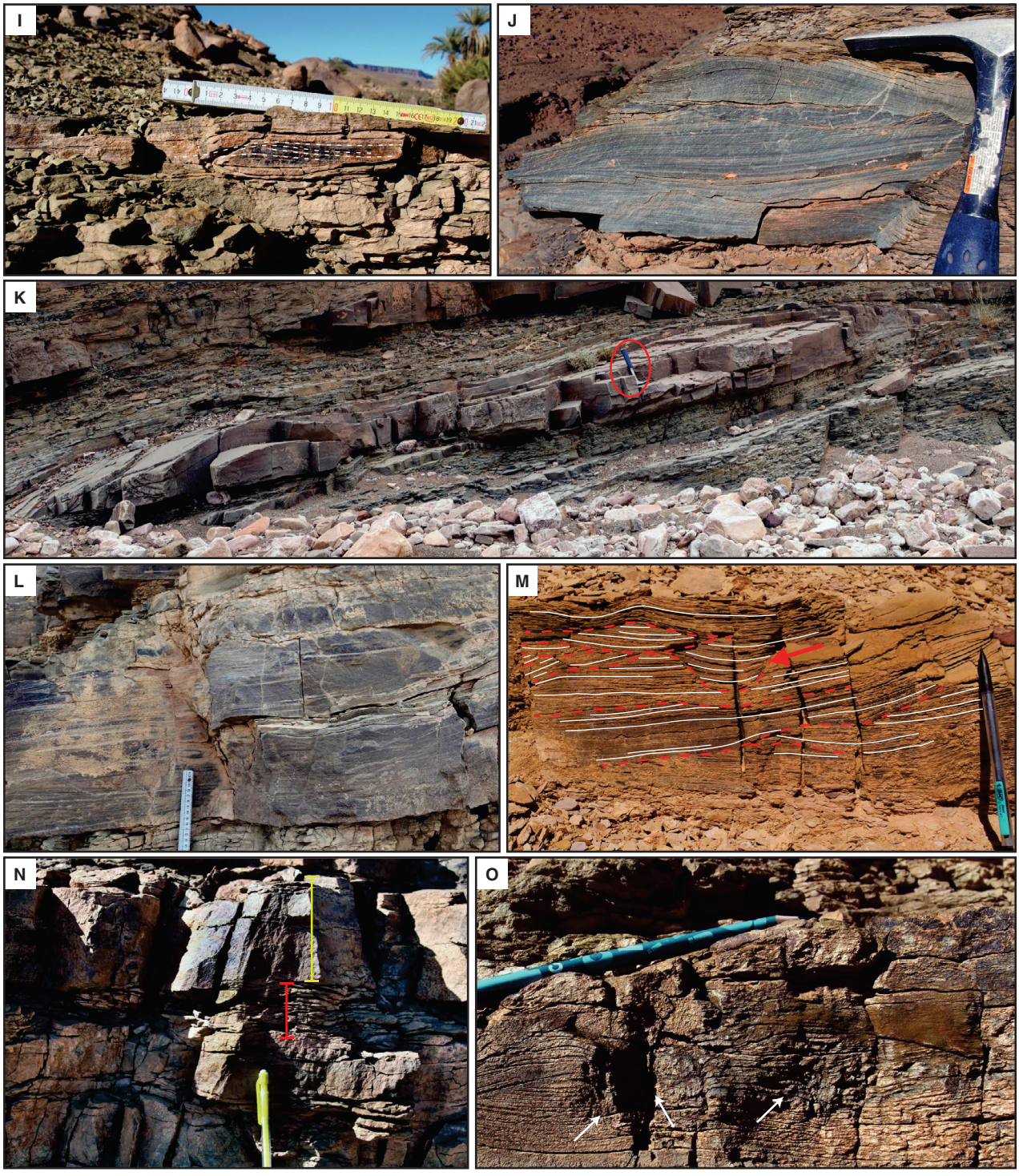

Fig. 5. Continued

of SL commonly displays an erosional base (*ca* decimetre deep). Usually, the sandstone parts of the SL are commonly thicker (*ca* decimetre thick) compared with the siltstone (*ca* centimetre thick). The transition between beds occurs as a gradational or erosive contact. Since SL are composed of several beds thicker at the centre than at the margins, commonly with a concave erosional base, the overall morphologies are elliptical with a scour base and a mound shape top. Two morphologies are then observed: (i) one with a scour base and a convex top; and (ii)

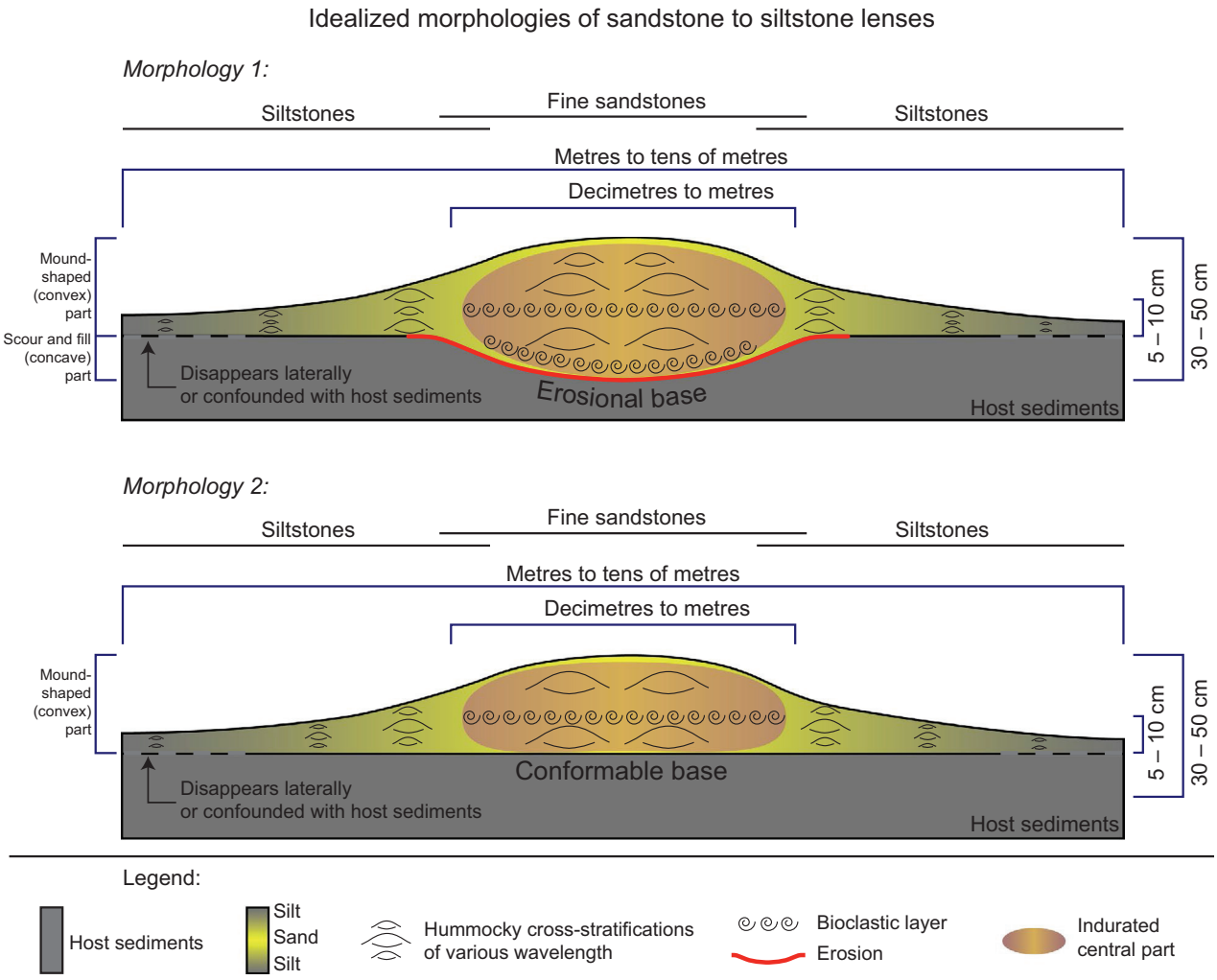

Fig. 6. Idealized sandstone to siltstone lenses (SL). Simplified drawing of the two observed morphologies of SL: (1) with a scour base; and (2) without a scour base. Both consist of fine-grained sandstones in their central part, which gradually pass laterally to siltstones. The overprinted brownish central part highlights the more cemented part of the SL, which is composed of coarser grain size (here, fine-grained sandstones and bioclast layers).

one without a scour base but also a convex top (Fig. 6).

Sandstone to siltstone lenses are formed of a stack of scour and drape HCS with varying wavelengths (Figs 6, 7A, 7B and 7C) (centimetre to multi-decimetre scale). A peculiar organization of HCS throughout the lenses is observed: (i) vertically, the SL are formed of a stack of HCS with various wavelengths (Fig. 7A and C); and (ii) laterally, HCS generally have a larger wavelength at the centre (sandy part) of the lenses than at their margins (silty part) (Fig. 7A and B). In places, oblique cross-stratifications are also observed in SL (Fig. 7E to G). The beds constituting the SL are formed by repeated changes in size of the HCS wavelength. Each couplet of larger to smaller HCS (vertically), or bioclastic layers to sandy HCS (vertical white triangle Fig. 7A and C), shows a lateral extension of a few metres. The boundary between the sandstone parts (centre) and siltstone parts (lateral) commonly appears sharp (visually) (Fig. 8). The sharp boundary of SL is due to the cementation, which is emphasized in the sandy and bioclastic parts. Usually, several SL can be observed on the same stratigraphic level and in places are laterally connected by a thin fine-grained sandstone layer (maximum of four connected SL observed across tens of metres width; Fig. 8A and E). On the surface of the beds, SL show a dominant south-east/north-west elongation (Fig. 7D). However, whatever the type of

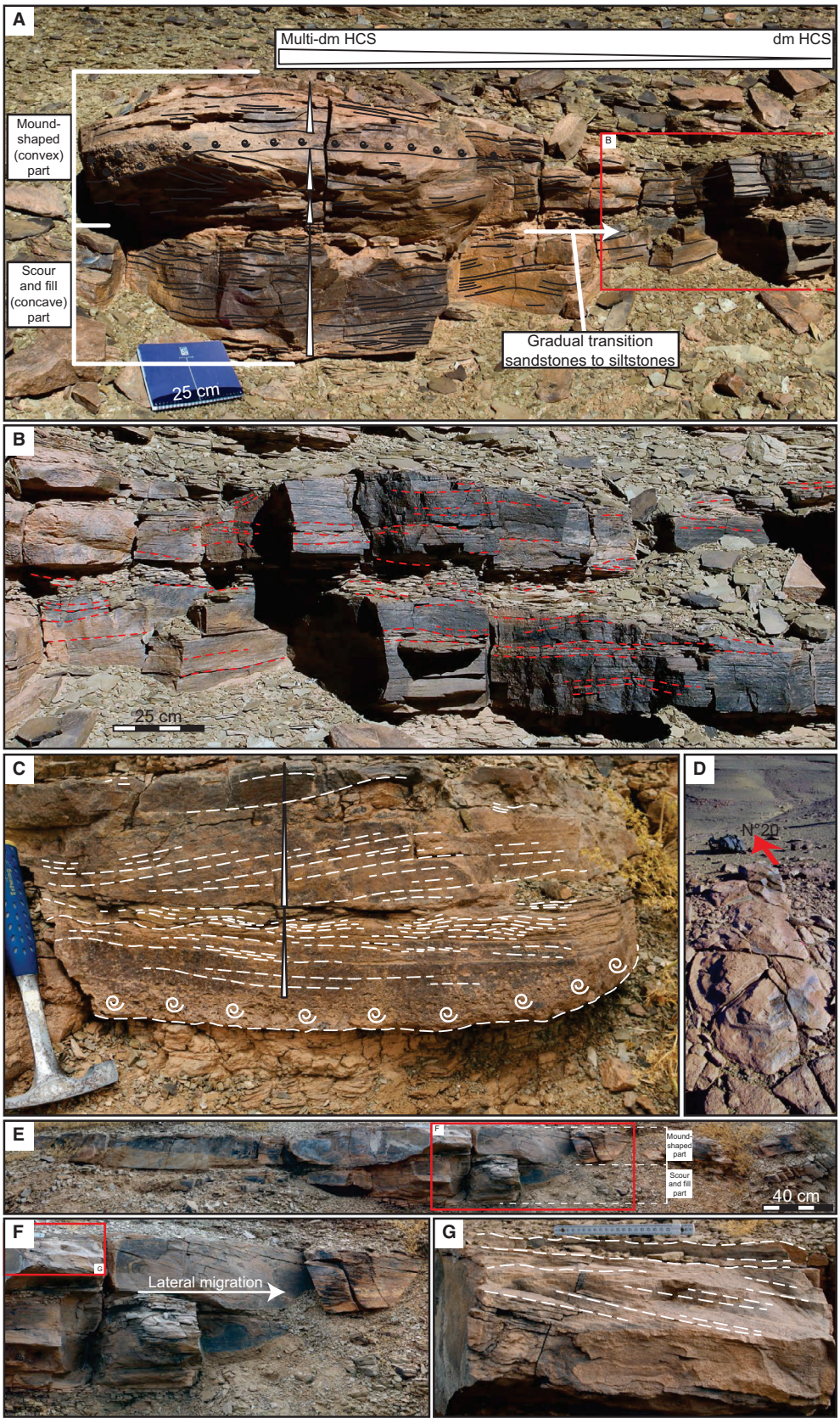

Fig. 7. Sandstone to siltstone lenses description. (A) Sandstone to siltstone lens (here SL1) in outcrop, which displays scour and drape HCS. The HCS vary in wavelength vertically and laterally. Each vertical white triangle corresponds to one unit. Morphology 1 is pointed out as well as the transition from sandstones to siltstones within the SL. In (A) and (C), the snail shell pattern indicates the bioclastic layers. (B) Lateral continuity of the SL in (A), which consists of scour and drape HCS with shorter wavelength compared with the central part in (A). (C) Characteristic vertical alternation of larger to smaller (white triangle) wavelength of HCS through a sandstone to siltstone lens. Hammer is 28 cm. (D) The view on surface bed of a sandstone to siltstone lens shows that they are elongated along a proximal–distal axis; here, a N20° direction was measured in agreement with the orientation of the sedimentary system (Fig. 1). The orange coloured body is *ca* 2·5 m long (E) Typical morphology 1 of one sandstone to siltstone lens (here observed in SL2) displaying oblique cross-stratifications [magnified in (F) and (G)] interpreted as structures of lateral migration of the locus of deposition after a certain angle of repository is attained between the central part of the sedimentary bodies and their lateral parts.

SL, there is a continuity from their centre with the lateral (less, or not cemented) sediments; thus, the lateral boundary of the SL with the surrounding sediment is gradational, fine-grained sandstones passing to siltstones (Figs 6, 7A, 7B, 8A and 8E).

Based on their composition and grain size, three types of sandstone to siltstone lenses were distinguished: (i) bioclastic lenses (SL1; Fig. 8B); (ii) mixed lenses (SL2; Fig. 8C); and (iii) sandy lenses (SL3; Fig. 8D). Type SL1 (Fig. 8B) records thick (up to 15 cm) bioclastic discontinuous layers that can locally fill erosional gutters within the sandy central part. Bioclasts have a size ranging from 0·5 to 5·0 cm, but are not graded. These bioclastic lags occur in different positions within the SL, at their base, in their middle part and rarely at their top. Their lateral extension corresponds to that of the more cemented part of the SL. Type SL2 (Fig. 8C) is defined as containing thin (centimetre-thick), commonly discontinuous bioclastic lags with millimetre to centimetre bioclasts. Type SL3 (Fig. 8D) corresponds to SL composed almost entirely of a fine-sandy fraction with a minor contribution of bioclasts, which are deposited as thin millimetre lags or are isolated in the sandstone part. The two morphologies described in Fig. 6 are present for the three types of SL.

Interpretation

Sandstone to siltstone lenses are almost only constituted by scour and drape HCS. However, HCS as well as swaley cross-stratifications (SCS) may display common characteristics with sedimentary structures formed under supercritical flows, such as antidunes, chutes and pools or cyclic steps (e.g. Alexander *et al.*, 2001; Lang & Winsemann, 2013; Cartigny *et al.*, 2014). The difficulty in the distinction between HCS/SCS versus antidunes/chutes and pools/cyclic steps has already been pointed out as a source of errors for palaeoenvironmental reconstructions (e.g. Prave & Duke, 1990; Rust & Gibling, 1990; Cotter & Graham, 1991). Alexander *et al.* (2001) led an experimental study in order to give key criteria of recognition of sedimentary structures generated by supercritical flows. Patterns only observed in supercritical-related flow deposits were as follows: (i) high-angle stratifications dipping downstream corresponding to rapid migration of the bedforms when the flow pass from supercritical to subcritical; and (ii) a dominance of subhorizontal laminae in the vertical section orthogonal to the flow. Cartigny *et al.* (2014) mentioned that chutes and pools may mimic HCS and noted that the preservation of the entire chute and pool structures is promoted by a high aggradation rates. The SL exhibit several types of stratifications such as subhorizontal laminae, trough and hummocky stratifications. The SL were observed in all possible cross-sections (parallel to perpendicular to the palaeoflow orientation) and the same patterns are observed independently from the plan of observation. In the outcrops parallel to the palaeoflow (south-east/north-west), neither dominantly upstream dipping laminae (as observed in cyclic steps) nor high-angle downstream dipping was observed. Similarly, in section perpendicular to the flow, no dominance of subhorizontal laminae was observed (as described by Alexander *et al.*, 2001 for antidunes) and subhorizontal laminae are always associated with trough cross-strata and hummocky cross-strata. Therefore, the stratifications observed in SL are interpreted here as HCS (scour and drape) rather than linked to supercritical flows. According to most previous studies (e.g. Harms, 1979; Dott & Bourgeois, 1982; Yang *et al.*, 2005, 2006; Quin, 2011), HCS are considered as storm depositional structures preferably generated and preserved between the storm-weather

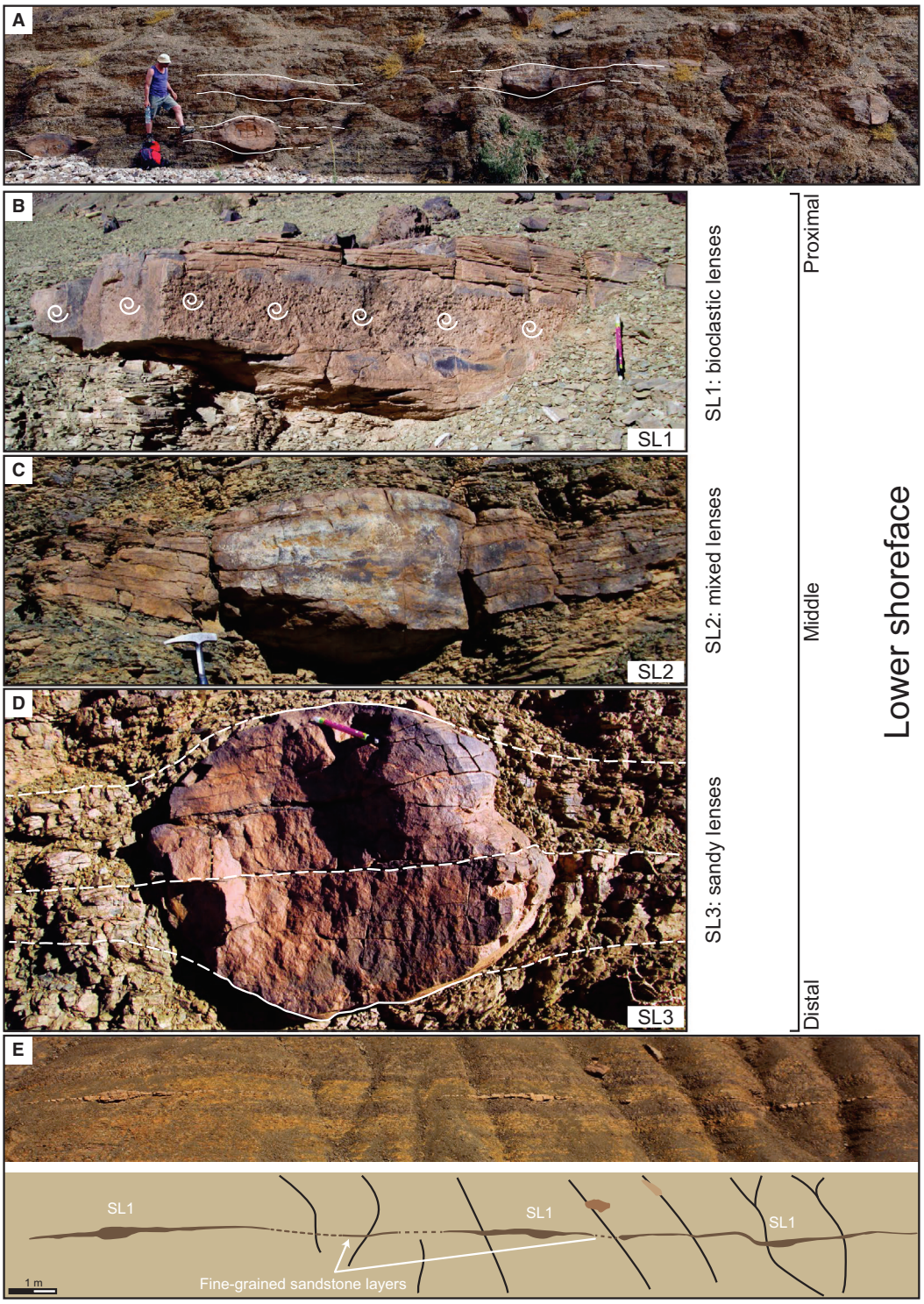

Fig. 8. (A) Sandstone to siltstone lenses (here SL2) in outcrop showing that deposits are very localized, although a lateral continuity of these bodies with the surrounding commonly occurs as here underlain by the white line (person for scale is 1·75 m). (B) SL1 (bioclastic lens) here exhibiting a 10 cm thick bioclastic layer in its centre (the snail shell pattern indicates the bioclastic layer). SL1 is typical of the proximal lower shoreface. (C) SL2 (mixed lens), typical of the middle lower shoreface. Hammer head is 15 cm. (D) SL3 (sandy lens) is found in the distal lower shoreface–proximal offshore. The lateral continuity of the cemented sandstone part of the SL with its siltstone part is shown with the white lines. Pen is 14 cm long. (E) Sandstone to siltstone lenses (here SL1) connected to one another by a fine-grained sandstone level, which corresponds to the sandy layers fringing the mound-shaped part.

wave base (SWWB) and the fair-weather wave base (FWWB; McLane, 1995). Differences in oscillatory structure wavelengths between the centre of SL (decimetre-scale to multi-decimetre-scale) and the lateral (centimetre-scale to decimetre-scale) can be explained by the grain-size difference (Cummings *et al.*, 2009). The cross-stratified part (Fig. 7E to G) sometimes observed in the upper part of SL is interpreted as lateral migration of the locus of deposition after a certain angle of repository is attained between the central part of the sedimentary bodies and its lateral parts (i.e. a maximum height of the sandy accumulation was attained, and the locus of deposition is forced to shift) because it occurs in sandy modern turbidite lobes (e.g. Gervais *et al.*, 2006). The SL consist of different units (i.e. couplets large to small HCS constituting one bed; Fig. 7A and C), suggesting either that the sandstone to siltstone lenses are formed: (i) by numerous amalgamated storm events; or (ii) that the record of storm intensity at the sea floor was modulated by a process other than the storm. Distribution of SL on outcrops (Fig. 8A and E) and on bed surfaces (Fig. 7D) shows that deposition is very localized. It is therefore highly improbable that successive (two to eight) storm events have deposited sands on exactly the same small area of a few square metres. It appears more probable that SL have resulted from a single storm event rather than numerous events. The absence of both muddy deposits and bioturbation between two successive units also suggests a fast, continuous deposition, and that one SL corresponds to one single storm event as suggested by the step by step diagram (Fig. 9).

The three types of sandstone to siltstone lenses (SL 1 – SL 2 – SL 3; see Table 1) commonly occur in FZ2. The SL are therefore typical of the lower shoreface. Type SL3 is commonly found with F4, SL2 with F5 and SL1 with F6/F7. Thus, SL1 (Fig. 8B) belongs to the proximal, SL2 (Fig. 8C) to the intermediate and SL3 (Fig. 8D) to the distal lower shoreface. Only few SL3 were observed in the proximal offshore (FZ1).

Development of the depositional model

In application of Walther's law (1894), facies succession and facies zone succession in the studied sections can provide information on how the facies and facies zones were spatially disposed along a proximal to distal transect, thus reinforcing their interpretation in terms of palaeoenvironmental significance. An example is shown in Fig. 10 that makes it evident that the succession FZ1–FZ2–FZ3–FZ4 (and the facies they contain) corresponds to palaeoenvironmental zones that can be placed in a model of deposition from the proximal offshore to the foreshore (Fig. 11). The outcrop analysis shows a dominance of FZ3 and FZ4 in the south-east of Zagora (Fig. 1A), while in the north-west of Zagora (Fig. 1A), FZ1 and FZ2 are dominant. This analysis implies a south-east (proximal) to north-west (distal) axis for the progradation of the system and a south-west/north-east shoreline orientation. A return to a facies zone belonging to deeper environment on top of facies shallowing upward bedsets implies a rupture in the characteristic facies succession as predicted by Walther's law (1894) that can be defined as a transgressive surface bounding a parasequence. Consequently, parasequences related to relative sea-level changes can be identified throughout the sections, and parasequences of different scales are recognized in the uppermost Fezouata and Zini formations (Fig. 10). They are here defined as elementary, small-scale, medium-scale and large-scale parasequences (Van Wagoner, 1995).

DEPOSITIONAL MODEL: A POTENTIAL TIDE MODULATION?

The main sedimentary features of the Fezouata and Zini formations are oscillatory structures pointing to fair-weather wave and storm-wave dominance on the sedimentation. The interpretation of storm-wave dominance in this studied interval is supported by: (i) a landward coarsening in grain size; (ii) the presence of planar bedding and tabular cross-beds (berms) in the foreshore; (iii) tens of metre-wide erosional surfaces interpreted as reactivation surfaces in the foreshore formed during storms (beach cusps); and (iv) oscillatory structures in most facies, from small-scale to large-scale wave ripples, HCS (mainly scour and drape, few accretionary) and SCS. Many authors have already studied wave-dominated systems, and the facies model for these coastal environments is now well-constrained (e.g. Davies & Moses, 1964; Bluck, 1967; Goldring & Bridges, 1973; Harms, 1979; Heward, 1981; Brenchley & Newall, 1982; Dott & Bourgeois, 1982; Davis & Hayes, 1984; Davis Jr, 1985; Brenchley *et al.*, 1986; Boyd *et al.*, 1992; Dumas & Arnott, 2006; Plint, 2010). However, not all sedimentary structures and all bedding architectures can be explained by only wave and storm action.

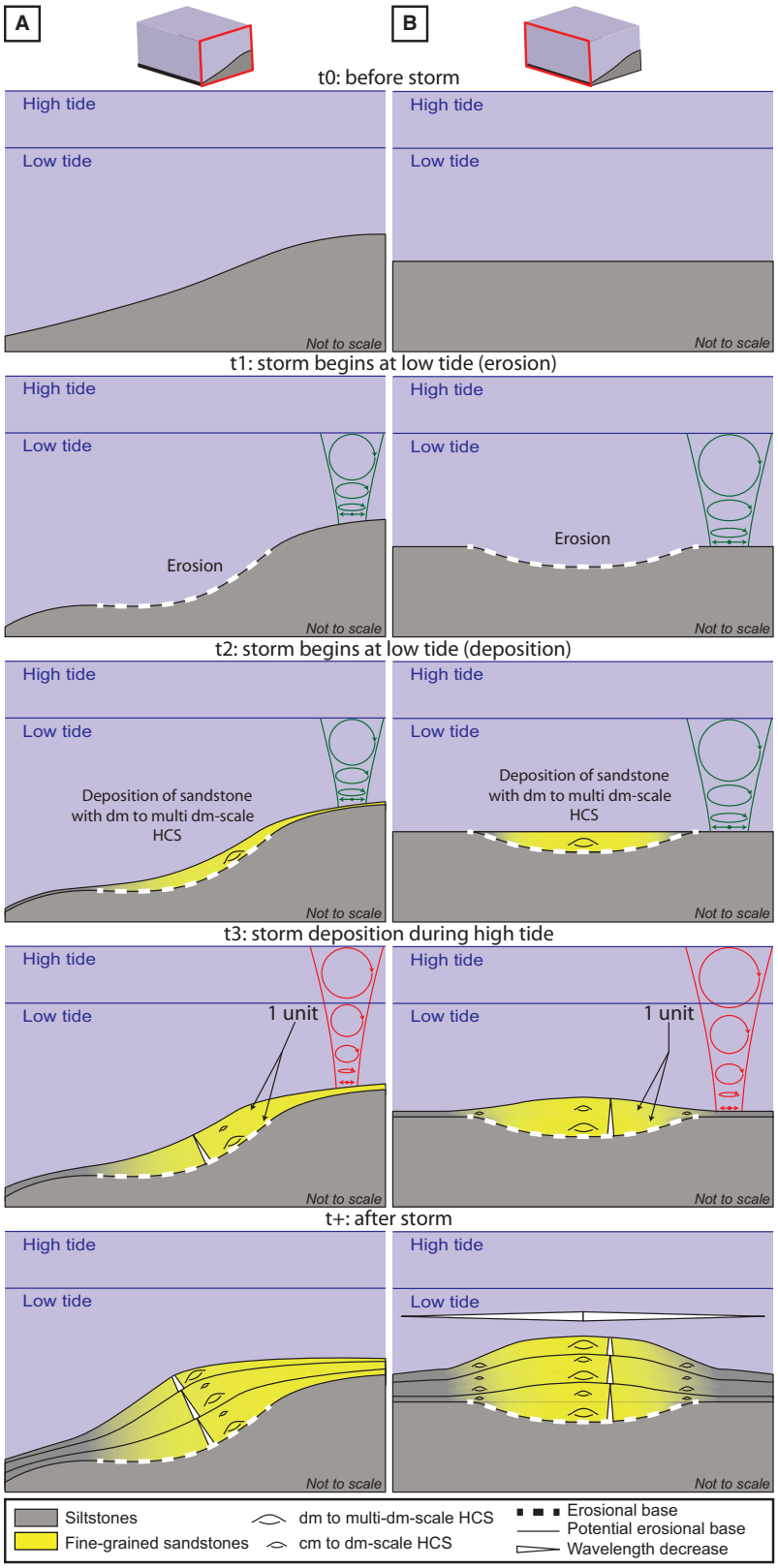

Fig. 9. Step by step diagram explaining the genesis of the sandstone to siltstone lenses, their sedimentary structures and their morphology with two views: (A) orthogonal and (B) parallel to the shore. The general shape of the SL, commonly having a geometry of scour and fill, suggests that erosion took place both orthogonally and parallel to the coastline probably during low tide, thus forming depressions filled-in during the subsequent tidal cycles.

According to the standard definitions, foreshore to shoreface deposits accumulate to form rather homogenous sandstone bodies without well-defined bedding planes due to a continuous regime of accumulation at the coast. Only the reactivation surfaces (often beach cusps) formed during storms interrupt sediment accumulation. In the Lower Ordovician successions of the central Anti-Atlas, the foreshore environments are uncommon and characterized by the alternation of bioturbated intervals with wave ripples (F11) and more massive sandstone beds with parallel or low-angle tabular stratifications (F10). Furthermore, peculiar features, unlike those in a purely storm-wave dominated system, are observed in the studied successions: (i) cyclical changes in both grain and structure size within a single storm event (here SL; Fig. 12A), cyclical organization at the transition between F1 and F2 (Fig. 12B and C), in fair-weather conditions with alternation of smaller and larger wavelength of wave ripples (Fig. 12D); (ii) local erosion in SCS interpreted as gutter (laminae in SCS rarely dip more than 10°; Leckie & Walker, 1982) (Fig. 5M); (iii) deep internal erosion in the sandstone to siltstone lenses, i.e. within the storm deposits themselves (Fig. 13A and B); (iv) discontinuous sandstone layers (Figs 4B, 4C and 8) in all environments that can locally form sandstone to siltstone lenses (Figs 6, 7A, 7E and 8). Moreover, in distal environments, the deposition is discontinuous with the formation of silty to fine-sandy lobes (F3; Fig. 5C); and (v) simultaneous aggradation–progradation of the wave ripples alternating with purely aggrading wave ripples (Fig. 13E). The latter observation suggests that, during one storm event, periods with oscillation dominantly controlling sediment deposition (aggradation; Fig. 13F) alternated with periods during which combined flow (progradation; Fig. 13F) controlled sediment accumulation (Fig. 13D). As observed in Fig. 13F, the change from one hydrodynamic regime to the other seems to be gradual. It is proposed here that the studied interval was wave-storm-dominated, but indirectly tide-modulated (Dashtgard *et al.*, 2012).

Changes in sea-level during tidal cycles would change the size of wave orbitals interacting with the sediment surface (Fig. 12E). At low tide, water depth is reduced; oscillation at the sea floor is expected to be of higher amplitude than at high tide, if tidal range is important. This implies that, during a storm event, larger oscillatory structures would be generated at low tide than at high tide (Fig. 13E and F). The observed changes in the amplitude of oscillation structures (or changes in grain size in the sandstone to siltstone lenses, with coarse bioclastic layers alternating with fine sandstones) characterize storm deposits in this study (Fig. 12A). Furthermore, SL are formed by two to eight cycles (Fig. 7) and for diurnal tide cycles, this would correspond to one to four days of storm. This duration is comparable with that of modern storms (Dolan *et al.*, 1988). Similarly, velocity of storm currents at the sea floor is expected to be higher during low tide than during high tide, implying that erosion would be more frequently recorded during falling tide than during rising tide, thus possibly explaining the decimetre-scale gutters commonly observed at the bottom or at the centre of SL1 (Fig. 13A to C) which correspond to one storm event. Moreover, changes in sea-level related to tide cycles would continuously change the storm equilibrium profile during the storms. Thus, erosion is not only recorded as gutter casts, but could also create an irregular topography along the sea floor, with zones of erosion and of deposition (Fig. 9), explaining that the Lower Ordovician sediments are generally deposited with a mound shape with or without a scour base (Figs 6, 7A, 7E and 9) and that storm deposits most commonly form discontinuous layers (Fig. 4B and C).

In a wave-dominated coastal system modulated by tidal cycles, the wave breaking zone moves on the intertidal zone, from the high-tide beach to the low-tide beach during falling tide and, conversely, from low-tide beach to high-tide beach during rising tide, thus forming surf bars (when submerged) or wave breaking bars (when located at the sea-level). A modern equivalent of this type of coastal system can be observed in northern France (Fig. 14A). Breaking or surf bars are both characteristic of the intertidal zone, where plane or low-angle parallel stratifications are formed (Fig. 14B). In topographical lows, large-scale and small-scale oscillation structures are generated when the intertidal zone is partly or fully submerged (Fig. 14B). This could explain the atypical coastal facies (F10 – F11), where oscillation structures are sandwiched between parallel stratifications (Fig. 4K). The morphology of the intertidal zone with disconnected surface bars and topographical lows at their back are only formed in macro-tidal systems (Short, 1991; Masselink & Short, 1993) and it can imply that both tide currents and storm back-currents are channelized (i.e. rip currents in channels or

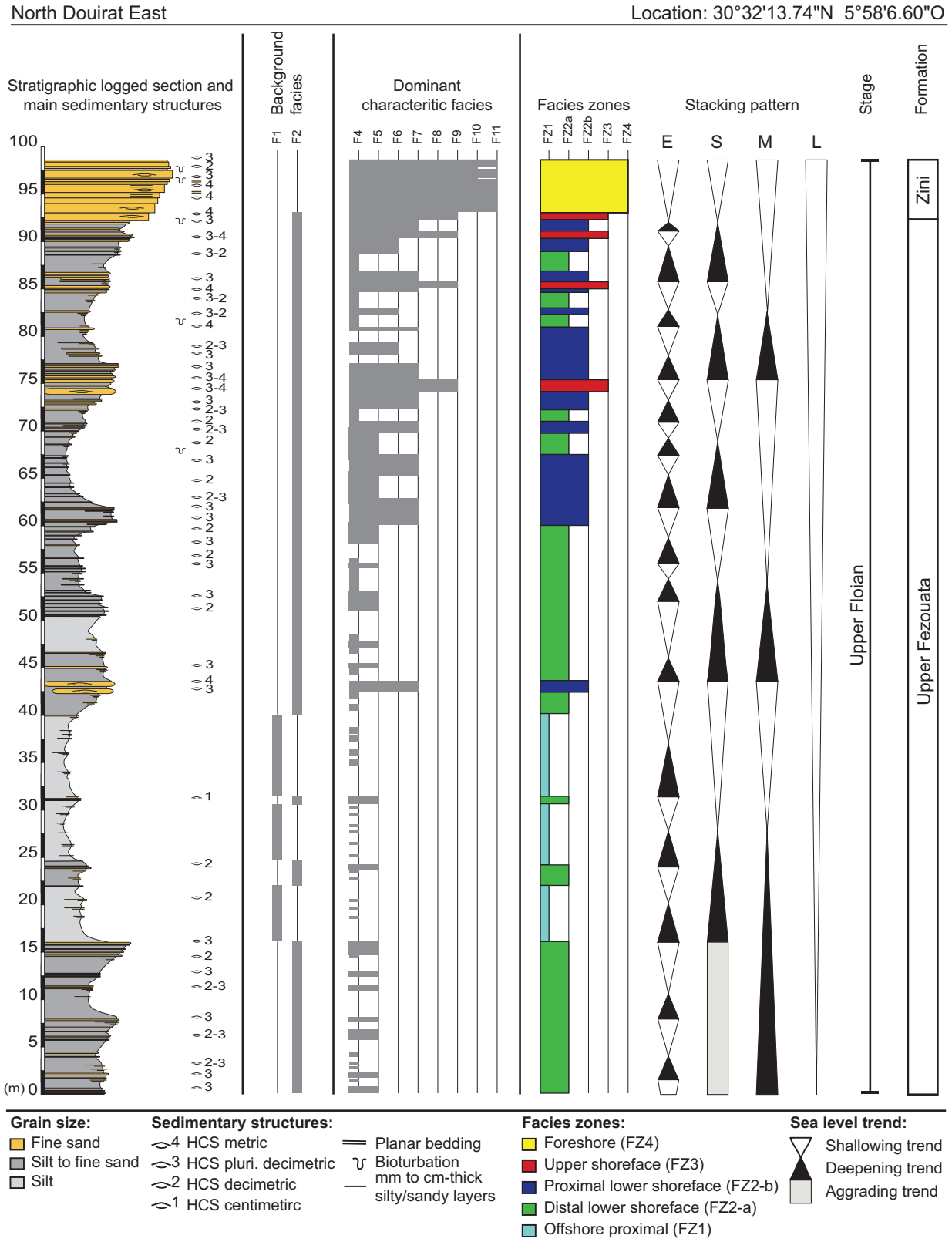

Fig. 10. Detailed section of the uppermost Fezouata and Zini formations (location: North Douirat East; Fig. 1A) with lithology, sedimentary structures, dominant facies and facies zone. According to the proposed facies model, elementary, small-scale, medium-scale and large-scale parasequences are identified, which suggest regressive and transgressive phases.

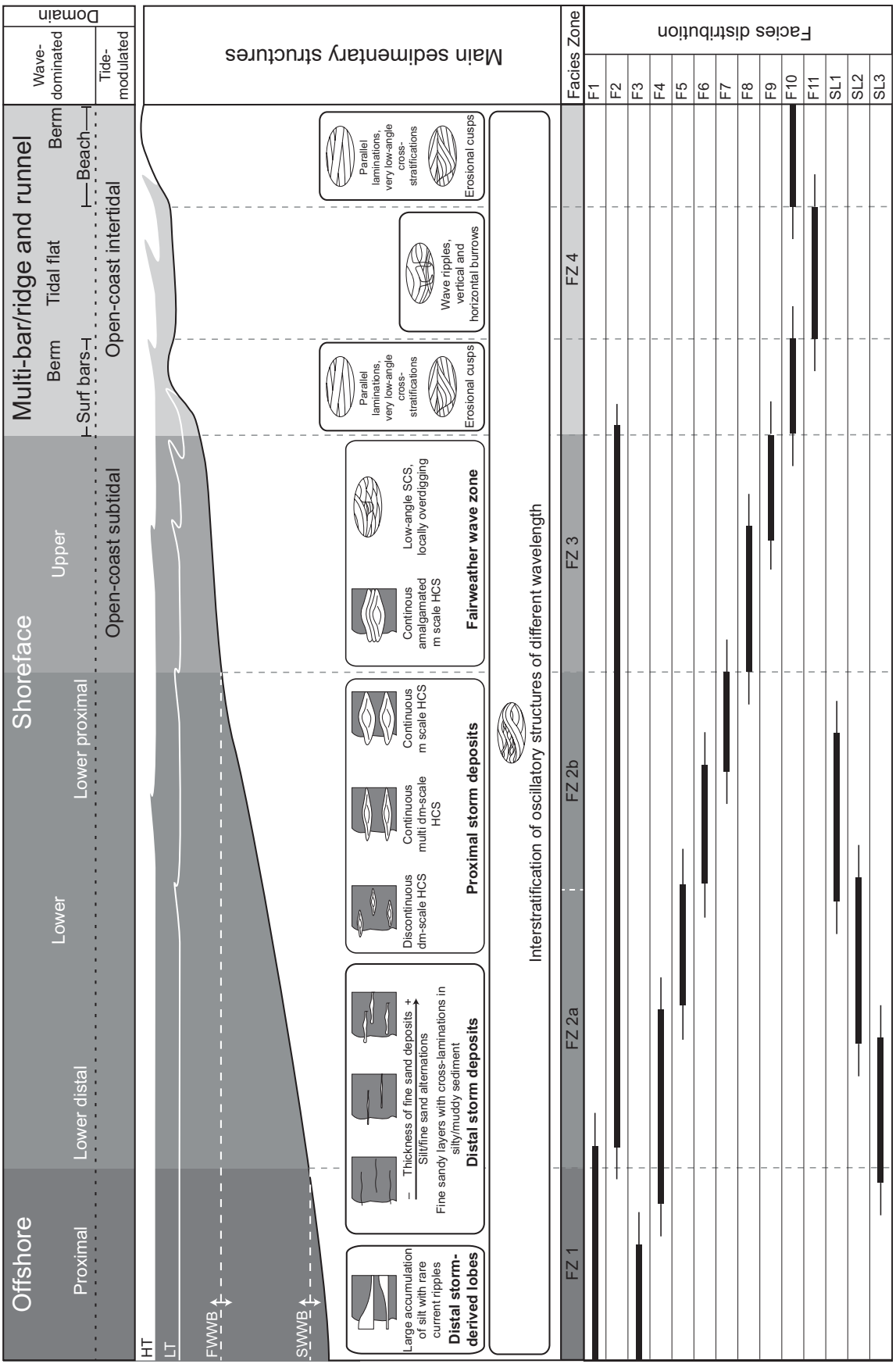

Fig. 11. Facies model for a wave-dominated, tide-modulated epicontinental system based on the Lower Ordovician horizontal and vertical facies distribution in the Fezouata and Zini formations.

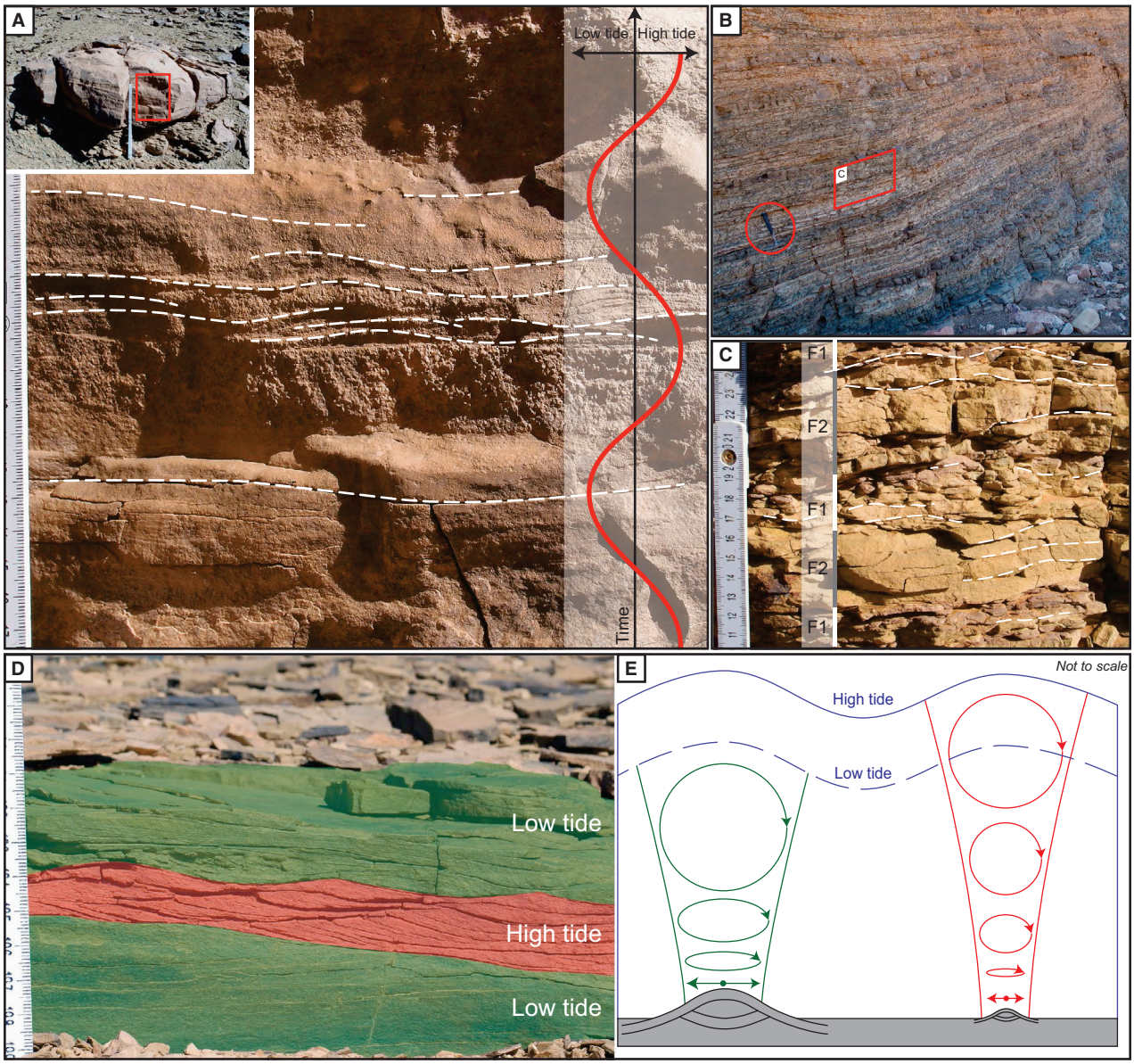

Fig. 12. (A) Cyclical changes in grain size in a sandstone to siltstone lens. The finest sediments are interpreted as being deposited during high tide, while the coarser sediments are deposited during low tide. (B) and (C) represent the characteristic cyclical organization in the lower part of facies zone 2. Cyclicity can be observed on both grain size and oscillatory structure size. Grain size varies from coarse siltstones (Facies 1) to fine sandstones (Facies 2), whereas wavelength of oscillatory structures alternates from decimetric to multi-decimetric. Coarse siltstones are associated with decimetric structures (Facies 1), fine sandstones with multi-decimetric structures (Facies 2). (D) Large and small wave ripples are commonly observed alternating in the sandy layers. (E) During high tide, wave orbits are attenuated on the sea floor, generating smaller wave ripples than during low tide.

Fig. 13. (A) and (B) Bioclastic infills of gutters in SL1. (C) Gutters are interpreted as generating during falling tide, eroding pre-existent sedimentary structures. (D) During storm events, the combination of oscillation and currents can vary during tidal cycles. At high tide, oscillation is weakened, implying that current may be better expressed in the sedimentary structures, thus creating combined oscillation–flow structures. (E) and (F) At low tide, oscillation dominates over currents, and mainly aggrading oscillation structures form. This process results in aggrading–prograding wave ripples (red lines) stacked between HCS (green lines).

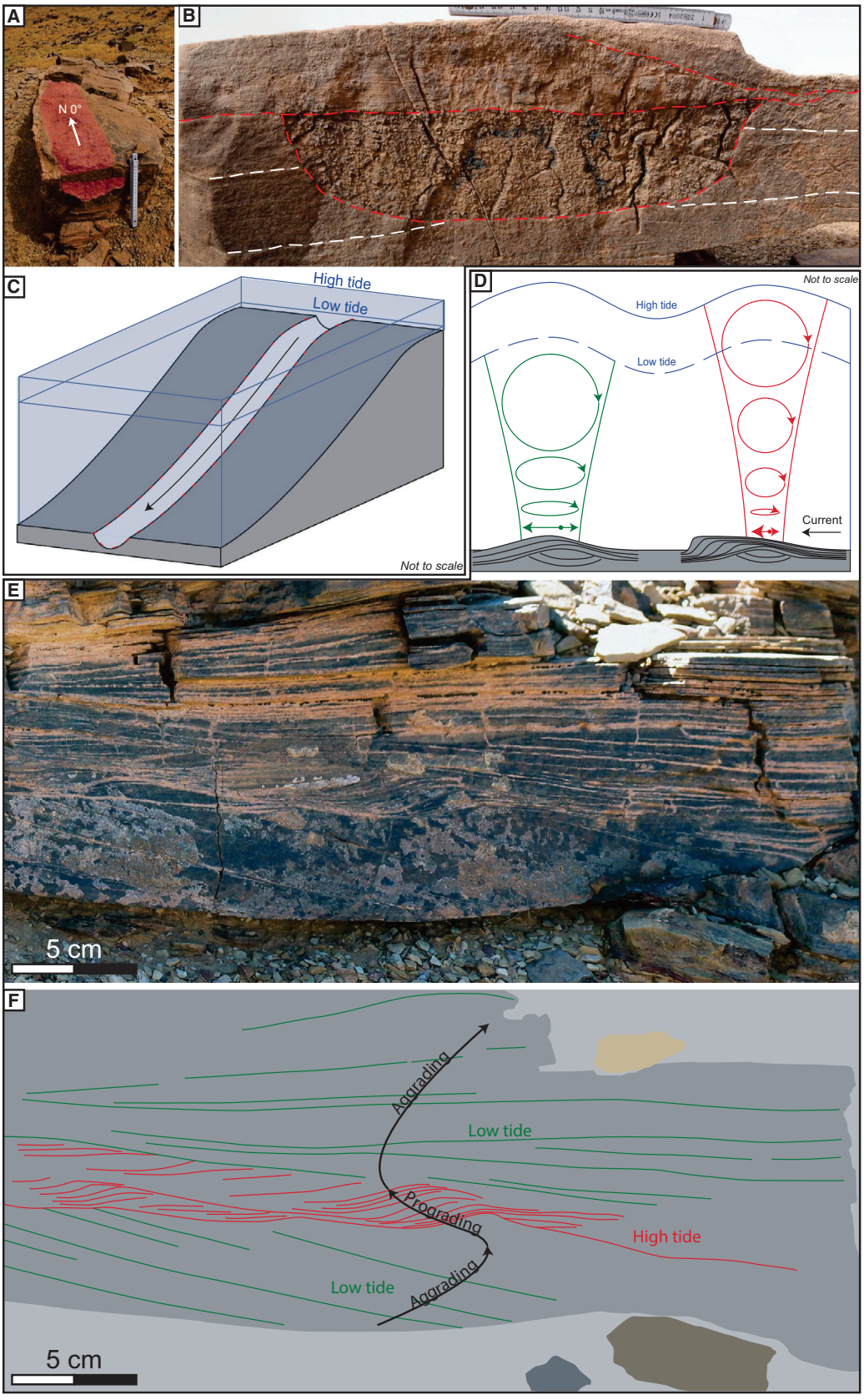

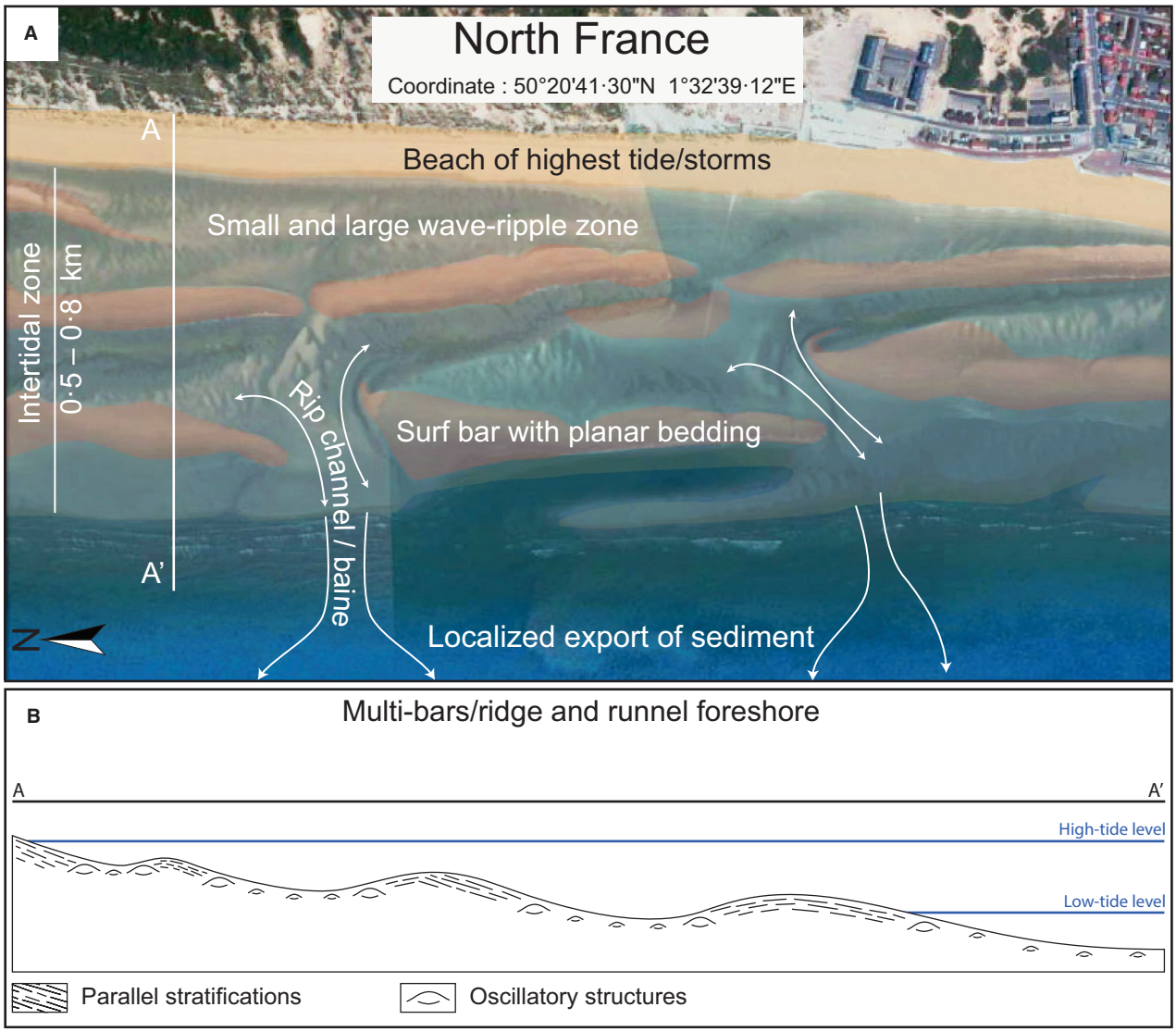

Fig. 14. (A) Satellite view in Google Earth, north of the Baie de Somme (northern France), showing a wave-dominated, tide-modulated coast. The intertidal zone is characterized by several surf bars. The surf bars are characterized by parallel stratifications due to wave breaking, and surrounded by topographical lows characterized by small and large oscillatory structures. These topographical lows act as tidal channels during rising or falling sea-level. Surf bars are disconnected from one another, thus allowing the tidal currents to be localized in rip current channels. During storms, strong rip currents may be responsible for the localized export of sediment seaward, thus possibly explaining that in the Lower Ordovician of the Anti-Atlas, the general organization of the deposits is characterized by discontinuous sedimentary bodies. (B) A simplified east–west transect of the intertidal zone (A) with the characteristic sedimentary structures and morphologies. The migration of the surf bars on the intertidal zone implies that small-scale and large-scale oscillatory structures will be sandwiched between low-angle parallel stratifications as observed in the facies (F10 and F11; FZ4) of the Zini Formation.

baines), thus focusing transport of the sediments seaward (Fig. 14A) (Shepard *et al.*, 1941; Short, 1985; Aagaard *et al.*, 1997; MacMahan *et al.*, 2006). This mechanism is probably contributing to form laterally discontinuous deposits as commonly recorded in the Lower Ordovician of the central Anti-Atlas.

Tide ranges were classified into three categories by Davies & Moses (1964): micro-tidal (<2 m), meso-tidal (2 to 4 m), macro-tidal (>4 m) and mega-tidal (>8 m). Macro-tidal beaches could be separated into two distinctive groups, and a third intermediate case (Short, 1991; Masselink & Short, 1993). End members are 'higher

wave, planar, uniform slope' and 'moderate waves, multi-bars'. The intermediate one is 'low wave beach and tidal flat'. The studied Lower Ordovician deposits probably belong to a system, where the coastal environment corresponds to the 'moderate waves, multi-bars' (ridge and runnel) macro-tidal beaches. Macro-tidal beaches showing 'moderate waves and multi-bars', as shown in Fig. 14, consist of small-scale and large-scale oscillatory structures alternating with large surf bars characterized by low-angle parallel stratifications. Evolution of this kind of coastal environment by migration of the surf bars would sandwich small-scale and large-scale oscillatory structures between low-angle parallel stratifications as observed in the Zini Formation. Current ripples, tidal channels and tidal bundles, as well as flaser, wavy or lenticular beddings, are missing in both the Fezouata and the Zini formations. The only possibly tide-generated sedimentary structures could be the tangential cross-bedded sandstones observed in one place in the Zini Formation (Fig. 4J), which could eventually be interpreted as the bottom part of tidal dunes. The SL frequently display internal erosion surfaces (Fig. 13A and B); thus, each tidal cycle could not be preserved through SL. Furthermore, the general sedimentation in the Lower Ordovician succession is mainly constituted of laterally discontinuous deposits, which imply that tidal cycles would not be recorded everywhere. However, the hypothesis that the studied deposits belong to a macro-tidal beach system is in agreement with a dominance of wave-related structures and the scarcity of typical tidal sedimentary structures and geometries in such a context (Dashtgard *et al.*, 2009, 2012). Through this study, the prolongation of the 'moderate waves, multi-bars' model (Short, 1991; Masselink & Short, 1993) is then proposed up to proximal offshore environments. Other authors have already observed hybrid sedimentary systems up to offshore environment in the rock record (e.g. Basilici *et al.*, 2011, 2012; Vakarelov *et al.*, 2012; Rossi & Steel, 2016). However, the Lower Ordovician of the Anti-Atlas is the first sedimentary system exhibiting storm and wave structures and geometries, which indirectly record a tide modulation. The other described examples of hybrid systems are characterized by a clear expression of both processes (waves and tides) with distinctly expressed wave and tide sedimentary structures.

Early Palaeozoic times were characterized by tides of higher amplitudes than today (Scrutton & Hipkin, 1973), due to the shorter Earth–Moon distance and hence faster Earth rotation (Lambeck, 1978, 2005; Scrutton, 1978). In the Anti-Atlas, the Lower Ordovician succession filled the intracratonic basin created by the rifting phase between Avalonia continent and Gondwanaland (Fig. 2) (Cocks & Torsvik, 2004). The proximity of Avalonia and Gondwana, separated by a wide shallow epicontinental sea, could be responsible for a significant effect of resonance (Davis Jr & Dalrymple, 2012) that increased tidal range (Cram, 1979). Other sedimentary successions from Early Palaeozoic report mixed wave and tide processes, for example the Cambro-Ordovician successions of Brazil (Basilici *et al.*, 2011) and of Algeria (Ghienne *et al.*, 2007), the Upper Ordovician of China (Fan *et al.*, 2004) or the Upper Ordovician of Morocco (Loi *et al.*, 2010). Brenchley & Newall (1982) also described SL similar to those described in the present study in the Middle Ordovician of England (Shropshire) and interpreted these sedimentary bodies as deposited under ebb-forced, storm back-currents, localized by reef barriers. Moreover, in the central Anti-Atlas, the middle Cambrian Tabanite Group (below the Fezouata Formation; Fig. 1) and the Middle Ordovician First Bani Group (above the Zini Formation; Fig. 2) both exhibit typical combined wave and tide sedimentary structures (field observations; Marante, 2008). Furthermore, Ghienne *et al.* (2007) have identified the influence of both waves and tides in the Lower Ordovician succession of Algeria. Therefore, it is likely that in the Zagora area, the Lower Ordovician succession was also influenced by both waves and tides.

PALAEOENVIRONMENT OF THE LOWER ORDOVICIAN FEZOUATA BIOTA

Processes responsible for exceptional preservation of soft-body tissues in the fossil record are still under investigation. However, the fossils of the Moroccan Fezouata *Lagerstätte* could exhibit, according to Gaines *et al.* (2012), characteristic features of a Burgess Shale-type preservation. Processes of organic matter degradation (decay) were stopped early, and authigenic minerals replaced soft tissues (Gaines *et al.*, 2008). Rapid burial is one key factor for organic matter preservation in order to escape oxidation by oxygen, sulphate reduction or other processes of organic matter oxidation (e.g. Froelich *et al.*, 1979; Allison, 1988; Briggs & Kear, 1994; Allison & Brett, 1995; Butterfield, 1995;

Gaines *et al.*, 2005). Exceptionally preserved soft-body tissues are found in thin layers of muddy sediment that are covered by centimetre-thick coarser, sandy deposits (Vaucher *et al.*, 2016). This fact implies that the fossil-rich layers correspond to peculiar stratigraphic levels and cannot be found throughout the entire Lower Ordovician succession (Martin *et al.*, 2016). The fact that these layers are only found in F1 when associated with F4 (distal tempestites) suggests that burial by storm deposits is required, but that energy was not high enough to rework fossil assemblages that can thus be preserved *in situ* (Martin *et al.*, 2016; Vaucher *et al.*, 2016). As previously mentioned, the dominant depositional geometry in most of the environment is mound-shaped as is the case for the SL, which implies that thick amounts of sediment can be deposited rapidly. The fast deposition of sediment appears to be a key factor to initiate the exceptional preservation in the Fezouata Formation. These conditions are fulfilled in the most distal storm-influenced zone (distal lower shoreface; Fig. 11).

Van Roy *et al.* (2010) described the environment of the Fezouata Biota as deep water and of low energy, whereas coarser sediments were interpreted as distal tempestites. This study suggests a shallower setting in agreement with Lefebvre & Botting (2007) who analysed assemblage composition of stylophoran echinoderms from the Fezouata Formation. This shallower setting is proposed here to be close to/above the limit of the storm-weather wave base. In terms of water depth, 30 to 70 m is suggested (Immenhauser, 2009).

CONCLUSIONS

The Fezouata and the Zini formations were subdivided into 14 facies, all grouped in four facies zones, namely the proximal offshore, the lower shoreface, the open-coast subtidal-upper shoreface and the intertidal-foreshore (respectively, FZ1 to FZ4). The Lower Ordovician succession records offshore to foreshore environments dominated by oscillatory structures. Tidal effects can only be recognized by the modulation of oscillatory structures during sea-level fluctuations induced by tidal cycles, and no diagnostic tidal sedimentary structures are present.

A new model of deposition for a wave-dominated, tide-modulated siliciclastic system is proposed. The two main characteristics of such a depositional environment are as follows: (i) the deposits are fundamentally discontinuous, at different scales and for different water depths (from the intertidal-foreshore to the offshore); and (ii) the deposits indirectly record tidally controlled cyclical changes in sea-level, and their expression depends on the position along the siliciclastic shelf.

This study revealed one of the very few wave-dominated and tide-modulated shallow epicontinental seas recording foreshore to offshore environments. The few examples described in the geological record focus only on proximal environments (e.g. Basilici *et al.*, 2011, 2012) but could exist in modern environments (e.g. Yang *et al.*, 2005; Dashtgard *et al.*, 2009, 2012). Only Vakarelov *et al.* (2012) described a wave-dominated and tide-influenced system from proximal offshore to foreshore environment by the recognition of both wave-generated and tide-generated sedimentary structures.

This study provides key data on the sedimentological context associated with exceptional preservation in the Early Ordovician Fezouata Biota. Rapid burial during storm events in a relatively distal environment seems to be a prerequisite for the *in situ* preservation of organisms by inhibiting their early decay.

ACKNOWLEDGEMENTS

The authors would like to thank the Agence National de la Recherche (EM, Grant Number RALI 197; 'The Rise of Animal Life (Cambrian-Ordovician): organisation and tempo') and CNRS-CNRST Cooperation Project VALORIZ for financial support. We are grateful to N. Allaire, A. Bachnou, K. El Hariri, J.-C. Gutiérrez-Marco, A. Hafid, R. Lerosey-Aubril, M. Masrour, E. Nardin, A. Prieur, E. Robert, T. Servais, T. Vandenbroucke, J. Vannier, P. V. Roy, M. Vidal and D. Vizcaïno for their precious help in the field and/or for fruitful discussions. We are also thankful to the Associate Editor Mariano Marzo as well as S. Dashtgard, P. Plink-Björklund, V. Rossi and two anonymous reviewers for their sensible remarks that helped us to improve the quality of the manuscript.

REFERENCES

Aagaard, T., **Greenwood, B.** and **Nielsen, J.** (1997) Mean currents and sediment transport in a rip channel. *Mar. Geol.*, **140**, 25–45.

Alexander, J., **Bridge, J.S.**, **Cheel, R.J.** and **Leclair, S.F.** (2001) Bedforms and associated sedimentary structures

formed under supercritical water flows over aggrading sand beds. *Sedimentology*, **48**, 133–152.

Allen, P.A. (1997) *Earth Surface Processes*. Blackwell Science, London, UK, 404 pp.

Allison, P.A. (1988) Konservat-Lagerstatten: cause and classification. *Paleobiology*, **14**, 331–344.

Allison, P.A. and **Brett, C.E.** (1995) *In situ* benthos and paleo-oxygenation in the Middle Cambrian Burgess Shale, British Columbia, Canada. *Geology*, **23**, s79–s1082.

Avigad, D., **Kolodner, K.**, **McWilliams, M.**, **Persing, H.** and **Weissbrod, T.** (2003) Origin of northern Gondwana Cambrian sandstone revealed by detrital zircon SHRIMP dating. *Geology*, **31**, 227–230.

Bambach, R.K., **Knoll, A.H.** and **Wang, S.C.** (2004) Origination, extinction, and mass depletions of marine diversity. *Paleobiology*, **30**, 522–542.

Basilici, G., **de Luca, P.H.V.** and **Oliveira, E.P.** (2011) A depositional model for a wave-dominated open-coast tidal flat, based on analyses of the Cambrian-Ordovician Lagarto and Palmares formations, north-eastern Brazil. *Sedimentology*, **59**, 1613–1639.

Basilici, G., **de Luca, P.H.V.** and **Poire, D.G.** (2012) Hummocky cross-stratification-like structures and combined-flow ripples in the Punta Negra Formation (Lower-Middle Devonian, Argentine Precordillera): a turbiditic deep-water or storm-dominated prodelta inner-shelf system?. *Sed. Geol.*, **267**, 73–92.

Billeaud, I., **Tessier, B.** and **Lesueur, P.** (2009) Impacts of late Holocene rapid climate changes as recorded in a macrotidal coastal setting (Mont-Saint-Michel Bay, France). *Geology*, **37**, 1031–1034.

Bluck, B.J. (1967) Sedimentation of beach gravels; examples from South Wales. *J. Sed. Res.*, **37**, 128–156.

Boote, D.R.D., **Clark-Lowes, D.D.** and **Traut, M.W.** (1998) Palaeozoic petroleum systems of North Africa. *Geol. Soc. London. Spec. Publ.*, **132**, 7–68.

Boyd, R., **Dalrymple, R.** and **Zaitlin, B.A.** (1992) Classification of clastic coastal depositional environments. *Sed. Geol.*, **80**, 139–150.

Brenchley, P.J. and **Newall, G.** (1982) Storm-influenced inner-shelf sand lobes in the Caradoc (Ordovician) of Shropshire, England. *J. Sed. Petrol.*, **52**, 1257–1269.

Brenchley, P.J., **Romano, M.** and **Gutierrez-Marco, J.C.** (1986) Proximal and distal hummocky cross-stratified facies on a wide Ordovician shelf in Iberia. Shelf Sands and Sandstones. In: *Canadian Society of Petroleum Geologists* (Eds R.J. Knight and J.R. McLean), **2**, pp. 241–255. Canadian Society of Petroleum Geologists, Calgary, AB, Canada. Memoir 11.

Briggs, D.E.G. and **Kear, A.J.** (1994) Decay and mineralization of shrimps. *Palaios*, **9**, 431–456.

Butterfield, N.J. (1995) Secular distribution of Burgess-Shale-type preservation. *Lethaia*, **28**, 1–13.

Carr, I.D. (2002) Second-order sequence stratigraphy of the Palaeozoic of North Africa. *J. Pet. Geol*, **25**, 259–280.

Cartigny, M.J.B., **Ventra, D.**, **Postma, G.** and **van Den Berg, J.H.** (2014) Morphodynamics and sedimentary structures of bedforms under supercritical-flow conditions: New insights from flume experiments. *Sedimentology*, **61**, 712–748.

Chauhan, P.P.S. (2000) Bedform association on a ridge and runnel foreshore: implications for the hydrography of a macrotidal estuarine beach. *Journal of Coastal Research*, **16**, 1011–1021.

Choubert, G. (1942) Constitution et puissance de la série primaire de l'Anti-Atlas. *CR Acad. Sci. Paris*, **215**, 445–447.

Cocks, L.R.M. and **Torsvik, T.H.** (2004) Major terranes in the Ordovician. In: *The Great Ordovician Biodiversification Event*. (Eds B.D. Webby, F. Paris, M.L. Droser and I.G. Percival), pp. 61–67. Columbia University Press, New York.

Cotter, E. and **Graham, J.R.** (1991) Coastal plain sedimentation in the late Devonian of Southern Ireland; hummocky cross-stratification in fluvial deposits? *Sediment. Geol.*, **72**, 201–224.

Coward, M. and **Ries, A.** (2003) Tectonic development of North African basins. *Geol. Soc. London. Spec. Publ.*, **207**, 61–83.

Cram, J.M. (1979) The influence of continental shelf width on tidal range: paleoceanographic implications. *J. Geol.*, **87**, 441–447.

Cummings, D.I., **Dumas, S.** and **Dalrymple, R.W.** (2009) Fine-grained versus coarse-grained wave ripples generated experimentally under large-scale oscillatory flow. *J. Sed. Res.*, **79**, 83–93.

Dalrymple, R.W. (1992) Tidal depositional systems. In : *Facies Models: Response to Sea Level Change* (Eds R.G. Walker and P.J. Noel), pp. 195–218. Geol. Assoc. Can., St. John's, Newfoundland, Canada.

Dalrymple, R.W., **Baker, E.K.**, **Harris, P.T.** and **Hughes, M.**, (2003). Sedimentology and stratigraphy of a tide-dominated, foreland–basin delta (Fly River, Papua New Guinea). In: *Tropical Deltas of Southeast Asia–Sedimentology, Stratigraphy, and Petroleum* (Eds F.H. Sidi, D. Nummedal, P. Imbert, H. Darman and H.W. Posamentier), SEPM Spec. Publ. Number, Tulsa, OK, USA, **76**, pp. 147–173

Dashtgard, S.E., **Gingras, M.K.** and **MacEachern, J.A.** (2009) Tidally modulated shorefaces. *J. Sed. Res.*, **79**, 793–807.

Dashtgard, S.E., **MacEachern, J.A.**, **Frey, S.E.** and **Gingras, M.K.** (2012) Tidal effects on the shoreface: towards a conceptual framework. *Sed. Geol.*, **279**, 42–61.

Davies, J. and **Moses, C.A.** (1964) A morphogenic approach to world shorelines. *Zeitschrift fur Geomorphologie*, **8**, 127–142.

Davis, R.A., Jr and **Hayes, M.O.** (1984) What is a wave-dominated coast? *Mar. Geol.*, **60**, 313–329.

Destombes, J. (1962) Stratigraphie et paléogéographie de l'Ordovicien de l'Anti-Atlas (Maroc). *Un essai de synthèse. Bull. Soc. Géol. Fr.*, **7**, 453–460.

Destombes, J., **Hollard, H.** and **Willefert, S.** (1985) Lower Palaeozoic rocks of Morocco. In: *Lower Palaeozoic Rocks of North-western and West-central Africa*. (Ed. C.H. Holland), pp. 91–336. Wiley, New-York, Chichester, Brisbane.

Dolan, R., **Lins, H.** and **Hayden, B.** (1988) Mid-Atlantic coastal storms. *J. Coastal Res.*, **4**, 417–433.

Dott, R. and **Bourgeois, J.** (1982) Hummocky stratification: significance of its variable bedding sequences. *Geol. Soc. Am. Bull.*, **93**, 663–680.

Dumas, S. and **Arnott, R.W.C.** (2006) Origin of hummocky and swaley cross-stratification - The controlling influence of unidirectional current strength and aggradation rate. *Geology*, **34**, 1073–1076.

Fabre, J. (1988) Les séries paléozoïques d'Afrique: une approche. *J. Af. Earth Sci. (and the Middle East)*, **7**, 1–40.

Fan, D., **Li, C.** and **Wang, P.** (2004) Influences of storm erosion and deposition on rhythmites of the upper Wenchang Formation (Upper Ordovician) around Tonglu, Zhejiang Province, China. *J. Sed. Res.*, **74**, 527–536.

Fildani, A. and **Normark, W.R.** (2004) Late Quaternary evolution of channel and lobe complexes of Monterey Fan. *Mar. Geol.*, **206**, 199–223.

Froelich, P.N., **Klinkhammer, G.P.**, **Bender, M.L.**, **Luedtke, N.A.**, **Heath, G.R.**, **Cullen, D.**, **Dauphin, P.**, **Hammond, D.**, **Hartman, B.** and **Maynard, V.** (1979) Early oxidation of organic matter in pelagic sediments of the eastern equatorial Atlantic: suboxic diagenesis. *Geochimi. Cosmochim. Acta*, **43**, 1075–1090.

Gaines, R.R., **Kennedy, M.J.** and **Droser, M.L.** (2005) A new hypothesis for organic preservation of Burgess Shale taxa in the middle Cambrian Wheeler Formation, House Range, Utah. *Palaeogeogr. Palaeoclimatol. Palaeoecol.*, **220**, 193–205.

Gaines, R.R., **Briggs, D.E.G.** and **Zhao, Y.L.** (2008) Cambrian Burgess Shale-type deposits share a common mode of fossilization. *Geology*, **36**, 755–758.

Gaines, R.R., **Hammarlund, E.U.**, **Hou, X.**, **Qi, C.**, **Gabbott, S.E.**, **Zhao, Y.**, **Peng, J.** and **Canfield, D.E.** (2012) Mechanism for Burgess Shale-type preservation. *Proc. Nat. Acad. Sci. USA*, **109**, 5180–5184.

Gasquet, D., **Roger, J.**, **Chalot-Prat, F.**, **Hassenforder, B.**, **Baudin, T.**, **Chevremont, P.**, **Razin, P.**, **Benlakhdim, A.**, **Mortaji, A.** and **Benssaou, M.** (2001) Carte géologique du Maroc au 1/50 000. Feuille De Tamazrar. *Mémoire explicatif. Notes et mémoires du Service géologique du Maroc*, **415** bis, 1–95.

Gervais, A., **Savoye, B.**, **Mulder, T.** and **Gonthier, E.** (2006) Sandy modern turbidite lobes: a new insight from high resolution seismic data. *Mar. Pet. Geol.*, **23**, 485–502.

Geyer, G. and **Landing, E.** (2006) Latest Ediacaran and Cambrian of the Moroccan Atlas regions. *Beringeria Special Issue*, **6**, 7–46.

Ghienne, J.F., **Boumendjel, K.**, **Paris, F.**, **Videt, B.**, **Racheboeuf, P.** and **Salem, H.A.** (2007) The Cambrian-Ordovician succession in the Ougarta Range (western Algeria, North Africa) and interference of the Late Ordovician glaciation on the development of the Lower Palaeozoic transgression on northern Gondwana. *Bull. Geosci.*, **82**, 183–214.

Goldring, R. and **Bridges, P.** (1973) Sublittoral sheet sandstones. *J. Sed. Res.*, **43**, 736–747.

Hampson, G.J. and **Storms, J.E.A.** (2003) Geomorphological and sequence stratigraphic variability in wave-dominated, shoreface-shelf parasequences. *Sedimentology*, **50**, 667–701.

Harms, J. (1979) Primary sedimentary structures. *Annu. Rev. Earth Planet. Sci.*, **7**, 227.

Heward, A.P. (1981) A review of wave-dominated clastic shoreline deposits. *Earth-Sci. Rev.*, **17**, 223–276.

Hine, A.C. (1979) Mechanisms of berm development and resulting beach growth along a barrier spit complex. *Sedimentology*, **26**, 333–351.

Hollard, H. and **Choubert, G.** (1985) Carte Géologique du Maroc, 1/1000000. *Ministère de l'Energie et des Mines, Direction de la Géologie, Editions du Service Géologique du Maroc*

Ichaso, A.A. and **Dalrymple, R.W.** (2009) Tide- and wave-generated fluid mud deposits in the Tilje Formation (Jurassic), offshore Norway. *Geology*, **37**, 539–542.

Immenhauser, A. (2009) Estimating palaeo-water depth from the physical rock record. *Earth-Sci. Rev.*, **96**, 107–139.

Inman, D.L. and **Guza, R.T.** (1982) The origin of swash cusps on beaches. *Mar. Geol.*, **49**, 133–148.

Davis Jr, R.A. (1985) Beach and nearshore zone. In: *Coastal Sedimentary Environments* (Ed. R.A. Davis Jr), pp. 379–444. Springer –Verlag, New York.

Davis Jr, R.A. and **Dalrymple, R.W.**, Eds, (2012) *Principles of Tidal Sedimentology*. Springer, New York, 607 p.

Lambeck, K. (1978) The Earth's Palaeorotation. In: *Tidal Friction and the Earth's Rotation*. (Eds P. Brosche and J. Sündermann), pp. 145–153. Springer, Berlin, Heidelberg.

Lambeck, K. (2005) *The Earth's Variable Rotation: Geophysical Causes and Consequences*. Cambridge University Press, New York, 464 p.

Lang, J. and **Winsemann, J.** (2013) Lateral and vertical facies relationships of bedforms deposited by aggrading supercritical flows: from cyclic steps to humpback dunes. *Sediment. Geol.*, **296**, 36–54.

Leckie, D.A. and **Walker, R.G.** (1982) Storm-and tide-dominated shorelines in Cretaceous Moosebar-Lower Gates interval - outcrop equivalents of Deep Basin gas trap in western Canada. *AAPG Bul.*, **66**, 138–157.

Lefebvre, B. and **Botting, J.P.** (2007) First report of the mitrate Peltocystis cornuta Thoral (Echinodermata, Stylophora) in the Lower Ordovician of central Anti-Atlas (Morocco). *Ann. Pal.*, **93**, 183–198.

Li, C., **Wang, P.**, **Daidu, F.**, **Bing, D.** and **Tiesong, L.** (2000) Open-coast intertidal deposits and the preservation potential of individual laminae: a case study from east-central China. *Sedimentology*, **47**, 1039–1051.

Loi, A., **Ghienne, J.F.**, **Dabard, M.P.**, **Paris, F.**, **Botquelen, A.**, **Christ, N.**, **Elaouad-Debbaj, Z.**, **Gorini, A.**, **Vidal, M.**, **Videt, B.** and **Destombes, J.** (2010) The Late Ordovician glacio-eustatic record from a high-latitude storm-dominated shelf succession: the Bou Ingarf section (Anti-Atlas, Southern Morocco). *Palaeogeogr. Palaeoclimatol. Palaeoecol.*, **296**, 332–358.

MacMahan, J.H., **Thornton, E.B.** and **Reniers, A.J.H.M.** (2006) Rip current review. *Coast. Eng.*, **53**, 191–208.

Marante, A. (2008) *Architecture et dynamique des systèmes sédimentaires silico-clastiques sur "la plate-forme géante" nord-gondwanienne. L'Ordovicien moyen de l'Anti-Atlas marocain*, Unpublished PhD Thesis, Université Michel Montaigne Bordeaux 3, Bordeaux, France.

Martin, E., **Lefebvre, B.**, **Pittet, B.**, **Vannier, J.**, **Bachnou, A.**, **Hariri, K.**, **Hafid, A.**, **Masrour, M.**, **Noailles, F.**, **Nowak, H.**, **Servais, T.**, **Vandenbroucke, T.A.**, **Van Roy, P.**, **Vidal, M.** and **Vizcaïno, D.** (2014) The Fezouata Biota (Central Anti-Atlas, Morocco): Biostratigraphy and associated environmental conditions of an Ordovician Burgess Shale. In: *STRATI 2013* (Eds R. Rocha, J. Pais, J.C. Kullberg and S. Finney), Springer Geology, pp. 419–423. Springer International Publishing, Heidelberg.

Martin, E.L.O., **Pittet, B.**, **Gutiérrez-Marco, J.-C.**, **Vannier, J.**, **El Hariri, K.**, **Lerosey-Aubril, R.**, **Masrour, M.**, **Nowak, H.**, **Servais, T.**, **Vandenbroucke, T.R.A.**, **Van Roy, P.**, **Vaucher, R.** and **Lefebvre, B.** (2016) The Lower Ordovician Fezouata Konservat-Lagerstätte from Morocco: age, environment and evolutionary perspectives. *Gondwana Res.*, **34**, 274–283.

Masselink, G. and **Anthony, E.J.** (2001) Location and height of intertidal bars on macrotidal ridge and runnel beaches. *Earth Surf. Proc. Land.*, **26**, 759–774.

Masselink, G. and **Short, A.D.** (1993) The effect of tide range on beach morphodynamics and morphology: a conceptual beach model. *J. Coastal Res.*, **9**, 785–800.

Masselink, G., **Kroon, A.** and **Davidson-Arnott, R.G.D.** (2006) Morphodynamics of intertidal bars in wave-dominated coastal settings — A review. *Geomorphology*, **73**, 33–49.

McLane, M. (1995) *Sedimentology*. Oxford University Press, New York; Oxford, 423 pp.

Meyers, S.R. and **Peters, S.E.** (2011) A 56 million year rhythm in North American sedimentation during the Phanerozoic. *Earth Planet. Sci. Lett.*, **303**, 174–180.

Myrow, P.M. and **Southard, J.B.** (1996) Tempestite deposition. *J. Sediment. Res.*, **66**, 875–887.

Plink-Björklund, P. (2008) Wave-to-tide process change in a Campanian Shoreline Complex, Chimney Rock Tongue, Wyoming/Utah. In: *Recent advances in Models of Siliciclastic Shallow-Marine Stratigraphy* (Eds G.J. Hampson, R.J. Steel and P.M. Burgess and R.W. Dalrymple), SEPM Spec. Publ., **90**, 265–291.

Plint, A.G. (2010) Wave-and storm-dominated shoreline and shallow-marine systems. In: *Facies Models* (Eds R.W. Dalrymple and N.P. James), 4th edn, pp. 167–200. Geol. Assoc. Canada, St John's.

Prave, A.R. and **Duke, W.L.** (1990) Small-scale hummocky cross-stratification in turbidites: a form of antidune stratification? *Sedimentology*, **37**, 531–539.

Quin, J.G. (2011) Is most hummocky cross-stratification formed by large-scale ripples? *Sedimentology*, **58**, 1414–1433.

Rossi, V.M. and **Steel, R.J.** (2016) The role of tidal, wave and river currents in the evolution of mixed-energy deltas: example from the Lajas Formation (Argentina). *Sedimentology*, **63**, 824–864.

Rust, B.R. and **Gibling, M.R.** (1990) Three-dimensional antidunes as HCS mimics in a fluvial sandstone: the Pennsylvanian South Bar Formation near Sydney, Nova Scotia. *J. Sediment. Res.*, **60**, 540–548.

Scrutton, C.T. (1978) Periodic growth features in fossil organisms and the length of the day and month. In: *Tidal Friction and the Earth's Rotation*. (Eds P. Brosche and J. Sündermann), pp. 154–196. Springer, Berlin, Heidelberg.

Scrutton, C.T. and **Hipkin, R.G.** (1973) Long-term changes in the rotation rate of the Earth. *Earth-Sci. Rev.*, **9**, 259–274.

Servais, T., **Lehnert, O.**, **Li, J.**, **Mullins, G.L.**, **Munnecke, A.**, **Nuetzel, A.** and **Vecoli, M.** (2008) The Ordovician Biodiversification: revolution in the oceanic trophic chain. *Lethaia*, **41**, 99–109.

Servais, T., **Owen, A.W.**, **Harper, D.A.T.**, **Kröger, B.** and **Munnecke, A.** (2010) The great ordovician biodiversification event (GOBE): the palaeoecological dimension. *Palaeogeogr. Palaeoclimatol. Palaeoecol.*, **294**, 99–119.

Shepard, F.P., **Emery, K.O.** and **La Fond, E.C.** (1941) Rip currents a process of geological importance. *J. Geol.*, **49**, 337–369.

Short, A.D. (1985) Rip-current type, spacing and persistence, Narrabeen Beach, Australia. *Mar. Geol.*, **65**, 47–71.

Short, A. (1991) Macro-meso tidal beach morphodynamics: an overview. *J. Coastal Res.*, **7**, 417–436.

Smith, A. (1997) Estimates of the Earth's spin (geographic) axis relative to Gondwana from glacial sediments and paleomagnetism. *Earth-Sci. Rev.*, **42**, 161–179.

Torsvik, T.H. and **Cocks, L.R.M.** (2013) Gondwana from top to base in space and time. *Gondwana Res.*, **24**, 999–1030.

Vakarelov, B.K., **Ainsworth, R.B.** and **MacEachern, J.A.** (2012) Recognition of wave-dominated, tide-influenced shoreline systems in the rock record: variations from a microtidal shoreline model. *Sed. Geol.*, **279**, 23–41.

Van Roy, P., **Orr, P.J.**, **Botting, J.P.**, **Muir, L.A.**, **Vinther, J.**, **Lefebvre, B.**, **El Hariri, K.** and **Briggs, D.E.** (2010) Ordovician faunas of Burgess Shale type. *Nature*, **465**, 215–218.

Van Roy, P., **Briggs, D.E.G.** and **Gaines, R.R.** (2015) The Fezouata fossils of Morocco; an extraordinary record of marine life in the Early Ordovician. *J. Geol. Soc.*, **172**5, 541–549.

Van Wagoner, J.C. (1995) Overview of sequence stratigraphy of foreland basin deposits: Terminology, summary of papers, and glossary of sequence stratigraphy. In: *Sequence Stratigraphy of Foreland Basin Deposits* (Ed. J. C. Van Wagoner and G. T. Bertman), Am. Assoc. Petrol. Geol. Mem., Tulsa, OK, USA, **64**, 137–223

Vaucher, R., **Martin, E.L.O.**, **Hormière, H.** and **Pittet, B.** (2016) A genetic link between *Konzentrat-* and *Konservat-Lagerstätten* in the Fezouata Shale (Lower Ordovician, Morocco). *Palaeogeogr. Palaeoclimatol. Palaeoecol.*, **460**, 24–34.

Veevers, J. (2005) Edge tectonics (trench rollback, terrane export) of Gondwanaland-Pangea synchronized by supercontinental heat. *Gondwana Res.*, **8**, 449–456.

Walther, J. (1894) *Einleitung in die Geologicals Historische Wissenschaft, Bd 3, Lithogenesis der Gegenwart*. Fischerverlag, Jena, pp. 535–1055. .

Williams, I., **Goodge, J.**, **Myrow, P.**, **Burke, K.** and **Kraus, J**. (2002) *Large-scale Sediment Dispersal Associated with the Late Neoproterozoic Assembly of Gondwana*. 16th Australian Geological Convention Adelaide, Australia, **67**, 238.

Yang, B.C. and **Chun, S.S.** (2001) A seasonal model of surface sedimentation on the Baeksu open-coast intertidal flat, southwestern coast of Korea. *Geosci. J.*, **5**, 251–262.

Yang, B.C., **Dalrymple, R.** and **Chun, S.** (2005) Sedimentation on a wave-dominated, open-coast tidal flat, south-western Korea: summer tidal flat - winter shoreface. *Sedimentology*, **52**, 235–252.

Yang, B.C., **Dalrymple, R.W.** and **Chun, S.** (2006) The significance of hummocky cross-stratification (HCS) wavelengths: evidence from an open-coast tidal flat, South Korea. *J. Sed. Res.*, **76**, 2–8.

Manuscript received 19 October 2015; revision accepted 27 September 2016

III) Corrélations stratigraphiques

Une interprétation en terme de séquences de dépôt est proposée dans cette partie pour les différentes coupes stratigraphiques mentionnées dans l'article précédent. L'identification des séquences est rendue possible par l'application du modèle de faciès proposé par Vaucher et al. (sous presse) (Chapitre II). Les séquences identifiées sont ensuite corrélées entre les coupes étudiées (Fig. 2.1). Afin de fournir la corrélation la plus parcimonieuse, l'interprétation de certaines séquences (en terme d'ordre de séquences) de la figure 10 de l'article précédent (Vaucher et al., sous presse) a été modifiée.

Les séquences élémentaires (sensu Strasser et al., 1999) (E) (environ 2 à 5 m d'épaisseur) correspondent au plus petit cycle identifiable des variations de faciès sédimentaires. Dans la région de Zagora, elles sont le plus souvent constituées de bancs finement lités dont la base silteuse est associée à des structures sédimentaires oscillatoires de petite longueur d'onde (centimétrique à décimétrique). Vers le haut, ces petites séquences passent progressivement à des sables fins formant des bancs plus épais, dans lesquels s'observent des structures sédimentaires oscillatoires de plus grande longueur d'onde (pluri-décimétrique à métrique).

Les petites séquences (S) sont identifiées comme un ensemble de plusieurs séquences élémentaires (généralement 2 à 5). Les petites séquences ont typiquement une épaisseur comprise entre 10 et 20 m. Elles sont formées à la base par des séquences élémentaires à dominance silteuse et au sommet par des séquences élémentaires à dominance gréseuse. Les moyennes séquences (M ; voir aussi *medium scale sequences* Fig. 3 de l'article précèdent) sont formées par 2 ou 3 petites séquences résultant en une épaisseur de 25 à 50 m. Ces dernières sont définies comme étant composées à la base par des petites séquences dominées par des silts et à leur sommet par des petites séquences composées majoritairement par des grès. Enfin, les grandes séquences (L ; voir aussi *large scale sequences* Fig. 3 de l'article précèdent) sont formées généralement de 3 moyennes séquences et ont une épaisseur allant de 75 à 140 m. Les grandes séquences sont composées de moyennes séquences à la base plus silteuses et au sommet plus gréseuses. Chaque coupe stratigraphique a donc été interprétée en terme de séquences élémentaires, petites, moyennes et grandes servant de base aux corrélations des localités étudiées. Sur la base du modèle sédimentaire de dépôt proposé (Fig. 11 de l'article précèdent), les coupes stratigraphiques ont été interprétées en fonction des changements d'environnements de dépôt répondant aux changements relatifs du niveau de la mer. Un exemple d'interprétation est donné dans la figure 10 (Chapitre II ; Vaucher et al., sous presse). La même procédure a été réalisée pour les dix autres coupes stratigraphiques et une corrélation entre elles est proposée (Fig. 2.1) en tenant compte de la hiérarchie des séquences et des changements latéraux des faciès sédimentaires.

La succession sédimentaire de l'Ordovicien inférieur représente environ 15,4 Ma. (Cohen et al., 2013). Cet intervalle sédimentaire est constitué de quatre cycles

transgression-régression à très long terme (voir *large - scale sequences* Fig. 3 ; Vaucher et al., sous presse ; Chapitre II), impliquant une durée moyenne de 3,85 ma par séquence. Par conséquent, ces séquences correspondent à des séquences de 2ème- ou 3ème-ordre sensu Vail et al. (1991). Les formations de Fezouata et de Zini sont subdivisées en vingt-six cycles de changements relatifs à moyen terme du niveau de la mer (M et *medium - scale sequences* Fig. 3 ; Vaucher et al., sous presse ; Chapitre II). Avec une durée moyenne d'environ 592 ka (Fig. 3 ; Vaucher et al., sous presse ; Chapitre II), elles correspondent probablement à des variations du niveau de la mer du 3ème - 4ème ordre.

L'intervalle étudié en détail des formations supérieures des Fezouata et du Zini se compose de 1 séquence grande (L ; Fig. 1.2), correspondant ainsi à une durée estimée de 3,85 ma, pendant laquelle 3 séquences moyennes (M ; Fig. 2.1) sont déposées. Ainsi, une durée moyenne d'environ 1,28 ma est calculée pour les séquences moyennes qui correspondent probablement à des fluctuations du niveau de la mer du 3ème ordre. Les moyennes séquences sont constituées de 2 à 3 petites (S ; Fig. 2.1) séquences, ce qui leur donne une durée d'environ 604 à 426 ka (séquences de 4ème ordre), éventuellement résultant de cycles de d'excentricité. Les séquences petites regroupent entre 2 et 5 séquences élémentaires (E ; Fig. 2.1), donnant respectivement des durées entre 302 et 85 ka pour les séquences élémentaires (séquences du 4ème - 5ème ordre). Cependant, les séquences élémentaires sont difficiles et parfois impossibles à corréler d'une coupe stratigraphique à l'autre (Fig. 2.1), même à courte distance. Par exemple, entre Nord Douirat Ouest (150 - 168 m) et Nord Douirat Est (63 - 75 m) (Fig. 2.1), séparés par seulement 2 km, la corrélation des séquences élémentaires n'est souvent pas réalisable. Cela suggère des changements de faciès latéraux sur de courtes distances et les corps gréseux qui sont généralement interprétés comme la partie régressive des séquences élémentaires sont discontinus à l'échelle du kilomètre. Par conséquent, les intervalles gréseux sont probablement déposés sous forme de lobes, et les séquences à petite échelle peuvent résulter du déplacement latéral de ces lobes (processus autocyclique ; Cecil, 2003), même si une surimpression par des changements allocycliques du niveau de la mer ne peut pas être exclue. La corrélation des coupes stratigraphiques suggère une orientation du système sédimentaire avec des environnements plus proximaux au Sud-Est et des conditions plus distales dans le Nord-Ouest. L'augmentation générale des sédiments à grains fins (argiles et silts) vers le Nord-Ouest et l'augmentation des sédiments sableux vers le Sud-Est est en accord avec un système dominé par la houle où l'offshore reçoit les sédiments les plus boueux (e.g. Heward, 1981 ; Davis Jr & Hayes, 1984 ; Boyd et al., 1992). La corrélation proposée suggère également une morphologie très plate de la plateforme qui correspond à une rampe siliciclastique à faible angle.

L'organisation sédimentaire d'un système dominé par la houle mais modulé par la marée, tel qu'il est observé dans les formations des Fezouata et du Zini a des implications sur la continuité des unités gréseuses et donc sur la qualité potentielle réservoir d'un tel environnement de dépôt. Dans le cas d'un matériel sédimentaire grossier et homogène

(ex : sable), la porosité et la perméabilité vont être plus importantes en comparaison d'un sédiment très fin (ex : silt-argile) (e.g. Koltermann & Gorelick, 1995 ; Kamann et al., 2007). La corrélation entre les différentes coupes stratigraphiques de ce système sédimentaire dominé par la houle et modulé par la marée met en évidence la très faible extension verticale et latérale des corps gréseux. Ce système présentant une granulométrie très fine (argiles-silts) sur la majeure partie de la succession sédimentaire, les seules couches sédimentaires ayant un potentiel intérêt en terme de capacité réservoir seraient les unités les plus gréseuses, mais ces dernières de par leurs géométries en lobes peu épais et d'extension limitée, en feraient des réservoirs de faible capacité. Par ailleurs, les lobes étant déconnectés les uns des autres, l'extension des unités réservoir serait réduite. Le Faciès F3 (silts à sable fins ; Vaucher et al., sous presse) est constitué de niveaux silto-gréseux amalgamés, mais le dépôt en lobe de ce faciès, avec une épaisseur maximale de 8 m pour une extension horizontale de quelques centaines de mètres, fait de ce faciès des unités réservoir de petite taille. Bien que les faciès sédimentaires constituant la Formation du Zini (F10 et F11 ; Vaucher et al., sous presse) sont exclusivement gréseux et donc d'un intérêt réservoir, cette dernière présente une épaisseur maximale d'une dizaine de mètres. F10 et F11 sont les faciès sédimentaires ayant la plus grande extension géographique (dans la région de Zagora) et même si la Formation du Zini reste discontinue à l'échelle plurikilométrique (Fig. 1.12 ; Chapitre I), cet intervalle sédimentaire a le potentiel le plus important en terme de réservoir. Cependant, il n'en est pas de même pour la Formation du Zini affleurant plus au Sud-Ouest (Fig. 1.12 ; Chapitre I). En effet d'après Destombes et al. (1985), cette formation peut atteindre une épaisseur de plus de 350 m sur plusieurs centaines de kilomètres. D'après les caractéristiques des faciès sédimentaires constituant la Formation du Zini dans la région de Zagora, son équivalent au Sud-Ouest (Fig. 1.12 ; Chapitre I) serait potentiellement d'un plus grand intérêt en terme de réservoir.

Fig. 2.1. *Corrélations des coupes stratigraphies de la partie supérieure de l'Ordovicien inférieur (Formations des Fezouata et du Zini) dans la région de Zagora. Les localités correspondent à celles mentionnées dans la Fig. 1 de Vaucher et al. (sous presse). M : medium scale sequences et L : large scale sequences, se réfèrent à la Fig. 3 de Vaucher et al. (sous presse). Se référer à la version électronique de la thèse pour une meilleure lecture.*

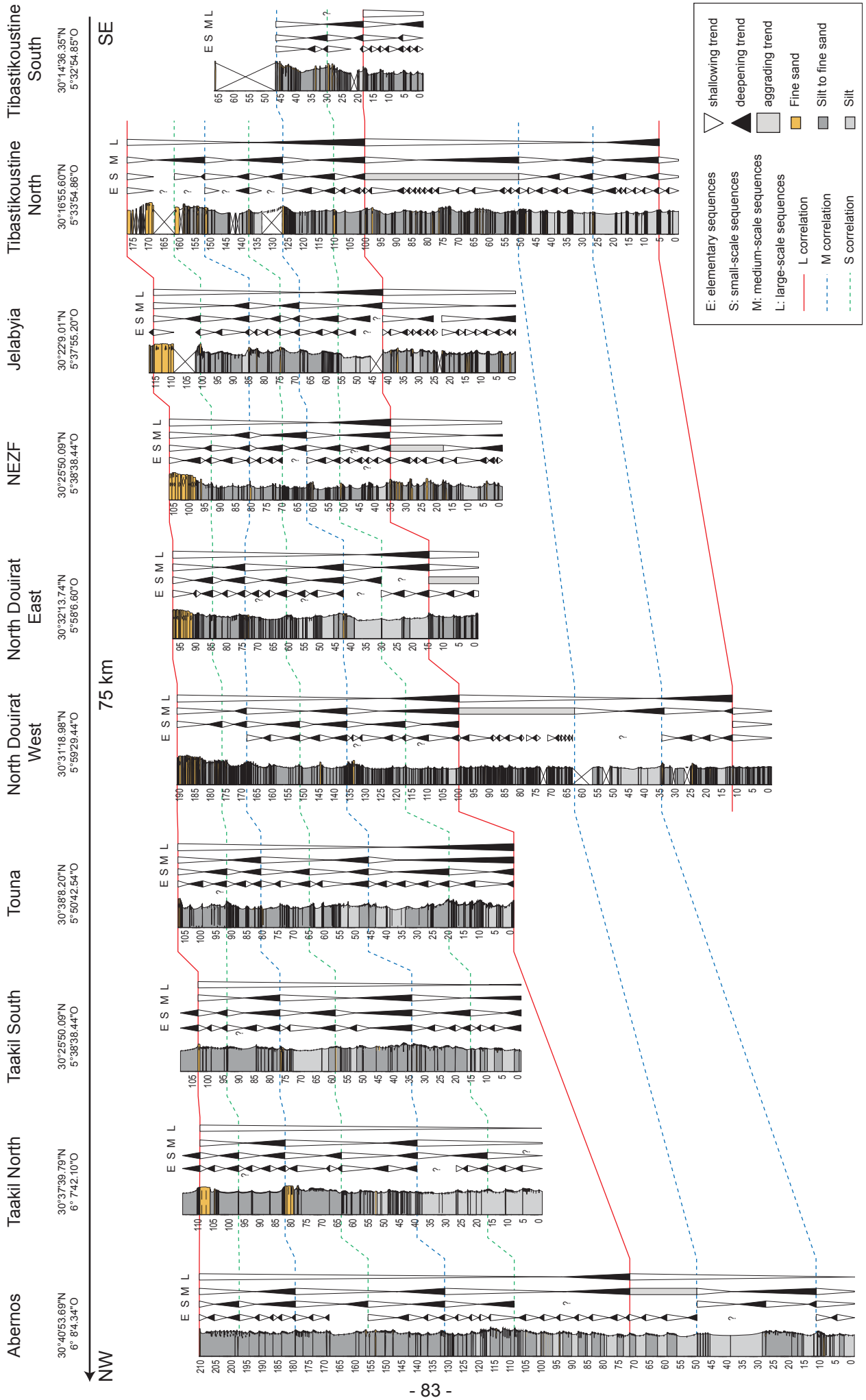
Abemos
30°40'53.69"N
6° 8'4.34"O
Taakil North
30°37'39.79"N
6° 7'42.10"O
Taakil South
30°25'50.09"N
5°38'38.44"O
Touna
30°38'8.20"N
5°50'42.54"O
North Douirat West
30°31'18.98"N
5°59'29.44"O
North Douirat East
30°32'13.74"N
5°58'6.60"O
NEZF
30°25'50.09"N
5°38'38.44"O
Jelabyia
30°22'9.01"N
5°37'55.20"O
Tibastikoustine North
30°16'55.60"N
5°33'54.86"O
Tibastikoustine South
30°14'36.35"N
5°32'54.85"O
NW
SE
75 km
E S M L
E: elementary sequences
S: small-scale sequences
M: medium-scale sequences
L: large-scale sequences
shallowing trend
deepening trend
aggrading trend
Fine sand
Silt to fine sand
Silt
L correlation
M correlation
S correlation

Références

Boyd, R., Dalrymple, R., Zaitlin, B.A., 1992. Classification of clastic coastal depositional environments. Sedimentary Geology, 80(3–4): 139-150.

Cecil, C.B., 2003. The concept of autocyclic and allocyclic controls on sedimentation and stratigraphy, emphasizing the climatic variable. In: C.B. Cecil, T.N. Edgar (Eds.), Climate Controls on Stratigraphy. SEPM Special Publication.

Cohen, K.M., Finney, S.M., Gibbard, P.L., Fan, J.-X., 2013. The ICS International Chronostratigraphic Chart. Episodes, 36, 3, 199-204.

Davis Jr, R.A., Hayes, M.O., 1984. What is a wave-dominated coast? Marine Geology, 60(1–4): 313-329.

Destombes, J., Hollard, H., Willefert, S., 1985. Lower Palaeozoic rocks of Morocco. Lower Palaeozoic rocks of the world, 4: 157-184.

Heward, A.P., 1981. A review of wave-dominated clastic shoreline deposits. Earth-Science Reviews, 17(3): 223-276.

Kamann, P.J., Ritzi, R.W., Dominic, D.F., Conrad, C.M., 2007. Porosity and Permeability in Sediment Mixtures. Groundwater, 45(4): 429-438.

Koltermann, C.E., Gorelick, S.M., 1995. Fractional packing model for hydraulic conductivity derived from sediment mixtures. Water Resources Research, 31(12): 3283-3297.

Strasser, A., Pittet, B., Hillgärtner, H., Pasquier, J.-B., 1999. Depositional sequences in shallow carbonate-dominated sedimentary systems: concepts for a high-resolution analysis. Sedimentary Geology, 128(3–4): 201-221.

Vail, P.R., Audemard, F., Bowman, S.A., Eisner, P.N., Perez- Cruz, C., 1991. The stratigraphic signatures of tectonics, eustasy and sedimentology — an overview. In: G. Einsele, W. Ricken, A. Seilacher (Eds.), Cycles and Events in Stratigraphy. Springer, Berlin, pp. 617–659.

Vaucher, R., Pittet, B., Hormière, H., Martin, E.L.O., Lefebvre, B., sous presse. A wave-dominated, tide-modulated model for the Lower Ordovician of the Anti-Atlas, Morocco. Sedimentology.

Chapitre III :

Origine des Konzentrat- et des Konservat-Lagerstätten de la Formation des Fezouata

«Aucun organisme complètement mou ne peut se conserver»

Charles Darwin

I) Résumé :

Dans la partie centrale de l'Anti-Atlas (Maroc, région de Zagora), la Formation des Fezouata a livré des gisements fossilifères à préservation exceptionnelle (*Lagerstätten*) correspondant aux étapes initiales de la Grande Biodiversification Ordovicienne. Ces *Lagerstätten* contiennent des fossiles remarquables à la fois par leur abondance et leur qualité de conservation. Bien que la préservation exceptionnelle des organismes à corps mous se limite à quelques intervalles stratigraphiques dans la Formation des Fezouata, d'autres niveaux fossilifères ne contenant que des bioclastes sont aussi présents. Replacés dans un modèle sédimentaire de dépôt préalablement établi (*cf*. Chapitre II), les fossiles à préservation exceptionnelle ont été interprétés comme des assemblages autochtones enfouis par des dépôts de tempête, à proximité de la limite d'action des vagues de tempête. Dans cette zone, la composante courant de tempête est réduite par rapport aux environnements proximaux. Ainsi, une oscillation faible, mais dominante, est enregistrée comme en témoignent les rides d'oscillations associées à ces dépôts. En revanche, les accumulations bioclastiques ont été préservées dans des environnements plus proximaux (mais toujours en dessous de la zone d'action des vagues de beau temps). Dans ce contexte plus proximal marqué par des structures oscillatoires de grande longueur d'onde qui suggèrent une forte houle, l'action des courants de retour de tempête est également forte, comme le suggère la désarticulation des bioclastes. On retrouve ces bioclastes dans des dépôts gréseux lenticulaires de quelques dizaines de centimètres d'épaisseur et de quelques mètres de largeur et de longueur. Ce type de dépôt lenticulaire présente généralement une base érosive et un sommet convexe, ce qui lui confère un aspect en lobe ou en lobe-chenal (si la base érosive est présente). Une grande quantité de sédiment est ainsi déposée rapidement, ce qui est à l'origine de l'enfouissement rapide très localisé du matériel allochtone sur le fond marin.

A partir d'observations sédimentologiques et paléontologiques, les intervalles contenant des fossiles à préservation exceptionnelle sont donc interprétés comme des *Konservat-Lagerstätten* (KsL), tandis que les accumulations bioclastiques sont considérées comme des *Konzentrat-Lagerstätten* (KzL). Ainsi, les assemblages fauniques enregistrés dans les KsL sont interprétés comme de potentielles biocénoses, dans lesquelles les organismes ont subi un enfouissement rapide par des tempestites distales. D'un autre côté, les assemblages contenus dans les KzL seraient plus susceptibles de correspondre à des thanatocénoses, dans lesquelles les organismes auraient été transportés par le courant de retour des tempêtes. Dans ce chapitre, une origine commune pour la formation des KsL et des KzL est mise en avant. Ces deux types de *Lagerstätten* sont tous deux liés à l'action des tempêtes, mais sont formés à des profondeurs différentes.

II) Article :

A genetic link between Konzentrat- and Konservat-Lagerstätten in the Fezouata Shale (Lower Ordovician, Morocco)

Auteurs : **Romain Vaucher**, Emmanuel L.O. Martin, Hélène Hormière, Bernard Pittet

Article publié dans *Palaeogeography, Palaeoclimatology, Palaeoecology*

Année : 2016 Volume : 460 Pages : 24 - 34

DOI : http://dx.doi.org/10.1016/j.palaeo.2016.05.020

Palaeogeography, Palaeoclimatology, Palaeoecology 460 (2016) 24–34

Contents lists available at ScienceDirect

Palaeogeography, Palaeoclimatology, Palaeoecology

journal homepage: www.elsevier.com/locate/palaeo

A genetic link between *Konzentrat-* and *Konservat-Lagerstätten* in the Fezouata Shale (Lower Ordovician, Morocco)

Romain Vaucher *, Emmanuel L.O. Martin, Hélène Hormière, Bernard Pittet

Univ Lyon, Université Claude Bernard Lyon 1, ENS de Lyon, CNRS, UMR 5276 LGL-TPE, F-69622 Villeurbanne, France

ARTICLE INFO

Article history:
Received 22 July 2015
Received in revised form 13 May 2016
Accepted 19 May 2016
Available online 20 May 2016

Keywords:
Lagerstätte
Storm deposits
Sandstone lenses
Fezouata Biota
Lower Ordovician

ABSTRACT

In the central Anti-Atlas (Morocco; Zagora region), the Fezouata Shale has yielded an extraordinary fossil *Lagerstätte* documenting the initial stages of the Great Ordovician Biodiversification Event. This *Lagerstätte* contains abundant and exceptionally well-preserved fossils (EPF) exhibiting soft-bodied preservation as well as "hard", mineralized parts of extinct organisms. While soft-bodied preservation in the Fezouata Shale is confined to a few stratigraphic intervals, other fossiliferous intervals contain only shelly fossils in sandstone lenses (SL). Placed in the context of a previously established depositional model, EPF are interpreted as autochthonous assemblages buried by storm deposits, close to storm wave-base. There, the current component of storms is reduced compared to proximal settings and weak oscillation is dominant resulting in the record of oscillation ripples. In contrast, bioclastic accumulations were generated upslope in shallower, more proximal lower shoreface environments. There, the current component of storms was significant, as suggested by the disarticulation of skeletal remains. Bioclastic materials are localized in SL, which are lenses a few tens of centimeters in thickness and a few meters in width and length. These lenses commonly display erosive bases and convex tops, resulting in a lobate or a channel-lobe morphology. A large amount of sediment was thus rapidly deposited, resulting in the rapid burial of allochthonous material across a strongly localized surface of the sea floor.
Integrating both sedimentological and paleontological evidence, intervals yielding EPF are considered as *Konservat-Lagerstätten* (KsL), in contrast with bioclastic accumulations defined as *Konzentrat-Lagerstätten* (KzL). Thus, KsL assemblages are interpreted to approximate biocenoses, in which organisms experienced rapid burial by distal tempestites, while KzL assemblages more likely correspond to thanatocenoses, locally deposited by storm back-currents. Here, a genetic link between KsL and KzL is suggested within the Fezouata Shale. Both types of *Lagerstätten* were related to storm activity, but at different depths.

1. Introduction

The Great Ordovician Biodiversification Event (GOBE) is one of the most important radiations of the Phanerozoic Eon. The GOBE began some 35 million years after the Cambrian Explosion, during the Early Ordovician (ca. 485.4–470 Ma; Bambach et al., 2004; Servais et al., 2008, 2010) and is characterized by an exponential diversification of classes within phyla that appeared during the Cambrian (e.g. Harper, 2006; Servais et al., 2008, 2010). Paleontologists have recognized a major gap in the record of soft-bodied faunas spanning the late Cambrian (Furongian) to the Middle Ordovician (Darriwilian). Middle to Late Ordovician *Konservat-Lagerstätten* are rare and post-date the initial stages of the GOBE (e.g., Briggs et al., 1991; Liu et al., 2006; Aldridge et al., 2007; Young et al., 2007; Botting et al., 2011). The recent discovery of a late Tremadocian *Konservat-Lagerstätte* in Morocco (Zagora region; Van Roy et al., 2010, 2015a, 2015b; Martin et al., 2014, in press) in the lower part of the Fezouata Shale (Martin et al., in press) (Fig. 1A) is thus of prime importance for understanding the rise of animal life (Van Roy et al., 2010). According to Van Roy et al. (2015a), these fossils may display characteristics of Burgess Shale-type (BST) preservation, as also suggested by more recent findings (Marti Mus, 2016–in this issue). If so, their preservation resulted from a combination of favorable sedimentary conditions: rapid burial in fine-grained sediment, early inhibition of microbial activity, low concentrations in both sulfate (in the global ocean) and oxygen (in the bottom waters) (Gaines et al., 2012). However, a second type of *Lagerstätte* also occurs in the Fezouata Shale, represented by massive bioclastic accumulations in dm-thick layers (*Konzentrat-Lagerstätte*).

The aim of this paper is to present the sedimentological field analyses performed in the Lower Ordovician deposits of the Zagora area in order to illustrate that the sedimentological processes involved in the

* Corresponding author.
E-mail addresses: romain.vaucher@univ-lyon1.fr (R. Vaucher), emmanuel.martin@univ-lyon1.fr (E.L.O. Martin), helene.hormiere@ens-lyon.fr (H. Hormière), bernard.pittet@univ-lyon1.fr (B. Pittet).

http://dx.doi.org/10.1016/j.palaeo.2016.05.020
0031-0182/

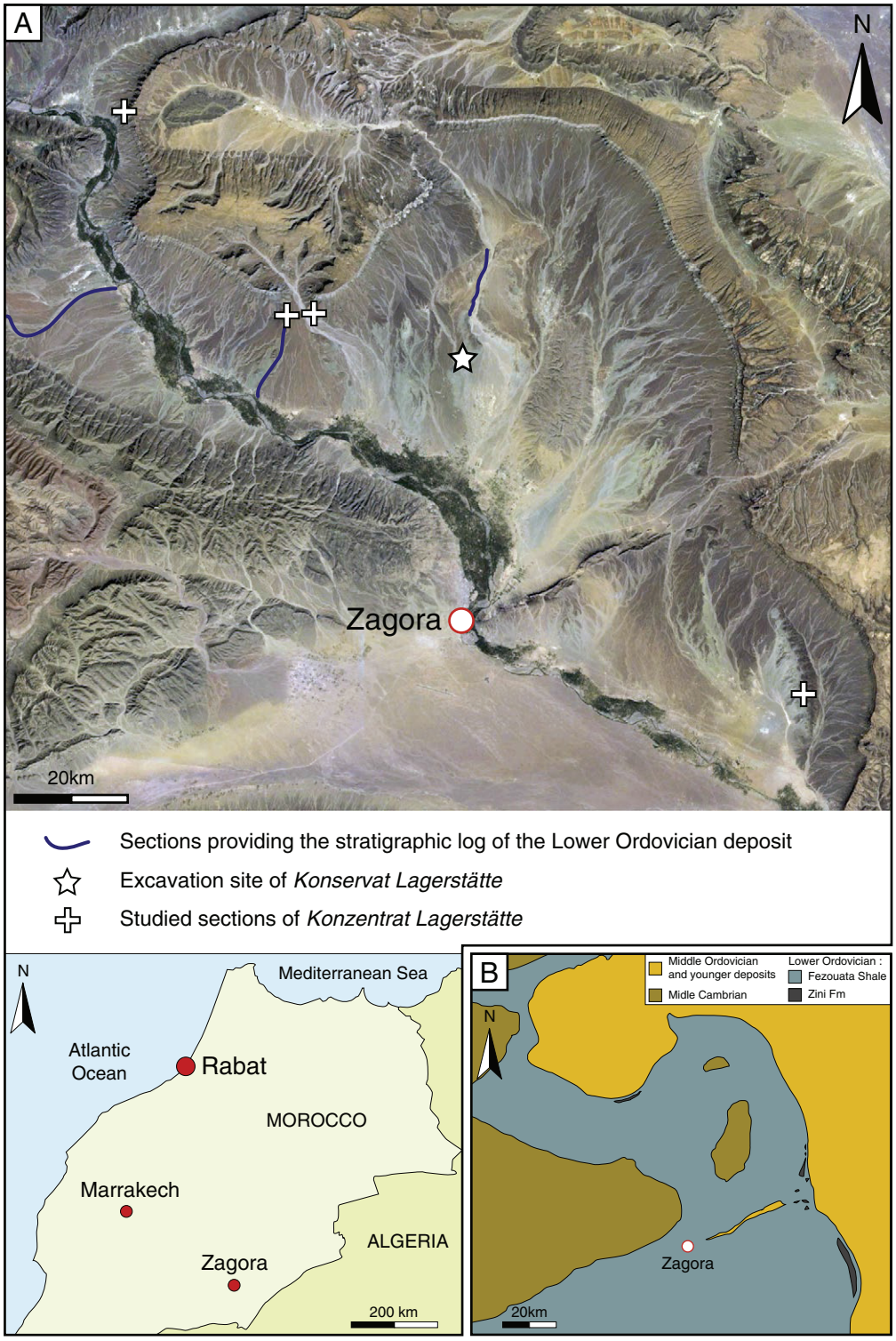

Fig. 1. (A) Satellite image (Google Earth) of the study area. (B) Geological map of the Zagora area modified from Destombes (1989).

formation of these two types of *Lagerstätten* are part of the same depositional system. Both are associated with different water depths in a storm-dominated sedimentary environment.

2. Geological setting

By the end of the Precambrian, the Pan-African Orogeny had resulted in the formation of Gondwana. This supercontinent was located in the southern hemisphere and extended from the South Pole to the Equator. Oceanic expansion during the Cambrian led to the rise of mean sea level, thus creating shallow epicontinental seas on the Gondwanan margins (Destombes et al., 1985; Fabre, 1988; Boote et al., 1998; Carr, 2002; Coward and Ries, 2003) and a long-term transgression took place at the beginning of the Ordovician (Meyers and Peters, 2011).

At the end of the Cambrian, the initiation of a rifting phase in the western part of Gondwana resulted in the northward drift of Avalonia and the opening of the Rheic Ocean (Cocks and Torsvik, 2004). The entire Lower Ordovician succession of Morocco was deposited on the

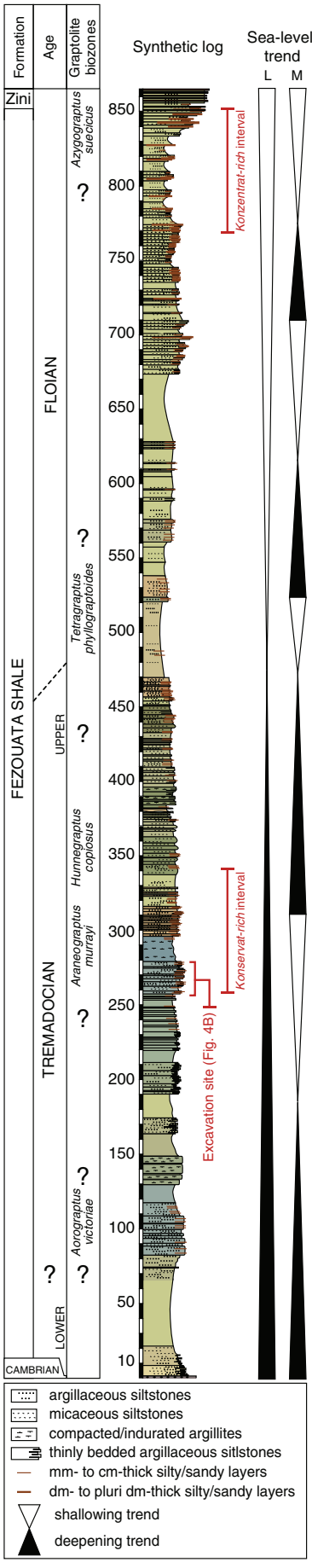

rifted margin of Gondwana (Cocks and Torsvik, 2004), and is now well-exposed in the central part of the Anti-Atlas Mountains of Morocco (Fig. 1B). Lower Ordovician deposits exhibit a wide geographic distribution of ca. 800 km from Tan-Tan to Erfoud (Destombes et al., 1985). In the Zagora region, the Fezouata Shale (Tremadocian to Floian in age) consists of ca. 900 m (Fig. 2) of quartz-rich siltstones locally overlain by massive black sandstones characteristic of the Zini Formation (late Floian) (Destombes, 1962; Martin et al., in press). Recently, the Lower Ordovician succession was interpreted to have been deposited in a storm-wave dominated sedimentary environment (Martin et al., in press; Fig. 3), but modulated by tides (see Vaucher and Pittet, 2014; Vaucher et al., 2015, submitted for publication). Tidal action is indirectly recorded in both the Fezouata Shale and the Zini Formation by the modification of storm-wave generated structures during their geneses. However no strictly tidally generated structures are present.

3. Material and methods

In January 2014, a large palaeontological excavation campaign was organized in the late Tremadocian series (*Araneograptus murrayi* graptolite Zone, Martin et al., in press; Gutiérrez-Marco and Martin, 2016–in this issue; *messaoudensis-trifidum* acritarch assemblages, Nowak et al., 2016–in this issue) of the Zagora area. The aim of this campaign was to collect in situ assemblages of exceptionally preserved fossils typical of the Lower Ordovician Fezouata Biota, which occur abundantly within several discrete horizons (Van Roy et al., 2010, 2015a, 2015b; Martin et al., in press). The excavation site is located on a hillside (Bou Izargane) covering an area of ca. 2000 m^2 (Fig. 4A). Twenty-two excavations were conducted, and all known levels yielding EPF were incorporated into a detailed stratigraphic log. Elsewhere in the Zagora area, a second type of fossiliferous horizon, which occurs only in the upper part of the Fezouata Shale, was also investigated: 77 sandstone lenses containing mm- to dm-thick bioclastic lags were analyzed from four distinct Lower Ordovician (Floian) sections (Figs. 1–2). Sandstone lenses were classified according to their bioclastic content (amount, clast size and thickness of bioclastic layers). The two types of fossil-rich intervals (with and without exceptional preservation of soft tissues) encountered in the Fezouata Shale (Figs. 1–2) were subjected to sedimentological analyses in the field, and their lithology, grain size, sedimentary structures and bed geometries were described.

4. Results and interpretations

4.1. Levels with soft-tissue preservation

4.1.1. Description

Bou Izargane, a 20-m high hill (Fig. 4A) yielding exceptionally well-preserved fossils (EPF; Van Roy et al., 2010, 2015a, 2015b; Martin et al., in press), consists of deposits of late Tremadocian age (Fig. 4B; *A. murrayi* biozone, Martin et al., in press; Gutiérrez-Marco and Martin, 2016–in this issue; *messaoudensis-trifidum* acritarchs assemblages, Nowak et al., 2016–in this issue). The sedimentary succession (Figs. 2–4A) is characterized by two alternating facies associations. The first one (FA1) is dominated by argillaceous siltstones and thin (mm-thick) claystones with sparse intercalations of siltstones (mm-thick). Argillaceous siltstones and siltstones display symmetrical cross-laminations of cm-scale wavelength (Fig. 3C) and claystones are devoid of sedimentary structures. The second facies association (FA2) consists of very fine sands that display hummocky cross-stratification (HCS) with dm-scale wavelength (Fig. 4C). The sandy layers (cm-thick) are commonly made of three parts (Fig. 4D): (1) a poorly sorted base displaying

Fig. 2. Composite stratigraphic section of Lower Ordovician deposits in the Zagora area. Fossil rich-intervals are shown; interpretation on sea level trends, L: long-term relative sea level; M: medium-term relative sea level; graptolite biozonation from Gutiérrez-Marco and Martin (2016–in this issue).

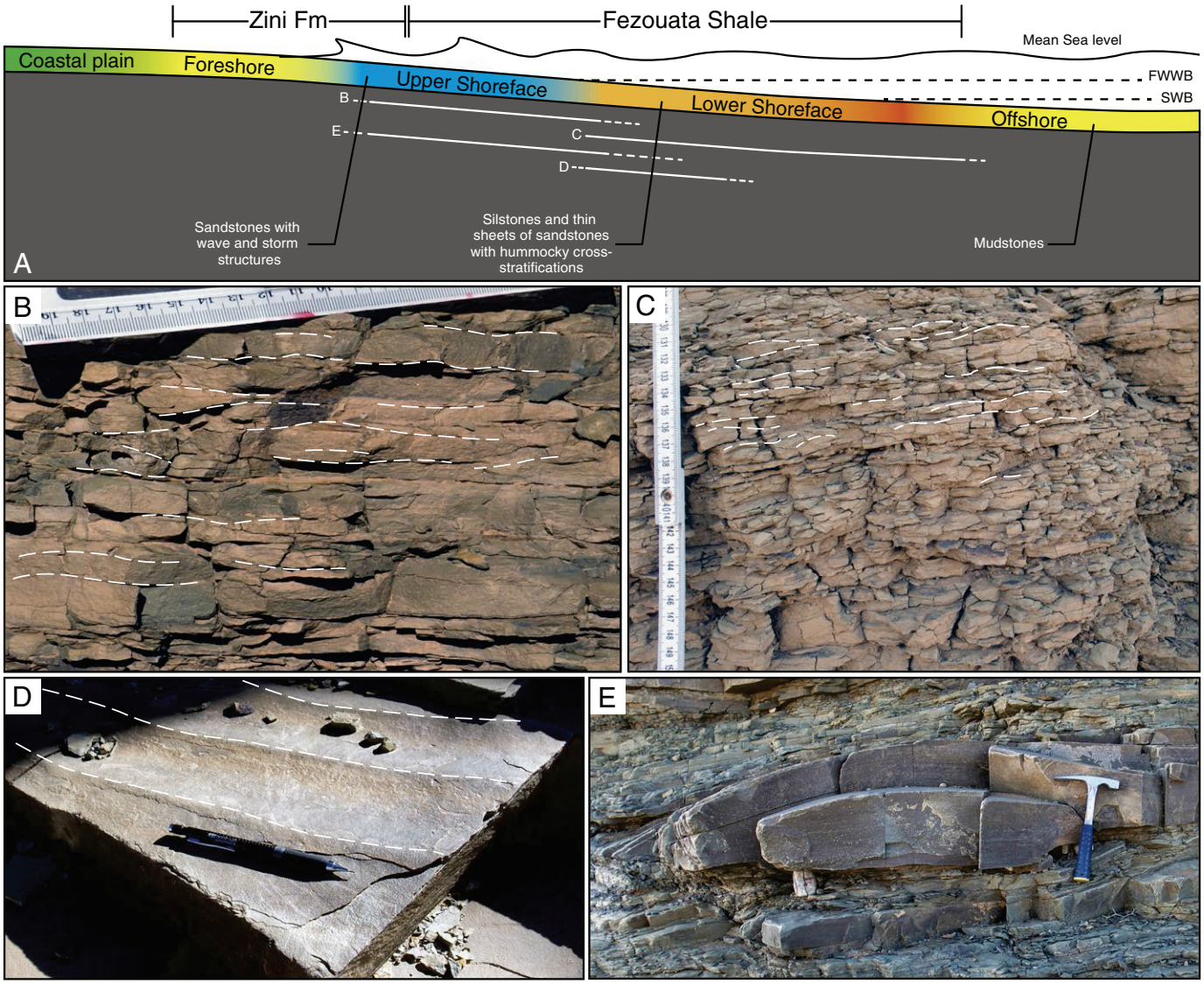

Fig. 3. (A) Simplified palaeoenvironmental reconstitution of the Fezouata Shale and the Zini Formation (modified from Martin et al., in press). Overview of sedimentary background and structures displayed in the Fezouata Shale. (B) Coarse siltstones consist of the sedimentary background in proximal lower shoreface environments that display wave-formed structures of dm-scale of wavelength. (C) Argillaceous siltstones dominated sedimentary background in the distal lower environments, which exhibit wave-formed structures of cm-scale of wavelength. (D) 2D symmetrical wave ripples and (E) accretionary HCS occurring in the proximal lower shoreface environments.

upward fining from coarse to fine sands (in Fig. 4D orange dots are iron-stained ooids); (2) an intermediate part with mostly plane parallel lamination, with a base comprised of fine-grained quartz sand; and (3) an upper part displaying small-scale HCS of dm-scale wavelength consisting of fine-grained sandstones to siltstones. The sandy deposits of FA2 are discontinuous at the meter- to decimeter-scale, with an overall flattened lobe shape. The 22 excavations containing EPF were incorporated onto a detailed stratigraphic log (Fig. 4B). In the Bou Izargane section, EPF consistently occur in the three intervals (from bottom to top, ca 1.5, 3 and 3.5 m thick respectively), which show a more important quantity and thicker sandy layers (cm-scale thick) of FA2 (Fig. 4B). Fossils are commonly disarticulated without exceptional preservation (Fig. 4E), but sometimes preserved as EPF (Fig. 4F). In these three intervals, the distribution of EPF is not random: they consistently occur at the top of the finest grained thin layers (claystones or argillaceous siltstones) of FA1 (Fig. 4G), and immediately below the coarser-grained sandy layers of FA2.

4.1.2. Interpretation

The succession of sedimentary structures in the sandy layers in FA2 from Part 1 (bottom) to Part 3 (top) can be interpreted as a distal storm sequence deposited under a wax and wane flow close to the storm wave base (SWB) (e.g. Harms, 1979; Brenchley and Newall, 1982; Dott and Bourgeois, 1982; Aigner, 1985; Duke, 1985; Duke et al., 1991). Part 1 corresponds to the basal part of a storm sequence deposited during the waxing phase of the storm flow. The transition to Part 2 suggests a decreasing flow velocity (waning flow). However, plane parallel laminae indicate that flow velocity was still high. The presence of HCS indicates that the deposition of Part 3 resulted from a mechanism mainly controlled by oscillation and thus suggests a decrease of the current component during waning flow (plane parallel bedding evolving into oscillatory structures). The laterally discontinuous aspect of storm deposits and their general flattened lobe-shaped morphology both indicate very localized deposition of the sandy layers. The background sedimentation (FA1) is dominated by argillaceous siltstones to siltstones, probably resulting from the gravitational settling of fine-grained particles of continental origin. FA1 displays symmetrical cross-laminations of small wavelength (cm-scale) (Fig. 3C). This indicates oscillation processes (e.g. Nichols, 2009) at the sea-floor during low-intensity storm conditions due to the collapse of storm orbits on the sea-floor (Allen, 1997) during and/or after deposition. The alternations of argillaceous siltstones (with rare claystones) dominated intervals (FA1) and

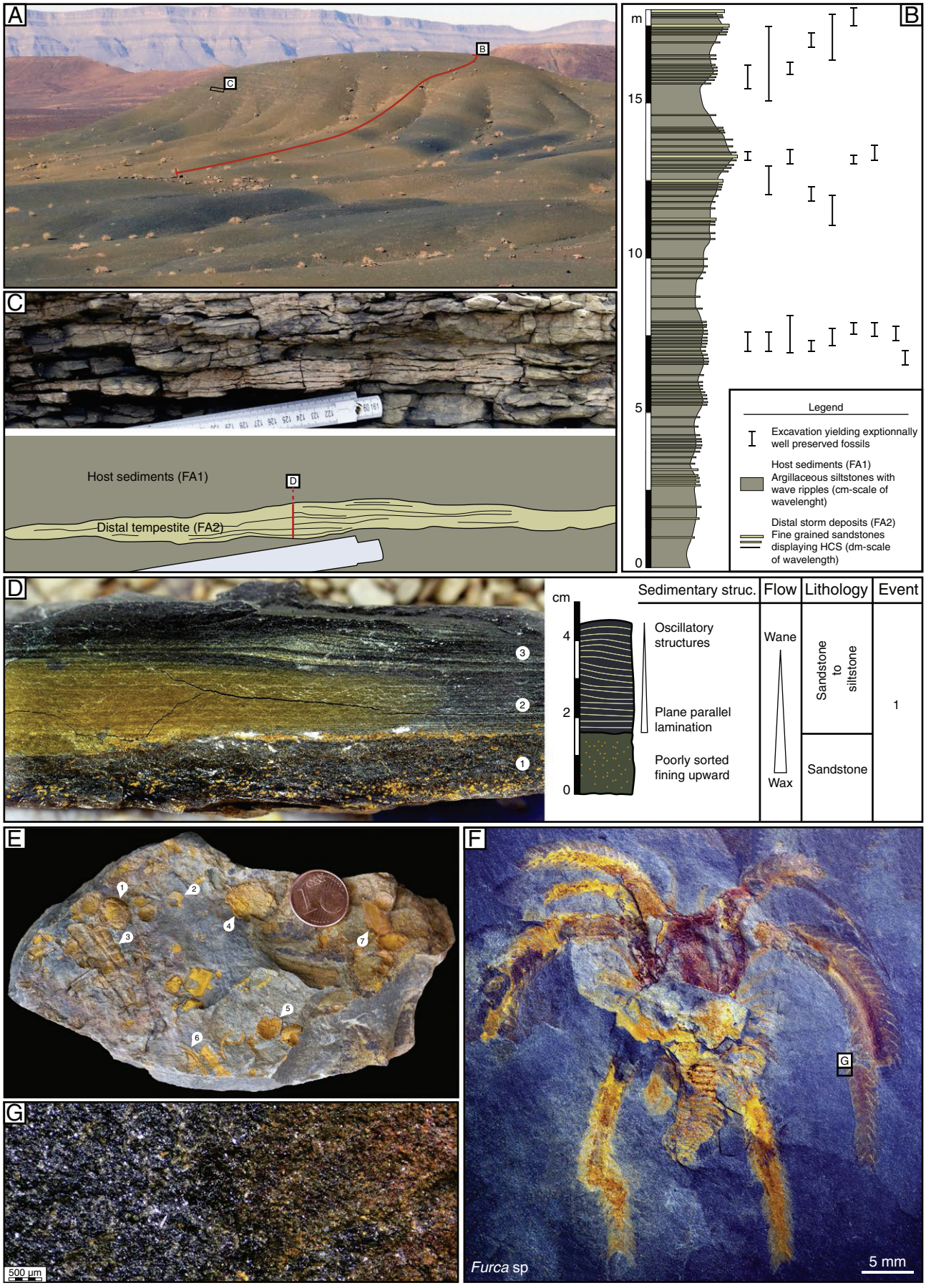
A
B
C
C
Host sediments (FA1)
D
Distal tempestite (FA2)
B
m
15
10
5
0
Legend
Excavation yielding exptionnally well preserved fossils
Host sediments (FA1) Argillaceous siltstones with wave ripples (cm-scale of wavelenght)
Distal storm deposits (FA2) Fine grained sandstones displaying HCS (dm-scale of wavelength)
D
3
2
1
cm
4
2
0
Sedimentary struc.
Oscillatory structures
Plane parallel lamination
Poorly sorted fining upward
Flow
Wane
Wax
Lithology
Sandstone to siltstone
Sandstone
Event
1
E
1
2
3
4
5
6
7
F
G
Furca sp
5 mm
G
500 µm

sandstones (FA2), suggest a depositional setting that lays below the fair weather wave base (FWWB) and above SWB (e.g. Davies, 1964; Bluck, 1967; Goldring and Bridges, 1973; Dumas and Arnott, 2006; Plint, 2010), and corresponds to lower shoreface environments (Fig. 3A) (sensu McLane, 1995).

4.2. Shell beds

4.2.1. Description

Shell accumulations primarily occur in the upper part of the Fezouata Shale (Fig. 2). Bioclastic material occurs as layers (from mm- to dm-thick) inside sandstone lenses (SL) (Fig. 5A). SL have a lobate or a channel-lobe morphology (concave erosive base and lobate top), ranging in width from 55 cm to 9 m (average of 3 m) and in thickness from 15 cm to 1 m (average 50 cm). Bioclastic layers uniformly occur within the thickest intervals of the SL, which is also the most indurated zone. SL are interstratified in coarse siltstones displaying symmetrical cross-laminations (dm-scale wavelength) (Fig. 3B–D) as well as HCS (Fig. 3E). SL are a stack of units (8 maximum), each consisting of three distinct parts (Fig. 5B): (1) a basal part formed of a bioclastic lag without obvious sedimentary structures; (2) an intermediate part consisting of fine- to medium-grained sandstones with plane parallel laminae; and (3) an upper part consisting of fine- to medium-grained sandstones showing accretionary or scour-and-drape HCS of decimeters- to meter-scale wavelength. Each unit is separated from the other by an erosion surface (Fig. 5B). Since SL are composed by several units, the bioclastic part may occur at different positions throughout the SL. Commonly, the bioclastic part is present at the base or in the center of the SL, whereas it is rarely observed in the upper unit of the SL. The bioclasts are unsorted and no soft tissues are preserved (Fig. 5C–D). Gastropods, brachiopods, bivalves and fragments of trilobites form the main component of the fauna in the bioclastic parts. SL have been classified according to the relative amount of bioclasts and to the thickness of the bioclastic layers. Three types of SL are distinguished: dm-thick bioclastic layer (SL1); cm-to pluri-cm thick bioclastic layers (SL2); and isolated bioclasts or mm-thick lags (SL3).

4.2.2. Interpretation

On the basis of the sedimentary structures (and their dimensions) and associated grain-size, each complete unit (consisting of three identified parts) of the SL can be interpreted as the typical sequence of a storm event in a lower shoreface environment (e.g. Allen, 1970; Komar and Miller, 1975; Harms, 1979; Kreisa, 1981; Brenchley and Newall, 1982; Dott and Bourgeois, 1982; Kreisa and Bambach, 1982; Aigner, 1985; Duke et al., 1991). Their basal bioclastic part was likely deposited during storm peak, which corresponds to the waxing flow (Kreisa and Bambach, 1982; Aigner, 1985). The transition to finer sediments in Part 2 suggests decreasing, but still rapid flow of the storm back current (start of the waning phase during the storm). Part 3 corresponds to the end of the storm event, when oscillatory flow overcomes back-current flow to generate oscillatory structures. SL formed by up to 8 units therefore correspond to the stack of successive storm events, or alternatively, as hypothesized by Vaucher et al. (submitted for publication) to the modulation of storm intensity by tides, each unit corresponding to one tide cycle and SL to single storm events. SL are interstratified in a host sediment which consists of coarse siltstones displaying symmetrical cross-laminations and HCS pointing out oscillatory processes (waves and storms) (e.g. Nichols, 2009). SL1 is associated with wave ripples of dm-scale of wavelength (Fig. 3D) and HCS of m-scale wavelength (Fig. 3E); SL2 is found with wave ripples of dm-scale of wavelength and HCS of multi dm-scale wavelength; and SL3 is observed with wave ripples of cm- to dm-scale wavelength with HCS of dm-scale wavelength. Environmental conditions necessary to produce the SL were clearly shallower than those associated with the formation of EPF levels. The wavelengths of both HCS in storm sequences and wave ripples in the host sediment are longer than in EPF layers, due to the stronger interaction of the wave orbits on the seafloor (Heward, 1981; Davis and Hayes, 1984; Boyd et al., 1992; Yang et al., 2006; Plint, 2010). The decrease in bioclastic content within the SL, as well as the decrease in wavelength of oscillatory structures in both the host sediment and the SL suggest a decreasing impact of the storms related to the increase of the water depth (e.g. Aigner, 1985). This implies that SL1 formed more proximally in the lower shoreface than SL2, while SL3 occurred in the distal part of the lower shoreface (Fig. 3A).

5. Discussion

Originally, the term "*Lagerstätte*" (plural *Lagerstätten*) comes from mining terminology used to describe a rock of economic interest (Seilacher, 1990). Applied to paleontology, this term describes stratigraphic units containing exceptionally well-preserved or remarkably abundant fossils (Seilacher, 1970; Allison, 1988a). Commonly, two types of *Lagerstätten* are distinguished: one related to the exceptional preservation of the fossils, and one to their concentration (e.g. Seilacher et al., 1985; Seilacher, 1990; Speyer and Brett, 1991; Briggs, 2007). Sedimentary rocks yielding soft-bodied fossils are conservation deposits, so called *Konservat-Lagerstätten* (sensu Seilacher, 1970). In this case, not only the hard parts but also the soft tissues can be preserved. This unusual preservation of soft tissues is related to a combination of favorable depositional, environmental and/or early diagenetic conditions for the preservation or mineral replication of soft tissue (e.g. Froelich et al., 1979; Allison, 1988b; Briggs and Kear, 1994; Allison and Brett, 1995; Butterfield, 1995; Gaines et al., 2005). On the other hand, sediments with a high fossil abundance are concentration deposits, which are referred as *Konzentrat-Lagerstätte* (sensu Seilacher, 1970). These two types of *Lagerstätten* are considered as end-members of a spectrum of preservation (Allison and Briggs, 1991a, 1991b). This study highlights two different types of fossil occurrences in the Lower Ordovician Fezouata Shale of Morocco: EPF and shell beds. According to the above-mentioned definitions, EPF horizons correspond to a *Konservat-Lagerstätte* (KsL) in which the quality of the fossil preservation is abnormally good, and shell beds to a *Konzentrat-Lagerstätte* (KzL), which is characterized by a large quantity of articulated and/or fragmented skeletal remains.

In the Fezouata Shale (Fig. 2), these two types of fossil-rich intervals are linked to storm deposits (Figs. 4–5). In the Zagora area, late Tremadocian EPF are never observed within the claystones and argillaceous siltstone layers corresponding to the background sedimentation (FA1). Their distribution is apparently restricted to the top of these units, immediately below the coarser sediments (FA2) deposited during the waxing phase of storms. Similarly, the shelly layers of SL were formed during the waxing phase of storms. Shell accumulation in SL corresponds to the basal part of the storm sequence, when the velocity is maximum and leads to the deposition of the unsorted coarser

Fig. 4. (A) Hillock of the excavation site (location red star Fig. 1). (B) Detailed section of the excavation site. The different excavation holes yielding exceptionally preserved specimens of the Fezouata Biota are placed along the log. All fossils were found in 3 distinct levels dominated by fine sandy sandstone (from bottom to top, ca 1.5, 3 and 3.5 m thick respectively). (C) Distal tempestite on the outcrop yielding exceptionally well preserved fossils; host sediments: siltstones displaying wave ripples with a cm-scale wavelength; distal tempestite: fine-grained sandstones displaying small HCS with dm-scale wavelength. (D) Section of a distal storm deposit and detailed section showing a waxing-and-waning flow deposit; 1: waxing phase; 2–3: waning phase. (E) Biomineralized fossil accumulations from interval yielding EPF; 1: bivalve; 2: *Ranorthis* sp. (brachiopod); 3: *Cavernolites* sp. (hyolithid); 4 & 5: undetermined brachiopod; 6: Librigena of trilobite with a genal spine 7: Cephalic doublure of a large asaphid trilobite (F) *Furca* sp. (marrellomorph arthropod; AA-BIZ31-OI-39, collections of the Cadi Ayyad University, Marrakech; modified from Martin et al., in press). (G) Orange part of the picture corresponds to a spine of *Furca* sp.; the exceptional preservation of soft tissues occurs in argillaceous siltstones.

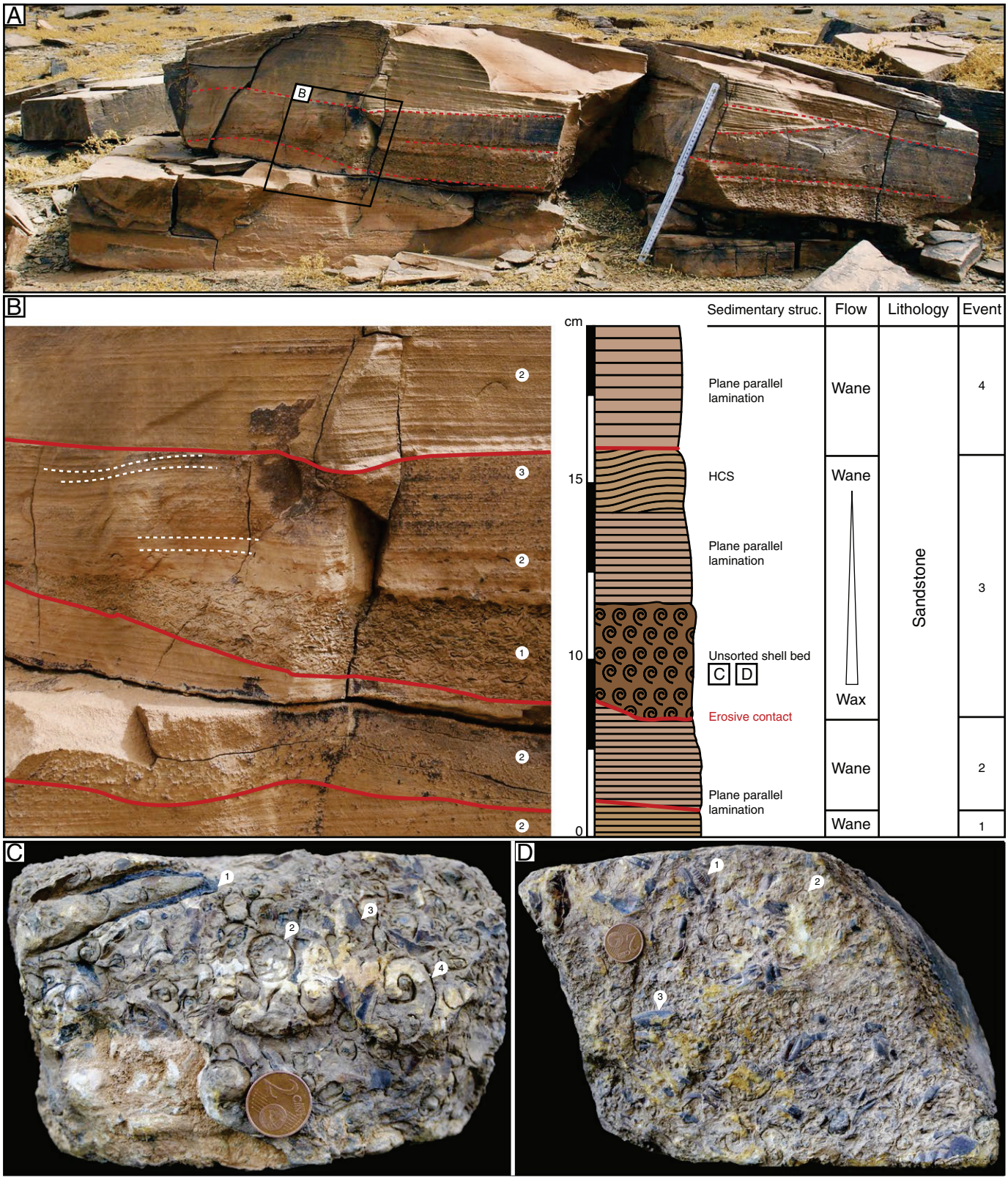

Fig. 5. (A) Proximal storm deposits containing *Konzentrat-Lagerstätte*; host sediments: coarse siltstones to fine-grained sandstones displaying wave ripples with a dm-scale wavelength (Fig. 3D); storm deposits: medium-grained sandstones showing HCS with a m-scale wavelength (red dotted line: erosive contact). (B) Detailed section showing several wax-and-wane flow deposits recording at the bottom of event 3 in a *Konzentrat-Lagerstätte*; 1: waxing phase; 2–3: waning phase. (C) Surface of Shell bed; 1: *Cavernolites* sp. (hyolithid); 2: undetermined gastropod; 3: undetermined hyolithid; 4: *Carcassonnella* sp. (gastropod). (D) Surface of Shell bed; 1: *Pradoella* sp. (trilobite); 2: undetermined gastropod; 3: Cephalic doublure of a large asaphid trilobite.

material of the sequence (e.g. Kreisa and Bambach, 1982; Aigner, 1985). Sedimentological analysis of the Fezouata Shale suggests that KsL and KzL can be both assigned to a lower shoreface environment, but with KsL in a more distal position than KzL (Fig. 6). In terms of water depth, 30–70 m are suggested for the depositional environment of KsL and 10–30 m for KzL (Immenhauser, 2009).

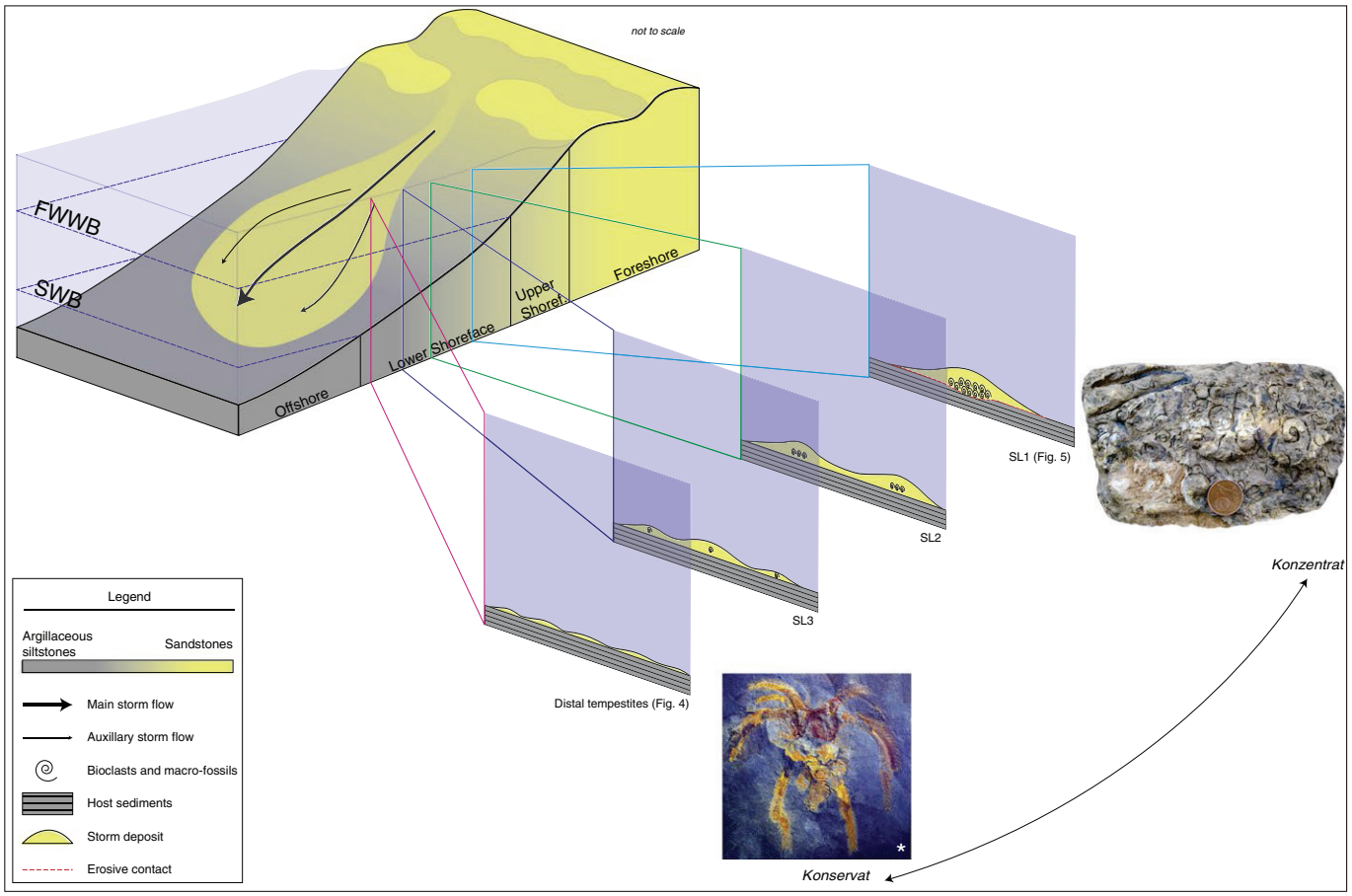

Fig. 6. Distribution of storm deposits (from SL1 to distal tempestites) in the lower shoreface (between the FWWB and the SWB) environment showing the genetic link between *Konzentrat*- and *Konservat-Lagerstätten* in the Fezouata Shale. *: *Furca* sp. (marrellomorph arthropod AA-BIZ31-OI-39, modified from Martin et al., in press).

Both types of fossil-rich occurrences in the Fezouata Shale are related to rapid burial or obrution events. This implies that a sufficiently thick amount of sediment was deposited very rapidly during a storm event (Martin, 1999). Obrution deposits appear to be the most common type of KsL (Brett, 1990, 1995) and preservation potential of soft tissues within them is especially high when rapid accumulation occurs in a quiet background sedimentary context (Brett et al., 1997). In shallower settings, wave activity continuously reworks previously deposited sediments. Commonly, organisms buried by obrution deposits experience little to no transport (Brett et al., 2012).

In the Fezouata Shale, the exceptional preservation observed in the KsL is in good agreement with the lower velocity of the storm flows compared to proximal settings. The fine-grained sandy layers (several cm-thick) deposited in the distal lower shoreface during storm events have enough velocity to rapidly bury the organisms, but not enough to transport them seaward (e.g. Aigner, 1985). However, if the sudden burial of communities by distal storm deposits appears as a necessary prerequisite for the occurrence of EPF in the Fezouata Shale (hence their non-random distribution), it cannot explain alone the preservation of soft parts. Distal storm deposits probably sealed sea-floors characterized by—at least temporarily—relatively inhospitable environmental conditions (e.g. low concentrations in oxygen; see Botting, 2016–in this issue; Lefebvre et al., 2016–in this issue; Martin et al., 2016–in this issue-a, b). Moreover, the absence of EPF within the deposits associated with the background sedimentation suggests that, although inhospitable sea-bottom conditions were necessary, they were alone not sufficient for the exceptional preservation of organisms and soft-tissues. Consequently, the Fezouata KsL can be interpreted as probably resulting from the combination of at least two processes, which together promoted the early inhibition of microbial activity (Gaines et al., 2012): a background sedimentation in a quiet, dysoxic to anoxic setting (FA1), interrupted by (fortuitous) repetitive burials of the sea-floor by distal storm deposits (FA2). After Martin et al. (in press), environmental conditions prevailing in the Fezouata KsL would be relatively similar to those occurring in the two Cambrian Guanshan and Chengjiang KsL (e.g. Hu, 2005; Hu et al., 2010; MacKenzie et al., 2015).

In some rare instances, EPF are separated from the overlying distal storm deposits by a thin (mm-thick) muddy layer. It is not clear if the absence of such a thin layer in most occurrences of EPF is original or if it results from its subsequent erosion. When present, this thin layer of background sediment (FA1) could suggest that the overlying storm deposit sealed a more or less freshly killed autochthonous community. Such a pre-obrution, mass-mortality was possibly caused by inhospitable sea-bottom conditions (e.g. anoxia).

In proximal storm deposits, KzL consist of shelly fossils, with skeletal remains occurring in the shell beds being either complete (e.g. echinoderms, see Allaire et al., 2015; Martin et al., 2015) or commonly fragmented. KzL are also obrution deposits (here storm deposits). In general, the component of allochthonous fauna in shell beds is generally high in proximal deposits and decreases seaward (Reineck et al., 1968). The high abundance of shelly fragments is likely explained by interludes of reduced sedimentation and/or repeated winnowing before being sealed during a storm event (e.g. Brett et al., 2008; Dattilo et al., 2008). It can be assumed that fully articulated organisms were buried close to their life habitat, whereas disarticulated to fragmented ones were probably transported seaward, or were already dead and subject to prior decay (Martin et al., 2016–in this issue-a). However, some experimental studies (Allison, 1986; Kidwell and Baumiller, 1990; Kerr

and Twitchett, 2004) suggest that soft-bodied and lightly sclerotized organisms (e.g. ophiuroids) can resist disarticulation for several hours in a tumbler and that fragmentation potential is largely controlled by the extent of decay prior to transport. Other examples of KzL exist in the geological record and are also formed by current activity as in the Middle Triassic (ophiuroid beds; Radwański, 2002; Zatoń et al., 2008), in the Middle Jurassic (ammonite rich intervals; Zatoń and Marynowski, 2010), in the Late Jurassic (bivalve rich intervals; Kin et al., 2013) and in the Late Cretaceous of Poland (crinoid rich intervals; Salamon et al., 2009).

In the Lower Ordovician of the Zagora area, the whole succession shows that sedimentary structures linked to storm and wave oscillation (Fig. 3) largely dominate over those formed by currents (e.g. Martin et al., in press; Vaucher et al., submitted for publication). The collapse of wave orbits on the seafloor generated oscillatory currents (e.g. Bagnold and Taylor, 1946; Perillo et al., 2014), which were not able to transport material over large distance; it only reworked the sediment locally, in contrast to unidirectional currents that can transport material for large distances. KzL exhibit evidence of current, and they can be considered as thanatocenoses. The rare current structures and the small wave ripples seen in the KsL are suggestive of a very reduced (if any) transport: the fauna can therefore be considered as living or having lived in situ or close to its burial site, and the KsL thus likely approximate to original biocoenoses.

Sedimentological analysis of the Fezouata *Lagerstätte* provides evidence that rapid burial (here storm deposits) is a necessary prerequisite condition for exceptional fossil preservation in the Fezouata Shale. Indeed, the known levels containing EPF are always related to storm deposits whereas the finest intervals devoid of storm deposits did not yield EPF. However, rapid burial alone cannot account for the preservation of soft tissues. In most other BST *Lagerstätten*, the exceptional preservation of organic remains results from the combination of multiple processes, including not only a rapid burial, but also e.g. oxygen-deficient conditions and low sulfate concentrations (see Jorgensen, 1982; Allison, 1988b; Butterfield, 1995; Gaines et al., 2005, 2012). Such environmental conditions would occur -at least episodically- in the Fezouata *Lagerstätte*. Low oxygenation can be inferred by both the presence of "dwarfed" benthic faunas (Ebbestad, 2016–in this issue; Lefebvre et al., 2016–in this issue), the absence of infaunal bivalves in the *A. murrayi* biozone (Polechova, 2016–in this issue), and preliminary geochemical data (Martin et al., 2016–in this issue-a). However, further studies are still required to better understand the precise environmental and taphonomic conditions, which favored the onset of exceptional preservation in the Fezouata *Lagerstätte*.

6. Conclusion

Sedimentological analysis of the Fezouata Shale (Tremadocian–Floian) in the Zagora area reveals the existence of two types of fossil-rich intervals: KsL and KzL horizons. KsL are characterized by exceptionally well-preserved fossils, and KzL, by shell beds. KsL intervals occur at the top of argillaceous siltstone beds and are consistently overlain by storm deposits (fine-grained sandstones) in the distal lower shoreface environment close to SWB. KzL are part of waxing storm deposits in the proximal lower shoreface environment. The KzL contain only hard skeletal fossils, mainly gastropods, bivalves, brachiopods, and fragments of trilobites. Both soft and mineralized remains of organisms are preserved in KsL. During storm events, sediment was transported from coastal environments and deposited seaward, burying in situ communities in distal settings (KsL), and concentrating skeletal remains of both living or dead organisms in more proximal settings (KzL). Consequently, fossil rich-intervals occur in different environments (proximal and distal lower shoreface), but the same process (storms) was associated with their formation. Relatively inhospitable sea-bottom conditions, such as low concentrations in both oxygen and sulfate have probably contributed to promote the exceptional preservation of fossil soft-tissues in KsL.

Acknowledgments

This work was supported by the ANR (Agence National de la Recherche) project "Rise of Animal Life (Cambrian-Ordovician): organisation and tempo" (grant number RALI 197) and by the CNRS-CNRST cooperation project VALORIZ. Ninon Allaire, Khadija El Hariri, Bertrand Lefebvre, Rudy Lerosey-Aubril, Elise Nardin, Abel Prieur, Emmanuel Robert, Thomas Servais, Thijs Vandenbroucke, Jean Vannier, Muriel Vidal, Daniel Vizcaïno, Guillaume Suan and Corentin Gibert are thanked for their precious help in the field and fruitful scientific discussions. We are also thankful to the managing guest-editor of this special issue Bertrand Lefebvre (Villeurbanne), to the guest editor Peter Van Roy (Yale University), and to the three reviewers Carlton E. Brett (University of Cincinnati), Robert R. Gaines (Pomona College) and an anonymous reviewer for their precious comments that helped us improve the overall quality of the manuscript.

References

Aigner, T., 1985. Storm Depositional Systems. Springer, Berlin Heidelberg.
Aldridge, R.J., Gabbott, S.E., Theron, J.N., 2007. The Soom Shale, Palaeobiology II. Blackwell Science Ltd, pp. 340–342.
Allaire, N., Lefebvre, B., Martin, E., Nardin, E., Vaucher, R., 2015. Taphonomy of new *Rhopalocystis* assemblages in the Lower Ordovician of the Zagora area (central Anti-Atlas, Morocco). In: Zamora, S., Rábano, I. (Eds.), Progress in Echinoderm Palaeobiology. Cuadernos Del Museo Geominero Vol. 19, pp. 21–26.
Allen, J.R.L., 1970. Physical Processes of Sedimentation. American Elsevier Pub. Co.
Allen, P.A., 1997. Earth Surface Processes. Blackwell Science, London, UK.
Allison, P.A., 1986. Soft-bodied animals in the fossil record: the role of decay in fragmentation during transport. Geology 14, 979–981.
Allison, P.A., 1988a. Konservat-Lagerstatten: cause and classification. Paleobiology 331–344.
Allison, P.A., 1988b. The role of anoxia in the decay and mineralization of proteinaceous macro-fossils. Paleobiology 14, 139–154.
Allison, P.A., Brett, C.E., 1995. *In situ* benthos and paleo-oxygenation in the Middle Cambrian Burgess Shale, British Columbia, Canada. Geology 23, 1079–1082.
Allison, P.A., Briggs, D.E.G., 1991a. Taphonomy of non-mineralized tissues. In: Allison, P.A., Briggs, D.E.G. (Eds.), Taphonomy: Releasing the Data Locked in the Fossil Record. Plenum Press, New-York, pp. 26–70.
Allison, P.A., Briggs, D.E.G., 1991b. The Taphonomy of Soft-Bodied Animals. In: Donovan, S.K. (Ed.), The Processes of Fossilization. Belhaven Press, London, pp. 120–140.
Bagnold, R.A., Taylor, G., 1946. Motion of waves in shallow water. Interaction between waves and sand bottoms. Proceedings of the Royal Society of London A: Mathematical, Physical and Engineering Sciences. The Royal Society, pp. 1–18.
Bambach, R.K., Knoll, A.H., Wang, S.C., 2004. Origination, extinction, and mass depletions of marine diversity. Paleobiology 30, 522–542.
Bluck, B.J., 1967. Sedimentation of beach gravels; examples from South Wales. J. Sediment. Res. 37, 128–156.
Boote, D.R.D., Clark-Lowes, D.D., Traut, M.W., 1998. Palaeozoic petroleum systems of North Africa. Geol. Soc. Lond., Spec. Publ. 132, 7–68.
Botting, J.P., 2016. Diversity and ecology of sponges in the Early Ordovician Fezouata Biota, Morocco. Palaeogeogr. Palaeoclimatol. Palaeoecol. 460, 75–86.
Botting, J.P., Muir, L.A., Sutton, M.D., Barnie, T., 2011. Welsh gold: a new exceptionally preserved pyritized Ordovician biota. Geology 39, 879–882.
Boyd, R., Dalrymple, R., Zaitlin, B.A., 1992. Classification of clastic coastal depositional environments. Sediment. Geol. 80, 139–150.
Brenchley, P.J., Newall, G., 1982. Storm-influenced inner-shelf sand lobes in the Caradoc (Ordovician) of Shropshire, England. J. Sediment. Res. 52.
Brett, C.E., 1990. Obrution Deposits. In: Briggs, D.E.G., Crowther, P.R. (Eds.), Palaeobiology: A Synthesis. Blackwell Scientific, London, pp. 239–243.
Brett, C.E., 1995. Sequence stratigraphy, biostratigraphy, and taphonomy in shallow marine environments. PALAIOS 10, 597–616.
Brett, C.E., Moffat, H.A., Taylor, W.L., 1997. Echinoderm taphonomy, taphofacies, and Lagerstätten. In: Waters, J.A., Maples, C.G. (Eds.), Geobiology of Echinoderms. Paleontological Society Papers Vol. 3, pp. 147–190.
Brett, C.E., Kirchner, B.T., Tsujita, C.J., Dattilo, B.F., 2008. Depositional dynamics recorded in mixed siliciclastic-carbonate marine successions: insights from the Upper Ordovician Kope Formation of Ohio and Kentucky, USA. In: Pratt, B.R., Holmden, C. (eds.), Dynamics of Epeiric Seas. Geol. Assoc. Can. Spec. Pap., 48, 73–102
Brett, C.E., Zambito, J.J., Hunda, B.R., Schindler, E., 2012. Mid-Paleozoic trilobite Lagerstätten: models of diagenetically enhanced obrution deposits. PALAIOS 27, 326–345.
Briggs, D.E.G., 2007. Exceptionally preserved fossils. In: Briggs, D.E.G., Crowther, P.R. (Eds.), Palaeobiology II. Blackwell Science Ltd, Oxford, pp. 328–332.
Briggs, D.E.G., Kear, A.J., 1994. Decay and mineralization of shrimps. PALAIOS 9, 431–456.
Briggs, D.E.G., Bottrell, S.H., Raiswell, R., 1991. Pyritization of soft-bodied fossils: Beecher's trilobite bed, Upper Ordovician, New York State. Geology 19, 1221–1224.

Butterfield, N.J., 1995. Secular distribution of Burgess-Shale-type preservation. Lethaia 28, 1–13.
Carr, I.D., 2002. Second-order sequence stratigraphy of the Palaeozoic of North Africa. J. Pet. Geol. 25, 259–280.
Cocks, L.R.M., Torsvik, T.H., 2004. 2004. Major Terranes in the Ordovician. In: Webby, B.D., Droser, M.L., Paris, F., Percival, I.G. (Eds.), The Great Ordovician Biodiversification Event. Columbia University Press, New York, pp. 61–67.
Coward, M., Ries, A., 2003. Tectonic development of North African basins. Geol. Soc. Lond., Spec. Publ. 207, 61–83.
Dattilo, B.F., Brett, C.E., Tsujita, C.J., Fairhurst, R., 2008. Sediment supply versus storm winnowing in the development of muddy and shelly interbeds from the Upper Ordovician of the Cincinnati region, USA. Can. J. Earth Sci. 45, 243–265.
Davies, J.L., 1964. A morphogenic approach to world shorelines. Z. Geomorphol. 8, 127–142 ((Sonderheft) (1964)).
Davis Jr., R.A., Hayes, M.O., 1984. What is a wave-dominated coast? Mar. Geol. 60, 313–329.
Destombes, J., 1962. Stratigraphie et paléogéographie de l'Ordovicien de l'Anti-Atlas (Maroc). Un essai de synthèse. Bull. Soc. Geol. Fr. 7, 453–460.
Destombes, J., 1989. Carte Géologique du Maroc - Zagora - Coude du Dra - Hamada du Dra, 1/200000. Ministère de l'Energie et des Mines, Direction de la Géologie, Editions du Service Géologique du Maroc.
Destombes, J., Hollard, H., Willefert, S., 1985. Lower Palaeozoic rocks of Morocco. In: Holland, C.H. (Ed.), Lower Palaeozoic Rocks of the World. 4. Lower Palaeozoic of North Western-Central Africa. Wiley, New York, pp. 91–336.
Dott, R., Bourgeois, J., 1982. Hummocky stratification: significance of its variable bedding sequences. Geol. Soc. Am. Bull. 93, 663–680.
Duke, W.L., 1985. Hummocky cross-stratification, tropical hurricanes, and intense winter storms. Sedimentology 32, 167–194.
Duke, W.L., Arnott, R.W.C., Cheel, R.J., 1991. Shelf sandstones and hummocky cross-stratification — new insights on stormy debate. Geology 19, 625–628.
Dumas, S., Arnott, R.W.C., 2006. Origin of hummocky and swaley cross-stratification — the controlling influence of unidirectional current strength and aggradation rate. Geology 34, 1073–1076.
Ebbestad, J.O.R., 2016. Gastropoda, Tergomya and Paragastropoda (Mollusca) from the Lower Ordovician Fezouata Formation, Morocco. Palaeogeogr. Palaeoclimatol. Palaeoecol. 460, 87–96 (in this issue).
Fabre, J., 1988. Les séries paléozoïques d'Afrique: une approche. J. Afr. Earth Sci. 7, 1–40.
Froelich, P.N., Klinkhammer, G.P., Bender, M.L., Luedtke, N.A., Heath, G.R., Cullen, D., Dauphin, P., Hammond, D., Hartman, B., Maynard, V., 1979. Early oxidation of organic matter in pelagic sediments of the eastern equatorial Atlantic: suboxic diagenesis. Geochim. Cosmochim. Acta 43, 1075–1090.
Gaines, R.R., Kennedy, M.J., Droser, M.L., 2005. A new hypothesis for organic preservation of Burgess Shale taxa in the middle Cambrian Wheeler Formation, House Range, Utah. Palaeogeogr. Palaeoclimatol. Palaeoecol. 220, 193–205.
Gaines, R.R., Hammarlund, E.U., Hou, X., Qi, C., Gabbott, S.E., Zhao, Y., Peng, J., Canfield, D.E., 2012. Mechanism for Burgess Shale-type preservation. Proc. Natl. Acad. Sci. 109, 5180–5184.
Goldring, R., Bridges, P., 1973. Sublittoral sheet sandstones. J. Sediment. Res. 43.
Gutiérrez-Marco, J.-C., Martin, E.L.O., 2016. Biostratigraphy and palaeoecology of Lower Ordovician graptolites from the Fezouata Shale (Moroccan Anti-Atlas). Palaeogeogr. Palaeoclimatol. Palaeoecol. 460, 35–49 (in this issue).
Harms, J., 1979. Primary sedimentary structures. Annu. Rev. Earth Planet. Sci. 7, 227.
Harper, D.A.T., 2006. The Ordovician biodiversification: setting an agenda for marine life. Palaeogeogr. Palaeoclimatol. Palaeoecol. 232, 148–166.
Heward, A.P., 1981. A review of wave-dominated clastic shoreline deposits. Earth Sci. Rev. 17, 223–276.
Hu, S.X., 2005. Taphonomy and palaeoecology of the Early Cambrian Chengjiang biota from eastern Yunnan, China. Berl. Paläobiol. Abh. 7, 1–197.
Hu, S., Zhu, M., Steiner, M., Luo, H., Zhao, F., Liu, Q., 2010. Biodiversity and taphonomy of the Early Cambrian Guanshan biota, eastern Yunnan. Sci. China Earth Sci. 53, 1765–1773.
Immenhauser, A., 2009. Estimating palaeo-water depth from the physical rock record. Earth Sci. Rev. 96, 107–139.
Jorgensen, B.B., 1982. Mineralization of organic matter in the sea bed-the role of sulphate reduction. Nature 296, 643–645.
Kerr, T.J.V., Twitchett, R.J., 2004. Experimental decay and disarticulation of *Ophiura texturata*: implications for the fossil record of ophiuroids. In: Heinzeller, T., Nebelsick, J.H. (Eds.), Echinoderms: Munchen. Balkema, Leiden, pp. 439–446.
Kidwell, S.M., Baumiller, T., 1990. Experimental disintegration of regular echinoids: roles of temperature, oxygen, and decay thresholds. Paleobiology 16, 247–271.
Kin, A., Gruszczyński, M., Martill, D., Marshall, J.D., Błażejowski, B., 2013. Palaeoenvironment and taphonomy of a Late Jurassic (Late Tithonian) Lagerstätte from central Poland. Lethaia 46, 71–81.
Komar, P.D., Miller, M.C., 1975. The initiation of oscillatory ripple marks and the development of plane-bed at high shear stresses under waves. J. Sediment. Res. 45.
Kreisa, R.D., 1981. Storm-generated sedimentary structures in subtidal marine facies with examples from the Middle and Upper Ordovician of southwestern Virginia. J. Sediment. Res. 51.
Kreisa, R.D., Bambach, R.K., 1982. The role of storm processes in generating shell beds in paleozoic shelf environments. In: Einsele, G., Seilacher, A. (Eds.), Cyclic and Event Stratification. Springer, Berlin Heidelberg, pp. 200–207.
Lefebvre, B., Allaire, N., Guensburg, T.E., Hunter, A.W., Kouraïss, K., Martin, E.L.O., Nardin, E., Noailles, F., Pittet, B., Sumrall, C.D., Zamora, S., 2016. Palaeoecological aspects of the diversification of echinoderms in the Lower Ordovician of central Anti-Atlas, Morocco. Palaeogeogr. Palaeoclimatol. Palaeoecol. 460, 97–121.
Liu, H.P., McKay, R.M., Young, J.N., Witzke, B.J., McVey, K.J., Liu, X., 2006. A new Lagerstätte from the middle Ordovician St. Peter formation in Northeast Iowa, USA. Geology 34, 969–972.
MacKenzie, L.A., Hofmann, M.H., Junyuan, C., Hinman, N.W., 2015. Stratigraphic controls of soft-bodied fossil occurrences in the Cambrian Chengjiang Biota Lagerstätte, Maotianshan Shale, Yunnan Province, China. Palaeogeogr. Palaeoclimatol. Palaeoecol. 420, 96–115.
Marti Mus, M., 2016. A hyolith with preserved soft parts from the Ordovician Fezouata Konservat-Lagerstätte of Morocco. Palaeogeogr. Palaeoclimatol. Palaeoecol. 460, 122–129.
Martin, R.E., 1999. Taphonomy: A Process Approach. Cambridge University Press, Cambridge.
Martin, E., Lefebvre, B., Pittet, B., Vannier, J., Bachnou, A., Hariri, K., Hafid, A., Masrour, M., Noailles, F., Nowak, H., Servais, T., Vandenbroucke, T.A., Van Roy, P., Vidal, M., Vizcaïno, D., 2014. The Fezouata biota (Central Anti-Atlas, Morocco): biostratigraphy and associated environmental conditions of an Ordovician Burgess Shale. In: Rocha, R., Pais, J., Kullberg, J.C., Finney, S. (Eds.), STRATI 2013. Springer International Publishing, pp. 419–423.
Martin, E., Lefebvre, B., Vaucher, R., 2015. Taphonomy of a stylophoran-dominated assemblage in the Lower Ordovician of Zagora area (central Anti-Atlas, Morocco). In: Zamora, S., Rabano, I. (Eds.), Progress in Echinoderm Palaeobiology. Cuadernos del Museo Geominero Vol. 19, pp. 95–100.
Martin, E.L.O., Lerosey-Aubril, R., Vannier, J., 2016a. Palaeoscolecid worms from the Lower Ordovician Fezouata Lagerstätte, Morocco: palaeoecological and palaeogeographical implications. Palaeogeogr. Palaeoclimatol. Palaeoecol. 460, 130–141 (in this issue a).
Martin, E.L.O., Vidal, M., Vizcaïno, D., Vaucher, R., Sans-Jofre, P., Lefebvre, B., Destombes, J., 2016b. Biostratigraphic and palaeoenvironmental controls on the trilobite associations from the Lower Ordovician (Fezouata formations) of the central Anti-Atlas, Morocco. Palaeogeogr. Palaeoclimatol. Palaeoecol. 460, 142–154 (2016–in this issue b).
Martin, E.L.O., Pittet, B., Gutiérrez-Marco, J.-C., Vannier, J., El Hariri, K., Lerosey-Aubril, R., Masrour, M., Nowak, H., Servais, T., Vandenbroucke, T.R.A., Van Roy, P., Vaucher, R., Lefebvre, B., 2016. The Lower Ordovician Fezouata Konservat-Lagerstätte from Morocco: age, environment and evolutionary perspectives. Gondwana Res. (in press).
McLane, M., 1995. Sedimentology. Oxford University Press, New York; Oxford.
Meyers, S.R., Peters, S.E., 2011. A 56 million year rhythm in North American sedimentation during the Phanerozoic. Earth Planet. Sci. Lett. 303, 174–180.
Nichols, G., 2009. Sedimentology and Stratigraphy. second ed. Blackwell, Oxford.
Nowak, H., Servais, T., Pittet, B., Vaucher, R., Akodad, M., Gaines, R.R., Vandenbroucke, T.R.A., 2016. Palynomorphs of the Fezouata Formation (Lower Ordovician, Morocco): age and environmental constraints of the Fezouata Biota. Palaeogeogr. Palaeoclimatol. Palaeoecol. 460, 62–74.
Perillo, M.M., Best, J.L., Yokokawa, M., Sekiguchi, T., Takagawa, T., Garcia, M.H., 2014. A unified model for bedform development and equilibrium under unidirectional, oscillatory and combined-flows. Sedimentology 61, 2063–2085.
Plint, A., 2010. Wave-and storm-dominated shoreline and shallow-marine systems. Facies Models 4, 167–200.
Polechova, M., 2016. Bivalve fauna from the Fezouata Formation (Lower Ordovician) of Morocco and its significance for palaeobiogeography, palaeoecology and early diversification of bivalves. Palaeogeogr. Palaeoclimatol. Palaeoecol. 460, 155–169.
Radwański, A., 2002. Triassic brittlestar beds of Poland: a case of *Aspiduriella ludeni* (v. Hagenow, 1846) and *Arenorbis squamosus* (E. Picard, 1858). Acta Geol. Pol. 52, 395–410.
Reineck, H.E., Dörjes, J., Gadow, S., Hertweck, G., 1968. Sedimentologie, Faunenzonierung und Faziesabfolge vor der Ostküste der inneren Deutschen Bucht. Senckenb. Lethaea 49, 261–305.
Salamon, M.A., Gorzelak, P., Borszcz, T., Gajerski, A., Kaźmierczak, J., 2009. A crinoid concentration Lagerstätte in the Turonian (Late Cretaceous) *Conulus* Bed (Miechów-Wolbrom area, Poland). Geobios 42, 351–357.
Seilacher, A., 1970. Begriff und Bedeutung der Fossil-Lagerstätten. Neues Jb. Geol. Paläontol. Monat. 1970, 34–39.
Seilacher, A., 1990. Taphonomy of Fossil-Lagerstätten: overview. Paleobiology 266–270.
Seilacher, A., Reif, W.E., Westphal, F., Riding, R., Clarkson, E.N.K., Whittington, H.B., 1985. Sedimentological, ecological and temporal patterns of fossil Lagerstätten [and discussion]. Philos. Trans. R. Soc. Lond. B 311, 5–24.
Servais, T., Lehnert, O., Li, J., Mullins, G.L., Munnecke, A., Nuetzel, A., Vecoli, M., 2008. The Ordovician biodiversification: revolution in the oceanic trophic chain. Lethaia 41, 99–109.
Servais, T., Owen, A.W., Harper, D.A.T., Kröger, B., Munnecke, A., 2010. The Great Ordovician Biodiversification Event (GOBE): the palaeoecological dimension. Palaeogeogr. Palaeoclimatol. Palaeoecol. 294, 99–119.
Speyer, S.E., Brett, C.E., 1991. Taphofacies controls: Background and episodic processes in fossil assemblage preservation. In: Allison, A., Briggs, D.E.G. (Eds.), Taphonomy: Releasing Data Locked in the Fossil Record, Topics in Geobiology, pp. 501–545.
Van Roy, P., Orr, P.J., Botting, J.P., Muir, L.A., Vinther, J., Lefebvre, B., El Hariri, K., Briggs, D.E., 2010. Ordovician faunas of Burgess Shale type. Nature 465, 215–218.
Van Roy, P., Briggs, D.E.G., Gaines, R.R., 2015a. The Fezouata fossils of Morocco; an extraordinary record of marine life in the Early Ordovician. J. Geol. Soc. 172, 541–549.
Van Roy, P., Daley, A.C., Briggs, D.E.G., 2015b. Anomalocaridid trunk limb homology revealed by a giant filter-feeder with paired flaps. Nature 522, 77–80.
Vaucher, R., Pittet, B., 2014. A Peculiar Wave-dominated siliciclastic system in the Fezouata and Zini formations, Lower Ordovician, Morocco: a possible tide influence? 19th International Sedimentological Congress, Geneva, Switzerland, p. 711

Vaucher, R., Hormière, H., Pittet, B., 2015. Genesis of sandstone lenses in a wave-dominated, tide-modulated siliciclastic system (Fezouata Fm, Lower Ordovician, Morocco). 31st IAS Meeting of Sedimentology, Kraków, Poland, p. 556.

Vaucher, R., Pittet, B., Hormière, H., Martin, E.L.O., Lefebvre, B., 2016. A wave-dominated, tide-modulated model for the Lower Ordovician of the Anti-Atlas, Morocco. Sedimentology (submitted for publication).

Yang, B.C., Dalrymple, R.W., Chun, S., 2006. The significance of hummocky cross-stratification (HCS) wavelengths: evidence from an open-coast tidal flat, South Korea. J. Sediment. Res. 76, 2–8.

Young, G.A., Rudkin, D.M., Dobrzanski, E.P., Robson, S.P., Nowlan, G.S., 2007. Exceptionally preserved Late Ordovician biotas from Manitoba, Canada. Geology 35, 883–886.

Zatoń, M., Marynowski, L., 2010. Konzentrat-Lagerstätte-type carbonate concretions from the uppermost Bajocian (Middle Jurassic) of the Częstochowa area, South-Cental Poland. Geol. Q. 48, 339–350.

Zatoń, M., Salamon, M.A., Boczarowski, A., Sitek, S., 2008. Taphonomy of dense ophiuroid accumulations from the Middle Triassic of Poland. Lethaia 41, 47–58.

CHAPITRE IV :

STRUCTURES SÉDIMENTAIRES ASSOCIÉES À DES ENVIRONNEMENTS MÉGA- ET MACRO-TIDAUX DOMINÉS PAR LA HOULE

«La houle mord la terre: elle ne lui pardonne pas de briser sa course»

Sylvain Tesson

Ce chapitre contient deux articles concernant des environnements actuels :

(1) Berck-Plage (Pas-de-Calais ; France) :

Bedforms in a tidally modulated ridge and runnel shoreface (Berck-Plage; North France): implications for the geological record

(2) Cap-Ferret (Gironde ; France) :

Hummocky bedforms in the intertidal zone as the results of supercritical flows and wave-wave interference?

I) Résumé de l'article concernant Berck-Plage :

Les plages et avant-plages sous l'influence de la houle et modulées par l'action de la marée correspondent à des environnements côtiers particuliers. Leurs géomorphologies générales ainsi que les structures sédimentaires associées résultent de l'action combinée de la houle et de la marée. L'identification de ces environnements atypiques dans des successions sédimentaires anciennes demeure difficile. L'analyse d'un environnement mégatidal semi-diurne actuel dans le Nord de la France (Berck-Plage) a permis de fournir de nouveaux critères de reconnaissance pour ce type de système côtier hybride dans le fossile. Une étude de terrain ainsi qu'une cartographie numérique ont été réalisées à marée basse lors de la marée du siècle en mars 2015. La zone intertidale est caractérisée par une succession de plusieurs bancs de sables parallèles à la côte et qui sont définis comme des barres (topographie positive) et des bâches (topographie négative). L'étude de terrain de cette zone a révélé sept types de structures sédimentaires : des rides de courant 3D ; des rides asymétriques 3D ; des rides symétriques 2D ; des petites dunes symétriques 2D ; des grandes dunes symétriques 2D ; des grandes dunes symétriques 3D et des structures planes. Ces dernières sont principalement observées aux sommets des barres, tandis que les six autres types de structures sédimentaires se retrouvent plus communément dans les bâches ou sur le flanc des barres. La comparaison effectuée avec des études expérimentales sur la genèse de structures sédimentaires prouve que les paramètres des courants nécessaires pour produire ces structures sédimentaires correspondent à un courant oscillatoire (à l'exception des rides de courant 3D, qui sont formées par un courant unidirectionnel). Cette étude confirme la prédominance des structures oscillatoires dans la zone intertidale, ce qui est relativement inattendu dans un contexte mégatidal et montre clairement que les processus de houle sont plus énergiques que ceux liés aux marées, lorsque les deux processus coexistent. Cette étude suggère que la géomorphologie côtière induit la réfraction de la houle, ce qui joue un rôle majeur dans la distribution et l'agencement des structures sédimentaires au sein de la zone intertidale. La réfraction de la houle est probablement à l'origine de la formation des dunes symétriques 3D, qui miment la morphologie externe des stratifications entrecroisées en mamelons (HCS). La description de ces sept types de structures sédimentaires, ainsi que l'analyse de leur répartition latérale et verticale montrent une répartition similaire des structures entre chaque couple de barres/bâches. Ces observations ont permis de proposer une séquence stratigraphique idéalisée pour un environnement mégatidal dominé par la houle qui sera utilisable pour la reconnaissance d'environnements similaires dans une succession sédimentaire ancienne.

II) Article :

Bedforms in a tidally modulated ridge and runnel shoreface (Berck-Plage; North France): implications for the geological record

Auteurs : **Romain Vaucher**, Bernard Pittet, Sophie Passot, Philippe Grandjean, Thomas Humbert, Pascal Allemand

Article soumis pour publication à *Continental Shelf Research*

Abstract

Tidally modulated shorefaces (TMS) correspond to peculiar costal environments. The general morphology and the expressed bedforms are provided by the interplay of both tides and waves. The recognition of TMS in the fossil record still remains a difficult task. The study of one mega-tidal modern TMS in the north of France (Berck-Plage) provides new key criteria to identify this kind of coastal system in the rock record. Field investigation and digital mapping were realized at lowest tide during the tide of the century in March 2015. The intertidal zone is characterized by a succession of several sand banks shore parallel that are defined as ridges and runnels. Seven distinct dominant bedforms are recognized: 3D current ripples, 3D asymmetrical ripples, 2D symmetrical ripples, 2D small symmetrical dunes, 2D large symmetrical dunes, 3D symmetrical dunes and upper stage plane beds. The upper stage plane bedding mainly composed the ridges while the six other bedforms are commonly found within the runnels or on the flanks of the ridges. Comparison with previous studies proves that the necessary flow parameters for generating these bedforms belong to an oscillatory flow except for the 3D current ripples, which are formed by a unidirectional flow. This study confirms (1) the dominance of oscillatory structures through the intertidal zone, which is not expected in a mega-tidal context and show that waves processes are more powerful than tide processes for bedforms generation; (2) the occurrence of topographic highs (ridges) induce wave refraction, which plays a major role in the bedform distribution and genesis, especially for the 3D symmetrical dunes that mimic the external shape of hummocky cross-stratified structures. The description of the bedforms as well as their lateral and vertical repartition shows repeated patterns of distribution between two ridges thus helping to predict an idealized stratigraphic sequence for TMS.

Keywords waves, tides, ridge and runnel, bedforms, stratigraphy, wave refraction

1. Introduction

Waves and tides are the two main processes acting either separately or together on the formation of sedimentary structures, their repartitions and the geomorphology of coastal systems. Facies models for wave-dominated (e.g. Allen, 1997; Clifton et al., 1971; Davis Jr, 1985; Davis Jr and Hayes, 1984; Harms, 1979; McLane, 1995; Plint, 2010) and tide-dominated (Dalrymple, 1992; Dalrymple, 2003; Davis and Dalrymple, 2012) sedimentary systems are now well constrained in the literature. Recent studies have shown how the co-influence of waves and tides can be recognized in the rock record at different scales, from the sedimentary structures to the general stratigraphic succession in sedimentary sequences (e.g. Basilici et al., 2011; Basilici et al., 2012; Rossi and Steel, 2016; Vakarelov et al., 2012; Vaucher et al., in press). Modern environments have been also investigated (e.g. Dashtgard et al., 2009; Dashtgard et al., 2012; Yang and Chun, 2001; Yang et al., 2005; Yang et al., 2006; Yang et al., 2008) and the double influence (waves and tides) was clearly pointed out by sedimentological and/or ichnological evidences. However, these studies on modern environments are mainly based on boxcore analysis, thus giving a vertical (temporal) view to the observations. In order to constrain the spatial distribution of sedimentary bodies and their associated bedforms in a tidally modulated modern shoreface (TMS; *sensu* Dashtgard et al., 2009), the Berck-Plage mega-tidal beach in northern France was investigated. It allows providing the spatial repartition of the different bedforms in order to reconstruct an idealized temporal, stratigraphic succession expected in TMS. The studied area is characterized by several shore-parallel sand banks that are *ca.* 1 m high (from trough to crest) and spaced from each other by *ca.* 200 m. This beach morphology, called ridge and runnel, was first described by King and Williams (1949). These peculiar beaches were subject to numerous publications that mainly describe their coastal dynamics (e.g. Anthony et al., 2005; Anthony et al., 2004; Battiau-Queney et al., 2003; Kroon and Masselink, 2002; Lashteh Neshaei et al., 2009; Levoy et al., 1998; Levoy et al., 2000; Masselink, 2004; Masselink and Anthony, 2001; Masselink et al., 2006; Reichmüth and Anthony, 2007; 1991; Short, 1984; Sipka and Anthony, 1999; Stépanian and Levoy, 2003; van Houwelingen et al., 2006; Voulgaris et al., 1998; Wijnberg and Kroon, 2002). However, the associated bedforms generated over the ridges and runnels have less been investigated. Only Chauhan (2000) has studied the different bedforms occurring in such environments. A newly established nomenclature proposed by Perillo et al. (2014a) is applied and adapted for the description of the bedforms present in the intertidal zone of Berck-Plage.

In this study we propose (1) to describe the bedforms generated in a ridge and runnel mega-tidal context using field investigations and ortho-images analysis, and thus to analyze their spatial distribution; (2) to interpret the bedforms in term of physical processes; and (3) to propose an idealized stratigraphic succession of sedimentary structures, applicable to the rock record, for the intertidal zone of TMS.

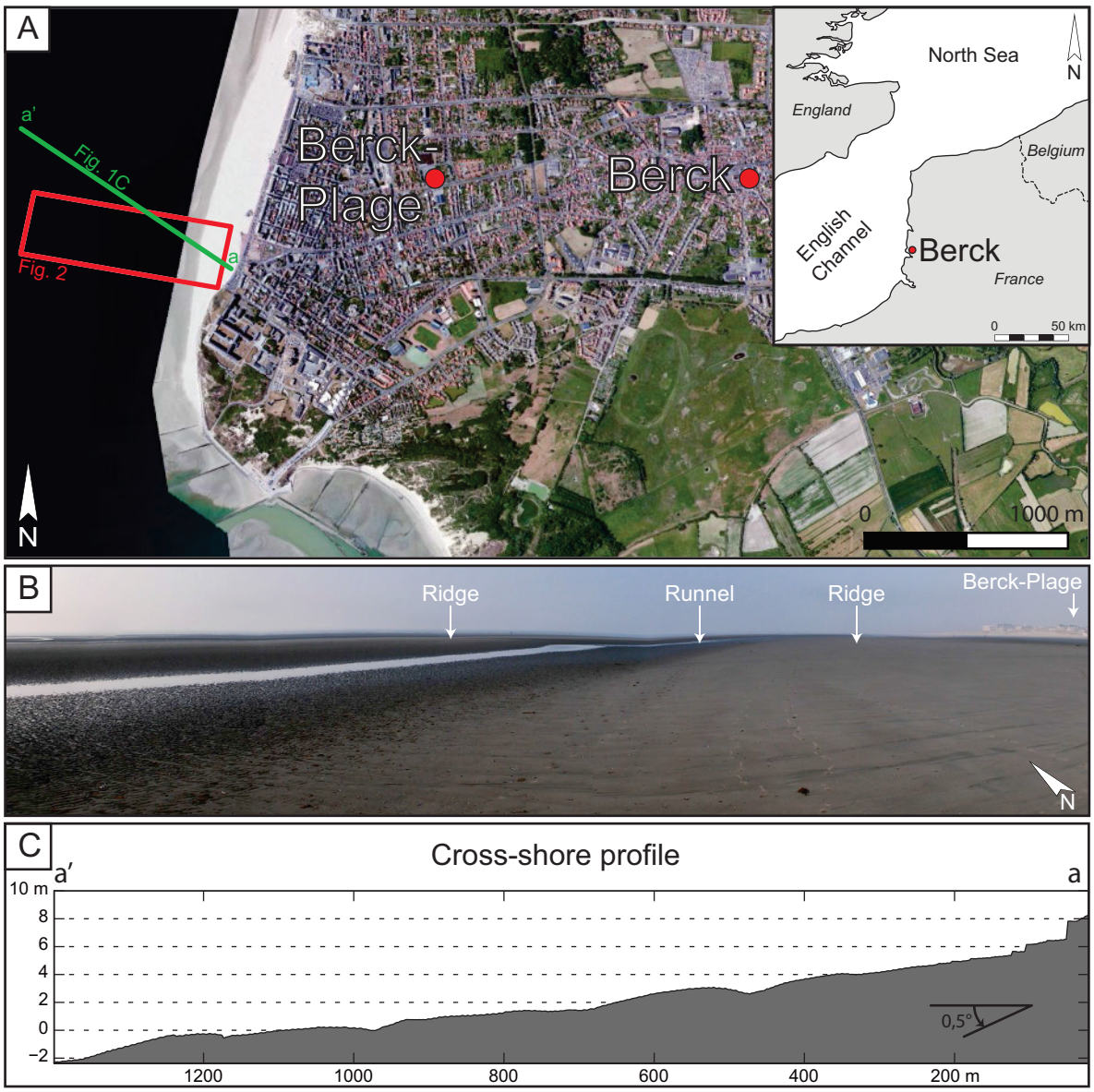

Fig. 1. *(A) Satellite image of the study area, from Bing Maps. The study area is a part of the intertidal zone of Berck-Plage (North France) orientated in N-S axis on the English Channel side; red rectangle: location of the ortho-images (see Fig. 2) achieved on the area, covering an area of ca. 0.58 km². (B) Part of the intertidal zone of Berck-Plage at low tide displaying ridge and runnel morphology. (C) Cross-shore profile of the intertidal zone showing the ridge and runnel morphology.*

2. Study area

The beach of Berck-Plage (Fig. 1A) is part of the Côte d'Opale in the northern part of France (Pas-de-Calais department) on the English Channel and is elongated on a N-S axis. This beach is submitted to moderate waves (fair-weather waves are < 1.5 m high; storm waves are *ca*. 2 – 4 m high; e.g. Augris et al., 2004). A mega-tidal range (spring tidal range of 8.3 m; Anthony et al., 2004) is recorded due to the geographical position of the beach (close to the northern extremity of the English Channel; Fig. 1A), which promotes the resonance effect of the tides (e.g. Cram, 1979; Davis and Dalrymple, 2012). Macro-tidal beaches are defined by a tidal range > 4 m but if the tidal range can reach up to 8

m, a classification as mega-tidal is applied (e.g. Levoy et al., 2000). Macro- and mega-tidal beaches are widespread on all continents, mainly in protected environments even if some are located in exposed environments (oceans) (Short, 1991). Macro- or mega-tidal beaches can be classified in three distinctive groups: (1) Higher Wave, Planar, Uniform Slope; (2) Moderate Waves, Multi Bar and; (3) Low Wave Beach and Tidal Flat (Short, 1991). Multi bar, or ridge and runnel beaches were first described by King and Williams (1949). This kind of beach is constituted of fine to medium sands, shows a 0.5 – 0.6° intertidal gradient, and presents several bars disconnected from each other (Short, 1991). The bars usually occur between the mean highest (MHTL) and the mean lowest tide levels (MLTL), have a height < 1 m and are spaced from 50 to 150 m. Several surveys of multi barred costal environments tend to suggest that positions and dimensions of the bars are relatively stable through times (Hale and McCann, 1982; King, 1972). Intuitively, the ridges was supposed to be formed by swash action during a stationary water levels (King, 1972), however a more recent study (Masselink and Anthony, 2001) suggests that both swash and surf processes acting together are responsible for the development and stability of the ridge and runnel geomorphology. This explanation is supported by the fact that the ridges are mainly present close to the mid-tide level where the water level is never stationary. Associated with these large bars, several bedforms (ripples and dunes) generated by oscillatory-, unidirectional- or combined-flows are also present and can be interpreted in terms of hydrodynamic conditions and relative water depth according to the tidal state and wave action.

The intertidal zone of Berck-Plage consists of well-sorted fine to medium grained quartz and bioclasts, has a general slope angle of *ca*. 0.5°, and displays numerous linear shore parallel banks. The Berck-Plage intertidal zone can thus be considered as a ridge and runnel beach (Fig. 1B and C). Five ridges are observed, which display a general asymmetry with a steeper landward than seaward slope. The different troughs (runnels) between two ridges act as channels during rising and falling tide.

3. Methods

The intertidal zone of Berck-Plage was investigated and analyzed during the tide of the century (tide coefficient: 119) occurring the 21st March 2015, under fair-weather conditions. Wave parameter for the incident waves were: 10 - 8 m of wavelength (L); 5 - 8 s of period (T); 0.5 - 1 m of wave height (H). The different bedforms were described in the field during the lowest tide levels. The spatial distribution and mapping of the observed bedforms were realized on ortho-images (Fig. 2), which covered an area of *ca.* 0.58 km^2 ranging from the MHTL to the MLTL.

Ortho-images

Bedforms distribution

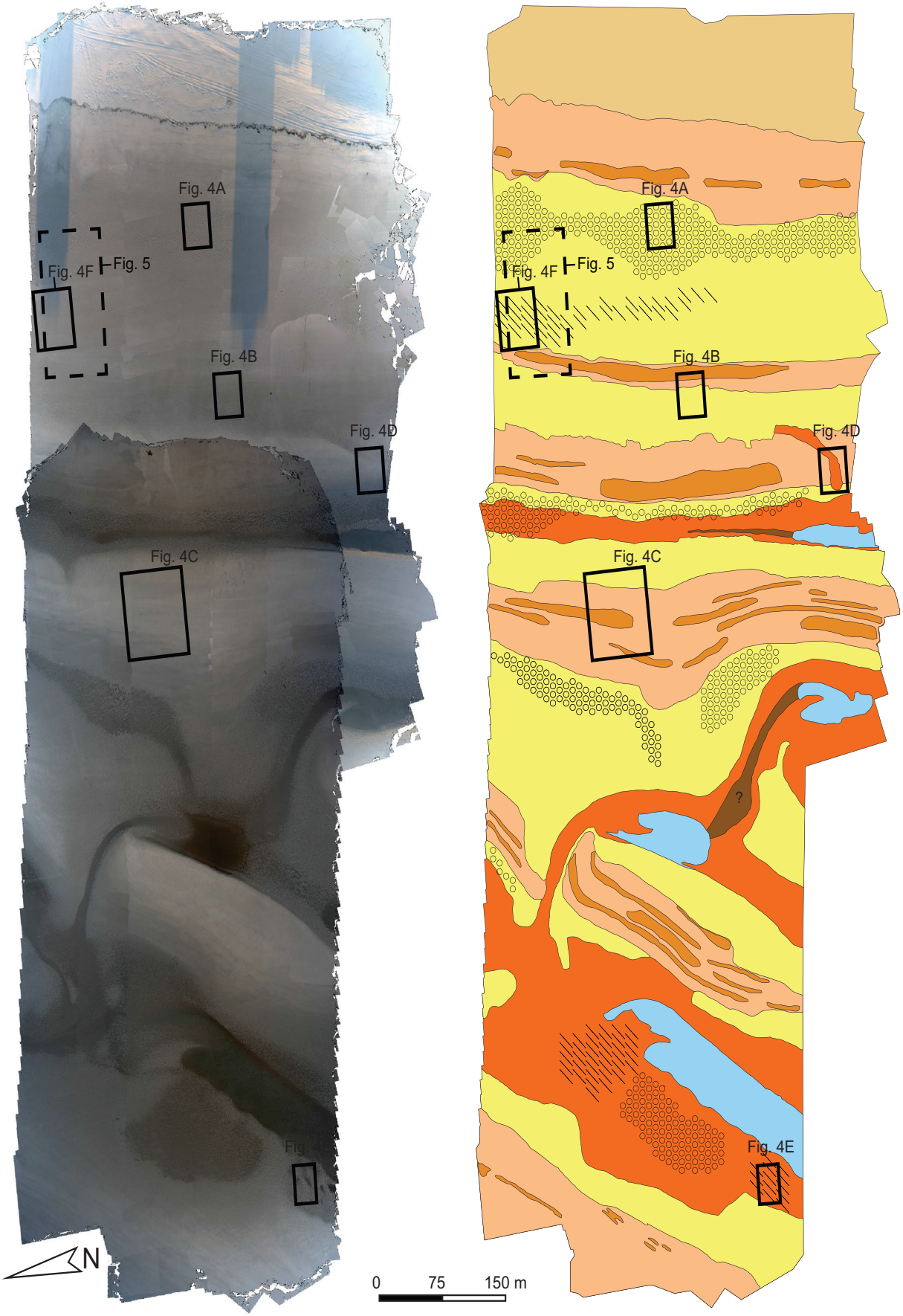

Fig. 2. *Ortho-images (left) and bedform distribution (right) in the studied intertidal zone. 3D CR (3D Current Ripples); 3D CR-pp (3D Current Ripples poorly preserved); 3D AR (3D Asymmetrical Ripples); 2/2.5D SR (2/2.5D Symmetrical ripples); 2D SSD (2D Symmetrical Medium Ripples); USPB (Upper Stage Plane Bed); 3D SD (3D Symmetrical Dunes); 2D SD (2D Symmetrical Dunes).*

3.1. Images acquisition

Images were acquired by UAV flights. The surveys were performed using DRELIO, an UAV based on a multi-rotor platform. It is equipped for nadir photography with a reflex camera Nikon D700 with a focal length of 35 mm, taking every 2 seconds one 12 Mpix photo stored in JPEG fine format. The flight in cruise limb is realized in automatic mode at an elevation of 100m above the intertidal zone. During the cruise limb, DRELIO follows a programmed path that has been prepared and downloaded in its memory just before takeoff. Before each flight, 15 highly visible targets were distributed in the study area. These targets are circular red disks of 23 cm in diameter. They are georeferenced with post-processed Differential GPS (DGPS), using a Topcon HiPer II GNSS receiver. During each flight more than 250 images were taken. The resolution of the images was around 2 cm.

Images were processed using the MicMac chain in order to obtain DEM and ortho-images of each flight. MicMac (acronym for “Multi-Images Correspondances, Méthodes Automatiques de Corrélation”) is an open-source photogrammetric software suite developed by IGN® for computing 3D models from sets of images (Pierrot Deseilligny, 2015; Pierrot Deseilligny and Clery, 2011). The process is realized in four steps. During the first one, tie points are computed on the images using the SIFT++ algorithm. The result of this step is a list of the position of the tie points on each image. In the second step, the external orientation and the intrinsic calibration of the camera are computed assuming a Fraser’s radial model of distortion. The results of this step are a set of parameters of distortion and a relative position and orientation of the camera for each image. The third step consists in a dense matching between the images that overlap in order to produce the DEM of the whole surface at a resolution close of the resolution of the image, i.e. 2 cm in this case. In the last step, the ortho-image is computed at the same resolution than the DEM. Finally the ortho-images and the DEM are georeferenced in a Lambert93 projection using the position and elevation of the targets visible on the ortho-image. The planimetric precision of the georeferencing is better than 5 cm. The overall precision in elevation has the same level of confidence from the differences between GPS measurements and elevation measured on the DEM. As the beach is very flat and with very small topographic features (less than 5 cm), the precision of the shape of these features in elevation is probably bad. Despite this problem, the shape in plan of the sedimentary features remains precise.

3.2. Bedform nomenclature

Recently, several experimental studies were performed on the genesis of bedforms under unidirectional-, oscillatory- and combined-flows (Cummings et al., 2009; Dumas et al., 2005; Perillo et al., 2014a; Perillo et al., 2014b; Perillo et al., 2014c). In this study, the bedforms described in the intertidal zone follow the classification provided from Perillo et al. (2014a) and was adapted when the bedforms were not present in their study:

- 3D Current Ripples (3D CR)
- 3D Asymmetrical Ripples (3D AR)
- 2/2.5D Symmetrical Ripples (2/2.5SD)
- 2D Symmetrical Small Dune (2D SSD)
- Upper-Stage Plan Bed (USPB)
- 2D Symmetrical Dunes (2D SD)
- 3D Symmetrical Dunes (3D SD)
- Antidunes

Bedforms	This study					Dumas et al., (2005)					Perillo et al., (2014a)				
	λ(cm)	η(cm)	BI	Position along the intertidal zone	% of bedforms trough the intertidale zone	U_o (cm.s^{-1})	U_c (cm.s^{-1})	λ(cm)	η(cm)	BI	U_o (cm.s^{-1})	U_c (cm.s^{-1})	λ(cm)	η(cm)	BI
3D CR	15	2	7,5	Trough of runnel	0,6	Ø	>10	Ø	Ø	Ø	<15	>20	35	1,5	12
3D AR	15	5	3	Trough of runnel / bottom of ridge	12,4	<40	>10	11-21	1,2-2,9	8-12	15-50	Ø	22	2,5	9
2/2.5D SR	16	5	3,2	Slope / bottom of ridge	31,4	<40	>5	7-11	0,5-1,3	8-12	<30	<10	23	3,7	6,12
2D SSD	50	15	3,33	Top of the ridge	4,6	Abs.	Abs.	Abs.	Abs.	Abs.	Abs.	Abs.	Abs.	Abs.	Abs.
USPB	Ø	Ø	Ø	Top of the ridge	29,7	90-120 60	Ø 20	Ø	Ø	Ø	Ø	Ø	Ø	Ø	Ø
2D SD	120	20	6	Slope / bottom of ridge	3,7	40-100	<4	111-224	6-27	8-12	Abs.	Abs.	Abs.	Abs.	Abs.
3D SD	140	20-50	7-2,8	Slope / bottom of the ridge	13,7	50-90	<15	150-300	10-25	8-12	70-80	<20	70	6	11

Table 1. *Summarize of the observed bedforms and comparison with two experimental studies (Dumas et al., 2005 and Perillo et al., 2014a). 3D CR (3D Current Ripples); 3D AR (3D Asymmetrical Ripples); 2/2.5D SR (2/2.5D Symmetrical ripples); 2D SSD (2D Symmetrical Medium Ripples); USPB (Upper Stage Plane Bed); 3D SD (3D Symmetrical Dunes); 2D SD (2D Symmetrical Dunes). λ(cm) bedform wavelength; η(cm) bedform elevation; U_o (cm.s-1) velocity of oscillatory flow; U_c (cm.s^{-1}) velocity of unidirectional flow; BI (λη^{-1}) bedform index; Ø: no data; Abs.: Not observed*

Fig. 3. *Bedforms and associated bedforms in the field. (A) 3D Current Ripples; (B) 3D Asymmetrical Ripples; (C) 2/2.5 D Symmetrical ripples; (D) Antidunes in the center of the residual channel are associated with 3D Current Ripples (on left) and Upper Stage Plane Bed (on the right); (E) 2D symmetrical Dunes associated with 3D Asymmetrical Ripples and Upper Stage Plane is also present on top right corner (white bar in the red circle in 20 cm); (F) 3D Symmetrical Dunes associated to 2/2.5 D Symmetrical ripples in the troughs (person for scale is 1.75 m high); (G) Association of bedforms in a runnel at the junction of two ridges, 3D Symmetrical Dunes are covered by 2/2.5 D Symmetrical ripples, 3D Current Ripples or 3D Asymmetrical Ripples. Note that 3D CR evolve as delta-like sediment accumulation within the trough (doted white line); (H) 3D Symmetrical Dunes, locally the hummocks are flattened (-f) and so replaced by Upper Stage Plane Bed. 2/2.5 D Symmetrical ripples are preserved in the troughs (white bar in the red circle in 20 cm).*

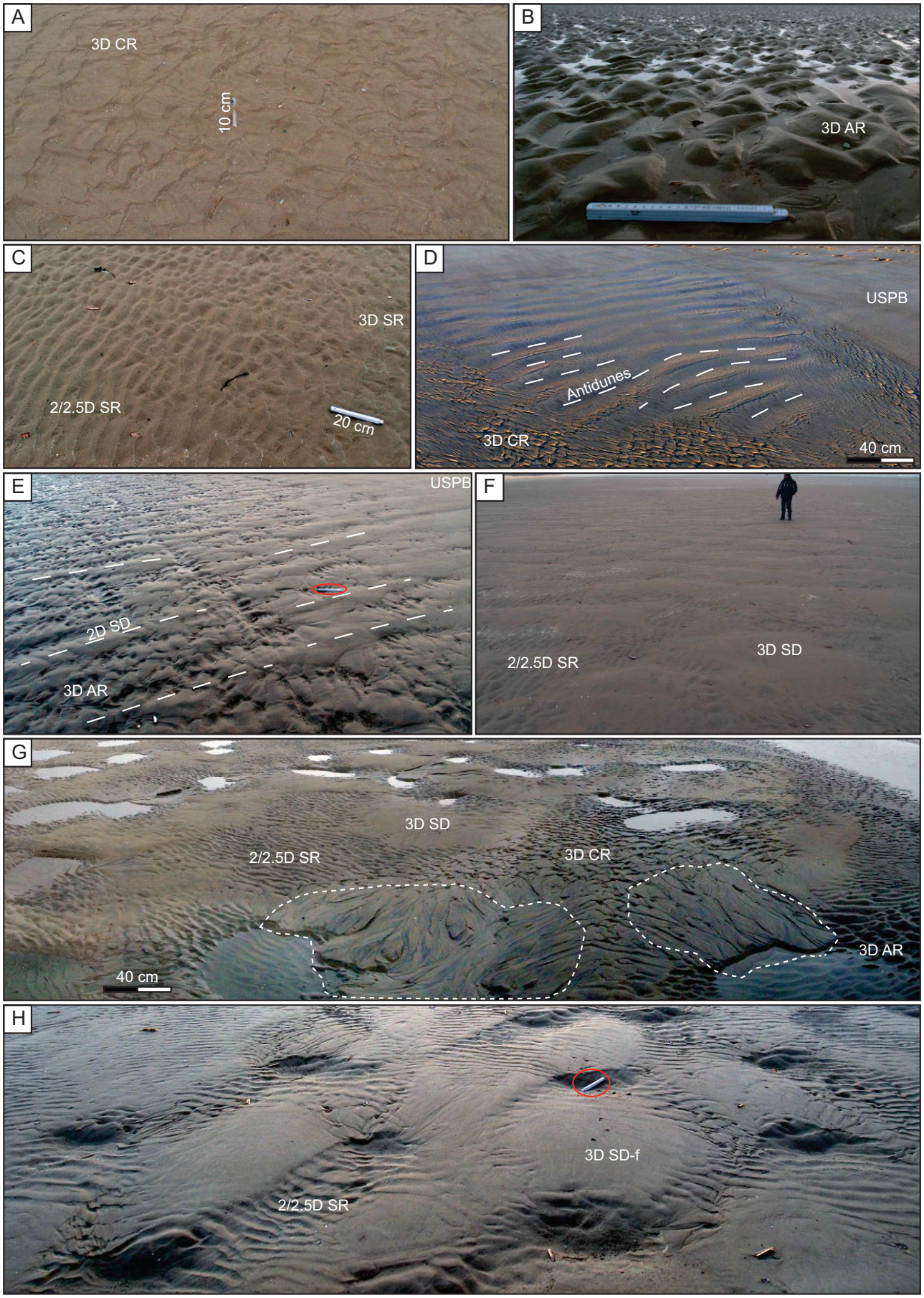
A
3D CR
10 cm
B
3D AR
C
3D SR
2/2.5D SR
20 cm
D
USPB
Antidunes
3D CR
40 cm
E
USPB
2D SD
3D AR
F
2/2.5D SR
3D SD
G
3D SD
2/2.5D SR
3D CR
3D AR
40 cm
H
3D SD-f
2/2.5D SR

The descriptions of the bedforms take into account the crest-to-crest spacing (or wavelength), the elevation (from trough to crest), sediment grain size, bedform symmetry/asymmetry and their general geometry (2D, 2.5D, 3D). Due to the homogeneous nature of the sediments that is deposited in the intertidal zone, no internal sedimentary structures are clearly visible. Once the bedforms described, a map of their distribution (Fig. 2) was achieved under SIG software (Quantion SIG) in order to constrain their relationship to each other.

4. Bedform descriptions and interpretations

Field analysis and ortho-images (Fig. 2) have permitted to define 8 bedforms (Figs. 3 and 4) in the intertidal zone of Berck Plage. Their main characteristics are summarized in Table 1, and compared to the description given by Dumas et al. (2005) and Perillo et al. (2014a). The observed bedforms are all constituted of fine to medium grained quartz. Two bedforms are only found on the ridges, two in the runnels, and four are generally encountered at the transition runnel - ridge.

4.1. 3D CR

Asymmetrical sedimentary structures are present, which are few centimeters high and display a mean crest-to-crest length of *ca.* 10 cm (Figs. 3A, D and G). The crest morphology is sinuous and these bedforms, only present in the lowest part of the runnel, are the less frequently observed in Berck-Plage. Generally, these bedforms are still submerged even during the lowest tidal state. The asymmetrical characteristics of these bedforms suggest they are formed by a unidirectional flow (e.g. Dumas et al., 2005; Harms, 1979; Perillo et al., 2014a). They are described as 3D Current Ripples (3D CR; *sensu* Perillo et al., 2014a). The current ripples can feed the troughs of larger bedforms to form small delta-*like* sediment accumulations (Fig. 3G).

4.2. 3D AR

Quasi-asymmetrical/asymmetrical structures of *ca.* 5 cm high and showing wavelengths of *ca.* 15 – 20 cm are observed (Figs. 3B, 4D and 4E). The crests are discontinuous and not straight. These bedforms are mainly orientated along NW-SE and SW-NE axes and are usually found laterally to the 3D CR on the bottom of the ridges still in the runnel part of the intertidal zone. These bedforms point to a combined-flow (oscillatory dominating) origin (e.g. Dumas et al., 2005; Harms, 1979; Perillo et al., 2014a). They are described as 3D Asymmetrical Ripples (3D AR; *sensu* Perillo et al., 2014a).

4.3. 2/2.5D SR

Symmetrical structures, few centimeters high, exhibiting a wavelength of 15 to 20 cm, orientated along a N-S axis are also frequently observed (Figs. 3B, 3C, 3G, 4A, 4B and 4F). The crests are continuous and straight (2D) and/or continuous but not straight (2.5D). These bedforms are usually present at the transition between the ridge and the runnel, higher on the slope of the ridges than the 3D AR. An oscillatory flow is responsible

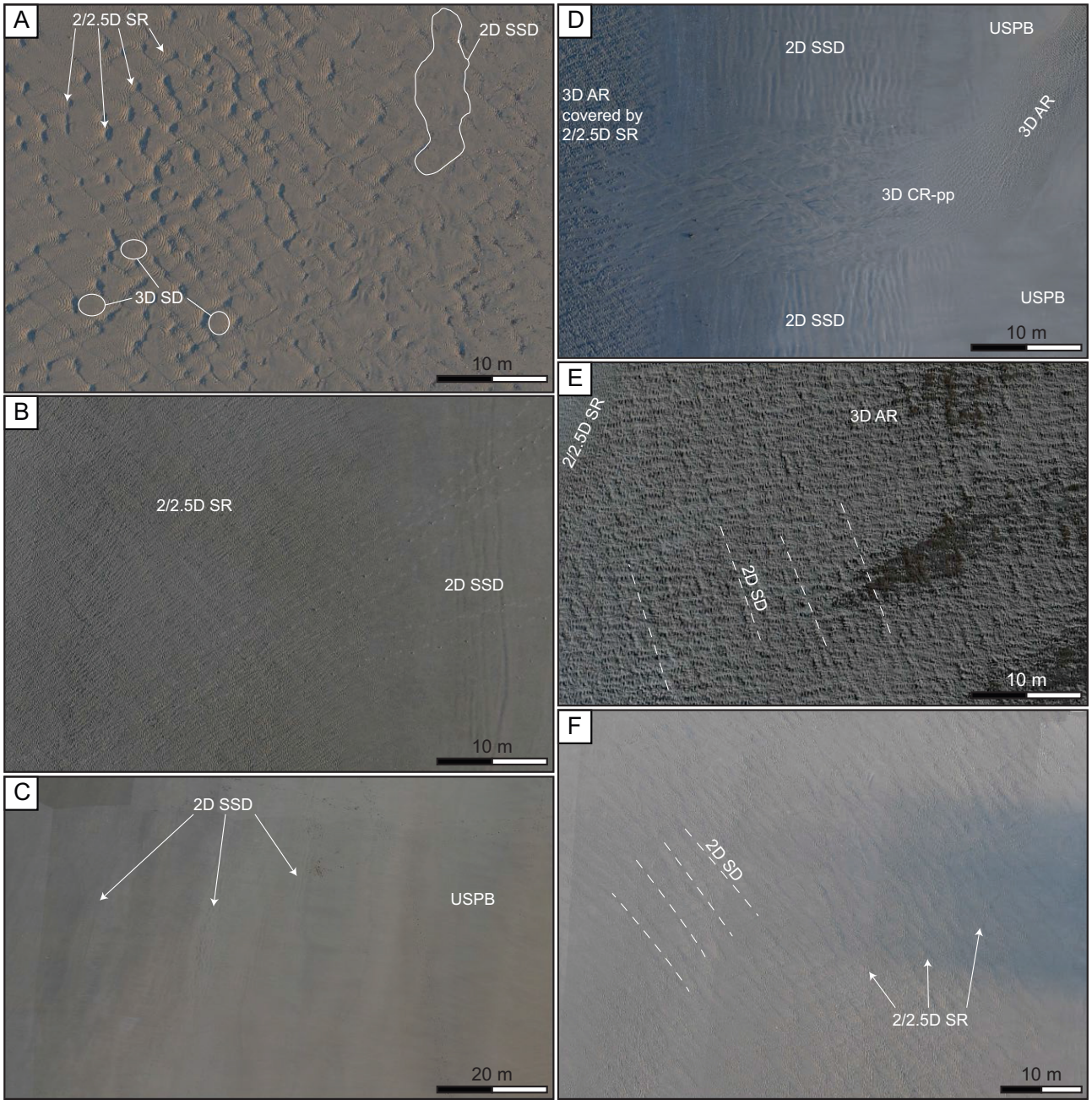

Fig. 4. *Bedforms and associated bedforms on the ortho-images. (A) 3D Symmetrical Dunes associated with 2/2.5 D Symmetrical ripples and 2D Small Symmetrical dunes (B) Transition from 2/2.5 D Symmetrical ripples (on left) to 2D Symmetrical Small Dunes (on the right); (C) Upper Stage Plane Bed associated to locally preserved 2D Small Symmetrical Dunes; (D) Transition from 3D Asymmetrical Ripples covered by 2D Symmetrical Ripples to 2D Small Symmetrical Dunes to Upper Stage Plane Bed; (E) 2D Symmetrical Dunes covered by 3D Asymmetrical Ripples, 2/2.5D Symmetrical Ripples are also present on the top left corner; (F) 2D Symmetrical Dunes with 2/2.5D Symmetrical Ripples within the troughs. Note that a meshed aspect is observed on pictures A, B, E and F.*

for the formation of these bedforms (e.g. Dumas et al., 2005; Harms, 1979; Perillo et al., 2014a). They are described as 2D/2.5D Symmetrical Ripples (2/2.5D SR; *sensu* Perillo et al., 2014a).

4.4. 2D SSD

Symmetrical structures, *ca.* 10 cm high, and showing a wavelength of *ca.* 50 cm can be observed at the transition ridge-runnel (Figs. 4A, 4B, 4C and 4D). They are elongated in a N-S direction. According to their symmetrical morphology an oscillatory flow is suggested for their formation (e.g. Dumas et al., 2005; Harms, 1979; Perillo et al., 2014a). However, concerning their names, regarding to their dimensions they can be classified either as dunes or ripples by Perillo et al. (2014a) (Table 1). Here these bedforms are described as 2D Symmetrical Small Dune (2D SSD) in order to be consistent with the used nomenclature. Intermediate bedforms such as 2D SSD, even if they can be physically generated, were not observed in the experimental study of Dumas et al. (2005). However, bedforms equivalent to 2D SSD were present, but not classified, in the experimental study of Perillo et al. (2014a).

4.5. USPB

Flat beds are the main observed bedforms on the ridges (Figs. 1B, 3D, 4C, 4D). These bedforms could result from an absence of sediment movement or to a high sediment movement generated by a high velocity current (oscillatory and/or unidirectional flow) (e.g. Dumas et al., 2005; Perillo et al., 2014a). According to the context (an intertidal zone) submitted to constant swash and surf processes, these bedforms are interpreted to be Upper Stage Plane Bed (USPB; *sensu* Perillo et al. 2014a) resulting from a high velocity current (swash and back-swash).

4.6. 2D SD

Large symmetrical structures, *ca*. 20 cm high, displaying a wavelength of *ca.* 120 cm are present in the runnels and are aligned along a NW-SE axis (Figs. 3E, 4E and 4F). Their crests are almost straight and continuous. These bedforms commonly occur at the transition between the ridge and the runnels. A combined-flow (dominance of the oscillatory component) is suggested for their genesis (e.g. Dumas et al., 2005; Harms, 1979; Perillo et al., 2014a). They correspond to the Symmetrical Large Ripples of Dumas et al. (2005) and are here described as 2D Symmetrical Dunes (2D SD) according to the nomenclature of Perrillo et al. (2014a). 2D SD can be observed associated with 2/2.5D SD (Fig. 4F) and 3D AR (Figs. 3E and 4E), these latter being mainly preserved within the trough of the 2D SD even if some are locally present on their crest.

4.7. 3D SD

Large symmetrical structures, 20 – 50 cm high and with a wavelength of *ca.* 140 cm, are present in the runnels (Figs. 3F, 3G, 3H and 4A). These bedforms have a general morphology of isolated hummocks, mainly aligned on the NW-SE and SW-NE axes. Hummocks display a dominance of rhombohedral spacing to each other, according to the classification of Allen (1985). These bedforms are most commonly located on the seaward side of the ridges slope, and preferentially at their extremities. A combined-flow (dominance of the oscillatory component) is proposed for their genesis (e.g. Dumas et al., 2005; Harms, 1979; Perillo et al., 2014a). There are described as 3D Symmetrical Dunes (3D SD; *sensu* Perillo et al. 2014a). 3D SD are observed associated to 2/2.5D SD (Figs.

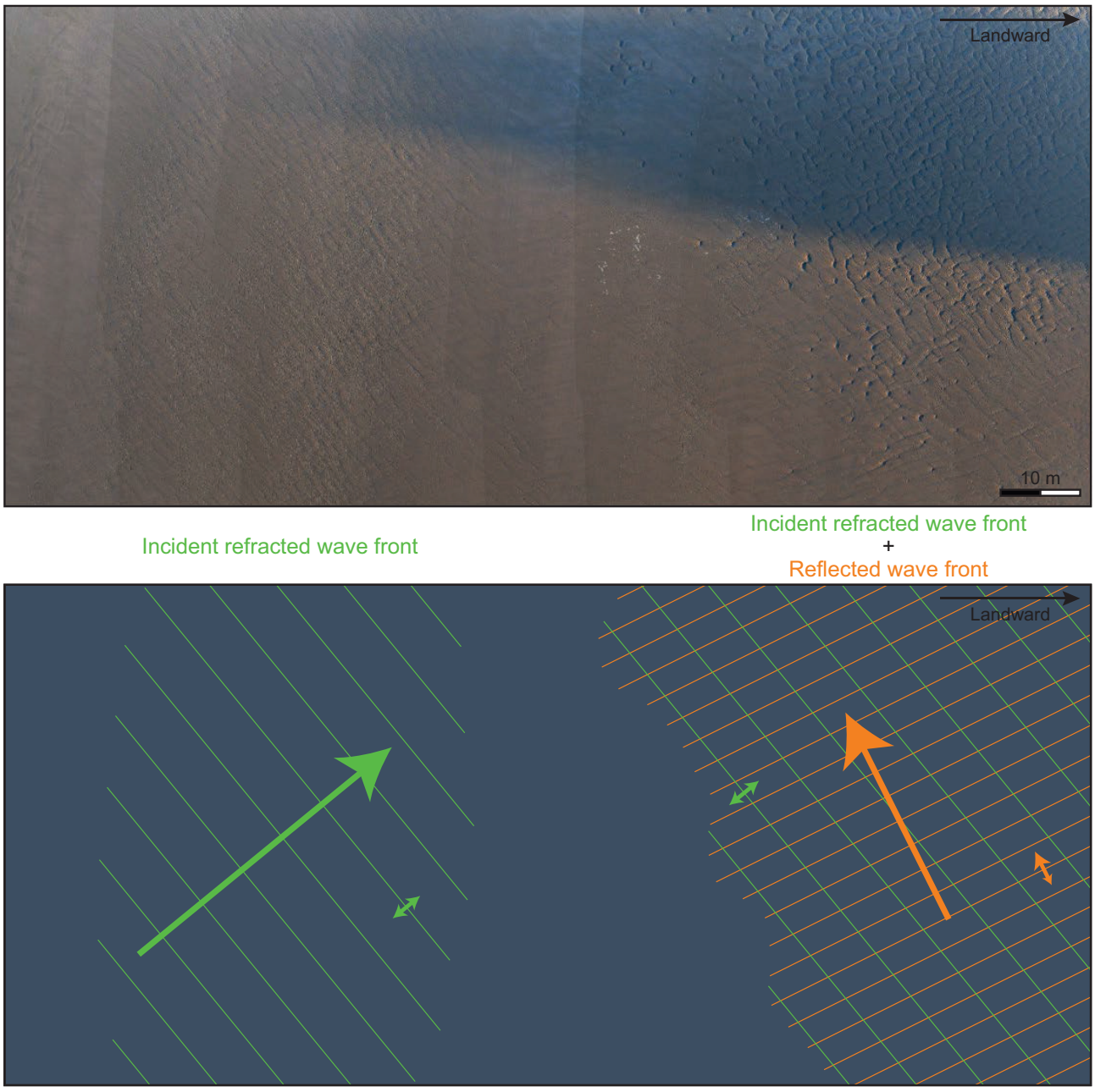

Fig. 5. *Meshed aspect of a runnel. This peculiar organization is likely explained by wave refraction. The incoming refracted wave (in green) formed NW-SE orientated 2D SD. By swashing on the beach with a certain angle, the wave is reflected, thus interfering with the incoming wave and creating the meshed aspect observed in the picture above. This meshed aspect is also visible in pictures in Figures 4A, B, E and F.*

3F, 3G, 3H), to 3D AR (Fig. 3G) or 3D CR (Fig. 3G), which all are mainly preserved within the trough of the 3D SD even some are locally present on the top of the hummocks. The 3D SD often exhibits a flattened hummock part (Fig. 3H; 3D SD-f) when located close to zones with dominant USPB bedforms.

4.8. Antidunes

Slightly asymmetrical bedforms, of *ca.* 5 cm high and with a 20 - 30 cm of wavelength were observed during their genesis within a channel crossing a ridge (Fig. 3D). At this location, the ebb-flow velocity was high and stationary waves were present. Theses bedforms are considered as antidunes (e.g. Alexander et al., 2001; Cartigny et al., 2014) formed by supercritical flows. Antidunes were rarely observed and no record of such bedforms was provided by the ortho-images.

4.9. Meshed organization of the bedforms

The bedforms observed in the runnels commonly display an organization as a grid that is well visible on ortho-images (Figs. 4A, B, E, F and 5). Sometimes well marked (Fig. 4E), sometimes less visible (Fig. 4B), the grid organization suggests two orientations of the bedforms, once with two oscillations of the same intensity, once with one dominant and one accessory oscillations. This organization in grid is also well marked when 3D SD are present giving a dominantly rhombohedral organization of these bedforms (Figs. 4A and 5).

5. Discussion

5.1. Bedform genesis

The bedforms and their distributions observed at low tide slack give an overview of the processes acting during a tidal cycle. From the trough of the runnels to the crest of the ridges the following bedforms occur: 3D CR, 3D AR, 2D SR, 2D SSD, then USPB. The pattern of bedform distribution is likely the same for each couplet of ridge-runnel (Figs. 2 and 6). 3D AR and 3D SR are more frequent in the outer part of the intertidal zone. According to Dumas et al. (2005) and Perillo et al. (2014a), the succession of bedforms from the top of the ridge to the center of the runnel suggests a transition from oscillatory-related (USPB) to oscillatory (2D SSD; 2D SR), to combined-oscillatory dominating (3D AR), and then to unidirectional flows (3D CR; Antidunes). USPB results of a high flow velocity, here considered as formed by the swash and back-swash of the waves on the ridges due to the collapse of the waves when their wave orbital is unsteady during decreasing water depth. 2D SSD as well as 2D SR need an oscillatory flow for their formation. It can be assumed

that they share the same flow parameters but, in order to explain their significantly different wavelength, shallower settings are inferred for 2D SSD. Furthermore, their position from the crest of the ridge to the slope of the runnel is always the same: USPB, 2D SSD then 2D SR (Figs. 2 and 6). 3D AR bedforms require an oscillatory dominating combined-flow for their formation. Since 3D AR are only observed without overprinted bedforms during the slack of low tide, it may be hypothesized that these bedforms are formed during the falling tide. The oscillatory motion responsible of 3D AR is wave activity, and according to their distribution (at the ridge-runnel transition), the unidirectional motion component of the combined-flow is provided by the ebb flow. 3D AR and 3D CR bedforms are mostly observed in the outer part of the intertidal zone where the ebb unidirectional flow is more important. The only pure unidirectional flow bedfrom generated corresponds to the 3D CR, interpreted as the final runoff of the ebb flow, which reworks material of the freshly formed 3D AR.

2D SD and 3D SD bedforms, which either are overprinted or truncated by other bedforms, are interpreted as being formed during rising tide. During the slack of high

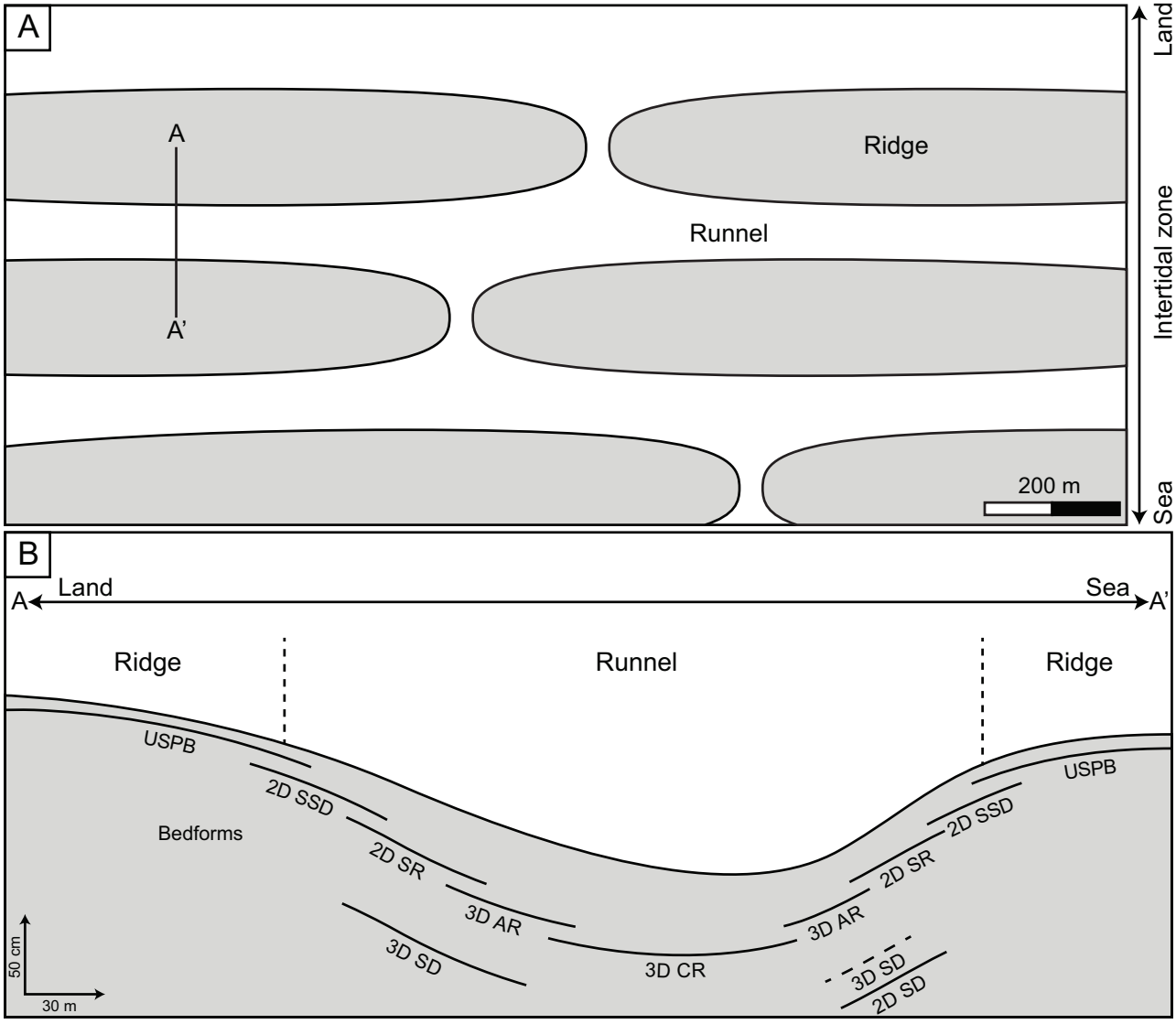

Fig. 6. *(A) Simplified representation of the intertidal ridge and runnel zone of Berck Plage, (B) Distribution of the bedforms observed during the slack of low tide through a ridge and runnel.*

tide, waves continuously pass over the submerged ridges and runnels, USPB is thus generated on the beach while oscillatory structures are formed in the submerged intertidal zone. Larger oscillatory structures (e.g. 2D SSD) are formed when and where the water depth is reduced (crest of the ridges), while smaller oscillatory structures (e.g. 2D SR) are generated under more important water depth (in the trough of the runnels). Furthermore, as explained by Beji and Battjes (1993), the wave frequency increases when passing over a submerged ridge. A diminution of the wavelength of the oscillatory structures is expected to occur from the trough of the runnel to the crest of the ridges but also between each landward couplet of ridge and runnel.

The Berck-Plage intertidal zone almost exclusively (*ca.* 95%; Table 1) consists of wave dominated sedimentary structures (except the 3D CR, which result in the runoff of the ebb flow). Dominance of oscillatory generated sedimentary structures in a macro- or mega-tidal context can be explained according to e.g. Reichmüth and Anthony (2007). The long residence time of wave processes during neap tides allows stronger offshore wave energy dissipation, while during spring tides larger waves are favored. Consequently, in both cases, wave flow largely exceeds tide flow. This implies that the potential of preservation of sedimentary tide-related structures is weaker than those formed by waves or storms (Li et al., 2000). This observation of a dominance of wave generated bedforms in a mega-tidal context have already be pointed out in a Canadian modern environment (Dashtgard et al., 2009; Dashtgard et al., 2012) but also recognized in the fossil record (Vaucher et al., in press).

5.2. Timing of bedform genesis

Across the intertidal zone of Berck-Plage eight bedforms were described and most of them are always found associated to other bedforms as it is shown in Figures 3B, C, D, F, G and H. Two examples of timing of bedform genesis are highlighted in Figure 7. Close to the shoreline of highest tide, 2D SR are mainly observed within the troughs of the 3D SD and the USPB replace the hummocky part of the 3D SD (Fig. 7A). According to the vertical (temporal) pattern, the 3D SD that are either overprinted by 2D SR or by UPSB, must have been generated first (during high tide). Once the falling tide start, 2D SR are generated and thus overprint the 3D SD (Fig. 7A). The sea level is still falling, and swash and back-swash process now act on the seafloor forming UPSB that flattened the zone (replacing the hummocky part of the 3D SD) and preserved the 2D SD within the trough of the 3D SD. Examples of some bedforms occurring within a runnel are given on Figure 7B. UPSB is present on the top of the ridge (top left corner of the picture) while 2D SD are observed on the slope of the runnel (a grid aspect occur due to the two observed orientations of the 2D SR) and 3D AR are limited to the central part of the runnel. 3D CR are not visible on the picture but occur under the residual submerged zone. 2D SR showing an orientation parallel to the runnel are considered to be formed during high tide (1 in Fig. 7) when the

ridges are still submerged. Sea-level continuing to fall (2), the ridge is close to be exposed and USPB are formed on the top of the ridges. When the ridge is fully exposed the runnel still allows wave propagation and thus 2D SR are formed that are orthogonally aligned with the runnel (2). In (3) the water is close to its lowest level, and unidirectional current increases, thus generating 3D AR and then 3D CR (when oscillatory process ceases).

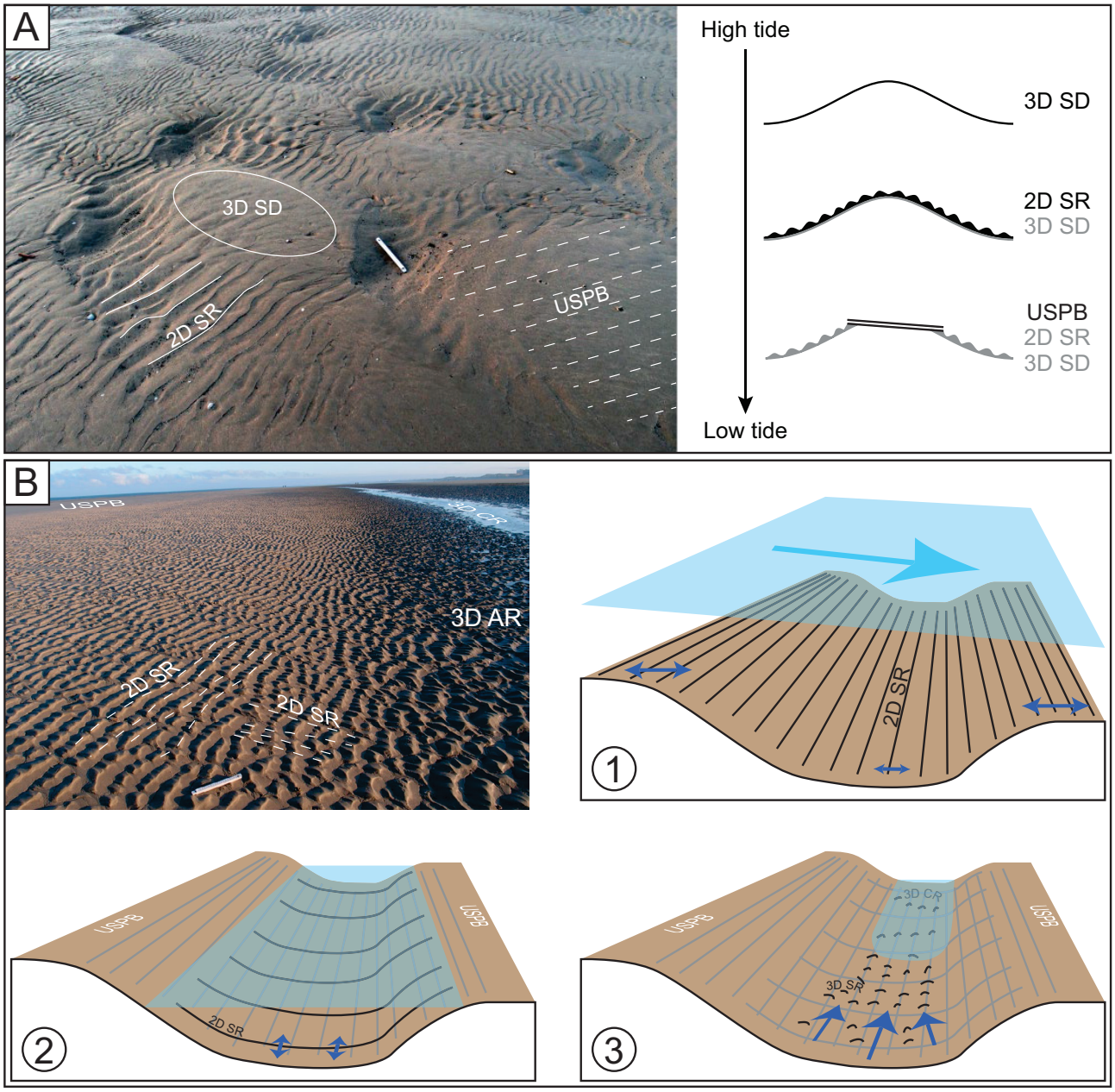

Fig. 7. *(A) Bedform succession observed close to the shoreline of highest tide. 2D SR are mainly observed within the troughs of the 3D SD, and the USPB replace the hummocky part of the 3D SD. The 3D SD are generated during high tide and then, during falling tide, 2D SR are generated. Sea level continuing to fall, swash process and back-swash process form UPSB, flattening the zone and preserving the 2D SD within the trough of the 3D SD. (B) Bedforms occurring within a runnel. UPSB is present on the ridge (top left corner) while 2D SD are observed on the slope of the runnel and 3D AR are limited to the central part of the runnel. 3D CR are not shown on the picture but occur under the small still submerged zone. 2D SR showing an orientation parallel to the runnel are considered to be formed during high tide (1). Sea-level falling, the ridge is close to be exposed and USPB are formed on the top of the ridges (2). When the ridge is fully exposed, the runnel still allows wave propagation and thus 2D SR are formed and are orthogonally aligned with the runnel (2). In (3), water is close to its lowest level and, during this step, unidirectional current has increased, thus generating 3D AR and then 3D CR (when oscillatory process ceases)*

Flow parameters being defined for the eight bedforms occurring in the intertidal zone of Berck-Plage, a hypothesis for their timing of generation can be proposed. In Figure 8, a step-by-step diagram is proposed to explain the spatial and temporal bedform genesis during falling- or rising-tide. During Step 1 (slack of high tide; Fig. 8) the runnel-ridge-runnel zone is fully submerged, thus the incident waves mostly generate small symmetrical-quasi-asymmetrical ripples (2/2.5 SR) across the entire submerged zone (Fig. 7B). Step 2 corresponds to the beginning of the falling-tide (Fig. 8). In this second step the ridge is still submerged but the water level has decreased. Thus larger symmetrical oscillatory structures (2D SSD) are formed at the top of the ridges (shallower conditions) (Figs. 4C and D), and the rest of the submerged zone is still dominated by 2/2.5D SR (deeper conditions) (Fig. 7B). The position through the intertidal zone of the 2D SD and the 3D SD (Figs. 2, 6 and 7A), which are both always overprinted by other bedforms (e.g. USPB, 2D SR; Figs. 3E, F, G, H, 4A, E, F, and 7A) are hypothesized to be formed during the falling- and/or the rising-tide. They are here considered to be generated during Step 2 and Step 3 because during Step 1, water depth and flow parameters of the incident waves would not allow such bedforms to be generated (the genesis of the 3D SD is discussed further in the text). In Step 3, the runnels are still submerged and the ridge is now exposed. In this configuration, swash and back swash processes occur on the seaward slope of the runnel thus forming plane stratifications (USPB), while the incoming waves will form oscillatory structures such as 2D SSD in the shallower part and 2/2.5D SR in the deeper part of the runnel (Fig. 8). The landward runnel will play a role of channel for the ebb-flow or flood-flow and a weak but still present oscillation occurs within the landward runnel promoting the formation of oscillatory- (2D SR) and combined-flow ripples (3D AR) on the border of the channel and current ripples (3D CR) at its center (Fig. 7B). The final or initial step of the diagram consists of the slack of low tide (Fig. 8). Step 4 exposed the landward runnel as well as the ridge. Swash and back swash processes still act on the seaward slope at the coastline but at a lower position than in Step 3 thus moving down the zone where USPB are formed. 2D SSD and 2/2.5D SR are still formed but their area of distribution is lower and seaward than in Step 3.

The bedform genesis through a tidal cycle shows that several successive bedforms can occur in a defined location during a tide cycle (Figs. 7 and 8). This implies that bedforms successively generated during a tidal cycle can theoretically be preserved in stratigraphic sedimentary successions. However, their potential of preservation is extremely weak as tide and wave intensity continuously varies. The most frequently recorded bedforms would probably be the USPB as the process responsible for its formation is the most powerful of those acting on the intertidal zone, and because the position of this swash/back-swash zone continuously changes along the intertidal zone during a tide cycle. The seven observed bedforms are bedforms generated during fair-weather, which implies that they could be eroded during each storm and then not being recorded (Immenhauser, 2009). However, several possibilities exist in order to preserved these bedforms: (1) the cross-

shore migration of the ridges (e.g. Grunnet and Ruessink, 2005; Ruessink and Kroon, 1994; Ruessink and Terwindt, 2000) through the intertidal zone implies that the seven bedforms can potentially be stacked together; and/or (2) a fast relative sea level rise combined with a high sediment input (e.g. Wheatcroft, 1990).

The recognition of such bedform pattern along an ancient sedimentary succession would be helpful for the paleoenvironmental reconstruction since they are diagnostics

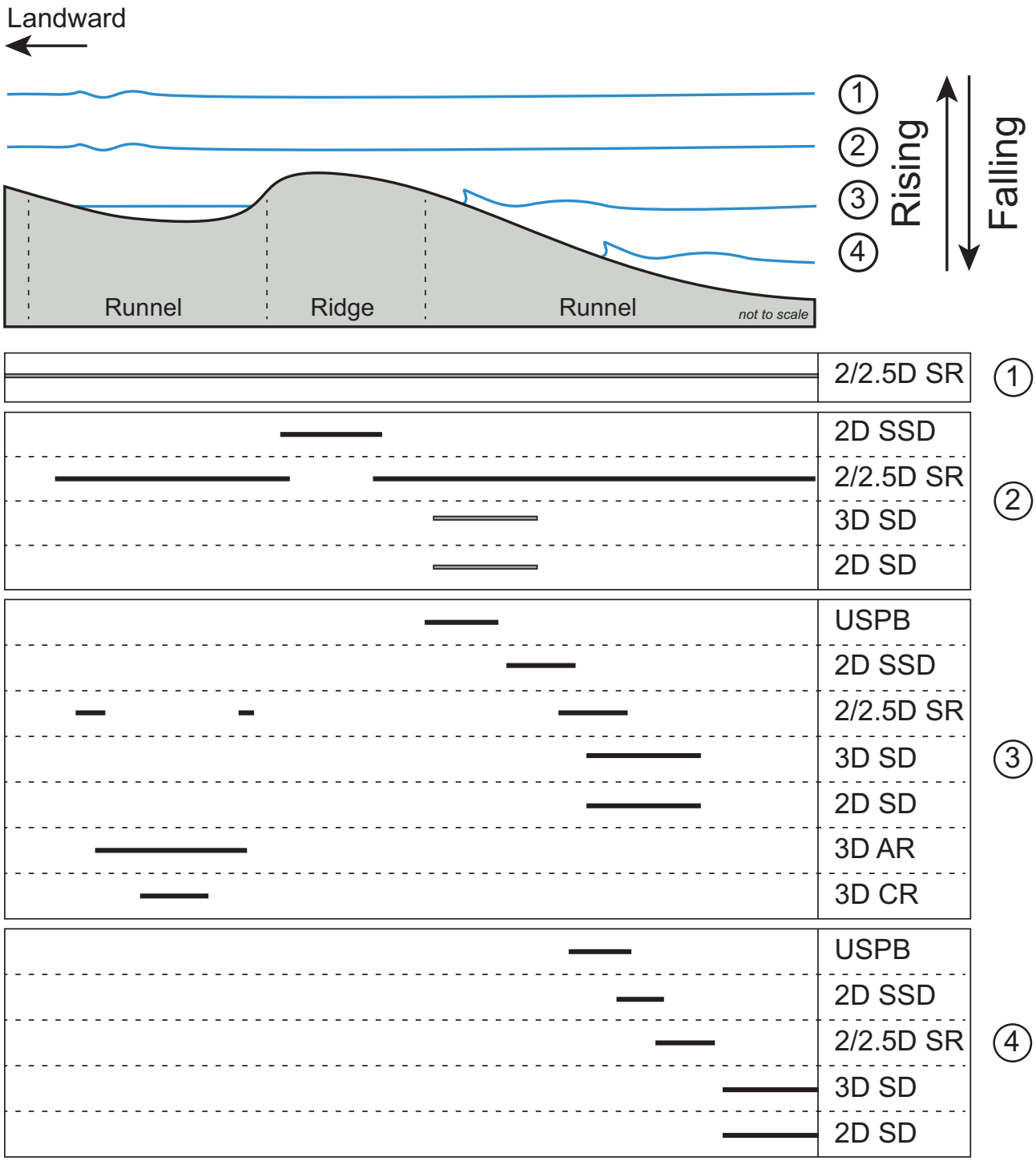

Fig. 8. *Bedform generation during a tidal cycle. 3D CR (3D Current Ripples); 3D AR (3D Asymmetrical Ripples); 2/2.5D SR (2/2.5D Symmetrical ripples); 2D SSD (2D Symmetrical Medium Ripples); USPB (Upper Stage Plane Bed); 3D SD (3D Symmetrical Dunes); 2D SD (2D Symmetrical Dunes). Black lines correspond to demonstrated bedform occurrence. Grey lines correspond to hypothesized bedform occurrence.*

of wave dominated tidally influenced environments but lacking of typical tidal structures (e.g. tidal dunes, flaser, wavy or lenticular beddings) because almost all bedforms are the results of oscillation (wave). Such bedform pattern has been recognized in the Lower Ordovician sedimentary succession of Morocco (Zini Formation). The Zini Formation was deposited in a storm- wave-dominated tide-modulated environment and exhibits very similar sedimentary structures than those described in the present study (Vaucher et al., in press). Symmetrical and slightly asymmetrical oscillatory sedimentary structures of various sizes sandwiched between dominantly low-angle or plane-parallel stratifications are observed in the Zini Formation.

5.3. Effect of the ridges on bedform wavelength

Bedforms are the expression of a flow (e.g. oscillatory, unidirectional or combined in water or air) at the sediment surface. In this study, the coastal environment is characterized by a ridge and runnel geomorphology, which differs from an unbarred low angle slope in a wave- or storm-dominated coast. This may have an impact on the incident wave edges and thus on the bedform distribution and shape. Masselink et al. (2006) proposed that the ridges result from the combined action of surf and swash processes succeeding during the tidal cycle. These ridges have been investigated northward of Berck-Plage, testifying to be relatively stable trough time in this area (even during storm conditions) (Levoy et al., 1998). However, in the continuity of Berck-Plage toward the north in the Netherlands, several surveys were realized and a succession of ridge genesis and degeneration occurs at a year scale: (1) generation near the shore; (2) migration seaward; and finally (3) degeneration (Grunnet and Ruessink, 2005; Ruessink and Kroon, 1994; Ruessink and Terwindt, 2000). Ridges may locally be destroyed during storm event but no cross-shore migration occurs (Sedrati and Anthony, 2007). The main process acting on the morphology of barred nearshore is the wave, and the responses of the bars are different according to the type, the intensity and the duration of the incident wave (Masselink et al., 2006). Ridge and runnel morphologies may display a considerable role in the bedform genesis. For example, experiments in laboratory (e.g. Beji and Battjes, 1993) describe the decrease of the wave amplitude associated with the generation of bound harmonics when a surface wave propagates over a submerged bar. Since the oscillatory flow is affected by positive topographies (ridges), the consequent generated bedforms will be also affected respectively to their positions across the intertidal zone (i.e. crest, slope or through):

$$\lambda = 0.65 d_o \quad (1)$$

where λ corresponds to the mean wavelength of the sedimentary structures formed under oscillatory flow and d_0 is the bottom orbital diameter, which is mainly a function of wave amplitude and water depth (Clifton, 1976; Komar, 1974). The coefficient 0.65 is commonly

used for oscillatory flow, however this value may differs to 0.7 (Yang et al., 2006) or to 0.82 (in the case of a combined flow; Perillo et al., 2014a). Furthermore, the bottom orbital velocity (U_o) responsible for the generation of oscillatory structures depends on the wave celerity (*c*). This quantity is provided by the dispersion relation:

$$c = \sqrt{\frac{g.L}{2\pi}.\tanh\left(\frac{2\pi.D}{L}\right)} \quad (2)$$

where *L* is the wavelength of the wave and *D* is the water depth. In this study the area is subjected to mega-tides, which imply that *D* constantly move up and down, thus modifying *c*, d_0 and by consequence λ of the generated bedforms.

5.4. Wave refraction and the meshed organization of the bedforms

The dependence of wave velocity on water depth mainly implies two phenomena when wave fronts get close to the shoreline: the decrease of the wavelength and the refraction of waves (Bühler, 2009; Landau and Lifshitz, 1987). This latter can be introduced from equation (2), where the wave celerity (*c*) is found to be reduced when the water depth (*D*) decreases. If we consider a swell arriving with an angle θ on a slopping beach (Fig. 9A), the part of the wave front located where the sea is shallower will travel at a smaller speed than the part of the wave front lying where the sea is deeper. This causes the wave crests to change their orientation until they become aligned with isobaths so that each part of the wave front then travels at the same speed in a direction that is perpendicular to the coast (Bascom, 1980).

The complex bathymetry observed in Berck-Plage and characterized by ridges and

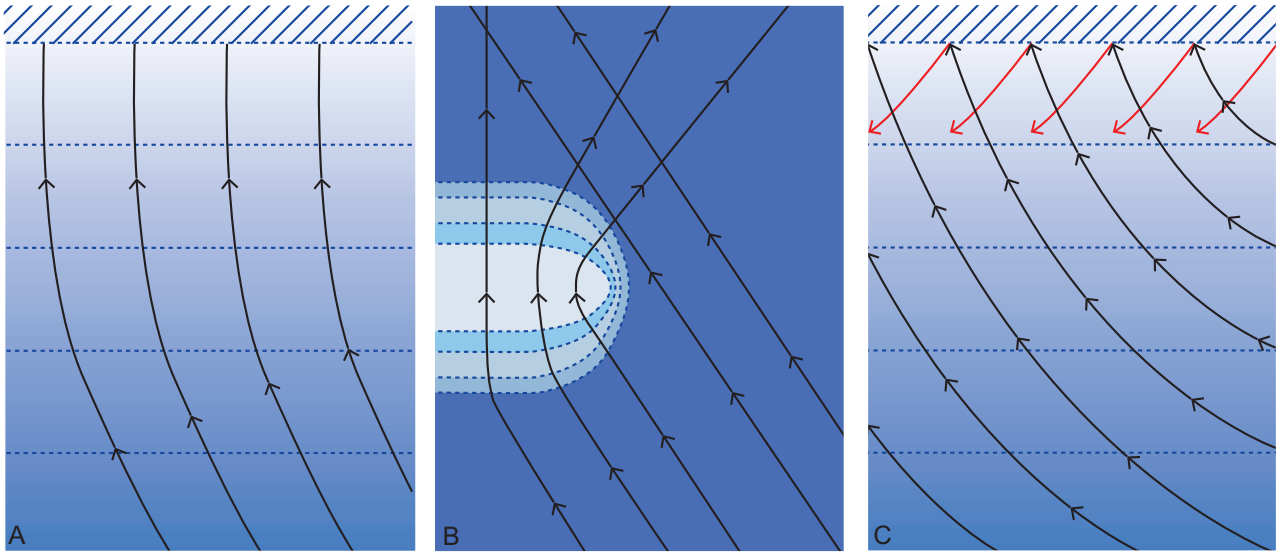

Fig. 9. *Three possible cases where waves are refracted. Black lines correspond to rays that are perpendicular to wave crests. Blue dotted lines are isobaths. Colors are associated to water depth: the darker the blue color is, the deeper the sea is. (A) Case of a slopping bottom uniform in one direction: wave refraction leads to the alignment of wave crests with the coast. (B) Ideal case of a ridge lying on a flat bottom: wave refraction leads to the generation of two wave fronts that propagate in different directions. (C) Case of a ridge lying of an uniform slopping bottom that shows the cross of the wave front at the coast.*

runnels can be responsible for the refraction of incoming waves when a shallow water regime takes place (either due to a strong amplitude of the waves, or to a low sea level). In particular (Figs. 2B and 9B) the extremities of the ridges will change the orientation of one part of the wave front whereas another part of the wave front keeps its initial direction of propagation. This refraction may lead: (1) to the propagation in the runnel part of two wave fronts that cross and act together over the seafloor (Fig. 9B); and/or (2) to force the incoming wave to swash with a certain angle and thus to be reflected (Fig. 9C). This mechanism could very likely explain the meshed aspect of the intertidal zone (as shown on Figs. 4A, B, E, F and 5). In this assumption, the dominant axis of bedform orientation can be inferred to the incoming wave with larger bottom orbital velocities or to the interaction of an incoming wave with the reflected swash. This effect due to the existence of ridges could also explain the genesis of the 3D SD structures observed in runnels either (1) as a result of a combined oscillatory flow mechanism, which is the sum of the contributions of two wave fronts and/or (2) as the results of the interaction between an incoming wave and the reflected swash.

Based on the literature (e.g. Cummings et al., 2009; Dumas et al., 2005; Perillo et al., 2014a), 3S SD are commonly formed under a dominating oscillatory flows with bottom orbital velocities ranging from: $50 < U_o < 100$ cm.s^{-1}. This range of bottom orbital velocities is common for storm condition on open continental shelves (e.g. Cummings et al., 2009 and references herein). According to the wave parameters described earlier in this study, the conditions during the observations of the intertidal zone were of fair-weather. However, bottom orbital velocities have not been measured, thus it is not excluded that bottom orbital velocities ranging from 50 to 100 cm.s^{-1} were present during the survey. By making the assumption that such U_o (50 - 100 cm.s^{-1}) were present, the 3D SD are expected to be formed uniformly all over the intertidal zone. However, the distribution is not uniform through the intertidal zone (Figs. 2 and 6). Then, U_o ranging from 50 to 100 cm.s^{-1} were possibly not present, and another process must be invoked to explain the genesis and patchy distribution of the 3D SD: the wave refraction leading to a wave-wave interference. The 3D SD bedforms have been observed elsewhere in France (Cap Ferret, Gironde; Côte Sauvage, Charente) (Fig. 10). Berck-Plage, Cap Ferret as well as Côte Sauvage, display all a irregular coastal morphologies (e.g. ridge and runnel, baines/rip channels), which are able to refract in the nearshore a part of the incident wave edge. In Cap Ferret but also in Côte Sauvage, the 3D SD are only observed within the baine system and are absent from the rest of the coast. Thus, these peculiar coastal morphologies probably promote the formation of 3D SD by wave refraction. All the observations of 3D SD in the three mentioned localities were all made during fair-weather conditions.

This 3D SD are characterized by a dome-*like* or hummock morphology, and are separated from each other by troughs (swales), and thus have an overall external morphology comparable to the hummocky cross-stratifications (HCS; e.g. Dott and Bourgeois, 1982; Harms et al., 1975). Unfortunately, the homogeneous grain size did not

allow us to observe the internal laminations in the 3D SD.

In this study, a wave-wave interaction is suggested for generating a combined oscillatory motion of particles at the sea floor, thus resulting in large, mostly symmetrical bedforms having common characteristics with HCS, and formed in the intertidal zone during fair-weather conditions. This would imply that HCS-*like* bedforms are not only diagnostic of storm deposits in the fossil record but can result from a wave-wave interference that can occur at various depths. The exact motion of the particles remains unknown, and further investigations are required especially concerning the bottom orbital velocities that occur during the formation of the 3D SD in order to confirm that low bottom orbital velocities can be responsible of the formation of the 3D SD in area characterized by wave-wave interference.

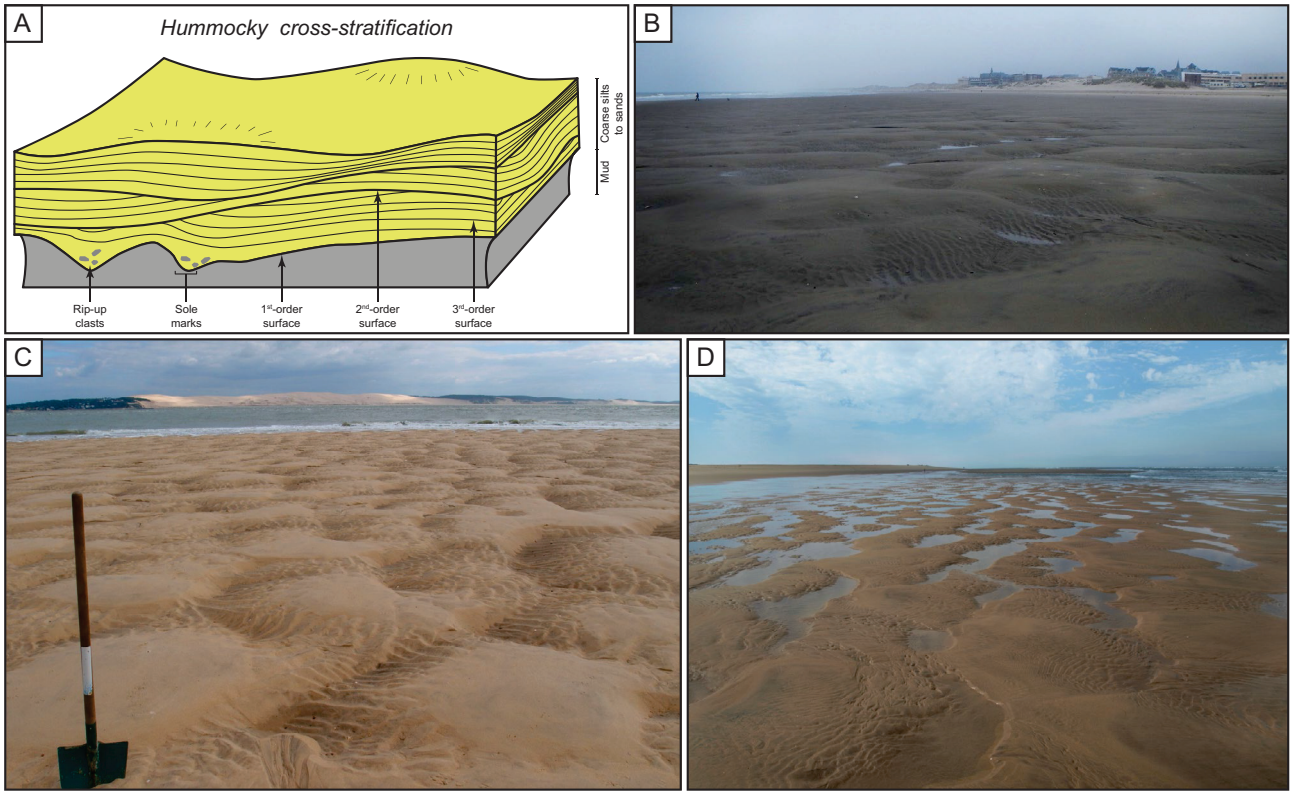

Fig. 10. *(A) Idealized hummocky cross-stratification (modified after Harms et al., 1975), internal hummock and swale stratifications are shown, as well as the classic dome-like external morphology. 3D SD observed in the intertidal zone of Berck-Plage (B), of the Cap-Ferret (Gironde Department, France) (C) and of the Côte Sauvage close to Oléron Island (Charente Department, France) (D), which all externally mimic hummocky cross-stratifications. In these three localities, these bedforms are only observed where peculiar coastal morphologies (presence of ridges, baines, rip channels) are able to refract the incoming waves, and thus to generate wave-wave interferences.*

6. Conclusion

The study of the intertidal zone of Berck-Plage has permitted to define and to map seven types of dominant bedforms (3D CR; 3D AR; 2D SR; 2D SSD; 2D SD; 3D SD; USPB) observed at low tide, which occur during fair-weather conditions. The analysis of the seven defined bedforms allows us to characterize the flow parameters responsible of both their formation and distribution. The findings confirm the dominance of bedforms having oscillatory flow affinities even if the area was submitted to mega-tides (tide of the century). The survey in this area has permitted to propose a timing of formation for each encountered bedform. The stacking pattern of the bedforms can be translated as a stratigraphic succession and thus be applied for ancient sedimentary succession as keys of recognition for wave-dominated tidally modulated proximal environment when no pure tide generated structures are present. Complex geomorphology of costal environments (here ridge and runnel) induces wave refraction that likely explains the grid organization of the bedforms as well as the formation of 3D SD that share common external characteristics with hummocky cross-stratifications. It appears that 3D SD (HCS-*like*) could be formed under lower bottom orbital velocities than previously proposed in the literature by wave-wave interference that creates a combined motion of particles on the seafloor.

Acknowledgements

This research did not receive any specific grant from funding agencies in the public, commercial, or not-for-profit sectors. We are thankful to _____ and _____ for their sensible remarks that helped us to improve the quality of the manuscript.

References

Alexander, J., Bridge, J.S., Cheel, R.J., Leclair, S.F., 2001. Bedforms and associated sedimentary structures formed under supercritical water flows over aggrading sand beds. Sedimentology, 48(1): 133-152.

Allen, J.R.L., 1985. Principles of Physical Sedimentology. London, Allen & Unwin, 272 pp.

Allen, P.A., 1997. Earth Surface Processes. Blackwell Science, London, UK, 404 pp.

Anthony, E.J., Levoy, F., Monfort, D., Degryse-Kulkarni, C., 2005. Short-term intertidal bar mobility on a ridge-and-runnel beach, Merlimont, northern France. Earth Surface Processes and Landforms, 30(1): 81-93.

Anthony, E.J., Levoy, F., Monfort, O., 2004. Morphodynamics of intertidal bars on a megatidal beach, Merlimont, Northern France. Marine Geology, 208(1): 73-100.

Augris, C., Clabaut, P., Costa, S., Gourmelon, F., Latteux, B., 2004. Evolution morpho-sédimentaire du domaine littoral et marin de la Seine-Maritime. Conseil Général de la Seine-Maritime, EDF, 2d. Ifremer, Bilans et Perspectives, Ifremer, 159 p.

Bascom, W., 1980. Waves and beaches; the dynamics of the ocean surface, (Revised an. ed).

Basilici, G., De Luca, P.H.V., Oliveira, E.P., 2011. A depositional model for a wave-dominated open-coast tidal flat, based on analyses of the Cambrian–Ordovician Lagarto and Palmares formations, north-eastern Brazil. Sedimentology, 59(5): 1613-1639.

Basilici, G., de Luca, P.H.V., Poire, D.G., 2012. Hummocky cross-stratification-like structures and combined-flow ripples in the Punta Negra Formation (Lower-Middle Devonian, Argentine Precordillera): A turbiditic deep-water or storm-dominated prodelta inner-shelf system? Sedimentary Geology, 267: 73-92.

Battiau-Queney, Y., Billet, J.F., Chaverot, S., Lanoy-Ratel, P., 2003. Recent shoreline mobility and geomorphologic evolution of macrotidal sandy beaches in the north of France. Marine Geology, 194(1–2): 31-45.

Beji, S., Battjes, J.A., 1993. Experimental investigation of wave propagation over a bar. Coastal Engineering, 19(1): 151-162.

Bühler, O., 2009. Waves and Mean Flows. Cambridge University Press.

Cartigny, M.J.B., Ventra, D., Postma, G., van Den Berg, J.H., 2014. Morphodynamics and sedimentary structures of bedforms under supercritical-flow conditions: New insights from flume experiments. Sedimentology, 61(3): 712-748.

Chauhan, P.P.S., 2000. Bedform Association on a Ridge and Runnel Foreshore: Implications for the Hydrography of a Macrotidal Estuarine Beach. Journal of Coastal Research, 16(4): 1011-1021.

Clifton, H.E., 1976. Wave-generated structures: a conceptual model. in Davis, J.R.A.,

and Ethrington, R.L., eds., Beach and Nearshore Processes: Society of Economic Paleontologists and Mineralogists, Special Publication(24): 126-148.

Clifton, H.E., Hunter, R.E., Phillips, R.L., 1971. Depositional structures and processes in the non-barred high-energy nearshore. Journal of Sedimentary Research, 41(3).

Cram, J.M., 1979. The influence of continental shelf width on tidal range: paleoceanographic implications. The Journal of Geology: 441-447.

Cummings, D.I., Dumas, S., Dalrymple, R.W., 2009. Fine-grained versus coarse-grained wave ripples generated experimentally under large-scale oscillatory flow. Journal of Sedimentary Research, 79(1-2): 83-93.

Dalrymple, R.W., 1992. Tidal depositional systems. Facies models: Response to sea level change: 195-218.

Dalrymple, R.W., 2003. Sedimentology and stratigraphy of a tide-dominated, foreland-basin delta (Fly River, Papua New Guinea).

Dashtgard, S.E., Gingras, M.K., MacEachern, J.A., 2009. Tidally modulated shorefaces. Journal of Sedimentary Research, 79(11-12): 793-807.

Dashtgard, S.E., MacEachern, J.A., Frey, S.E., Gingras, M.K., 2012. Tidal effects on the shoreface: Towards a conceptual framework. Sedimentary Geology, 279: 42-61.

Davis Jr, R.A., 1985. Beach and nearshore zone, Coastal sedimentary environments. Springer, pp. 379-444.

Davis Jr, R.A., Hayes, M.O., 1984. What is a wave-dominated coast? Marine Geology, 60(1–4): 313-329.

Davis, R.A.J., Dalrymple, R.W., 2012. Principles of tidal sedimentology. Springer.

Dott, R., Bourgeois, J., 1982. Hummocky stratification: significance of its variable bedding sequences. Geological Society of America Bulletin, 93(8): 663-680.

Dumas, S., Arnott, R.W.C., Southard, J.B., 2005. Experiments on Oscillatory-Flow and Combined-Flow Bed Forms: Implications for Interpreting Parts of the Shallow-Marine Sedimentary Record. Journal of Sedimentary Research, 75(3): 501-513.

Grunnet, N.M., Ruessink, B.G., 2005. Morphodynamic response of nearshore bars to a shoreface nourishment. Coastal Engineering, 52(2): 119-137.

Hale, P.B., McCann, S.B., 1982. Rhythmic topography in a mesotidal, low-wave-energy environment. Journal of Sedimentary Petrology, 52: 415-429.

Harms, J., 1979. Primary sedimentary structures. Annual Review of Earth and Planetary Sciences, 7: 227.

Harms, J.C., Southard, J.B., Spearing, D.R., Walker, R.G., 1975. Depositional environments as interpreted from pri- mary sedimentary structures and stratification sequences. SEPM Short Course, 2.

Immenhauser, A., 2009. Estimating palaeo-water depth from the physical rock record. Earth-

Science Reviews, 96(1): 107-139.

King, C.A.M., 1972. Beaches and Coasts, 2nd edition. Edward Arnold, London.

King, C.A.M., Williams, W.W., 1949. The Formation and Movement of Sand Bars by Wave Action. The Geographical Journal, 113: 70-85.

Komar, P.D., 1974. Oscillatory ripple marks and the evaluation of ancient wave conditions and environments. Journal of Sedimentary Research, 44(1): 169-180.

Kroon, A., Masselink, G., 2002. Morphodynamics of intertidal bar morphology on a macrotidal beach under low-energy wave conditions, North Lincolnshire, England. Marine Geology, 190(3–4): 591-608.

Landau, L., Lifshitz, E., 1987. Fluid Mechanics. volume 6 of Courses of Theoretical Physics. 2nd edition, Pergamon Press, Oxford.

Lashteh Neshaei, M.A., Holmes, P., Gholipour Salimi, M., 2009. A semi-empirical model for beach profile evolution in the vicinity of reflective structures. Ocean Engineering, 36(17–18): 1303-1315.

Levoy, F., Anthony, E., Barusseau, J.-P., Howa, H., Tessier, B., 1998. Morphodynamique d'une plage macrotidale à barres. Comptes Rendus de l'Académie des Sciences - Series IIA - Earth and Planetary Science, 327(12): 811-818.

Levoy, F., Anthony, E.J., Monfort, O., Larsonneur, C., 2000. The morphodynamics of megatidal beaches in Normandy, France. Marine Geology, 171(1–4): 39-59.

Li, C., Wang, P., Daidu, F., Bing, D., Tiesong, L., 2000. Open-coast intertidal deposits and the preservation potential of individual laminae: a case study from east-central China. Sedimentology, 47(5): 1039-1051.

Masselink, G., 2004. Formation and evolution of multiple intertidal bars on macrotidal beaches: application of a morphodynamic model. Coastal Engineering, 51(8–9): 713-730.

Masselink, G., Anthony, E.J., 2001. Location and height of intertidal bars on macrotidal ridge and runnel beaches. Earth Surface Processes and Landforms, 26(7): 759-774.

Masselink, G., Kroon, A., Davidson-Arnott, R.G.D., 2006. Morphodynamics of intertidal bars in wave-dominated coastal settings — A review. Geomorphology, 73(1–2): 33-49.

McLane, M., 1995. Sedimentology. Oxford university press, New York; Oxford, 423 pp.

Perillo, M.M., Best, J., Garcia, M.H., 2014a. A New Phase Diagram for Combined-Flow Bedforms. Journal of Sedimentary Research, 84(4): 301-313.

Perillo, M.M., Best, J.L., Yokokawa, M., Sekiguchi, T., Takagawa, T., Garcia, M.H., 2014b. A unified model for bedform development and equilibrium under unidirectional, oscillatory and combined-flows. Sedimentology, 61(7): 2063-2085.

Perillo, M.M., Prokocki, E.W., Best, J.L., García, M.H., 2014c. Bed form genesis from bed defects under unidirectional, oscillatory, and combined flows. Journal of Geophysical

Research: Earth Surface, 119(12): 2635-2652.

Pierrot Deseilligny, M., 2015. Apero, Pastis and Other Beverages in a Nutshell! <http://logiciels.ign.fr/IMG/pdf/docmicmac-2.pdf>.

Pierrot Deseilligny, M., Clery, I., 2011. Apero, AN Open Source Bundle Adjusment Software for Automatic Calibration and Orientation of Set of Images. International Archives of the Photogrammetry, Remote Sensing and Spatial Information Sciences, 38: 269-276.

Plint, A.G., 2010. Wave-and storm-dominated shoreline and shallow-marine systems. In: R.W. Dalrymple, N.P. James (Eds.), Facies models. Geol. Assoc. Canada, St John's, pp. 167-200.

Reichmüth, B., Anthony, E.J., 2007. Tidal influence on the intertidal bar morphology of two contrasting macrotidal beaches. Geomorphology, 90(1–2): 101-114.

Rossi, V.M., Steel, R.J., 2016. The role of tidal, wave and river currents in the evolution of mixed-energy deltas: Example from the Lajas Formation (Argentina). Sedimentology, 63(4): 824-864.

Ruessink, B.G., Kroon, A., 1994. The behaviour of a multiple bar system in the nearshore zone of Terschelling, the Netherlands: 1965–1993. Marine Geology, 121(3): 187-197.

Ruessink, B.G., Terwindt, J.H.J., 2000. The behaviour of nearshore bars on the time scale of years: a conceptual model. Marine Geology, 163(1–4): 289-302.

Sedrati, M., Anthony, E.J., 2007. Storm-generated morphological change and longshore sand transport in the intertidal zone of a multi-barred macrotidal beach. Marine Geology, 244(1–4): 209-229.

Short, A., 1991. Macro-meso tidal beach morphodynamics: An overview. Journal of Coastal Research: 417-436.

Short, A.D., 1984. Beach and nearshore facies: Southeast Australia. Marine Geology, 60(1–4): 261-282.

Sipka, V., Anthony, E.J., 1999. Morphology and hydrodynamics of a macrotidal ridge and runnel beach under modal low wave conditions. Journal de Recherche Océanographique, 24: 25-31.

Stépanian, A., Levoy, F., 2003. Séquences d'évolution morphodynamique des barres intertidales d'une plage macrotidale : l'exemple d'Omaha beach (Normandie, France). Oceanologica Acta, 26(2): 167-177.

Vakarelov, B.K., Ainsworth, R.B., MacEachern, J.A., 2012. Recognition of wave-dominated, tide-influenced shoreline systems in the rock record: Variations from a microtidal shoreline model. Sedimentary Geology, 279: 23-41.

van Houwelingen, S., Masselink, G., Bullard, J., 2006. Characteristics and dynamics of

multiple intertidal bars, north Lincolnshire, England. Earth Surface Processes and Landforms, 31(4): 428-443.

Vaucher, R., Pittet, B., Hormière, H., Martin, E., Lefebvre, B., in press. A wave-dominated, tide-modulated model for the Lower Ordovician of the Anti-Atlas, Morocco. Sedimentology.

Voulgaris, G., Simmonds, D., Michel, D., Howa, H., Collins, M.B., Huntley, D.A., 1998. Measuring and Modelling Sediment Transport on a Macrotidal Ridge and Runnel Beach: An Intercomparison. Journal of Coastal Research, 14(1): 315-330.

Wheatcroft, R.A., 1990. Preservation potential of sedimentary event layers. Geology, 18(9): 843-845.

Wijnberg, K.M., Kroon, A., 2002. Barred beaches. Geomorphology, 48(1–3): 103-120.

Yang, B., Chun, S.S., 2001. A seasonal model of surface sedimentation on the Baeksu open-coast intertidal flat, southwestern coast of Korea. Geosciences Journal, 5(3): 251-262.

Yang, B., Dalrymple, R., Chun, S., 2005. Sedimentation on a wave-dominated, open-coast tidal flat, south-western Korea: summer tidal flat - winter shoreface. Sedimentology, 52(2): 235-252.

Yang, B., Dalrymple, R.W., Chun, S., 2006. The significance of hummocky cross-stratification (HCS) wavelengths: Evidence from an open-coast tidal flat, South Korea. Journal of Sedimentary Research, 76(1-2): 2-8.

Yang, B., Gingras, M.K., Pemberton, S.G., Dalrymple, R.W., 2008. Wave-generated tidal bundles as an indicator of wave-dominated tidal flats. Geology, 36(1): 39-42.

III) Résumé de l'article concernant Arcachon :

La zone intertidale du Cap-Ferret (Sud-Ouest de la France) est un environnement côtier dominé par l'action de la houle sous influence de marée semi-diurne macrotidale. A travers cette zone intertidale, des morphologies sédimentaires en dômes rappelant celles de stratifications entrecroisées en mamelons (HCS) sont observées à marée basse. Ces dernières présentent une longueur d'onde d'environ 1,2 m pour une élévation d'environ 30 cm. Ces mamelons sont uniquement formés lorsque la houle incidente présente une hauteur significative. Les stratifications internes de ces dômes sont en creux, sub-planes, tangentielles, tabulaires et en *hummocks*. Les stratifications tabulaires et tangentielles sont caractérisées par des foresets progradants qui montrent des variations d'angles de leur pente. Les bottomsets des stratifications tangentielles sont la plupart du temps érosifs, d'où un aspect de surcreusement basal. Ces mamelons ont été jusqu'alors généralement considérés comme étant des HCS en accrétion latérale formées par la houle en condition de beau temps durant un cycle de marée. Cependant, les sets de laminations observés partagent plus de caractéristiques communes avec ceux formés par des flux supercritiques dans des simulations analogiques. Ces morphologies particulières ont été observées à la zone de transition surf-swash où le reflux des vagues ayant déferlé peut atteindre des conditions supercritiques. Ce type de flux peut expliquer les structures internes mais pas l'aspect général en dôme (structure 3D) de ces morphologies. Afin d'expliquer la formation localisée de ces mamelons, une réfraction de la houle initiée par la géomorphologie côtière non linéaire (présence de baïnes) génère des fronts d'ondes croisés qui seront à l'origine de la structure 3D des dômes. Cette étude propose que, en conditions supercritiques, le reflux des vagues agissant à la transition surf-swash associé à une réfraction de la houle sur la côte génère des morphologies en dôme mimant celle des HCS.

IV) Article :

Hummocky bedforms in the intertidal zone as the results of supercritical flows and wave-wave interference?

Auteurs : **Romain Vaucher**, Bernard Pittet, Thomas Humbert, Serge Ferry

Article en preparation

Abstract

The intertidal zone of Cap-Ferret (SW of France) is a costal wave dominated, tidally modulated environment with a semidiurnal macro-tidal range displaying peculiar dome-like bedforms reminiscent of the hummocky cross-stratifications (HCS). These bedforms are recognized at low tide across the intertidal zone, and exhibit a wavelength of *ca*. 1.2 m and an elevation of *ca*. 30 cm. They only occur when incident wave height is significant. The internal stratifications are characterized by trough stratifications, sub-planar stratifications, tangential stratifications, tabular stratifications, as well as hummocky-like stratifications. The tabular and tangential stratifications are characterized by a set of prograding foresets that almost always show variations in their steepness. Downcutting in the bottomsets of the tangential stratifications is commonly observed. These bedforms were previously classified as HCS with lateral accretion formed under fair-weather conditions during a tide cycle. However, the displayed sets of laminae observed in the bedforms share more characteristics with those formed by supercritical-flows observed in flume experiments. These peculiar bedforms are observed at the surf-swash transition zone where backwash flows are supercritical. This type of flow alone could explain the internal architecture but not the general distribution as dome-like (3D) bedforms. In order to explain the localized formation of such bedforms a wave-wave interference initiated by the geomorphology (i.e. baine) of the coastal environment is hypothesized. This study proposes that supercritical-flow occurring at the surf-swash transition zone and wave-wave interference generate dome-like bedforms that can morphologically mimic hummocky cross-stratifications.

Keywords waves, tides, dome-like bedforms, supercritical flow, HCS, wave refraction

1. Introduction

Intertidal zones dominated by wave action display a panel of sedimentary structures such as symmetrical / asymmetrical ripples or dunes, upper stage plane beds, where all these structures can be diachronically and/or synchronically formed and overprinted each other (e.g. Chauhan, 2000; Vaucher et al., submitted). Peculiar bedforms with a dome-like external shape also occur (Fig. 1). They are commonly named megaripples or hydraulic dunes with current process affinities (e.g. Chauhan, 2000; Gallagher, 2003; Swales et al., 2006; Larsen et al., 2015). However, these peculiar bedforms tend to be formed only when the incoming wave reach a significant height, and are therefore linked to wave action rather than to current processes (e.g. Dabrio, 1982; Chauhan, 2000). Such dome-like external morphologies likely resemble to the 3D Symmetrical Dunes (3D SD *sensu* Perillo et al., 2014) observed across the intertidal zone of Berck-Plage (Vaucher et al., submitted). However for the Cap-Ferret, according to their external morphology and internal structures, these bedforms were interpreted as hummocky cross-stratifications (HCS) of fair-weather by Thiry-Bastien (2002) and Ferry (2015) that display both vertical and lateral accretion.

HCS were firstly observed by Campbell (1966), and then described by Harms et al. (1975) who defined this peculiar sedimentary structure (Fig. 2) by the following points: (1) its large size (normally with wavelengths of 1 to 5 m and heights up to 0.5 m); (2) the cross-stratifications exhibit no preferential orientation; (3) the structure includes lower bounding surfaces of sets, which are erosional and dip at low angles; (4) it includes laminations that laterally vary in thickness; and (5) the steepness of the internal laminations typically diminishes upwards. However, the internal stratifications of the dome-like bedforms share common characteristics with those formed under supercritical flow conditions (antidunes, cyclic steps, chutes-and-pools; e.g. Cartigny et al., 2014). Several studies were led on sedimentary structures either formed by supercritical-flows in flume experiments (e.g. Alexander et al., 2001; Cartigny et al., 2014), or described in various ancient and modern environments (e.g. Schmincke et al., 1973; Langford and Bracken, 1987; Marren et al., 2009; Ghienne et al., 2010; Lang et al., 2012; Lang and Winsemann, 2013), or were digitally modelled (e.g. Hughes and Stewart, 1961; Broome and Komar, 1979; Brocchini and Peregrine, 1996; Baldock and Holmes, 1999; Longo et al., 2002). The only study that linked the dome-like sedimentary structures and supercritical flows in modern coastal environments is the study by Broome and Komar (1979) but these authors did not describe the internal sedimentary structures of these bedforms. As highlighted by Alexander et al. (2001) precautions must be taken for the distinction between sedimentary structures formed under supercritical-flows and HCS, because the organization of the laminations in these two types of bedforms display very similar patterns.

In the present study peculiar dome-like bedforms of *ca.* 1.2 m of wavelength with an elevation of *ca.* 30 cm are recognized through the intertidal zone of Cap-Ferret (Gironde

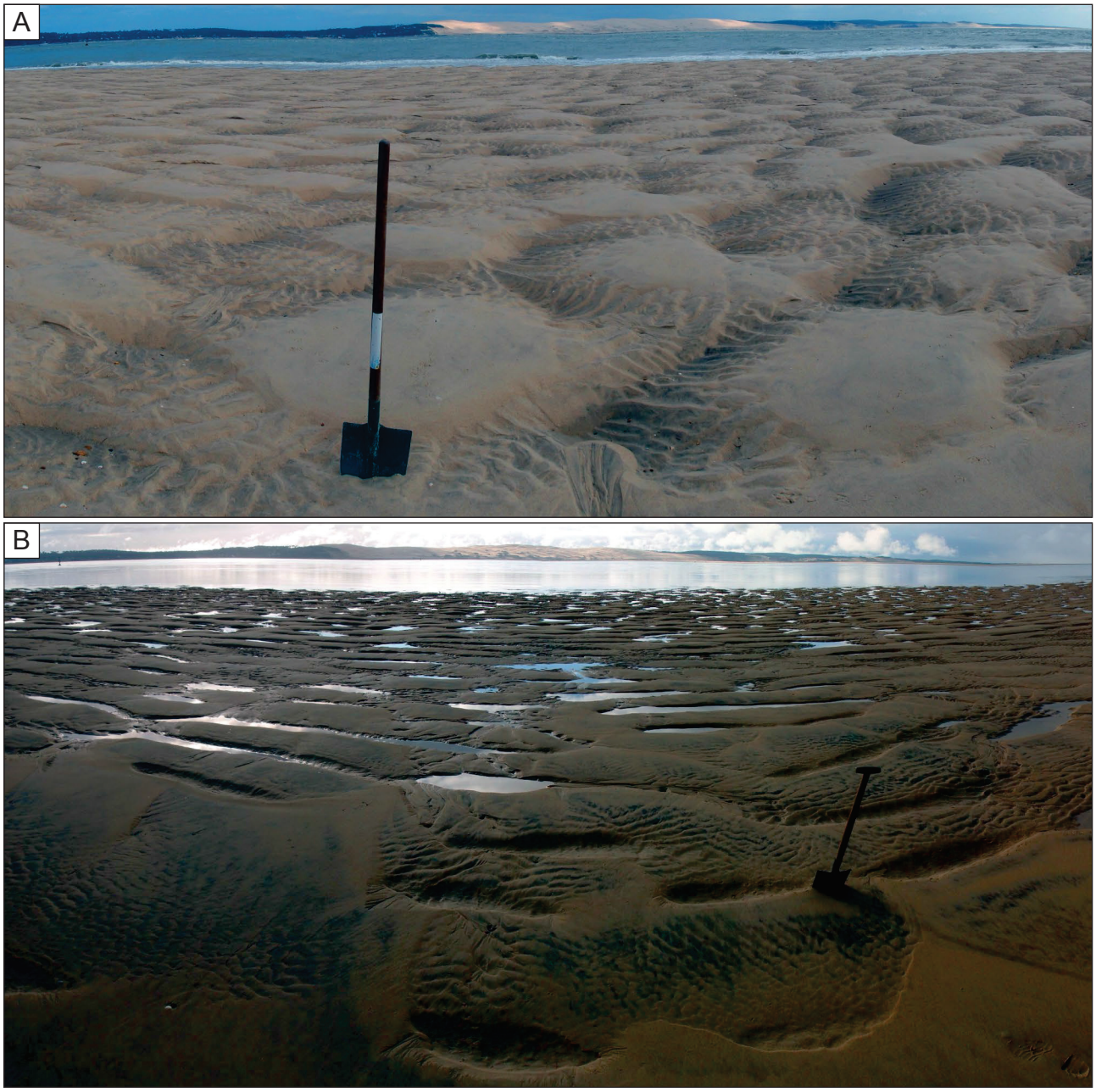

Fig. 1. *(A) Typical dome-like morphologies with an elevation of ca. 30 cm. These bedforms showing an important elevation are mainly observed around the mid-tide level. Note that the the troughs commonly display small-scale symmetrical or asymmetrical bedforms with linear / quasi-linear crests. (B) Bedforms with a lunated or elongated shape and an elevation of ca. 10 cm. This more flattened bedforms are mainly observed close to the lowest and highest tide levels (here lowest). Note that relics of small-scale symmetrical or asymmetrical ripples with linear / quasi-linear crests are visible. (A) and (B) have a wavelength of 1 - 1.5 m.*

department; SW France; Fig. 1 and 3). These bedforms exhibit sets of laminae, which can belong either to HCS (Harms et al., 1975) or to supercritical-flow deposits (e.g. Alexander et al., 2001; Cartigny et al., 2014). This study aims to discuss the formation of these bedforms and proposes that the internal cross-stratifications are derived from a backwash supercritical-flow at the surf-swash transition and that their dome-like external shape is the result of a wave-wave interference during fair-weather conditions induced where an irregular, curved costal geomorphology is observed.

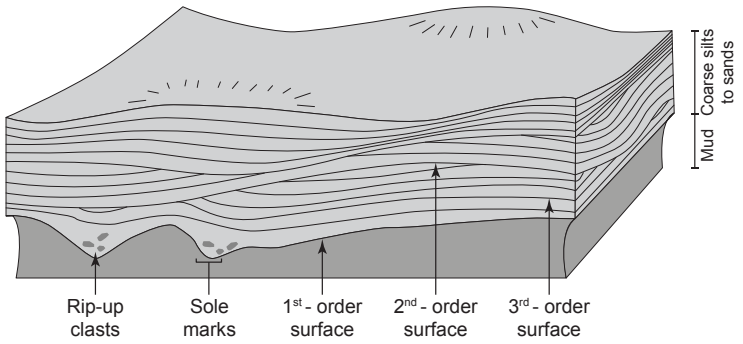

Fig. 2. *Hummocky-cross stratifications (HCS) and their different orders of surfaces (modified after Harms et al., 1975)*

2. Study area

The Cap-Ferret is located in the southwestern part of France in the Gironde department on the Atlantic coast (Figs. 3A and 3B). The beach system is elongated N-S and corresponds to a sand-spit that progrades with numerous associated baines / rip-channels due to the long-shore drift oriented toward the south initiated by the oceanic swell from the northwest (e.g. Thauront, 1994; Cayocca, 1996). The western part of the Cap-Ferret is under the dominance of the ocean swell while its eastern part is dominated by the tides. The tide range is macrotidal with a maximum spring tide range of 4.6 m and fair weather waves are 1 – 1.5 m height (e.g. Thauront, 1994; Cayocca, 1996). The beach system is mainly composed of medium grained quartz, but thinner grains and bioclasts are also present. During field investigations wave height (H) was < 2 m for a period (T) of 8 - 10 s (these values were evaluated during fieldwork, but not precisely measured).

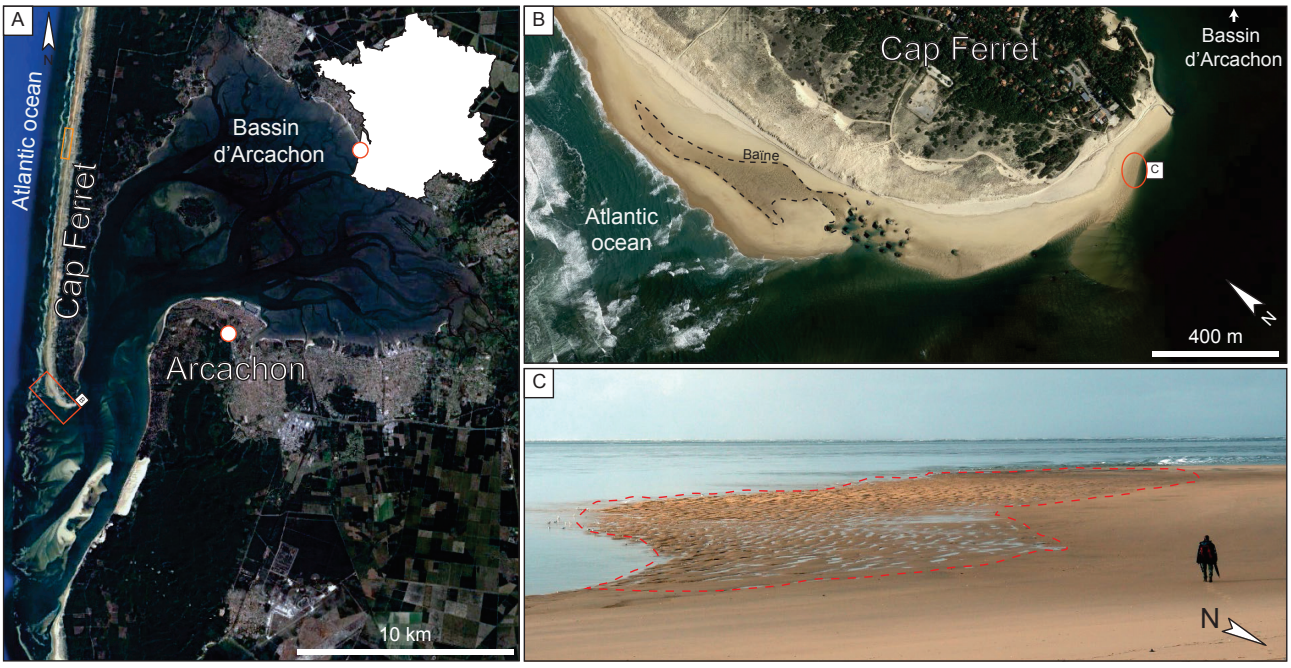

Fig. 3. *(A) Map of the study area (Google Earth image), the Cap-Ferret in located is the south-west of France; orange rectangle corresponds to the Plage du Truc Vert. (B) Satellite picture of the tip of the Cap-Ferret, which is formed of baine systems prograding toward the south. This picture is dated from march 2015, the actual coastal geomorphology is slightly different (see. Fig. 4). (C) Intertidal zone at the tip of the Cap-Ferret at low tide exhibiting dome-like bedforms. The red dashed line highlights the zone where the dome-like bedforms are observed at low tide. Note that they occur in a zone where the coastline is not straight, but curvated.*

3. Methods

The choice of the Cap-Ferret as study area is due to the presence of peculiar dome-like bedforms across the intertidal zone (Thiry-Bastien, 2002). These bedforms do not occur exclusively in this area, but the grain size heterogeneity here allows the observations of their internal stratifications. The coastal environment of the Cap-Ferret was investigated from 8th to 11th of March 2016. Tide coefficient were 101 to 116 giving respectively a tidal range of 3.72 to 4.31 m between the lowest and highest tide levels. In order to (1) describe and, (2) understand the timing of genesis of these peculiar sedimentary structures 20 trenches were realized at low tide (Fig. 4). Four sites were investigated and three of them were located at the tip of the Cap-Ferret. The fourth one was located northward on the beach called *La Plage du Truc Vert* (Fig. 3A). Several trenches were realized on the same dome-like bedforms (Figs. 4A and 4B). All the trenches were photographed, and the orientation of the trenches as well as the direction of progradation of the foresets observed in the dome-like bedforms was measured (Fig. 4C).

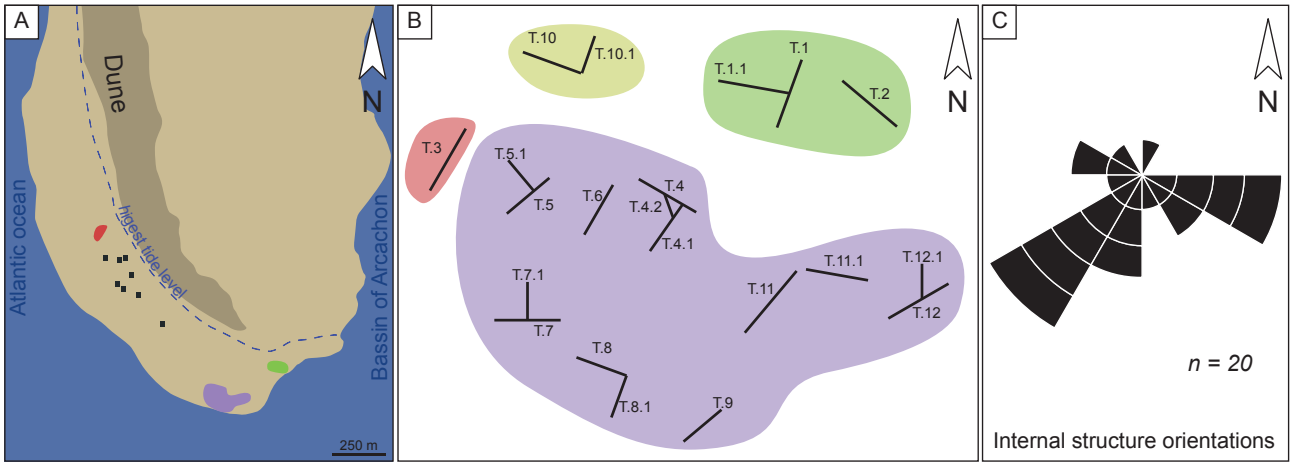

Fig. 4. *(A) Simplified map of the study area showing the different investigated zones. Black squares are World War 2 bunkers. Zones in red, purple and green referrer to (B). (B) Orientations of the trenches and their relationship to each other. Note that the yellowish zone is not present on (A), as this zone was located toward the north on the Plage du Truc Vert (see Fig. 3A for location). (C) Internal structure (foreset) orientations suggest two preferential orientations, toward the southwest and the east.*

4. Results

The intertidal zone of Cap-Ferret exhibits large bedforms with a dominant dome-like external shape separated from each other by troughs (Fig. 1A). Other large bedforms also occur that have a lunate to elongated shape (Fig. 1B). The mean wavelength of the bedforms is *ca.* 1.2 m with an elevation, from trough to crest, of *ca.* 30 cm. Their distribution across the intertidal zone is very patchy. These bedforms were more commonly observed when wave height (H) reaches a significant height estimated to > 1 m. Although no precise data were available to quantify wave height, dome-like bedforms were absent in some of the 4 sites and size of the area where they form reduced when wave heights were very

weak as it was the case the 8th and 11th of March 2016. Conversely, the abundance of these bedforms was high and size of the area of their formation large the 9th and the 10th of March during a windy period that generated high waves (visually estimated between 1.5 to 2 m). Externally, these large-scale bedforms display a smooth hummocky part while the troughs are commonly covered by small (dm-scale of wavelength) symmetrical or asymmetrical bedforms with linear / quasi-linear crests (Fig. 1A). Two types of external morphology are recognized: (1) one with an important elevation showing a convex upper surface of the bedforms (Fig. 1A), and (2) the other with a reduced elevation and a flat upper surface of the bedforms (Fig. 1B). Commonly the more domed bedforms are observed close to the mid tide level, while the more flattened bedforms occur close to the highest and to the lowest tide levels. The trenches revealed the internal architecture of the bedforms, which are characterized by:

- Trough stratifications (Fig. 5A)
- Hummocky-like stratifications (Fig. 5A)
- Tangential stratifications (Fig. 5B, C and F)
- Tabular stratifications (Fig. 5D)
- Sub-planar stratifications (Fig. 5F)

The trough stratifications (Fig. 5A) are concave laminations and the hummocky-like stratifications are convex laminations (Fig. 5A), giving together a reminiscent aspect of HCS (Harms et al., 1975). Tangential stratifications are oblique incurved laminations with a bottom tangential contact (Fig. 5B, C and F). Tabular stratifications are angular parallel laminations (Fig. 5D). Sub-planar stratifications are sub-horizontal plane parallel laminations (Fig. 5E). The tangential cross-stratifications are organized as prograding foresets that commonly show variations in their steepness (Fig. 5F). A basal downcutting in the bottomsets is commonly observed (Fig. 5B, C and F). Examples of five trenches from the 20 realized are shown in Figure 6. Troughs and hummocky-like stratifications, when occurring, commonly display a set of stratifications in vertical accretion that can evolve to tangential prograding foresets (Fig. 6A, 6B, 6C and 6D). Tangential stratifications are the more frequently observed stratifications, and sometimes the bedforms are almost exclusively constituted of tangential stratifications (Fig. 6E). The bedforms only constituted by tangential stratifications have an aspect very similar to current megaripples/dunes (e.g. Dalrymple, 1984; Berné et al., 1988). However, variations in steepness of the tangential stratifications (Fig. 5F and 6) as well as the downcutting in the bottomsets (Fig. 5F, 6E) are important difference with current megaripples/dunes. The less frequent types of lamination encountered are the trough and hummocky-like stratifications. The sidewalls of the troughs separating the dome-like commonly display tabular stratifications that can reach an important angle of steepness (*ca.* 40°; Fig. 5D, 6C and 6D). The direction of all the progradational structures was measured when two trenches crosscut the same bedforms

(Fig. 4B). The internal stratifications are preferentially directed to the east-southeast and southwest, but foreset progradation can also occur in any other direction (Fig. 4C).

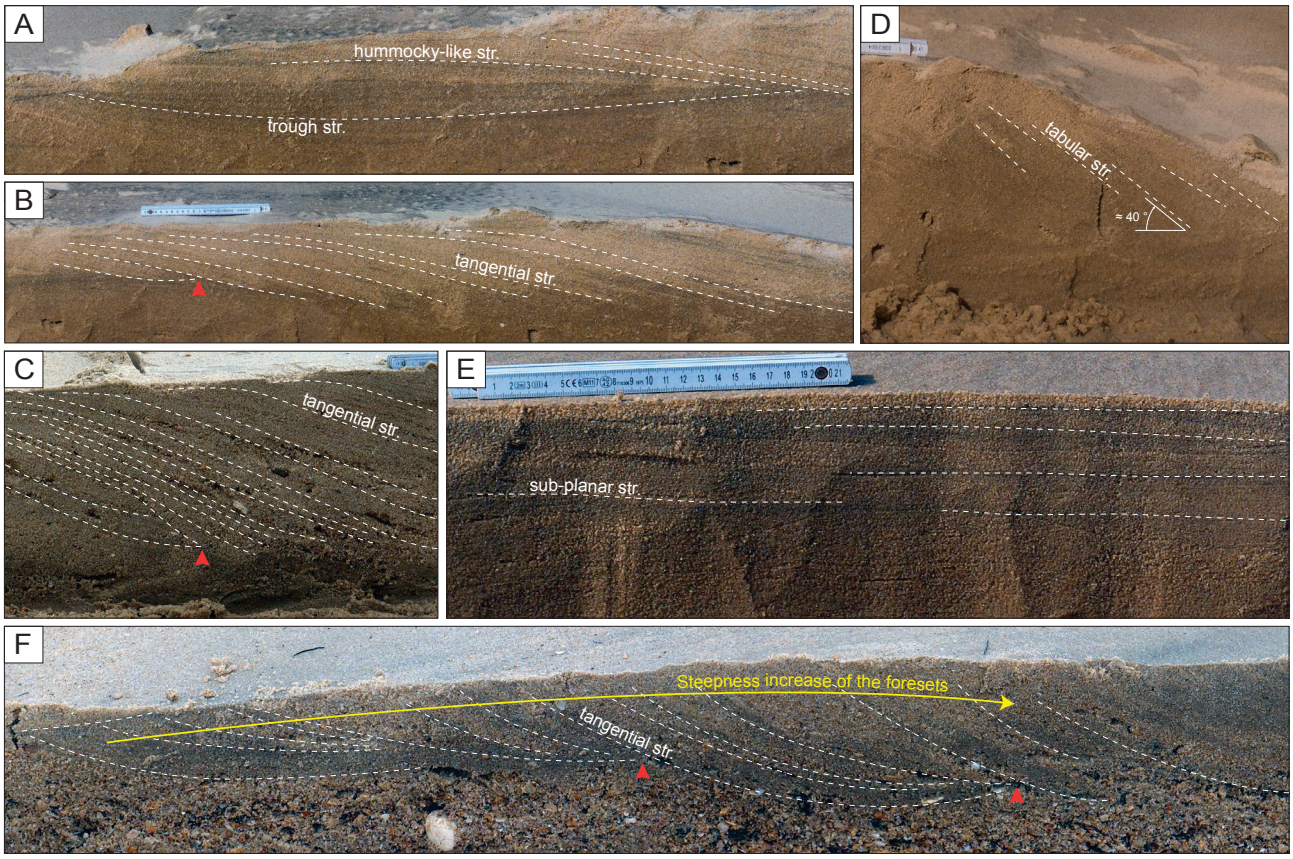

Fig. 5. *Internal stratifications in the dome-like bedforms. (A) Trough and hummocky-like stratifications. (B) and (C) highlight the tangential stratifications that mainly composed the dome-like bedforms. Note that the downcutting in the bottomsets of the tangential stratifications commonly from one another (pointed out by the red triangles). (D) Tabular stratifications can reach an angle of ca. 40°. Such stratifications almost exclusively occur on the sidewalls of the troughs separating the domes. (E) Sub-planar stratifications. (F) Tangential stratifications commonly display variations of steepness of the foresets (yellow arrow). The downcutting in of the bottomsets is well marked on this bedforms (pointed out by the red triangles). Str.: stratifications.*

Fig. 6. *Sedimentary structures in five examples of trench. T.X.Y is the trench number according to Fig. 4B. (A) to (C) show internal stratifications mainly displaying a set of trough stratifications, which can laterally pass to a set of tangential stratifications. Note that basal downcutting of the bottomsets as well as variations of steepness of the foresets may occur. (D) Tangential stratifications are the main stratifications in these bedforms. Note that a scour is fulfilled by tangential stratifications, which are overlain by subplanar stratifications. (E) These bedforms are exclusively composed by a set of tangential stratifications displaying steepness variations of the foresets. Locally downcutting in the bottomsets occurs. Green arrows show the vertical accretion. Orange arrows show the lateral accretion associated to the steepness variations of the foresests. Red triangles point out the basal downcutting of the bottomsets and the blue ones the tabular stratifications. Str.: stratifications.*

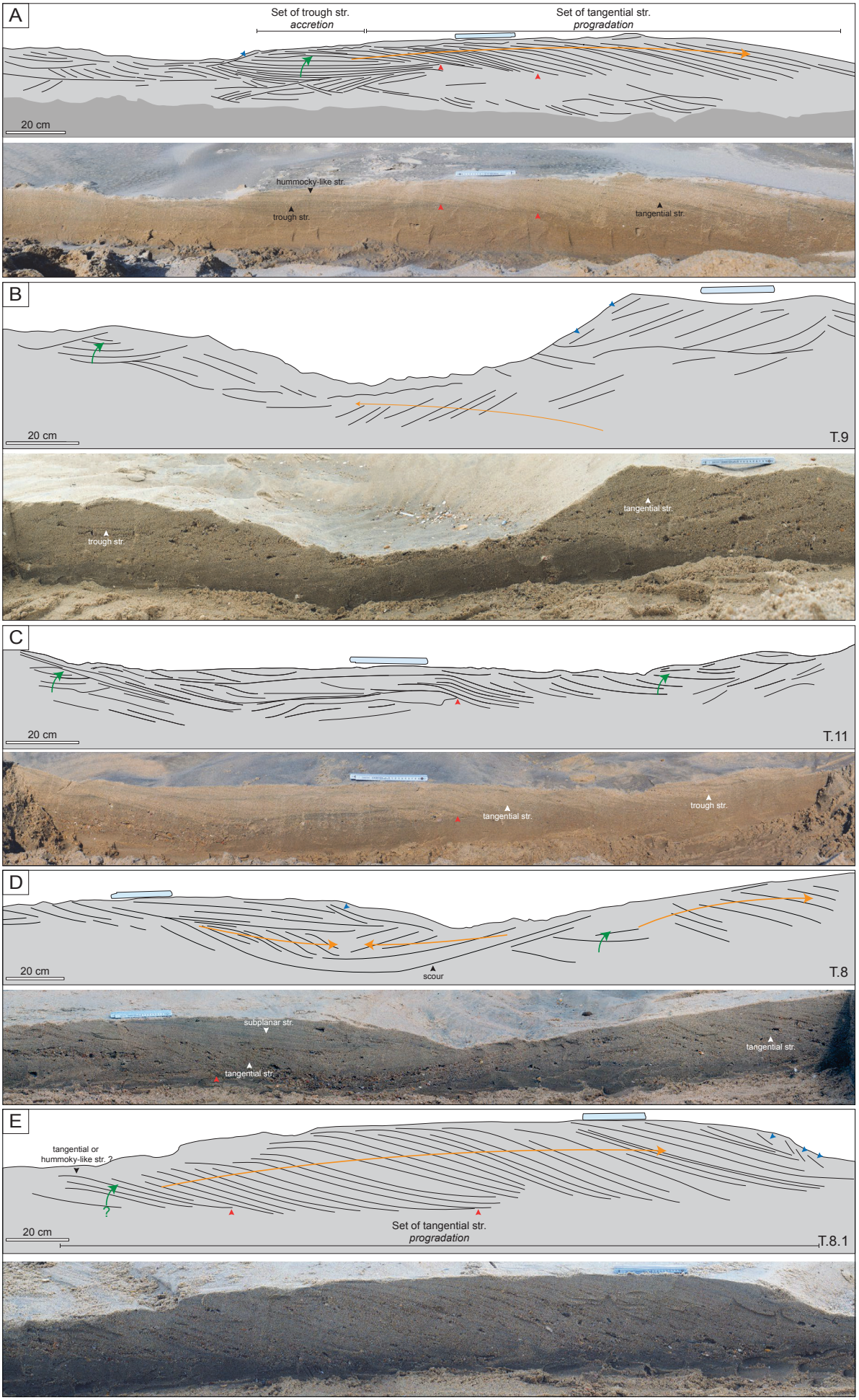
A
Set of trough str.
accretion
Set of tangential str.
progradation
20 cm
hummocky-like str.
trough str.
tangential str.
B
20 cm
T.9
tangential str.
trough str.
C
20 cm
T.11
tangential str.
trough str.
D
20 cm
scour
T.8
subplanar str.
tangential str.
tangential str.
E
tangential or
hummoky-like str. ?
?
20 cm
Set of tangential str.
progradation
T.8.1

5. Discussion

Thiry-Bastien (2002) and Ferry (2015) observed these dome-like bedforms across the intertidal zone of the Cap-Ferret and interpreted them as HCS in lateral accretion, because showing sediment vertical accretion (as in classical HCS; e.g. Harms et al., 1975; Dumas et al., 2005) and lateral accretion. HCS are peculiar sedimentary structures often considered as diagnostic of storm events on the continental shelf when recognized in the fossil record (e.g. Harms et al., 1975; Dott and Bourgeois, 1982; Duke, 1985). Since HCS are prone to be generated from the nearshore to the storm wave base, and mainly preserved between the fair-weather and the storm wave-base, these sedimentary structures are powerful tools for paleoenvironmental reconstructions (e.g. Yang et al., 2006). These sedimentary structures are widely recognized through the rock record (e.g. Harms et al., 1975; Brenchley and Newall, 1982; Dott and Bourgeois, 1982; Allen, 1985; Duke, 1985; Brenchley et al., 1986; Greenwood and Sherman, 1986; Cheel and Leckie, 1992; Yang et al., 2006; Mulder et al., 2009; Basilici et al., 2012; Vaucher et al., 2016; in press). However, the processes responsible for their formation have a half-century of debate and several flow parameters are invoked in the literature. According to the most recent reviews made by Quin (2011) and Morsilli and Pomar (2012) the main hypothesis for the formation of HCS and HCS-*like* are related to pure oscillatory-flow, to combined-unidirectional dominated-flow, to combined-oscillatory dominated-flow, to turbiditic-flow or to internal waves. Thiry-Bastien (2002) and Ferry (2015) inferred the trough cross-stratifications in vertical accretion as the results of wave interference while the lateral accretion would be initiated by an increase of the wave orbital influence on the seafloor during falling tide. However, this latter interpretation is not consistent with an oscillatory flow that generates horizontal back-and-forth currents. In the case of a wave-dominated tide-influenced proximal environment, at a given position the oscillation raises during falling tide and then the wavelength of the bedforms is expected to increase (Cummings et al., 2009) but not to form lateral accretion. However, this explanation does not account for the variations of the dip in the lamina sets as well as for the erosive, downcutting aspect of the bottomsets (Fig. 5E and 6).

According to their external morphologies the dome-like bedforms can be either classified as Lunate Megaripples (Clifton, 2006) as 3D Symmetrical Dunes (*sensu* Perillo et al., 2014) or as Hummocky Bedforms (*sensu* Dumas et al., 2005). Clifton (2006) described the internal stratifications as tangential cross-stratifications displaying a set of laminations that are either orientated seaward or landward. In the described bedforms of the Cap Ferret some laminations are tangentially cross-stratified (Fig. 6E), but not exclusively. Furthermore, the bottomsets are erosive and variations in the steepness of the forests occur (Fig. 5A, 5C, 5F, 6A and 6E), which is not the case in the study of Clifton (2006). Dumas et al. (2005) show that the hummocky bedforms experimentally generated under pure oscillatory flow display a set of classic isotropic hummock and swale morphologies,

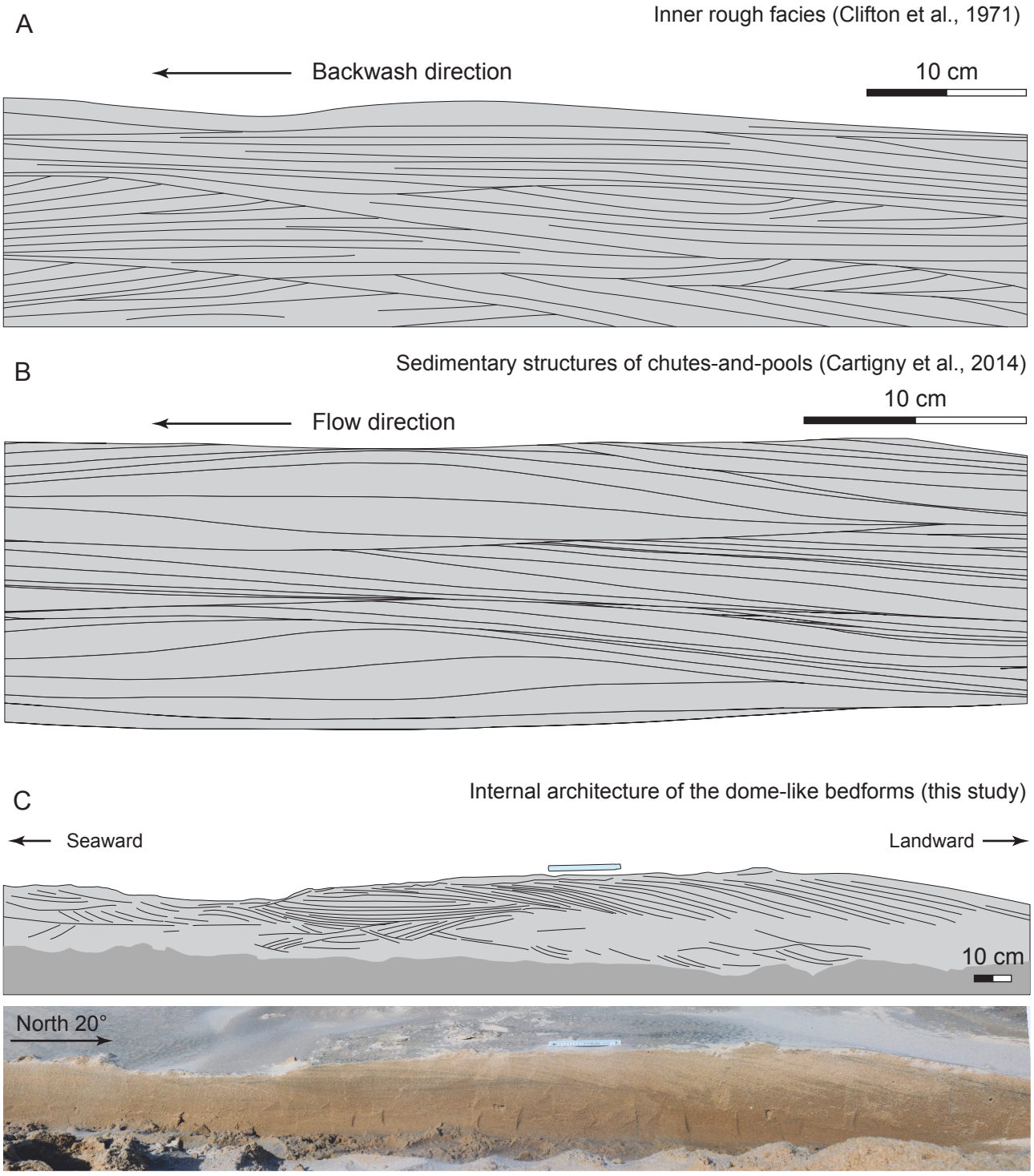

***Fig. 7**. Comparison of internal stratifications. The three examples commonly display the same sets of internal stratifications: trough, subplanar, tangential and hummocky-like stratifications. Note that tabular stratifications as well as downcutting of the bottomsets only occur in the bedforms analyzed in this study. (A) Inner rough facies (modified from Clifton et al., 1971). (B) Sedimentary structures of chutes-and-pools produced by a synthetic aggradation rate of 0.24 mm.s^{-1} (modified from Cartigny et al., 2014). (C) Internal stratifications of one dome-like bedform in the intertidal zone at the tip of the Cap-Ferret.*

which are diagnostic of the classical HCS (Harms et al., 1975). Dumas et al. (2005) also show that under combined flow (oscillatory dominated), the set of hummock and swale morphologies are anisotropic, giving a progradational aspect to the laminae in response to the current flow direction. Such morphologies very likely occur in the bedforms described in the intertidal zone of Cap-Ferret (Fig. 6A), but neither basal downcuttings in the bottomsets,

nor planar and tabular stratifications are observed in the flume experiments of Dumas et al. (2005).

Clifton et al. (1971) studied one modern high-energy nearshore environment, and defined several types of bedforms. One type of bedforms was named Inner Rough Facies. This type of bedforms displays symmetrical ripples parallel to the shore with a wavelength of *ca.* 50 cm, and likely occurs at the transition between the surf and the swash zone. The internal cross-stratifications of the inner rough facies are in troughs, in hummocks, and tangential. The foresets of the tangential stratifications prograde either seaward or landward, or both (Fig. 7A). This pattern likely resembles to the sets of laminae described in the present study (Fig. 6 and 7C) even if the wavelength of the bedforms in Clifton et al. (1971) is smaller than in the here-described bedforms. The authors mentioned that at the transition between the surf and the swash zone, the backwash seems to be dominant by comparison to the swash. Clifton et al. (1971) mentioned that the inner rough facies is of a great complexity and no unique interpretation for its formation is valid. They however suggest that the flow is very turbulent and likely due to the interference of the swash and backwash currents. The peculiar sets of internal stratifications have also morphological affinities with those formed under supercritical-flow in flume studies, especially with sedimentary structures associated to chutes-and-pools (Fig. 7B) (e.g. Alexander et al., 2001; Cartigny et al., 2014). Chutes-and-pools are formed by supercritical flows, which are defined by a *Froude number* > 1. This number is dimensionless and defined by the following relation: $Fr = U/(g.h)^{1/2}$ where (U) is the flow velocity, (g) the acceleration of gravity and (h) the flow depth. In supercritical flows the inertia dominates over the gravity. Chutes-and-pools are formed by supercritical flows, which are turbulent (*Reynolds number* > 2000) and unstable (*Vedernikov number* > 1) (Alexander et al., 2001; Cartigny et al., 2014). According to Cartigny et al. (2014) and references herein, chutes-and-pools consist of reaches where the flow rapidly accelerated (chute) finishing in a hydraulic jump followed by a long pool. In the pool the flow is tranquil, but accelerating and can either migrate downstream or upstream. Hydraulic jump is the transition zone, where the supercritical flow becomes subcritical. It is characterized by abrupt increase of the flow depth associated to a decrease in velocity (Cartigny et al., 2014). Alexander et al. (2001) note that a plane bedded area can separate chutes-and-pools. These authors show that sedimentary structures (Fig. 7B) formed by chutes-and-pools display hummocky, trough, tangential, and sub-planar stratifications that can be either aggrading or prograding (upstream and downstream). These internal stratifications very likely resemble to those formed in the inner rough facies (Fig. 7A) of Clifton et al. (1971) as well as to the stratifications observed in the bedforms of Cap-Ferret (Fig. 6 and 7C). Unfortunately, due to the narrowness of the used flumes for the experimental studies no external morphology of the bedforms generated under supercritical flow conditions was described (e.g. Alexander et al., 2001; Cartigny et al., 2014).

Our observations and those of Clifton et al. (1971) suggest that the analysed

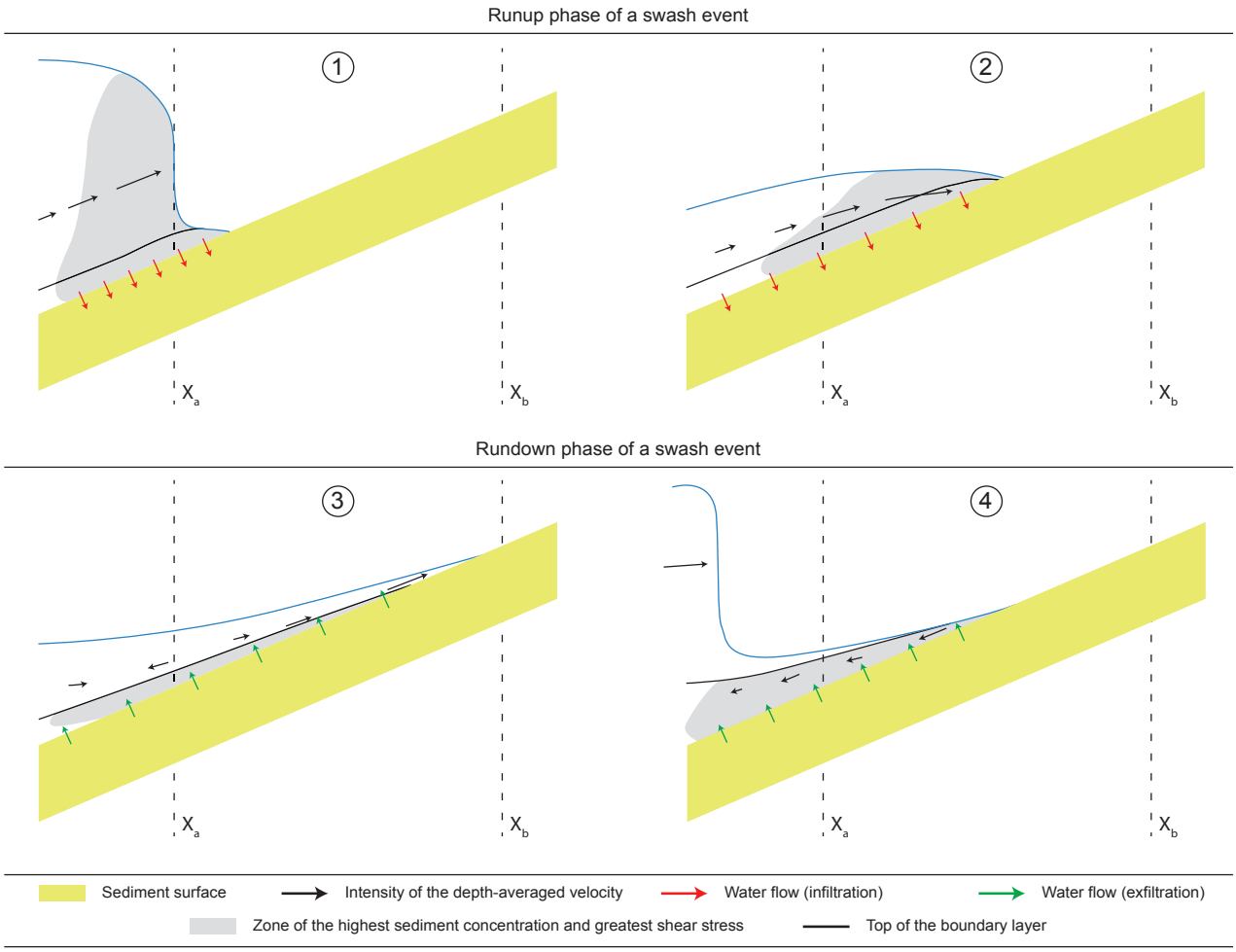

Fig. 8. *Runup and rundown phase of a swash event, after Brocchini and Baldock (2008). (1) Wave collapse; (2) Beginning of the runup ; (3) End of the runup and beginning of the rundown; and (4) Rundown and subsequent incoming wave.*

bedforms and inner rough facies form at the surf-swash transition zone, and share internal stratifications exhibiting affinities with sedimentary structures formed by supercritical-flows (Alexander et al., 2001; Cartigny et al., 2014). Even if Clifton et al. (1971) did not clearly invoke that supercritical-flows were responsible to form their inner rough facies, Broome and Komar (1979) did. The bedforms described by Broome and Komar (1979), which externally are similar to the inner rough facies of Clifton et al. (1971) (without internal cross-stratifications described) were inferred to supercritical flows resulting of the collision between backwash and the next incoming wave (Broome and Komar, 1979). More recently, a review made by Brocchini and Baldock (2008) explain how supercritical-flow conditions are reached at the surf-swash transition (Fig. 8) and distinguish 4 steps. Once the wave starts to collapse (Fig. 8; step 1), the water surface dips seaward and the general flow acceleration are directed offshore for the whole swash event. Therefore, the boundary layer is submitted to an adverse pressure gradient during the runup (swash) (Fig. 8; step 2). During this phase, water infiltration takes place into the sediments, thus thinning the boundary layer and removing water for the rundown (backwash). The combined actions of the latter mechanisms, the intense flow velocities and the thin boundary layer promote a great shear stress at the water-sediment interface to which is added the turbulence of the

wave collapse. This implies that the runup flow is charged in sediments. The reversal flow starts seaward and the pressure gradient strongly increases in the boundary layer (Fig. 8; step 3). At the transition between the runup and the rundown the flow velocity is almost nil, which means that the suspended sediments bring by the runup settled and sediments transport occurs as sheet-flow during the rundown. Exfiltration of water from the seafloor thickens the boundary layer and this effect is counterbalanced by the thinning effect of the favourable pressure gradient due to the next incoming wave. Thus, the backwash flow starts to be supercritical (Fig. 8; step 4). In Brocchini and Baldock (2008), the authors did not pay attention to the formed sedimentary structures, but now a parallel between this study and those led by Alexander et al. (2001) and Cartigny et al. (2014) can be achieved. The dome-like bedforms of the intertidal zone of the Cap-Ferret have internal cross-stratifications very similar to those related to chutes-and-pools and supercritical flow conditions can be reach at the surf-swash transition zone, which corresponds to the preferential zone of formation (and preservation) of the dome-like bedforms. Furthermore, the relation between the wave height is proportional to velocity of the swash, implying that for a reduce wave height the induced swash flow is slower and not able to generate supercritical backwash flow conditions (Baldock and Holmes, 1999). The interpretation of these dome-like bedforms as the result of supercritical flows is in agreement with the fact that these bedforms are less frequently generated when the height of the incident wave is very weak. However, the first interpretation of these bedforms as HCS with lateral accretion is correct since it was noted that chutes-and-pools may mimic the internal cross-stratifications of HCS (Alexander et al., 2001) but the fact that they result from wave interferences (Thiry-Bastien, 2002; Ferry, 2015) is unlikely. Concerning the hypothesis of Vaucher et al. (submitted) that the 3D SD of Berck-Plage are the result of wave-wave interferences generating a combined motion of particles on the seafloor may be erroneous. Since the 3D SD (Berck-Plage) and the dome-like bedforms (this study) are formed in the same environments both when wave height is not weak, the question of a common origin can be raised. However, due to the grain size homogeneity of Berck-Plage, no internal structures were observed. In this way, even if the dome-like bedforms of this study and the 3D SD of Berck-Plage share the same external morphologies it is not possible to affirm that they are formed by the same processes.

Sedimentary structures related to a supercritical-flow need a pre-built topography to be formed, even if the supercritical-flow can erode the seafloor, thus creating topographies. The Cap-Ferret coastal morphology induces wave front propagation in various directions (see further in this text). Wave-wave interferences could be responsible for the initiation of the dome-like bedforms, thus forming topographies that would be used after by the supercritical-flows to construct the dome-like bedforms and their internal sedimentary structures. Then, the hypothesis of a formation in two steps for these dome-like bedforms cannot be excluded. However, this would imply two successive mechanisms to form the dome-like bedforms. Since supercritical-flow can explain all the characteristics of the dome-

like bedforms, the hypothesis that the supercritical-flow is the only process responsible for the formation of dome-like bedforms is preferred.

The change of the dip in the lamina sets observed in the dome-like bedforms is most commonly coincident with the downcutting in the bottomsets. This pattern was only described in the literature by Thiry-Bastien (2002) and Ferry (2015). Indeed, the downcutting in the bottomsets is illustrated in several studies interested in wave dominated tidally modulated proximal environments (see Fig. 7A, 7C, 9E, 11C, 11D, 13E and 13F of Yang et al. (2005); Fig. 2 of Yang et al. (2006); Fig. 2B of Yang et al. (2008); Fig. 7A of Dashtgard et al. (2009); Fig. 5E, 5H, 11B and 12C of Dashtgard et al. (2012)) but this pattern was not mentioned or interpreted, or was attributed to tide current or to combined-flow. In our study but also in Yang et al. (2005; 2006; 2008) and Dashtgard et al. (2009; 2012), the investigated areas are under the influence of tides (macro- and megatidal range). This implies that during falling tide, the influence of the supercritical backwash flow on the sediment increases. This phenomenon could likely explain the downcutting in the bottomsets and why this pattern is not observed in flume experiments (e.g. Alexander et al., 2001; Cartigny et al., 2014) in which water level did not vary. Concerning the variations of steepness of the tangential stratifications, Alexander et al. (2001) and Cartigny et al. (2014) inferred this phenomenon to the migration of the hydraulic jump (upstream or downstream). Such migration of the hydraulic jump producing variations of steepness of tangential stratifications is well visible on Movie S3 (additional supporting information of Cartigny et al., 2014; click here for direct link). The establishment of tangential stratifications with variations of steepness can thus occur landward or seaward if the hydraulic jump migrated seaward or landward respectively. In this study internal stratifications are preferentially directed to the east-southeast and southwest, but foreset progradation can also occur in any other direction (Fig. 4C). However, Thiry-Bastien (2002) also measured the direction of foreset progradation and observed that it was preferentially toward the north. Thus, by comparison between this study and Thiry-Bastien (2002) no preferential orientation of foreset progradation can be highlighted. This phenomenon could likely be inferred to the swash and backwash that occur in every direction and to the hydraulic jump able to migrate upstream and downstream. If the downcutting in the bottomsets associated to the variations of steepness in the foresets seems to be diagnostic for the recognition of the surf-swash transition zone in a wave-dominated macrotidal context, the direction of progradation of the foresets is not meaningful.

Peculiar observations were made just before the low tide slack when the dome-like bedforms are still submerged under several centimetres of water. On the step-by-step Figure 9 realized in a baine, waves collapse on the right side of the picture and swashed in several directions according to their incident angle of propagation. Indeed, Vaucher et al. (submitted) show that peculiar costal geomorphologies (here one baïne) may induce propagation of different wave fronts across the intertidal zone. On Figure 9, three successive swashes occur. The first came from the right, the second from the left

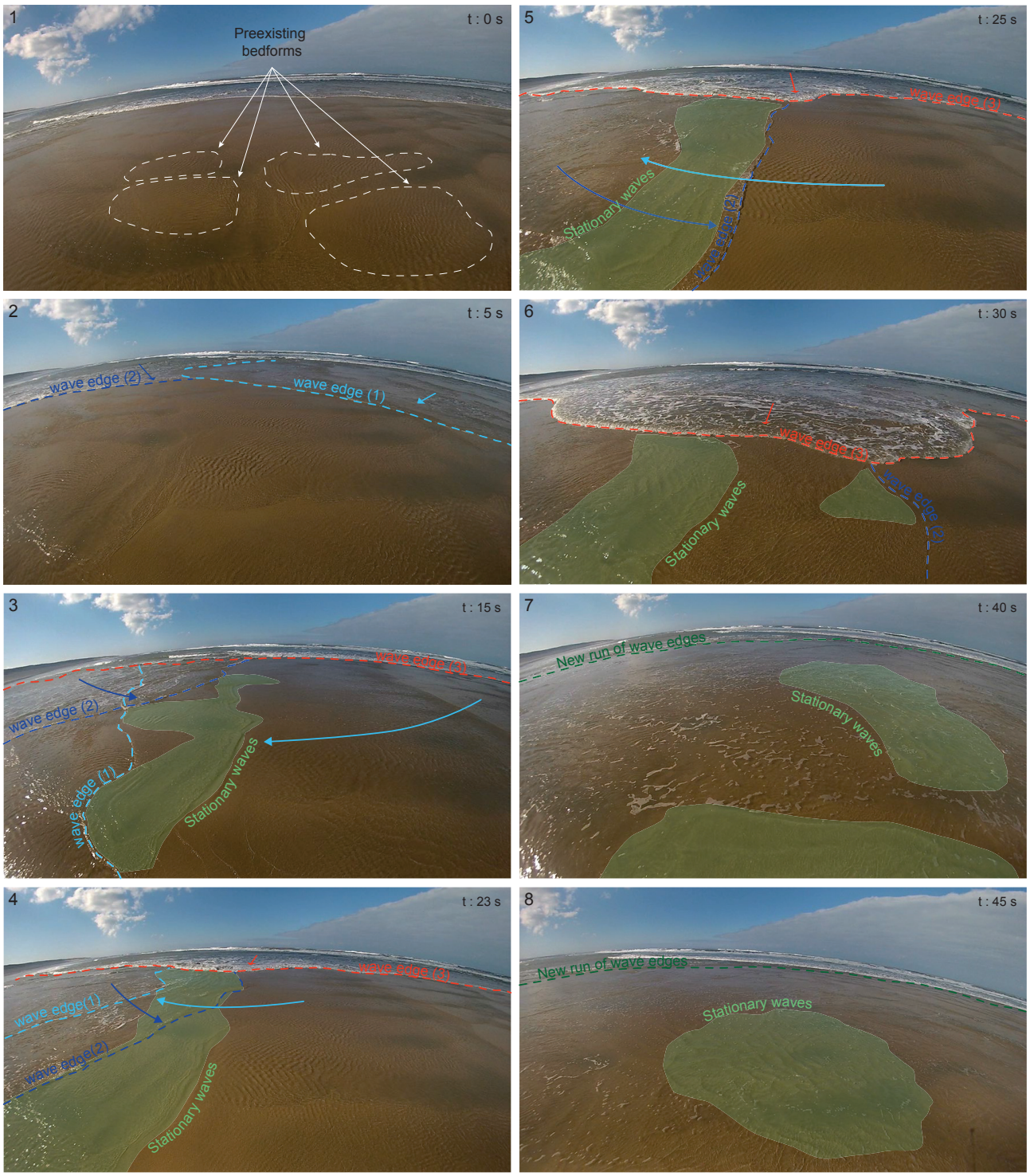

Fig. 9. *Step-by-step pictures of three incoming wave fronts through a baine close to the Plage du Truc Vert (location on Fig. 3A). Pictures are taken toward the south. The first wave front (light blue) came from the west, the second (dark blue) from the east and the third (red) from the south. Wave fronts generated stationary waves when passing over the troughs that separate the bedforms. Arrows show respective wave front propagations. The zones in light green correspond to the stationary wave areas. Step-by-step pictures start at t = 0s and end at t = 45s.*

and finally the third one from the front. Figure 9 clearly highlighted that stationary waves are formed in the troughs separating the dome-like bedforms and in various orientations as wave fronts pass over the troughs. Since stationary waves are supercritical flows (Alexander et al., 2001; Cartigny et al., 2014) it could likely explain a part of the variations of the dip in the sets of the laminae. Furthermore, the stationary waves formed in the

troughs (hydraulic jumps) are very turbulent and thus likely explain the downcutting in the bottomsets.

When the water depth is reduced enough to exude (or emerge) the top of the dome-like bedforms, swash and backwash processes remobilize sediments from the top of the dome to the troughs separating the bedforms. This sediment remobilization produces an avalanching on the slope of the bedforms, thus forming delta-*like* morphologies likely responsible of the tabular stratifications (Fig. 5D) on the sidewalls of the troughs separating the dome. Since the water depth decreases during falling tide, the possibility to reach supercritical flow conditions in very shallow environment increases, thus the downcutting in the bottomsets but also the tabular stratifications could point to a tidal signature in a wave-dominated system.

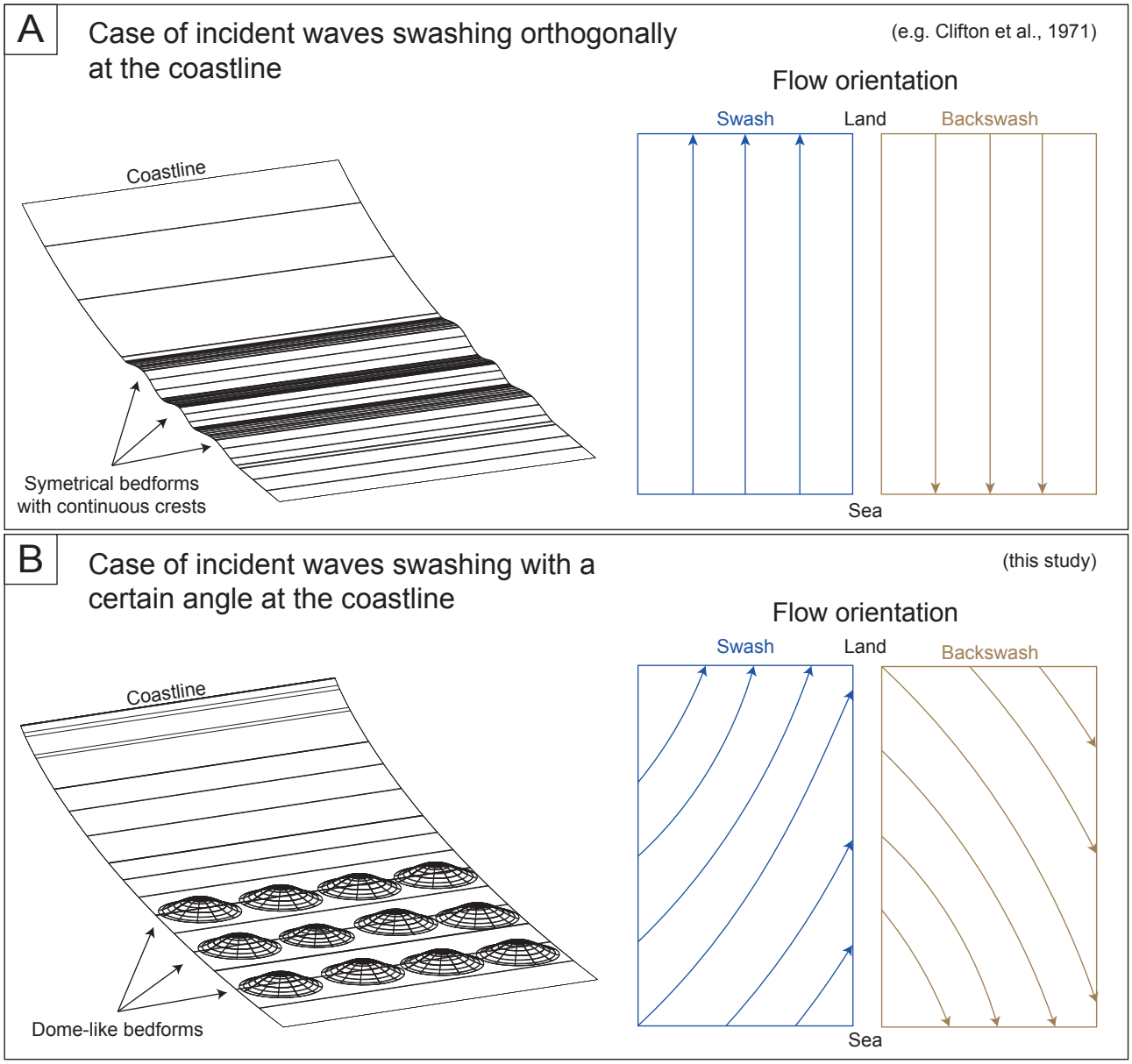

Fig. 10. *(A) Waves approach parallel to the coast and thus the swash and the backwash flows share the same orientation, which is orthogonal to the coastline. In this case the created bedforms exhibit continuous crests. (B) Waves approach the coast with a certain angle. The swash is not orthogonally according to the coastline and induces wave reflection implying that backswash has a different direction than the swash. This phenomenon could likely explain why 3D rather than 2D bedforms are form.*

The dominant axis of wave propagation in the Cap-Ferret is northwest. This implies that waves approach the coast with an important angle. Furthermore, the costal geomorphology of the zone corresponds to numerous systems of baine, which means that the seafloor topography across the intertidal zone is very irregular. Therefore, as mentioned in Vaucher et al. (submitted) the wave will spread and swash in several directions (refracted by the topography, likely explained by the dispersion relation). By swashing with a certain angle means that the backwash will also be also oriented as well. In the study led by Clifton et al. (1971) the costal morphology is simpler with a classic gently dipping uniform slope and the wave swashed orthogonally to the coast. This latter phenomenon implies that the swash and backwash likely share the same orientations at the coast and could explain the continuous crested aspect of the inner rough facies (Fig. 10A). Differently here, the swash and thus the backwash occur in several directions (Fig. 10B) and can explain the occurrence of 3D bedforms in Cap-Ferret rather than 2D bedforms as described by Clifton et al. (1971). Indeed, as backwash induced flow spread in all directions, interferences between backwash and incoming surf are not favourable to form sub-linear crested bedforms (Fig. 10).

Even if the dome-like morphologies are most commonly observed, two types of morphologies are recognized. One appears more flattened than the other (Fig. 1). Commonly, the more domed morphologies are observed at the mid tide level (Fig. 1A) while the more flattened bedforms occur close to the highest and to the lowest tide levels (Fig.1B). At lowest and highest tide levels, the time residence of the sea level is longer compared to the mid tide level. This implies that swash process acts during longer time at lowest and at highest tide level than at mid tide level. Since swash and backwash are very powerful processes for sediment mobilization it seems logical that bedforms occurring close to the lowest and the highest tide level are more prone to be flattened than those occurring close to the mid tide level. The flattened effect is produced by the sediment mobilization from the top of the dome, fulfilling the troughs that separate the bedforms. As shown previously, swash and thus backwash can occur in several directions. This implies that sediment mobilization occurs in every direction. The fulfil effect can be recognized across the trenches giving opposite senses of progradation to the sets of tangential laminations (Fig. 6D) or giving a festoon aspect to the displayed sets of stratifications (Fig. 6C). The example in Figure 6D highlights that once the trough is fulfilled by sediment that came from the top of the dome, sub-planar stratifications (Fig. 6D) can occur if water depth is reduced enough. At that moment, swash and backwash processes occur, thus forming sub-planar stratifications due to a high rate of sediment mobilization (e.g. Perillo et al., 2014). In this way the distribution of the two types of bedform elevations could be induced by the average time that the bedforms are under the influence of swash.

The symmetrical (sometimes asymmetrical) bedforms with quasi-linear crests of a decimetre scale of wavelength can be interpreted as 2D Symmetrical Bedforms (2D SR of Perillo et al., 2014) resulting from a weak oscillation. Since the dome-like bedforms are

formed at the surf-swash transition zone and that they are covered of 2D SR, it implies that dome-like bedforms are generated first. The surf-swash transition zone switches seaward and landward twice a day, implying that for a given position across the intertidal zone, the dome-like bedforms are formed in very shallow conditions with a limited extension. Once formed and the tide is still rising, the dome-like bedforms stop to be generated in a given position and thus 2D SR can be formed on the seafloor under deeper conditions, overprinting the freshly created domes (Fig. 1A).

Since the more domed bedforms are preserved close to the mid-tide level it likely explains why the 2D SR are also well preserved at this location (Fig. 1A), compared to the 2D SR appearing as relics on the bedforms observed close to the highest and lowest tide levels (Fig. 1B). Perillo et al. (2014) mentioned that 2R SR bedforms are generated perpendicularly to the oscillatory flow. However, the 2D SR bedforms (Fig. 1A) exhibit a large panel of crest directions (almost at 180°). This could be in agreement with a wave propagation occurring in all directions, likely induced by the costal geomorphology.

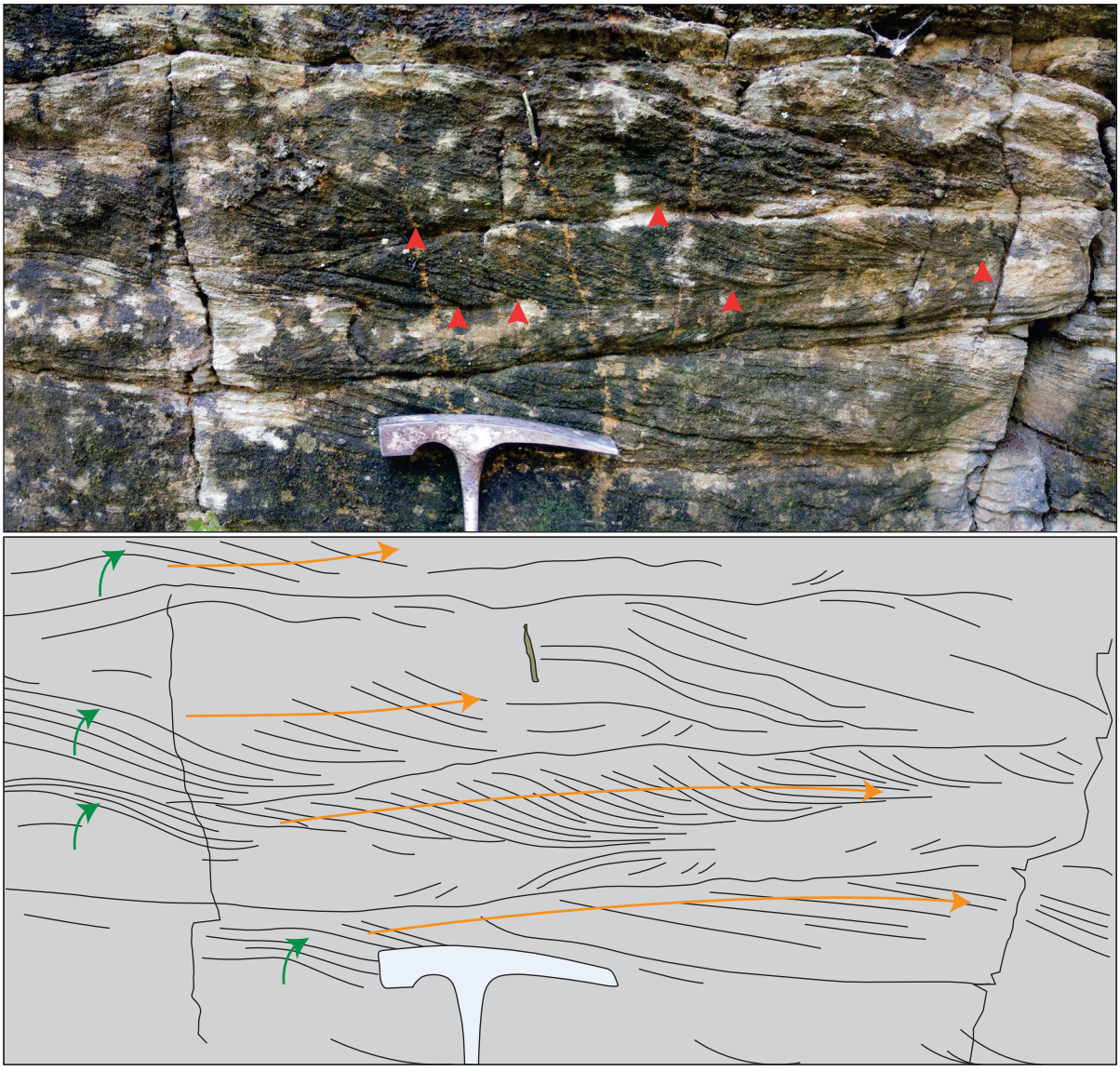

Fig. 11. *The cliffs of Crémieu (Rhône department; France) consist of crinoidal jurassic limestones. Similar sedimentary structures to those observed at the Cap-Ferret are observed here. Green arrows show the vertical accretion given a HCS aspect to the stratifications; orange arrows point out the lateral progradation with common changes in foreset steepness. Red triangles highlight basal the downcutting in the bottomsets.*

However, the dome-like bedforms freshly formed constitute a very irregular seafloor topography that possibly interfere with the oscillatory motion, which could also led to the formation of 2D SR with crest orientations in various directions.

The inner rough facies (Clifton et al., 1971) shows a narrow cross-shore extension of *ca.* 15 m while in the case of the Cap-Ferret, even if the distribution is patchy, the cross-shore extension is larger. As it was shown previously in this study the zone of formation of the dome-like bedforms is at the surf-swash transition. In the case of a micro-tidal range environment, the zone does not much switch seaward or landward during a tide cycle. However, the Cap-Ferret is a macro-tidal environment, which implies than the surf-swash transition zone importantly (several hundred meters) switch seaward and landward twice a day.

All the patterns of internal sedimentary structures observed in the intertidal zone of the Cap-Ferret are recognized in the fossil record. In Crémieu (Rhône department; France), cliffs exposed jurassic crinoidal limestones (Bajocian) (Thiry-Bastien, 2002). Figure 11 show similar sedimentary structures to those formed in Cap-Ferret. These structures were interpreted by Thiry-Bastien (2002) as HCS (for the vertical accretion part) with lateral accretion pointing to very shallow and proximal environments. The paleoenvironmental significance when recognized in the fossil record remains correct but the inferred mechanism for the formation of this HCS-*like* structures is questionable. Even if the wave motion initiates the swash and the backwash, the dome-like bedforms are likely not induced by oscillatory flows but result from supercritical flows. Furthermore, the recognition of the downcutting in the bottomsets in this ancient sedimentary succession suggests that tide processes also occur, as already inferred by Thiry-Bastien (2002).

Since this study is in preparation, further analyses are needed to validate the hypothesis presented here. In order to confirm that these dome-like bedforms are the result of supercritical flows, measurements of current velocity as well as wave height and orientation should be taken *in situ* following, for example, the methodologies led by Bastide (2011) to characterize the different wave parameters, especially to define if supercritical flows conditions are reached. Even if the turbidity and the current are very high at the tip of the Cap-Ferret, information about the timing of formation of the sedimentary structures (2D SR vs dome-like bedforms) need to confirmed by direct observations or by using a Multibeam Echosounder (see Hendershot et al., 2016). Furthermore, information of what happens at high tide should be also confirmed by direct observations or by using underwater camera in order to estimate if the dome-like bedforms are in part formed by wave-wave interferences and to estimate on which distance backwash flow stays in supercritical conditions. Concerning wave-wave interference effect, analogic and/or numerical simulations must be achieved to constrain what is the exact motion of particles on the seafloor. In order to prove that the variation of water depth is responsible for the downcuttings observed in the bottomsets, supercritical flow experiments that include changes in water depth should be led. Further details are provided in Chapter V.

6. Conclusion

The Cap-Ferret intertidal zone exhibited peculiar bedforms, which are here firstly described and interpreted in term of processes. Dome-like bedforms with a wavelength of *ca.* 1.2 m and an elevation of *ca.* 30 cm are characterized by trough-, planar-, tangential-, tabular-, and hummocky-stratifications. This preliminary study proposes that these bedforms are generated at the surf-swash transition zone by the backwash. If wave height is important enough, the induced swash and backwash can reach supercritical conditions. When these conditions are reached, sedimentary structures formed by chutes-and-pools occur, explaining the internal stratifications recognized in these bedforms. The external (3D) dome-like morphologies are attributed to the fact that swash and backwash flows occur in several directions, which is not favourable to form sub-linear (2D) crested bedforms. This study also suggests that the recognition of such sedimentary structures in the sedimentary record could be used as a tool for paleoenvironmental reconstruction pointing to the surf-swash transition zone. The downcutting in the bottomsets is proposed to be one criteria for identifying tide influence in ancient wave-dominated sedimentary successions.

Acknowledgements

This research did not receive any specific grant from funding agencies in the public, commercial, or not-for-profit sectors. We are thankful to _____ and _____ for their sensible remarks that helped us to improve the quality of the manuscript.

References

Alexander, J., Bridge, J.S., Cheel, R.J., Leclair, S.F., 2001. Bedforms and associated sedimentary structures formed under supercritical water flows over aggrading sand beds. Sedimentology, 48(1): 133-152.

Allen, P.A., 1985. Hummocky cross-stratifications is not produced purely under progressive gravity-waves. Nature, 313(6003): 562-564.

Baldock, T.E., Holmes, P., 1999. Simulation and prediction of swash oscillations on a steep beach. Coastal Engineering, 36(3): 219-242.

Basilici, G., de Luca, P.H.V., Poire, D.G., 2012. Hummocky cross-stratification-like structures and combined-flow ripples in the Punta Negra Formation (Lower-Middle Devonian, Argentine Precordillera): A turbiditic deep-water or storm-dominated prodelta inner-shelf system? Sedimentary Geology, 267: 73-92.

Bastide, J., 2011. Morphodynamique et enjeux d'aménagement des franges littorales d'un estuaire macrotidal tempéré : la Baie de Somme, Picardie, France, Unpublished PhD thesis, Université du littoral côte d'Opale, Dunkerque, 332 pp.

Berné, S., Auffret, J.-P., Walker, P., 1988. Internal structure of subtidal sandwaves revealed by high-resolution seismic reflection. Sedimentology, 35(1): 5-20.

Brenchley, P.J., Newall, G., 1982. Storm-influenced inner-shelf sand lobes in the Caradoc (Ordovician) of Shropshire, England. Journal of Sedimentary Research, 52(4).

Brenchley, P.J., Romano, M., Gutierrez-Marco, J.C., 1986. Proximal and distal hummocky cross-stratified facies on a wide Ordovician shelf in Iberia. 241-255.

Brocchini, M., Baldock, T.E., 2008. Recent advances in modeling swash zone dynamics: Influence of surf-swash interaction on nearshore hydrodynamics and morphodynamics. Reviews of Geophysics, 46(3).

Brocchini, M., Peregrine, D.H., 1996. Integral flow properties of the swash zone and averaging. Journal of Fluid Mechanics, 317: 241-273.

Broome, R., Komar, P.D., 1979. Undular hydraulic jumps and the formation of backlash ripples on beaches. Sedimentology, 26(4): 543-559.

Campbell, C.V., 1966. Truncated wave-ripple lamina. Journal of Sedmentary Petrology, 36: 825–828.

Cartigny, M.J.B., Ventra, D., Postma, G., van Den Berg, J.H., 2014. Morphodynamics and

sedimentary structures of bedforms under supercritical-flow conditions: New insights from flume experiments. Sedimentology, 61(3): 712-748.

Cayocca, F., 1996. Modélisation morphodynamique d'une embouchure tidale : application aux passes d'entrée du Bassin d'Arcachon, Unpublished PhD thesis, University Bordeaux 1, Bordeaux, France, 426 pp.

Chauhan, P.P.S., 2000. Bedform Association on a Ridge and Runnel Foreshore: Implications for the Hydrography of a Macrotidal Estuarine Beach. Journal of Coastal Research, 16(4): 1011-1021.

Cheel, R.J., Leckie, D.A., 1992. Coarse-grained storm beds of the Upper Cretaceous Chungo Member (Wapiabi Formation), southern Alberta, Canada. Journal of Sedimentary Research, 62(6).

Clifton, H.E., 2006. A re-examination of facies models for clastic shorelines. In: H.W. Posamentier, R.G. Walker (Eds.), Facies Model Revisited. SEPM, Special Publication, vol. 84, pp. 293-337.

Clifton, H.E., Hunter, R.E., Phillips, R.L., 1971. Depositional structures and processes in the non-barred high-energy nearshore. Journal of Sedimentary Research, 41(3).

Cummings, D.I., Dumas, S., Dalrymple, R.W., 2009. Fine-grained versus coarse-grained wave ripples generated experimentally under large-scale oscillatory flow. Journal of Sedimentary Research, 79(1-2): 83-93.

Dabrio, C.J., 1982. Sedimentary structures generated on the foreshore by migrating ridge and runnel systems on microtidal and mesotidal coasts of S. Spain. Sedimentary Geology, 32(1–2): 141-151.

Dalrymple, R.W., 1984. Morphology and internal structure of sandwaves in the Bay of Fundy. Sedimentology, 31(3): 365-382.

Dashtgard, S.E., Gingras, M.K., MacEachern, J.A., 2009. Tidally modulated shorefaces. Journal of Sedimentary Research, 79(11-12): 793-807.

Dashtgard, S.E., MacEachern, J.A., Frey, S.E., Gingras, M.K., 2012. Tidal effects on the shoreface: Towards a conceptual framework. Sedimentary Geology, 279: 42-61.

Dott, R., Bourgeois, J., 1982. Hummocky stratification: significance of its variable bedding sequences. Geological Society of America Bulletin, 93(8): 663-680.

Duke, W.L., 1985. Hummocky cross-stratification, tropical hurricanes, and intense winter storms. Sedimentology, 32(2): 167-194.

Dumas, S., Arnott, R.W.C., Southard, J.B., 2005. Experiments on Oscillatory-Flow and Combined-Flow Bed Forms: Implications for Interpreting Parts of the Shallow-Marine Sedimentary Record. Journal of Sedimentary Research, 75(3): 501-513.

Ferry, S., 2015. Influence du cycle de marée sur les HCS littoraux. Données comparées de plages actuelles et de séquences côtières anciennes., 15ème Congrès Français de Sédimentologie, Chambery, France.

Gallagher, E.L., 2003. A note on megaripples in the surf zone: evidence for their relation to steady flow dunes. Marine Geology, 193(3–4): 171-176.

Ghienne, J.F., Girard, F., Moreau, J., Rubino, J.L., 2010. Late Ordovician climbing-dune cross-stratification: A signature of outburst floods in proglacial outwash environments? Sedimentology, 57(5): 1175-1198.

Greenwood, B., Sherman, D.J., 1986. Hummocky cross-stratification in the surf zone: flow parameters and bedding genesis. Sedimentology, 33(1): 33-45.

Harms, J.C., Southard, J.B., Spearing, D.R., Walker, R.G., 1975. Depositional environments as interpreted from pri- mary sedimentary structures and stratification sequences. SEPM Short Course, 2.

Hendershot, M.L., Venditti, J.G., Bradley, R.W., Kostaschuk, R.A., Church, M., Allison, M.A., 2016. Response of low-angle dunes to variable flow. Sedimentology, 63(3): 743-760.

Hughes, B.A., Stewart, R.W., 1961. Interaction between gravity waves and a shear flow. Journal of Fluid Mechanics, 10(3), pp. 385–400.

Lang, J., Dixon, R.J., Le Heron, D.P., Winsemann, J., 2012. Depositional architecture and sequence stratigraphic correlation of Upper Ordovician glaciogenic deposits, Illizi Basin, Algeria. Geological Society, London, Special Publications, 368(1): 293-317.

Lang, J., Winsemann, J., 2013. Lateral and vertical facies relationships of bedforms deposited by aggrading supercritical flows: From cyclic steps to humpback dunes. Sedimentary Geology, 296: 36-54.

Langford, R., Bracken, B., 1987. Medano Creek, Colorado, a model for upper-flow-regime fluvial deposition. Journal of Sedimentary Petrology, 57(5): 863-870.

Larsen, S.M., Greenwood, B., Aagaard, T., 2015. Observations of megaripples in the surf zone. Marine Geology, 364: 1-11.

Longo, S., Petti, M., Losada, I.J., 2002. Turbulence in the swash and surf zones: a review. Coastal Engineering, 45(3–4): 129-147.

Marren, P.M., Russell, A.J., Rushmer, E.L., 2009. Sedimentology of a sandur formed by multiple jökulhlaups, Kverkfjöll, Iceland. Sedimentary Geology, 213(3–4): 77-88.

Morsilli, M., Pomar, L., 2012. Internal waves vs. surface storm waves: a review on the origin of hummocky cross-stratification. Terra Nova, 24(4): 273-282.

Mulder, T., Razin, P., Faugeres, J.C., 2009. Hummocky cross-stratification-like structures in deep-sea turbidites: Upper Cretaceous Basque basins (Western Pyrenees, France). Sedimentology, 56(4): 997-1015.

Perillo, M.M., Best, J., Garcia, M.H., 2014. A New Phase Diagram for Combined-Flow Bedforms. Journal of Sedimentary Research, 84(4): 301-313.

Quin, J.G., 2011. Is most hummocky cross-stratification formed by large-scale ripples? Sedimentology, 58(6): 1414-1433.

Schmincke, H.-U., Fisher, R.V., Waters, A.C., 1973. Antidune and chute and pool structures in the base surge deposits of the Laacher See area, Germany. Sedimentology, 20(4): 553-574.

Swales, A., Oldman, J.W., Smith, K., 2006. Bedform geometry on a barred sandy shore. Marine Geology, 226(3–4): 243-259.

Thauront, F., 1994. Les transits sédimentaires subtidaux dans les passes internes du Bassin d'Arcachon, Unpublished PhD thesis, Unversity Bordeaux 1, Bordeaux, France, 304 pp.

Thiry-Bastien, P., 2002. Stratigraphie séquentielle des calcaires bajociens de l'Est de la France (Jura - Bassin de Paris), Unpublished PhD Thesis, Université Claude Bernard Lyon 1, 411 pp.

Vaucher, R., Martin, E.L.O., Hormière, H., Pittet, B., 2016. A genetic link between Konzentrat- and Konservat-Lagerstätten in the Fezouata Shale (Lower Ordovician, Morocco). Palaeogeography, Palaeoclimatology, Palaeoecology, 460: 24-34.

Vaucher, R., Pittet, B., Hormière, H., Martin, E.L.O., Lefebvre, B., in press. A wave-dominated, tide-modulated model for the Lower Ordovician of the Anti-Atlas, Morocco. Sedimentology.

Vaucher, R., Pittet, B., Passot, S., Grandjean, P., Humbert, T., Allemand, P., submitted. Bedforms in a tidally modulated ridge and runnel shoreface (Berck-Plage; North France): implications for the geological record. Continental Shelf Research.

Yang, B., Dalrymple, R., Chun, S., 2005. Sedimentation on a wave-dominated, open-coast

tidal flat, south-western Korea: summer tidal flat - winter shoreface. Sedimentology, 52(2): 235-252.

Yang, B., Dalrymple, R.W., Chun, S., 2006. The significance of hummocky cross-stratification (HCS) wavelengths: Evidence from an open-coast tidal flat, South Korea. Journal of Sedimentary Research, 76(1-2): 2-8.

Yang, B., Gingras, M.K., Pemberton, S.G., Dalrymple, R.W., 2008. Wave-generated tidal bundles as an indicator of wave-dominated tidal flats. Geology, 36(1): 39-42.

CHAPITRE V :

PERSPECTIVES ET CONCLUSIONS

I) Perspectives

Les perspectives sont subdivisées en deux parties. La première partie concerne les perspectives associées à la succession sédimentaire de l'Ordovicien inférieur décrite dans les Chapitres II et III et la deuxième partie discutera des perspectives concernant l'analyse des environnements actuels du Chapitre IV.

a. Chapitre II et III : environnements anciens (Ordovicien inférieur)

i. Géochimie

Deux lentilles gréseuses (*cf. sandstone lenses* Chapitres II et III) ont été échantillonnées afin d'effectuer des analyses en éléments majeurs, mineurs, traces et Terres Rares. Le protocole analytique mis en place par Dr. Sylvain Pichat (ENS de Lyon) est détaillé dans l'**Annexe 1.** L'échantillonnage a été réalisé du centre des lentilles à leur périphérie. Certains des résultats (**Annexe 2**) sont brièvement mis en forme dans la figure 5.1. Bien que les résultats ne soient pas encore interprétés, on note que tous les éléments majeurs, traces ou Terres Rares présentent une concentration décroissante à mesure que l'on se rapproche du centre des lentilles, à l'exception du Li, Mn, Ca, Sr et Fe qui augmentent de la périphérie vers le centre des lentilles (Fig. 5.1). Cette appauvrissement relatif à mesure que l'on se rapproche du centre de la lentille pourrait être en lien avec la circulation des fluides qui ont cimenté ces lentilles entre les parties les plus poreuses (centre de la lentille) et moins poreuses (périphérie de la lentille). L'augmentation relative en Ca et Sr est intuitivement expliquée par l'abondance de bioclastes à squelette carbonaté présents au centre des lentilles. Cependant, l'augmentation relative de la concentration en Li, Mn, et Fe au centre des lentilles pourrait quant à elle être la signature de fluides hydrothermaux, possiblement liés à l'expansion de l'océan Rhéique.

Une question intéressante d'un point de vue paléontologique serait de déterminer quand ces fluides hydrothermaux ont circulé. En effet, par analogie avec l'Actuel, de nombreux écosystèmes hyper-spécialisés sont associés à de tels échappements de fluides dans les fonds océaniques. Il serait donc intéressant d'analyser plus en détail ces résultats, afin de (1) contraindre l'origine de ces fluides ; (2) de dater leur mise en place, car potentiellement, ces fluides ont pu avoir un rôle dans la mise en place des écosystèmes des Fezouata. Toutefois, une connaissance plus pointue du comportement des éléments analysés est impérative afin d'effectuer des comparaisons avec les travaux réalisés sur les circulations de fluides hydrothermaux. Une circulation hydrothermale pourrait être aussi mise en évidence par la présence de minéraux tels que l'adulaire ou la monazite qui auraient pu précipiter aux centres des lentilles. La formation de l'adulaire, par exemple, pourrait être datée par K/Ar permettant de contraindre la mise en place de cette circulation fluide. La Formation des Fezouata est riche en micas et, de ce fait, une chloritisation de

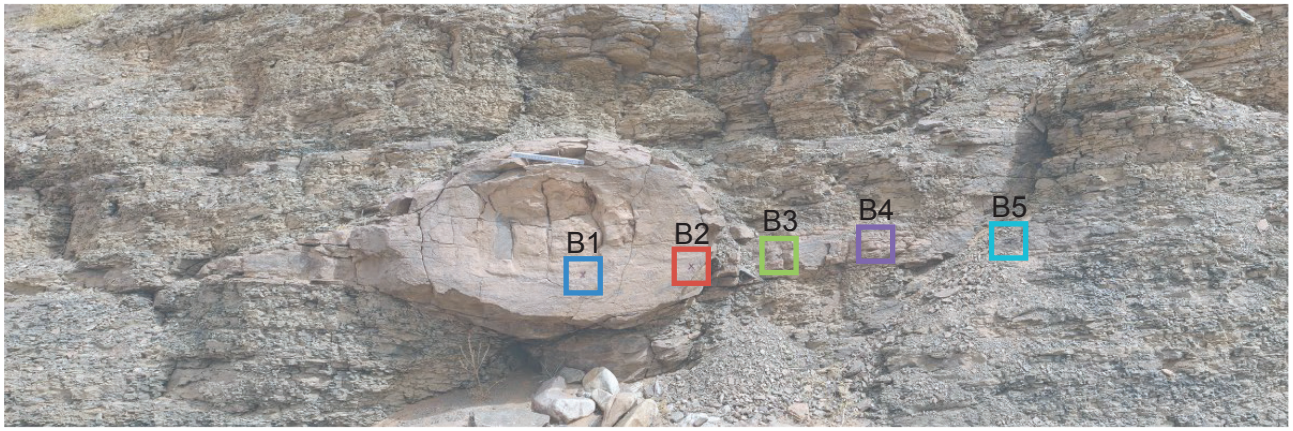

Eléments traces

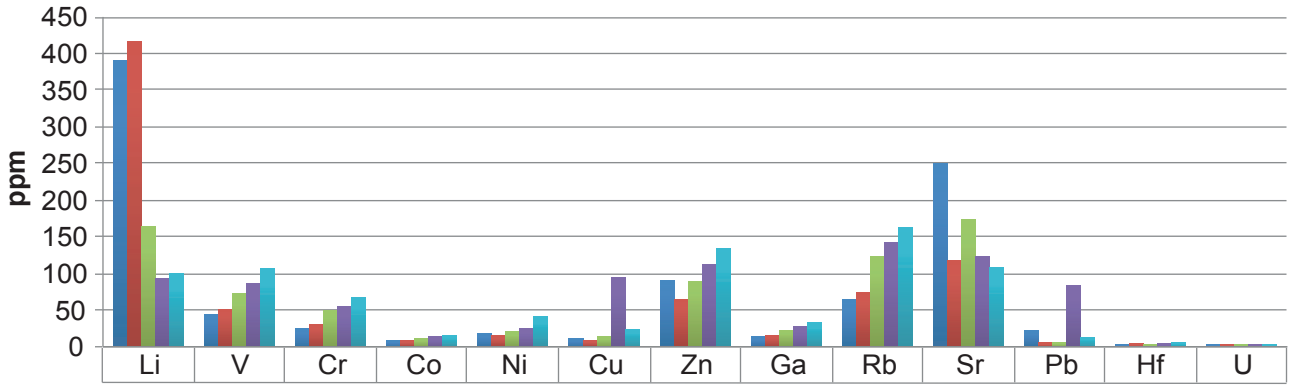

Eléments majeurs

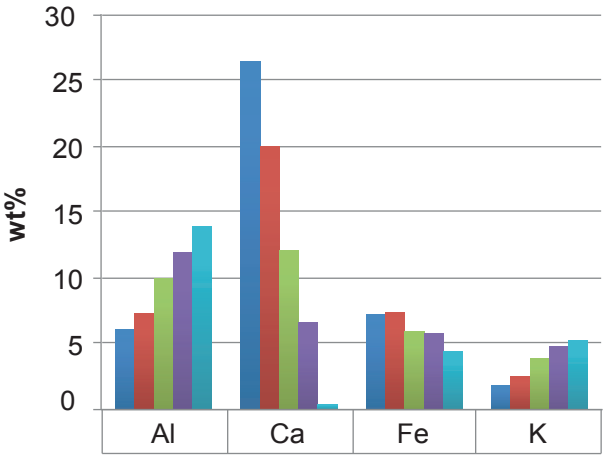

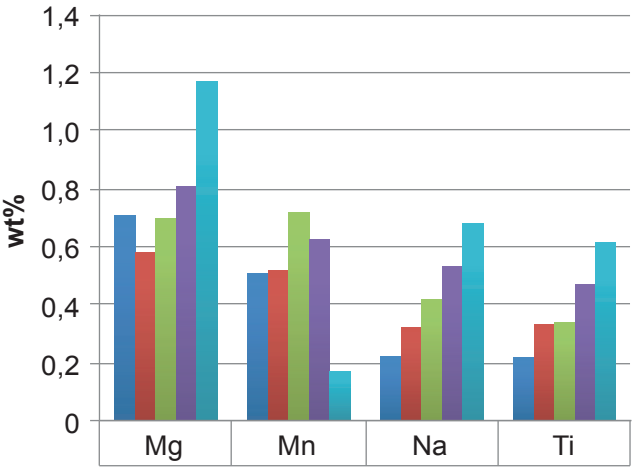

Terres Rares

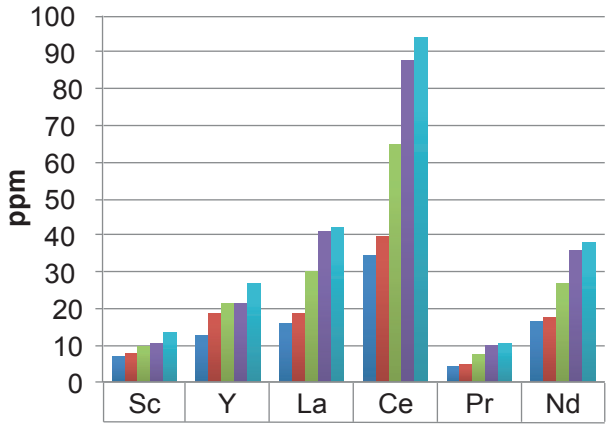

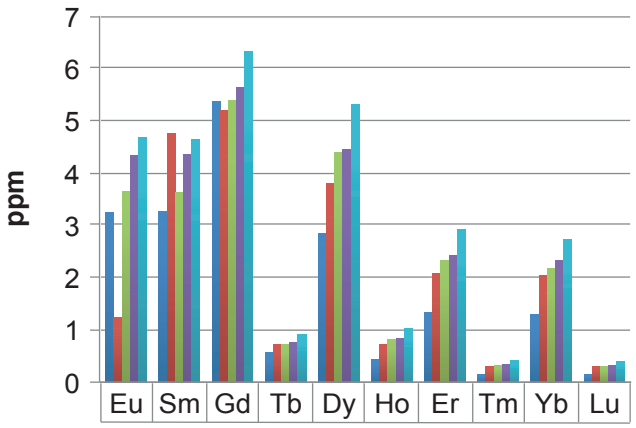

Fig. 5.1. *Résultats des analyses géochimiques effectuées sur une lentille gréseuse de la coupe Nord Douirat Est. Chaque élément est associées à cinq couleurs qui correspondent aux différentes positions B1 à B5 sur la lentille gréseuse.*

ces derniers aux centres des lentilles permettrait aussi d'argumenter l'hypothèse d'une circulation de fluides hydrothermaux. Cette chloritisation pourrait être également datée, ce qui permettrait d'estimer le moment de la mise en place de ces circulations.

ii. Localités d'intérêts paléontologiques

L'élaboration d'un modèle sédimentaire de dépôt pour l'Ordovicien inférieur de la région de Zagora (*cf.* Chapitre II) a permis de contraindre la distribution paléoenvironnementale et stratigraphique des gisements fossilifères à préservation exceptionnelle (*cf.* Chapitre III). Sur la base de ce modèle, une prospection pourrait être réalisée : (1) dans d'autres localités de la plaine des Ternata (au Nord de Zagora), mais aussi (2) dans d'autres régions paléogéographiques.

La Formation des Fezouata s'étend sur plus de 600 km, de Tan-Tan, au Sud-Ouest, à Erfoud, au Nord-Est (*cf.* Chapitres I et II). Les faciès sédimentaires associés aux gisements à préservation exceptionnelle étant désormais bien établis dans la région de Zagora, il serait intéressant, d'un point de vue paléontologique, de tester ce modèle dans d'autres localités, plus jeunes ou plus anciennes, afin de découvrir de potentiels nouveaux assemblages fauniques. La découverte de tels gisements permettrait ainsi d'appréhender l'évolution temporelle des assemblages fauniques et, par conséquent, apporterait de précieux renseignements sur les étapes initiales de la Grande Biodiversification Ordovicienne. Dans la région de Zagora, les localités de Abernoss, Taakil Nord, Taakil Sud et Touna sont les localités idéales pour prospecter dans des niveaux floiens car elles présentent les faciès sédimentaires caractéristiques qui sont associés à la préservation exceptionnelle. Pour des niveaux trémadociens potentiellement plus anciens que ceux découverts actuellement, la zone d'affleurement de la Formation des Fezouata située entre le Jebel Tibastikoustine et celui de Jebel Adafan serait idéale (Est - Sud Est de Zagora). Plus loin au nord-est, entre Tazzarine et Alnif et plus précisément dans le secteur de Taichoute, des gisements pourraient être découverts. En effet, un niveau à échinodermes, ainsi qu'une lentille à anomalocarides ont été découverts récemment. Leur position stratigraphique n'est pour l'instant pas précisée, même si un âge floien est probable car le Trémadocien est quasiment absent dans cette région (Fig. 1.12 ; S & BL). Il serait donc intéressant de tester si le modèle sédimentaire de dépôt développé dans la région de Zagora est valide dans le cadre d'une prospection paléontologique dans une autre région de l'Anti-Atlas (Taichoute).

Dans un contexte paléogéographique très différent, la Formation Santa Rosita (Cambrien, Etage 10 – Ordovicien, Trémadocien) représente, d'un point de vue paléontologique et sédimentologique, un analogue potentiellement plus ancien de la

Formation des Fezouata. Cette formation sédimentaire affleure en Amérique du Sud, au nord-ouest de l'Argentine et au sud de la Bolivie. En effet, la découverte d'un *Apankura machu* (Membre Casa Colorada, Formation de Santa Rosita) ainsi que celle d'un marrellomorphe d'âge trémadocien inférieur (Formation de Floresta) constituent des indices intéressants, qui invitent à la poursuite de la prospection de gisements à préservation exceptionnelle sud-américains. Pour plus de détails concernant cette problématique, un projet d'étude en collaboration avec Dr. Luis Buatois (Université de Saskatchewa ; Canada) et Dr. Emilio Vaccari (Univerisité National de Cordoba ; Argentine) est présenté dans l'**Annexe 3**.

iii. Localités d'intérêts sédimentologiques

Comme mentionné dans les Chapitres I et II, la Formation du Zini fait environ 10 m d'épaisseur dans la région de Zagora alors qu'elle peut en atteindre plus de 350 m dans le Sud-Ouest du Maroc (région de Tilesoun ; *cf.* Chapitre I). Une étude de la Formation du Zini plus au Sud serait très intéressante afin de comprendre l'origine d'une telle variation d'épaisseur et mettre en évidence, par exemple, un éventuel contrôle tectono-structural de la distribution des unités gréseuses du Zini, en lien avec l'histoire extensive du bassin des « Fezouata » suite au rifting cambrien. Par ailleurs, le modèle sédimentaire de dépôt pourrait alors être testé et validé pour des environnements plus gréseux et donc probablement plus proximaux que ceux généralement analysés au cours de cette thèse. Les observations faites dans l'actuel pourraient potentiellement être utilisées pour contraindre encore mieux dans le fossile l'effet de la modulation de la marée sur des environnements côtiers dominés par la houle.

D'autres localités pourraient faire l'objet d'études sédimentologiques, notamment la Formation de Staithes (Pliensbachien, Yorkshire, Royaume-Uni) ainsi que le Miocène affleurant près de Saint-Nazaire-en-Royans le long de la Bourne (limite entre le département de l'Isère et de la Drôme ; France) au croisement entre la D351 et la D76A. Ces deux formations enregistrent une dominance de la houle mais une influence de la marée semble y être néanmoins présente. Ces deux formations présentent des rides symétriques (de longueur d'onde décimétrique à métrique) présentant deux phases (accrétion verticale et latérale), comme dans le cas des structures observées à Arcachon. En effet, ces rides commencent en accrétion verticale (rides de houle ou HCS) puis évoluent en accrétion latérale donnant cet aspect de progradation, phénomène que l'on retrouve dans les morphologies en dôme dans la zone intertidale du Cap-Ferret mais aussi dans la succession sédimentaire de Crémieu. En effet, ce phénomène a été mis en avant dans le Chapitre IV comme étant caractéristique d'une influence de la marée dans un contexte dominé par la houle.

b. Chapitre IV : environnements actuels

i. Caractérisation *in situ* et localités d'intérêts potentiels

Des simulations numériques et analogiques sont envisagées pour faire suite aux travaux sur l'Actuel. Afin de mieux contraindre les paramètres physiques impliqués lors des simulations proposées plus loin dans ce chapitre, il paraît important de caractériser les processus en jeu de façon précise. En effet les paramètres suivants doivent être calibrés *in situ* :

- longueur d'onde de la houle
- fréquence de la houle
- hauteur de la houle
- vitesses de fond (oscillatoires et/ou unidirectionnelles) liées à la houle
- granulométrie du sédiment
- vitesses liées aux courants de marée
- quantification de la dérive littorale
- analyse des stratifications internes de morphologies sédimentaires formées à la zone de transition *surf-swash,* présentant un aspect 2D/2.5D comme c'est le cas à la plage de Vert Bois (Ile d'Oléron, Charente, France)

Dans un premier temps il serait nécessaire d'effectuer une mission de suivi sur une longue période (un cycle mortes-eaux vives-eaux par exemple) et de ne pas effectuer des missions ponctuelles. En effet, un suivi sur du moyen terme permettrait d'acquérir suffisamment de données pour les confronter à nos hypothèses : flux supercritiques et/ou interférentiel de houle. Cela permettrait aussi d'être plus précis concernant la hauteur des vagues nécessaire à la formation de ces morphologies en dômes. Afin de contraindre les différents paramètres de la houle un courantomètre houlographe S4 ADW pourrait être utilisé. En effet, cet appareil permet de mesurer la direction et l'intensité horizontale de la houle. Les différentes mesures de courants pourraient être réalisées à l'aide d'un courantomètre hydroacoustique (ex : *Acoustic Doppler Current Profiler*) qui permet d'obtenir la direction et l'intensité des courants en se basant sur l'énergie acoustique réfléchie par les particules contenues dans l'eau. Un suivi de l'évolution des morphologies sédimentaires au cours d'un cycle de marée pourrait être réalisé à l'aide d'un sonar à multifaisceaux, ce qui fournirait un aspect dynamique à l'analyse. Ce sonar permettrait de réaliser des cartes topographiques du fond à différents moments, permettant ainsi de contraindre l'évolution de ces morphologies en dômes au cours d'un cycle de marée. Dans tout les cas, un suivi de l'évolution des structures internes *in situ* paraît peu réalisable et donc une simulation analogique semble plus adéquate. La combinaison de ces mesures couplée *à* l'observations des structures sédimentaires rendrait plus robuste les hypothèses

émises au cours de ce travail (Chapitre IV).

Des morphologies en dôme similaires à celles observés sur la pointe du Cap Ferret se forment dans d'autres zones intertidales, telles que :

- La plage de Vert Bois (Ile d'Oléron, Charente, France)
- La Pointe de la Presqu'île d'Arvert (Charente-Maritime, France)
- La plage de Silloh (North West, Angleterre)
- La plage de Trouville-sur-Mer (Normandie, France)

Une étude comparée des structures internes de ces dômes, ainsi que des conditions hydrodynamiques permettant leur formation pourrait être envisagée afin de mieux contraindre leur genèse et de valider les hypothèses formulées dans ce travail.

ii. Simulations numériques

Des simulations numériques sont en cours, en collaboration avec Dr. Thomas Humbert (Ecole Supérieur de Physique et Chimie Industrielle). Les environnements actuels du Chapitre IV (Berck-Plage et le Cap-Ferret) présentent des géomorphologies non-linéaires qui induisent la propagation des fronts d'ondes de houle dans toutes les directions (ondes réfractées par les topographies). Ainsi, à travers les zones intertidales de Berck-Plage et du Cap-Ferret, les fronts d'ondes vont se croiser et donc interférer. Actuellement, le mouvement des masses d'eau au fond ainsi que le mouvement des sédiments associés à cette interférence n'est pas connu. Bien que les morphologies sédimentaires observées à marée basse à la pointe du Cap-Ferret aient été interprétées comme étant le résultat de flux supercritiques, il n'est pas exclu que le croisement des ondes de houles ait une influence sur la genèse de ces structures sédimentaires, du moins dans leur stade initial de formation. Afin de mieux contraindre l'interaction de deux fronts de houles sur le sédiment, un code numérique préliminaire est en développement. Dans ce code, deux longueurs d'ondes de houles sont incrémentées avec un angle d'incidence et une amplitude fixés. Ces deux ondes vont être lancées sur une matrice de points représentant le fond marin présentant une pente (l'angularité de la pente peut être variée). Une granulométrie fixe ou en gradient est ensuite associée à cette matrice. En transformant la relation de dispersion d'onde (voir équation 2 ; Chapitre I), une vitesse au fond, dépendante de la longueur d'onde en surface ainsi que de l'amplitude va être calculée. La profondeur limite de déferlement qui est fonction du diamètre de l'orbital et de la profondeur d'eau va être calculée respectivement par rapport à l'onde. En prenant en compte la vitesse au fond calculée, du type d'écoulement (turbulent ou laminaire), de la vitesse de mise en mouvement des particules en fonction de leur diamètre (en les assumant sphériques) et de la densité du fluide dans lequel elles se trouvent, le code calcule alors

des longueurs d'ondes de structures sédimentaires associées à un courant oscillatoire pour une profondeur et une granulométrie donnée. Pour l'instant le code est prometteur mais l'effet d'un croisement d'onde n'est pas encore très bien contraint numériquement et il serait probablement nécessaire de créer un code numérique progressif plutôt que statique.

iii. Simulations analogiques

En complément des simulations numériques, une expérimentation analogique serait d'un grand intérêt afin de caractériser les structures sédimentaires internes formées. Plusieurs paramètres pourraient être alors testés afin d'estimer (1) l'effet d'un croisement d'ondes et (2) l'effet d'un croisement d'ondes initiant un flux supercritique, tels que :

- L'angle d'incidence d'un front d'onde par rapport à un autre
- La pente du système
- La variation de la profondeur
- La granulométrie des sédiments transportés

Dans l'idéal, il faudrait un bassin expérimental de forme carrée plutôt qu'un canal. Cela permettrait l'observation des structures sédimentaires en 3D à la surface du sédiment, ce qui n'est majoritairement pas le cas pour les études expérimentales sur les laminations internes de structures sédimentaires. Il est impératif que ce dispositif expérimental permette aussi l'observation en section des structures sédimentaires formées afin de contrôler le lien entre les morphologies externes et leurs structures internes. Le problème d'échelle devra être impérativement pris en compte car les bassins expérimentaux n'ont pas toujours la possibilité de reproduire des phénomènes océaniques à l'échelle 1:1. Ce type d'expérience pourrait être conduit par exemple au sein du Ludwig-Franzius-Institut für Wasserbau, Ästuar- und Küsteningenieurwesen (Université d'Hanovre ; Allemagne) qui dispose d'un nouveau bassin pouvant faire varier l'angle d'incidence de la houle et qui présente un fond sableux.

II) Conclusions

Ce travail de thèse a eu pour but principal de caractériser des environnements sédimentaires hybrides (houle-marée) dans des systèmes anciens et actuels. Les différentes études se sont focalisées dans des systèmes où la houle (de beau temps ou de tempête) est le processus dominant, mais où l'action des marées est également présente. En deuxième lieu, le contexte paléoenvironnemental associé à la Grande Biodiversification Ordovicienne dans l'Anti-Atlas marocain a pu être précisé. Les zones étudiées furent :

- L'Anti-Atlas marocain et plus particulièrement les formations des Fezouata et du Zini (Ordovicien inférieur) dans la région de Zagora (Maroc)
- La zone intertidale de Berck-Plage (Pas-de-Calais) dans le nord de la France
- La zone intertidale du Cap-Ferret (Gironde) dans le sud-ouest de la France

Les principales conclusions des études effectuées sur l'Ordovicien inférieur marocain sont :

(1) Les formations des Fezouata et du Zini sont subdivisées en 14 faciès sédimentaires eux-mêmes groupés en 4 zones de faciès : l'offshore proximal, l'avant-plage inférieure, l'avant-plage supérieure, la zone intertidale-plage. L'Ordovicien inférieur de la région de Zagora enregistre des environnements de dépôt allant de l'offshore à la plage avec une dominance de l'action de la houle. L'effet de la marée est exclusivement mis en évidence par modulation de l'action de l'houle lors des fluctuations du niveau de la mer au cours d'un cycle de marée et aucune structure tidale classique n'est présente. Un nouveau modèle sédimentaire de dépôt pour un système dominé par la houle et modulé par la marée est donc proposé. Les deux principales caractéristiques d'un tel environnement de dépôt sont : (i) les dépôts sont discontinus à toutes échelles et à toutes profondeurs (de la zone intertidale-plage à l'offshore) ; et (ii) les dépôts enregistrent indirectement des changements du niveau de la mer en lien avec les cycles tidaux qui s'exprimeront de différentes façons en fonction de la bathymétrie. Cette étude a permis de mettre en évidence l'un des rares systèmes dominés par la houle, modulés par la marée, enregistrant des environnements de la zone intertidale-plage jusqu'à l'offshore.

(2) L'analyse sédimentologique de la Formation des Fezouata (Tremadocien-Floien) dans la région de Zagora révèle l'existence de deux types d'intervalles riches en fossiles: les *Konservat-Lagerstätten* (Ksl) et *Konzentrat-Lagerstätten* (Kzl). Les KsL sont caractérisés par des fossiles à préservation exceptionnelle, et les KzL par des niveaux coquilliers. Les intervalles à KsL se situent au sommet de niveaux silto-argileux recouverts par des dépôts de tempête (grès à grains fins). Les KsL sont retrouvés dans des environnements d'avant-plage inférieure distale proche de la limite d'action des vagues de tempête. Les KzL font partie des dépôts de tempête de l'avant-plage inférieure proximale. Les KzL contiennent exclusivement des débris coquilliers, principalement des gastéropodes, des bivalves, des brachiopodes et des fragments de trilobites. Les restes d'organismes à corps mous et minéralisés sont préservés dans les KsL. Pendant les tempêtes, les sédiments sont transportés depuis les environnements côtiers vers le large. Ces sédiments vont enfouir des communautés *in situ* dans des milieux distaux (KsL), et concentrer des restes squelettiques d'organismes vivants (ou déjà morts) dans des environnements plus proximaux (KzL). Par conséquent, les intervalles fossilifères se retrouvent dans différents environnements (avant-plage inférieure proximale ou distale),

mais le même processus (tempête) est associé à leur formation. Des conditions au fond de la mer relativement inhospitalières, telles que des concentrations faibles en oxygène et en sulfate, ont probablement contribué à favoriser la préservation exceptionnelle des tissus mous dans les KsL.

Les conclusions principales en lien avec les études dans les environnements actuels sont :

(3) L'analyse de la zone intertidale de Berck-Plage a permis de définir et de cartographier sept types de structures sédimentaires observées à marée basse durant des conditions de beau temps (3D CR : rides de courants 3D ; 3D AR : rides asymétriques 3D ; 2D SR : rides symétriques 2D ; 2D SSD : petites dunes symétriques 2D ; 2D SD : dunes symétriques 2D ; 3D SD : dunes symétriques 3D et USPB : stratifications planes parallèles). L'analyse de ces sept types de structures sédimentaires a permis de caractériser les paramètres d'écoulement responsables de leur formation et de leur distribution. Les résultats confirment la prédominance de structures sédimentaires ayant des affinités avec un courant oscillatoire, bien que la zone d'étude soit soumise à l'action des marées (marnage mégatidal). Cette étude a permis de proposer une chronologie pour la formation et la distribution de chaque structure sédimentaire. L'agencement vertical peut être ainsi traduit comme équivalent d'une succession stratigraphique. Celle-ci peut être appliquée à d'anciennes successions sédimentaires comme critère de reconnaissance pour des environnements proximaux dominés par la houle et modulés par la marée lorsqu'aucune structure d'origine purement tidale n'est générée. La géomorphologie non-linéaire des environnements côtiers (ici en barres-et-bâches) induisant la réfraction de la houle explique vraisemblablement l'organisation en maille des structures sédimentaires, ainsi que la formation des 3D SD. Les 3D SD partagent des caractéristiques externes communes aux stratifications entrecroisées en mamelons (HCS). Il semblerait donc que ces 3D SD (HCS-*like*) pourraient être formés à des vitesses orbitales inférieures à celles proposées précédemment dans la littérature, et résultant ainsi de l'interférence d'ondes de houle qui crée un mouvement combiné des particules sédimentaires sur le fond marin.

(4) La zone intertidale du Cap-Ferret présente des structures sédimentaires particulières en dôme (morphologiquement similaire aux 3D SD observés à Berck-Plage) qui sont ici décrites et interprétées en terme de processus. Ces morphologies sédimentaires ont une longueur d'onde de *ca.* 1,2 m et une élévation de *ca*. 30 cm. Ces dernières se caractérisent par des stratifications en creux, planes, tangentielles, tabulaires et mamelonnées. Cette étude préliminaire propose que ces structures en dôme soient générées à la zone de transition *surf-swash* par le reflux des vagues. En fonction de la hauteur des vagues, si celle-ci est suffisamment importante, le flux induit -et donc le reflux- peuvent atteindre des conditions supercritiques. Lorsque ces conditions sont

atteintes, des structures sédimentaires formées par des *chutes-and-pools* peuvent avoir lieu, expliquant les différents types de stratifications internes reconnues. Ces morphologies en dôme (structures 3D) s'expliquent par le fait que l'écoulement du flux et du reflux se produit dans des directions différentes, ce qui n'est pas favorable pour former des structures sédimentaires à crêtes quasi-linéaires. Cette étude suggère également que la reconnaissance de telles structures sédimentaires dans l'enregistrement sédimentaire pourrait être utilisée comme outil de reconstruction paléoenvironnementale pointant la zone de transition *surf-swash*. De plus, l'aspect érosif des *bottomsets* est proposé comme critère de reconnaissance de l'influence de la marée pour des environnements sédimentaires dominés par la houle.

نهاية

ANNEXES

Annexe 1 : Protocole expérimental des analyses géochimiques

Sample dissolution

Samples were analyzed for a suite of major, minor, and trace elements (Al, Ca, Fe, K, Mg, Na, Ti, Mn, Ba, Li, Rb, Sr, V, Cr, Cu, Zn, Pb, Ga, Hf, U, and REE). All acids were distilled in a DST-1000 (Savillex) sub-boiling system. Water used is Milli-Q water. All containers were acid-cleaned. Samples dissolution and preparation for analyses were made in a class 1000 clean laboratory.

Around 50 g of sample was first dried and ground. Approximately 100 mg of sample powder was used for analyses. Sample powder was humidified with *ca.* 1ml of Milli-Q H_2O to avoid projections. 1ml of concentrated HNO3 was added to the powder dropwise to let CO_2 evolve. The sample was then dissolved in a 2:1 mixture of concentrated HF:HNO_3 (v:v) for 48h at 120°C and evaporated to dryness. A 1:1 mixture of 70% $HClO_4$: concentrated HNO_3 was added to the sample and evaporated at 200°C until fumes of perchloric acid are evolved. 4 ml of HCl 6N were added and evaporated to dryness after 24h at 120°C in closed vials. This step helps to remove potential leftover fluorides. The sample was then converted to nitric form with a few drops of concentrated HNO_3 and evaporated to dryness. The sample was finally brought back into solution in 5 ml HNO_3 4N. The solution was centrifuged to check that there were no remaining particles. Aliquots were taken for the various analyses.

Analysis

Al, Ca, Fe, K, Mg, Mn, Na, Ti, Ba, Ga, Ni, and Pb were measured by Inductively-Coupled Plasma Optical Emission Spectrometry (ICP-OES, Thermo iCAP). Li, V, Cr, Mn, Co, Ni, Cu, Zn, Ga, Rb, Sr, Hf, Pb, U, and REE were measured by Quadrupole Inductively-Coupled Plasma Mass-Spectrometry (Q-ICP-MS, Agilent 7500cx). Two dilutions were used for ICP-OES measurements, and three for the Q-ICP-MS measurements. These dilutions allowed us to cover a large range of concentrations as well as a duplication of most measurements. A procedural blank was measured for each of the two sets of analyses. The blank contributions were always negligible.

Internal corrections of instrumental drift were made using Sc for ICP-OES measurements and Rh or In for Q-ICP-MS measurements.

Reference materials MAG-1 (USGS) and HISS-1 (NRCC) were used to assess the quality of the measurements. We used the REE values of Waheed et al. (2007) for HISS-1. Most measured values agreed within less than 8.4% (2σ) with the certified values for both MAG-1 and HISS-1, and less than 6.3% for REE that were measured on an independent run. However, for Gd the values measured in MAG-1 were 13.3% higher than the certified value. For Ca in MAG-1, the average value was in agreement with the certified value, but there was a rather large dispersion (18.6%, 2σ, N = 6). This might be due to the low Ca content of MAG-1 compared to some of our samples. For Mn, some of the samples measurements by Q-ICP-MS were higher than the range of the calibration curve as were those of MAG-1. For MAG-1, the Q-ICP-MS values were 9.7 to 16.3% lower than the certified value. These values are in agreement with the difference we found between the Q-ICP-MS and ICP-OES results for Mn on the same sample.

Reference

Waheed, S., Rahman, A., Siddique, N., Ahmad, S., 2007. Rare Earth and Other Trace Element Content of NRCC HISS-1 Sandy Marine Sediment Reference Material. Geostandards and Geoanalytical Research, 31(2): 133-141.

Trace elements

sa.	sa, g	Li	Li (2)	V	V (2)	Cr	Cr (2)	Mn	Mn (2)	Co	Ni_corr	Ni (2)	Cu	Cu (2)	Zn (2)	Ga	Ga (2)	Rb (2)	Sr (2)	Hf	Hf (2)	Pb	Pb (2)	U
name	g	(ppm)	(ppm)	(ppm)	(ppm)	(ppm)	(ppm)	(ppm)	(ppm)	(ppm)	(ppm)	(ppm)	(ppm)	(ppm)	(ppm)	(ppm)	(ppm)	(ppm)	(ppm)	(ppm)	(ppm)	(ppm)	(ppm)	(ppm)
A1	0,1080	122	119,1	39,3	37,9	23,7	23,8	3251	3098	4,7	11,5	15,4	9,9	8,0	75,5	14,1	14,2	60,5	133,4	6,8	8,3	8,5	7,8	1,9
A2	0,1000	75	79,4	35,2	37,2	17,2	18,8	2737	2782	6,1	12,3	16,3	9,4	9,3	59,0	13,9	15,2	68,6	449,0	4,4	5,1	174,2	179,2	2,0
A3	0,1050	49	53,1	57,4	59,2	34,5	35,5	112	106	6,7	25,6	27,8	14,3	14,1	79,3	21,7	22,2	107,6	72,4	11,6	13,0	19,0	18,4	3,4
B1	0,1099	391	404,2	43,6	45,0	24,4	26,4	4176	4233	8,4	18,3	22,0	11,1	10,5	90,7	13,5	14,7	64,1	250,5	2,1	2,7	22,5	23,6	2,7
B2	0,0982	417	414,2	51,0	48,8	30,6	31,3	4363	4076	8,6	15,0	18,5	8,8	8,6	64,6	15,9	16,0	74,6	117,7	4,3	4,6	5,2	5,1	2,3
B3	0,1147	164	170,2	72,4	72,1	49,2	50,0	6145	5840	10,9	20,7	22,5	13,6	14,4	89,3	22,6	23,9	122,9	173,3	3,4	4,0	5,8	6,4	2,1
B4	0,1030	93	86,9	86,9	86,4	55,2	53,4	5223	4692	13,5	25,3	25,1	94,0	97,2	111,6	27,4	28,2	142,8	122,5	4,1	4,8	83,9	89,2	2,5
B5	0,1030	100	96,6	107,3	107,3	66,7	66,5	1476	1347	16,0	41,3	39,9	23,4	23,4	134,5	32,7	33,7	162,5	108,5	5,4	6,1	12,9	13,7	2,9

REE

sa.	sa. wt.	Sc	Y	La	Ce	Pr	Nd	Eu	Sm	Gd	Tb	Dy	Ho	Er	Tm	Yb	Lu
name	g	(ppm)	(ppm)	(ppm)	(ppm)	(ppm)	(ppm)	(ppm)	(ppm)	(ppm)	(ppm)	(ppm)	(ppm)	(ppm)	(ppm)	(ppm)	(ppm)
A1	0,1080	5,8	18,2	22,4	48,2	5,5	20,1	1,2	4,5	4,8	0,7	3,8	0,6	2,0	0,2	1,7	0,2
A2	0,1000	6,8	22,2	28,0	64,1	7,3	26,4	3,4	3,4	5,9	0,8	4,6	0,8	2,4	0,3	2,3	0,3
A3	0,1050	10,3	26,3	28,2	60,5	7,3	25,9	3,0	3,1	4,7	0,7	4,8	0,9	2,9	0,4	2,9	0,4
B1	0,1099	6,9	12,8	16,1	34,4	4,2	16,6	3,2	3,3	5,4	0,6	2,8	0,4	1,3	0,2	1,3	0,2
B2	0,0982	7,7	18,7	18,6	39,7	4,6	17,5	1,2	4,8	5,2	0,7	3,8	0,7	2,1	0,3	2,0	0,3
B3	0,1147	9,8	21,5	30,2	64,8	7,4	26,9	3,6	3,6	5,4	0,7	4,4	0,8	2,3	0,3	2,2	0,3
B4	0,1030	10,4	21,4	41,0	87,7	10,0	35,8	4,3	4,3	5,6	0,8	4,5	0,8	2,4	0,3	2,3	0,3
B5	0,1030	13,4	27,0	42,1	93,9	10,4	37,9	4,7	4,6	6,3	0,9	5,3	1,0	2,9	0,4	2,7	0,4

Major elements

sa.	Al	Ca	Fe	K	Mg	Mn	Na	Ti	Ba	Ga*	Ni*	Pb*
name	(wt%)	(wt%)	(wt%)	(wt%)	(wt%)	(wt%)	(wt%)	(wt%)	(ppm)	(ppm)	(ppm)	(ppm)
A1	5,74	26,5	4,77	2,17	0,48	0,40	0,22	0,28	349	168	-3	171
A2	5,41	23,9	3,77	2,19	0,42	0,32	0,22	0,26	359	136	-5	427
A3	10,04	2,0	3,90	3,55	0,86	0,01	0,63	0,47	483	195	15	265
B1	6,04	26,4	7,25	1,84	0,71	0,51	0,22	0,22	317	162	5	194
B2	7,25	19,9	7,36	2,47	0,58	0,52	0,32	0,33	421	205	-1	235
B3	9,92	12,1	5,95	3,84	0,70	0,72	0,42	0,34	892	205	9	255
B4	11,91	6,6	5,76	4,80	0,81	0,62	0,53	0,47	1156	226	15	378
B5	13,92	0,4	4,39	5,25	1,17	0,17	0,68	0,61	846	308	37	319

* do not use, close to detection limits

= above calib. curve range

(2): measurement made with a different dilution and different measurement session

A1 to A3: A1 center of one lens; A3 lateral host sediment

B1 to B5: B1 center of one lens; B5 lateral host sediment

Annexe 3 : Projet postdoctoral

Proyecto científico postdoctoral

Paleoambientes sedimentarios relacionados al Gran Evento Biodiversificación del Ordovícico (GOBE) en el Noroeste de Argentina

Sedimentología y Paleontología

En colaboración con :

Dr. Luis Buatois (Universidad de Saskatchewa ; Canada)
Dr. Emilio Vaccari (Universidad Nacional de Córdoba ; Argentina)

Paleoambientes sedimentarios relacionados al Gran Evento biodiversificación del Ordovícico (GOBE) en el Noroeste de Argentina

Sedimentología y Paleontología

Objetivos

Objetivo principal

El objetivo principal de este estudio postdoctoral es precisar los paleoambientes de la Formación Santa Rosita (Cámbrico - Ordovícico Temprano). La sucesión sedimentaria de la Formación Santa Rosita contiene yacimientos de preservación excepcional de invertebrados marinos de cuerpo blando que documentan los primeros pasos del Gran Evento de Diversificación Ordovícico (GOBE). Una vez que se definan las facies sedimentarias que permiten esta conservación, se espera contribuir al reconocimiento de las preferencias ecológico-ambientales de los organismos, a comprender mejor la forma en que se conservan y, en última instancia, a identificar nuevas localidades fosilíferas.

Objetivos específicos

1. Analizar la sedimentología de la Formación Santa Rosita con el fin de caracterizar los paleoambientes generales.
2. Definir las facies sedimentarias, las tendencias proximal-distal, así como la paleobatimetría relativa y establecer un modelo depositacional para la Formación Santa Rosita.
3. Definir la relación entre los niveles fosilíferos y la sucesión sedimentaria a través de un análisis tafonómico, con el fin de entender si corresponden a asociaciones autóctonas o transportadas.
4. Identificar cómo se han conservado los fósiles (por ejemplo, asociados a matas microbianas, entierro rápido por depósitos turbidíticos o de tormenta, etc.).
5. Comparación de las comunidades y sus paleoambientes asociados con localidades similares (por ejemplo, Formación Fezouata, Marruecos).
6. Correlacionar a través de estratigrafía secuencial y bioestratigrafía las distintas secciones de las formaciones Santa Rosita y Floresta, con el fin de definir la paleogeografía de la cuenca y los potenciales niveles fosilíferos de preservación excepcional dentro de la misma.

Problemática

El Gran Evento de Biodiversification Ordovícico (GOBE) es una de las radiaciones más importantes del Eon Fanerozoico. El GOBE comenzó durante el Ordovícico inferior (ca. 485.4 – 470 Ma; Bambach et al., 2004; Servais et al., 2008; 2010) unos 35 millones de años después de la explosión del Cámbrico, y se caracteriza por una exponencial diversificación a nivel de las clases y ordenes de los phyla que aparecieron durante el Cámbrico (pe, Harper, 2006; Servais et al., 2008; 2010). A pesar de que existe un gran volumen de información respecto a la diversificación de organismos con esqueletos mineralizados, se ha reconocido un gran vacío en el registro de las faunas de cuerpo blando que abarca desde el Cámbrico tardío (Furongiano) hasta el Ordovícico medio (Darriwiliano). Los *Konservat-Lagerstätten* del Ordovícico medio y tardío son raros y posteriores a las etapas iniciales del GOBE (p.ej, Briggs et al., 1991; Liu et al., 2006;. Aldridge et al., 2007; Young et al., 2007; Botting et al., 2011). Recientemente, fue hallado un *Lagersttätte* en la Formación Fezouata del Ordovícico Inferior (Tremadociano tardío)

en Marruecos (por ejemplo, Van Roy et al., 2010; 2015; Martin et al., 2016; Lefebvre et al., 2016). Este yacimiento excepcional reveló la presencia de varios organismos con afinidades cámbricas (por ejemplo. *Furca* sp. Fig. 1A). Sobre la base de hallazgos recientes, dos potenciales *Lagersttätten* más antiguos podrían existir en Argentina. A partir del hallazgo del artrópodo no-mineralizado *Apankura* (Miembro Casa Colorada de la Formación Santa Rosita, zona de Tilcara; Vaccari et al., 2004; Fig. 1B) se presumen que el más antiguo podría estar desarrollado en el Cámbrico tardío (Furongiano). El más joven podría ser Ordovícico temprano (Tremadociano tardío temprano, Tr2) en virtud del registro de *Furca* sp. (Formación Floresta, Salta; Aris y Palomo, 2014; Fig. 1C). Algunos restos de *Furca* sp. también han sido hallados en el Miembro de Alfaricto (Tremadociano temprano; quebrada Arenal; Formación Santa Rosita). El interés paleontológico de estos posibles *Lagersttätten* en Argentina es muy grande, ya que no existen *Lagersttäten* ordovícicos previos a los de Formación Fezouata del Tremadociano superior (Tr3) - Floiano de Marruecos y los *Lagersttäten* del Cámbrico tardío son realmente raros en el mundo. Hasta el momento, estas unidades con fósiles de preservación excepcional son los únicos potenciales *Lagersttäten* en Argentina y en América del Sur.

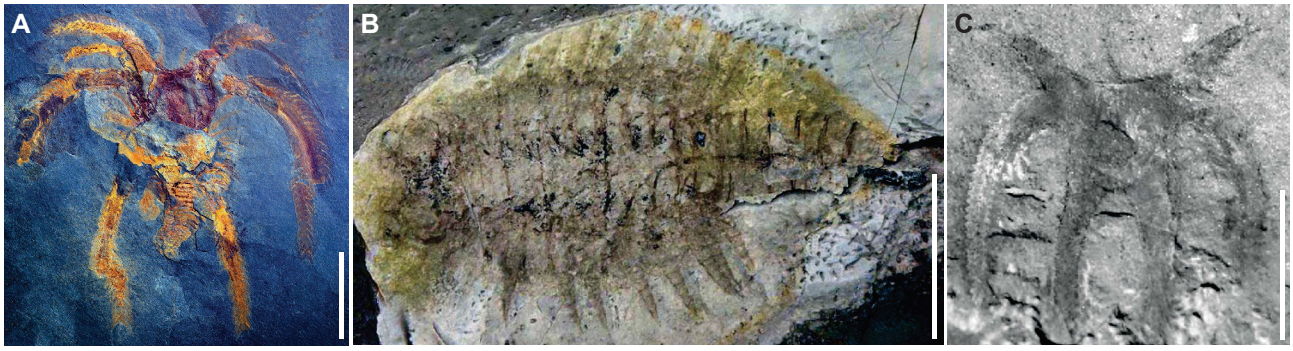

Fig.1.*(A) Furca sp. Fezouata Fm, MoroccoTremadocianotardio; Martin et al., 2016); (B) Apankura machu, (Casa Colorada Member, Santa Rosita Formation; Vaccari et al., 2004); y (C) Furca sp. Floresta Fm, Argentina (Tremadociano temprano; Aris y Palomo, 2014). Escalar: 1 cm.*

Por lo expuesto, los afloramientos de Cámbrico superior - Ordovícico inferior del noroeste de Argentina brindan buenas perspectivas para localizar yacimientos con preservación excepcional. Los mismos resultarían de importancia científica capital para caracterizar la diversificación de los metazoos durante el período Cambro-Ordovícico y completar el conocimiento sobre marco ambiental de la misma (Fig.2). Por otro lado, la posibilidad de comparar el contexto ambiental de la Formación Santa Rosita con los depósitos de aguas más profundas de la Formación Floresta permitirá comprender la distribución de la fauna a través de un gradiente ambiental y, por lo tanto, abordar los posibles controles de la misma.

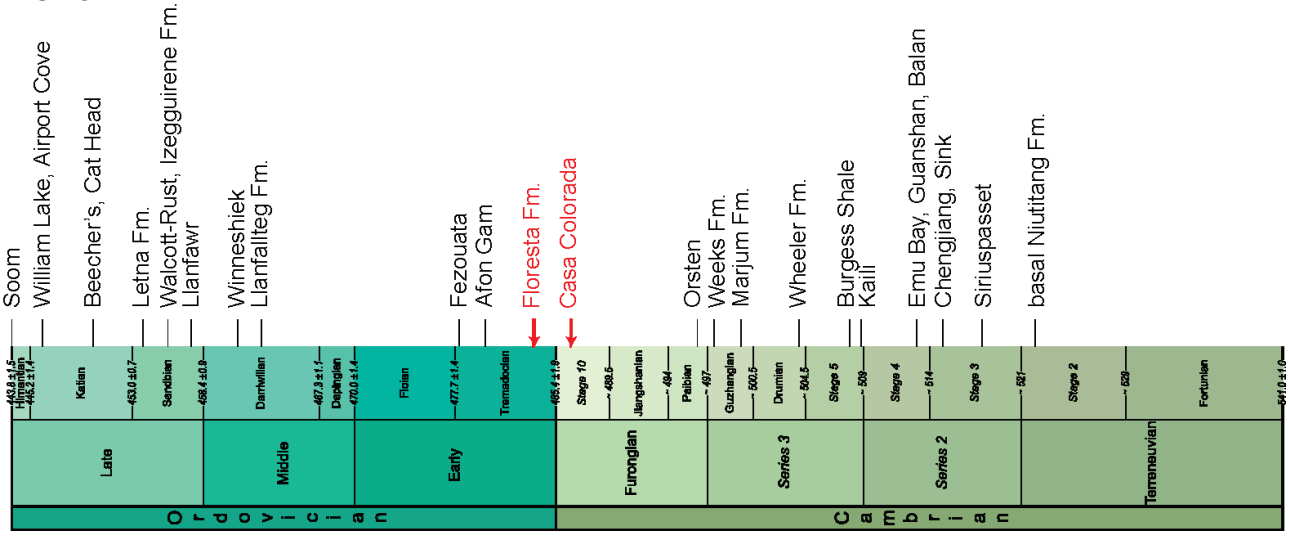

Fig. 2. *Posición estratigráfica de los Konservat-Lagersttäteconocidos del Cambro-Ordovicico (modificado de Van Roy et al., 2015)*

A través de este proyecto postdoctoral pretendemos precisar el marco paleoambiental del GOBE en Argentina utilizando un enfoque basado en estudios sedimentológicos de detalle y su comparación con el contexto ambiental en que tuvo lugar la explosión Cámbrica. Se realizará un análisis paleoambiental para (1) definir las facies sedimentarias que contienen fósiles en la formación de Santa Rosita, (2) determinar si las asociaciones de fósiles son paleocomunidades o asociaciones transportadas, (3) proporcionar criterios sedimentológicos para correlacionar distintas secciones Cambro-Ordovícico y (4) prospectar otras localidades con este interés paleontológico.

Marco general

Las sucesiones silicoclásticas del Paleozoico inferior del Noroeste de Argentina fueron depositadas en una cuenca de retro-arco a lo largo del margen occidental de Gondwana (Fig. 3) a ca. 30 ° S de latitud (ver Buatois y Mangano, 2003; Buatois et al., 2006 y citas allí). La sucesión Cámbrico Superior-Ordovícico Inferior (Fig. 4) fue depositada en ambientes marinos abiertos dominados por olas, alternados por la incisión de valles fluviales y estuarios dominados por mareas. Buatois et al., (2006) han estudiado la estratigrafía de los depósitos del Ordovícico Inferior en el área de Alfarcito (miembros Alfarcito y Rupasca de Formación Santa Rosita) y las facies sedimentarias que se describen indican ambientes relativamente poco profundos (entre la base de olas tormenta y la base de olas de buen tiempo). Si bien no se han realizado estudios sedimentológicos de detalle la Formación Floresta es el equivalente estratigráfico hacia el sur del Miembro Rupasca.

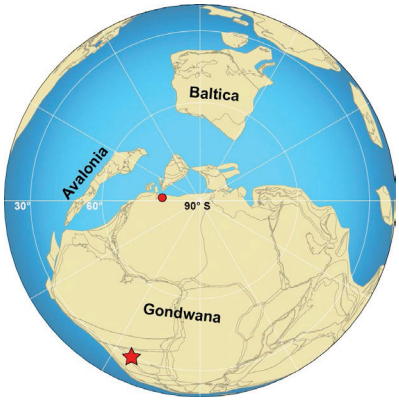

Fig. 3. *Mapa paleogeográfica del Ordovícico Temprano (estrella roja : afloramiento argentinos de interés; punto rojo : Fm Fezouata).*

Series	Stages	Stage slices	Intervals used	Biostratigraphy			Lithostratigraphy	
				Trilobites	Conodonts	Graptolites	East	West
Ordovician	Tremadocian	Tr2	Tr2	*B. tetragonalis*	*P. deltifer*	*Bryograptus*	Rupasca	
				Kainella teiichi				
		Tr1	Late Tr1	*Kainella meridionalis*	*C. angulatus*	?	Santa Rosita Fm: Alfarcito	Guayoc Chico Gr.
				Kainella andina ?		*R. f. anglica*		
			Early Tr1	*J. keideli keideli* ?	*lapetognathus*	*A. matanensis*		
Cambrian	Stage 10		Furongian	*P. (N.) frequens argentina*			Santa Rosita Fm: Pico de Halcón	
					C. proavus		Casa Colorada	Lampazar Fm
				?	?		Tilcara	Padrioc Fm

Fig. 4. *Cuadro de correlación de las unidades mencionadas (Balseiro y Waisfeld, 2013)*

Localidades de interés

La Formación Santa Rosita aflora extensamente en la Sierra Altos de Tilcara desde las cercanías de Tumbaya al sur hasta la localidad de Huacalera al norte. A lo largo de esta sierra se han encontrado algunos fósiles de preservación excepcional (FPE), entre ellos, *Apankura machu* (Vaccari et al., 2004) del Miembro Casa Colorada (Furongiano), y *Furca* sp (Vaccari, com. pers.) en el Miembro Alfarcito (Tremadociano inferior Tr2) en la quebrada del Arenal. Así, el área de Alfarcito-Arenal es de una importancia primordial para este proyecto. Por otra parte, *Furca* sp. fue también hallado en la Formación Floresta en la Sierra de Mojotoro al sur de la ciudad de Salta. Dado el potencial que esta unidad tiene para el hallazgo de FPE se levantaran varias secciones, entre ellas Chachapoyas, Tres Cerritos, Autódromo, Villa Floresta y Miraflores. Estas localidades enumeradas son estratigráficamente discontinuas debido a la cubierta vegetal, pero se centraran los trabajos en la cantera de Cerámica Alberdi en la localidad de Floresta. Luego del análisis sedimentológico en las diferentes localidades, se prestará especial atención a los que contienen el FPE (para una comparación ver análasis del *Lagersttäten* Fezouata en

Vaucher et al., 2016; en prensa), estos serán luego volcados en un modelo depositacional y se presentará un esquema de correlación. La Formación Floresta es un equivalente estratigráfico del Miembro Rupasca de la Formación Santa Rosita (Moya, 1988; Buatois et al., 2006; Balseiro y Waisfeld, 2013). Esta unidad está muy bien expuesta en el área de Alfarcito-Arenal, lo que permitirá realizar estudios sedimentológicos de detalle en varias secciones a lo largo de la sierra Altos de Tilcara. La correlación entre la Formación Santa Rosita y Formación Floresta se realizará mediante (1) la estratigrafía secuencial, (2) el análisis de facies, (3) graptolitos y (4) biozonas de trilobites.

Habilidades necesarias

La mayor parte del trabajo se basará en los datos adquiridos en el campo (registros estratigráficos, muestreo, toma de fotográfías, medición de secciones (orientación, espesor), etc.). El análisis de facies se realizará con la metodología habitual en estos estudios. En este sentido la experiencia adquirida durante mi formación de grado y durante el desarrollo de los trabajos de campo en el marco de mi tesis doctoral en sedimentología de campo (tanto en ambientes silicoclástico como carbonáticos), facies, análisis de microfacies, interpretación estratigrafía secuencial son fundamentales para el éxito de este proyecto.
La ejecución de eta propuesta tendrá lugar en el Centro de Investigaciones en Ciencias de la Tierra (CONICET-UNC). El CICTERRA cuenta con gabinetes para investigadores y becarios, un gabinete para preparación de macrofósiles equipado con lápiz neumático y lupa binocular y un laboratorio para tratamiento de materiales con ácidos. El CICTERRA dispone de vehículos utilitarios 4x4 e instrumental básico de campaña. También cuenta con un laboratorio con equipamiento para preparación de muestras geológicas (LABGEO) y a acceso a la biblioteca electrónica de SECyT.

References

Aldridge, R.J., Gabbott, S.E. and Theron, J.N. (2007) The Soom Shale. In: *Palaeobiology II*, pp. 340-342. Blackwell Science Ltd.

Aris, M.J. and Palomo, M. (2014) Primer registro de una fauna Ordovícica 'tipo Burgess Shale'en Argentina y Sudamérica. In: *XIX Congreso Geológico Argentino, Córdoba*.

Balseiro, D. and Waisfeld, B.G. (2013) Ecological instability in Upper Cambrian–Lower Ordovician trilobite communities from Northwestern Argentina. *Palaeogeography, Palaeoclimatology, Palaeoecology*, **370,** 64-76.

Bambach, R.K., Knoll, A.H. and Wang, S.C. (2004) Origination, extinction, and mass depletions of marine diversity. *Paleobiology*, **30,** 522-542.

Botting, J.P., Muir, L.A., Sutton, M.D. and Barnie, T. (2011) Welsh gold: A new exceptionally preserved pyritized Ordovician biota. *Geology*, **39,** 879-882.

Briggs, D.E.G., Bottrell, S.H. and Raiswell, R. (1991) Pyritization of soft-bodied fossils: Beecher's trilobite bed, Upper Ordovician, New York State. *Geology*, **19,** 1221-1224.

Buatois, L.A. and Mángano, M.G. (2003) Sedimentary facies, depositional evolution of the Upper Cambrian–Lower Ordovician Santa Rosita formation in northwest Argentina. *Journal of South American Earth Sciences*, **16,** 343-363.

Buatois, L.A., Zeballo, F.J., Albanesi, G.L., Ortega, G., Vaccari, E. and Mángano, M.G. (2006) Depositional Environments and Stratigraphy of the Upper Cambrian-Lower Ordovician Santa Rosita Formation at the Alfarcito area, Cordillera Oriental, Argentina: Integration of biostratigraphic data within a sequence stratigraphic framework. *Latin American Journal of Sedimentology and Basin Analysis*, **13,** 65 - 95.

Harper, D.A.T. (2006) The Ordovician biodiversification: setting an agenda for marine life. *Palaeogeography, Palaeoclimatology, Palaeoecology*, **232,** 148-166.

Lefebvre, B., El Hariri, K., Lerosey-Aubril, R., Servais, T. and Van Roy, P. (2016) The Fezouata Shale (Lower Ordovician, Anti-Atlas, Morocco): A historical review. *Palaeogeography, Palaeoclimatology, Palaeoecology*.

Liu, H.P., McKay, R.M., Young, J.N., Witzke, B.J., McVey, K.J. and Liu, X. (2006) A new Lagerstätte from the Middle Ordovician St. Peter formation in northeast Iowa, USA. *Geology*, **34,** 969-972.

Martin, E.L.O., Pittet, B., Gutiérrez-Marco, J.-C., Vannier, J., El Hariri, K., Lerosey-Aubril, R., Masrour, M., Nowak, H., Servais, T., Vandenbroucke, T.R.A., Van Roy, P., Vaucher, R. and Lefebvre, B. (2016) The Lower Ordovician Fezouata Konservat-Lagerstätte from Morocco: Age, environment and evolutionary perspectives. *Gondwana Research*, **34,** 274-283.

Moya, M.C. (1988) Lower ordovician in the southern part of the argentine eastern cordillera. In: *The Southern Central Andes: Contributions to Structure and Evolution of an Active Continental Margin* (Eds H. Bahlburg, C. Breitkreuz and P. Giese), pp. 55-69. Springer Berlin Heidelberg, Berlin, Heidelberg.

Servais, T., Lehnert, O., Li, J., Mullins, G.L., Munnecke, A., Nuetzel, A. and Vecoli, M. (2008) The Ordovician Biodiversification:

revolution in the oceanic trophic chain. *Lethaia*, **41,** 99-109.
Servais, T., Owen, A.W., Harper, D.A.T., Kröger, B. and Munnecke, A. (2010) The great ordovician biodiversification event (GOBE): the palaeoecological dimension. *Palaeogeography, Palaeoclimatology, Palaeoecology*, **294,** 99-119.
Vaccari, N.E., Edgecombe, G.D. and Escudero, C. (2004) Cambrian origins and affinities of an enigmatic fossil group of arthropods. *Nature*, **430,** 554-557.
Van Roy, P., Briggs, D.E.G. and Gaines, R.R. (2015) The Fezouata fossils of Morocco; an extraordinary record of marine life in the Early Ordovician. *J. Geol. Soc.*, **172,** 541-549.
Van Roy, P., Orr, P.J., Botting, J.P., Muir, L.A., Vinther, J., Lefebvre, B., el Hariri, K. and Briggs, D.E. (2010) Ordovician faunas of Burgess Shale type. *Nature*, **465,** 215-218.
Vaucher, R., Martin, E.L.O., Hormière, H. and Pittet, B. (2016) A genetic link between Konzentrat- and Konservat-Lagerstätten in the Fezouata Shale (Lower Ordovician, Morocco). *Palaeogeography, Palaeoclimatology, Palaeoecology*.
Vaucher, R., Pittet, B., Hormière, H., Martin, E. and Lefebvre, B. (in press) A wave-dominated, tide-modulated model for the Lower Ordovician of the Anti-Atlas, Morocco. *Sedimentology*.
Young, G.A., Rudkin, D.M., Dobrzanski, E.P., Robson, S.P. and Nowlan, G.S. (2007) Exceptionally preserved Late Ordovician biotas from Manitoba, Canada. *Geology*, **35,** 883-886.

Annexe 4 :

The Lower Ordovician Fezouata Konservat-Lagerstätte from Morocco: Age, environment and evolutionary perspectives

Auteurs : Emmanuel L.O. Martin, Bernard Pittet, Juan-Carlos Gutiérrez-Marco, Jean Vannier, Khadija El Hariri, Rudy Lerosey-Aubril, Moussa Masrour, Hendrik Nowak, Thomas Servais, Thijs R.A. Vandenbroucke, Peter Van Roy, **Romain Vaucher**, Bertrand Lefebvre

Article publié dans *Gondwana Research*

Année : 2016 Volume : 34 Pages : 274 - 283

DOI : http://dx.doi.org/10.1016/j.gr.2015.03.009

Gondwana Research 34 (2016) 274–283

Contents lists available at ScienceDirect

Gondwana Research

journal homepage: www.elsevier.com/locate/gr

The Lower Ordovician Fezouata Konservat-Lagerstätte from Morocco: Age, environment and evolutionary perspectives

Emmanuel L.O. Martin [a,*], Bernard Pittet [a], Juan-Carlos Gutiérrez-Marco [b], Jean Vannier [a], Khadija El Hariri [c], Rudy Lerosey-Aubril [a], Moussa Masrour [d], Hendrik Nowak [e], Thomas Servais [e], Thijs R.A. Vandenbroucke [e], Peter Van Roy [f], Romain Vaucher [a], Bertrand Lefebvre [a]

[a] UMR CNRS 5276 Laboratoire de Géologie de Lyon, Terre, Planètes, Environnement (LGLTPE), Géode, campus LyonTech-la Doua, Université Lyon 1, 2 rue Dubois, 69622 Villeurbanne cedex, France
[b] Instituto de Geociencias (CSIC, UCM), José Antonio Novais 12, E-28040 Madrid, Spain
[c] Département de Géologie, Faculté des Sciences et Techniques, Université Cadi-Ayyad, BP 549, 40000 Marrakesh, Morocco
[d] Département de Géologie, Faculté des Sciences, Université Ibn Zohr, Cité Dakhla, BP 8106, 80060 Agadir, Morocco
[e] UMR CNRS 8198 Evo-Eco-Paléo, bâtiment SN5, Cité Scientifique, Université Lille 1, 59655 Villeneuve d'Ascq cedex, France
[f] Department of Geology and Geophysics, Yale University, P.O. Box 208109, New Haven, CT 06520-8109, USA

ARTICLE INFO

Article history:
Received 14 December 2014
Received in revised form 31 March 2015
Accepted 31 March 2015
Available online 6 May 2015

Handling Editor: I.D. Somerville

Keywords:
Konservat-Lagerstätten
Sedimentology
Ordovician
Gondwana
Morocco
Fezouata

ABSTRACT

The Lower Ordovician Fezouata Konservat-Lagerstätte from southern Morocco has been one of the major palaeontological discoveries of the last decade. It provides a unique insight into one of the most critical periods in the evolution of marine life: the Cambrian–Ordovician transition. However, its potential for deciphering key trends in animal diversification was hitherto largely limited by major uncertainties concerning its stratigraphic position, age and environmental setting. Based on extensive fieldwork, fossil evidence, and facies recognition, our study provides clarification on these three crucial issues. Exceptional preservation is limited to two intervals within the Fezouata Shale. Graptolites indicate a late Tremadocian age for the Fezouata Konservat-Lagerstätte as a whole, which is supported by biostratigraphical evidence provided by acritarchs. Sedimentological features and reconstructed patterns of relative sea-level changes indicate relatively shallow-water environmental conditions, under distal storm influence, in an offshore to lower shoreface siliciclastic ramp setting. The Fezouata Biota represents a unique and exceptional window into the palaeobiodiversity in open-marine conditions, thus contrasting with the other Ordovician Konservat-Lagerstätten presently known. In our analyses of this new set of data, we pave the way for accurate temporal, faunal and environmental comparisons with other Lower Palaeozoic Konservat-Lagerstätten, and unlock the full potential of the Fezouata Biota to better understand the processes and scenarios of early animal radiations.

1. Introduction

The Cambrian–Ordovician time interval (c. 541–443 Ma) is characterised by the evolution and radiation of animals that led to irreversible changes in marine ecosystems (Bambach et al., 2007; Vannier et al., 2007; Butterfield, 2011; Erwin and Valentine, 2013). Triggered by complex interacting factors (Smith and Harper, 2013; Maruyama et al., 2014; Santosh et al., 2014; Zhang et al., 2014), the Cambrian Explosion is the initial visible phase of animal diversification and is defined by the appearance in the fossil record of a wide spectrum of new anatomies and functionalities, and by complex ecological systems that have no counterparts in the Precambrian (Erwin et al., 2011; Shu et al., 2014). This evolutionary and ecological revolution is evidenced by several early to middle Cambrian Konservat-Lagerstätten (*sensu* Seilacher, 1970; termed "Lagerstätten" below; Fig. 1), which have yielded abundant and diverse remains of both shelly and non-biomineralised organisms such as those of Chengjiang (Hou et al., 2004; Zhao et al., 2009), Sirius Passet (Peel and Ineson, 2011), Emu Bay (Paterson et al., 2015), or the Burgess Shale (Caron and Jackson, 2008). They provide detailed information on the anatomy, lifestyles, and behaviours of early animals and also on their interactions within the evolving trophic web (Dunne et al., 2008; Vannier, 2011). Postdating the Cambrian Explosion, the Great Ordovician Biodiversification Event (GOBE) represents the second major burst in marine biodiversity. During most of the Ordovician Period, a sustained exponential diversification took place within almost all animal phyla (Harper, 2006; Servais et al., 2008, 2010). Unlike the Cambrian Explosion, the GOBE is primarily recognised from diversity

* Corresponding author. Tel.: +33 472432834.
E-mail addresses: emmanuel.martin@univ-lyon1.fr (E.L.O. Martin), bernard.pittet@univ-lyon1.fr (B. Pittet), jcgrapto@ucm.es (J.-C. Gutiérrez-Marco), jean.vannier@univ-lyon1.fr (J. Vannier), elhariri@fstg-marrakech.ac.ma (K. El Hariri), leroseyaubril@gmail.com (R. Lerosey-Aubril), moussamasrour5@gmail.com (M. Masrour), hendrik.nowak@etudiant.univ-lille1.fr (H. Nowak), thomas.servais@univ-lille1.fr (T. Servais), thijs.vandenbroucke@univ-lille1.fr (T.R.A. Vandenbroucke), peter.vanroy@yale.edu (P. Van Roy), romain.vaucher@univ-lyon1.fr (R. Vaucher), bertrand.lefebvre@univ-lyon1.fr (B. Lefebvre).

http://dx.doi.org/10.1016/j.gr.2015.03.009
1342-937X/

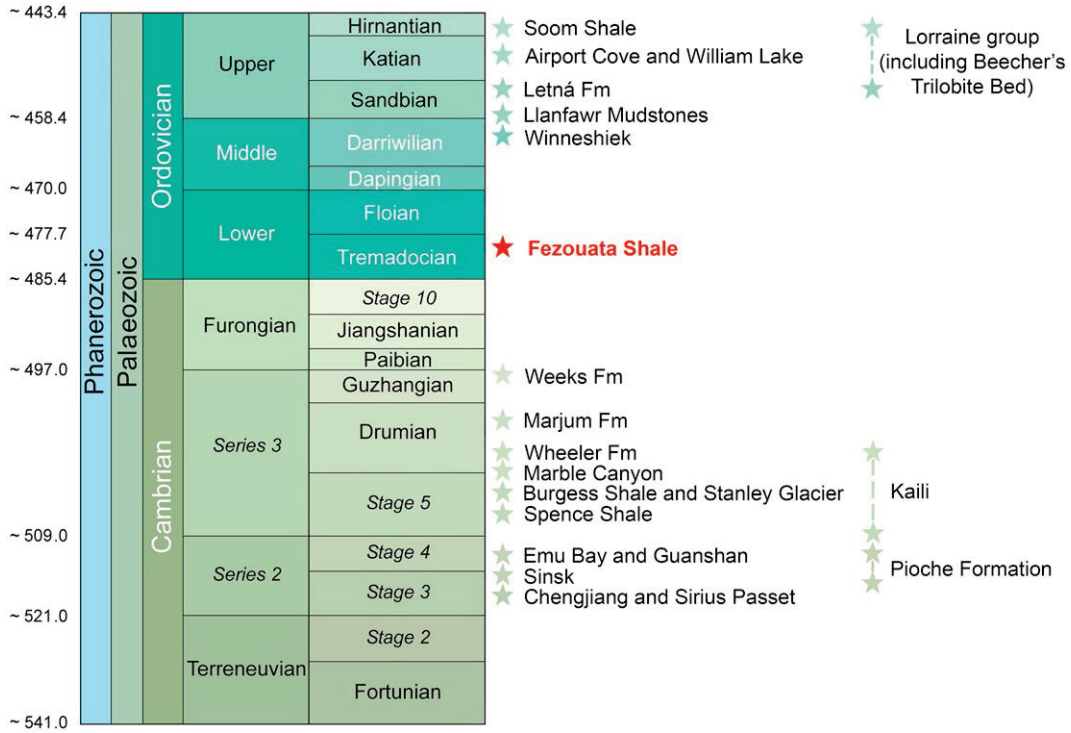

Fig. 1. Stratigraphic distribution of the main diverse exceptionally preserved faunas from the Cambrian and the Ordovician. Numerical ages in Ma.

analyses based on the fossil record of shelly faunas and microfossils. Indeed, Ordovician Lagerstätten are rare and most of them occur in the Upper Ordovician, long after the initial stages of the GOBE (Fig. 1). Moreover, they typically contain low diversity faunas that lived in restricted marine environments (e.g. Beecher's Trilobite Bed from the Lorraine Group, Farrell et al., 2013; Soom Shale, Gabbott, 1998; William Lake Biota of Manitoba, Young et al., 2007).

The recent discovery of a Burgess Shale-type Lagerstätte in the Lower Ordovician of Morocco (Zagora area, Central Anti-Atlas, Fig. 2A; Van Roy et al., 2010) provided unexpected and unprecedented

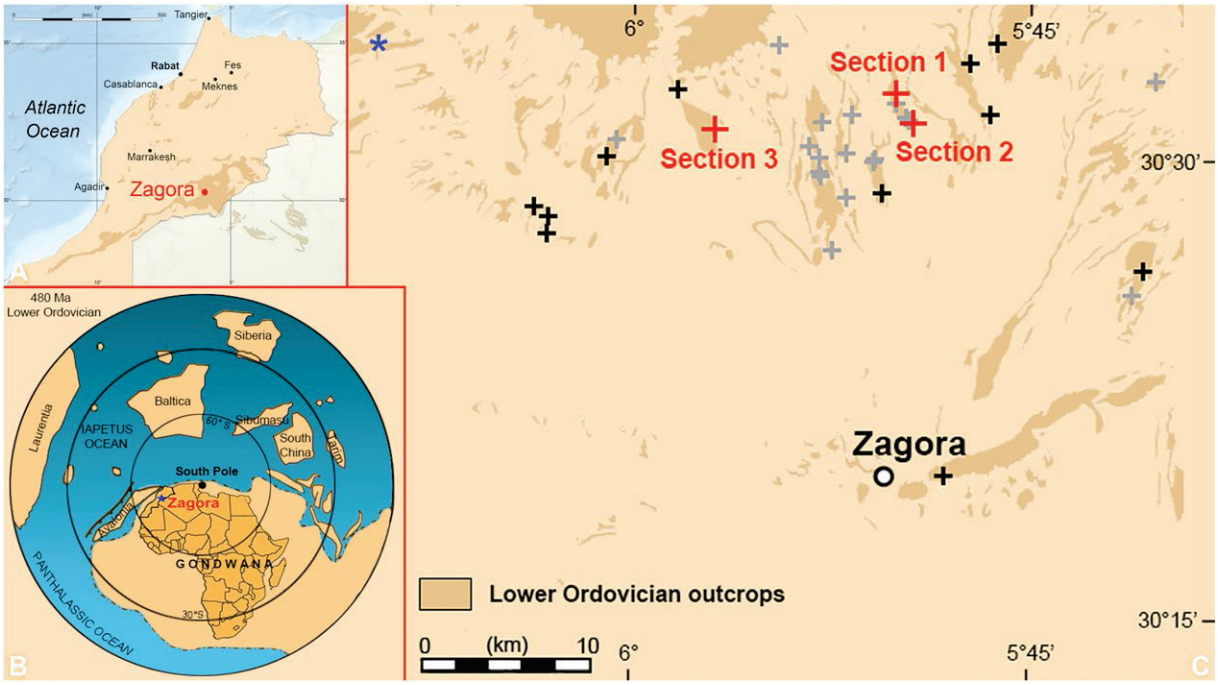

Fig. 2. A, Lower Ordovician outcrops of northern Morocco and location of Zagora; B, Palaeogeography of Africa (blue star represents Zagora) in the Early Ordovician (modified from Cocks and Torsvik, 2004; Torsvik and Cocks, 2011); and C, Lower Ordovician outcrops in the Zagora area. Small black crosses indicate logged sections and red crosses the three key sections used to build the composite stratigraphic column (Fig. 4). Small grey crosses and blue asterisk indicate the inspected and non-inspected localities that yielded EPF respectively (Van Roy et al., 2010; modified).

possibilities to obtain high-resolution information on both the aftermath of the Cambrian Explosion and the very beginning of the Ordovician radiation event. Although still largely undescribed, the diverse fossil assemblages of the Fezouata Biota (Fig. 3) are characterised by the co-occurrence of organisms typical of Cambrian Burgess Shale-type biotas (Van Roy et al., 2010), such as anomalocaridids (Van Roy and Briggs, 2011; Gaines et al., 2012a; Van Roy et al., 2015) and some demosponges (Botting, 2007) with classical Ordovician faunal elements. The biomineralised component of the Fezouata Biota is dominated by trilobites (e.g. Destombes, 1972; Rábano, 1990; Henry et al., 1992; Vidal, 1998a,b; Chatterton and Fortey, 2008; Fortey, 2009, 2011a,b) and echinoderms (Ubaghs, 1963; Chauvel, 1966, 1969, 1971a,b, 1978; Chauvel and Régnault, 1986; Donovan and Savill, 1988; Lefebvre and Botting, 2007; Noailles et al., 2010; Sumrall and Zamora, 2011). The fauna also contains a great abundance of xiphosurid arthropods (Van Roy et al., 2010), palaeoscolecidan worms, annelids (machaeridians, Vinther et al., 2008), molluscs (Babin and Destombes, 1990; Horný, 1997; Kröger and Lefebvre, 2012), hyolithids (Marek, 1983; Valent et al., 2013), brachiopods (Havliček, 1971; Mergl, 1981, 1988), and conularids (Destombes et al., 1985). Graptolites are also abundant but have not been studied in detail so far (Destombes and Willefert, 1959; Willefert in Destombes et al., 1985; Aceñolaza et al., 1996). Despite this remarkable diversity, two main obstacles have so far limited the impact of the Fezouata Lagerstätte. First, most fossils were collected from isolated excavations lacking an accurate positioning within the lithological succession. This led Van Roy et al. (2010) to hypothesise that the Fezouata Lagerstätte could span a time period of almost 10 Myr (late Tremadocian to late Floian). Second, major uncertainties remained concerning the environmental setting of the Fezouata Biota, especially in terms of bathymetry, energy and oxygenation. The Lower Ordovician succession in the Zagora area has remained virtually unstudied since the pioneering work of Destombes et al. (1985). Based on extensive fieldwork in the Zagora area, new fossil studies, and facies recognition, we here provide clarification on these two crucial chronological and environmental issues, making it possible for the first time 1) to establish precise comparisons with other Lower Palaeozoic Lagerstätten and 2) to test the potential of the Fezouata Lagerstätte in resolving the pace and amplitude of the animal diversification in the Early Palaeozoic.

2. Geological setting

In the Anti-Atlas of south-eastern Morocco, the Cambrian–Ordovician transition is exposed in the Ternata plain, 30 km north of Zagora. The Guzhangian (Cambrian series 3) sandstones of the Tabanite Group are unconformably overlain by the Tremadocian to Floian (Lower Ordovician) deposits of the Lower Fezouata, the Upper Fezouata, and the Zini formations, which, together with the Tachilla Formation (Middle Ordovician), form the Outer Feijas Group (Destombes et al., 1985; Geyer and Landing, 2006). The Lower and Upper Fezouata formations constitute a thick (up to 1200 m) and rather monotonous sequence dominated by silty and micaceous argillites. A glauconitic and ferruginous horizon has often been used as a possible lithological marker for the boundary between the two formations, which have been regarded as Tremadocian and Floian in age respectively (Destombes et al., 1985). However, this horizon is missing in the Zagora area, where the Fezouata Lagerstätte is located. Consequently, the Lower and Upper Fezouata formations are here considered together as a single lithological unit: the Fezouata Shale, which is topped by the sandstone-dominated Zini Formation (Destombes, 1962; Destombes et al., 1985).

During the Early Ordovician, the Anti-Atlas was located on the southern margin of Gondwana and situated in the southern hemisphere at high latitudes (c. 65°S), relatively close to the South Pole (Fig. 2B, Cocks and Torsvik, 2004; Torsvik and Cocks, 2011, 2013). The Lower Ordovician sediments were deposited in a rifting context associated with the northward drift of Avalonia away from the Gondwanan palaeocontinent (Cocks and Torsvik, 2004).

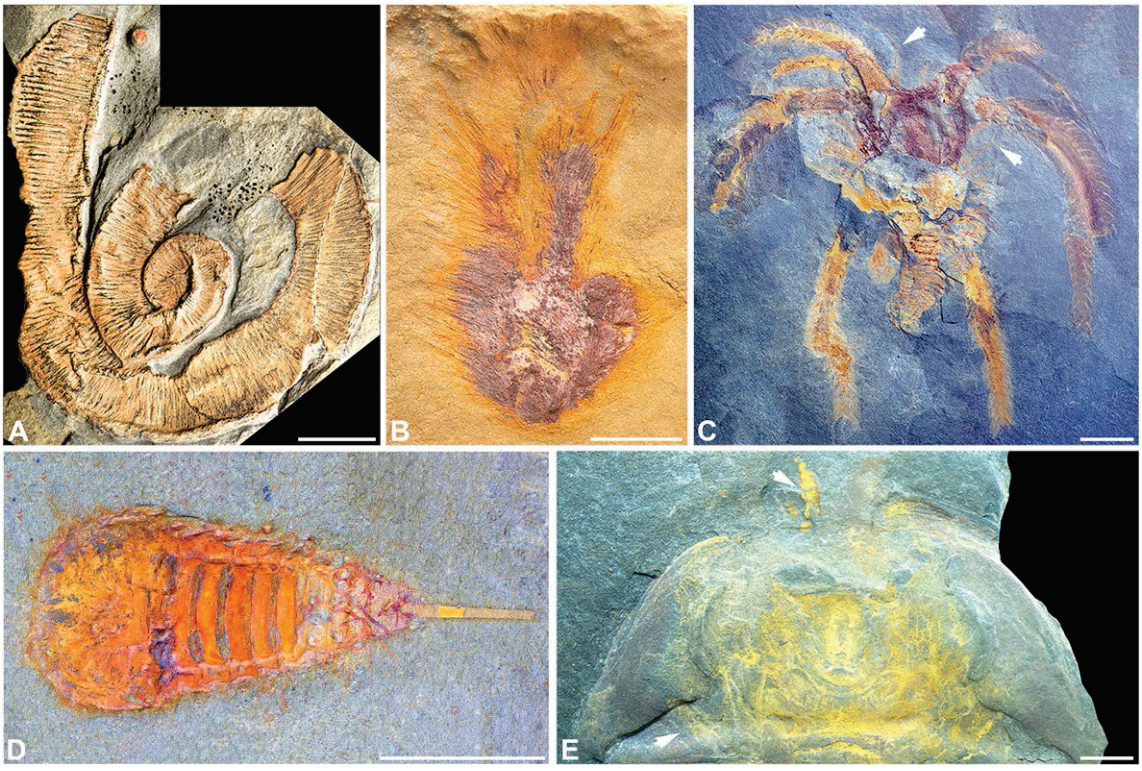

Fig. 3. Examples of exceptionally preserved fossils from the Fezouata Biota (latest Tremadocian; Zagora area, Morocco). A, undetermined palaeoscolecid worm, AA-BGF2-OI-1; B, *Pirania auraeum* Botting, 2007, demosponge, AA-JBZ-OI-115; C–E, arthropods with preserved appendages (arrows); C, *Furca* sp. (Marrellomorpha), AA-BIZ31-OI-39; D, Xiphosuran (Chelicerata) with fully segmented opisthosoma, FSL 712 411; E, *Bavarilla* sp. (Trilobita), AA-BIZ15-OI-16. All specimens were photographed under alcohol. Scale bars: A–C, 5 mm; D–E, 2 mm.

3. Material and methods

3.1. Exceptional preservation

The Fezouata Lagerstätte is a Konservat-Lagerstätte that is by definition characterised by the occurrence of exceptionally well-preserved fossils (EPF). In the Fezouata Lagerstätte, EPF were soft-bodied and lightly sclerotised organisms (e.g. worms, sponges, arthropods) that are usually preserved via pyritisation and subsequent weathering to iron oxides, giving the fossils a reddish colour. EPF typically display more or less complete anatomical (e.g. digestive structures) and exoskeletal features (e.g. arthropod appendages).

3.2. Fieldwork

The whole Lower Ordovician succession exposed in the Zagora area (Central Anti-Atlas, Morocco; Fig. 2C) was logged at a decimetre scale from fourteen different sections (black and red crosses on Fig. 2C). Data were compiled in a single, synthetic c. one thousand-metre-thick stratigraphic column. All localities yielding EPF mentioned in the original contribution of Van Roy et al. (2010) were included in this study, except one located c. 15 km west of the main outcrop area (blue asterisk on Fig. 2C). EPF localities were carefully located and positioned along the stratigraphic column based on their lithological characteristics (colour, composition, marker beds) and faunal elements (mostly graptolites, trilobites, and to a lesser extent echinoderms). Graptolites were collected throughout the succession, but particular attention was paid to horizons yielding EPF. Changes in lithology and sedimentary structures were observed throughout the succession and were used to reconstruct short-term and long-term relative sea-level changes. EPF and graptolites were photographed using a Nikon D3X camera (with a Micro-Nikkor AF 60 mm f/2.8D macrolens) and a Leica MZ12.5 microscope, equipped with a Leica integrated digital camera. When necessary, fossils were immersed under dilute ethanol in order to enhance contrast and avoid reflective spots. All fossil specimens are deposited in the collections of the Cadi Ayyad University, Marrakesh (Faculté des Sciences et Techniques, Guéliz; sample number prefix AA), except for one, which is deposited in the palaeontological collections of Lyon 1 University, Villeurbanne (sample number prefix FSL).

4. Results and interpretations

4.1. Stratigraphic distribution and age of the Fezouata Biota

The lithology of the Fezouata Shale Formation is fairly homogeneous and largely dominated by fine-grained siliciclastic deposits, except in its lowermost and uppermost parts. The lower part of the Fezouata Shale is characterised by a transgression from a foreshore environment, whereas its upper part records a regressive trend. The distribution of EPF throughout the thousand-metre-thick Fezouata Shale shows that exceptional preservation occurs within a restricted interval in the lower part of the succession. Fig. 4 summarises the stratigraphic distribution of graptolites across this interval and its facial characteristics (colour, lithology, sedimentary structures). About three hundred well-preserved graptolite specimens were collected, identified, and used for dating the lower part of the Fezouata Shale. Graptolites also occur locally as monospecific mass-occurrences of *Araneograptus murrayi* (Hall) and "*Tetragraptus*" *bulmani* Thomas. The facies evolution within the entire succession and the structural context of the Lower Ordovician in the area of Zagora are beyond the scope of this contribution and will be the subjects of a separate study.

The studied succession is rather homogeneous, being composed of mainly thinly-bedded argillites with frequent intercalations of silts and millimetre- to centimetre-thick silty to sandy beds. Facies variations consist of slight differences in argillite composition (e.g. presence of silts or micas), or in diagenesis (e.g. induration, bedding). EPF are restricted to a 70-metre-thick interval developed between 260 and 330 m above the basal contact with the Guzhangian Tabanite Group and are usually found in relatively fine facies, the beds overlying them being coarser. They occur within two distinct intervals of c. 25 (interval 1) and 15 (interval 2) metres in thickness respectively, separated by a c. 30-metre-thick interval where only biomineralised remains are found (e.g. brachiopod shells, echinoderm skeletons, trilobite carapaces).

Eleven graptolite species have been recognised through the studied succession (Fig. 5). These include the index species of the *A. murrayi* and *Hunnegraptus copiosus* graptolite biozones, which are the uppermost graptolite zones of the Tremadocian (Loydell, 2012). *A. murrayi* occurs in great abundance from 240 to 295 m above the base of the Fezouata Shale. EPF-bearing Interval 1 falls within the *A. murrayi* Biozone. EPF-bearing Interval 2 mainly belongs to the upper part of the *A. murrayi* Biozone. Only the uppermost part of this interval corresponds to the following *H. copiosus* Biozone, as indicated by the first occurrence of *H. copiosus*. EPF-bearing intervals 1 and 2 are thus both of late Tremadocian age and correlate with the Tr3 substage of Bergström et al. (2009).

4.2. Environmental setting of the Fezouata Biota

Ripple marks, hummocky cross-stratification (HCS), and normally-graded tempestites are repeatedly found throughout the section, including in the two intervals with EPF (Fig. 6A–D). These sedimentary structures are interpreted as being induced by storm wave action on the sea floor (Harms et al., 1975; Duke, 1985; Duke et al., 1991; Gupta, 1998) and suggest a depositional environment at or above storm wave-base. However, HCS observed in the studied succession are only at a millimetre- to centimetre-scale, whereas they can reach several decimetres elsewhere in the succession (e.g., near the contact with the Zini Formation). These small-scale HCS suggest a relatively shallow depositional environment, most probably located within the offshore to lower shoreface (as defined by McLane, 1995; Fig. 6E).

Three long-term cycles of relative sea-level fluctuations are recognised in the entire Fezouata Shale, but only the first and the second of them are documented in the presented section (Fig. 4). All are composed of a transgressive phase marked by an evolution from silt-dominated to clay-dominated intervals and a regressive phase marked by the opposite trend. Exceptional preservation occurs at the end of the regressive phase of the first cycle and at the beginning of the transgressive phase of the second cycle (Fig. 4). Additionally, facies changes towards more argillaceous sedimentary deposits and fewer silty tempestites, or towards more silty argillites interrupted by more frequent silty or fine-sandy tempestites are interpreted as transgressive and regressive phases of short-term cycles respectively. Two of them are associated with the preservation of EPF.

5. Discussion

5.1. Exceptional preservation: stratigraphic distribution and environmental factors

The distribution of EPF within the Fezouata Shale is restricted to two narrow stratigraphic intervals, which contradicts earlier assessments (Van Roy et al., 2010) that exceptional preservation occurs throughout the Fezouata Shale. This is a common point shared with most major Cambrian and Ordovician Lagerstätten in which exceptional preservation is limited to a relatively narrow stratigraphic interval, ranging from a few metres – e.g. Sinsk (Russia; Ivantsov et al., 2005), Emu Bay (Australia; Gehling et al., 2011), the Spence Shale (USA; Liddell et al., 1997), the Burgess Shale (Canada; Collom et al., 2009), or the Llanfawr Mudstones (UK; Botting et al., 2011) – to a few tens of metres, as in Chengjiang (China; Babcock and Zhang, 2001), the Pioche Shale (USA; Moore and Lieberman, 2009), Wheeler Formation (USA; Brett et al.,

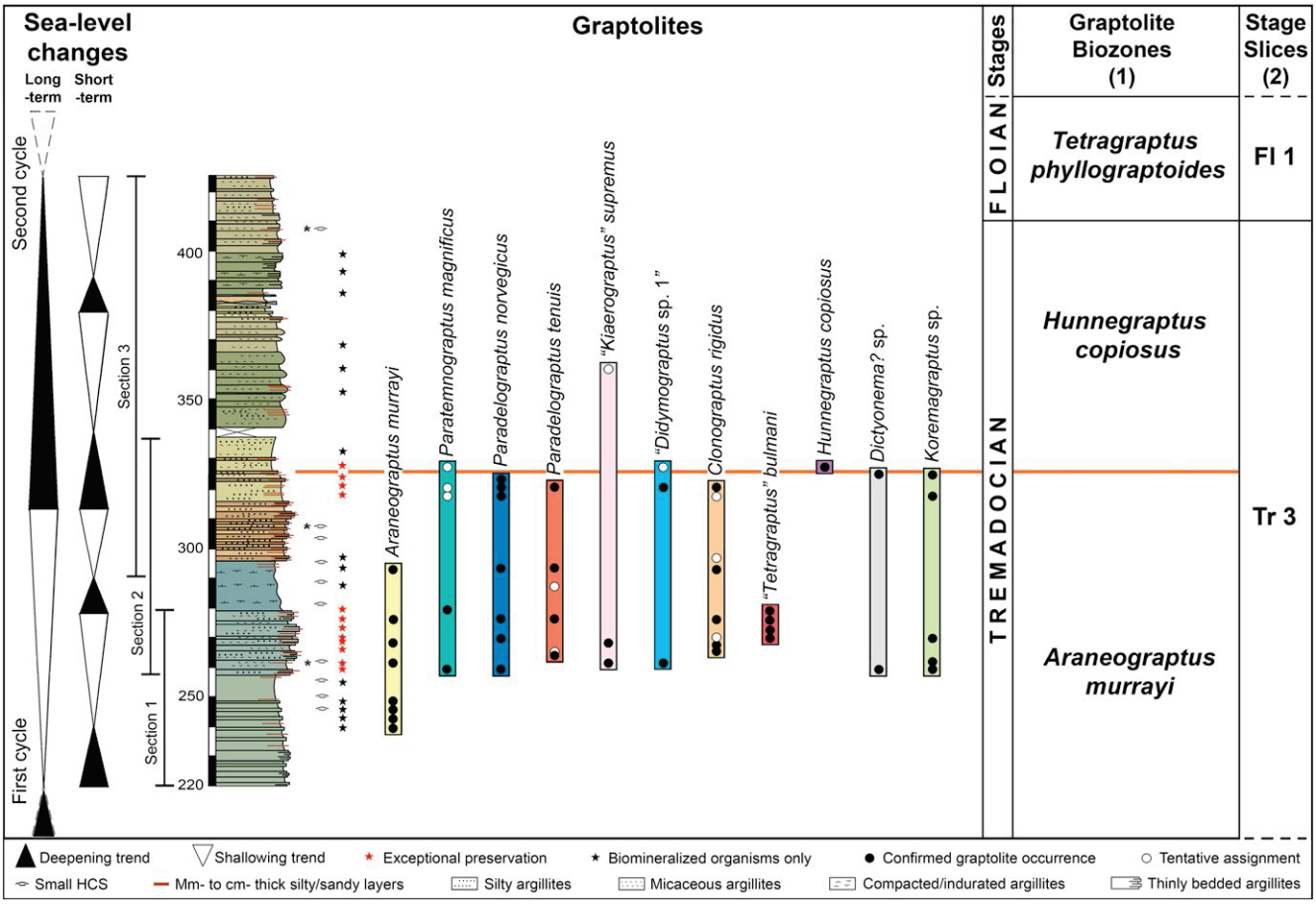

Fig. 4. Partial composite section of the Fezouata Shale (Lower Ordovician, Zagora area) showing the distribution of Exceptionally Preserved Fossils (EPF; red stars) and the vertical range of diagnostic graptolites. Right columns modified from (1) Loydell (2012) and (2) Bergström et al. (2009). The colours in the logged section roughly correspond to the colours of outcropping rocks.

2009), or the Soom Shale (South Africa; Aldridge et al., 1994). An exception is the Guanshan Biota (China; Hu et al., 2010), which seems to occur throughout the entire Wulongqing Formation, which can reach up to 60 m in thickness. Environmental conditions maintained over a relatively short timespan may account for the preservation of EPF within a narrow stratigraphic interval (Hagadorn, 2002). Exceptional preservation is often associated with the rapid burial of organisms, which is supposed to promote oxygen restriction and to favour the preservation of soft tissues and lightly sclerotised features (Gaines et al., 2012b). Different mechanisms of entombment have been proposed. For example, a mostly turbiditic origin is often suggested for the mudrock–siltstones of the Burgess Shale (Gabbott et al., 2008), with probably a rhythmic deposition from waxing and waning density currents (Gabbott and Zalasiewicz, 2009). Recent studies of the Burgess Shale communities (Caron and Jackson, 2008; Caron, 2009) show that the fauna was mostly preserved *in situ* and only moderately disturbed by the event of burial. Most organisms were buried *in situ* by distal mudflow events. In Chengjiang, a typical sedimentary succession is recognised (Hu, 2005). It consists of background layers dominated by hemipelagic mud, which are interrupted by event layers that contain soft-bodied fossils. These event layers are generated by bottom-flowing density currents, which are responsible for the burial of the fauna.

Although storms played an important role in the overall depositional mode of the Fezouata Shale (as indicated by the presence of numerous HCS and tempestites), the storm waves seem to have had a limited influence on the relatively distal deposits that contain EPF. Indeed, storm currents were weak in this area, as attested by the relatively small scale of the HCS found, resulting from a mainly oscillatory movement at the seafloor. The animal communities of the Fezouata Shale were probably buried *in situ* during storm events, which mobilised more proximally a large amount of coarser sediments. Between two storm events, the background sedimentation resulted from the decantation of mud suspended by wave action. It is not associated with any sedimentological structures, such as HCS and tempestites. This depositional scenario would be comparable to the one invoked for the Chengjiang and other Burgess Shale-type Lagerstätten (Gaines et al., 2012b).

The geochemical context of the Fezouata Shale has not yet been explored and will be investigated on fresh rocks obtained from drill cores (in progress). No detailed information is available on the redox conditions that prevailed at the water–sediment interface and within the sediment. However, the presence of iron oxides in the majority of the weathered EPF suggests that an early mineralisation of pyrite took place on both soft and sclerotised tissues and was induced by microbial activity under anaerobic conditions (Gabbott et al., 2004; Vinther et al., 2008; Van Roy et al., 2010). The exceptional preservation of giant anomalocaridids in silica-chlorite concretions is unusual among Burgess Shale-type Lagerstätten and possibly involved the dissolution of volcanic ashes in the sediment (Gaines et al., 2012a). Field observations indicate that bioturbation associated with EPF-bearing intervals was limited to mostly narrow horizontal burrows, very close to the water–sediment interface. This supports a low infaunal activity, possibly related to dysoxic/anoxic conditions within the sediment.

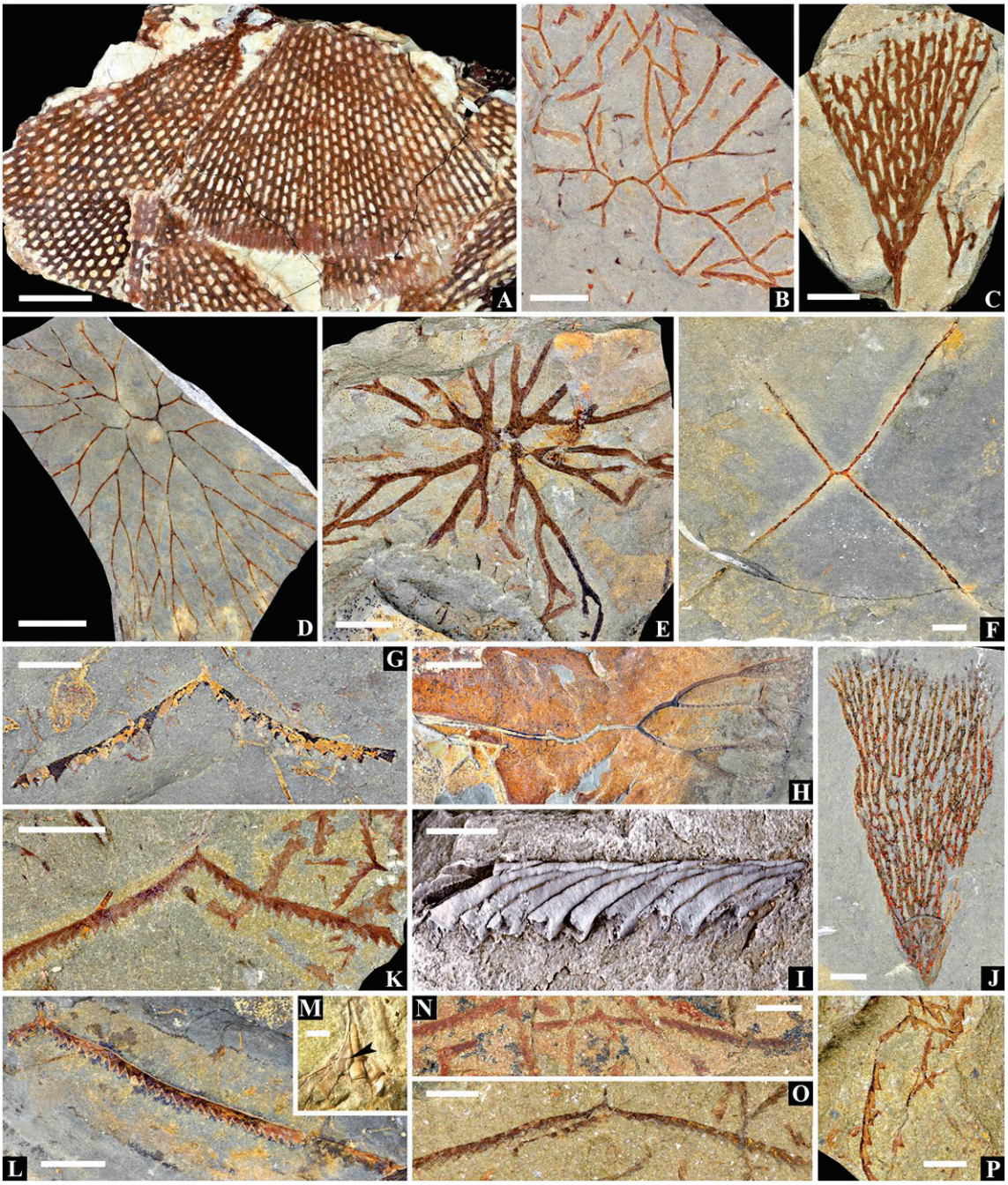

Fig. 5. Graptolites of the Fezouata Biota (late Tremadocian; Zagora area, Morocco). A, *Araneograptus murrayi* (Hall, 1865), AA-BIZ3-OI-35 showing nematularium (upper left) and distal end on another young colony (centre-right); B, *Paradelograptus tenuis* Lindholm, 1991, AA-OFTa-OI-23; C, *Koremagraptus* sp., AA-FETi-OI-1; D, *Clonograptus rigidus* (Hall, 1858), AA-JTZb-OI-19; E, *Paradelograptus norvegicus* (Monsen, 1937), AA-JTZ-OI-10; F, "*Tetragraptus*" *bulmani* Thomas, 1973, AA-BIZ13-OI-9; G, "*Didymograptus* sp. 1" (cf. Lindholm, 1991), AA-BIZ31-OI-40; H–I, *Paratemnograptus magnificus* (Pritchard, 1892), fragment of a large rhabdosome (F, AA-BZG-OI-13) and detail of a stipe showing plaited thecal structure (triad budding without bithecae), AA-BIZ13-OI-10; J, *Dictyonema*? sp., AA-BZG-OI-14; K–M, "*Kiaerograptus*" *supremus* Lindholm, 1991, K = AA-BGF2-OI-7; L = AA-BGF2-OI-6, with detail of the proximal end (M) showing sicular bitheca (arrow); N–O, *Hunnegraptus copiosus* Lindholm, 1991, N = AA-JBZ-OI-117; O = AA-JBZ-OI-116; and P, *Paradelograptus* sp., AA-JTZ-OI-9. All specimens, except A, H, I and M, were photographed under alcohol. Scale bars: A, D, and H, 20 mm; E, 10 mm; C, F, K, L, and J, 5 mm; B, G, N, and O, 3 mm; I, and P, 2 mm; and M, 0.5 mm.

5.2. Dating the Fezouata Lagerstätte

Graptolites (*A. murrayi* and *H. copiosus* biozones) indicate a late Tremadocian age for the EPF-bearing intervals of the Fezouata Shale. Therefore, the Fezouata Lagerstätte does not extend to the Floian as suggested previously (Van Roy et al., 2010). It cannot be entirely ruled out that *H. copiosus* occurs lower in the stratigraphy. As the base of the *H. copiosus* Biozone is defined by the First Appearance Datum of this biozonal marker graptolite (Egenhoff et al., 2004), a larger portion of the interval 2 may belong to the *H. copiosus* Biozone. However, the resulting changes would be of little significance regarding the age of the Fezouata Biota, which would remain late Tremadocian (Tr3 of Bergström et al., 2009).

The only excavation that was not re-studied in detail (blue asterisk in Fig. 2C) yielded the graptolite *Clonograptus* along with the trilobite *Dikelokephalina brenchleyi*. Both would suggest a late Tremadocian age (Fortey, 2009, 2011b).

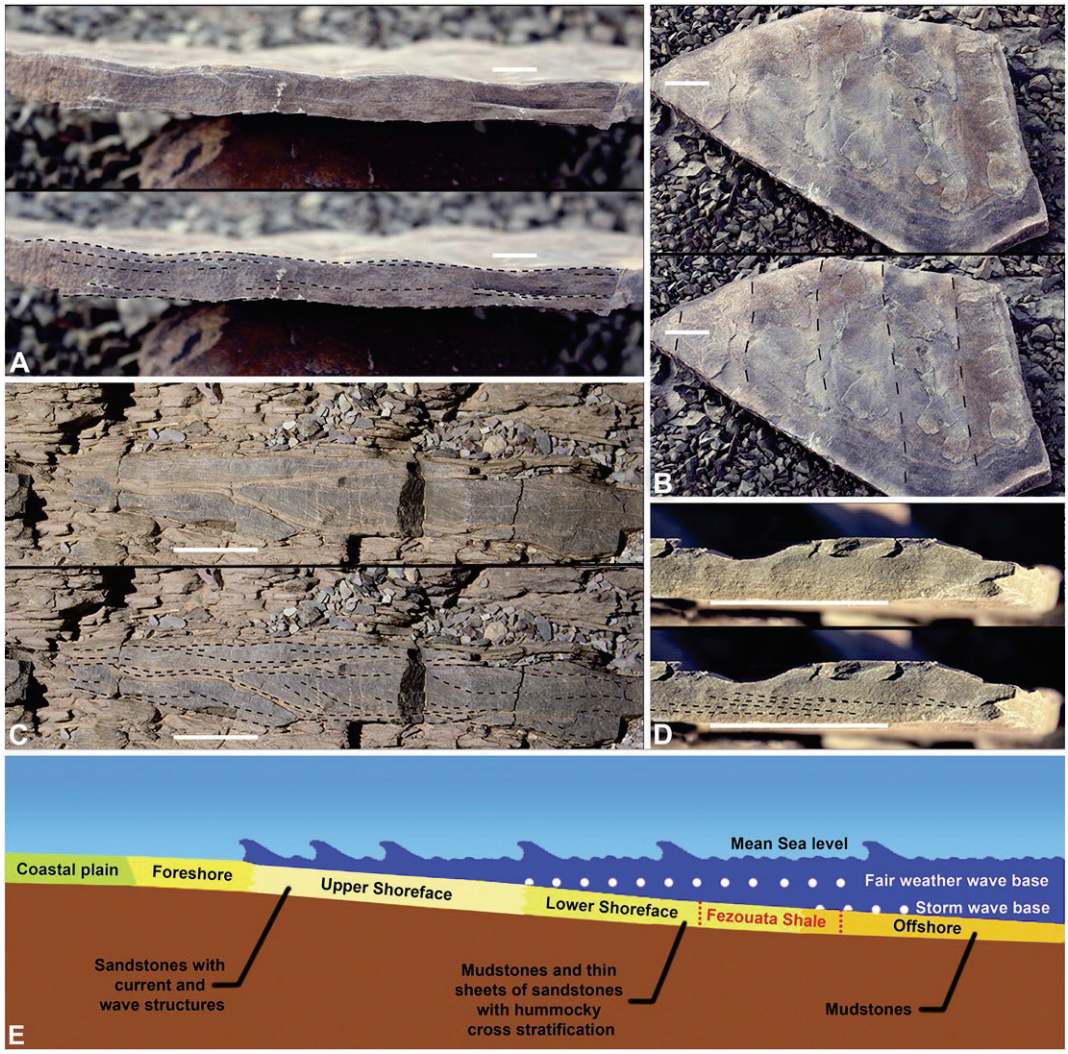

Fig. 6. Typical sedimentary structures used to characterise the palaeoenvironment of the Fezouata Shale. A–B, 2D-wave ripples in a distal tempestite, in section and slab surface, respectively. C, small, centimetre-scale hummocky cross stratifications (HCS) from the top of the section. D, thin, possibly wave-induced cross-laminated structures in a distal silty tempestite. E, general palaeoenvironmental reconstruction for the Fezouata Shale deposition. Terminology of depth zones follows the definition of McLane (1995). Scale bars: A–B, 1 cm; and C–D, 3 cm.

Graptolites are both abundant and well preserved throughout the Fezouata Shale (Fig. 5). They are reliable markers for dating and correlations, especially in the Ordovician (Webby et al., 2004; Sadler et al., 2009). The graptolite assemblages of the Fezouata Shale are dominated by planktonic forms that are assumed to have lived in epipelagic niches (Cooper et al., 1991, 2012a), with a small percentage of rooted benthic dendroids (Fig. 5C and J). The planktonic ones have a cosmopolitan distribution and have been widely used for global correlations. They occur in Scandinavia (Lindholm, 1991), North America (Williams and Stevens, 1991; Maletz, 1997; Jackson and Lenz, 2003), South America (Maletz and Egenhoff, 2001; Ortega and Albanesi, 2005), China (Feng et al., 2009) and southwestern Europe (Aceñolaza et al., 1996; Pillola et al., 2008).

Microfossils, such as acritarchs, chitinozoans, and conodonts, are also accurate biostratigraphic markers, but their study requires fresh material (e.g. from well drillings or boreholes; Elaouad-Debbaj, 1988) for high-resolution dating. Acritarchs typical of the late Tremadocian to lower Floian *messaoudensis–trifidum* assemblage occur in the lower part of the Fezouata Shale below and within EPF-bearing interval 1. This particular acritarch assemblage indicates a late Tremadocian age, correlating to the top of the *A. murrayi* and the base *H. copiosus* graptolite biozones (Molyneux et al., 2007). Cuttings from a drill, which presumably crosses the Fezouata Shale, about 300 km southwest of Zagora, yielded comparable acritarch assemblages equally pointing to a late Tremadocian age (Nowak et al., 2015).

5.3. Environmental setting: implications

Sedimentological features indicate that the Fezouata Shale was deposited above storm wave-base, in a relatively shallow, open-marine environment (offshore to lower shoreface, Fig. 6e). Based on comparisons with the depth of storm influence in modern oceans (Immenhauser, 2009), a palaeodepth ranging from 50 to 150 m is proposed for the depositional area of the Fezouata Shale. The Fezouata Biota also delivers interesting indications of water depths. Based on the characteristics of the mitrate (Echinodermata, Stylophora) *Peltocystis cornuta* from the Fezouata Formation, Lefebvre and Botting (2007) concluded that the environment was shallow and of moderately high energy. In addition, non-calcareous algae are present in the fauna (Van Roy et al., 2010), but they might also have been transported in from shallower waters. Thus, their presence should be considered with caution and is not a reliable depth indicator. In this respect, the visual systems of the articulated benthic trilobites are probably more useful. All trilobites of this stratigraphic interval seem to have eyes (except *Ampyx* cf. *priscus*; Vidal, 1998a,b). This would suggest that there must have been at least some visible light, but not necessarily enough for

photosynthesis. As a consequence, a maximum depth of 150 m might be overestimated, given the low insolation received in high latitudes (Kirk, 2011). The weak contrasts in lithology and facies throughout the cycles of short- and long-term sea-level changes indicates relatively low-amplitude sea-level fluctuations and thus, a relatively stable sea level close to storm wave-base over a relatively long time span (at least from the *A. murrayi* to the *H. copiosus* biochrons that represent a duration of about 2 Myr; Cooper et al., 2012b).

The palaeoenvironmental setting (open shelf close to the limit between the lower shoreface and the offshore) of the Fezouata Biota differs markedly from that of all Ordovician Lagerstätten presently known (Fig. 1), which are associated with particular marine environments. Indeed, the Winneshiek Biota (USA) lived in a possible estuarine embayment (Liu et al., 2006), the Beecher's Trilobite Bed (USA) was deposited under dysoxic conditions in an environment of deposition of distal turbidites (Farrell et al., 2013), the Llanfawr mudstones (UK) represented deep-water or abyssal environments (Botting et al., 2011), the Letná Formation (Czech Republic; Fatka et al., 2013), the Airport Cove and William Lake (Canada; Young et al., 2007) were located in shallow peritidal settings and the Soom Shale (South Africa) was close to a retreating ice front (Aldridge et al., 2001).

Therefore, the Fezouata Lagerstätte opens a unique and exceptional window into the marine biodiversity within open-marine environments during the Early Ordovician and makes it possible for the first time to establish accurate comparisons with the older well-documented open-marine exceptional biotas from the Cambrian. Among them, the Burgess Shale (Canada; Collom et al., 2009), Kaili (China; Zhao et al., 2005), Sinsk (Russia; Ivantsov et al., 2005), and Sirius Passet (Greenland; Ineson et al., 2011) Lagerstätten are associated with distal offshore environments, whereas the Emu Bay Shale Lagerstätte (Australia; Gehling et al., 2011) is characterised by a relative nearshore setting affected by the tectonics of an active margin. In terms of environmental setting, the Fezouata Lagerstätte may best compare with the Guanshan and Chengjiang Lagerstätten (Hu, 2005; Hu et al., 2010; MacKenzie et al., 2015), although the environmental conditions that prevailed at Chengjiang are still debated (see Zhao et al., 2012). A lower shoreface/offshore depositional environment has been inferred for these three localities, in which early diagenetic pyritization represents the dominant mode of soft-tissue preservation (Gabbott et al., 2004; Van Roy et al., 2010; Vinther et al., 2008).

Another important characteristic of the Fezouata Lagerstätte is its high latitudinal position (c. 65°S) compared with that of other Ordovician and Cambrian Lagerstätten (Fig. 2B, Cocks and Torsvik, 2004; Torsvik and Cocks, 2011). The Hirnantian Soom Shale Lagerstätte (South Africa) was previously thought to be located at 60°S, but more recent palaeogeographic reconstructions suggest a much lower latitude (i.e. 35°S; Whittle et al., 2007; Torsvik and Cocks, 2013). Unlike the Soom Shale (Gabbott, 1998), no glaciogenic sediments are associated with the Fezouata Biota. This raises the important question of the climatic conditions and seawater temperature that prevailed and may have influenced the diversity and composition of the Fezouata Biota. Nevertheless, the very nature of the global climate state during the Early and Middle Ordovician is under discussion (Trotter et al., 2008; Vandenbroucke et al., 2009; Nardin et al., 2011; Turner et al., 2011).

5.4. A Late Tremadocian Lagerstätte : evolutionary perspectives

The Fezouata Biota is a key source of information for understanding the biotic turnover that took place during the Cambrian–Ordovician transition, i.e. after the Cambrian Explosion and before the GOBE. The co-existence of Burgess Shale-type faunal elements (such as marrellomorphs and anomalocaridids) with remarkably derived, typical post-Cambrian organisms (such as crinoids, ostracods and xiphosurids) indicates that the transition between the Cambrian and Palaeozoic Evolutionary Faunas (Sepkoski, 1979) was more complex and extended than hitherto realised. Moreover, the presence of several surprisingly advanced forms in the biota, such as xiphosurid arthropods, machaeridians, or cheloniellids (Van Roy et al., 2010), suggests that at least in some non-biomineralised groups, the GOBE started earlier than previously thought. This supports the idea that, rather than being two distinct events, the Cambrian Explosion and the GOBE might in fact represent different phases of the same dynamic of diversification (Droser and Finnegan, 2003; Van Roy et al., 2010).

6. Conclusions

Exceptional preservation in the Fezouata Shale is restricted to two relatively narrow intervals that belong to the upper Tremadocian (*A. murrayi* to basalmost *H. copiosus* graptolite biozones). The animal communities of the Fezouata biota lived in an open-marine environment, in a relatively shallow setting (offshore to lower shoreface transition) close to the storm wave-base. Organisms were very likely buried *in situ* during storm events, with a background sedimentation resulting from the decantation of mud suspended by wave action. By offering better chronological and environmental constraints, our results reveal the potential of the Fezouata Biota for understanding the early steps of animal life. Future investigations will concentrate on the identification of the taphonomic and/or abiotic factors controlling the restricted stratigraphic distribution of EPF within the thousand-metre-thick Fezouata Shale.

Acknowledgments

This work is part of the ANR (Agence Nationale de la Recherche) research project entitled “The Rise of Animal Life (Cambrian–Ordovician): organisation and tempo” (grant number RALI 197) and of the CNRS-CNRST cooperation project VALORIZ (grant number 52943). J. C. G-M thanks MINECO (project CGL2012-39471) and P. V. R. the National Science Foundation (grant EAR 1053247) for financial support. The authors are particularly grateful to C. E. Brett (Cincinnati), M. Williams (Leicester), A. Rushton (London), and I. D. Somerville (Dublin) for reviewing the manuscript and making many helpful remarks. We also thank Abdel Azizi, Ali Bachnou, Ahmid Hafid, Khaoula Kouraïss, Mohamed “Ou Saïd” Ben Moula, Elise Nardin, Fleur Noailles, Abel Prieur, Roland and Véronique Reboul, Emmanuel Robert, Muriel Vidal, Daniel Vizcaïno and the numerous French and Moroccan student volunteers for assistance in the field and Carlos Alonso (Madrid) for photography.

References

Aceñolaza, F.G., Aceñolaza, G.F., Esteban, S.B., Gutiérrez-Marco, J.C., 1996. Estructuras nemales de *Araneograptus murrayi* (J. Hall) (graptolito del Ordovícico Inferior) y actualización del registro perigondwánico de la especie. Memorias del XII Congreso Geológico de Bolivia, Tarija, pp. 681–689.

Aldridge, R.J., Theron, J.N., Gabbott, S.E., 1994. The Soom Shale: a unique Ordovician fossil horizon in South Africa. Geology Today 10, 218–221.

Aldridge, R.J., Gabbott, S.E., Theron, J.N., 2001. The Soom Shale. In: Briggs, D.E.G., Crowther, P.R. (Eds.), Palaeobiology II. Blackwell Science, Oxford, pp. 340–342.

Babcock, L.E., Zhang, W.-T., 2001. Stratigraphy, paleontology and depositional setting of the Chengjiang Lagerstätte (Lower Cambrian), Yunnan, China. In: Peng, S.-C., Babcock, L.E., Zhu, M.-Y. (Eds.), Cambrian System of South China. University of Science and Technology of China Press, Hefei, pp. 66–86.

Babin, C., Destombes, J., 1990. Les mollusques bivalves et rostroconches ordoviciens de l'Anti-Atlas marocain: intérêt paléogéographique de leur inventaire. Géologie Mediterranéenne 17, 243–261.

Bambach, R.K., Bush, A.M., Erwin, D.H., 2007. Autecology and the filling of ecospace: key metazoan radiations. Palaeontology 50, 1–22. http://dx.doi.org/10.1111/j.1475-4983.2006.00611.x.

Bergström, S.M., Chen, X., Gutiérrez-Marco, J.C., Dronov, A., 2009. The new chronostratigraphic classification of the Ordovician System and its relations to major regional series and stages and to $\delta^{13}C$ chemostratigraphy. Lethaia 42, 97–107. http://dx.doi.org/10.1111/j.1502-3931.2008.00136.x.

Botting, J.P., 2007. “Cambrian” demosponges in the Ordovician of Morocco: insights into the early evolutionary history of sponges. Geobios 40, 737–748. http://dx.doi.org/10.1016/j.geobios.2007.02.006.

Botting, J.P., Muir, L.A., Sutton, M.D., Barnie, T., 2011. Welsh gold: a new exceptionally preserved pyritized Ordovician biota. Geology 39, 879–882. http://dx.doi.org/10.1130/G32143.1.
Brett, C.E., Allison, P.A., DeSantis, M.K., Liddell, W.D., Kramer, A., 2009. Sequence stratigraphy, cyclic facies, and Lagerstätten in the Middle Cambrian Wheeler and Marjum formations, Great Basin, Utah. Palaeogeography, Palaeoclimatology, Palaeoecology 277, 9–33. http://dx.doi.org/10.1016/j.palaeo.2009.02.010.
Butterfield, N.J., 2011. Animals and the invention of the Phanerozoic Earth system. Trends in Ecology & Evolution 26, 81–87. http://dx.doi.org/10.1016/j.tree.2010.11.012.
Caron, J.-B., 2009. The Greater Phyllopod Bed community, historical variations and quantitative approaches. In: Caron, J.-B., Rudkin, D. (Eds.), A Burgess Shale Primer: History, Geology and Research Highlights. The Burgess Shale Consortium, Toronto, pp. 52–58.
Caron, J.-B., Jackson, D.A., 2008. Paleoecology of the Greater Phyllopod Bed community, Burgess Shale. Palaeogeography, Palaeoclimatology, Palaeoecology 258, 222–256. http://dx.doi.org/10.1016/j.palaeo.2007.05.023.
Chatterton, B.D.E., Fortey, R.A., 2008. Linear clusters of articulated trilobites from Lower Ordovician (Arenig) strata at Bini Tin Zoulin North of Zagora, southern Morocco. Cuadernos del Museo Geominero 9, 73–78.
Chauvel, J., 1966. Echinodermes de l'Ordovicien du Maroc. Cahiers de Paléontologie. Editions du CNRS, Paris (120 pp.).
Chauvel, J., 1969. Les échinodermes macrocystellides de l'Anti-Atlas marocain. Bulletin de la Société Géologique et Minéralogique de Bretagne C1, 21–32.
Chauvel, J., 1971a. *Rhopalocystis ubaghsi*: un échinoderme éocrinoïde du Trémadocien de l'Anti-Atlas marocain. Mémoires du BRGM 73, 43–49.
Chauvel, J., 1971b. Les échinodermes carpoïdes du Paléozoïque inférieur marocain. Notes du Service Géologique du Maroc 31, 49–60.
Chauvel, J., 1978. Compléments sur les échinodermes du Paléozoïque marocain (diploporites, éocrinoïdes, édrioastéroïdes). Notes du Service Géologique du Maroc 39, 27–78.
Chauvel, J., Régnault, S., 1986. Variabilité du genre *Rhopalocystis* Ubaghs, éocrinoïde du Trémadocien de l'Anti-Atlas marocain. Geobios 19, 863–870.
Cocks, L.R.M., Torsvik, T.H., 2004. Major terranes in the Ordovician. In: Webby, B.D., Paris, F., Droser, M.L., Percival, I.G. (Eds.), The Great Ordovician Biodiversification Event. Columbia University Press, New York, pp. 61–67.
Collom, C.J., Johnston, P.A., Powell, W.G., 2009. Reinterpretation of "Middle" Cambrian stratigraphy of the rifted western Laurentian margin: Burgess Shale Formation and contiguous units (Sauk II megasequence), Rocky Mountains, Canada. Palaeogeography, Palaeoclimatology, Palaeoecology 277, 63–85. http://dx.doi.org/10.1016/j.palaeo.2009.02.012.
Cooper, R., Fortey, R.A., Lindholm, K., 1991. Latitudinal and depth zonation of early Ordovician graptolites. Lethaia 24, 199–218.
Cooper, R.A., Rigby, S., Loydell, D.K., Bates, D.E.B., 2012a. Palaeoecology of the Graptoloidea. Earth-Science Reviews 112, 23–41. http://dx.doi.org/10.1016/j.earscirev.2012.01.001.
Cooper, R.A., Sadler, P.M., Hammer, O., Gradstein, F.M., 2012b. Chapter 20 — the Ordovician Period. In: Gradstein, F.M., Ogg, J.G., Schmitz, M.D., Ogg, G.M. (Eds.), The Geologic Time Scale. Elsevier, Boston, pp. 489–523.
Destombes, J., 1962. Stratigraphie et paléogéographie de l'Ordovicien de l'Anti-Atlas (Maroc). Un essai de synthèse. Bulletin de la Société Géologique de France 7, 453–460.
Destombes, J., 1972. Les trilobites du sous-ordre des Phacopina de l'Ordovicien de l'Anti-Atlas (Maroc). Notes et Mémoires du Service Géologique du Maroc 240, 1–113.
Destombes, J., Willefert, S., 1959. Sur la présence de *Dictyonema* dans le Tremadoc de l'Anti-Atlas (Maroc). Comptes Rendus de l'Académie des Sciences de Paris 249, 1246–1247.
Destombes, J., Hollard, H., Willefert, S., 1985. Lower Palaeozoic rocks of Morocco. In: Holland, C.H. (Ed.), Lower Palaeozoic Rocks of North-Western and West-Central Africa. Wiley, New-York, Chichester, Brisbane, pp. 91–336.
Donovan, S.K., Savill, J.J., 1988. *Ramseyocrinus* (Crinoidea) from the Arenig of Morocco. Journal of Paleontology 62, 283–285.
Droser, M.L., Finnegan, S., 2003. The Ordovician radiation: a follow-up to the Cambrian explosion? Integrative and Comparative Biology 43, 178–184. http://dx.doi.org/10.1093/icb/43.1.178.
Duke, W.L., 1985. Hummocky cross-stratification, tropical hurricanes, and intense winter storms. Sedimentology 32, 167–194.
Duke, W.L., Arnott, R.W.C., Cheel, R.J., 1991. Shelf sandstones and hummocky cross-stratification: new insights on a stormy debate. Geology 19, 625–628.
Dunne, J.A., Williams, R.J., Martinez, N.D., Wood, R.A., Erwin, D.H., 2008. Compilation and network analyses of Cambrian food webs. PLoS Biology 6, e102. http://dx.doi.org/10.1371/journal.pbio.0060102.
Egenhoff, S.O., Maletz, J., Erdtmann, B.-D., 2004. Lower Ordovician graptolite biozonation and lithofacies of southern Bolivia: relevance for palaeogeographic interpretations. Geological Magazine 141, 287–299. http://dx.doi.org/10.1017/S0016756804009239.
Elaouad-Debbaj, Z., 1988. Acritarches et chitinozoaires du Trémadoc de l'Anti-Atlas central (Maroc). Revue de Micropaléontologie 31, 85–128.
Erwin, D.H., Valentine, J.W., 2013. The Cambrian Explosion: The Construction of Animal Biodiversity. Roberts and Company Publishers, Greenwood Village (416 pp.).
Erwin, D.H., Laflamme, M., Tweedt, S.M., Sperling, E.A., Pisani, D., Peterson, K.J., 2011. The Cambrian conundrum: early divergence and later ecological success in the early history of animals. Science 334, 1091–1097. http://dx.doi.org/10.1126/science.1206375.
Farrell, U.C., Briggs, D.E., Hammarlund, E.U., Sperling, E.A., Gaines, R.R., 2013. Paleoredox and pyritization of soft-bodied fossils in the Ordovician Frankfort Shale of New York. American Journal of Science 313, 452–489. http://dx.doi.org/10.2475/05.2013.02.
Fatka, O., Lerosey-Aubril, R., Budil, P., Rak, š., 2013. Fossilised guts in trilobites from the Upper Ordovician Letná Formation (Prague Basin, Czech Republic). Bulletin of Geosciences 88, 95–104. http://dx.doi.org/10.3140/bull.geosci.1329.
Feng, H.-Z., Li, M., Zhang, Y.-D., Erdtmann, B.-D., Li, L.-X., Wang, W.-H., 2009. Succession and global correlation of Late Tremadoc graptolite zones from South China. Science in China Series D: Earth Sciences 52, 287–299.
Fortey, R.A., 2009. A new giant asaphid trilobite from the Lower Ordovician of Morocco. Memoirs of the Association of Australasian Palaeontologists 37, 9–16.
Fortey, R.A., 2011a. The first known complete lichakephalid trilobite, Lower Ordovician of Morocco. Memoirs of the Association of Australasian Palaeontologists 42, 1–7.
Fortey, R.A., 2011b. Trilobites of the genus *Dikelokephalina* from Ordovician Gondwana and Avalonia. Geological Journal 46, 405–415. http://dx.doi.org/10.1002/gj.1275.
Gabbott, S.E., 1998. Taphonomy of the Ordovician Soom Shale Lagerstätte: an example of soft tissue preservation in clay minerals. Palaeontology 41, 631–667.
Gabbott, S., Zalasiewicz, J., 2009. Sedimentation of the Phyllopod Bed within the Cambrian Burgess Shale Formation. In: Caron, J.-B., Rudkin, D. (Eds.), A Burgess Shale Primer: history, geology and research highlights. The Burgess Shale Consortium, Toronto, pp. 307–318.
Gabbott, S.E., Hou, X.-G., Norry, M.J., Siveter, D.J., 2004. Preservation of Early Cambrian animals of the Chengjiang biota. Geology 32, 901–904. http://dx.doi.org/10.2110/10.1130/G20640.1.
Gabbott, S.E., Zalasiewicz, J., Collins, D., 2008. Sedimentation of the Phyllopod Bed within the Cambrian Burgess Shale Formation of British Columbia. Journal of the Geological Society 165, 307–318. http://dx.doi.org/10.1144/0016-76492007-023.
Gaines, R.R., Briggs, D.E.G., Orr, P.J., Van Roy, P., 2012a. Preservation of giant anomalocaridids in silica-chlorite concretions from the Early Ordovician of Morocco. Palaios 27, 317–325. http://dx.doi.org/10.2110/palo.2011.p11-093r.
Gaines, R.R., Hammarlund, E.U., Hou, X., Qi, C., Gabbott, S.E., Zhao, Y., Peng, J., Canfield, D.E., 2012b. Mechanism for Burgess Shale-type preservation. Proceedings of the National Academy of Sciences 109, 5180–5184. http://dx.doi.org/10.1073/pnas.1111784109.
Gehling, J.G., Jago, J.B., Paterson, J.R., García-Bellido, D.C., Edgecombe, G.D., 2011. The geological context of the Lower Cambrian (Series 2) Emu Bay Shale Lagerstätte and adjacent stratigraphic units, Kangaroo Island, South Australia. Australian Journal of Earth Sciences 58, 243–257. http://dx.doi.org/10.1080/08120099.2011.555487.
Geyer, G., Landing, E., 2006. Latest Ediacaran and Cambrian of the Moroccan Atlas regions. Beringeria Special Issue 6, 7–46.
Gupta, A., 1998. Primordial storms: an overview of depositional environments in Mid-Late Proterozoic platforms of India. Gondwana Research 1, 291–298. http://dx.doi.org/10.1016/S1342-937X(05)70840-6.
Hagadorn, J.W., 2002. Burgess Shale-type localities: the global picture. In: Bottjer, D.J., Etter, W., Hagadorn, J.W., Tang, C.M. (Eds.), Exceptional fossil preservation—a unique view on the evolution of marine life. Columbia University Press, New York, pp. 61–89.
Hall, J., 1858. Note upon the genus *Graptolithus*, and description of some remarkable new forms from the shales of the Hudson River group, discovered in the investigations of the Geological Survey of Canada, under the direction of Sir W. E. Logan. Canadian Naturalist and Quarterly Journal of Science 3, 139–150 161–177.
Hall, J., 1865. Graptolites of the Quebec group. In: Dawson Brothers (Ed.), Figures and descriptions of Canadian organic remains. Geological Survey of Canada, Montreal (151 pp.).
Harms, J.C., Southard, J.B., Spearing, D.R., Walker, R.G., 1975. Depositional Environments as Interpreted from Primary Sedimentary Structures and Stratification Sequences. Short course No. 2. Society of Economic Paleontologists and Mineralogists, Dallas (161 pp.).
Harper, D.A.T., 2006. The Ordovician biodiversification: setting an agenda for marine life. Palaeogeography, Palaeoclimatology, Palaeoecology 232, 148–166. http://dx.doi.org/10.1016/j.palaeo.2005.07.010.
Havlíček, V., 1971. Brachiopodes de l'Ordovicien du Maroc. Notes et Mémoires du Service Géologique du Maroc 230, 1–135.
Henry, J.L., Vizcaïno, D., Destombes, J., 1992. Evolution de l'œil et hétérochronie chez les trilobites ordoviciens *Ormathops* Delo, 1935 et *Toletanaspis* Rabano, 1989 (Dalmanitidae, Zeliszkellinae). Paläontologische Zeitschrift 66, 277–290.
Horný, R.J., 1997. Ordovician Tergomya and Gastropoda (Mollusca) of the Anti-Atlas (Morocco). Acta Musei Nationalis Pragae B 53, 37–78.
Hou, X., Aldridge, R.J., Bergström, J., Siveter, D.J., Siveter, D.J., Feng, X., 2004. The Cambrian Fossils of Chengjiang, China: The Flowering of Early Animal Life. Blackwell Science, Oxford (256 pp.).
Hu, S.X., 2005. Taphonomy and palaeoecology of the Early Cambrian Chengjiang biota from Eastern Yunnan, China. Berliner Paläobiologische Abhandlungen 7, 1–197.
Hu, S., Zhu, M., Steiner, M., Luo, H., Zhao, F., Liu, Q., 2010. Biodiversity and taphonomy of the Early Cambrian Guanshan biota, eastern Yunnan. Science China Earth Sciences 53, 1765–1773. http://dx.doi.org/10.1007/s11430-010-4086-9.
Immenhauser, A., 2009. Estimating palaeo-water depth from the physical rock record. Earth-Science Reviews 96, 107–139.
Ineson, J.R., Peel, J.S., Bentley, S., 2011. Geological and depositional setting of the Sirius Passet Lagerstätte (Early Cambrian), North Greenland. Canadian Journal of Earth Sciences 48, 1259–1281. http://dx.doi.org/10.1139/e11-018.
Ivantsov, A.Y., Zhuravlev, A.Y., Leguta, A.V., Krassilov, V.A., Melnikova, L.M., Ushatinskaya, G.T., 2005. Palaeoecology of the Early Cambrian Sinsk biota from the Siberian Platform. Palaeogeography, Palaeoclimatology, Palaeoecology 220, 69–88. http://dx.doi.org/10.1016/j.palaeo.2004.01.022.
Jackson, D.E., Lenz, A.C., 2003. Taxonomic and biostratigraphical significance of the Tremadoc graptolite fauna from northern Yukon territory, Canada. Geological Magazine 140, 131–156.
Kirk, J.T.O., 2011. Light and Photosynthesis in Aquatic Ecosystems. 3rd edition. Cambridge University Press, Cambridge (662 pp.).
Kröger, B., Lefebvre, B., 2012. Palaeogeography and palaeoecology of early Floian (Early Ordovician) cephalopods from the Upper Fezouata Formation, Anti-Atlas, Morocco. Fossil Record 15, 61–75. http://dx.doi.org/10.1002/mmng.201200004.
Lefebvre, B., Botting, J.P., 2007. First report of the mitrate *Peltocystis cornuta* Thoral (Echinodermata, Stylophora) in the Lower Ordovician of central Anti-Atlas (Morocco). Annales de Paleontologie 93, 183–198. http://dx.doi.org/10.1016/j.annpal.2007.06.003.

Liddell, W., Wright, S., Brett, C., 1997. Sequence Stratigraphy and Paleoecology of the Middle Cambrian Spence Shale in Northern Utah and Southern Idaho. Brigham Young University Geology Studies 42 pp. 59–78.
Lindholm, K., 1991. Ordovician graptolites from the early Hunneberg of Southern Scandinavia. Palaeontology 34, 283–327.
Liu, H.P., McKay, R.M., Young, J.N., Witzke, B.J., McVey, K.J., Liu, X., 2006. A new Lagerstätte from the Middle Ordovician St. Peter Formation in northeastern Iowa, USA. Geology 34, 969–972. http://dx.doi.org/10.1130/G22911A.1.
Loydell, D.K., 2012. Graptolite biozone correlation charts. Geological Magazine 149, 124–132. http://dx.doi.org/10.1017/S0016756811000513.
MacKenzie, L.A., Hofmann, M.H., Junyuan, C., Hinman, N.W., 2015. Stratigraphic controls of soft-bodied fossil occurrences in the Cambrian Chengjiang Biota Lagerstätte, Maotianshan Shale, Yunnan Province, China. Palaeogeography, Palaeoclimatology, Palaeoecology 420, 96–115. http://dx.doi.org/10.1016/j.palaeo.2014.11.006.
Maletz, J., 1997. Arenig biostratigraphy of the Pointe-de-Lévy slice, Quebec Appalachians, Canada. Canadian Journal of Earth Sciences 34, 733–752.
Maletz, J., Egenhoff, S.O., 2001. Late Tremadoc to early Arenig graptolite faunas of southern Bolivia and their implications for a worldwide biozonation. Lethaia 34, 47–62.
Marek, L., 1983. The Ordovician hyoliths of Anti-Atlas (Morocco). Sborník Národního Muzea v Praze 39, 1–36.
Maruyama, S., Sawaki, Y., Ebisuzaki, T., Ikoma, M., Omori, S., Komabayashi, T., 2014. Initiation of leaking Earth: an ultimate trigger of the Cambrian explosion. Gondwana Research 25, 910–944. http://dx.doi.org/10.1016/j.gr.2013.03.012.
McLane, M., 1995. Sedimentology. Oxford University Press, Oxford (423 pp.).
Mergl, M., 1981. The genus *Orbithele* (Brachiopoda, Inarticulata) from the Lower Ordovician of Bohemia and Morocco. Vestník Ústredního Ústavu Geologického 56, 287–292.
Mergl, M., 1988. *Incorthis* (Orthida, Brachiopoda) from the Lower Ordovician (Arenig) of Morocco. Casopis pro Mineralogii a Geologii 33, 199–200.
Molyneux, S.G., Raevskaya, E., Servais, T., 2007. The *messaoudensis–trifidum* acritarch assemblage and correlation of the base of Ordovician Stage 2 (Floian). Geological Magazine 144, 143–156. http://dx.doi.org/10.1017/S0016756806002676.
Monsen, A., 1937. Die Graptolithenfauna im Unteren Didymograptusschiefer (Phyllograptusschiefer) Norwegens. Norsk Geologisk Tidsskrift 16, 57–266.
Moore, R.A., Lieberman, B.S., 2009. Preservation of Early and Middle Cambrian soft-bodied arthropods from the Pioche Shale, Nevada, USA. Palaeogeography, Palaeoclimatology, Palaeoecology 277, 57–62. http://dx.doi.org/10.1016/j.palaeo.2009.02.014.
Nardin, E., Goddéris, Y., Donnadieu, Y., Le Hir, G., Blakey, R.C., Pucéat, E., Aretz, M., 2011. Modeling the Early Paleozoic long-term climatic trend. Geological Society of America Bulletin 123, 1181–1192. http://dx.doi.org/10.1130/B30364.1.
Noailles, F., Lefebvre, B., Guensburg, T.E., Hunter, A.W., Nardin, E., Sumrall, C.D., Zamora, S., 2010. New echinoderm-Lagerstätten from the Lower Ordovician of central Anti-Atlas (Zagora area, Morocco): a Gondwanan perspective of the Great Ordovician Biodiversification Event. In: Reich, M., Reitner, J., Roden, V., Thuy, B. (Eds.), Echinoderm Research 2010. Universitätsverlag Göttingen, Göttingen, pp. 77–78.
Nowak, H., Akodad, M., Lefebvre, B., Servais, T., 2015. Discovery of the *messaoudensis–trifidum* acritarch assemblage (upper Tremadocian–lower Floian, Lower Ordovician) in the subsurface of Morocco. Estonian Journal of Earth Sciences 64, 80–83. http://dx.doi.org/10.3176/earth.2015.14.
Ortega, G., Albanesi, G.L., 2005. Tremadocian graptolite–conodont biostratigraphy of the South American Gondwana margin (Eastern Cordillera, NW Argentina). Geologica Acta 3, 355–371.
Paterson, J.R., Edgecombe, G.D., Jago, J.B., 2015. The "great appendage" arthropod *Tanglangia*: biogeographic connections between early Cambrian biotas of Australia and South China. Gondwana Research 27, 1667–1672. http://dx.doi.org/10.1016/j.gr.2014.02.008.
Peel, J.S., Ineson, J.R., 2011. The Sirius Passet Lagerstätte (Early Cambrian) of North Greenland. Palaeontographica Canadiana 31, 109–118.
Pillola, G.L., Piras, S., Serpagli, E., 2008. Upper Tremadoc–Lower Arenig? Anisograptid–Dichograptid fauna from the Cabitza Formation (Lower Ordovician, SW Sardinia, Italy). Revue de Micropaléontologie 51, 167–181.
Pritchard, G.B., 1892. On a new species of Graptolitidae (*Temnograptus magnificus*). Proceedings of the Royal Society of Victoria 4, 56–58.
Rábano, I., 1990. Trilobites del Museo Geominero. I. *Platypeltoides magrebiensis* n. sp. (Asaphina, Nileidae), del Ordovícico inferior del Anti-Atlas central (Marruecos). Boletín Geológico y Minero 101, 21–27.
Sadler, P.M., Cooper, R.A., Melchin, M., 2009. High-resolution, early Paleozoic (Ordovician–Silurian) time scales. Geological Society of America Bulletin 121, 887–906. http://dx.doi.org/10.1130/B26357.1.
Santosh, M., Maruyama, S., Sawaki, Y., Meert, J.G., 2014. The Cambrian explosion: plume-driven birth of the second ecosystem on Earth. Gondwana Research 25, 945–965. http://dx.doi.org/10.1016/j.gr.2013.03.013.
Seilacher, A., 1970. Begriff und Bedeutung der Fossil-Lagerstätten. Neues Jahrbuch für Geologie und Paläontologie Monatshefte 1970, 34–39.
Sepkoski, J.J., 1979. A kinetic model of Phanerozoic taxonomic diversity II. Early Phanerozoic families and multiple equilibria. Paleobiology 5, 222–251.
Servais, T., Lehnert, O., Li, J., Mullins, G.L., Munnecke, A., Nützel, A., Vecoli, M., 2008. The Ordovician biodiversification: revolution in the oceanic trophic chain. Lethaia 41, 99–109. http://dx.doi.org/10.1111/j.1502-3931.2008.00115.x.
Servais, T., Owen, A.W., Harper, D.A.T., Kröger, B., Munnecke, A., 2010. The Great Ordovician Biodiversification Event (GOBE): the palaeoecological dimension. Palaeogeography, Palaeoclimatology, Palaeoecology 294, 99–119. http://dx.doi.org/10.1016/j.palaeo.2010.05.031.
Shu, D., Isozaki, Y., Zhang, X., Han, J., Maruyama, S., 2014. Birth and early evolution of metazoans. Gondwana Research 25, 884–895. http://dx.doi.org/10.1016/j.gr.2013.09.001.
Smith, M.P., Harper, D.A.T., 2013. Causes of the Cambrian explosion. Science 341, 1355–1356. http://dx.doi.org/10.1126/science.1239450.
Sumrall, C.D., Zamora, S., 2011. Ordovician edrioasteroids from Morocco: faunal exchanges across the Rheic Ocean. Journal of Systematic Palaeontology 9, 425–454. http://dx.doi.org/10.1080/14772019.2010.499137.
Thomas, D.E., 1973. Two new graptolites from Victoria, Australia. Geological Magazine 109, 529–532.
Torsvik, T.H., Cocks, L.R.M., 2011. The Palaeozoic palaeogeography of central Gondwana. Geological Society, London, Special Publications 357, 137–166. http://dx.doi.org/10.1144/SP357.8.
Torsvik, T.H., Cocks, L.R.M., 2013. Gondwana from top to base in space and time. Gondwana Research 24, 999–1030. http://dx.doi.org/10.1016/j.gr.2013.06.012.
Trotter, J.A., Williams, I.S., Barnes, C.R., Lecuyer, C., Nicoll, R.S., 2008. Did cooling oceans trigger Ordovician biodiversification? Evidence from conodont thermometry. Science 321, 550–554. http://dx.doi.org/10.1126/science.1155814.
Turner, B.R., Armstrong, H.A., Holt, P., 2011. Visions of ice sheets in the Early Ordovician greenhouse world: evidence from the Peninsula Formation, Cape Peninsula, South Africa. Sedimentary Geology 236, 226–238. http://dx.doi.org/10.1016/j.sedgeo.2011.01.009.
Ubaghs, G., 1963. *Rhopalocystis destombesi* n. gen., n. sp., éocrinoïde de l'Ordovicien inférieur (Trémadocien supérieur) du Sud marocain. Notes du Service Géologique du Maroc 23, 25–39.
Valent, M., Corbacho, J., Martínez, D., 2013. Hyolith localities of Zagora region (Morocco). Upper Fezouata Formation (Lower Ordovician). Batalleria 19, 20–23.
Van Roy, P., Briggs, D.E.G., 2011. A giant Ordovician anomalocaridid. Nature 473, 510–513. http://dx.doi.org/10.1038/nature09920.
Van Roy, P., Daley, A.C., Briggs, D.E.G, 2015. Anomalocaridid trunk limb homology revealed by a giant Ordovician filter-feeder with paired lateral flaps. Nature http://dx.doi.org/10.1038/nature14256 advance online publication.
Van Roy, P., Orr, P.J., Botting, J.P., Muir, L.A., Vinther, J., Lefebvre, B., el Hariri, K., Briggs, D.E.G., 2010. Ordovician faunas of Burgess Shale type. Nature 465, 215–218. http://dx.doi.org/10.1038/nature09038.
Vandenbroucke, T.R.A., Armstrong, H.A., Williams, M., Zalasiewicz, J.A., Sabbe, K., 2009. Ground-truthing Late Ordovician climate models using the paleobiogeography of graptolites. Paleoceanography 24, 1–19. http://dx.doi.org/10.1029/2008PA001720.
Vannier, J., 2011. Gut contents as direct indicators for trophic relationships in the Cambrian marine ecosystem. PloS One 7, e52200. http://dx.doi.org/10.1371/journal.pone.0052200.
Vannier, J., Steiner, M., Renvoise, E., Hu, S.-X., Casanova, J.-P., 2007. Early Cambrian origin of modern food webs: evidence from predator arrow worms. Proceedings of the Royal Society B: Biological Sciences 274, 627–633. http://dx.doi.org/10.1098/rspb.2006.3761.
Vidal, M., 1998a. Trilobites (Asaphidae et Raphiphoridae) de l'Ordovicien inférieur de l'Anti-Atlas, Maroc. Palaeontographica Abteilung A 251, 39–77.
Vidal, M., 1998b. Le modèle des biofaciès à trilobites: un test dans l'Ordovicien inférieur de l'Anti-Atlas, Maroc. Comptes Rendus de l'Académie des Sciences, Series IIA, Earth and Planetary Science Letters 327, 327–333. http://dx.doi.org/10.1016/S1251-8050(98)80051-7.
Vinther, J., Van Roy, P., Briggs, D.E.G., 2008. Machaeridians are Palaeozoic armoured annelids. Nature 451, 185–188. http://dx.doi.org/10.1038/nature06474.
Webby, B.D., Paris, F., Droser, M.L., Percival, I.A. (Eds.), 2004. The Great Ordovician Biodiversification Event. Columbia University Press, New York (496 pp.).
Whittle, R.J., Gabbott, S.E., Aldridge, R.J., Theron, J.N., 2007. Taphonomy and palaeoecology of a Late Ordovician caryocaridid from the Soom Shale Lagerstätte, South Africa. Palaeogeography, Palaeoclimatology, Palaeoecology 251, 383–397. http://dx.doi.org/10.1016/j.palaeo.2007.04.006.
Williams, S.H., Stevens, R.K., 1991. Late Tremadoc graptolites from western Newfoundland. Palaeontology 34, 1–47.
Young, G.A., Rudkin, D.M., Dobrzanski, E.P., Robson, S.P., Nowlan, G.S., 2007. Exceptionally preserved Late Ordovician biotas from Manitoba, Canada. Geology 35, 883–886. http://dx.doi.org/10.1130/G23947A.1.
Zhang, X., Shu, D., Han, J., Zhang, Z., Liu, J., Fu, D., 2014. Triggers for the Cambrian explosion: hypotheses and problems. Gondwana Research 25, 896–909. http://dx.doi.org/10.1016/j.gr.2013.06.001.
Zhao, Y., Zhu, M., Babcock, L.E., Yuan, J., Parsley, R.L., Peng, J., Yang, X., Wang, Y., 2005. Kaili Biota: a taphonomic window on diversification of metazoans from the basal Middle Cambrian: Guizhou, China. Acta Geologica Sinica 79, 751–765. http://dx.doi.org/10.1111/j.1755-6724.2005.tb00928.x.
Zhao, F., Caron, J.-B., Hu, S., Zhu, M., 2009. Quantitative analysis of taphofacies and paleocommunities in the Early Cambrian Chengjiang Lagerstätte. Palaios 24, 826–839. http://dx.doi.org/10.2110/palo.2009.p09-004r.
Zhao, F., Hu, S., Caron, J.-B., Zhu, M., Yin, Z., Lu, M., 2012. Spatial variation in the diversity and composition of the Lower Cambrian (Series 2, Stage 3) Chengjiang Biota, Southwest China. Palaeogeography, Palaeoclimatology, Palaeoecology 346–347, 54–65. http://dx.doi.org/10.1016/j.palaeo.2012.05.02.

Annexe 5 :

Biostratigraphic and palaeoenvironmental controls on the trilobite associations from the Lower Ordovician Fezouata Shale of the central Anti-Atlas, Morocco

Auteurs : Emmanuel L.O. Martin, Muriel Vidal, Daniel Vizcaïno, **Romain Vaucher**, Pierre Sansjofre, Bertrand Lefebvre, Jacques Destombes

Article publié dans *Palaeogeography, Palaeoclimatology, Palaeoecology*

Année : 2016 Volume : 460 Pages : 142 - 154

DOI : http://dx.doi.org/10.1016/j.palaeo.2016.06.003

Palaeogeography, Palaeoclimatology, Palaeoecology 460 (2016) 142–154

Contents lists available at ScienceDirect

Palaeogeography, Palaeoclimatology, Palaeoecology

journal homepage: www.elsevier.com/locate/palaeo

Biostratigraphic and palaeoenvironmental controls on the trilobite associations from the Lower Ordovician Fezouata Shale of the central Anti-Atlas, Morocco

Emmanuel L.O. Martin [a,*], Muriel Vidal [b], Daniel Vizcaïno [c], Romain Vaucher [a], Pierre Sansjofre [b], Bertrand Lefebvre [a], Jacques Destombes [d]

[a] Univ Lyon, Université Claude Bernard Lyon 1, ENS de Lyon, CNRS, UMR 5276 LGL-TPE, F-69622 Villeurbanne, France
[b] UMR 6538 Domaines Océaniques, IUEM-UBO, CNRS, Brest University, Place Copernic, 29280 Plouzané, France
[c] 7, rue Jean Baptiste Chardin, Maquens, 11090, Carcassonne, France
[d] 19, rue de la Fon de Madran, 33600 Pessac, France

ARTICLE INFO

Article history:
Received 31 October 2015
Received in revised form 2 June 2016
Accepted 5 June 2016
Available online 7 June 2016

Keywords:
Trilobita
Biostratigraphy
Sedimentology
Geochemistry
Fezouata Shale
Lower Ordovician

ABSTRACT

Trilobites are a major component of both biomineralized and soft-bodied assemblages of the Fezouata Biota, central Anti-Atlas, Morocco. Trilobite taxa of the Fezouata Shale (Tremadocian–Floian) in the Zagora area are typical of Lower Ordovician communities from shallow shelf environments, and show strong affinities with Early Ordovician assemblages from the Montagne Noire (southern France). Dramatic variations in both taxonomic composition and taphonomic attributes, together with the sedimentological facies changes, allow us to discriminate the palaeoenvironmental versus stratigraphic control on trilobite assemblages. Three communities are described along an onshore–offshore profile, namely the pilekiid-bavarillid, *Agerina* and raphiophorid biofacies. Additionally, three stratigraphic assemblages are identified: assemblage 1 is confined to the late Tremadocian, assemblage 2 ranges from late Tremadocian to middle Floian and assemblage 3 is restricted to the Floian. The higher diversity of some levels is explained by storm-induced inputs of debris from taxa living in adjacent environments. Additionally, control of relative seal level variation on some peculiarities of the trilobite fauna (specific endemicity, lack of some expected taxa) is evidenced in the Fezouata Shale. Finally, temporary dysoxic events are highlighted by preliminary geochemical analyses, probably allowing episodic exceptional preservation.

1. Introduction

A comprehensive historical review of the Fezouata Shale study has been recently published (Lefebvre et al., 2016a-in this issue), so that only the historical discoveries concerning the trilobite fauna are highlighted herein. The Lower Ordovician of the Anti-Atlas (Morocco; Fig. 1B) is one of the few successions, worldwide, documenting the early stages of the Great Ordovician Biodiversification Event. In the last 50 years, the shales of the Lower and Upper Fezouata formations (early Tremadocian to late Floian; Fig. 1D) have yielded abundant and diverse biomineralized assemblages of marine invertebrates dominated by trilobites, associated with articulate brachiopods, echinoderms, graptolites and molluscs (Destombes et al., 1985). In the early 2000s, the discovery of exceptionally preserved remains of soft-bodied organisms in the Lower Ordovician of the Zagora area (central Anti-Atlas) dramatically altered the views on the tempo and patterns of the major diversification of metazoans in Early Palaeozoic times (Van Roy et al., 2010). The Burgess Shale type Fezouata Biota includes a mixture of taxa typical of early to middle Cambrian Lagerstätten (e.g., anomalocaridids, marrellomorphs) and the earliest occurrences of typical post-Cambrian organisms, previously known from younger strata (e.g., cirriped crustaceans, eurypterids, highly derived xiphosurids; Van Roy et al., 2015).

In the Zagora area, levels with exceptional preservation are restricted to two narrow stratigraphic intervals within the Fezouata Shale, which corresponds to a monotonous series of argillites about 850 m thick (Fig. 2; Martin et al., 2016). Recent advances in graptolite biostratigraphy in the central Anti-Atlas indicate that the main, lower level with exceptional preservation corresponds to a ~70 m thick interval at the top of the *Araneograptus murrayi* Zone (late Tremadocian), whereas the second, upper level is only ~15 m thick and occurs about 200 m above, in the? *Baltograptus jacksoni* Zone (middle Floian; Gutiérrez-Marco and Martin, 2016-in this issue). After the discovery of the Fezouata Biota, successive field campaigns were organized from 2003 to 2015, and abundant, new material was collected in the Lower Ordovician of

* Corresponding author.
E-mail addresses: emmanuel.martin@univ-lyon1.fr (E.L.O. Martin), Muriel.Vidal@univ-brest.fr (M. Vidal), daniel.vizcaino@wanadoo.fr (D. Vizcaïno), romain.vaucher@univ-lyon1.fr (R. Vaucher), Pierre.SansJofre@univ-brest.fr (P. Sansjofre), bertrand.lefebvre@univ-lyon1.fr (B. Lefebvre), jacquesdestombes@free.fr (J. Destombes).

http://dx.doi.org/10.1016/j.palaeo.2016.06.003
0031-0182/

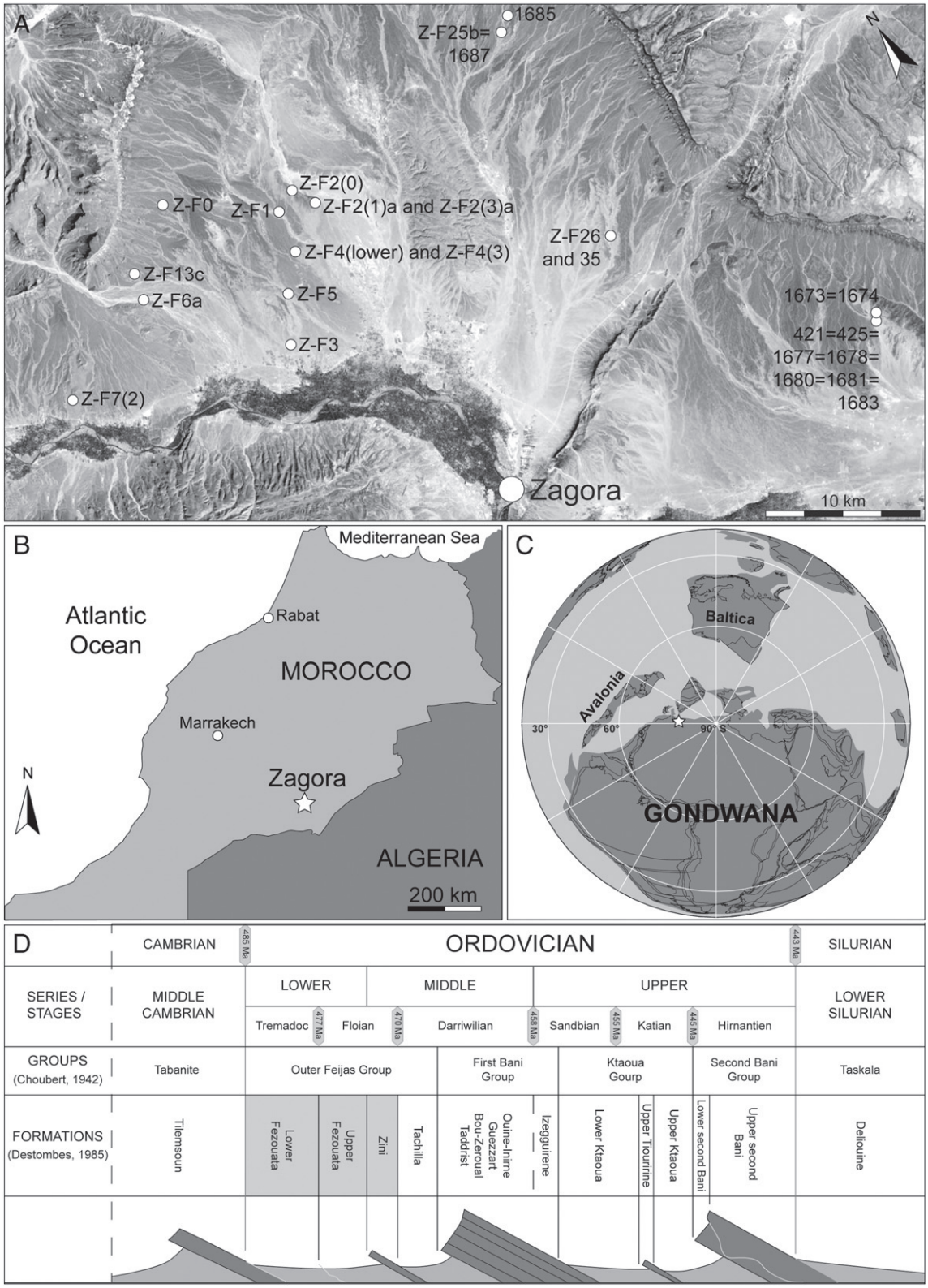

Fig. 1. (A) Satellite image (Google Earth) of the studied area, locations and names of the excavations are indicated. (B) General map of Morocco showing the location of Zagora, the studied area (white star). (C) Palaeogeographic map for Early Ordovician time (ca. 480 Ma) modified from BugPlates (see Torsvik, 2009). (D) Lithostratigraphical units of the Ordovician in the central Anti-Atlas modified from Destombes (1971).

the Zagora area. This material was recently replaced within both its biostratigraphic and environmental contexts (Gutiérrez-Marco and Martin, 2016-in this issue; Lehnert et al., 2016-in this issue; Nowak et al., 2016-in this issue; Vaucher et al., 2016-in this issue).

These newly acquired data, along with the material originally collected by Jacques Destombes in the second half of the 20th century, make it possible to describe with unprecedented detail the assemblages of Early Ordovician trilobites from the central Anti-Atlas, and to discuss

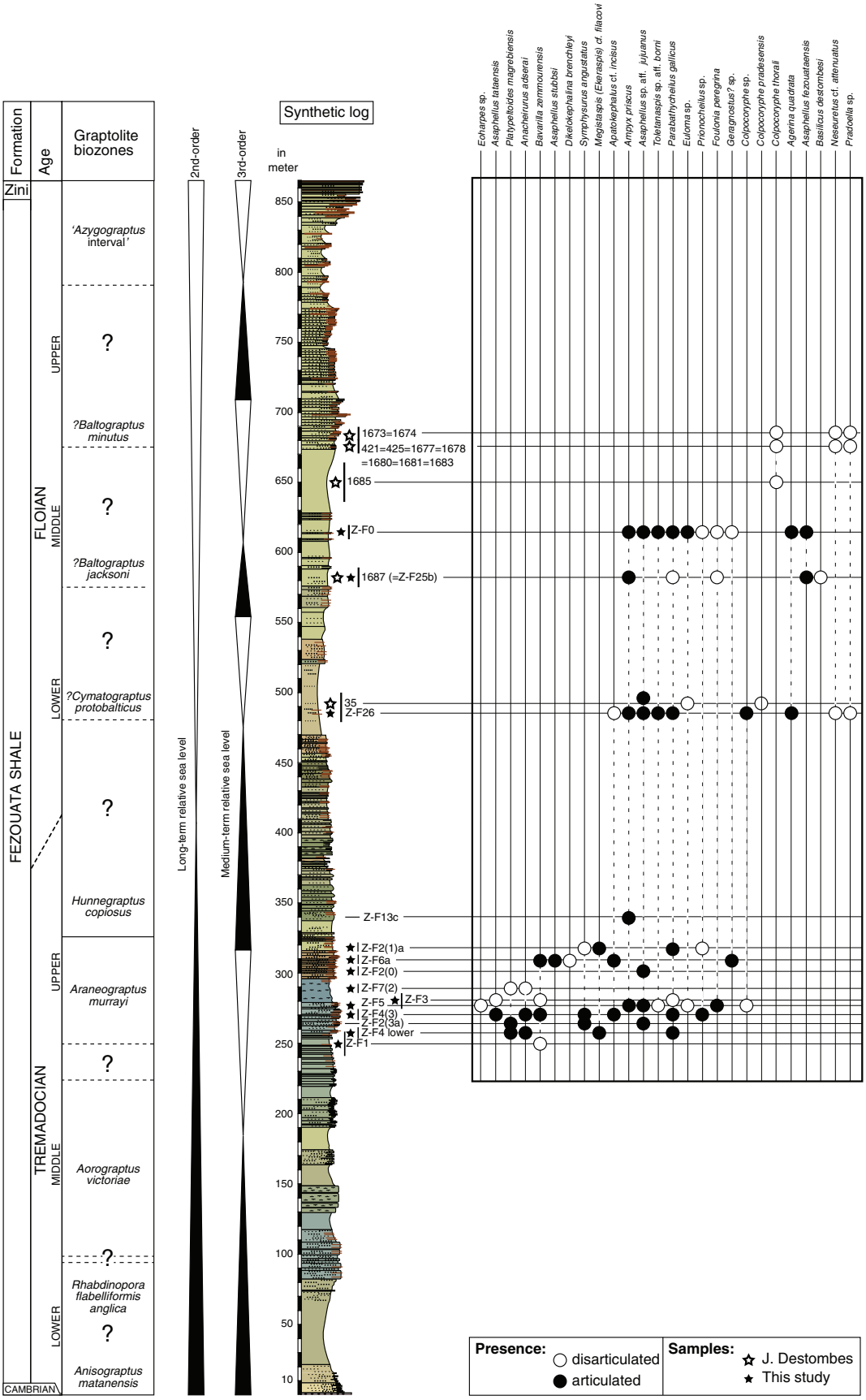

Fig. 2. Biostratigraphy of the trilobite fauna from the Lower Ordovician Fezouata Shale. The stratigraphic column of the Fezouata Shale is a composite from various sections (see Martin et al., 2016). Localities were replaced according to Lefebvre et al. (2016b-in this issue). Graptolite biozonations (Gutiérrez-Marco and Martin, 2016-in this issue) are also indicated. Black spots indicate articulated specimens, while white spots indicate disarticulated ones.

their variations through time and space in this area. Trilobites are one of the major groups of marine invertebrates in the Fezouata Shale, both in terms of abundance and diversity (Destombes et al., 1985; Vidal, 1996, 1998a, 1998b). Moreover, trilobites occur both in "classic" fossiliferous levels yielding biomineralized remains throughout the section and in the horizons with exceptional preservation, in which trilobite soft-parts (e.g., gut) and lightly sclerotized portions of their bodies (e.g., appendages) can be preserved (Van Roy et al., 2010).

Although the systematics of trilobites from the Fezouata Shale is still partly underway, their biostratigraphy, palaeoecology and palaeobiogeography can be discussed and compared with previous trilobite-based studies achieved in other areas and/or slightly younger stratigraphic intervals (e.g., Fortey and Cocks, 2003; Turvey, 2005; Mergl, 2006; Zhou et al., 2011; Adrain, 2013). Consequently, the aims of this paper are: (1) to analyse the variations through time of the successive Early Ordovician trilobite assemblages of the Zagora area, and to propose a trilobite-based biozonation correlated to that established on graptolites; (2) to discuss the spatial distribution of trilobite assemblages in the Lower Ordovician of the central Anti-Atlas, and to identify trilobite biofacies along a depth-related profile; and (3) to discuss the palaeobiogeographic affinities of the Moroccan trilobite assemblages with other high-latitude, Early Ordovician faunas from peri-Gondwanan areas (e.g., Bohemia, Montagne Noire, Wales).

2. Historical background

In Morocco, the first Ordovician trilobites were reported successively in the Djebilet hills (*Calymene*; Barthoux, 1924), in Oulmès area (*Trinucleus*; Termier, 1927) and in the High-Atlas (*Placoparia*; Roch, 1930). The presence of Ordovician rocks in the Anti-Atlas, was first mentioned by Neltner (1929), based on the presence of the trilobite *Trinucleus* in the Tafilalt area. Similarly, the existence of the Ordovician system in the western (Jbel Tachilla, Tiznit area; Bigot and Dubois, 1931) and central Anti-Atlas (Jbel Bani, Foum Zguid area; Bondon *in* Termier, 1936) was established by the discovery of trilobite remains assigned to *Acidaspis buchi* and *Homalonotus* sp., respectively.

In the Anti-Atlas (and in Morocco), the first Early Ordovician trilobites were collected in the 1930s in the Agdz area (Jbel Kissane) by Jacques Bondon and identified as *Onchometopus* cf. *volborthi* by Pierre Pruvost (*in* Roch, 1939), who suggested a late Tremadocian age. Two specimens of large trilobites (*O.* cf. *volborthi* and *Ogygia desiderata*) from the Lower Ordovician of the Agdz area were figured by Termier and Termier (1950: pl. 193, figs. 1-2). The Tremadocian age of the large specimens from Agdz was questioned by most authors, who reinterpreted them as more likely 'Arenig' or 'Skiddawian', i.e. Floian (Choubert, 1946, 1951, 1952; Choubert and Termier, 1947; Termier and Termier, 1947, 1950; Roch, 1950; Choubert et al., 1952). However, a new fossil site discovered East of Agdz (Tansikht bridge), yielded through successive field campaigns from 1952 to 1954, a diverse trilobite assemblage definitively interpreted as late Tremadocian by Pierre Hupé (*in* Choubert et al., 1955) and consisting of *Asaphellus* cf. *homfrayi*, *Asaphopsis* sp., *Parapilekia* cf. *olesnaensis* and *Platypeltoides croftii*.

From the late 1950s to the late 1990s, Jacques Destombes collected thousands of Early Palaeozoic fossils during the mapping of Cambro-Ordovician rocks for the series of 1:200000 geological maps of the Anti-Atlas. Several late Tremadocian levels yielding large trilobites were identified by Destombes (1960) in the Agdz-Zagora area. A more detailed account of trilobite diversity in the Lower Ordovician of the central Anti-Atlas was provided by Destombes (1967), who mentioned the occurrence of *Asaphellus*, *Bavarilla*, *Beltella*, *Dikelokephalina*, Orometopidae, *Pharostomina*, *Pilekia*, *Platypeltoides*?, Raphiophoridae and *Symphysurus* in the Tremadocian, and of *Ampyx*, *Apatokephalus*, *Asaphus*? and undetermined asaphids, *Bathycheilus*, *Bavarilla*, *Ceraurinella*, *Colpocoryphe*, *Euloma*, *Neseuretus*, *Plesiomegalaspis*, *Prionocheilus*, *Pterygometopus* and *Symphysurus*, in the Floian. In the "Zemmour area" (Northern Mauritania), Destombes et al. (1969) described a small trilobite fauna including *Bavarilla zemmourensis*, *Megistaspis* (*Ekeraspis*) sp., *Nileus deynouxi*, *Parapilekia sougyi*, *Platypeltoides* sp., and *Prionocheilus* sp. A relatively complete overview of trilobite diversity in the Lower Ordovician of the Anti-Atlas was later provided by Destombes et al. (1985) and Destombes (2006a, 2006b, 2006c, 2006d, 2006e, 2006f, 2006g, 2006h, 2006i, 2006j), who listed 11 and 25 taxa in the lower and upper parts of the Fezouata Shale, respectively (see also Vidal, 1998b).

Systematic descriptions of trilobites have focused mainly on the more diverse assemblages from the upper part of the Fezouata Shale (Floian), with contributions on phacopids (Destombes, 1972), calymenids (Vidal, 1996), asaphids and raphiophorids (Vidal, 1998a), and asaphids (Corbacho and Vela, 2010). In contrast, the description of the trilobite fauna from the lower part of the Fezouata Shale (late Tremadocian) is far less advanced. It was originally undertaken by the late Wolfgang Hammann, who died before it could be completed. So far, only a few late Tremadocian taxa have been described (Rabano, 1990; Fortey, 2009, 2011a, 2011b; Corbacho and Vela, 2011). No synthetic description of trilobite assemblages from the whole Fezouata Shale has been achieved yet, thus preventing any attempt of detailed comparison with other Early Ordovician trilobite faunas from high-latitude peri-Gondwanan areas, such as Avalonia, England and Wales (Fortey and Owens, 1978, 1987, 1991; Owens et al., 1982), Bohemia, Czech Republic (e.g. Mergl, 2006), or the Montagne Noire, France (e.g. Vizcaïno and Álvaro, 2002). Although the primary aims of this study are to focus on the biostratigraphy, palaeoecology and palaeobiogeography of trilobites from the Lower Ordovician of the central Anti-Atlas, several hundred specimens were identified up to generic, and when possible, specific level. However, their systematic description will be treated elsewhere.

3. Geological context

In Early Ordovician times, the Anti-Atlas was part of the northern Gondwanan margin, which was located at high latitudes (ca. 65°S; Fig. 1C) in the southern hemisphere, relatively close to the South Pole (Cocks and Torsvik, 2004; Torsvik and Cocks, 2011, 2013). The thick Lower Ordovician succession of the central Anti-Atlas was deposited in a rifting context, related to the opening of the Rheic Ocean and the drift of Avalonia away from the Gondwanan supercontinent (Cocks and Torsvik, 2004).

The Ordovician succession of the Anti-Atlas was originally subdivided into four main lithostratigraphic units by Choubert (1942), which were later formally described as groups by Destombes (1971; Fig. 1D): (1) the External Feijas Group (Tremadocian–early Darriwilian); (2) the First Bani Group (early Darriwilian–early Sandbian); (3) the Ktaoua Group (early Sandbian–late Katian); and (4) the Second Bani Group (late Katian–Hirnantian). The name of the lower part of the succession ("Feijas") refers, in southern Morocco, to the depressed and elongated areas, which occur between the middle Cambrian sandstones of the Tilemsoun Formation (Tabanite Group, Cambrian Series 3) and the Middle Ordovician sandstones of the First Bani Group (Destombes et al., 1985; Geyer and Landing, 2006). Four main subdivisions were identified by Destombes (1962, 1970, 1971) within the External Feijas Group: (1) the Lower Fezouata Shale Formation (early to late Tremadocian); (2) the Upper Fezouata Shale Formation (early to late Floian); (3) the Zini Sandstone Formation (late Floian); and (4) the Tachilla Shale Formation (early Darriwilian).

In the eastern Anti-Atlas, the boundary between the Lower and Upper Fezouata Shale formations corresponds to a glauconitic and ferruginous horizon, probably associated with a maximum flooding surface (Destombes et al., 1985). In the central Anti-Atlas, however, this lithological marker bed is absent, and the two lowermost Ordovician formations cannot be distinguished (Destombes et al., 1985; Destombes, 2006a, 2006b, 2006c, 2006d, 2006e, 2006f, 2006g,

2006h, 2006i, 2006j). For this reason, the term "Fezouata Shale" was proposed by Martin et al. (2016), for the thick (~850 m), monotonous Early Ordovician succession of the Zagora area, consisting of silty and micaceous argillites, and laterally equivalent to both the Lower and Upper Fezouata Shale formations.

The thickness of the Lower Ordovician series varies along the Anti-Atlas, and it reaches its maximum value (~900 m) in the Ternata plain (N. of Zagora) in the central part of the Anti-Atlas. In this area, the Fezouata Shale rests unconformably on the middle Cambrian (Guzhangian) Tabanite Group (Fig. 1). The siltstones of the Fezouata Shale were almost exclusively deposited in proximal offshore to lower shoreface environments (Martin et al., 2016; Vaucher et al., submitted for publication, 2016-in this issue). In the central Anti-Atlas, the late Floian deposits of the uppermost part of the Fezouata Shale and of the overlying Zini Sandstone Formation both record a shallowing upward sequence, with a gradual transition from lower shoreface to foreshore environments (Vaucher et al., 2016-in this issue). Both the Fezouata Shale and the Zini Sandstone exhibit centimeter- to meter-scale oscillatory structures (e.g. wave ripples, hummocky cross stratification), indicating that sedimentation was chiefly controlled by storms and waves (Vaucher et al., 2016-in this issue), but with the subsidiary influence of tides (Vaucher et al., submitted for publication).

4. Material and methods

4.1. Fieldwork

The whole Lower Ordovician succession exposed in the Zagora area (central Anti-Atlas, Morocco) was logged, at a decimeter scale, from fourteen different sections (see Martin et al., 2016). Data were compiled into a single, synthetic stratigraphic column ~900 meter-thick (Vaucher et al., 2016-in this issue; Fig. 2). All localities yielding exceptionally preserved fossils (EPF) mentioned in the original contribution of Van Roy et al. (2010) were included, except one located c. 15 km west of the main outcrop area. EPF localities were carefully located and positioned along the stratigraphic column, based on their lithological characteristics (colour, composition, marker beds) and faunal elements (mostly graptolites, trilobites, and to a lesser extent echinoderms). Graptolites were collected throughout the succession, but particular attention was paid to horizons yielding EPF (Gutiérrez-Marco and Martin, 2016-in this issue). Changes in lithology and sedimentary structures were observed throughout the succession and were used to reconstruct short-term and long-term relative sea-level changes.

4.2. The trilobite material

This study is based on 485 complete and incomplete trilobite specimens, sampled throughout the Fezouata Shale and derived from 19 different stratigraphic levels (Figs. 1A, 2). Each sample was identified down to the species level, when possible. All specimens were whitened with ammonium chloride and observed with a binocular microscope. When necessary, camera lucida sketches and photographs were produced, for purposes of comparison with material published in the literature. All trilobite occurrences reported by Jacques Destombes (2006a, 2006b, 2006c, 2006d, 2006e, 2006f, 2006g, 2006h, 2006i, 2006j) from other regions of the Anti-Atlas were also plotted on the log, when correlations were possible.

Each identifiable trilobite sclerite was counted according to the MNI protocol used to obtain the number of individuals in each sample (Gilinsky and Bennington, 1994). The state of completeness and the parts preserved were also taken into account.

All studied specimens are deposited in the collections of the Cadi Ayyad University, Marrakesh (Faculté des Sciences et Techniques, Guéliz; sample number prefix AA), and in the palaeontological collections of Lyon 1 University, Villeurbanne (FSL).

4.3. Definition of a depth-related zonation

A relative depth zonation for Early Ordovician trilobite assemblages of the Zagora area was defined, based on the sedimentological data obtained from the field (e.g. lithology, grain sizes, sedimentary structures, and biostratinomy). In the Fezouata Shale, two different types of fossiliferous beds are identified (Vaucher et al., 2016-in this issue). The first type consists of fine to medium grained sands, associated with hummocky cross-stratifications (HCS) of meter-scale wavelength and is considered to represent proximal storm deposits. It commonly yields disarticulated specimens, even for species considered as endobenthic. The second type, which especially contains EPF and/or articulated biomineralized remains, corresponds to a quiet muddy background environment, covered by the most distal storm deposits (several centimeter-thick). The distal storm deposits of the Fezouata Shale consist of fine grained sands displaying HCS of decimeter-scale wavelength and were deposited under waxing-and-waning flow activity with potential transport of skeletal material derived from more proximal environments. Three main, partly overlapping zones were defined along a proximal-distal profile: (1) lower shoreface; (2) transition zone; and (3) proximal offshore (Fig. 3). As mentioned above, the typical coastal linear zonation (e.g. McLane, 1995) is modified in the Fezouata Shale, because of the influence of tides. Detailed definitions of the lower shoreface and proximal offshore settings in the Zagora area were given by Vaucher et al. (submitted for publication).

In this peculiar depositional context, lower shoreface environments are characterized by siltstones displaying wave ripples (with a decimeter-scale wavelength), with intercalations of fine, 5 to 15-centimeter-thick, sandy storm deposits. The following trilobite localities can be assigned to these settings: 421 = 425 = 1677 = 1678 = 1680 = 1681 = 1683; 1673 = 1674; Z-F2(0), Z-F3, Z-F4(3), Z-F4(lower excavation), Z-F5 and Z-F6a.

Proximal offshore environments correspond to argillaceous siltstones showing wave ripples (with a centimeter-scale wavelength) and thin (1–5 centimeter-thick) intercalations of coarse silty to fine sandy storm deposits. Trilobite levels associated with such offshore conditions correspond to localities 35, 1685, Z-F7(2) and Z-F26.

Finally, the sedimentological features observed in the transition zone (defined herein) are a mixture of those typical of both more distal (proximal offshore) and more proximal (lower shoreface) environments. In the Zagora area, several trilobite levels are associated with this intermediate, transitional setting: 1687 = Z-F25b, Z-F0, Z-F1, Z-F2(1)a, Z-F2(3a) and Z-F13c.

4.4. Geochemical data

Chemical analyses were performed in order to investigate the presence of any significant difference between levels with exceptional preservation and those recording background sedimentation. Because of the intense surface weathering of Ordovician outcrops in Morocco, an alteration of the original chemical signal is likely. Consequently, only a limited number of surface samples (six) was selected for this preliminary geochemical analysis (Trace Element and Organic carbon isotopes, $\delta^{13}C_{org.}$ analysis). All samples were collected from the same 18 meter-thick section, at Bou Izargane hill (Z-F4), about 20 km N of Zagora. This locality has yielded three fossiliferous levels, all located between 270 and 290 m above the base of the Ordovician, i.e. within the main, lower interval with exceptional preservation (*A. murrayi* Zone, late Tremadocian; Figs. 2, 4).

The stratigraphically lowest sample (Gc1) was extracted from a small lens (Z-F4 lower excavation, *Anatifopsis* lens; Fig. 4), where diverse and abundant remains of biomineralized invertebrates were collected: bivalves, brachiopods, conularids, graptolites, mitrate stylophorans (*Anatifopsis*), and trilobites.

The next three samples were extracted 10 m above, from a slightly younger stratigraphic interval (Z-F4(3)). One of them (Gc3) was

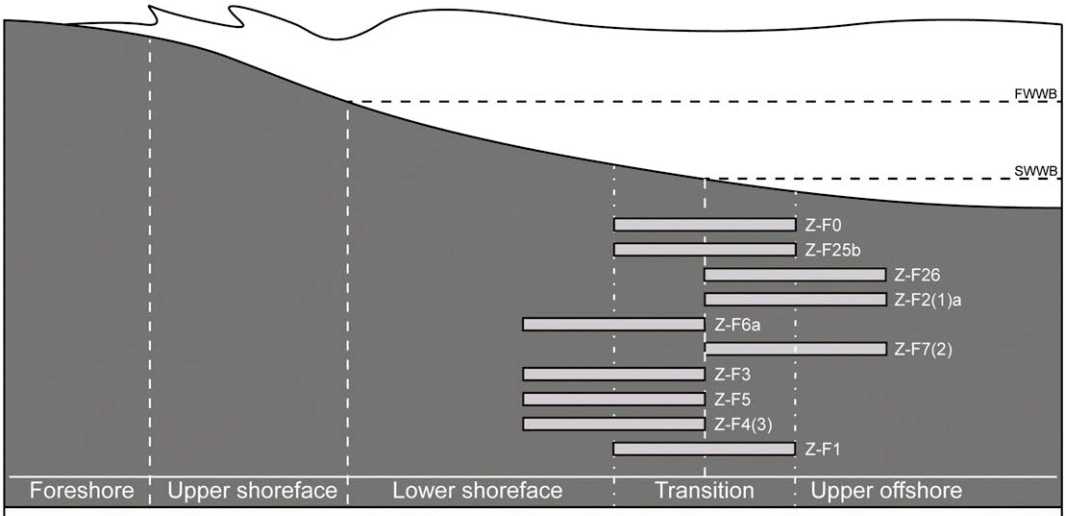

Parabathycheilus gallicus	N=13	n=4	31	15	54
Asaphellus sp. aff. *jujuanus*	N=16	n=3	6	44	50
Toletanaspis sp. aff. *borni*	N=5	n=2	0	60	40
Ampyx priscus	N=26	n=4	19	12	69
Colpocoryphe sp.	N=2	n=1	0	0	100
Agerina quadrata	N=30	n=2	0	90	10
Asaphellus fezouataensis	N=6	n=2	0	100	0
Euloma sp.	N=6	n=1	0	100	0
Megistaspis (Ekeraspis) cf. *filacovi*	N=4	n=2	75	25	0
Prionocheilus sp.	N=3	n=1	100	0	0
Geragnostus? sp.	N=1	n=1	100	0	0
Apatokephalus cf. *incisus*	N=2	n=2	100	0	0
Asaphellus tataensis	N=1	n=1	100	0	0
Platypeltoides magrebiensis	N=2	n=1	100	0	0
Anacheirurus adserai	N=39	n=1	100	0	0
Bavarilla zemmourensis	N=26	n=2	100	0	0
Asaphellus stubbsi	N=5	n=1	100	0	0
Symphysurus angustatus	N=3	n=1	100	0	0
Number of specimens (N) and of localities (n)			**Repartition of articulated specimens (%)**		

uncleared affinities | upper offshore affinities | transition affinities | lower shoreface affinities

Fig. 3. Definition of trilobite biofacies along an onshore–offshore transect. Depth zonations follow Vaucher et al. (2016-in this issue, submitted for publication). Only articulated trilobites were considered in determining distribution patterns. The number of articulated trilobites (N) and the number of different stratigraphic levels (n) in which they occur are also indicated. Distribution of each articulated species is given in percent.

collected within a level yielding fossils with exceptionally preserved soft-tissue: graptolites, marrellomorphs (*Furca*), cornute stylophorans (*Hanusia*, *Thoralicystis*), and trilobites exhibiting antennae and/or appendages (*Anacheirurus*, *Bavarilla*). The other samples were extracted from the barren deposits located below (Gc2) and above (Gc4) the level with exceptional preservation.

The last two samples were collected 5 m above, from the stratigraphically highest fossiliferous interval (Z-F4, upper excavation).

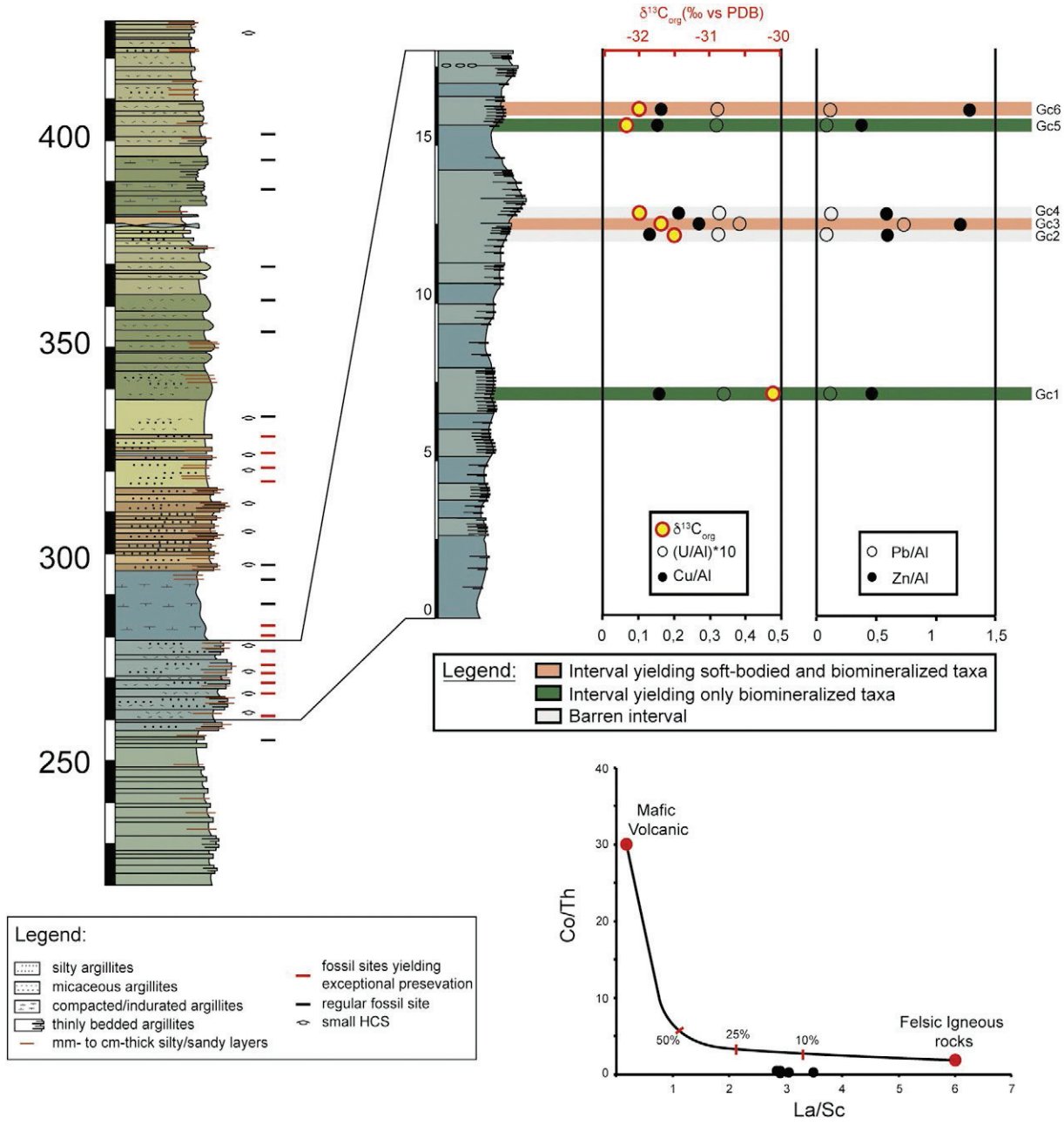

Fig. 4. Geochemical analysis performed on the first Late Tremadocian interval of the Fezouata Shale yielding soft-bodied taxa (*Araneograptus murrayi* biozone; Martin et al., 2016). Stratigraphic columns are modified from Vaucher et al. (2016-in this issue). Stratigraphic positions of the six selected samples are indicated: unfossiliferous samples in grey, biomineralized fossiliferous samples in green, lagerstätte samples in red. Trace metals and U (ppm) are presented along the profile normalized to Al (%) and Organic carbon isotopes analyses are reported in per mil (vs PDB). Values of different possible rock sources and of the samples are also plotted in a Co/Th Vs La/Sc diagram.

The first one (Gc5) was extracted from a level yielding poorly preserved remains of biomineralized organisms (brachiopods, graptolites and trilobites), whereas the second one (Gc6) was collected within a level with exceptional preservation (appendages of anomalocaridids, graptolites, marrellomorphs, palaeoscolecid worms and trilobites).

All samples were cut, avoiding any fractures or secondary crystallisation and ground in an agate mortar, until having a grain size lower than 145 μm. For trace element analysis, about 100 mg of ground bulk powder was digested with 5% (*v*/v) acetic acid. Rare earth and other trace element concentrations were measured with an Element 2 ICP–MS at the Pôle Spectrométrie Océan (PSO, Brest). For $\delta^{13}C_{org}$, samples were decarbonated in 6 N HCl overnight at room temperature, followed by 2 h at 80 °C. Residues were washed with distilled water, centrifuged and dried at 50 °C. Around 1 mg of decarbonated powder was then analysed using a EA coupled to a Delta V Plus Thermo Fisher mass spectrometer. Analytical precision is ±0.2‰ (2σ).

5. Results

5.1. Distribution of trilobite assemblages through time and space

The 485 specimens examined were assigned to 26 different species and 21 genera, belonging to the 15 families listed in Table 1.

Several of these species are endemic to the Anti-Atlas: *Asaphellus fezouataensis*, *A. stubbsi*, *A. tataensis*, *Basilicus destombesi*, *Bavarilla zemmourensis*, *Dikelokephalina brenchleyi*, and *Platypeltoides magrebiensis*. Moreover, it is very likely that specimens identified as *Euloma* sp.,

Table 1
List of the 26 trilobite species identified in the Lower Ordovician Fezouata Shale. Family of each species and references of their systematic description are also provided.

Family	Genus	Species	References
Agnostidae	*Geragnostus*	sp.	
Asaphidae	*Asaphellus*	*fezouataensis*	Vidal (1998a)
	Asaphellus	sp. aff. *jujuanus*	Harrington (1937)
	Asaphellus	*stubbsi*	Fortey (2009)
	Asaphellus	*tataensis*	Vidal (1998a)
	Basilicus	*destombesi*	Vidal (1998a)
	Megistapis (*Ekeraspis*)	cf. *filacovi*	Bergeron (1888)
Bathycheilidae	*Parabathycheilus*	*gallicus*	Dean (1965)
Bavarillidae	*Bavarilla*	*zemmourensis*	Destombes et al. (1969)
Calymenidae	*Colpocoryphe*	*pradesensis*	Courtessole et al. (1985)
	Colpocoryphe	*thorali*	Dean (1966)
	Colpocoryphe	sp.	
	Neseuretus	cf. *attenuatus*	Gigout (1951)
	Pradoella	sp.	
Cheiruridae	*Anacheirurus*	*adserai*	Vela and Corbacho (2007)
	Foulonia	*peregrina*	Dean (1966)
Dalmanitidae	*Toletanaspis*	sp. aff. *borni*	(Dean, 1966)
Dikelokephalinidae	*Dikelokephalina*	*brenchleyi*	Fortey (2011a)
Eulomidae	*Euloma*	sp.	
Harpididae	*Eoharpes*	sp.	
Leiostegiidae	*Agerina*	*quadrata*	Dean (1966)
Nileidae	*Platypeltoides*	*magrebiensis*	Rabano (1990)
	Symphysurus	*angustatus*	Boeck (1838)
Pharostomatidae	*Prionocheilus*	sp.	
Raphiophoridae	*Ampyx*	*priscus*	Thoral (1935)
Remopleuridiidae	*Apatokephalus*	cf. *incisus*	Dean (1966)

the uppermost Floian part of the Fezouata Shale (from about 700 to 850 m above the base of the Ordovician) have been less intensively sampled and have thus yielded fewer specimens than the two main intervals investigated. Pending more intensive sampling, the trilobite assemblages from both the earliest Tremadocian and late Floian intervals remain too poorly known to be included in the present analysis.

In the Fezouata Shale, three distinct trilobite assemblages were identified (Fig 2).

Assemblage 1 is strictly limited to the *A. murrayi* Zone. It was observed in the following localities (Fig. 2): Z-F1, Z-F2(1a), Z-F2(3a), Z-F3, Z-F4 (lower excavation), Z-F4(3), Z-F5, Z-F6a, and Z-F7(2). It includes eight species: *Anacheirurus adserai*, *Asaphellus stubbsi*, *A. tataensis*, *Bavarilla zemmourensis*, *Dikelokephalina brenchleyi*, *Megistaspis* (*Ekeraspis*) cf. *filacovi*, *Platypeltoides magrebiensis* and *Symphysurus angustatus*.

Assemblage 2 was evidenced in various localities ranging from the late Tremadocian (*A. murrayi* Zone) to the middle Floian (?*B. jacksoni* Zone). It occurs in the following localities (Fig. 2): 35, 1687 = Z-F25b, Z-F0, Z-F2(0), Z-F2(1a), Z-F2(3a), Z-F3, Z-F4 (lower excavation), Z-F4(3), Z-F5, Z-F6a, Z-F13c and Z-F26. It includes 10 species: *Ampyx priscus*, *Apatokephalus* cf. *incisus*, *Asaphellus* sp. aff. *jujuanus*, *Colpocoryphe* sp., *Euloma* sp. *Foulonia peregrina*, *Geragnostus* ? sp., *Parabathycheilus gallicus*, *Prionocheilus* sp. and *Toletanaspis* sp. aff. *borni*.

Finally, assemblage 3 is apparently restricted to the early–middle Floian time interval (?*C. protobalticus* to ?*B. jacksoni* zones; Fig. 2). It was identified in the following localities: 35, 412 = 425 = 1677 = 1678 = 1680 = 1681 = 1683, 1673 = 1674, 1685, 1687 = Z-F25b, Z-F0 and Z-F26. It comprises seven species: *Agerina quadrata*, *Asaphellus fezouataensis*, *Basilicus destombesi*, *Colpocoryphe pradesensis*, *C. thorali*, *Neseuretus* cf. *attenuatus* and *Pradoella* sp.

Pradoella sp. and *Toletanaspis* sp. belong to new species, yet awaiting formal description (in progress).

Although systematics is not the primary aim of this work, two points have to be stressed. First, pilekiid trilobites of the Fezouata Shale were assigned to different species of the genus *Lehua* (junior synonym of *Anacheirurus*) by Corbacho and Vela (2011). However, a single morphological type of pilekiid was identified in our material and assigned to a unique species *Anacheirurus adserai* (Vela and Corbacho, 2007). Second, all leiostegiid specimens from the Fezouata Shale appear to be conspecific with the Montagne Noire species, originally described as *Hoekaspis*? *quadrata* by Dean (1966) and here assigned to the genus *Agerina*.

The distribution of the 26 trilobite taxa identified in the Lower Ordovician of the Zagora area is clearly neither homogeneous nor random within the Fezouata Shale, but rather results from the complex interaction of both macroevolutionary and environmental factors. The putative influence of several of these factors is discussed below. Regarding the overall trilobites fauna, the Tremadocian levels of the Fezouata Shale (from 250 to 350 m, Fig. 2) display 8 endemic species over 19 (42.1%), while only 5 species over 17 (29.4%) are specific to the Anti-Atlas during the Floian (from 480 m to 700 m).

5.1.1. Trilobite biostratigraphy: evolution through time

The 26 trilobite taxa examined in this study were collected from two main stratigraphic intervals (Fig. 2): a lower (~100 meter-thick) late Tremadocian interval (*A. murrayi* Zone and base of the overlying *H. copiosus* Zone), and about 120 m above it, a larger (230 meter-thick) early to middle Floian interval (?*C. protobalticus* to ?*B. jacksoni* zones). The two intervals have 10 species in common. The stratigraphically lower one yielded 19 species, whereas 17 taxa were observed in the upper fossiliferous interval.

Trilobites are extremely rare in the lowermost part of the Fezouata Shale (early and middle Tremadocian; Destombes et al., 1985). Consequently, the few available specimens were not included in this study. The stratigraphic intervals located near the Tremadocian–Floian boundary (from about 350 to 470 m above the base of the Ordovician) and in

5.1.2. Trilobite biofacies: a depth control on assemblages

Fortey (1975a, 1975b) was one of the first to highlight a depth control on trilobite communities. He also defined trilobite biofacies patterns by studying trilobite assemblage variation along onshore–offshore transects. Similar studies have been undertaken in the Ordovician, Silurian, and Devonian (for example Fortey and Owens, 1978, 1987; Cocks and Fortey, 1988; Chlupáč, 1983, 1987; Zhou et al., 2011; Carlucci and Westrop, 2015). In the Lower Ordovician of Spitzbergen, Fortey and Owens (1978) described a basinward succession of illaenid-cheirurid, nileid, and olenid communities close to the palaeoequator, and of *Neseuretus*, raphiophorid and olenid communities at high palaeolatitudes. Most of the Tremadocian trilobite assemblages in higher latitude and siliciclastic settings of Bohemia might be compared with the illaenid-cheirurid biofacies originally described in lower palaeolatitudes (Mergl, 2006).

In order to discriminate biofacies in the Fezouata Shale, we used the relative abundance of trilobites for each locality to carry out a cluster analysis. The first analysis was based on both articulated and disarticulated remains but did not provide consistent results. However, distinct groups can be eventually recognized when using the relative abundance of articulated remains only. Cluster analysis is a well established method for defining biofacies (Ludvigsen et al., 1986; Balseiro et al., 2011), as it groups the different trilobites species according to the shared similarity in distribution (in this case, the pattern of distribution of articulated specimens along a proximal–distal transect). This analysis was performed using the software Past 3.07 (Hammer et al., 2001). The dendrogram was obtained using the square root of the Bray–Curtis similarity index with the Ward grouping method. Because the metric used is ultrametric with binary data and possibly with abundance data (which means that there are no reversals in the clustering; Legendre and Legendre, 2012), it is suitable for Ward's method (Balseiro et al., 2011).

Three different trilobite biofacies were distinguished in the Lower Ordovician of the Zagora area, based on the depth-related zonation defined above (see Section 4.3), and the distribution of articulated trilobites observed in the various localities (Fig. 3).

The most proximal trilobite biofacies displays lower shoreface affinities and includes the following nine species: *Anacheirurus adserai*, *Apatokephalus* cf. *incisus*, *Asaphellus stubbsi*, *A. tataensis*, *Bavarilla zemmourensis*, *Megistaspis* (*Ekeraspis*) cf. *filacovi*, *Platypeltoides magrebiensis*, *Prionocheilus* sp. and *Symphysurus angustatus*. The co-occurrence of both pilekiid (*Anacheirurus*) and bavarillid (*Bavarilla*) representatives appears to be diagnostic of this biofacies. This is also the case with the proximal association in the Tremadocian of Bohemia (Mergl, 2006). This proximal assemblage occupies a palaeogeographic position along a proximal–distal transect analogous to that of the illaenid-cheirurid biofacies (Fortey, 1975b).

The second biofacies is mainly restricted to intermediate environmental conditions around the storm wave base, and comprises three species: *Agerina quadrata*, *Asaphellus fezouataensis* and *Euloma* sp. Named *Agerina* biofacies in this study, it is characterized by the eponymous genus, which occurs with representatives of the Eulomidae family, such as *Euloma* in the Fezouata Shale or *Proteuloma* in analogous environment from Bohemia (Mergl, 2006). The onshore–offshore position of the *Agerina* biofacies is similar to that of the nileid biofacies (as proposed by Mergl, 2006).

Finally, a third trilobite biofacies occurs in the most distal settings (upper offshore) of the Fezouata Shale and is characterized by two species: *Ampyx priscus* and *Colpocoryphe* sp. Associated with depth-tolerant asaphid species, this assemblage corresponds to the raphiophorid biofacies (Fortey and Owens, 1978) previously described in Morocco (Vidal, 1998b).

Depth-related affinities are unclear for at least three taxa: articulated specimens of *Asaphellus* sp. aff. *jujuanus* and *Toletanaspis* sp. aff. *borni* are found both in transition zone and upper offshore environments, while articulated individuals of *Parabathycheilus gallicus* were observed in both offshore and shoreface deposits.

The first proximal assemblage, with pilekiids and bavarillids in the lower shoreface, and the second one, in transitional environment observed in the Fezouata Shale (*Agerina* biofacies), have many similarities with those described in the same stratigraphic levels from Bohemia (Mergl, 2006), though *Platypeltoides* appears to have shallower affinities in Morocco than in Bohemia. Representatives of the Olenid biofacies, which are supposed to dominate deeper and oxygen-deficient settings adjacent to palaeoocean, are missing both in the Lower Ordovician of Bohemia and in the Fezouata Shale. To explain this absence, Mergl (2006) suggests that the depositional setting of Bohemia during the Ordovician was too shallow as well as too oxygenated, and thus unsuited for olenids. In the Fezouata Shale, geochemical analyses show at least temporary dysoxic conditions on the sea floor (see Section 5.2), nevertheless sedimentary analysis (see Section 4.3) and trilobite biofacies highlight together that the deposit environments of the Fezouata Shale belong to the proximal part of the shelf, far from the continental slope and deep ocean environments.

5.1.3. Trilobite assemblages: allochthonous vs. autochthonous assemblages

In the five localities of the Zagora area yielding more than 15 specimens of Early Ordovician trilobites palaeoecological aspects of the assemblages were investigated: especially the autochthonous/allochthonous nature of the associations (i.e. biocoenosis vs. thanatocoenosis, Fig. 5).

Although only few trilobite assemblages could be analysed for this purpose, their stratigraphic distribution is relatively wide, with late Tremadocian (Z-F4(3) and Z-F5), early Floian (Z-F26), and middle Floian (Z-F0 and Z-F25b) localities. In these assemblages, the number of taxa varies from five (Z-F25b), to seven (Z-F4(3) and Z-F5), nine (Z-F26), and ten (Z-F0).

All five investigated trilobite assemblages display both articulated and disarticulated exoskeletons. Moreover, in a single locality, co-occurring taxa show contrasting environmental affinities with different depth-related habits (Fig. 3). This suggests that these five assemblages all probably result from a combination of both autochthonous and allochthonous elements, transported from nearby settings (Fig. 5). To test this hypothesis, articulated and disarticulated trilobites were plotted separately for each locality. As a result, all taxa that are preserved as articulated and disarticulated remains, turned out to have transition and/or offshore affinities, whereas trilobites that are only preserved as disarticulated remains had shoreface and/or transition affinities (Fig. 5).

In Z-F0, the articulated trilobite assemblage is dominated by taxa with transition setting affinities (*Agerina*, *Euloma*, *Ampyx*, and *Asaphellus*), in accordance with the sedimentological data. Similarly, in Z-F25b and Z-F26, the analysis of the community structure and field-based sedimentological evidence both suggest a transitional to proximal offshore setting for this locality. The interpretation of the Z-F5 is more problematic. The trilobite assemblage suggests a proximal offshore environment, whereas sedimentological data rather indicate more proximal environmental conditions (lower shoreface for Z-F5). It is thus very likely that Z-F5 and Z-F25b were both located in a quiet, offshore environment, occasionally disturbed by storm events, which could occasionally introduce allochthonous, often disarticulated trilobites living in more proximal environments (Vaucher et al., 2016-in this issue). Correlatively, this implies that, if too many storm events were stacked together, the resulting sedimentological signal would then be biased and would suggest deposition in more proximal environments.

Differences in relative depths possibly explain the dramatically distinct compositions of the two contemporaneous trilobite assemblages from Z-F4(3) and Z-F5 (late Tremadocian, *A. murrayi* Zone). Z-F4(3) is the oldest and unique locality yielding trilobites with strict shoreface affinities. In contrast, the trilobite community of Z-F5 is typical of deep, offshore settings. It shows striking similarities with the younger (early Floian) Z-F26 assemblage, which was associated with similar, offshore environments. In such relatively deep settings, downslope transported elements are usually rare and not diverse (one to four species) and communities are dominated by autochthonous taxa, such as *Ampyx priscus*.

5.1.4. Affinities with Early Ordovician trilobite faunas

Most genera of trilobites occurring in the Fezouata Shale were widespread in temperate to high palaeolatitudes during the Early Ordovician (e.g. *Agerina*, *Apatokephalus*, *Asaphellus*, *Dikelokephalina*, *Geragnostus*, *Platypeltoides*). In contrast, the distribution of calymenacean genera was restricted to (peri)Gondwanan regions (e.g. *Bavarilla*, *Colpocoryphe*, *Neseuretus*, *Parabathycheilus* and *Pradoella*). Those genera are distinctive of proximal to median shelf environments from Avalonia, Bohemia, Armorica and Gondwana continent during the Lower Ordovician (Fortey and Cocks, 2003). Among coeval assemblages of trilobites from these high latitude, peri-Gondwanan terranes, the faunas from the Lower Ordovician of the Zagora area display strong affinities with the Montagne Noire (southern France), as indicated by the shared occurrence of several species: *Agerina quadrata*, *Ampyx priscus*, *Colpocoryphe pradesensis*, *C. thorali*, *Foulonia peregrina* and *Parabathycheilus gallicus*. Two of them, *Ampyx priscus* and *Parabathycheilus gallicus*, are characterized by a long stratigraphic range in the Anti-Atlas, extending from the late Tremadocian (*A. murrayi* Zone) to the middle Floian (?*B. jacksoni*). Similarly, in the Montagne Noire, these two taxa show relatively large stratigraphic extensions (Vizcaïno et al., 2001). In that region, *A. priscus* is known from the Saint-Chinian (late Tremadocian) to the Landeyran Formation, and *Parabathycheilus gallicus* is recorded in both the Foulon (middle Floian) and Landeyran formations (late Floian). Consequently, *Ampyx* has a slightly longer range in the Montagne Noire, whereas that of *Parabathycheilus* is shorter. The late Floian trilobite faunas from the Landeyran Formation show strong affinities with the slightly older Floian assemblages of the Zagora area, with for example the occurrence of three common species: *Agerina quadrata*, *Foulonia peregrina* and *Colpocoryphe thorali*. Both in Morocco and in the Montagne Noire, the stratigraphic occurrence of *C. thorali* is preceded by that of a closely related species: *C. pradesensis*. In the Montagne Noire, *Colpocoryphe pradesensis* (originally assigned to *Platycalymene* by Courtessole et al., 1983) occurs in the la Maurerie Formation (early Floian), and in Morocco, it was documented in Destombes locality 35 (early Floian).

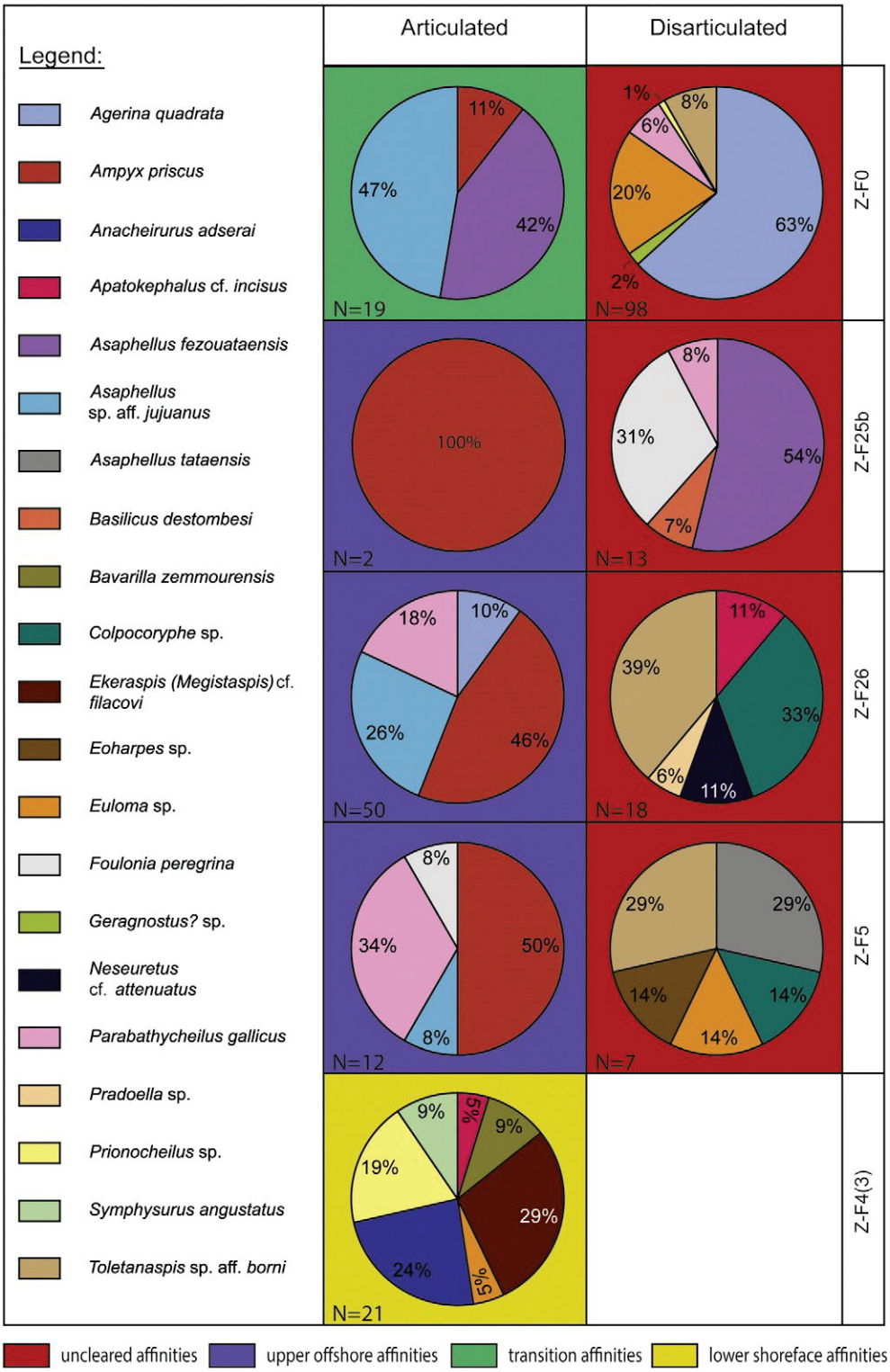

Fig. 5. Relative abundance of articulated (left column) against disarticulated (right column) specimens in different excavations. Only excavations yielding more than 15 specimens were taken into account. The numbers of articulated and disarticulated trilobites (N) per locality are indicated. Depth affinities are inferred from the biofacies defined in Fig. 3.

The observation of the same succession of closely related species in the two regions supports the existence of common evolutionary trends and strong faunal exchanges between them.

However, significant differences also exist between the trilobite faunas from Morocco and those of southern France. First, faunal elements adapted to deep platform settings (i.e. *Bohemilla* (*Fenniops*), *Cyclopyge*, *Degamella*, *Pricyclopyge*) are present in the Montagne Noire (Vizcaïno et al., 2001), whereas they are absent in the central Anti-Atlas. Their absence in Morocco is in good agreement with sedimentological data, all suggesting that the depositional environment of the Fezouata Shale was relatively shallow, from lower shoreface to upper offshore and probably never reached the most distal part of the shelf (see above, Section 4.3; Vaucher et al., 2016-in this issue). Consequently, the absence of deeper water trilobites in the Anti-Atlas probably results from the original absence of corresponding outer shelf environments in this region and/or the absence of exchanges with an oceanic basin.

A second major difference concerns the absence of the genus *Taihungshania* in the Zagora area, whereas it is one of the most common faunal elements in the latest Tremadocian–early Floian time interval in the Montagne Noire (Vizcaïno and Álvaro, 2002). *Taihungshania* is a typical (peri)Gondwanan trilobite, with a relatively wide palaeobiogeographic distribution: for example, it was reported in China (Lu, 1975 ; Turvey, 2005), Iran (Ghobadi Pour et al., 2007), Turkey (Dean, 1971), Oman (Fortey et al., 2011), Sardinia (Pillola, pers. comm.), and Montagne Noire (Courtessole et al., 1985). In all these regions, *Taihungshania* occurs in shallow shelf environments (Turvey, 2005; Zhou et al., 2011). Consequently, its absence in the Anti-Atlas cannot be simply explained by environmental conditions (Vidal, 1998a), but it more likely suggests that this area was isolated, with restricted communications (and faunal exchanges) with other (peri)Gondwanan regions, at least during the late Tremadocian time interval. In detail, the endemicity rates are similarly high in both late Tremadocian (50% of endemic species in Z-F4(3); 33.3% in Z-F5; 40% in Z-F6a) and middle Floian localities (40% of endemic species in Z-F25b; 33.3% in Z-F0). By contrast, endemicity is much lower in the early Floian with only 22.2% of endemic species in the locality Z-F26. This evolution of endemicity rates mirrors the relative sea level variations. Indeed, a transgressive trend is recorded from the late Tremadocian to the early Floian, while a regression takes place from the early Floian up to the late Floian (Fig. 2). Thus, the most endemic communities are found in shallower facies of the Fezouata Shale, while the less endemic ones are observed in the deepest facies. A similar correlation was already highlighted in the Ordovician of Wales (Fortey and Owens, 1978, 1987).

5.2. Geochemical data: understanding the environmental context

Geochemical analyses performed on samples extracted from six distinct levels (Fig. 4), all located within the lower interval with exceptional preservation (late Tremadocian, *A. murrayi* Zone) at Bou Izargane, offer the possibility to take into account additional data on environmental conditions, independent of those deduced from the analysis of sedimentology and trilobite assemblages.

The six carbon isotopes on the organic matter show a clear trend towards more negative values from −30.2 to −32.0‰, which are consistent with the $\delta^{13}C_{org}$ compilation presented in Hayes et al. (1999) and with the low $\delta^{13}C_{carb}$ for the same stratigraphic interval in Argentina (Bergström et al., 2009). Trace elements show relatively low differences from one sample to another, with the exception of the two samples collected within the two horizons yielding exceptionally preserved trilobites (Gc6 and Gc3), and both characterized by high values in Zn. Moreover, one of these two levels (Gc3) is also enriched in Pb and, to a lesser extent, in both U and Cu (when normalized to Al).

These results suggest that the Gc3 fossiliferous level was deposited in a more reduced environment, with the possible influence of chemoautotrophic bacteria participating in the isotopic negative signal. Cu, Zn and Pb are elements highly sensitive to the sulphur cycle, thus suggesting high bacterial sulphate-reduction activity, leading to the rapid isolation of organic matter from oxidation. This “pyrite wall” may have acted as an oxidative sheltering armor. During later diagenesis and exhumation, oxidative weathering led to the replacement of this pyrite coating by iron oxide, liberating the sulphur as sulphate in the dissolved fluid porosity.

The differences observed between the Gc6 and Gc1 fossiliferous levels suggest the presence of a less reduced environment in Gc1, which did not yield any soft-tissue preservation. Alternatively, these differences could simply result from a better preservation of the original geochemical signal, as samples Gc2, Gc3 and Gc4 were obtained from more deeply excavated rocks (and thus, potentially less weathered) than samples Gc1, Gc5 and Gc6.

In summary, the two levels yielding exceptional preservation (e.g. trilobites with soft-tissue, antennae and/or appendages), Gc3 and Gc6, are both enriched in Zn, which suggests the occurrence of reducing environmental conditions. In contrast, the two levels yielding mineralized fossil remains (e.g. echinoderms, molluscs, trilobites), Gc1 and Gc5, have a geochemical signal very similar to that of barren layers (Gc2 and Gc4).

These geochemical analyses thus confirm periodical development of hypoxic/anoxic conditions in the lower part of the Fezouata Shale, which has been recently inferred to explain (1) mass mortality assemblages of deep-water graptolites (Gutiérrez-Marco and Martin, 2016-in this issue), sponges (Botting, 2016-in this issue), and palaeoscolecid worms in non-bioturbated horizons in the Fezouata Shale (Martin et al., 2016-in this issue), (2) dwarfed communities in some stylophoran beds (Lefebvre et al., 2016b-in this issue), and (3) the absence of infaunal bivalves (Polechová, 2016-in this issue).

Moreover, the Co/Th Vs La/Sc diagram makes it possible to identify the origin of the source rocks in the sediment (Fig. 4). On such a diagram, based on a mixing model between a mafic volcanic and a felsic igneous chemistry composition, the six examined samples from the Fezouata Shale all indicate a relatively similar, felsic igneous source rock. Consequently, this preliminary investigation does not support a hypothesis predicting that inputs of volcanic ashes would have favored diagenetic mineralization and exceptional preservation (Gaines et al., 2012).

6. Conclusions

Three temporally restricted trilobite assemblages were identified in the Fezouata Shale of the Zagora area, central Anti-Atlas: assemblage 1 is restricted to the late Tremadocian, assemblage 2 extends from the late Tremadocian to the middle Floian, and assemblage 3 is observed only the early–middle Floian. Consequently, though less precise than graptolites, trilobite assemblages can be used as a complementary stratigraphic tool in the Lower Ordovician of Morocco.

A dramatic faunal turnover takes place around the Tremadocian/Floian boundary, with the disappearance of several typical late Tremadocian taxa (e.g. *Anacheirurus*, *Bavarilla*, *Dikelokephalina*, *Platypeltoides*…), and their replacement by Floian (peri)Gondwanan assemblages dominated by Calymenidae (in particular, Reedocalymeninae and Colpocoryphinae).

The identification of three trilobite biofacies in the Fezouata Shale, comprising the newly recognized pilekiid-bavarillid biofacies, *Agerina* biofacies and the well known raphiophorid biofacies, is in good accordance with classic models describing the distribution of benthic taxa along an onshore-offshore transect. Moreover, a fourth trilobite biofacies (*Neseuretus* biofacies) was also described by Vidal (1998b) in the uppermost part of the Fezouata Shale (late Floian), from levels which were not studied here. This *Neseuretus* biofacies is typical of shallow shelf environments in (peri)Gondwanan regions (Fortey and Owens, 1978; Fortey and Morris, 1982; Turvey, 2005; Zhou et al., 2011).

This research also suggests that the highest diversity is observed in assemblages resulting from the mixing of autochthonous, distal communities with allochthonous elements from more proximal settings, transported downslope by storm waves.

Though palaeobiogeographic affinities of Tremadocian Moroccan assemblages with coeval faunas from Bohemia (Mergl, 2006), Avalonia (Owens et al., 1982; Fortey and Owens, 1991), and Baltica (Ebbestad, 1999) are evident at generic level, many species are endemic to the Anti-Atlas, probably because of the shallow environmental conditions of the Fezouata Shale. In contrast, early Floian assemblages of the Zagora area comprised much less endemic species (22.2% for the locality Z-F26), suggesting the existence of enhanced faunal exchanges due to a higher relative sea-level. The endemicity of most Tremadocian and middle Floian taxa, along with the absence of taihungshaniids from shallow environments, and of pelagic trilobites in the Lower Ordovician of the Zagora area all suggest that the Fezouata Shale was deposited in an episodically shallow basin. The induced temporary relative isolation of the

present day Anti-Atlas region during the earliest Ordovician is also accompanied by the occurrence of episodic dysoxic events, which facilitated exceptional preservation in some intervals of the Fezouata Shale, as supported by geochemical analyses. The scarcity of olenid trilobites (generally associated with oxygen-depleted environments), only reported in the lower part of the Fezouata Shale (Destombes et al., 1985) might result from the depositional environments of the Fezouata Shale, which despite being periodically affected by oxygen-depletion remained too shallow-water to host such trilobites. However, new field investigations are necessary to identify more precisely the stratigraphic position of olenid occurrences in the lowermost part of the Fezouata Shale. Finally, it is possible that the more sustained faunal exchanges documented in the early–middle Floian time interval were tectonically controlled and related to the widening of the basin.

Acknowledgments

The authors would like to thank the Agence National de la Recherche — RALI project (grant number ANR-11-BS56-0025; "Rise of Animal Life (Cambrian-Ordovician): organization and tempo"), and the CNRS-CNRST cooperation project VALORIZ (grant number 52943) for their financial support. This paper is a contribution to the IGCP project 591'The Early to Middle Palaeozoic Revolution', and of the team "Vie primitive, biosignatures, milieux extrêmes", UMR CNRS 5276 LGLTPE. Many important data on the stratigraphy and localities were obtained from M. Ben Moula (Taichoute), J.P. Botting and L. Muir (Llandrindod Wells), J.C. Gutiérrez-Marco (Madrid), R. and V. Reboul (Saint-Chinian), B. Pittet (Villeurbanne), E. Nardin (Toulouse), and P. Van Roy (Yale). Critical field assistance was provided by A. Azizi, A. Bachnou, M. Bajedoub, K. Kouraïss, A. Hafid, and K. El Hariri (Marrakesh), C. Jauvion, M. Martin, and J. Vannier (Villeurbanne), M. Masrour (Agadir), R. Lerosey-Aubril (Armidale), H. Nowak and T. Vandenbroucke (Villeneuve d'Ascq). The authors are particularly thankful to Rudy Lerosey-Aubril, Richard Fortey and Carlton Brett for reviewing the manuscript and making many helpful remarks.

Appendix A. Supplementary data

Supplementary data to this article can be found online at http://dx.doi.org/10.1016/j.palaeo.2016.06.003.

References

Adrain, J.M., 2013. A synopsis of Ordovician trilobite distribution and diversity. Geol. Soc. Lond. Mem. 38, 297–336.
Balseiro, D., Waisfeld, B.G., Buatois, L.A., 2011. Unusual trilobite biofacies from the Lower Ordovician of the Argentine Cordillera Oriental: new insights into olenid palaeoecology: unusual olenid biofacies in Argentina. Lethaia 44, 58–75. http://dx.doi.org/10.1111/j.1502-3931.2010.00224.x.
Barthoux, J.C., 1924. Les massifs de Djebilet et des Rehamna (Maroc). C. R. Acad. Sci. Paris 179, 504–506.
Bergeron, J., 1888. Sur la présence de la faune primordiale (Paradoxidien) dans les environs de Ferrals-les-Montagnes (Hérault). I. Etude stratigraphique. II. Etude paléontologique (en collaboration avec M. Munier-Chalmas). C. R. Acad. Sci. Paris 106, 375–377.
Bergström, S.M., Chen, X., Gutiérrez-Marco, J.C., Dronov, A., 2009. The new chronostratigraphic classification of the Ordovician System and its relations to major regional series and stages and to $\delta^{13}C$ chemostratigraphy. Lethaia 42, 97–107. http://dx.doi.org/10.1111/j.1502-3931.2008.00136.x.
Bigot, D., Dubois, G., 1931. Sur la présence de l'Ordovicien dans l'Anti-Atlas marocain. C. R. Acad. Sci. Paris 193, 282–293.
Boeck, C., 1838. Ubersicht der bisher in Norwegen gefundenen Formen der Trilobiten Familie. Gaea Norvegica L 138–145.
Botting, J.P., 2016. Diversity and ecology of sponges in the Early Ordovician Fezouata Biota, Morocco. Palaeogeog. Palaeoclimatol. Palaeoecol. 460, 75–86 (in this issue).
Carlucci, J.R., Westrop, S.R., 2015. Trilobite biofacies and sequence stratigraphy: an example from the Upper Ordovician of Oklahoma. Lethaia 48, 309–325.
Chlupáč, I., 1983. Trilobite assemblages in the Devonian of the Barrandian area and their relations to palaeoenvironments. Geol. Palaeontol. 17, 45–73.
Chlupáč, I., 1987. Ecostratigraphy of Silurian trilobite assemblages of the Barrandian area, Czechoslovakia. Newsl. Stratigr. 17, 169–186.
Choubert, G., 1942. Constitution et puissance de la série primaire de l'Anti-Atlas. C. R. Acad. Sci. Paris 215, 445–447.
Choubert, G., 1946. Aperçu de la géologie marocaine. Rev. Géogr. Maroc. 23, 1–19.
Choubert, G., 1951. Note sur la géologie de l'Anti-Atlas. Int. Geol. Congr. Lond. 14, 29–44 (1948).
Choubert, G., 1952. Histoire géologique du domaine de l'Anti-Atlas. Notes Mém. Serv. Géol. Maroc. 100, 77–194.
Choubert, G., Termier, H., 1947. Sur la stratigraphie de l'Ordovicien. C. R. Somm. Soc. Geol. France 16, 335–337.
Choubert, G., Clariond, L., Hindermeyer, J., 1952. Livret-guide de l'excursion C 36. Anti-Atlas central et oriental. 19ème Congrès géologique International Alger (1952) Maroc 11, pp. 1–89.
Choubert, G., Hindermeyer, J., Hupé, P., 1955. Découverte du Trémadoc dans l'Anti-Atlas (Maroc). C. R. Acad. Sci. Paris 241, 1592–1594.
Cocks, L.R.M., Fortey, R.A., 1988. Lower Palaeozoic facies and fauna around Gondwana. In: Audley-Charles, M.G., Hallam, A. (Eds.), Gondwana and Tethys. — Geological Society Special Publication 37, pp. 183–200.
Cocks, L.R.M., Torsvik, T.H., 2004. Major terranes in the Ordovician. In: Webby, B.D., Paris, F., Droser, M.L., Percival, I.G. (Eds.), The Great Ordovician Biodiversification Event. Columbia University Press, New York, pp. 61–67.
Corbacho, J., Vela, J.A., 2010. Giant trilobites from Lower Ordovician of Morocco. Batalleria 15, 3–32.
Corbacho, J., Vela, J.A., 2011. Revisión de las especies de *Lehua* de la región de Zagora (Marruecos). Batalleria 16, 46–49.
Courtessole, R., Marek, L., Pillet, J., Ubaghs, G., Vizcaïno, D., 1983. Calymenina, Echinodermata et Hyolitha de l'Ordovicien inférieur de la Montagne Noire (France méridionale). Mem. Soc. Etud. Sci. Aude 1–62.
Courtessole, R., Pillet, J., Vizcaïno, D., Eschard, R., 1985. Etude biostratigraphique et sédimentologique des formations arénacées de 1'Arenigien du Saint-Chinianais oriental (Hérault), versant sud de la Montagne Noire (France méridionale). Mem. Soc. Etud. Sci. Aude (5 pp.).
Dean, W.T., 1965. Revision of the Ordovician Trilobite genus *Bathycheilus* Holub. Sborník Národního Muzea V Praze 21 (B), pp. 1–10 (pls. l, 2).
Dean, W.T., 1966. The Lower Ordovician stratigraphy and trilobites of the Landeyran valley and neighbouring district of the Montagne Noire, south-western France. Bull. Br. Mus. (Nat. Hist.), Geol. 12, 245–353 (pls. 1–21).
Dean, W.T., 1971. The Lower Palaeozoic stratigraphy and faunas of the Taurus Mountains near Beyşehir Turkey. II. The trilobites of the Seydisehir Formation (Ordovician). Bulletin of the British Museum (Natural History). Geology 20, 3–24.
Destombes, J., 1960. Sur l'extension du Trémadoc dans le Sud marocain. C. R. Soc. Sci. Nat. Phys. Maroc. 3, 45–47.
Destombes, J., 1962. Stratigraphie et paléogéographie de l'Ordovicien de l'Anti-Atlas (Maroc): un essai de synthèse. Bull. Soc. Géol. France 7 (4), 453–460.
Destombes, J., 1967. Distribution et affinités des genres de trilobites de l'Ordovicien de l'Anti-Atlas (Maroc). C. R. Somm. Soc. Géol. France 1967, 133–134.
Destombes, J., 1970. Cambrien et Ordovicien. Notes Mém. Serv. Géol. Maroc. 229, 161–170.
Destombes, J., 1971. L'Ordovicien au Maroc. Essai de synthèse stratigraphique. Mém. Bur. Rech. Géol. Min. 73, 237–263.
Destombes, J., 1972. Les trilobites du sous-ordre des Phacopina de l'Ordovicien de l'Anti-Atlas (Maroc). Notes Mém. Serv. Géol. Maroc. 240, 114.
Destombes, J., 2006a. Carte géologique au 200 000 de l'Anti-Atlas marocain. Paléozoïque inférieur. Cambrien moyen et supérieur-Ordovicien-base du Silurien. Sommaire général sur les Mémoires explicatifs des cartes géologiques au 1/200 000 de l'*Anti*-Atlas marocain. Notes Mém. Serv. Géol. Maroc. 515 (149 pp.).
Destombes, J., 2006b. Carte géologique au 1/200 000 de l'Anti-Atlas marocain. Paléozoïque inférieur. Cambrien moyen et supérieur-Ordovicien-base du Silurien. Feuille Zagora-Coude du Dra. Mémoire explicatif, Chapitre A [written in 1983]. Notes Mém. Serv. Géol. Maroc. 273 (bis, 36 pp.).
Destombes, J., 2006c. Carte géologique au 1/200 000 de l'Anti-Atlas marocain. Paléozoïque inférieur. Cambrien moyen et supérieur-Ordovicien-base du Silurien. Feuille Bou Haiara- Zegdou. Mémoire explicatif, Chapitre B [written in 1983]. Notes Mém. Serv. Géol. Maroc. 259 (bis, 30 pp.).
Destombes, J., 2006d. Carte géologique au 1/200 000 de l'Anti-Atlas marocain. Paléozoïque inférieur. Cambrien moyen et supérieur-Ordovicien-base du Silurien. Feuille Jbel Saghro-Dadès. Mémoire explicatif, Chapitre C [written in 1983]. Notes Mém. Serv. Géol. Maroc. 161 (bis, 41 pp.).
Destombes, J., 2006e. Carte géologique au 1/200 000 de l'Anti-Atlas marocain. Notice explicative. Paléozoïque inférieur. Cambrien moyen et supérieur-Ordovicien-base du Silurien. Feuille Todrha- Maïder. Mémoire explicatif, Chapitre D [written in 1985]. Notes Mém. Serv. Géol. Maroc. 243 (bis, 58 pp.).
Destombes, J., 2006f. Carte géologique au 200 000 de l'Anti-Atlas marocain. Paléozoïque inférieur (Cambrien moyen et supérieur-Ordovicien-base du Silurien). Feuille Tafilalt-Taouz. Mémoire explicatif, Chapitre E (Anti-Atlas oriental) [written in 1987]. Notes Mém. Serv. Géol. Maroc. 244 (bis, 69 pp.).
Destombes, J., 2006g. Carte géologique au 1/200 000 de l'Anti-Atlas marocain. Paléozoïque inférieur: Cambrien moyen et supérieur-Ordovicien-base du Silurien. Feuille Telouet Sud, Ouarzazate, Alougoum, Agadir-Tissinnt. Mémoire explicatif, Chapitre F [written in 1988]. Notes Mém. Serv. Géol. Maroc. 138 (bis, 43 pp.).
Destombes, J., 2006h. Carte géologique au 1/200 000 de l'*Anti*-Atlas marocain. Paléozoïque inférieur (Cambrien moyen et supérieur-Ordovicien-base du Silurien). Feuille Foum el Hassane-Assa. Mémoire explicatif, Chapitre H (Flanc sud de l'Anti-Atlas occidental et des plaines du Dra) [written in 2001]. Notes Mém. Serv. Géol. Maroc. 159 (bis, 35 pp.).
Destombes, J., 2006i. Carte géologique au 1/200 000 de l'Anti-Atlas marocain. Paléozoïque inférieur: Cambrien moyen-Ordovicien-base du Silurien. Feuille Goulimine-Dra inférieur au 1/200 000, feuille Fask au 1/100 000 (Anti-Atlas occidental, Maroc).

Mémoire explicatif, Chapitre I [written in 2002]. Notes Mém. Serv. Géol. Maroc. 90 (bis A, 34 pp.).
Destombes, J., 2006j. Carte géologique au 1/200 000 de l'Anti-Atlas marocain. Paléozoïque inférieur: Cambrien moyen-Ordovicien-base du Silurien. Feuille régions de Tan-Tan–Jbel Zini (Province de Tarfaya). Mémoire explicatif, Chapitre J (Anti-Atlas sud-occidental au sud de l'oued Dra) [written in 2003]. Notes Mém. Serv. Géol. Maroc. 90 (bis B, 29 pp.).
Destombes, J., Sougy, J., Willefert, S., 1969. Révisions et découvertes paléontologiques (brachiopodes, trilobites et graptolites) dans le Cambro-Ordovicien du Zemmour (Mauritanie septentrionale). Bull. Soc. Géol. Fr. 7 (11), 185–206.
Destombes, J., Hollard, H., Willefert, S., 1985. Lower Palaeozoic rocks of Morocco. In: Holland, C.H. (Ed.), Lower Palaeozoic Rocks of the World 4. Wiley, New York, pp. 91–336.
Ebbestad, J.O.R., 1999. Trilobites of the Tremadoc Bjørkåsholmen Formation in the Oslo region, Norway. Fossils Strata 47 (188-pp.).
Fortey, R.A., 1975a. The Ordovician trilobites of Spitsbergen II. Asaphidae, Nileidae, Raphiophoridae and Telephinidae of the Valhallfonna Formation. Nor. Polarinst. Skr. 162, 1–207.
Fortey, R.A., 1975b. Early Ordovician trilobite communities. Fossils Strata 4, 339–360.
Fortey, R.A., 2009. A new giant asaphid trilobite from the Ordovician of Morocco. Mem. Aust. Assoc. Palaeontol. 37, 9–16.
Fortey, R.A., 2011a. Trilobites of the genus *Dikelokephalina* from Ordovician Gondwana and Avalonia. Geol. J. 46, 405–415. http://dx.doi.org/10.1002/gj.1275.
Fortey, R.A., 2011b. The first known complete lichakephalid trilobite, Lower Ordovician of Morocco. Mem. Assoc. Aust. Palaeontol. 42, 1–7.
Fortey, R.A., Cocks, L.R.M., 2003. Palaeontological evidence bearing on global Ordovician–Silurian continental reconstructions. Earth Sci. Rev. 61, 245–307. http://dx.doi.org/10.1016/S0012-8252(02)00115-0.
Fortey, R.A., Morris, S.F., 1982. The Ordovician trilobite *Neseuretus* from Saudi Arabia and the palaeogeography of the fauna related to Gondwanaland in the earliest Ordovician. Bull. Br. Mus., Nat. Hist. (Geol.) 36, 63–75.
Fortey, R.A., Owens, R.M., 1978. Early Ordovician (Arenig) stratigraphy and fauna of the Carmarthen district, south-west Wales. Bulletin of the British Museum (Natural History). Geology 30 (3), 225–294.
Fortey, R.A., Owens, R.M., 1987. The Arenig Series in South Wales: Stratigraphy and palaeontology. bulletin of the British Museum (Natural History). Geology 41 (3), 169–307.
Fortey, R.A., Owens, R.M., 1991. A trilobite fauna from the highest Shineton Shales in Shropshire, and the correlation of the latest Tremadoc. Geol. Mag. 128, 437–464.
Fortey, R.A., Heward, A.P., Miller, G.C., 2011. Sedimentary facies and trilobite and conodont faunas of the Ordovician Rann Formation, Ras Al Khaimah, United Arab Emirates. GeoArabia. J. Middle East Petrol. Geosci. 16, 127–152.
Gaines, R.R., Briggs, D.E.G., Orr, P.J., Van Roy, P., 2012. Preservation of giant anomalocaridids in silica-chlorite concretions from the Early Ordovician of Morocco. PALAIOS 27, 317–325. http://dx.doi.org/10.2110/palo.2011.p11-093r.
Geyer, G., Landing, E., 2006. Latest Ediacaran and Cambrian of the Moroccan Atlas regions. Beringeria Spec. Issue 6, 7–46.
Ghobadi Pour, M., Vidal, M., Hosseini-Nezhad, M., 2007. An Early Ordovician trilobite assemblage from the Lashkarak Formation, Damghan area, northern Iran. Geobios 40, 489–500.
Gigout, M., 1951. Etudes Géologiques sur la Meseta marocaine Occidentale (Arrière pays de Casablanca, Mazagan et Safi). Notes Mém. Serv. Géol. Maroc. 86, 1–490 (18 pl).
Gilinsky, N.L., Bennington, J.B., 1994. Estimating numbers of whole individuals from collections of body parts: a taphonomic limitation of the paleontological record. Paleobiology 20, 245–258.
Gutiérrez-Marco, J.-C., Martin, E.L.O., 2016. Biostratigraphy and palaeoecology of Lower Ordovician graptolites from the Fezouata Shale (Moroccan Anti-Atlas). Palaeogeogr. Palaeoclimatol. Palaeoecol. 460, 35–49 (in this issue).
Hammer, Ø., Harper, D.A.T., Paul, D.R., 2001. Past: paleontological statistics software package for education and data analysis. Palaeontol. Electron. 4, 4–9 (http://palaeo-electronica.org/2001_1/past/issue1_01.htm).
Harrington, H.J., 1937. On some Ordovician fossils from northern Argentina. Geol. Mag. 74, 97–124.
Hayes, J.M., Strauss, H., Kaufman, A.J., 1999. The abundance of ^{13}C in marine organic matter and isotopic fractionation in the global biogeochemical cycle of carbon during the past 800 Ma. Chem. Geol. 161, 103–125.
Lefebvre, B., El Hariri, K., Lerosey-Aubril, R., Servais, T., Van Roy, P., 2016a. The Fezouata Shale (Lower Ordovician, Anti-Atlas, Morocco): A historical review. Palaeogeogr. Palaeoclimatol. Palaeoecol. 460, 7–23 (in this issue).
Lefebvre, B., Allaire, N., Guensburg, T.E., Hunter, A.W., Kouraïss, K., Martin, E.L.O., Nardin, E., Noailles, F., Pittet, B., Sumrall, C.D., Zamora, S., 2016b. Palaeoecological aspects of the diversification of echinoderms in the Lower Ordovician of central Anti-Atlas, Morocco. Palaeogeogr. Palaeoclimatol. Palaeoecol. 460, 97–121 (in this issue).
Legendre, P., Legendre, L., 2012. Numerical ecology, Third English Edition. Ed. Developments in Environmental Modelling. Elsevier, Amsterdam (990 pp.).
Lehnert, O., Nowak, H., Sarmiento, G.N., Gutiérrez-Marco, J.C., Akodad, M., Servais, T., 2016. Conodonts from the Lower Ordovician of Morocco — contributions to age and faunal diversity of the Fezouata Lagerstätte and peri-Gondwana biogeography. Palaeogeogr. Palaeoclimatol. Palaeoecol. 460, 50–61 (in this issue).
Lu, Y., 1975. Ordovician trilobite faunas of central and southwestern China. Palaeontol. Sin. New Ser. B 11, 1–463.
Ludvigsen, R., Westrop, S.R., Pratt, B.R., Tuffnell, P.A., Young, G.A., 1986. Dual biostratigraphy: zones and biofacies. Geosci. Can. 13, 139–154.
Martin, E.L.O., Lerosey-Aubril, R., Vannier, J., 2016. Palaeoscolecid worms from the Lower Ordovician Fezouata Lagerstätte, Morocco: Palaeoecological and palaeogeographical implications. Palaeogeogr. Palaeoclimatol. Palaeoecol. 460, 130–141 (in this issue).
Martin, E.L.O., Pittet, B., Gutiérrez-Marco, J.-C., Vannier, J., El Hariri, K., Lerosey-Aubril, R., Masrour, M., Nowak, H., Servais, T., Vandenbroucke, T.R.A., Van Roy, P., Vaucher, R., Lefebvre, B., 2016. The Lower Ordovician Fezouata Konservat–Lagerstätte from Morocco: Age, environment and evolutionary perspectives. Gondwana Res. 34, 274–283.
McLane, M., 1995. Sedimentology. Oxford University Press, Oxford (423 pp.).
Mergl, M., 2006. Tremadocian trilobites of the Prague Basin, Czech Republic. Acta Mus. Nat. Pragae, Ser. B, Hist. Nat. 62 (1–2), 1–70 (Praha. ISSN 0036–5343).
Neltner, L., 1929. Etat des connaissances actuelles sur la géologie du Maroc. C. R. 15ème. Congr. Géol. Int. Pretoria 2 (6), 550–556.
Nowak, H., Servais, T., Pittet, B., Vaucher, R., Akodad, M., Gaines, R.R., Vandenbroucke, T., 2016. Palynomorphs of the Fezouata Shale (Lower Ordovician, Morocco): Age and environmental constraints of the Fezouata Biota. Palaeogeogr. Palaeoclimatol. Palaeoecol. 460, 62–74 (in this issue).
Owens, R.M., Fortey, R.A., Cope, J.C.W., Rushton, A.W.A., Bassett, M.G., 1982. Tremadoc faunas from the Carmarthen district, South Wales. Geol. Mag. 119, 1–112.
Polechová, M., 2016. The bivalve fauna from the Fezouata Formation (Lower Ordovician) of Morocco and its significance for palaeobiogeography, palaeoecology and early diversification of bivalves. Palaeogeogr. Palaeoclimatol. Palaeoecol. 460, 155–169 (in this issue).
Rabano, I., 1990. Trilobites del Museo GeoMinero. I. *Platypeltoides magrebiensis* n. sp. (Asaphina, Nileidae), del Ordovícico inferior del Anti-Atlas central (Marruecos). Bol. Geol. Min. 101, 21–27.
Roch, E., 1930. Etudes géologiques dans la région méridionale du Maroc occidental. Mém. Serv. Géol. Maroc. 9, 1–542.
Roch, E., 1939. Description géologique des montagnes à l'Est de Marrakech. Notes Mém. Serv. Géol. Maroc. 51, 1–438.
Roch, E., 1950. Histoire stratigraphique du Maroc. Notes Mém. Serv. Géol. Maroc. 80, 1–435.
Termier, H., 1927. Observations nouvelles en Maroc central. C. R. Somm. Soc. Géol. France 9, 100–102.
Termier, H., 1936. Etudes géologiques sur le Maroc central et le Moyen-Atlas septentrional. Notes Mém. Serv. Géol. Maroc. 33, 1–1556.
Termier, H., Termier, G., 1947. Les principaux niveaux paléontologiques dans l'Ordovicien marocain. C. R. Somm. Soc. Géol. France 13, 254–256.
Termier, G., Termier, H., 1950. Paléontologie marocaine 2 (4). Invertébrés de l'Ere Primaire. Annélides, arthropodes, échinodermes, conularides et graptolithes. Notes Mém. Serv. Géol. Maroc. 79, 1–279.
Thoral, M., 1935. Contribution à l'Étude Paléontologique de l'Ordovicien Inférieur de la Montagne Noire et Révision Sommaire de la Faune Cambrienne de la Montagne Noire. Imprimerie de la Charité, Montpellier.
Torsvik, T.H., 2009. BugPlates: linking biogeography and palaeogeography [WWW document]. (URL) http://www.geodynamics.no/bugs/SoftwareManual.pdf.
Torsvik, T.H., Cocks, L.R.M., 2011. The Palaeozoic palaeogeography of central Gondwana. Geol. Soc. Lond., Spec. Publ. 357, 137–166. http://dx.doi.org/10.1144/SP357.8.
Torsvik, T.H., Cocks, L.R.M., 2013. Gondwana from top to base in space and time. Gondwana Res. 24, 999–1030. http://dx.doi.org/10.1016/j.gr.2013.06.012.
Turvey, S.T., 2005. Early Ordovician (Arenig) trilobite palaeoecology and palaeobiogeography of the South China Plate. Palaeontology 48, 519–547.
Van Roy, P., Orr, P.J., Botting, J.P., Muir, L.A., Vinther, J., Lefebvre, B., El Hariri, K., Briggs, D.E.G., 2010. Ordovician faunas of Burgess Shale type. Nature 465, 215–218. http://dx.doi.org/10.1038/nature09038.
Van Roy, P., Briggs, D.E., Gaines, R.R., 2015. The Fezouata fossils of Morocco; an extraordinary record of marine life in the Early Ordovician. J. Geol. Soc. 172, 541–549.
Vaucher, R., Martin, E.L.O., Hormière, H., Pittet, B., 2016a. A genetic link between Konzentrat- and Konservat-Lagerstätten in the Fezouata Shale (lower Ordovician, Morocco). Palaeogeogr. Palaeoclimatol. Palaeoecol. 460, 24–34 (in this issue).
Vaucher, R., Pittet, B., Martin, E.L.O., Hormière, H., Lefebvre, B., 2016b. A wave-dominated, tide-modulated model for the Lower Ordovician of the Anti-Atlas, Morocco. Sedimentology (submitted for publication).
Vela, J.A., Corbacho, J., 2007. A new species of *Lehua* from the Lower Ordovician of Dra Valley of Morocco. Batalleria 13, 75–80.
Vidal, M., 1996. Biofaciès à trilobites dans l'Ordovicien inférieur de l'Anti-Atlas, Maroc: paléoenvironnements et paléobiogéographie. Université de Rennes 1, Unpublished thesis, (142 pp).
Vidal, M., 1998a. Trilobites (Asaphidae et Raphiphoridae) de l'Ordovicien inférieur de l'Anti-Atlas, Maroc. Palaeontogr. Abt. A 251, 39–77.
Vidal, M., 1998b. Le modèle des biofaciès à trilobites: un test dans l'Ordovicien inférieur de l'Anti-Atlas, Maroc. C. R. Acad. Sci., Paris [Sci. terre planèt.] 327–333 (1998).
Vizcaïno, D., Álvaro, J.J., 2002. Adequacy of the Early Ordovician trilobite record in the southern Montagne Noire (France): biases for biodiversity documentation. Trans. R. Soc. Edinb. Earth Sci. 93. http://dx.doi.org/10.1017/S0263593300000493.
Vizcaïno, D., Álvaro, J.J., Lefebvre, B., 2001. The lower Ordovician of the southern Montagne Noire. Ann. Soc. Géol. Nord 8 (4), 213–220.
Zhou, Z.-Y., Bergström, J., Zhou, Z.-Q., Yuan, W.-W., Zhang, Y.-B., 2011. Trilobite biofacies and palaeogeographic development in the Arenig (Ordovician) of the Yangtze Block, China. Palaeoworld 20, 15–45.

Annexe 6 :

Palynomorphs of the Fezouata Shale (Lower Ordovician, Morocco): Age and environmental constraints of the Fezouata Biota

Auteurs : Hendrik Nowak, Thomas Servais, Bernard Pittet, **Romain Vaucher**, Mustapha Akodad, Robert R. Gaines, Thijs R.A. Vandenbroucke

Article publié dans *Palaeogeography, Palaeoclimatology, Palaeoecology*

Année : 2016 Volume : 460 Pages : 62 - 74

DOI : http://dx.doi.org/10.1016/j.palaeo.2016.03.007

Palaeogeography, Palaeoclimatology, Palaeoecology 460 (2016) 62–74

Contents lists available at ScienceDirect

Palaeogeography, Palaeoclimatology, Palaeoecology

journal homepage: www.elsevier.com/locate/palaeo

Palynomorphs of the Fezouata Shale (Lower Ordovician, Morocco): Age and environmental constraints of the Fezouata Biota

Hendrik Nowak [a,b,*], Thomas Servais [a], Bernard Pittet [c], Romain Vaucher [c], Mustapha Akodad [d], Robert R. Gaines [e], Thijs R.A. Vandenbroucke [a,f]

[a] UMR 8198 Evo-Eco-Paleo, CNRS, Université de Lille—Sciences et Technologies, Bâtiment SN5, Cité Scientifique, Avenue Paul Langevin, 59655 Villeneuve d'Ascq Cedex, France
[b] Naturmuseum Südtirol, Bindergasse 1, 39100 Bolzano-Bozen, Italy
[c] ENS-UMR 5276, CNRS, Université Lyon 1, Campus de la Doua, 2, rue Raphaël Dubois, 69622 Villeurbanne Cedex, France
[d] Faculté Pluridisciplinaire de Nador, Labo OLMAN-RL, FPN 300, Selouane, 67200, Nador, Morocco
[e] Geology Department, Pomona College, 185 E. Sixth Street, Claremont, CA 91711, USA
[f] Department of Geology, Ghent University, Krijgslaan 281/S8, 9000 Ghent, Belgium

ARTICLE INFO

Article history:
Received 13 October 2015
Received in revised form 12 February 2016
Accepted 6 March 2016
Available online 10 March 2016

Keywords:
Lower Ordovician
Morocco
Fezouata Shale
Acritarchs
Chitinozoans

ABSTRACT

The present study documents new palynological investigations of the Fezouata Shale from the Anti-Atlas (Morocco). Palynomorphs were extracted from samples collected from both outcrops and drill cuttings. Outcrop samples were taken near Zagora, and include some that were collected during excavation of stratigraphic horizons where exceptionally well-preserved fossils of the Fezouata Lagerstätte occur. Subsurface samples were taken from the AZ-1 (Adrar Zouggar Mountain) borehole, which was extracted some 300 km to the southwest of Zagora. The palynological samples yielded acritarchs, chitinozoans, scolecodonts, conodonts and fragments of graptolites. The abundance and quality of preservation of palynomorphs varies greatly, but rich and diverse assemblages were recovered from several samples. The diversity and composition of the assemblages points to an open shelf environment. Generally mixed preservation states suggest resedimentation or differential transport histories. The acritarchs can be assigned to the diagnostic *messaoudensis-trifidum* acritarch assemblage, which is typical of the Tremadocian/Floian boundary interval of the Gondwanan margin in high southern palaeolatitudes. The acritarch taxa present in some of the lower parts of the Fezouata Shale including levels of exceptional preservation can be attributed to sub-assemblages 1–2 of the *messaoudensis-trifidum* assemblage and thus point to a late Tremadocian age of the Fezouata Lagerstätte, confirming biostratigraphic data provided by graptolites of the *Araneograptus murrayi* graptolite biozone. Chitinozoans from the Fezouata Shale are from the *E. symmetrica* and *E. brevis* biozones and include various species that are well-known from several localities on the Gondwanan margin and from other palaeocontinents (Baltica, Laurentia, and South China), demarcating broad links between those regions. The coincidence between index fossils of these three groups, hitherto not all found in the same level, suggests that the age assignments of chitinozoan biozones may be in need of revision.

1. Introduction

The Fezouata Shale (Tremadocian to Floian in age) in the Anti-Atlas of southeastern Morocco has attracted much attention for its various fossils. Macrofossils found in this succession include graptolites, trilobites, echinoderms, brachiopods, various arthropods, hyolithids, conularids, demosponges, gastropods and cephalopods (Destombes et al., 1985, and references therein; Chauvel and Regnault, 1986; Donovan and Savill, 1988; Mergl, 1988; Rábano, 1990; Henry et al., 1992; Aceñolaza et al., 1996; Horný, 1997; Vidal, 1998a, 1998b; Van Roy and Tetlie, 2006; Lefebvre and Botting, 2007; Vela and Corbacho, 2007; Chatterton and Fortey, 2008; Vinther et al., 2008; Fortey, 2009, 2011, 2012; Corbacho and Vela, 2010, 2011, 2013; Noailles et al., 2010; Sumrall and Zamora, 2011; Van Roy and Briggs, 2011; Corbacho and López-Soriano, 2012; Kröger and Lefebvre, 2012; Valent et al., 2013; Valent and Corbacho, 2015; Van Roy et al., 2015b). Certain layers also contain soft-bodied fossils (Van Roy et al., 2010, 2015a, 2015b; Gaines et al., 2012; Martin et al., in press). Deposits bearing exceptional preservation are usually termed 'Lagerstätte', or more precisely 'Konservat-Lagerstätte' (Seilacher, 1970). The mode of preservation of the Fezouata Lagerstätte has not yet been precisely determined, owing to high degree of weathering of exposures in the Zagora area, but has been compared to Burgess Shale-type deposits characteristic of the Cambrian (Van Roy et al., 2010, 2015a). The Fezouata Lagerstätte is remarkable as it contains a biota with elements typical of Cambrian Burgess Shale-type faunas, as well as more 'modern' groups typical of the Palaeozoic Evolutionary Fauna *sensu* Sepkoski (1981, 1984) (Van Roy

* Corresponding author.
E-mail address: hendrik-nowak@web.de (H. Nowak).

http://dx.doi.org/10.1016/j.palaeo.2016.03.007
0031-0182/

et al., 2015a). Moreover, it was the first Lower Ordovician Konservat-Lagerstätte discovered, and is possibly the only post-Cambrian Lagerstätte that has been conserved via the Burgess Shale-type taphonomic pathway (Butterfield, 1995; Gaines et al., 2008; Gaines, 2014). Van Roy et al. (2010, p. 215) assumed that exceptional preservation occurred "from the top of the Lower Fezouata Formation through to the top of the Upper Fezouata Formation", but Martin et al. (in press) determined that the exceptional preservation is limited to certain layers within a ca. 80 m thick interval, near the top of the (Tremadocian) Lower Fezouata Formation. Since then it was found that the Lagerstätten bearing interval in the Lower Fezouata Formation is more restricted, while on the other hand exceptional preservation also occurs in the Upper Fezouata Formation (Lefevbre et al., 2016–in this issue; Gutiérrez-Marco and Martin, 2016–in this issue).

Palynomorphs, i.e. organic-walled microfossils, have been described previously from the Fezouata Shale. These first reports primarily concerned acritarchs and chitinozoans. Acritarchs are by definition of unknown origin (Evitt, 1963), but commonly are interpreted as cysts of unicellular algae. Chitinozoans are probably eggs of an unknown animal (Paris and Nõlvak, 1999), which occupied the mixed layer of early Palaeozoic oceans (Vandenbroucke et al., 2010a).

Acritarchs from the Fezouata Shale were first studied by Deunff (1968a, 1968b); Deunff in Destombes et al., 1985), who provided the first description of the now widely known genus *Arbusculidium*, and the first description of *Impluviculus milonii* (originally described as *Veryhachium miloni*) from the Fezouata material. Subsequently, Elaouad-Debbaj (1984, 1988) studied acritarchs and chitinozoans from the Lower Fezouata Formation and chitinozoans from the Upper Fezouata Formation. She described the chitinozoan *Lagenochitina destombesi* (Elaouad-Debbaj, 1988), which was later used by Paris (1990) as the index species for his lowermost chitinozoan biozone. In an unpublished PhD thesis, Snape (1993) identified a large number of palynomorph species and several assemblages in the Fezouata Shale, albeit from a small number of samples and with poor stratigraphic constraints. He compared one of his acritarch assemblages to the 'Watch Hill assemblage', which is now known as the *messaoudensis-trifidum* assemblage (Molyneux and Rushton, 1988; Servais and Molyneux, 1997). More recently, Nowak et al. (2015) provided a preliminary report on the *messaoudensis-trifidum* assemblage from borehole AZ-1 (Adrar Zouggar Mountain), in stratigraphic levels assigned to the Fezouata Shale.

The present study is part of a concerted effort to re-evaluate the Fezouata Shale in a new level of detail, using lithostratigraphy, biostratigraphy, geochemistry, palaeoecology, and to constrain the stratigraphic position of intervals containing exceptional preservation (Martin et al., in press). We here report on the palynology of the intervals bearing the Fezouata Lagerstätte, specifically acritarchs and chitinozoans, using material collected from outcrops of the Fezouata Shale from the part of the succession that has yielded exceptionally well-preserved fossils, as well as that collected from borehole AZ-1. Detailed logging and field observations allow us to integrate and constrain the palynological samples in a highly resolved, integrated stratigraphic framework.

2. Geological setting

During the early Palaeozoic, Africa was a part of the supercontinent Gondwana, and Morocco was located close to the South Pole. Around the Cambrian/Ordovician boundary, the Rheic Ocean opened between Avalonia and Gondwana, and Avalonia began moving northwards (Cocks and Fortey, 2009). The Lower Ordovician (Tremadocian to Floian) Fezouata Shale was deposited in an epicontinental sea on this newly rifted and subsiding margin of Gondwana. It is a succession of mudstones with quartz-rich siltstones and sandstones reaching a total thickness of about 900 m in the Zagora area (Destombes et al., 1985; Martin et al., in press; Vaucher et al., 2016–in this issue). It has a wide distribution in the Anti-Atlas, with the most prominent outcrops in the Draa Valley around Zagora (Destombes et al., 1985). Historically, the Fezouata Shale has been divided into a Lower Fezouata Formation (Tremadocian) and an Upper Fezouata Formation (Floian), but the distinctive horizon that defines the boundary is often absent, as for example in the Zagora area (Destombes, 1962). The Fezouata Shale unconformably overlies sediments of the Tabanite Group (Guzhangian, Cambrian Series 3; Geyer and Landing, 2006) and is locally overlain by the sandstones of the Zini Formation (upper Floian). The Fezouata and Zini formations are capped by an unconformity on which the Tachilla Formation (Darriwillian) was deposited. Together, the Fezouata, Zini, and Tachilla formations constitute the Outer Feijas Shale Group (Choubert, 1942). The Fezouata and the Zini formations were deposited under storm- and wave-dominance, but modulated by tidal action (Vaucher et al., 2016–in this issue).

3. Materials and methods

Outcrop samples were collected from various localities from the Ternata plain (the widened Draa valley) near Zagora (Fig. 1) during several field campaigns between 2012 and 2014. The respective sample levels were correlated using a detailed lithostratigraphical compound log, which was produced at the same time. The detailed log showing the position of the palynological samples (Fig. 2) corresponds to the interval spanning 240–330 m above the base of the Fezouata Shale in the compound log of the Lower Ordovician deposits (Vaucher et al., 2016–in this issue, their fig. 2). This includes the stratigraphic interval in the upper Lower Fezouata Formation yielding exceptionally preserved fossils (Martin et al., in press; Lefevbre et al., 2016–in this issue). It is centred around an easily recognizable, greyish blue, clay-dominated, *ca.* 20 m-thick interval (43 to 62 m in Fig. 2) that serves as a stratigraphic marker horizon to correlate the logs and position the various samples on the compound log. At Tizig Zaouine (30°31′04″N, 5°49′19″W), 28 samples (with prefix TZ-Paly) were taken that represent all of the stratigraphic interval bearing exceptionally preserved fossils. 17 samples (prefix FZ1) were taken during an excavation at Bou Izargane (30°29′59″N, 5°51′00″W). These samples are the product of a high-resolution (every ~10 cm) sampling in three quarries, representing a total thickness of about four metres. Samples from each quarry are grouped together in Fig. 2. Another five samples were collected at Tamroute (30°29′47″N, 5°53′15″W) (samples TVDB 12–041 to −045), and one sample each at Oued Beni Zoli (30°28′54″N, 5°52′03″W) (sample TVDB 12-046) and Oued Ouaoufraou (30°31′15″N, 5°56′44″W) (sample HN-FF05).

Surface-collected samples from Tizig Zaouine, Tamroute, Oued Beni Zoli, and Oued Ouaoufraou are characterized by deep weathering to a buff yellow colour, as is typical of near-surface Fezouata material (e.g. Van Roy et al., 2015a). By comparison, excavations at Bou Izargane reached less altered dark grey mudrocks from which the FZ1 samples were drawn. While samples from Bou Izargane have clearly been affected by weathering processes, as indicated by iron oxide staining along joints and cracks, the retention of some fraction of early diagenetic pyrite in most samples demonstrates that they were less affected by oxidative weathering than the other outcrop samples.

The borehole samples are cuttings from the AZ-1 borehole, which was drilled in 1963–64 at Adrar Zouggar Mountain, approximately 300 km southwest of Zagora. The drilling was executed by the petroleum company Petrofina for oil exploration, and attained a maximum depth of 3398.13 m. The interval between 624 m and 1134.8 m depth was assigned to the Fezouata Shale based on lithology (Fig. 3). This interval is overlain by 144 m of the Zini Formation and subsequently by the Tachilla Formation, according to the drill log.

The samples were processed by both standard palynological techniques and by using a low-manipulation technique employing hydrofluoric acid (similar to the method described by Butterfield and Harvey, 2012) with the objective to recover 'Small Carbonaceous Fossils' (SCFs). These are fragile, uncommon palynomorphs that are normally

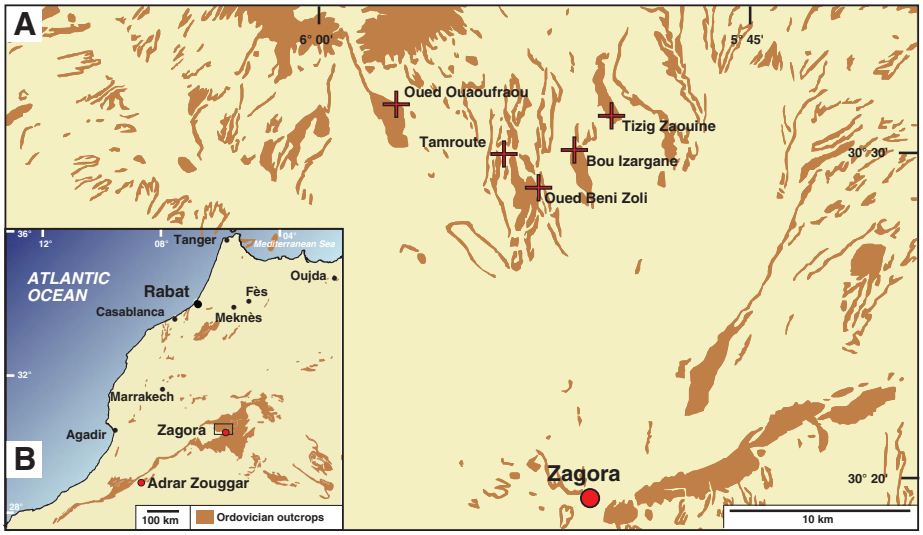

Fig. 1. Map of sampling sites.
Modified from supplementary information S1 of Van Roy et al. (2010). A) Ordovician outcrop areas around Zagora with marked sampled localities. B) section of the map of Morocco and adjacent areas showing the distribution of Ordovician outcrops and positions of Zagora and the Adrar Zouggar Mountain.

destroyed during standard processing, used to recover acritarchs and chitinozoans. The standard palynological technique involved treatment by hydrofluoric and hot hydrochloric acids, followed by centrifugation. Samples from Tizig Zaouine and Bou Izargane were treated using only the low-manipulation approach. Residues from the acid treatment were filtered at 51 or 63 μm (63 in the case of low-manipulation

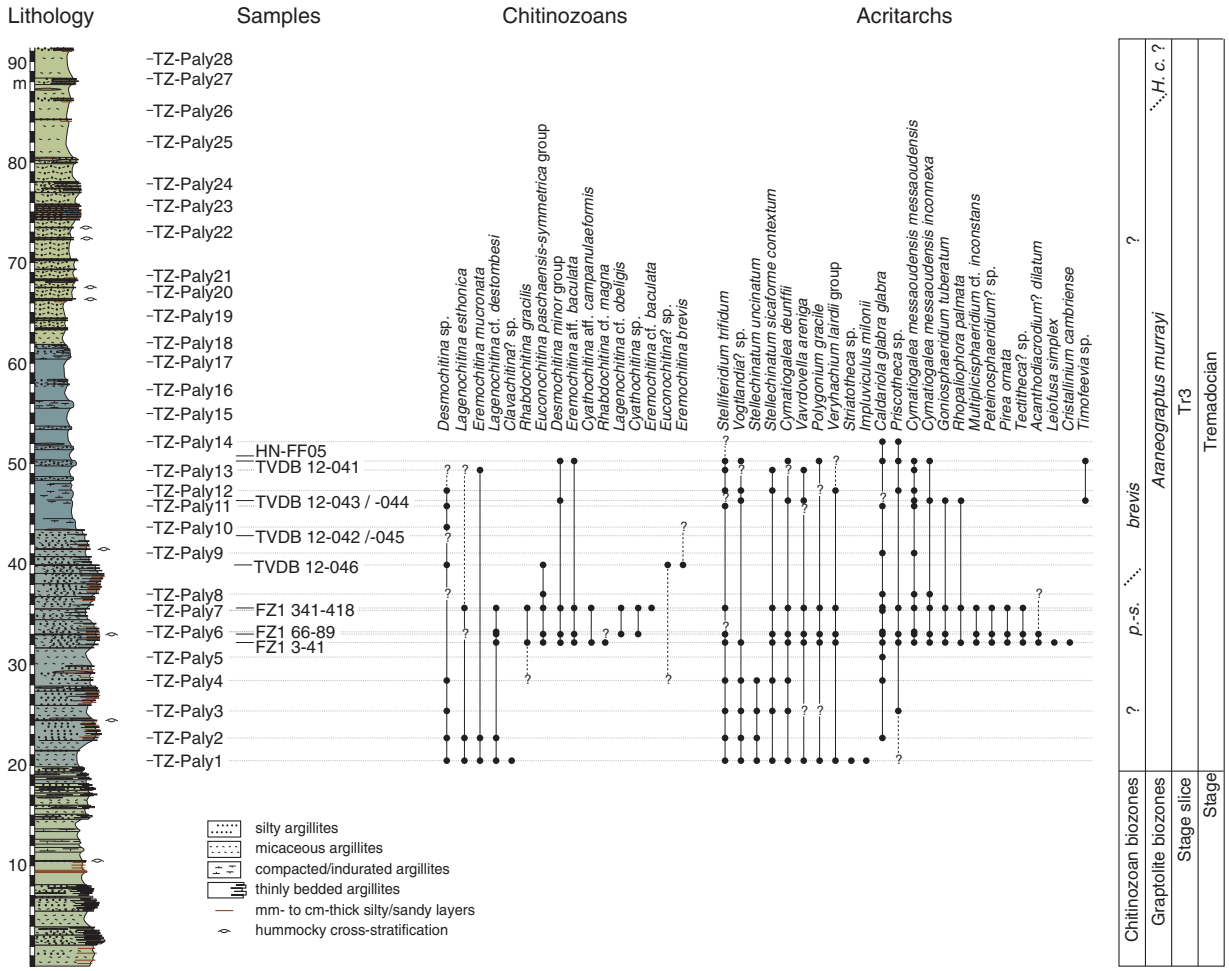

Fig. 2. Lithostratigraphy of the Fezouata Lagerstätte, positions of palynological samples, and ranges of selected acritarch and chitinozoan taxa. Lithostratigraphy of the Tizig Zaouine section, north of Zagora (see also Fig. 1). Graptolite biozonation according to Gutiérrez-Marco and Martin (2016–in this issue). *p.-s.* = *paschaensis-symmetrica*. *H. c.* = *Hunnegraptus copiosus*. Stage slice according to Bergström et al. (2009).

treatment of samples from the borehole, 51 in all other cases) and subsequently at 15 μm.

Microfossils were hand-picked from the larger fraction (>51 or 63 μm), then gold-coated and studied by Scanning Electron Microscopy (SEM). Palynological slides were produced from the 15 to 51 or 63 μm fraction. Images of acritarchs in the slides were taken using a Zeiss AxioCam ERc5s mounted on a Zeiss Axio Imager A2 transmitted light-microscope. All processed samples, slides and SEM preparations are stored in the collections of the Evo-Eco-Paleo department of the University of Lille, France.

4. Distribution of microfossils

4.1. Microfossils in the outcrops

In the lower part of the outcrop section at Tizig Zaouine (see Fig. 2), acritarchs and chitinozoans are present in varying abundance and diversity, and with poor to moderate preservation. Sample 15 and all samples above number 16 are devoid of organic matter, including palynomorphs. In contrast, all but four samples of the TZ-Paly batch—which were processed with a low-manipulation technique—yielded conodonts. The conodonts from the outcrops (i.e., at Tizig Zaouine and Bou Izargane) and the borehole are the focus of a study by Lehnert et al. (2016–in this issue).

Samples from the excavation at Bou Izargane are rich in well-preserved acritarchs and chitinozoans, including taxa not otherwise recorded in this area. The composition of their respective assemblages varies mostly in relative quantities.

Of five samples from Tamroute (TVDB 12-041 to -045), three yielded acritarchs and chitinozoans (and graptolite fragments), but chitinozoans are abundant and identifiable in only one sample (TVDB 12-041). The other two samples are barren, despite their stratigraphic position, which is approximately equivalent to two of the fossiliferous samples at the same locality.

The sample from Oued Beni Zoli (TVDB 12-046) is rich in acritarchs and chitinozoans, but acritarchs are too poorly preserved for confident identification and the chitinozoan diversity is limited.

A sample from Oued Ouaoufraou (HN-FF05) proved to be barren of palynomorphs.

Most samples yielding acritarchs and chitinozoans also contained graptolite fragments. Despite the use of the low-manipulation technique to recover Small Carbonaceous Fossils, such microfossils have not been recorded from our samples.

4.2. Microfossils in borehole AZ-1

In borehole AZ-1, most organic matter takes the form of indistinct opaque organic matter. Abundant, identifiable acritarchs are limited to the lower part of the Fezouata Shale, i.e. between 965 and 1100.65 m depth (34.15–169.8 m above the base of the Fezouata Shale; Fig. 3). A few, degraded acritarchs were also found in other samples, but samples from the interval between 699 and 749 m are barren. Complete specimens of chitinozoans are present from the top down to 965 m. Fragments occur in all samples except the lowermost one. Additionally, a few samples yielded graptolite fragments, conodonts and scolecodonts. Preliminary information on acritarchs from borehole AZ-1 was provided by Nowak et al. (2015). For a discussion of the conodonts, see Lehnert et al. (2016–in this issue).

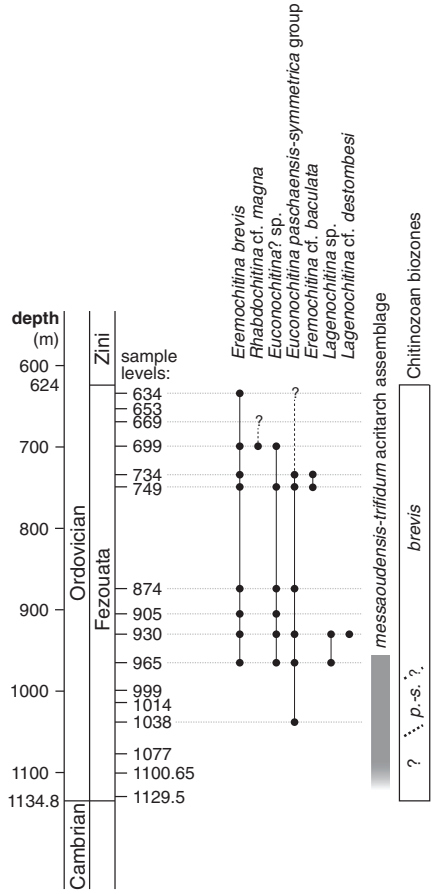

Fig. 3. Ranges of chitinozoan taxa in borehole AZ-1. Position of the *messaoudensis-trifidum* assemblage according to Nowak et al. (2015). *p.-s.* = *paschaensis-symmetrica*. The actual boundary between the *paschaensis-symmetrica* and *brevis* zones may lie higher, since the First Appearance Datum of *Eremochitina brevis* cannot be determined with certainty from the well cuttings due to probable mixing with overlying strata.

5. Acritarchs

The most common acritarch species in the studied outcrops (see Fig. 2) are *Stelliferidium trifidum* (Rasul, 1974) Fensome et al., 1990 (Fig. 4N), *Caldariola glabra glabra* (Martin, 1972) Molyneux *in* Molyneux and Rushton, 1988 (Fig. 4B), *Cymatiogalea deunffii* Jardiné et al., 1974 (Fig. 4C), *C. messaoudensis* Jardiné et al., 1974 with its two varieties *C. messaoudensis* var. *inconnexa* Servais and Molyneux, 1997 (Fig. 4E) and *C. messaoudensis* var. *messaoudensis* Jardiné et al., 1974 (Fig. 4F), and *Vogtlandia*? sp. (Fig. 4T). Frequently, when *C. deunffii* and *C. messaoudensis* are present, specimens that appear to represent a transitional state between the two are also observed (Fig. 4D), similar to specimens described by Servais and Molyneux (1997). Sphaeromorph acritarchs are omnipresent. Most of the latter would be assignable to the genus *Leiosphaeridia*, or defy identification because of poor preservation. They appear in all sizes (up to ~100 μm in diameter), and they are the most common type of acritarchs in the >51 μm size fraction. The following species are also fairly abundant where present: *Impluviculus milonii* (Deunff, 1968a) Loeblich and Tappan, 1969 (Fig. 4G), *Goniosphaeridium tuberatum* (Downie, 1958) Welsch, 1986 (Fig. 4H), *Multiplicisphaeridium* cf. *inconstans* Cramer and del Díez, 1977 (Fig. 4I), *Polygonium gracile* Vavrdová, 1966 *emend.* Jacobson and Achab, 1985 (Fig. 4K), *Tectitheca*? sp. (Fig. 4S), *Vavrdovella areniga* (Vavrdová, 1973) Loeblich and Tappan, 1976 (Fig. 4O), *Veryhachium lairdii* group Deflandre, 1946 *ex* Loeblich, 1970 (Fig. 4P), unidentified *Stelliferidium* and at least one species of *Priscotheca* (Fig. 4Q). *Stellechinatum sicaforme* Molyneux *in* Molyneux and Rushton, 1988 (Fig. 4M) occurs frequently, but in low abundance. Rare constituents are *Acanthodiacrodium*? *dilatum* Molyneux in Molyneux and Rushton, 1988 (Fig. 4A), *Cristallinium cambriense* (Slavíková, 1968) Vanguestaine, 1978, *Leiofusa simplex* (Combaz, 1967) Martin, 1975, *Pirea ornata* (Burmann, 1970) Eisenack et al., 1976 (Fig. 4J), *Rhopaliophora palmata* (Combaz and Péniguel, 1972) *emend.*

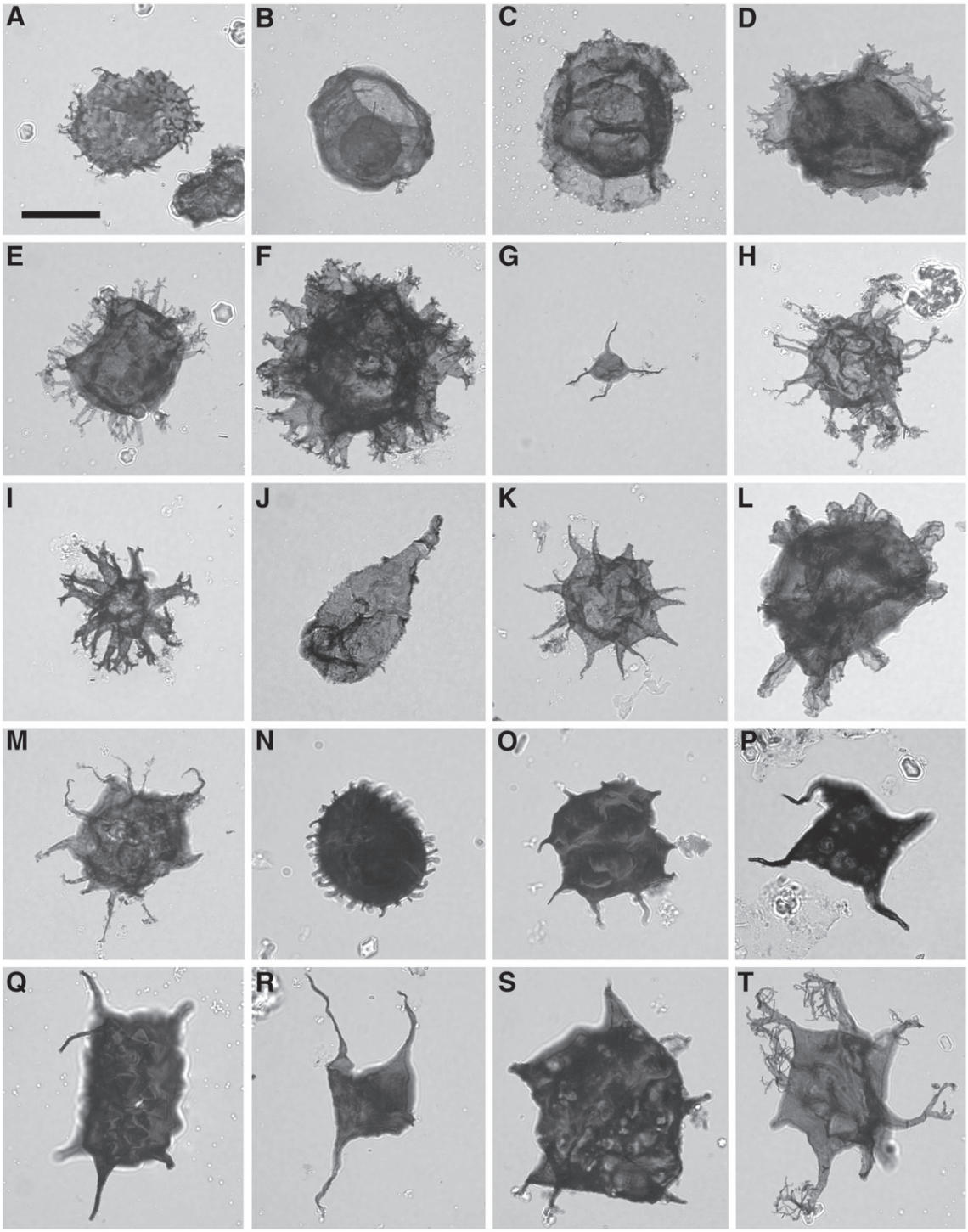

Fig. 4. Selected acritarchs from the Fezouata Shale near Zagora. Scale bar = 20 μm. Sample numbers are followed by slide numbers (in parentheses; s = standard maceration, lm = low-manipulation treatment) and England Finder Graticule coordinates. A) *Acanthodiacrodium*? *dilatum* Molyneux *in* Molyneux and Rushton, 1988; FZ1 3–4 (lm1), T51/3. B) *Caldariola glabra glabra* (Martin, 1972) Molyneux *in* Molyneux and Rushton, 1988; FZ1 4–5 (lm1), T37. C) *Cymatiogalea deunffii* Jardiné et al., 1974; FZ1 4–5 (lm1), N31/2. D) transient between *Cymatiogalea deunffii* (Downie, 1958) Martin, 1969 and *Cymatiogalea messaoudensis* Jardiné et al., 1974; TVDB 12-044 (s2), X33/2. E) *Cymatiogalea messaoudensis* Jardiné et al., 1974 var. *inconnexa* Servais and Molyneux, 1997; FZ1 13–16 (lm1), F51/3. F) *Cymatiogalea messaoudensis* var. *messaoudensis* Jardiné et al., 1974; FZ1 66–67 (lm1), G39/4. G) *Impluviculus milonii* (Deunff, 1968a) Loeblich and Tappan, 1969; TZ-Paly 1 (lm1), H42. H) *Goniosphaeridium tuberatum* (Downie, 1958) Welsch, 1986; FZ1 4–5 (lm1), V42/3. I) *Multiplicisphaeridium* cf. *inconstans* Cramer and Díez, 1977; FZ1 66–67 (lm1), G43. J) *Pirea ornata* (Burmann, 1970) Eisenack et al., 1976; FZ1 31–32 (lm1), P49/4. K) *Polygonium gracile* Vavrdová, 1966; FZ1 66–67 (1), P46. L) *Rhopaliophora palmata* (Combaz and Péniguel, 1972) emend. Playford and Martin, 1984; TVDB 12-044 (s1), L34. M) *Stellechinatum sicaforme* Molyneux *in* Molyneux and Rushton, 1988 var. *contextum* Servais and Molyneux, 1997; FZ1 3–4 (lm1), T51/2. N) *Stelliferidium trifidum* (Rasul, 1974) Fensome et al., 1990; TZ-Paly 4 (lm1), L48. O) *Vavrdovella areniga* (Vavrdová, 1973) Loeblich and Tappan, 1976; TZ-Paly 1 (lm1), H49. P) *Veryhachium lairdii* group Deflandre, 1946 ex Loeblich, 1970 sensu Servais et al., 2007; FZ1 76–80 (lm1), P34. Q) *Priscotheca* sp.; TZ-Paly 12 (lm1), D27. R) *Striatotheca* sp. TZ-Paly 1 (lm1), H34/4. S) *Tectitheca*? sp.; FZ1 3–4 (lm1), R39/2-R40/1. T) *Vogtlandia*? sp.; TZ-Paly 12 (lm1), P34/2.

Playford and Martin, 1984 (Fig. 4L), *Stellechinatum uncinatum* (Downie, 1958) Molyneux, 1987, *Striatotheca* sp. (Fig. 4R), *Timofeevia* sp., and an unidentified species of *Peteinosphaeridium*?, resembling specimens previously reported from Argentina as "*Peteinosphaeridium* cf. *P. bergstroemii* Staplin et al., 1965" by Achab et al. (2006; pl. II, figs 12, 13). In addition, several unidentified species of *Acanthodiacrodium*,

Baltisphaeridium, *Comasphaeridium*, *Goniosphaeridium*, *Lophosphaeridium*, *Polygonium* and *Micrhystridium* occur sporadically in the studied samples.

The assemblage of borehole AZ-1 is largely comparable (see Nowak et al., 2015). Apart from the rare species, *M.* cf. *inconstans* and *V. areniga* are not recorded from the borehole. *Stellechinatum sicaforme* is present in AZ-1, but was not reported by Nowak et al. (2015).

The acritarchs recovered from the Fezouata Shale include each of the typical elements of the *messaoudensis-trifidum* assemblage. This assemblage was originally described as the 'Watch Hill assemblage' by Molyneux and Rushton (1988) from the Lake District in northern England. It was named the '*trifidum* assemblage' by Fortey et al. (1991), the '*messaoudii-trifidum* assemblage' by Cooper et al. (1995) and subsequently corrected into the '*messaoudensis-trifidum* assemblage' by Servais and Molyneux (1997). The seven diagnostic species (or species groups) of the assemblage are *Acanthodiacrodium*? *dilatum*, *Caldariola glabra* s.l., *Cymatiogalea deunffii*, *C. messaoudensis*, *Stellechinatum sicaforme* s.l., *Stelliferidium trifidum* and *Vavrdovella areniga*. Each is present in the Fezouata Shale, although *A.*? *dilatum* is rare in the outcrop samples and is not observed in borehole samples. Similarly, *V. areniga* is not present in borehole samples.

5.1. Acritarch palaeobiogeography

After its original description from the English Lake District, the *messaoudensis-trifidum* assemblage was reported from other locations in England, Wales, Ireland, Belgium, Turkey, Argentina, Germany, the Czech Republic, Spain and Morocco (Snape, 1993; Molyneux et al., 2007 and references therein; Rubinstein et al., 2007; Aráoz, 2009; de la Puente and Rubinstein, 2009; Toro et al., 2010; Nowak et al., 2015). Aside from the Argentinean occurences, these localities correspond to positions at high southern latitudes during the Early Ordovician according to current palaeogeographical reconstructions (Fig. 5A) (Torsvik and Cocks, 2013). Individual taxa of the *messaoudensis-trifidum* assemblage have also been reported from Baltica and South China (Molyneux et al., 2007 and references therein; Wang et al., 2013a). Given that the reconstructed position of North Africa for the Early Ordovician is relatively close to other localities that yielded the *messaoudensis-trifidum* assemblage, its presence in Morocco is expected, but for a long time was overlooked. Vecoli and Le Hérissé (2004) stated that the *messaoudensis-trifidum* assemblage had not been reported from North Africa and suggested the reason might be a lack of late Tremadocian sediments, unaware that Snape (1993) had in fact noted similarities between the 'Watch Hill assemblage' and one assemblage from the Fezouata Shale in an unpublished PhD thesis.

The *messaoudensis-trifidum* assemblage was regarded as a part of the 'peri-Gondwana' 'Mediterranean' or 'cold-water' province (see Servais et al., 2003 for a discussion), which was originally defined by the presence of *Arbusculidium filamentosum*, *Coryphidium* and *Striatotheca* by Li (1987) in the Floian, in contrast to the 'warm-water' province marked by the genera *Aryballomorpha*, *Athabascaella* and *Lua* (Volkova, 1997). It is now clear that provincialism is not simply related to cold and warm-water environments. Nevertheless, the *messaoudensis-trifidum* assemblage is typical of the margin of Gondwana at high southern latitudes. The reader is referred to Molyneux et al. (2013) for a detailed review of acritarch palaeobiogeography in the Early Ordovician.

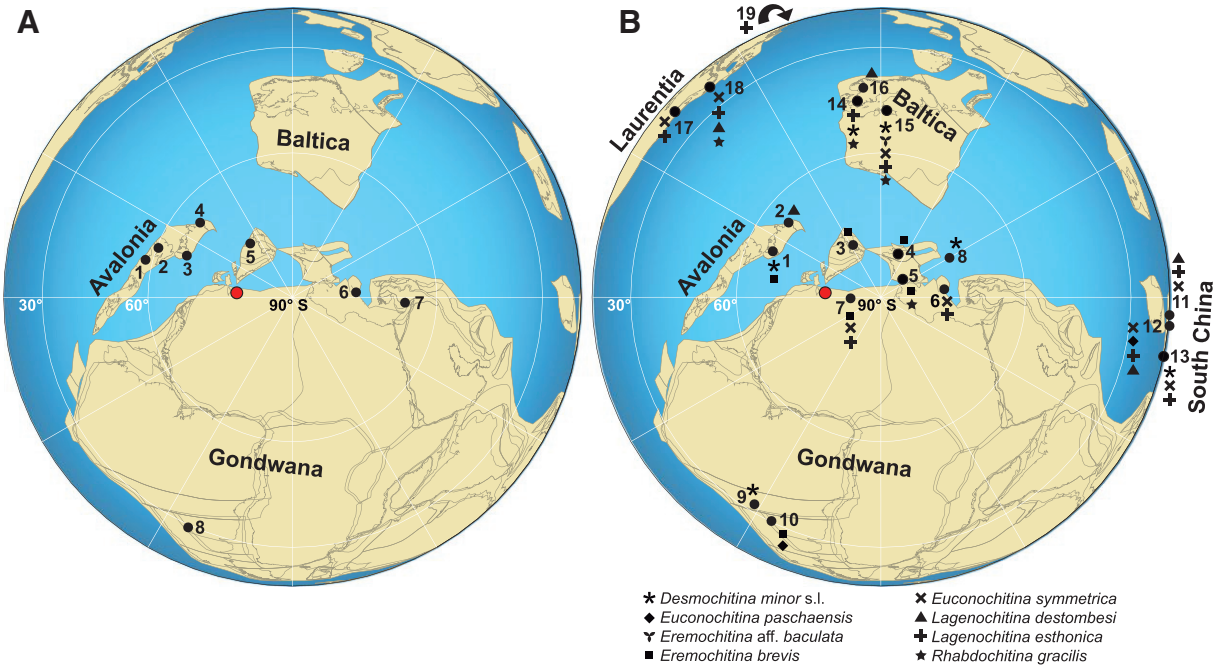

Fig. 5. Palaeogeographical reconstruction of the Early Ordovician (ca. 480 Ma). The base map was derived from BugPlates (see Torsvik, 2009). Red circle = Zagora. Black dots = areas with comparable palynomorphs. A) Distribution of the *messaoudensis-trifidum* acritarch assemblage. (1) Dingle Peninsula, Ireland (Connery and Higgs, 1999; Todd et al., 2000). (2) England, Wales and Isle of Man (Molyneux *in* Chadwick et al., 2001; Cooper and Molyneux, 1990; Molyneux, 1999; Molyneux and Dorning, 1989). (3) Ardennes, Belgium (Breuer and Vanguestaine, 2004; Vanguestaine and Servais, 2002). (4) Rügen, Germany (Servais and Katzung, 1993; Servais and Molyneux, 1997). (5) Sierra Morena, Spain (Mette, 1989, Servais and Mette, 2000). (6) Bohemia, Czech Republic (Fatka, 1993). (7) Southeastern Turkey (Dean and Martin, 1992; Martin, 1996). (8) Northwestern Argentina (de la Puente and Rubinstein, 2009; Rubinstein et al., 2007; Toro et al., 2010). B) Global distribution of chitinozoan species found in the Fezouata Shale during the Early Ordovician. (1) Belgium (Martin, 1969; Samuelsson and Verniers, 2000). (2) Rügen, Germany (Samuelsson, 1999; Samuelsson et al., 2000). (3) Serra do Buçaco, Portugal (Paris, 1981). (4) Mayenne and Orne areas, France (Paris, 1981). (5) Montagne Noire, France (Rauscher, 1968). (6) Bohemia, Czech Republic (Paris and Mergl, 1984; Fatka, 1993, 1999). (7) Algerian Sahara (Taugourdeau and de Jekhowsky, 1960; Benoît and Taugourdeau, 1961; Oulebsir and Paris, 1995). (8) Holy Cross Mountains, Poland (Chlebowski and Szaniawski, 1974). (9) Eastern Cordillera, Bolivia (Heuse et al., 1999). (10) Northwestern Argentina (Ottone et al., 1992; Achab et al., 2006; de la Puente, 2010; de la Puente and Rubinstein, 2009, 2013; Toro et al., 2010). (11) Hubei Province, China (Chen et al., 2008, 2009). (12) Hunan Province, China (Wang et al., 2013b). (13) Yunnan Province, China (Gao, 1986). (14) Skåne, Sweden (Grahn, 1980; Grahn and Nõlvak, 2007). (15) Tallinn, Estonia (Grahn, 1984; Hints and Nõlvak, 2006). (16) Oslo region, Norway (Owen et al., 1990). (17) Québec, Canada (Achab, 1980, 1986). (18) Western Newfoundland, Canada (Batten, 2000). (19) Spitsbergen, Norway (Bockelie, 1980).

5.2. Acritarch biostratigraphy

In general, the *messaoudensis-trifidum* assemblage ranges from the upper Tremadocian *Araneograptus murrayi* (British or Baltoscandic) to the lower Floian *Tetragraptus phyllograptoides* graptolite biozone (Molyneux et al., 2007). Higher biostratigraphic resolution is provided by the definition of five sub-assemblages by Cooper et al. (1995) (Fig. 6). The Tremadocian-Floian boundary presumably coincides with the boundary between sub-assemblages 4 and 5.

The assemblage recovered from the Fezouata Shale, both in the outcrop area near Zagora and in the borehole ~300 km southwest, contains none of the typical elements of assemblages above sub-assemblage 2, such as *Coryphidium* or triangular forms of *Veryhachium*. The presence of *Rhopaliophora palmata* in sample FZ1 13–16 provides an upper limit for the lower boundary of sub-assemblage 2. Because it is a rare species, its absence from lower strata is not diagnostic. The acritarchs of the Fezouata Shale therefore most probably represent sub-assemblage 2 and possibly sub-assemblage 1. The Fezouata assemblage as a whole is most comparable with the *messaoudensis-trifidum* assemblage from northern Germany (Servais and Molyneux, 1997), also attributed to the upper Tremadocian. The sub-assemblages 1 and 2 of the *messaoudensis-trifidum* assemblage have been correlated with the *A. murrayi* and *Hunnegraptus copiosus* graptolite zones (Cooper et al., 1995), also indicating that the Moroccan assemblage corresponds to the upper Tremadocian. The acritarch data are, thus, fully consistent with those provided by graptolite collections from outcrops, which indicate the *A. murrayi* graptolite biozone for the studied strata, with the boundary to the following *H. copiosus* Zone in the uppermost part, from which no palynomorphs were recovered (Martin et al., in press; Gutiérrez-Marco and Martin, 2016–in this issue).

6. Chitinozoans

The chitinozoan assemblages from both the outcrop (Figs. 2, 7) and borehole samples (Figs. 3, 8) are dominated by small species: *Eremochitina brevis* Benoît and Taugourdeau, 1961 (Fig. 8E,F), *Euconochitina* spp. and *Euconochitina*? sp. (Fig. 8D) in the borehole; *Euconochitina* spp., *Desmochitina minor* s.l. Eisenack, 1931 (Fig. 7A,E) and *Desmochitina* sp. (Fig. 7B) in outcrop. *Euconochitina* specimens show a range of morphological variation that encompasses *Eu. paschaensis* de la Puente and Rubinstein, 2009 (Figs. 7F, 8A,G) and *Eu. symmetrica* (Taugourdeau and de Jekhowsky, 1960) (Figs. 7G, 8B,C). The latter is distinguished from the former by a flaring collarette, a character that is not always preserved or easy to recognise. Because specimens in our material assignable to either of these two species seem to be end-members of a single population that also contains a morphological continuum of intermediary specimens, we here use a combined *Eu. paschaensis-symmetrica* group. *Euconochitina*? sp. in the present study closely resembles specimens from the Suri Formation in northwestern Argentina, figured by Achab et al. (2006; pl. V, figs 4, 9, 11, 12) as "*Conochitina* sp.".

Eremochitina aff. *baculata* Taugourdeau and de Jekhowsky, 1960 (Fig. 7K) dominates the assemblage in a single sample, FZ1 13–16, which yields one of the richest assemblages recovered in this study. This species is conspecific with specimens from the Leetse Formation at Tallinn, Estonia, figured by Nõlvak and Grahn (1993; pl. V, fig. E) as "*Eremochitina* sp." and by Hints and Nõlvak (2006; pl. IV, figs. 1-4, 10) as "*Eremochitina* sp. A, aff. *baculata*". A relatively small form of *Lagenochitina esthonica* Eisenack, 1955 (Fig. 7Q) is very abundant in samples FZ1 341–345 and 349–350. Similar specimens were reported by Hints and Nõlvak (2006; pl. IV, figs. 15-26) and from Argentina by de la Puente and Rubinstein (2009; pl. III, fig. 2) as "*Lagenochitina* cf. *longiformis* (Obut, 1995)".

Er. brevis is represented in the outcrop by a few specimens in sample TVDB 12-046 (Fig. 7M), and perhaps by fragments in lower strata. *Euconochitina*? sp. has a limited occurrence in some of the richer samples from Bou Izargane (Fig. 7H), which also yielded *Cyathochitina* aff. *campanulaeformis* (Eisenack, 1931) (Fig. 7C), *Cyathochitina* sp. (Fig. 7D), *Lagenochitina* cf. *obeligis* Paris, 1981 (Fig. 7O) and *Rhabdochitina cf. magna* Eisenack, 1931 (the latter also occurs in borehole samples, see Fig. 8I). The outcrop samples furthermore produced *Eremochitina cf. mucronata* Taugourdeau and de Jekhowsky, 1960 (Fig. 7N), which is smaller than typical for the species, *Clavachitina*? sp. (Fig. 7I) and *Rhabdochitina gracilis* Eisenack, 1962 (Fig. 7J). *Desmochitina* is absent in the borehole samples. Both the borehole and the outcrop samples contained poorly preserved specimens of *Eremochitina* that might pertain to *Er. baculata* (Figs. 7L, 8H), unidentified species of *Lagenochitina* (Fig. 8J), and a few specimens

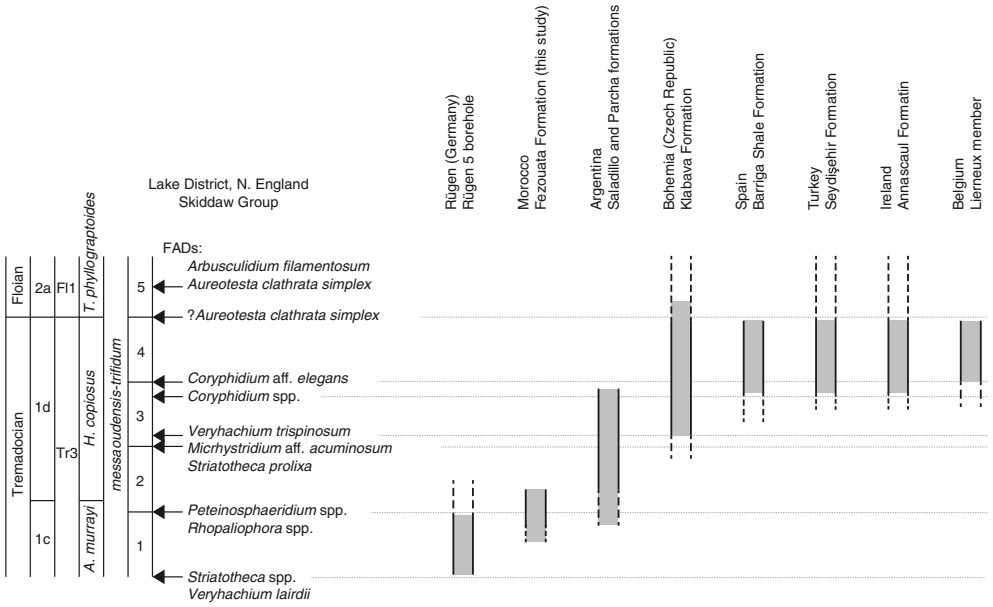

Fig. 6. Distribution of *messaoudensis-trifidum* sub-assemblages. Modified after Molyneux et al. (2007). Sub-assemblages following Cooper et al. (1995), Time Slices following Webby et al. (2004), Stage Slices following Bergström et al. (2009). Data on Argentina were taken from Rubinstein et al. (2007). *T. ph.* = *Tetragraptus phyllograptoides*.

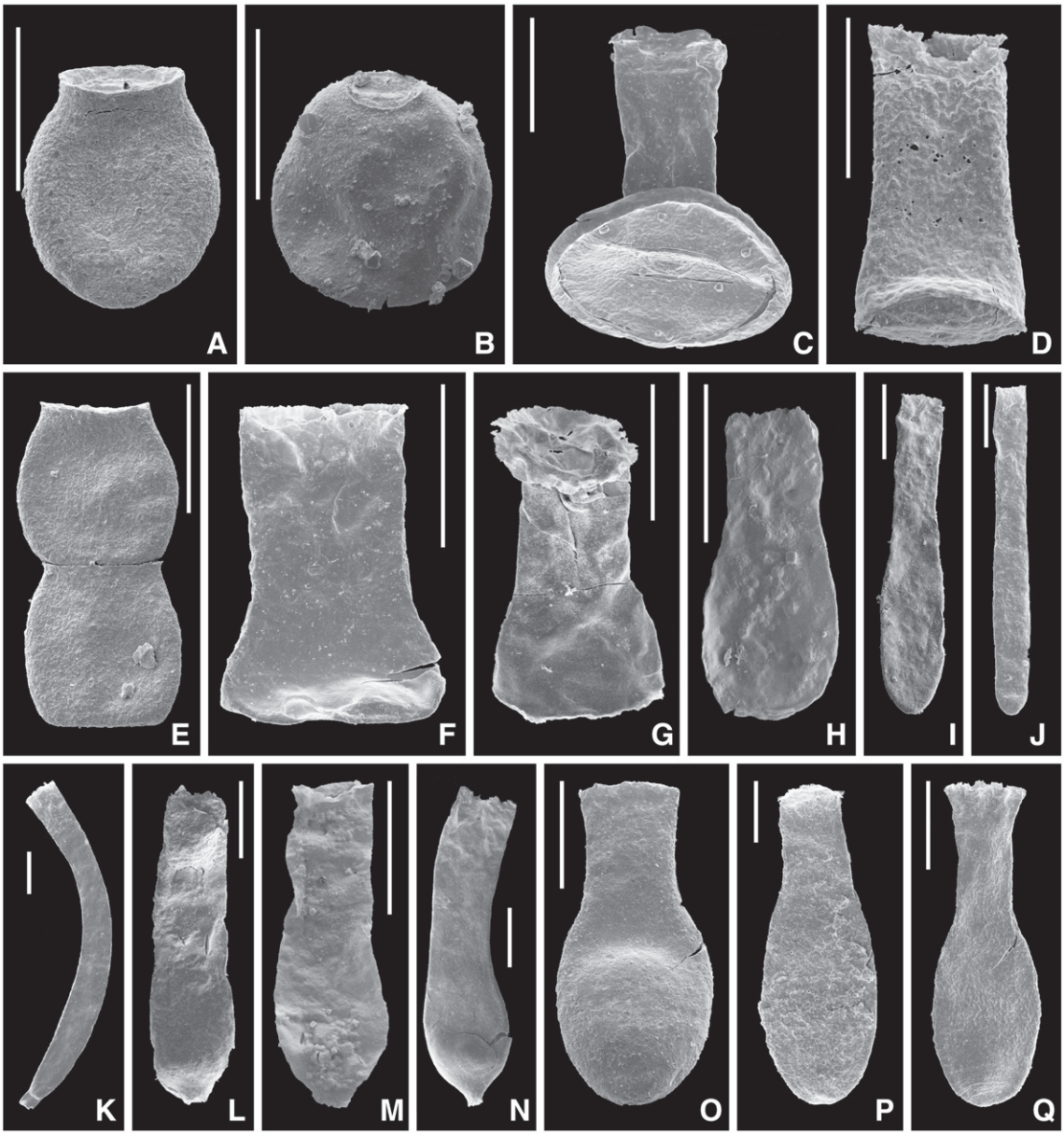

Fig. 7. Selected chitinozoans from the Fezouata Shale near Zagora. Scale bars = 100 μm. A) *Desmochitina minor* s.l. Eisenack, 1931; FZ1 356–360. B) *Desmochitina* sp.; TZ-Paly 1. C) *Cyathochitina* aff. *campanulaeformis* (Eisenack, 1931); FZ1 349–350. D) *Cyathochitina* sp., vesicle wall showing multiple microborings; FZ1 82–89. E) two chained individuals of *Desmochitina minor* s.l. Eisenack, 1931; FZ1 356–360. F–G) *Euconochitina paschaensis-symmetrica* group; F: specimen assignable to *Eu. paschaensis* de la Puente and Rubinstein, 2009; FZ1 13–16. G: specimen assignable to *Eu. symmetrica* (Taugourdeau and de Jekhowsky, 1960); FZ1 31–32. H) *Euconochitina*? sp.; TVDB 12-046. I) *Clavachitina*? sp.; TZ-Paly 1. J) *Rhabdochitina gracilis* Eisenack, 1962; FZ1 13–16. K) *Eremochitina* aff. *baculata* Taugourdeau and de Jekhowsky, 1960; FZ1 13–16. L) *Eremochitina* cf. *baculata* Taugourdeau and de Jekhowsky, 1960; TZ-Paly 10. M) *Eremochitina brevis* (Benoît and Taugourdeau, 1961); TVDB 12–046. N) *Eremochitina cf. mucronata* Taugourdeau and de Jekhowsky, 1960; TZ-Paly 2. O) *Lagenochitina* cf. *obeligis* Paris, 1981; FZ1 66–67. P) *Lagenochitina* cf. *destombesi* Elaouad-Debbaj, 1988; FZ1 4–5. Q) *Lagenochitina esthonica* Eisenack, 1955; FZ1 356–360.

resembling *L. destombesi* Elaouad-Debbaj, 1988, but differing in size or surface structure (Figs. 7P, 8K).

6.1. Chitinozoan palaeobiogeography

The chitinozoans identified in the Fezouata Shale show connections to assemblages from the subsurface of the neighbouring Algerian Sahara (Taugourdeau and de Jekhowsky, 1960; Benoît and Taugourdeau, 1961; Oulebsir and Paris, 1995), but also to the Lower Ordovician of other locations in peri-Gondwana (Czech Republic: Paris and Mergl, 1984; Fatka, 1993, 1999; Belgium: Martin, 1969; Samuelsson and Verniers, 2000; France: Rauscher, 1968; Paris, 1981; Holy Cross Mountains, Poland: Chlebowski and Szaniawski, 1974; Island of Rügen, Germany: Samuelsson, 1999, Samuelsson et al., 2000; Portugal: Paris, 1981), 'western' Gondwana (Argentina: Ottone et al., 1992; Achab et al., 2006; de la Puente and Rubinstein, 2009, 2013; de la Puente, 2010; Toro et al., 2010; Bolivia: Heuse et al., 1999), Baltica (Estonia: Grahn, 1984; Hints and Nõlvak, 2006; Norway: Owen et al., 1990; Sweden: Grahn, 1980; Grahn and Nõlvak, 2007), Laurentia (Quebec: Achab, 1980, 1986; Western Newfoundland: Batten, 2000; Spitsbergen: Bockelie, 1980) and South China (Hunan Province: Wang et al., 2013b; Hubei Province: Chen et al., 2008, 2009; Yunnan Province: Gao, 1986) (Fig. 5B). In terms of numbers of common species, the greatest agreement is with the Estonian assemblage, South China and Western Newfoundland.

Vandenbroucke et al. (2010a, 2010b, 2013) showed that the palaeogeographic distribution of Late Ordovician chitinozoan assemblages reflects palaeoclimatic belts. Except for *Eremochitina brevis*, which is restricted to peri-Gondwana, and *Er.* aff. *baculata*, which until now was only known from Estonia, the chitinozoans present in the

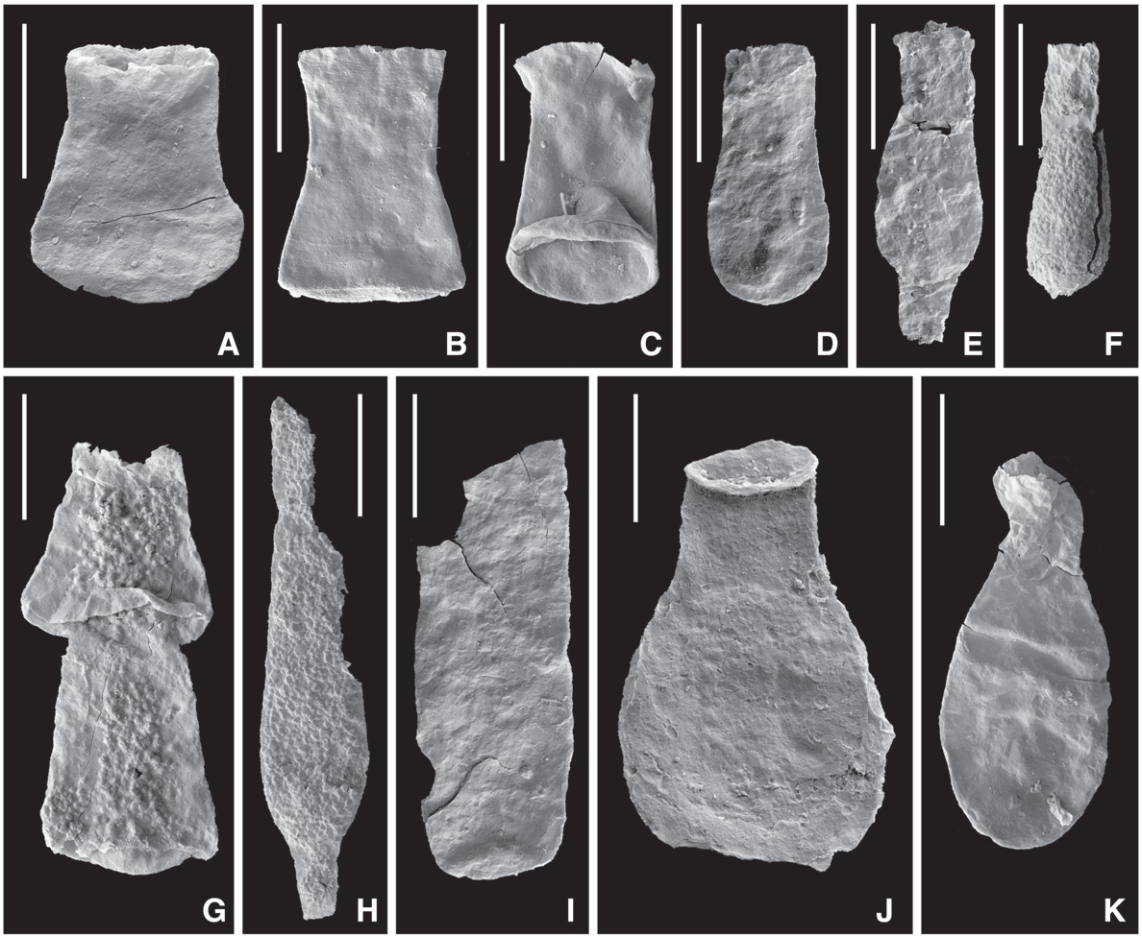

Fig. 8. Selected chitinozoans from the Fezouata Shale in the AZ-1 borehole. Scale bars = 100 μm. A–C,G) *Euconochitina paschaensis-symmetrica* group; A: specimen assignable to *Eu. paschaensis* de la Puente and Rubinstein, 2009; 965 m. B–C: specimen assignable to *Eu. symmetrica* (Taugourdeau and de Jekhowsky, 1960); 965 m. G: two chained individuals assignable to *Eu. paschaensis*; 930 m. D) *Euconochitina*? sp.; 749 m. E–F) *Eremochitina brevis* (Benoît and Taugourdeau, 1961); E: flattened specimen; 874 m, F: specimen with inflated chamber; 905 m. H) *Eremochitina* cf. *baculata* Taugourdeau and de Jekhowsky, 1960; 749 m. I) *Rhabdochitina* cf. *magna* Eisenack, 1931; 699 m. J) *Lagenochitina* sp., 1981; 930 m. K) *Lagenochitina* cf. *destombesi* Elaouad-Debbaj, 1988; 930 m.

Fezouata Shale seem to be characterized by widespread distribution. Pending more complete documentation and analyses of full assemblages through discrete timeslices, the Early Ordovician chitinozoan assemblages do not appear to demonstrate latitudinal constraints.

6.2. Chitinozoan biostratigraphy

A chitinozoan biozonation for Gondwana has been proposed by Paris (1990) and was subsequently calibrated against the current chronostratigraphic stages (Webby et al., 2004). Therein, the total range of *Lagenochitina destombesi* defines the lowermost biozone, representing the upper lower to lower upper Tremadocian. This was based on the discovery of the species in the Fezouata Shale by Elaouad-Debbaj (1988). However, the lower and upper boundaries of its range have not been established. The *L. destombesi* Zone was also adopted as the lowermost chitinozoan biozone in Baltoscandia (Nõlvak, 1999; Nõlvak et al., 2006) and South China (Chen et al., 2009). In Gondwana, it is followed in order by the *Lagenochitina conifundus* Zone, the *Euconochitina symmetrica* Zone, the *Eremochitina baculata* Zone and the *Er. brevis* Zone. The *symmetrica* to *brevis* zones were assigned to the Floian by Webby et al. (2004).

A major constituent of the chitinozoan assemblages in our study is the *Eu. paschaensis-symmetrica* group. According to de la Puente and Rubinstein (2009), *Eu. paschaensis* represents the *conifundus* Zone in Argentina. In our samples, the range of specimens assignable to *Eu. paschaensis* overlaps with that of *L.* cf. *destombesi*. Furthermore, *Eu. paschaensis* shows seamless transitions within populations to *Eu. symmetrica*, the index species of the biozone that follows the *conifundus* Zone in 'northern' Gondwana. In the same samples, *Eremochitina* aff. *baculata*, a species which is close to *Er. baculata*, is abundantly present, although no unambiguous examples of actual *Er. baculata* were recovered. A few specimens from slightly higher up in the stratigraphy are assignable to *Er. brevis*, which traditionally is taken to indicate a (late) Floian age, but still falls into the range of the *messaoudensis-trifidum* acritarch assemblage and the graptolite *A. murrayi*. In the borehole, *Er. brevis* also coincides with essentially the same acritarch assemblage, although not at its first downhole appearance, which would be more explicit. It is also interesting to note that in the borehole, the intervals with abundant acritarchs and chitinozoans respectively are hardly overlapping (and are most likely extended downwards due to mixing with cuttings from overlying strata in the drilling fluid), suggesting that, if the acritarch assemblages are coeval, the chitinozoans from the surface are probably for the most part older than those from the borehole.

Our data indicate an overlap between the ranges of *Eu. symmetrica* (as part of the *paschaensis-symmetrica* group) and *Er. brevis* (in the borehole and in sample TVDB 12-046). The overlapping ranges of these index fossils necessitate a redefinition of their respective biozones from total-range zones to partial-range zones (i.e., biozones defined to span the interval from the FAD of the index fossil to the FAD of the index fossil of the overlying biozone), which has become the standard way of defining chitinozoan biozones (Verniers et al., 1995; Vandenbroucke, 2008). Awaiting a formal redefinition of these

biozones, we have here established a local biozonation using the partial range zones for the *Eu. paschaensis-symmetrica* group and *Er. brevis*.

If we follow the calibrations in Webby et al. (2004), the chitinozoan ranges and biozones would point to a Floian age of the Fezouata Lagerstätte. However, this would be at odds with acritarch and graptolite biostratigraphy, which both clearly suggest a Tremadocian age (Martin et al., in press; Gutiérrez-Marco and Martin, 2016–in this issue). This example suggests that the chronostratigraphy and age assignments of chitinozoan biozones may be in need of revision (following a global survey of the co-occurrence of the index taxa and those of other fossil groups).

7. Preservation, taphonomy and palaeoenvironment

The acritarchs and chitinozoans of the Fezouata Shale show a mixture of preservational states with well-preserved and badly degraded specimens in the same samples. This pattern may point to exhumation and resedimentation or differential transport histories of individual fossils within single samples. This is consistent with regular disturbance by storms and thus with sedimentological interpretations of the Fezouata (Martin et al., in press; Vaucher et al., 2016–in this issue). The preservation also usually shows a variation between flattened and three-dimensional individuals within individual samples. In chitinozoans, the chamber often remains partially inflated, while the neck is compressed (e.g. Figs. 7D,O, 8F). In acritarchs, three-dimensionality is mostly retained in vesicles with a thick wall, and in larger (>50 μm) sphaeromorphs. Three-dimensional specimens are not equally distributed and are most common in samples from Bou Izargane and in borehole samples corresponding to 734, 905 and 940 m depths. This suggests temporal changes in the taphonomic histories of at least a part of the organic-walled microfossils, which might be related to the exceptional preservation of macrofossils in the same layers at Bou Izargane.

The surface and eventual ornamentation of chitinozoans is often abraded, although the taxon *Desmochitina minor* represents a notable exception in that it usually retains a granular surface to some degree. Some specimens of *Lagenochitina* also show a structured surface. The abrasion can be attributed to transport before burial and possibly, in some cases, resedimentation.

Chitinozoan vesicle walls are often perforated by microborings (Fig. 7D), sometimes heavily. Such microborings have been attributed to bacteria and fungi (Eisenack, 1973; Grahn, 1981). They might represent parasites on the living organism or digestion of shed shells (Wrona, 1980; Grahn, 1981). Vesicles with a high density of microborings are typically poorly preserved (abraded and fragmented), implying an extended period of exposure. Acritarchs rarely show microborings.

The chitinozoan assemblages are dominated by small species, while larger forms are rare except in samples FZ1 13–16 and TZ-Paly 1, 2 and 13. The sample FZ1 13–16 is particularly interesting, as it is directly adjacent to FZ1 19–20. Both samples yielded extremely abundant and well-preserved chitinozoans of mostly the same species (a few more in the latter case), but while the lower sample is dominated by the particularly large *Er.* aff. *baculata* and *Rhabdochitina gracilis*, these are rare in the overlying sample, and mostly represented by fragments. Such fragments of large tubular chitinozoans are relatively common in other samples too, while complete specimens are overall rare. This points to size sorting and possibly a higher tendency of long and narrow forms to break during transport (although the breaking of large vesicles can also partly be explained by a size dependant higher probability of fragmentation by the formation of cracks in the host rock and during the maceration process). The fact that chains of *D. minor* and *Eu. paschaensis* are observed (Figs. 7E, 8G), but none that include more than two individuals, is consistent with this pattern.

The best preserved acritarch assemblages from both outcrop and borehole samples are dominated by galeate and polygonomorph species, and generally show a rather high diversity of spiny forms. According to studies on the distribution of acritarch groups in relation to the distance from the shoreline, this indicates an open shelf environment, a fair distance away from the shore and not shallow (e.g. Li et al., 2004; Lei et al., 2012). This is in agreement with an offshore environmental setting close to storm wave-base interpreted by Martin et al. (in press) for the same stratigraphic interval of the Fezouata Shale. Nearshore assemblages are typically less diverse and dominated by smooth-walled forms and species of *Micrhystridium* with short spines (e.g. Stricanne et al., 2004).

Comparison of assemblages from Bou Izargane (FZ1) with those from approximately coeval horizons at Tizig Zaouine (TZ-Paly 5–7; see Fig. 2) suggests a pronounced effect of oxidative weathering on the organic palynomorph remains. The dark grey FZ1 samples yield the most diverse and abundant assemblages recovered from surface materials, and include the best states of preservation (Fig. 4, 7), while more intensely weathered samples from coeval strata at Tizig Zaouine yield primarily fragmented material with substantially reduced diversity of identifiable forms. These findings underscore the susceptibility of thin organic remains to degradation during oxidative weathering. They also support previous observations that the taphonomic expression of the soft-bodied macrofossils of the Fezouata Shale has been profoundly affected by oxidative weathering (Van Roy et al., 2010, 2015a), as also observed in the early Cambrian Chengjiang biota (Forchielli et al., 2014). It is not yet clear whether the absence of Small Carbonaceous Fossils is due to wheathering, or whether the taphonomy of the Fezouata Shale, even in Lagerstätten bearing strata, prevented their preservation in the first place. A currently planned drilling through a site with exceptional preservation might answer this question and others regarding the preservational mode of the Fezouata Lagerstätte, if unaltered material can be obtained.

While the presence/absence patterns of palynomorphs in the outcrop samples can mostly be attributed to surface weathering, the absence of palynomorphs at certain levels in the borehole cannot be explained as such, but the presence of opaque organic matter suggests the influence of alteration. The unequal distribution of acritarchs and chitinozoans means that either alteration affected the two groups differently, or that this pattern reflects original ecological and/or taphonomic effects. The differences in preservation are not related to conspicuous variations in lithology. Furthermore, the pattern is different between the Zagora and Adrar Zouggar areas, as the palynomorph assemblages in the borehole appear to be more stratigraphically restricted than those from the studied outcrops. Specifically, no acritarchs that are evidently younger and no chitinozoans that are evidently older than the studied outcrop interval were found in the borehole, but younger acritarch assemblages have been reported from the Upper Fezouata Formation (Deunff, 1968b; Snape, 1993), and older chitinozoans from the Lower Fezouata Formation (Elaouad-Debbaj, 1988).

8. Conclusions

The present palynological study focuses on the Lagerstätte in the Lower Fezouata Formation, i.e. the part of the succession bearing exceptionally preserved fossils. Two palynological techniques were used (a standard and a low-manipulation technique) which have yielded abundant and diverse acritarchs and chitinozoans, but no 'Small Carbonaceous Fossils'.

The presence of the *messaoudensis-trifidum* acritarch assemblage in this interval is confirmed. Acritarch assemblages from the outcrop and the borehole AZ-1 are overall comparable. They correspond to sub-assemblages 1–2 (in the outcrops mostly 2, possibly 1 in the lowest part) of the *messaoudensis-trifidum* assemblage, indicating a late Tremadocian age, which is in accordance with a previous assignment of the *A. murrayi* graptolite biozone to this interval. The occurrence of the *messaoudensis-trifidum* assemblage in the Early Ordovician of Morocco provides further evidence for its biogeographical

distribution on the margin of Gondwana at high latitudes (peri-Gondwana).

The chitinozoans of the Fezouata Shale show connections to other sites in peri-Gondwana, but also to western Gondwana, Baltica, Laurentia and South China. The chitinozoans from the levels attributed clearly to the late Tremadocian include the index species of the *Euconochitina symmetrica* and *Eremochitina brevis* biozones, which are so far considered to be indicative of the early and late Floian. These results indicate that the calibration between the chronostratigraphic stages and the chitinozoan biozonation for the Gondwanan margin may require revision.

Acknowledgements

We thank the ONHYM (Office National des Hydrocarbures et des Mines, Rabat, Morocco) for granting access to the borehole material and giving permission for publication. Peter Van Roy is acknowledged for providing outcrop samples. Laurence Debeauvais (CNRS, University of Lille) performed the acid treatment of rock samples. We also thank Wang Wenhui, G. Susana de la Puente and an anonymous reviewer for their constructive comments and suggestions. This study is financed as part of the RALI (Rise of Animal Life) project, which is funded by the ANR (Agence Nationale de la Recherche, France; grant number ANR-11-BS56-0025). This paper is a contribution to the IGCP project 591—'The Early to Middle Palaeozoic Revolution'.

References

Aceñolaza, F.G., Aceñolaza, G.F., Esteban, S.B., Gutiérrez-Marco, J.C., 1996. Estructuras nemales de *Araneograptus murrayi* (J. Hall)(graptolito del Ordovícico Inferior) y actualización del registro perigondwánico de la especie. Memorias Del XII Congreso Geológico de Bolivia, Tarija, pp. 681–689.

Achab, A., 1980. Chitinozoaires de l'Arenig inferieur de la formation de Lévis (Québec, Canada). Rev. Palaeobot. Palynol. 31, 219–239. http://dx.doi.org/10.1016/0034-6667(80)90028-7.

Achab, A., 1986. Assemblages de chitinozoaires dans l'Ordovicien inférieur de l'est du Canada. Can. J. Earth Sci. 23, 682–695.

Achab, A., Rubinstein, C.V., Astini, R.A., 2006. Chitinozoans and acritarchs from the Ordovician peri-Gondwana volcanic arc of the Famatina System, northwestern Argentina. Rev. Palaeobot. Palynol. 139, pp. 129–149. http://dx.doi.org/10.1016/j.revpalbo.2005.07.004.

Aráoz, L., 2009. Microfloras ordovícicas en Sierra de Zenta, Cordillera Oriental Argentina. Ser. Correl. Geol. 25, 37–94.

Batten, R.S.R., 2000. Biostratigraphy of the Lower Ordovician Chitinozoa of Western Newfoundland, Canada (M. Sc.). Memorial University of Newfoundland http://research.library.mun.ca/6542/ (accessed 10 June 2015).

Benoît, A., Taugourdeau, P., 1961. Quelques chitinozoaires de l'Ordovicien du Sahara. Rev. Inst. Fr. Pétrol. 16, 1403–1421.

Bergström, S.M., Chen, X., Gutiérrez-Marco, J.C., Dronov, A., 2009. The new chronostratigraphic classification of the Ordovician System and its relations to major regional series and stages and to δ13C chemostratigraphy. Lethaia 42, 97–107. http://dx.doi.org/10.1111/j.1502-3931.2008.00136.x.

Bockelie, T.G., 1980. Early Ordovician chitinozoa from Spitsbergen. Palynology 4, 1–14. http://dx.doi.org/10.1080/01916122.1980.9989198.

Breuer, P., Vanguestaine, M., 2004. The latest Tremadocian *messaoudensis-trifidum* acritarch assemblage from the upper part of the Lierneux Member (Salm Group, Stavelot Inlier, Belgium). Rev. Palaeobot. Palynol. 130, 41–58.

Burmann, G., 1970. Weitere organische Mikrofossilien aus dem unteren Ordovizium. Paläontol. Abh. 3, 289–332.

Butterfield, N.J., 1995. Secular distribution of Burgess-Shale-type preservation. Lethaia 28, 1–13.

Butterfield, N.J., Harvey, T.H.P., 2012. Small carbonaceous fossils (SCFs): a new measure of early Paleozoic paleobiology. Geology 40, 71–74. http://dx.doi.org/10.1130/G32580.1.

Chadwick, R.A., Jackson, D.I., Barnes, R.P., Kimbell, G.S., Johnson, H., Chiverrell, R.C., Thomas, G.S.P., Jones, N.S., Riley, N.J., Pickett, E.A., Young, B., Holliday, D.W., Ball, D.F., Molyneux, S.G., Long, D., Power, G.M., Roberts, D.H., 2001. Geology of the Isle of Man and its offshore area. Br. Geol. Surv. Res. Rep.

Chatterton, B.D.E., Fortey, R.A., 2008. Linear clusters of articulated trilobites from Lower Ordovician (Arenig) strata at Bini Tinzoulin, north of Zagora, southern Morocco. In: Rábano, I., Gozalo, R., Capdevila, D.G.-B. (Eds.), Advances in Trilobite Research, Cuadernos Del Museo Geominero. Instituto Geológico y Minero de España, Madrid, pp. 73–78.

Chauvel, J., Regnault, S., 1986. Variabilité du genre *Rhopalocystis* Ubaghs, eocrinoïde du trémadocien de l'anti-atlas marocain. Geobios 19, 863–870. http://dx.doi.org/10.1016/S0016-6995(86)80113-9.

Chen, X., Paris, F., Zhang, M., 2008. Chitinozoans from the Fenxiang Formation (Early Ordovician) of Yichang, Hubei Province, China. Acta Geol. Sin. 82, 287–294. http://dx.doi.org/10.1111/j.1755-6724.2008.tb00579.x.

Chen, X., Paris, F., Wang, X., Zhang, M., 2009. Early and Middle Ordovician chitinozoans from the Dapingian type sections, Yichang area, China. Rev. Palaeobot. Palynol. 153, 310–330. http://dx.doi.org/10.1016/j.revpalbo.2008.09.006.

Chlebowski, R., Szaniawski, H., 1974. Chitinozoa from the Ordovician conglomerates at Międzygórz in the Holy Cross Mts. Acta Geol. Pol. 24, 221–230.

Choubert, G., 1942. Constitution et puissance de la série primaire de l'Anti-Atlas. C. R. Acad. Sci. Paris 215, 445–447.

Cocks, L.R.M., Fortey, R.A., 2009. Avalonia: a long-lived terrane in the Lower Palaeozoic? Geol. Soc. Lond. Spec. Publ. 325, 141–155. http://dx.doi.org/10.1144/SP325.7.

Combaz, A., 1967. Un microbios du Trémadocien dans un sondage d'Hassi-Messaoud. Actes Soc. Linn. Bordeaux. 104, 1–26.

Combaz, A., Péniguel, G., 1972. Étude palynostratigraphique de l'Ordovicien dans quelques sondages du Bassin de Canning (Australie Occidentale). Bull. Cent. Rech. Pau SNPA 6, 121–167.

Connery, C., Higgs, K.T., 1999. Tremadoc-Arenig acritarchs from the Annascaul Formation, Dingle Peninsula, Co. Kerry, Ireland. Boll. Della Soc. Geol. Ital. 38, 133–154.

Cooper, A.H., Molyneux, S.G., 1990. The age and correlation of Skiddaw Group (early Ordovician) sediments in the Cross Fell inlier (Northern England). Geol. Mag. 127, 147–157. http://dx.doi.org/10.1017/S0016756800013832.

Cooper, A.H., Rushton, A.W.A., Molyneux, S.G., Hughes, R.A., Moore, R.M., Webb, B.C., 1995. The stratigraphy, correlation, provenance and palaeogeography of the Skiddaw Group (Ordovician) in the English Lake District. Geol. Mag. 132, 185–211. http://dx.doi.org/10.1017/S0016756800011742.

Corbacho, J., López-Soriano, F.J., 2012. A new asaphid trilobite from the Lower Ordovician (Arenig) of Morocco—Un nuevo trilobites asáfido del Ordovícico Inferior (Arenig) de Marruecos. Batalleria 17, 3–11.

Corbacho, J., Vela, J.A., 2010. Giant Trilobites from Lower Ordovician of Morocco. Batalleria 15, 3–32.

Corbacho, J., Vela, J.A., 2011. Revisión de las especies de *Lehua* de la región de Zagora (Marruecos). Batalleria 16, 46–49.

Corbacho, J., Vela, J.A., 2013. *Parvilichas marochii*: new genus and species of Lichidae from the Zagora Region (Morocco), Early Ordovician (Floian). *Scr. Mus*ei Geol. Semin. Barc. Ser. Palaeontol. 14, 3–13.

Cramer, F.H., Díez, M. del C.R., 1977. Late Arenigian (Ordovician) acritarchs from Cis-Saharan Morocco. Micropaleontology 23, 339–360.

de la Puente, G.S., 2010. Quitinozoos del Floiano (Ordovícico Inferior) del área de Santa Victoria, Cordillera Oriental, noroeste argentino: Sistemática. Ameghiniana 47, 217–238.

de la Puente, G.S., Rubinstein, C.V., 2009. Late Tremadocian chitinozoans and acritarchs from northwestern Argentina (Western Gondwana). Rev. Palaeobot. Palynol. 154, 65–78. http://dx.doi.org/10.1016/j.revpalbo.2008.12.006.

de la Puente, G.S., Rubinstein, C.V., 2013. Ordovician chitinozoans and marine phytoplankton of the Central Andean Basin, northwestern Argentina: a biostratigraphic and paleobiogeographic approach. Rev. Palaeobot. Palynol. 198, 14–26. http://dx.doi.org/10.1016/j.revpalbo.2012.03.007.

Dean, W.T., Martin, F., 1992. Ordovician biostratigraphic correlation in southern Turkey. In: Webby, B.D., Laurie, J.R. (Eds.), Global Perspectives on Ordovician Geology. Balkema, Rotterdam, pp. 195–203.

Deflandre, G., 1946. Hystrichosphaeridés II. Espèces du Secondaire et du Tertiaire. Fich. Micropaléontologique 6, *Arch. Orig. Centre Ddoc.* CNRS 3235, 860–1019.

Destombes, J., 1962. Stratigraphie et paléogéographie de l'Ordovicien de l'Anti-Atlas (Maroc). Un essai de synthèse. Bull. Soc. Géol. Fr. 7, 453–460.

Destombes, J., Hollard, H., Willefert, S., 1985. Lower Palaeozoic rocks of Morocco. In: Holland, C.H. (Ed.), Lower Palaeozoic of North-Western and West-Central Africa. Lower Palaeozoic Rocks of the World. John Wiley & Sons, Chichester, pp. 157–184.

Deunff, J., 1968a. Sur une forme nouvelle d'Acritarche possédant une ouverture polaire (*Veryhachium miloni* n. sp.) et sur la présence d'une colonie de *Veryhachium* dans le Trémadocien marocain. C. R. Seances Acad. Sci. D 267, 46–49.

Deunff, J., 1968b. *Arbusculidium*, genre nouveau d'acritarche du Trémadocien marocain. C.R. Somm. Séances Soc. Géol. Fr. 3, 101–102.

Donovan, S.K., Savill, J.J., 1988. *Ramseyocrinus* (Crinoidea) from the Arenig of Morocco. J. Paleontol. 62, 283–285.

Downie, C., 1958. An assemblage of microplankton from the Shineton Shales (Tremadocian). Proc. Yorks. Geol. Polytech. Soc. 31, 331–350. http://dx.doi.org/10.1144/pygs.31.4.331.

Eisenack, A., 1931. Neue Mikrofossilien des baltischen Silurs. I. Palaeontol. Z. 13, 74–118.

Eisenack, A., 1955. Chitinozoen, Hystrichosphären und andere Mikrofossilien aus dem *Beyrichia*-Kalk. Senckenb. Lethaea 36, 157–188.

Eisenack, A., 1962. Neotypen baltischer Silur-Chitinozoen und neue Arten. N. Jb. Geol. Paläont. (Abh.) 114, 291–316.

Eisenack, A., 1973. Kleinorganismen als Zerstörer säurefester organischer Substanzen und von Biophosphaten. Paläontol. Z. 47, 8–16. http://dx.doi.org/10.1007/BF02989558.

Eisenack, A., Cramer, F.H., Díez, M. del C.R., 1976. Katalog Der Fossilen Dinoflagellaten, Hystrichosphären Und Verwandten Mikrofossilien. Band IV Acritarcha 2. Teil. E. Schweizerbart'sche Verlagsbuchhandlung, Stuttgart.

Elaouad-Debbaj, Z., 1984. Acritarches et chitinozoaires de l'Arenig-Llanvirn de l'Anti-Atlas (Maroc). Rev. Palaeobot. Palynol. 43, 67–88. http://dx.doi.org/10.1016/0034-6667(84)90027-7.

Elaouad-Debbaj, Z., 1988. Acritarches et chitinozoaires du Trémadoc de l'Anti-Atlas central (Maroc). Rev. Micropaleontol. 31, 85–128.

Evitt, W.R., 1963. A discussion and proposals concerning fossil dinoflagellates, hystrichospheres, and acritarchs, II. Proc. Natl. Acad. Sci. U. S. A. 49, 298–302.

Fatka, O., 1993. Chitinozoans and acritarchs in latest Tremadoc-early Arenig sediments of the Prague Basin, Czech Republic. Spec. Pap. Palaeontol. 48, 29–36.
Fatka, O., 1999. Organic walled microfossils of the Barrandian area: a review. J. Czech Geol. Soc. 44, 31–42.
Fensome, R.A., Williams, G.L., Barss, M.S., Freeman, J.M., Hill, J.M., 1990. Acritarchs and Fossil Prasinophytes: An Index to Genera, Species and Infraspecific Taxa, AASP Contributions Series. American Association of Stratigraphic Palynologists Foundation.
Forchielli, A., Steiner, M., Kasbohm, J., Hu, S., Keupp, H., 2014. Taphonomic traits of clay-hosted early Cambrian Burgess Shale-type fossil Lagerstätten in South China. Palaeogeogr. Palaeoclimatol. Palaeoecol. 398, 59–85. http://dx.doi.org/10.1016/j.palaeo.2013.08.001.
Fortey, R.A., 2009. A new giant asaphid trilobite from the Lower Ordovician of Morocco. Assoc. Australas. Paleontol. Mem. 9.
Fortey, R.A., 2011. Trilobites of the genus *Dikelokephalina* from Ordovician Gondwana and Avalonia. Geol. J. 46, 405–415. http://dx.doi.org/10.1002/gj.1275.
Fortey, R.A., 2012. The first known complete Lichakephalid trilobite, lower Ordovician of Morocco. Assoc. Australas. Paleontol. Mem. 42, 1–7.
Fortey, R.A., Bassett, M.G., Harper, D.A.T., Hughes, R.A., Ingham, J.K., Molyneux, S.G., Owen, A.W., Owens, R.M., Rushton, A.W.A., Sheldon, P.R., 1991. Progress and problems in the selection of stratotypes for the bases of series in the Ordovician System of the historical type area in the UK. In: Barnes, C.R., Williams, S.H. (Eds.), Advances in Ordovician Geology. Geological Survey of Canada Paper, Geological Survey of Canada, pp. 5–25.
Gaines, R.R., 2014. Burgess Shale-type preservation and its distribution in space and time. In: Laflamme, M., Schiffbauer, J.D., Darroch, S. (Eds.), Reading and Writing of the Fossil Record: Preservational Pathways to Exceptional Fossilization. The Paleontological Society Papers Vol. 20, pp. 123–146.
Gaines, R.R., Briggs, D.E.G., Zhao, Y.L., 2008. Burgess Shale-type deposits share a common mode of fossilization. Geology 36, 755–758.
Gaines, R.R., Briggs, D.E.G., Orr, P.J., Van Roy, P., 2012. Preservation of giant anomalocaridids in silica-chlorite concretions from the Early Ordovician of Morocco. PALAIOS 27, 317–325. http://dx.doi.org/10.2110/palo.2011.p11-093r.
Gao, L.D., 1986. Lower Ordovician Chitinozoans from Wuding and Luquan, Yunnan Province. Prof. Pap. Stratigr. Palaeontol. 14, 133–152.
Geyer, G., Landing, E., 2006. Latest Ediacaran and Cambrian of the Moroccan Atlas regions. In: Geyer, G., Landing, E. (Eds.), Morocco 2006. Ediacaran–Cambrian Depositional Environments and Stratigraphy of the Western Atlas Regions. Explanatory Description and Field Excursion Guide, Beringeria Special Issue, pp. 7–46.
Grahn, Y., 1980. Early Ordovician Chitinozoa from Öland, Sveriges Geologiska Undersökning, Ser. C. Uppsala.
Grahn, Y., 1981. Parasitism on Ordovician Chitinozoa. Lethaia 14, 135–142. http://dx.doi.org/10.1111/j.1502-3931.1981.tb01914.x.
Grahn, Y., 1984. Ordovician chitinozoa from Tallinn, northern Estonia. Rev. Palaeobot. Palynol. 43, 5–31. http://dx.doi.org/10.1016/0034-6667(84)90025-3.
Grahn, Y., Nõlvak, J., 2007. Ordovician Chitinozoa and biostratigraphy from Skåne and Bornholm, southernmost Scandinavia—an overview and update. Bull. Geosci. 82, 11–26.
Gutiérrez-Marco, J.C., Martin, E.L.O., 2016. Biostratigraphy and palaeoecology of Lower Ordovician graptolites from the Fezouata Shale (Moroccan Anti-Atlas). Palaeogeogr. Palaeoclimatol. Palaeoecol. 460, 35–49 (in this issue)
Henry, J.-L., Vizcaïno, D., Destombes, J., 1992. Evolution de l'œil et hétérochronie chez les trilobites ordoviciens *Ormathops* Delo, 1935 et *Toletanaspis* Rabano, 1989 (Dalmanitidae, Zeliszkellinae). Paläontol. Z. 66, 277–290.
Heuse, T., Grahn, Y., Erdtmann, B.-D., 1999. Early Ordovician chitinozoans from the East Cordillera of Southern Bolivia. Rev. Micropaleontol. 42, 43–55. http://dx.doi.org/10.1016/S0035-1598(99)90175-7.
Hints, O., Nõlvak, J., 2006. Early Ordovician scolecodonts and chitinozoans from Tallinn, North Estonia. Rev. Palaeobot. Palynol. 139, 189–209.
Horný, R.J., 1997. Ordovician Tergomya and Gastropoda (Mollusca) of the Anti-Atlas (Morocco). Acta Mus. Natl. Pragae B 53, 37–78.
Jacobson, S.R., Achab, A., 1985. Acritarch biostratigraphy of the *Dicellograptus complanatus* graptolite zone from the Vaureal formation (Ashgillian), Anticosti Island, Quebec, Canada. Palynology 9, 165–198. http://dx.doi.org/10.1080/01916122.1985.9989294.
Jardiné, S., Combaz, A., Magloire, L., Peniguel, G., Vachey, G., 1974. Distribution stratigraphique des acritarches dans le paléozoïque du sahara algérien. Rev. Palaeobot. Palynol. 18, 99–129. http://dx.doi.org/10.1016/0034-6667(74)90012-8.
Kröger, B., Lefebvre, B., 2012. Palaeogeography and palaeoecology of early Floian (Early Ordovician) cephalopods from the Upper Fezouata Formation, Anti-Atlas, Morocco. Foss. Rec. 15, 61–75. http://dx.doi.org/10.1002/mmng.201200004.
Lefebvre, B., Botting, J.P., 2007. First report of the mitrate *Peltocystis cornuta* Thoral (Echinodermata, Stylophora) in the Lower Ordovician of central Anti-Atlas (Morocco). Ann. Paléontol. 93, 183–198. http://dx.doi.org/10.1016/j.annpal.2007.06.003.
Lefebvre, B., El Hariri, K., Lerosey-Aubril, R., Servais, T., Van Roy, P., 2016. The Fezouata Shale (Lower Ordovician, Anti-Atlas, Morocco): A historical review. Palaeogeogr. Palaeoclimatol. Palaeoecol. 460, 7–23. http://dx.doi.org/10.1016/j.palaeo.2015.10.048 (in this issue).
Lehnert, O., Nowak, H., Sarmiento, G.N., Gutiérrez-Marco, J.C., Akodad, M., Servais, T., 2016. Conodonts from the Lower Ordovician of Morocco -contributions to age and faunal diversity of the Fezouata Lagerstätte and peri-Gondwana biogeography. Palaeogeogr. Palaeoclimatol. Palaeoecol. 460, 50–61 (in this issue).
Lei, Y., Servais, T., Feng, Q., He, W., 2012. The spatial (nearshore–offshore) distribution of latest Permian phytoplankton from the Yangtze Block, South China. Palaeogeogr. Palaeoclimatol. Palaeoecol. 363–364, 151–162. http://dx.doi.org/10.1016/j.palaeo.2012.09.010.
Li, J., 1987. Ordovician acritarchs from the Meitan Formation of Guizhou province, southwest China. Palaeontology 30, 613–634.
Li, J., Servais, T., Yan, K., Zhu, H., 2004. A nearshore–offshore trend in acritarch distribution from the Early–Middle Ordovician of the Yangtze Platform, South China. Rev. Palaeobot. Palynol. 130, pp. 141–161. http://dx.doi.org/10.1016/j.revpalbo.2003.12.005.
Loeblich Jr., A.R., 1970. Morphology, ultrastructure and distribution of Paleozoic acritarchs. Proceedings of the North American Paleontological Convention. Chicago (1969), pp. 705–788.
Loeblich Jr., A.R., Tappan, H., 1969. Acritarch excystment and surface ultrastructure with descriptions of some Ordovician taxa. Rev. Esp. Micropaleontol. 1, 45–57.
Loeblich Jr., A.R., Tappan, H., 1976. Some new and revised organic-walled phytoplankton microfossil genera. J. Paleontol. 50, 301–308.
Martin, F., 1969. Les acritarches de l'Ordovicien et du Silurien belges: Détermination et valeur stratigraphique. Inst. R. Sci. Nat. Belg. Mém. 160, 1–175.
Martin, F., 1972. Les acritarches de l'Ordovicien inférieur de la Montagne Noire (Hérault, France). Bull. Inst. R. Sci. Nat. Belg. Sci. Terre 48, 1–61.
Martin, F., 1975. Acritarches du Cambro-Ordovicien du Massif du Brabant, Belgique. Bull. Inst. R. Sci. Nat. Belg. Sci. Terre 51, 1–33.
Martin, F., 1996. Recognition of the acritarch-based *trifidum* flora (Ordovician) in the absence of the eponymous species. Bull. Inst. R. Sci. Nat. Belg. Sci. Terre 66, 5–13.
Martin, E.L.O., Pittet, B., Gutiérrez-Marco, J.-C., Vannier, J., El Hariri, K., Lerosey-Aubril, R., Masrour, M., Nowak, H., Servais, T., Vandenbroucke, T.R.A., Van Roy, P., Vaucher, R., Lefebvre, B., 2016. The Lower Ordovician Fezouata Konservat-Lagerstätte from Morocco: age, environment and evolutionary perspectives. Gondwana Res. http://dx.doi.org/10.1016/j.gr.2015.03.009 (in press).
Mergl, M., 1988. *Incorthis* (Orthida, Brachiopoda) from the Lower Ordovician (Arenig) of Morocco. Čas. Mineral. Geol. 33, 199–200.
Mette, W., 1989. Acritarchs from Lower Paleozoic rocks of the western Sierra Morena, SW-Spain and biostratigraphic results. Geol. Palaeontol. 23, 1–19.
Molyneux, S.G., 1987. II. Appendix. Acritarchs and chitinozoa from the Arenig Series of south-west Wales. Bull. Br. Mus. Nat. Hist. Geol. 41, 309–364.
Molyneux, S.G., 1999. A reassessment of Manx Group acritarchs, Isle of Man. Geol. Soc. Lond. Spec. Publ. 160, 23–32. http://dx.doi.org/10.1144/GSL.SP.1999.160.01.03.
Molyneux, S.G., Dorning, K.J., 1989. Acritarch dating of latest Tremadoc-earliest Arenig (Early Ordovician) sediments in the Carmarthen District, South Wales. Geol. Mag. 126, 707–714.
Molyneux, S.G., Rushton, A.W.A., 1988. The age of the Watch Hill Grits (Ordovician), English Lake District: structural and palaeogeographical implications. Trans. R. Soc. Edinb. Earth Sci. 79, 43–69. http://dx.doi.org/10.1017/S0263593300014097.
Molyneux, S.G., Raevskaya, E., Servais, T., 2007. The *messaoudensis–trifidum* acritarch assemblage and correlation of the base of Ordovician Stage 2 (Floian). Geol. Mag. 144, 143–156.
Molyneux, S.G., Delabroye, A., Wicander, R., Servais, T., 2013. Biogeography of early to mid Palaeozoic (Cambrian–Devonian) microplankton, in: Harper, D.A.T, Servais, T. (Eds.), Early Palaeozoic Biogeography and Palaeobiogeography. Geol. Soc. Lond. Mem. 38, 365–397.
Noailles, F., Lefebvre, B., Guensburg, T.E., Hunter, A.W., Nardin, E., Sumrall, C.D., Zamora, S., 2010. New echinoderm-Lagerstätten from the Lower Ordovician of central Anti-Atlas (Zagora area, Morocco): a Gondwanan perspective of the Great Ordovician Biodiversification Event. In: Reich, M., Reitner, J., Roden, V., Thuy, B. (Eds.), Echinoderm Research. Universitätsverlag Göttingen, Göttingen, pp. 77–78.
Nõlvak, J., 1999. Ordovician chitinozoan biozonation of Baltoscandia. Acta Univ. Carol. Geol. 43, 287–290.
Nõlvak, J., Grahn, Y., 1993. Ordovician chitinozoan zones from Baltoscandia. Rev. Palaeobot. Palynol. 79, 245–269. http://dx.doi.org/10.1016/0034-6667(93)90025-P.
Nõlvak, J., Hints, O., Männik, P., 2006. Ordovician timescale in Estonia: recent developments. Proc. Est. Acad. Sci. Geol. 55, 95–108.
Nowak, H., Akodad, M., Lefebvre, B., Servais, T., 2015. Discovery of the *messaoudensis–trifidum* acritarch assemblage (upper Tremadocian–lower Floian, Lower Ordovician) in the subsurface of Morocco. Est. J. Earth Sci. 64, 80–83. http://dx.doi.org/10.3176/earth.2015.14.
Obut, O.T., 1995. New species of chitinozoans in the Ordovician of Moscow Syneclise. Geologija i geochimija osadotchnyh basseinov Sibirii, Novosibirsk 47–54 (in Russian).
Ottone, E.G., Toro, B.A., Waisfeld, B.G., 1992. Lower Ordovician palynomorphs from the Acoite Formation, Northwestern Argentina. Palynology 16, 93–116. http://dx.doi.org/10.1080/01916122.1992.9989409.
Oulebsir, L., Paris, F., 1995. Chitinozoaires ordoviciens du Sahara algérien: biostratigraphie et affinités paléogéographiques. Rev. Palaeobot. Palynol. 86, 49–68. http://dx.doi.org/10.1016/0034-6667(94)00098-5.
Owen, A.W., Bruton, D.L., Bockelie, J.F., Bockelie, T.G., 1990. The Ordovician successions of the Oslo region, Norway. Nor. Geol. Unders. Spec. Publ. 4, 3–54.
Paris, F., 1981. Les Chitinozoaires dans le Paléozoïque de Sud-Ouest de l'Europe: cadre géologique, étude systématique, biostratigraphie, Mémoire de la Société Geologique et Minéralogique de Bretagne. Rennes.
Paris, F., 1990. The Ordovician chitinozoan biozones of the Northern Gondwana domain. Rev. Palaeobot. Palynol. 66, 181–209. http://dx.doi.org/10.1016/0034-6667(90)90038-K.
Paris, F., Mergl, M., 1984. Arenigian chitinozoans from the Klabava formation, Bohemia. Rev. Palaeobot. Palynol. 43, 33–65. http://dx.doi.org/10.1016/0034-6667(84)90026-5.
Paris, F., Nõlvak, J., 1999. Biological interpretation and paleobiodiversity of a cryptic fossil group: the "chitinozoan animal". Geobios 32, 315–324. http://dx.doi.org/10.1016/S0016-6995(99)80045-X.
Playford, G., Martin, F., 1984. Ordovician acritarchs from the Canning Basin, Western Australia. Alcheringa Australas. J. Palaeontol. 8, 187–223. http://dx.doi.org/10.1080/03115518408618943.

Rábano, I., 1990. Trilobites del Museo GeoMinero. I. *Platypeltoides magrebiensis* n. sp. (Asaphina, Nileidae), del Ordovícico inferior del Anti-Atlas central (Marruecos). Bol. Geol. Min. 101, 21–27.
Rasul, S.M., 1974. The Lower Palaeozoic acritarchs *Priscogalea* and *Cymatiogalea*. Palaeontology 17, 41–63.
Rauscher, R., 1968. Chitinozoaires de l'Arenig de la Montagne Noire (France). Rev. Micropaleontol. 11, 51–60.
Rubinstein, C.V., de la Puente, G.S., Toro, B.A., Servais, T., 2007. The presence of the *messaoudensis-trifidum* acritarch assemblage (Upper Tremadocian–Floian) in the Central Andean Basin, north-western Argentina: calibration with chitinozoans and graptolite zonation. Acta Palaeontol. Sin. 46, 422.
Samuelsson, J., 1999. Ordovician Chitinozoa from Rügen, North-East Germany. Acta Univ. Carol. Geol. 43, 295–297.
Samuelsson, J., Verniers, J., 2000. Ordovician chitinozoan biozonation of the Brabant Massif, Belgium. Rev. Palaeobot. Palynol. 113, 105–129. http://dx.doi.org/10.1016/S0034-6667(00)00055-5.
Samuelsson, J., Verniers, J., Vecoli, M., 2000. Chitinozoan faunas from the Rügen Ordovician (Rügen 5/66 and Binz 1/73 wells), NE Germany. Rev. Palaeobot. Palynol. 113, 131–143. http://dx.doi.org/10.1016/S0034-6667(00)00056-7.
Seilacher, A., 1970. Begriff und Bedeutung der Fossil-Lagerstätten. N. Jb. Geol. Paläont. (Monatsh.) 1970, 34–39.
Sepkoski Jr., J.J., 1981. A factor analytic description of the Phanerozoic marine fossil record. Paleobiology 7, 36–53.
Sepkoski Jr., J.J., 1984. A kinetic model of Phanerozoic taxonomic diversity. III. Post-Paleozoic families and mass extinctions. Paleobiology 10, 246–267.
Servais, T., Katzung, G., 1993. Acritarch dating of Ordovician sediments of the Island of Rügen (NE-Germany). N. Jb. Geol. Paläont. (Monatsh.) 12, 713–723.
Servais, T., Mette, W., 2000. The *messaoudensis-trifidum* acritarch assemblage (Ordovician: late Tremadoc–early Arenig) of the Barriga Shale Formation, Sierra Morena (SW-Spain). Rev. Palaeobot. Palynol. 113, 145–163. http://dx.doi.org/10.1016/S0034-6667(00)00057-9.
Servais, T., Molyneux, S.G., 1997. The *messaoudensis-trifidum* acritarch assemblage (Ordovician: late Tremadoc–early Arenig) from the subsurface of Rügen (Baltic Sea, NE Germany). Palaeontogr. Ital. 84, 113–161.
Servais, T., Li, J., Molyneux, S.G., Raevskaya, E., 2003. Ordovician organic-walled microphytoplankton (acritarch) distribution: the global scenario. Palaeogeogr. Palaeoclimatol. Palaeoecol. 195, 149–172. http://dx.doi.org/10.1016/S0031-0182(03)00306-7.
Servais, T., Vecoli, M., Li, J., Molyneux, S.G., Raevskaya, E.G., Rubinstein, C.V., 2007. The acritarch genus *Veryhachium* Deunff 1954: Taxonomic evaluation and first appearance. Palynology 31, 191–203.
Slavíková, K., 1968. New finds of acritarchs in the Middle Cambrian of the Barrandian (Czechoslovakia). Věst. Ústř. Úst. Geol. 43, 199–205.
Snape, M.G., 1993. A Palynological Study of the Ordovician to Devonian Sediments of the Anti Atlas, Morocco (PhD) University of Sheffield http://etheses.whiterose.ac.uk/3536/ (accessed 11 March 2014).
Staplin, F.L., Jansonius, J., Pocock, S.A., 1965. Evaluation of some acritarchous hystrichosphere genera. N. Jb. Geol. Paläont. (Abh.) 123, 167–201.
Stricanne, L., Munnecke, A., Pross, J., Servais, 2004. Acritarch distribution along an inshore-offshore transect in the Gorstian (lower Ludlow) of Gotland, Sweden. Rev. Palaeobot. Palynol. 130, 195–216.
Sumrall, C.D., Zamora, S., 2011. Ordovician edrioasteroids from Morocco: faunal exchanges across the Rheic Ocean. J. Syst. Palaeontol. 9, 425–454. http://dx.doi.org/10.1080/14772019.2010.499137.
Taugourdeau, P., de Jekhowsky, B., 1960. Répartition et description des chitinozoaires siluro-dévoniens de quelques sondages de la CREPS, de la CFPA et de la SN Repal au Sahara. Rev. Inst. Fr. Pétrol. 9, 1199–1260.
Todd, S.P., Connery, C., Higgs, K.T., Murphy, F.C., 2000. An Early Ordovician age for the Annascaul Formation of the SE Dingle Peninsula, SW Ireland. J. Geol. Soc. 157, 823–833. http://dx.doi.org/10.1144/jgs.157.4.823.
Toro, B.A., Susana de la Puente, G., Rubinstein, C.V., 2010. New graptolite, chitinozoan and acritarch records from the Pascha-Incamayo area, Cordillera Oriental, Argentina. C.R. Palevol 9, 23–30. http://dx.doi.org/10.1016/j.crpv.2009.09.001.
Torsvik, T.H., 2009. BugPlates: linking biogeography and palaeogeography [WWW Document]. URL http://www.geodynamics.no/bugs/SoftwareManual.pdf (accessed 1 September 2014).
Torsvik, T.H., Cocks, L.R.M., 2013. New global palaeogeographical reconstructions for the Early Palaeozoic and their generation. Geol. Soc. Lond. Mem. 38, 5–24. http://dx.doi.org/10.1144/M38.2.
Valent, M., Corbacho, J., 2015. *Pauxillites thaddei* a new Lower Ordovician hyolith from Morocco. *Acta* Musei Natl. Pragae Ser. B Hist. Nat. 71, 51–54. http://dx.doi.org/10.14446/AMNP.2015.51.
Valent, M., Corbacho, J., Martínez, D., 2013. Hyolith localities of Zagora region (Morocco), Upper Fezouata Formation (Lower Ordovician). Batalleria 19, 20–23.
Van Roy, P., Briggs, D.E.G., 2011. A giant Ordovician anomalocaridid. Nature 473, 510–513. http://dx.doi.org/10.1038/nature09920.
Van Roy, P., Tetlie, O.E., 2006. A spinose appendage fragment of a problematic arthropod from the Early Ordovician of Morocco. Acta Palaeontol. Pol. 51, 239–246.
Van Roy, P., Orr, P.J., Botting, J.P., Muir, L.A., Vinther, J., Lefebvre, B., Hariri, K. El, Briggs, D.E.G., 2010. Ordovician faunas of Burgess Shale type. Nature 465, 215–218. http://dx.doi.org/10.1038/nature09038.
Van Roy, P., Briggs, D.E.G., Gaines, R.R., 2015a. The Fezouata fossils of Morocco; an extraordinary record of marine life in the Early Ordovician. J. Geol. Soc. 172, 541–549. http://dx.doi.org/10.1144/jgs2015-017.
Van Roy, P., Daley, A.C., Briggs, D.E.G., 2015b. Anomalocaridid trunk limb homology revealed by a giant filter-feeder with paired flaps. Nature 522, 77–80. http://dx.doi.org/10.1038/nature14256.
Vandenbroucke, T.R.A., 2008. An Upper Ordovician Chitinozoan Biozonation in British Avalonia (England & Wales). Lethaia 41, 275–294. http://dx.doi.org/10.1111/j.1502-3931.2007.00090.x.
Vandenbroucke, T.R.A., Armstrong, H.A., Williams, M., Paris, F., Sabbe, K., Zalasiewicz, J.A., Nõlvak, J., Verniers, J., 2010a. Epipelagic chitinozoan biotopes map a steep latitudinal temperature gradient for earliest Late Ordovician seas: implications for a cooling Late Ordovician climate. Palaeogeogr. Palaeoclimatol. Palaeoecol. 294, 202–219. http://dx.doi.org/10.1016/j.palaeo.2009.11.026.
Vandenbroucke, T.R.A., Armstrong, H.A., Williams, M., Paris, F., Zalasiewicz, J.A., Sabbe, K., Nõlvak, J., Challands, T.J., Verniers, J., Servais, T., 2010b. Polar front shift and atmospheric CO2 during the glacial maximum of the Early Paleozoic Icehouse. Proc. Natl. Acad. Sci. 107, 14983–14986. http://dx.doi.org/10.1073/pnas.1003220107.
Vandenbroucke, T.R.A., Armstrong, H.A., Williams, M., Paris, F., Sabbe, K., Zalasiewicz, J.A., 2013. Chapter 24 Late Ordovician zooplankton maps and the climate of the Early Palaeozoic Icehouse. Geol. Soc. Lond. Mem. 38, 399–405. http://dx.doi.org/10.1144/M38.24.
Vanguestaine, M., 1978. Critères palynostratigraphiques conduisant a la reconnaissance d'un pli couche revinien dans le sondage de Grand-Halleux. Ann. Soc Géol. Belg. 100, 249–276.
Vanguestaine, M., Servais, T., 2002. Early Ordovician acritarchs of the Lierneux Member (Stavelot Inlier, Belgium): stratigraphy and palaeobiogeography. Bull. Soc. Geol. Fr. 173, 561–568. http://dx.doi.org/10.2113/173.6.561.
Vaucher, R., Martin, E.L.O., Hormière, H., Pittet, B., 2016. A genetical link between *Konzentrat* and *Konservat Lagerstätten* in the Fezouata Formation (Lower Ordovician, Morocco): storm deposits as graves in early life. Palaeogeogr. Palaeoclimatol. Palaeoecol. 460, 24–34 (in this issue).
Vavrdová, M., 1966. Palaeozoic microplankton from central Bohemia. Čas. Mineral. Geol. 11, 409–414.
Vavrdová, M., 1973. New acritarchs from Bohemian Arenig (Ordovician). Věst. Ústř. Úst. Geol. 48, 285–289.
Vecoli, M., Le Hérissé, A., 2004. Biostratigraphy, taxonomic diversity and patterns of morphological evolution of Ordovician acritarchs (organic-walled microphytoplankton) from the northern Gondwana margin in relation to palaeoclimatic and palaeogeographic changes. Earth-Sci. Rev. 67, 267–311. http://dx.doi.org/10.1016/j.earscirev.2004.03.002.
Vela, J.A., Corbacho, J., 2007. A new species of *Lehua* from Lower Ordovician of Dra Valley of Morocco. Batalleria 13, 75–80.
Verniers, J., Nestor, V., Paris, F., Dufka, P., Sutherland, S., Van Grootel, G., 1995. A global Chitinozoa biozonation for the Silurian. Geol. Mag. 132, 651–666. http://dx.doi.org/10.1017/S0016756800018896.
Vidal, M., 1998a. Trilobites (Asaphidae et Raphiphoridae) de l'Ordovicien inférieur de l'Anti-Atlas, Maroc. Palaeontogr. Abt. A 251, 39–77.
Vidal, M., 1998b. Le modèle des biofaciès à Trilobites: un test dans l'Ordovicien inférieur de l'Anti-Atlas, Maroc. C.R. Acad. Sci., Ser. IIA-Earth Planet. Sci. 327, 327–333.
Vinther, J., Van Roy, P., Briggs, D.E.G., 2008. Machaeridians are Palaeozoic armoured annelids. Nature 451, 185–188. http://dx.doi.org/10.1038/nature06474.
Volkova, N.A., 1997. Paleogeography of phytoplankton at the Cambrian–Ordovician boundary. Paleontol. J. 31, 135–140.
Wang, W., Vecoli, M., Vandenbroucke, T.R.A., Feng, H., Li, L., Verniers, J., 2013a. Late Tremadocian–early Floian acritarchs from graptolitic shales of the Yinzhubu and Ningkuo formations of Yiyang, South China. Rev. Palaeobot. Palynol. 193, 1–14. http://dx.doi.org/10.1016/j.revpalbo.2013.01.005.
Wang, W., Feng, H., Vandenbroucke, T.R.A., Li, L., Verniers, J., 2013b. Chitinozoans from the Tremadocian graptolite shales of the Jiangnan Slope in South China. Rev. Palaeobot. Palynol. 198, 45–61. http://dx.doi.org/10.1016/j.revpalbo.2012.02.003.
Webby, B.D., Paris, F., Droser, M.L., Percival, I.G. (Eds.), 2004. The Great Ordovician Biodiversification Event, Critical Moments and Perspectives in Earth History and Paleobiology. Columbia University Press, New York.
Welsch, M., 1986. Die Acritarchen der höheren Digermul-Gruppe, Mittelkambrium bis Tremadoc, Ost-Finnmark, Nord-Norwegen. Palaeontogr. Abt. B 201, 1–109.
Wrona, R., 1980. Microarchitecture of the chitinozoan vesicles and its paleobiological significance. Acta Palaeontol. Pol. 25, 123–163.

Annexe 7 :

Taphonomy of new *Rhopalocystis* assemblages in the lower ordovician of the Zagora area (central Anti-Atlas, Morocco)

Auteurs : Ninon Allaire, Bertrand Lefebvre, Emmanuel Martin, Elise Nardin, **Romain Vaucher**

Chapitre publié dans *Progress in Echinoderm Palaeobiology*

Année : 2015 Pages : 21 - 26

S. Zamora & I. Rábano (eds.), *Progress in Echinoderm Palaeobiology.*
Cuadernos del Museo Geominero, 19. Instituto Geológico y Minero de España, Madrid. ISBN: 978-84-7840-961-7

TAPHONOMY OF NEW *RHOPALOCYSTIS* ASSEMBLAGES IN THE LOWER ORDOVICIAN OF THE ZAGORA AREA (CENTRAL ANTI-ATLAS, MOROCCO)

Ninon Allaire[1,2], Bertrand Lefebvre[2], Emmanuel Martin[2], Elise Nardin[3] and Romain Vaucher[2]

[1] UMR CNRS 8198 EvoEcoPaleo, Cité Scientifique, bâtiment SN5, Université Lille 1, 59655 Villeneuve d'Ascq, France. ninon.allaire@ed.univ-lille1.fr

[2] UMR CNRS 5276 LGLTPE, Université Lyon 1, 2 rue Raphaël Dubois, 69622 Villeurbanne cedex, France. bertrand.lefebvre@univ-lyon1.fr, emmanuel.martin@univ-lyon1.fr, romain.vaucher@univ-lyon1.fr

[3] UMR CNRS-IRD-UPS 5563 Géosciences Environnement Toulouse, Observatoire Midi-Pyrénées, 14 avenue Edouard Belin, 31400 Toulouse, France. elise.nardin@get.omp.eu

Keywords: Anti-Atlas, eocrinoids, Morocco, Ordovician, *Rhopalocystis*, taphonomy.

INTRODUCTION

Rhopalocystis is a Tremadocian (Early Ordovician) genus of eocrinoids (basal blastozoans), endemic to the Agdz-Zagora area in the central Anti-Atlas, Morocco. Isolated skeletal remains from the Valdemiedes Formation (Cambrian Series 2, Stage 4) of Spain were tentatively assigned to *Rhopalocystis* (Clausen, 2004). However, they more likely belong to a yet undescribed gogiid eocrinoid (S. Zamora, pers. comm., 2013). The morphology of *Rhopalocystis* is characterised by a mixture of plesiomorphic (e.g., epispires) and more advanced characters (e.g., theca organised into well-defined circlets of plates). Its phylogenetic position remains largely unresolved. *Rhopalocystis* was identified as a gogiid eocrinoid (Sprinkle, 1973; Broadhead, 1982), assigned to various groups of more derived blastozoans (e.g., Paul, 1988; Sumrall *et al.*, 2001; Nardin, 2007), or interpreted as a possible transitional form between blastozoans and crinoids (e.g., Ausich *et al.*, 2013; but see Ubaghs, 1963; Guensburg and Sprinkle, 2007).

Remains of *Rhopalocystis* were first collected in 1952 at Tansikht bridge (locality 1; Fig. 1A) during the field excursion of the 19th International Geological Congress (Ubaghs, 1963). However, specimens of *Rhopalocystis* from Tansikht bridge were not described by Choubert *et al.* (1953), who only reported on the presence of the associated glyptocystitid *Mimocystites* (= *Macrocystella*). Abundant specimens of *Rhopalocystis* were subsequently collected by Jacques Destombes (from 1959 to 1985) in several localities located E of the Jbel Bou Dehir, in Zagora area (localities 2, 3 and 5; Fig. 1A), W of Agdz (locality 4; Fig. 1A), and at Tansikht bridge (locality 1). This material was described in a series of papers by Ubaghs (1963), Chauvel (1971, 1978) and Chauvel and Régnault (1986). Ubaghs (1963) created the genus *Rhopalocystis* based on exquisitely preserved specimens collected at locality 2. All individuals were assigned to the type species, *R. destombesi*. Four additional species of *Rhopalocystis* were described by Chauvel (1971), based on new material collected at localities 2 (*R. grandis*, *R. zagoraensis*), 3 (*R.* sp. A), and 4 (*R. fraga*). Chauvel (1978) redescribed *R. zagoraensis* and identified three more species, based on new material from localities 1 (*R.* sp. C), 2 (*R. havliceki*), and 3 (*R.* sp. B). Finally, Chauvel and Régnault (1986) discussed the systematics of the different species assigned to *Rhopalocystis* and suggested the erection of two more taxa, based on new material from localities 2 and 5 (*R. dehirensis* and *R. lehmani*).

The aim of this paper is to describe three new *Rhopalocystis* assemblages (localities 6, 7, and 8) in the Lower Ordovician of the Zagora area and to discuss their taphonomy. Moreover, intensive field work conducted between 2012 and 2014 made it possible to obtain a detailed logging of the Lower Ordovician succession in the Zagora area,

and to place all known occurrences of *Rhopalocystis* in this revised stratigraphic framework (Fig. 1B). The morphological disparity within the genus *Rhopalocystis* and the validity of its 10 described species will not be investigated here, but will be treated elsewhere.

GEOLOGICAL CONTEXT

In the central Anti-Atlas (Morocco), the Lower Ordovician succession rests unconformably over the middle Cambrian sandstones of the Tabanite Group (Destombes *et al.*, 1985). In the Agdz-Zagora area, the Lower Ordovician sequence corresponds to a thick (1000 m), monotonous series of fine siltstones (Fezouata Shale, Tremadocian to late Floian), capped by the sandstones of the Zini Formation (latest Floian). In the last twelve years, successive field excursions in the Ternata plain (N. of Zagora) resulted in the detailed logging of the whole Lower Ordovician succession and the definition of a precise biostratigraphic framework based on both graptolites and acritarchs (Martin *et al.*, in press). All historical sites yielding remains of *Rhopalocystis* could be placed in this refined biostratigraphic framework: a late Tremadocian age (*A. murrayi* biozone) was confirmed for the three localities of the Ternata plain, E of Jbel Bou Dehir (localities 2, 3 and 5; Fig. 1B), and also for the two other sites, in the Agdz area (localities 1 and 4). Moreover, three new sites yielding abundant remains of *Rhopalocystis* (localities 6, 7, and 8; Fig. 1) were discovered in the Lower Ordovician of the Zagora area.

Locality 6 (Fig. 1) corresponds to a low cliff along the banks of a dry stream bed (oued), about 10 km NE of the small village of Beni Zoli and 21 km N of Zagora, in the western part of the Ternata plain (W of Jbel Bou Dehir). Laminated greenish siltstones have yielded a late Tremadocian assemblage (*A. murrayi* biozone) consisting in abundant remains of *Rhopalocystis* spp., associated with an extremely depauperate fauna comprising only rare specimens of the trilobite *Bavarilla* sp. In 2003, the exploitation of this site yielded 80 specimens deposited in the collections of Cadi-Ayyad University, Marrakesh (AA.TAM.OI.1-80).

Locality 7 (Fig. 1) is located 20 km NE of Zagora, in the eastern part of the Ternata plain (E of Jbel Bou Dehir). Abundant specimens of *Rhopalocystis* were collected in 2003-2004 by Roland and Véronique Reboul within large, massive lenses of bioclastic sandstones. No other faunal element was observed in these levels. The study material is deposited in the collections of the Musée des Confluences, Lyon (ML20.269379-382) and Lyon 1 University, Villeurbanne (FSL 711650, FSL 711160-163, FSL 712045). Locality 7 is indeed very close to Jacques Destombes' locality 1687 mentioned in Vidal (1998a, 1998b). Destombes' site corresponds to a distinct, concretion-bearing level occurring a few meters below, in the same area. The small alumino-siliceous concretions of locality 1687 have yielded an abundant and diverse assemblage comprising many bivalves (e.g., *Redonia michelae*), brachiopods, cephalopods (e.g., *Bathmoceras australe*, *Destombesiceras zagorense*, *Rioceras* sp.), conularians, echinoderms (e.g., *Anedriophus moroccoensis*, *Argodiscus espilezorum*, *Balanocystites primus*, *Balantiocystis regnelli*, *Lingulocystis* sp.), gastropods (e.g., *Carcassonnella courtessolei*, *Thoralispira* cf. *laevis*), graptolites, hyolithids (e.g., *Cavernolites senex*), machaeridians, trilobites (e.g., *Ampyx* sp., *Asaphellus fezouataensis*, *Basilicus* sp., cheirurids indet.) and other arthropods (e.g., *Eoduslia*, *Zagoracaris*). A mid to late Floian age has been generally assigned to this assemblage (Vidal, 1998a, 1998b; Van Roy, 2006; Sumrall and Zamora, 2011; Kröger and Lefebvre, 2012). However, the composition of the graptolite assemblage suggests that a latest Tremadocian age (*H. copiosus* biozone) is more likely (Martin *et al.*, in press). Consequently, a latest Tremadocian (or earliest Floian) age can be inferred for the overlying horizon yielding large *Rhopalocystis*-bearing concretions.

Locality 8 (Fig. 1) is located at the summit of a small hill, N of Jbel Tizagzaouine, about 2.2 km NE of locality 6 and 23 km N of Zagora, in the western part of the Ternata plain (W of Jbel Bou Dehir). Large fragments of massive lenses of bioclastic sandstones were collected in 2013-2014. They have yielded a late Tremadocian assemblage (*A. murrayi* biozone) comprising abundant specimens of *Rhopalocystis* spp., sometimes associated to large fragments of disarticulated trilobites. All available material is deposited in the collections of Cadi-Ayyad University, Marrakesh (AA.TISa.OI.1-24) and Lyon 1 University, Villeurbanne (FSL 712044).

TAPHONOMY

Taphonomic features of *Rhopalocystis* assemblages in the late Tremadocian of the Agdz-Zagora area were thoroughly investigated and discussed by Ubaghs (1963), who identified two main kinds of preservation. The first one

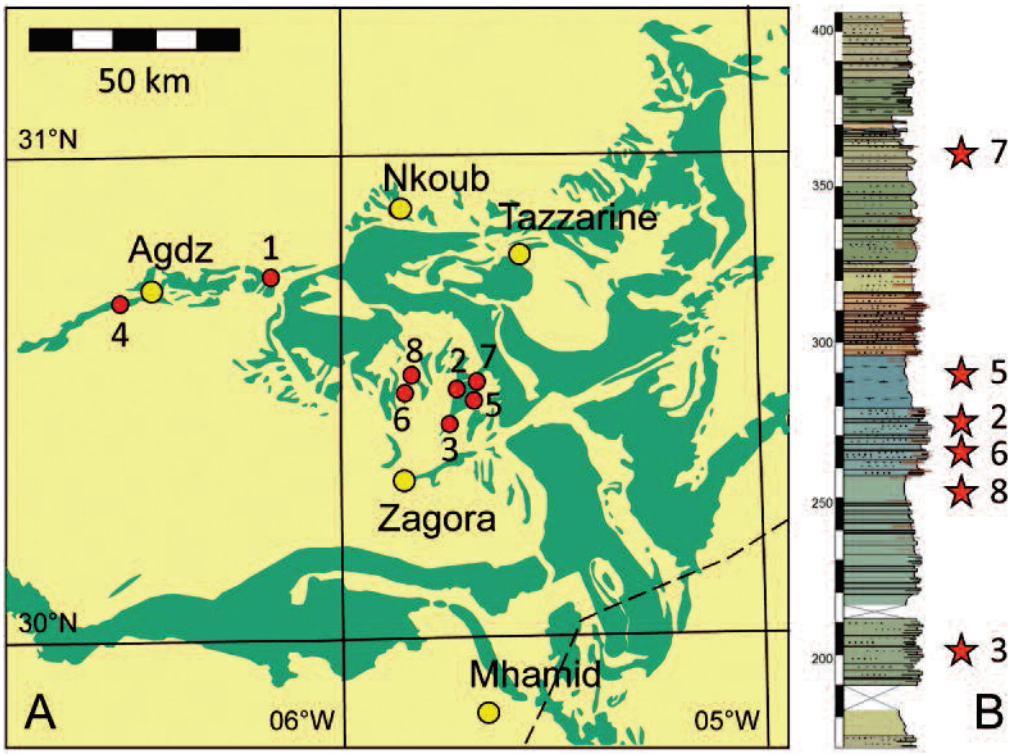

Figure 1. Location and stratigraphic position of *Rhopalocystis* assemblages. A. Simplified geological map of the central Anti-Atlas, Morocco. Ordovician outcrops are indicated in green. B. Partial log of the Lower Ordovician succession in the Zagora area (interval between 170 and 405 m above the unconformity between the Tabanite Group and the Fezouata Shale) showing the stratigraphic position of *Rhopalocystis* beds. Locality 1: Tansikht bridge (= Destombes locality 2082); locality 2: Jbel Bou Dehir (= Destombes localities 1157 and 1725); locality 3: Jbel Bou Dehir (= Destombes localities 1737, 1738 and 1750); locality 4: W. of Agdz (= Destombes locality 1773); locality 5: Jbel Bou Dehir (= Destombes locality 2367); locality 6: Tameraout, Z-F1; locality 7: Bou Chrebeb, Z-F25; locality 8: small hill, N of Jbel Tizagzaouine, Z-F12c.

corresponds to extremely dense accumulations of individuals in massive, bioclastic sandstones, and the second one, to more scattered individuals preserved in laminated siltstones. The three new *Rhopalocystis* assemblages confirm the existence of, at least, two main modes of preservation, but they also offer the opportunity to place them in their palaeoenvironmental context.

Both locality 7 and 8 have yielded type 1 assemblages of *Rhopalocystis* (Fig. 2A-F). They consist in densely packed accumulations of complete, fully articulated thecae in thick, lenticular beds of massive sandstones (Fig. 2C-F). Thecae do not exhibit any preferential orientation. Articulated portions of stems are sometimes preserved, either as isolated stumps, or still in connection with the theca (Fig. 2A, E). No distal extremities of stems have been observed. Brachioles are never preserved. In some other levels, complete thecae are less common and are associated with thousands of disarticulated thecal plates (Fig. 2B) and sometimes, large fragments of trilobites (Fig. 2A). In these levels, isolated skeletal elements consist almost exclusively of basal plates. Type 1 assemblages of *Rhopalocystis* are interpreted here as storm-generated levels of accumulation, resulting from the downslope transport and rapid burial of shallower communities. A similar interpretation was proposed by Vidal (1998a, 1998b) for the taphonomy of trilobite assemblages occurring (stratigraphically) a few meters above the *Rhopalocystis* horizon at locality 7.

The *Rhopalocystis* assemblage collected at locality 6 illustrates the second type of preservation (Fig. 2G-J) mentioned by Ubaghs (1963). Individuals are not preserved in clusters, but randomly distributed in fine, laminated

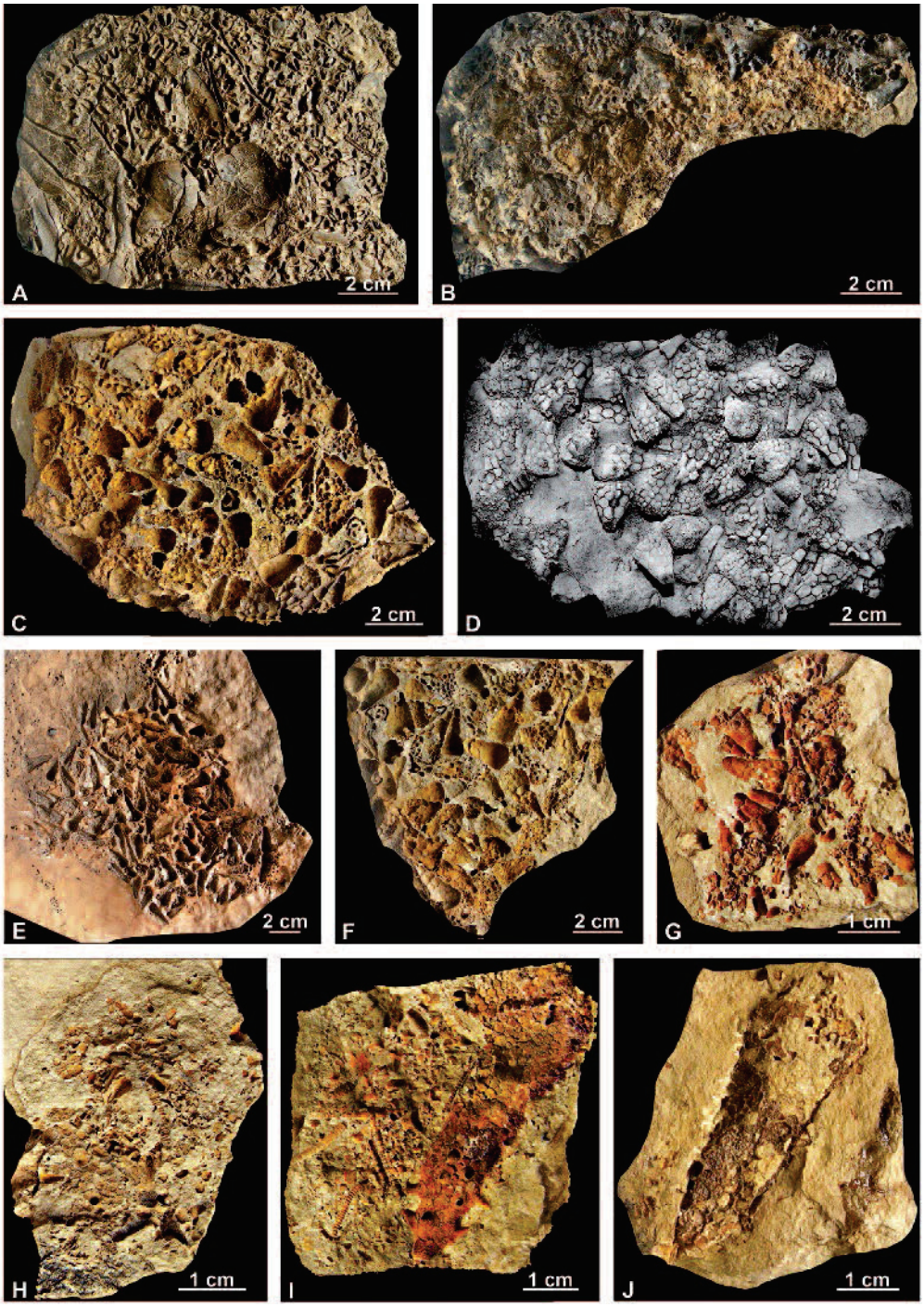

Figure 2.

siltstones (Fig. 2G). Their thecae are large to very large, but never complete, frequently slightly disarticulated and/or collapsed (Fig. 2I-J). Brachioles have not been observed. Fully articulated proximal parts of stems are often preserved in connection with the thecae. The siltstones also contain abundant disarticulated fragments of *Rhopalocystis* (different types of thecal plates, columnals and numerous smaller elements; Fig. 2H-I). Type 2 assemblages are here interpreted as distal storm-influenced deposits, resulting from the *in situ* disarticulation and slow burial of *Rhopalocystis*-dominated communities.

CONCLUSIONS

The discovery of three new *Rhopalocystis*-dominated assemblages confirms the existence of widespread eocrinoid meadows in shallow environmental conditions in the late Tremadocian of the Agdz-Zagora area. The absence or extreme rarity of associated benthic fauna (e.g., molluscs, trilobites) is a characteristic feature also observed in many fossil and modern echinoderm dense beds (Fujita and Ohta, 1989; Lefebvre, 2007; Zatoń *et al*., 2008). The abundant material collected at the new localities will offer the opportunity to reevaluate the systematics and morphological disparity within the genus *Rhopalocystis*.

Acknowledgements

This paper is a contribution of the ANR (Agence Nationale de la Recherche) research project entitled "The Rise of Animal Life (Cambrian-Ordovician): organisation and tempo" (RALI, coord. Jean Vannier). The authors are particularly grateful to Khadija El Hariri, Moussa Masrour, Fleur Noailles, Bernard Pittet, Roland and Véronique Reboul, and Daniel Vizcaïno for their assistance in the field, and also to Abel Prieur, for his valuable help with photographs. Samuel Zamora and James Sprinkle reviewed this manuscript and made many helpful remarks.

REFERENCES

Ausich, W.I., Rhenberg, E.C., Kammer, T.W. and Deline, B. 2013. Rooting the early crinoid diversification with the eocrinoid *Rhopalocystis*. *Geological Society of America Abstracts with Programs*, 45 (7), 109.

Broadhead, T.W. 1982. Reappraisal of class Eocrinoidea (Echinodermata). In Lawrence J.M. (Ed.), *Echinoderms: Proceedings of the International Conference, Tampa Bay*. Balkema, Rotterdam, 125-131.

Chauvel, J. 1971. *Rhopalocystis* Ubaghs: un échinoderme éocrinoïde du Trémadocien de l'Anti-Atlas marocain. *Mémoires du Bureau de Recherches Géologiques et Minières,* 73, 43-49.

Chauvel, J. 1978. Compléments sur les échinodermes du Paléozoïque marocain (diploporites, éocrinoïdes, édrioastéroïdés). *Notes du Service géologique du Maroc*, 39 (272), 27-78.

Chauvel, J. and Régnault, S. 1986. Variabilité du genre *Rhopalocystis* Ubaghs, éocrinoïde du Trémadocien de l'Anti-Atlas marocain. *Geobios*, 19, 863-870.

Choubert, G., Termier, H. and Termier, G. 1953. Présence du genre *Mimocystites* Barrande dans l'Ordovicien du Maroc. *Notes et Mémoires du Service géologique du Maroc*, 117, 137-143.

Clausen, S. 2004. New Early Cambrian eocrinoids from the Iberian Chains (NE Spain) and their role in nonreefal benthic communities. *Eclogae Geologicae Helvetiae*, 97 (3), 371-379.

Figure 2. Different types of preservation of *Rhopalocystis* spp., late Tremadocian, Zagora area (Morocco). All photographs show original specimens, with the exception of D (latex cast). A-F. Accumulations of *Rhopalocystis* spp. within lenses of bioclastic sandstones. A. Partially disarticulated thecae, portions of stems and isolated skeletal elements of *Rhopalocystis* sp., associated with large isolated pieces of trilobites, Z-F12c (AA.TISa.OI.10). B. Isolated plates and complete thecae of *Rhopalocystis destombesi*, Z-F12c (AA.TISa.OI.9). C, F. *Rhopalocystis destombesi*, Z-F25 (FSL 711650, part and counterpart). D. *Rhopalocystis destombesi*, Z-F25 (ML20-269382). E. *Rhopalocystis zagoraensis*, Z-12c (FSL 712044). G-J. *Rhopalocystis* spp. preserved in fine siltstones, Z-F1. G. Complete to slightly disarticulated thecae of *Rhopalocystis zagoraensis* (AA.TAM.OI.2). H-I. Part and counterpart of specimen AA.TAM.OI.21. H. Isolated skeletal elements of *Rhopalocystis* sp. I. Isolated plates of *Rhopalocystis* sp. and large complete theca of *Rhopalocystis havliceki*. J. Large complete theca of *Rhopalocystis havliceki* (AA.TAM.OI.13). Repositories: Université Cadi-Ayyad, Marrakesh, Morocco (AA), Université Lyon 1, Villeurbanne, France (FSL) and Musée des Confluences, Lyon (ML).

Destombes, J., Hollard, H. and Willefert, S. 1985. Lower Palaeozoic rocks of Morocco. In Holland C.H. (Ed.), *Lower Palaeozoic Rocks of the World, vol. 4: Lower Palaeozoic of North-Western and West-Central Africa*. John Wiley and Sons, New-York, 91-336.

Fujita, T. and Ohta, S. 1989. Spatial structure within a dense bed of the brittle star *Ophiura sarsii* (Ophiuroidea: Echinodermata) in the bathyal zone off Otsuchi, northeastern Japan. *Journal of the Oceanographical Society of Japan*, 45, 289-300.

Guensburg, T.E. and Sprinkle, J. 2007. Phylogenetic implications of the Protocrinoida: blastozoans are not ancestral to crinoids. *Annales de Paléontologie*, 93 (4), 277-290.

Kröger, B. and Lefebvre, B. 2012. Palaeogeography and palaeoecology of early Floian (Lower Ordovician) cephalopods from the Upper Fezouata Formation, Anti-Atlas, Morocco. *Fossil Record*, 15, 61-75.

Lefebvre, B. 2007. Early Palaeozoic palaeobiogeography and palaeoecology of stylophoran echinoderms. *Palaeogeography, Palaeoclimatology, Palaeoecology*, 245 (1), 156-199.

Martin, E., Pittet, B., Gutiérrez-Marco, J.C., Vannier, J., El Hariri, K., Lerosey-Aubril, R., Masrour, M., Nowak, H., Servais, T., Vandenbroucke, T., Van Roy, P., Vaucher, R. and Lefebvre, B. in press. The Lower Ordovician Fezouata Konservat-Lagerstätte from Morocco: age, environment and evolutionary perspectives. *Gondwana Research*.

Nardin, E. 2007. *La diversification des blastozoaires (Echinodermata) au Paléozoïque inférieur: aspects phylogénétiques, paléoécologiques et paléobiogéographiques*. Unpublished PhD thesis, Université de Bourgogne, Dijon, 532 pp.

Paul, C.R.C. 1988. The phylogeny of the cystoids. In Paul C.R.C. and Smith A.B. (Eds.), *Echinoderm Phylogeny and Evolutionary Biology*. Clarendon Press, Oxford, 199-213.

Sprinkle, J. 1973. *Morphology and Evolution of Blastozoan Echinoderms*. Special Publication, Museum of Comparative Zoology Harvard University, Cambridge, Massachusetts, 283 pp.

Sumrall, C.D. and Zamora, S. 2011. Ordovician edrioasteroids from Morocco: faunal exchanges across the Rheic Ocean. *Journal of Systematic Palaeontology*, 9 (3), 425-454.

Sumrall, C.D., Brochu, C.A. and Merck, J.W.Jr. 2001. Global lability, regional resolution, and majority-rule consensus bias. *Paleobiology*, 27, 254-261.

Ubaghs, G. 1963. *Rhopalocystis destombesi* n.g., n. sp. éocrinoïde de l'Ordovicien inférieur (Trémadocien supérieur) du Sud marocain. *Notes du Service géologique du Maroc*, 23 (172), 25-45.

Van Roy, P. 2006. *Non-trilobite arthropods from the Ordovician of Morocco*. Unpublished PhD thesis, Ghent University, Ghent (Belgium) 230 pp.

Vidal, M. 1998a. Le modèle des biofaciès à trilobites: un test dans l'Ordovicien inférieur de l'Anti-Atlas, Maroc. *Comptes-Rendus de l'Académie des Sciences, Paris, Sciences de la Terre et des planètes*, 327, 327-333.

Vidal, M. 1998b. Trilobites (Asaphidae et Raphiophoridae) de l'Ordovicien inférieur de l'Anti-Atlas, Maroc. *Palaeontographica Abteilung A*, 251, 39-77.

Zatoń, M., Salamon, M.A., Boczarowski, A. and Sitek, S. 2008. Taphonomy of dense ophiuroid accumulations from the Middle Triassic of Poland. *Lethaia*, 41 (1), 47-58.

Annexe 8 :

Taphonomy of new *Stylophoran*-dominated assemblage in the lower ordovician of the Zagora area (central Anti-Atlas, Morocco)

Auteurs : Emmanuel Martin, Bertrand Lefebvre, **Romain Vaucher**

Chapitre publié dans *Progress in Echinoderm Palaeobiology*

Année : 2015 Pages : 95 - 100

S. Zamora & I. Rábano (eds.), *Progress in Echinoderm Palaeobiology.*
Cuadernos del Museo Geominero, 19. Instituto Geológico y Minero de España, Madrid. ISBN: 978-84-7840-961-7

TAPHONOMY OF A STYLOPHORAN-DOMINATED ASSEMBLAGE IN THE LOWER ORDOVICIAN OF ZAGORA AREA (CENTRAL ANTI-ATLAS, MOROCCO)

Emmanuel Martin, Bertrand Lefebvre and Romain Vaucher

UMR CNRS 5276 LGLTPE, Université Lyon 1, 2 rue Raphaël Dubois, 69622 Villeurbanne cedex, France. emmanuel.martin@univ-lyon1.fr, bertrand.lefebvre@univ-lyon1.fr, romain.vaucher@univ-lyon1.fr

Keywords: Anti-Atlas, cornutes, Morocco, Ordovician, stylophorans, taphonomy.

INTRODUCTION

Echinoderms are a major component of benthic communities in the Lower Ordovician of central Anti-Atlas (Noailles *et al.*, 2010; Van Roy *et al.*, 2010). In the Fezouata Shale (Tremadocian-late Floian), stylophorans (cornutes and mitrates) are the most diverse group of echinoderms (24 taxa). Until recently, however, stylophorans were considered as extremely rare fossils in the Lower Ordovician of this region. From 1959 to 1991, a single specimen was collected, despite intensive fieldwork performed by Jacques Destombes. This specimen was found at Destombes' locality 1685 (Fig. 1; latest Tremadocian to earliest Floian) and described by Chauvel (1971) as the holotype of *Thoralicystis zagoraensis*. This cornute was associated to a diverse benthic assemblage dominated by bivalves, gastropods and trilobites (e.g., *Asaphellus fezouataensis, Colpocoryphe thorali*), associated with brachiopods (e.g., *Paurorthis tadristensis*), conularians, crinoids (*Ramseyocrinus* sp.), glyptocystitid rhombiferans (*Macrocystella bohemica*), and hyolithids (Chauvel, 1969; Havliček, 1971; Donovan and Savill, 1988; Vidal, 1998).

In the last twelve years, successive field campaigns in the Lower Ordovician of the Zagora area confirmed that stylophorans are a minor component of high-diversity benthic assemblages dominated by arthropods and molluscs. Stylophorans, however, also occur in mass occurrences in densely packed, low-diversity assemblages, within some well-defined, thin horizons (Lefebvre, 2007; Lefebvre and Botting, 2007). For example, Lefebvre (2007) figured a slab containing numerous specimens of the cornutes *Cothurnocystis* sp. and *Galliaecystis* sp. (locality Z-F3, late Tremadocian, *A. murrayi* biozone; Fig. 1). Two distinct stylophoran beds were reported by Lefebvre and Botting (2007) at locality Z-F2(1) (late Tremadocian, *A. murrayi biozone*; Fig. 1): a *Thoralicystis*-dominated horizon and, about two meters above it, a *Peltocystis*-dominated level. Lefebvre (2007) suggested that stylophoran beds observed in the Fezouata Shale of Zagora area were showing taphonomic features characteristic of taphofacies E as defined by Brett *et al.* (1997) for echinoderms, and were thus associated with relatively deep environmental conditions (outer shelf, slope; see also Van Roy *et al.*, 2010). In contrast, Lefebvre and Botting (2007) suggested that stylophoran beds were possibly associated with much shallower environmental conditions, closer to normal wave base (echinoderm taphofacies C).

The aims of this paper are to describe a new stylophoran-dominated assemblage in the Lower Ordovician of the Zagora area and to discuss its associated palaeoenvironmental context. A taphonomic classification dedicated to stylophorans is proposed here for the first time thus describing the taphonomy of the new assemblage. Finally, all published occurrences of stylophorans in the Lower Ordovician of Zagora area (central Anti-Atlas, Morocco) are

replaced in a new, refined biostratigraphic framework (Fig. 1B), based on field campaigns achieved in 2012-2014 (Martin *et al.*, in press).

GEOLOGICAL CONTEXT

The Fezouata Shale (Tremadocian-late Floian) represents the basal member of the Outer Feijas Group (Tremadocian-mid Darriwilian), which corresponds to a shale-dominated interval comprised between the sandstones of the middle Cambrian Tabanite Group and the sandstone-dominated units of the First Bani Group (late Darriwilian-early Sandbian; Destombes *et al.*, 1985; Gutiérrez-Marco *et al.*, 2003). In Zagora area, the Fezouata Shale corresponds to a 1000 m-thick, monotonous succession of fine-grained siltstones. In this area, a detailed logging of the Fezouata Shale and of the overlying Zini Formation (latest Floian) was achieved through a series of field campaigns organized between 2012 and 2014. Sedimentary structures typical of storm deposits (e.g., ripple marks, hummocky cross-stratification) were observed repeatedly, at different scales in all parts of the Lower Ordovician succession (Martin *et al.*, in press). Consequently, the general depositional context of the Fezouata Shale more likely corresponds to relatively shallow conditions (lower shoreface), at or above storm-wave base (Lefebvre and Botting, 2007; Martin *et al.*, in press), rather than to a deep, outer shelf setting (Lefebvre, 2007; Van Roy *et al.*, 2010; Gaines *et al.*, 2012).

Moreover, the detailed analysis of both graptolite and acritarch assemblages collected in the last twelve years in Zagora area offered the opportunity to better constrain the biostratigraphic framework of the Fezouata Shale (Martin *et al.*, in press). In this revised biostratigraphic scheme, most deposits formerly interpreted as early to mid Floian in age are now assigned to the *Hunnegraptus copiosus* biozone (latest Tremadocian). In Zagora area, all described occurrences of stylophoran-dominated beds in the Fezouata Shale are restricted to the *A. murrayi* biozone (late Tremadocian; Fig. 1B).

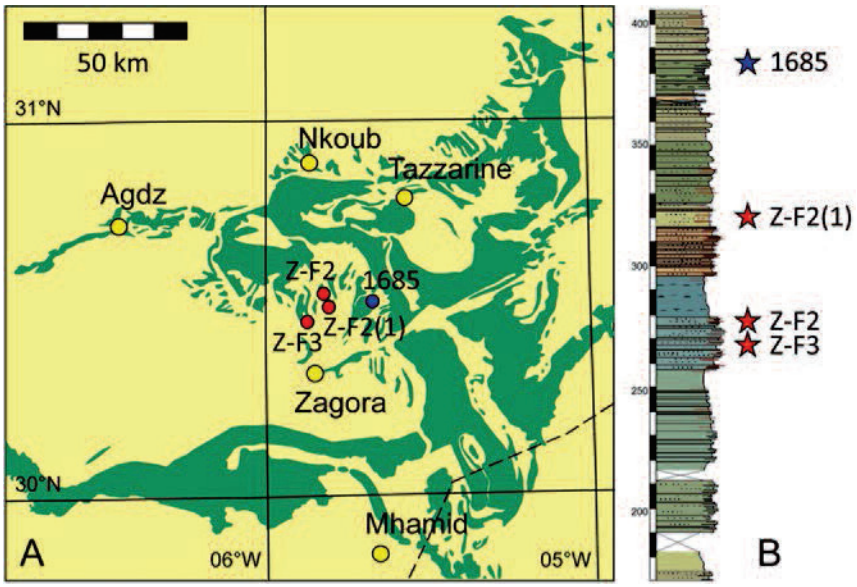

Figure 1. Location and stratigraphic positions of all stylophoran occurrences described in the Lower Ordovician of Zagora area. A. Simplified geological map of central Anti-Atlas, Morocco. Ordovician outcrops are indicated in green. B. Partial log of the Lower Ordovician succession in Zagora area (interval comprised between 170 and 405 m above the unconformity between the Tabanite Group and the Fezouata Shale) showing the stratigraphic positions of stylophoran beds (in red) and stylophorans occurring within diverse benthic assemblages (in blue). Z-F3: locality NE of Beni Zoli village (Lefebvre, 2007); Z-F2: Jbel Tizagzaouine (new assemblage); Z-F2(1): locality S of Jbel Tizagzaouine (Lefebvre and Botting, 2007); 1685: type-locality of *Thoralicystis zagoraensis* (Chauvel, 1971).

The new stylophoran-dominated assemblage reported here was collected from a single, thin, lens-shaped layer of beige siltstones at locality Z-F2, along the very steep slopes forming the eastern flank of Jbel Tizagzaouine. This site is located about 11 km NE of the village of Beni Zoli and 21 km N of Zagora, in the western part of the Ternata plain (W of Jbel Bou Dehir; Fig. 1A). The stylophoran bed was entirely quarried out in 2002-2003. This small lens yielded extremely abundant specimens of cornutes (over 500 individuals), all of them belonging to the same, yet undescribed species. One specimen of this large cornute from Jbel Tizagzaouine was reported as "undescribed Tremadoc boot-shaped form" and figured by Ware and Lefebvre (2007, p. 784, fig. 5.1-2). In Z-F2, the monospecific stylophoran assemblage is associated to a low diversity, depauperate fauna comprising fragments of large trilobites (Fig. 2H), along with rare articulate brachiopods, relatively common graptolites (e.g., *Paradelograptus norvegicus*) and, locally, clusters of tiny gastropods (Fig. 2C). The graptolite assemblage observed in locality Z-F2 suggests a late Tremadocian age for this level (*A. murrayi* biozone; Fig. 1B).

MATERIAL AND METHODS

The excavation of the Z-F2 stylophoran bed in 2002-2003 yielded 300 specimens (rock samples) containing more than 500 individuals belonging to the same undescribed species of large cornute (Fig. 2). Study material is deposited in the collections of the following public institutions: Cadi-Ayyad University, Marrakesh, 190 specimens (AA.JTZ.OI.1-6, AA.JTZ.OI.11-194), Musée des Confluences, Lyon, 9 specimens (ML20.269238-246), and Muséum d'Histoire naturelle, Nantes, 101 specimens (MHNN.P.045197-297). During fieldwork, sampling was performed as exhaustively as possible: all fossiliferous pieces of rock were collected, even those containing fragmentary, disarticulated material. A sampling bias towards better-preserved, fully articulated specimens is, however, likely. Indeed, minute isolated skeletal elements are less eye-catching, and the possibility that they were under-sampled cannot be excluded.

TAPHONOMY

Five taphonomic groups are defined here for stylophorans, based on the quality of preservation of the specimens. Similar taphonomic classifications have been already proposed for helicoplacoids (Dornbos and Bottjer, 2001) and ophiuroids (Zatoń *et al.*, 2008).

Group 1 includes all cornute specimens with (1) their distal aulacophore preserved, with cover plates articulated (or in close contact) to underlying ossicles; (2) their proximal aulacophore; and (3) a complete to slightly disarticulated theca. Cover plates are extremely delicate skeletal elements protecting the food groove of stylophorans (Ubaghs, 1968; Lefebvre, 2003). In cornutes, their preservation requires the rapid burial of live, *in situ* organisms (Lefebvre, 2007). Unlike cornutes, mitrates had the possibility to flex their distal aulacophore, so as to close their cover plates and thus protect their food groove in case of physical disturbance and/or danger (Parsley, 1988; Lefebvre, 2003). In mitrates, the recurved, distress position of the aulacophore greatly enhances the preservation potential of cover plates. Consequently, group 1 only includes mitrates preserved in life position, i.e. with their distal aulacophore held in extended position, over the sea floor (see e.g., Parsley and Gutiérrez-Marco, 2005; Lefebvre and Botting, 2007).

Group 2 corresponds to cornutes with (1) only their brachials (stylocone, ossicles) preserved (cover plates absent); (2) their proximal aulacophore; and (3) a complete to slightly disarticulated theca. In mitrates, group 2 includes all specimens with their distal aulacophore (brachials and cover plates) preserved in flexed, distress position.

Group 3 comprises stylophorans with (1) no distal aulacophore; (2) a complete or more or less dissociated proximal aulacophore; and (3) a complete to partly disarticulated theca.

Group 4 is defined for more or less strongly disarticulated stylophoran thecae, with no aulacophore articulated to them.

Group 5 is proposed for dissociated skeletal elements.

TAPHOFACIES

Three distinct types of preservation (taphofacies) can be identified in the stylophoran bed of locality Z-F2. The first taphofacies is restricted to the lowermost part of the lens, which consists in a thin, irregular layer (0-3 mm in thickness) of coarse siltstones. This level contains abundant isolated skeletal elements of cornutes (taphonomic group 5; Fig. 2G-

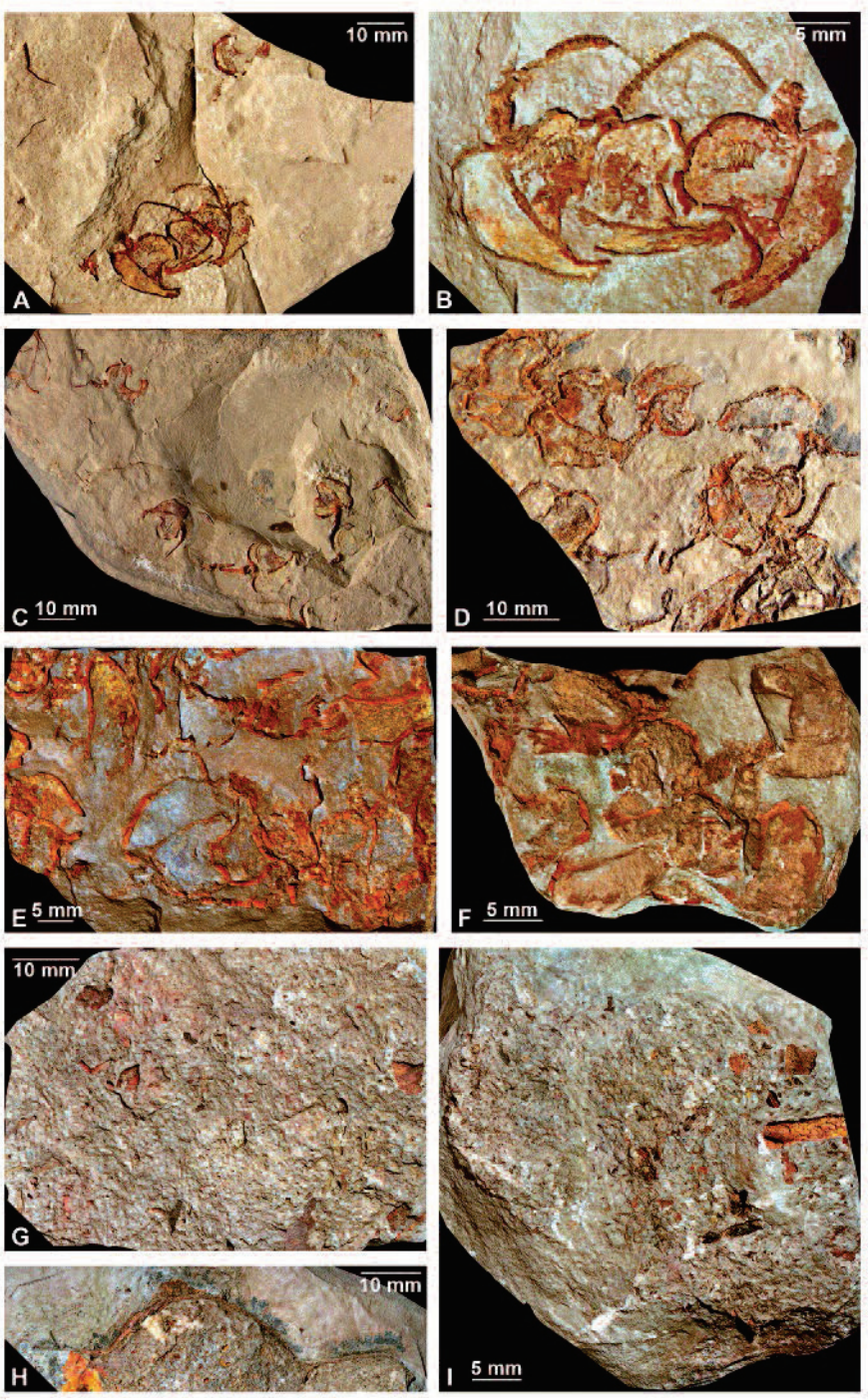

Figure 2.

I), sometimes sheltered under large pieces of disarticulated trilobites (Fig. 2H). The second taphofacies is observed in the overlying, thicker, irregular layer (2-5 mm in thickness) of finer siltstones. This horizon corresponds to a dense accumulation of hundreds of cornutes, piled on top of each other (Fig. 2D-F). In this level, individuals do not exhibit any preferential orientation, and about half of the specimens are upside-down. Most cornutes can be assigned to taphonomic group 2, although some individuals belonging to groups 1 and 3 are also present. The third taphofacies occurs in the overlying, thick, upper part of the stylophoran bed (10-30 mm in thickness), which consists in very fine siltstones. This level has yielded scattered, well-preserved specimens of cornutes, frequently associated with graptolites and clusters of tiny gastropods (Fig. 2A-C). In this layer, most individuals belong to taphonomic group 2. Specimens do not show any preferential orientation, and only a few cornutes are upside-down (Fig. 2B).

CONCLUSIONS

In their taphonomic classification of echinoderms, Brett *et al.* (1997) identified three main groups, based on the resistance of their skeleton to disarticulation. In this scheme, stylophorans belong to type 1 echinoderms (i.e., taxa characterized by loosely articulated skeletal elements; Brett *et al.*, 1997; Lefebvre, 2007). Experimental taphonomic studies on extant type 1 organisms (e.g., ophiuroids) indicate that their skeleton entirely disarticulates within a few days after death (Schäfer, 1972; Allison, 1990; Donovan, 1991). Freshly killed specimens of type 1 echinoderms, however, can endure high-energy conditions without severe disarticulation (Kerr and Twitchett, 2004; Gorzelak and Salamon, 2013). Consequently, the preservation of hundreds of exquisitely preserved specimens of cornutes in locality Z-F2 requires exceptional environmental conditions. The available sedimentological evidence (e.g., scoured bioclastic lag at the base of the lens, fining upward lithology) and the geological context of the Fezouata Shale (shallow deposits at or above storm wave base) both strongly suggest that the stylophoran bed of Jbel Tizagzaouine represents a storm deposit (taphofacies IIC of Brett *et al.*, 1997). The local accumulation of hundreds of specimens of cornutes very likely results from distal storm scour and redeposition of a para-autochtonous, monospecific community.

Acknowledgements

This paper is a contribution of the ANR (Agence Nationale de la Recherche) research project entitled "The Rise of Animal Life (Cambrian-Ordovician): organisation and tempo" (RALI, coord. Jean Vannier). The authors are particularly grateful to Myriam Lefebvre, Roland and Véronique Reboul, and Daniel and Framboise Vizcaïno for their assistance in the field, to Abel Prieur, for his help with photographs, and also to James Nebelsick and Samuel Zamora, for their constructive comments and corrections.

REFERENCES

Allison, P.A. 1990. Variation in rates of decay and disarticulation of Echinodermata: implications for theapplication of actualistic data. *Palaios*, 5, 432-440.

Brett, C.E., Moffat, H.A. and Taylor, W.L. 1997. Echinoderm taphonomy, taphofacies, and Lagerstätten. *Paleontological Society Papers*, 3, 147-190.

Chauvel, J. 1969. Les échinodermes macrocystellides de l'Anti-Atlas marocain. *Bulletin de la Société géologique et minéralogique de Bretagne (C)*, 1, 21-32.

Figure 2. Different types of preservation in the stylophoran bed of locality Z-F2 (Jbel Tizagzaouine, Zagora area), Lower Ordovician (late Tremadocian, *A. murrayi* biozone). All photographs show original specimens. A-C. Isolated cornutes in uppermost part of fossiliferous layer. A-B. MHNN.P.045281. A. Large slab showing four complete individuals and a few isolated skeletal elements. B. Cluster of three specimens: two of them are in lower aspect, one is in upper aspect. C. Large slab showing six complete individuals (all in lower aspect), associated with portions of other specimens, isolated plates, and numerous poorly preserved tiny gastropods, MHNN.P.045296. D-F. Accumulation layer full of complete cornutes. D. AA.JTZ.OI.5. E. AA-JTZ-OI-50. F. AA-JTZ-OI-14. G-I. Bioclastic lag at base of stylophoran bed. G. AA-JTZ-OI-50. H. MHNN.P.045295. I. AA-JTZ-OI-34. Repositories: Cadi-Ayyad University, Marrakesh (AA), Muséum d'Histoire naturelle, Nantes (MHNN).

Chauvel, J. 1971. Les échinodermes carpoïdes du Paléozoïque inférieur marocain. *Notes du Service géologique du Maroc*, 237, 49-60.

Destombes, J., Hollard, H. and Willefert, S. 1985. Lower Palaeozoic rocks of Morocco. In Holland C.H. (Ed.), *Lower Palaeozoic Rocks of the World, vol. 4: Lower Palaeozoic of North-Western and West-Central Africa*. John Wiley and sons, New-York, 91-336.

Donovan, S.K. 1991. The taphonomy of echinoderms: calcareous multi-element skeletons in the marine environment. In Donovan S.K. (Ed.), *The Processes of Fossilisation*. Belhaven Press, London, 241-269.

Donovan, S.K. and Savill, J.J. 1988. *Ramseyocrinus* (Crinoidea) from the Arenig of Morocco. *Journal of Paleontology*, 62, 283-285.

Dornbos, S.Q. and Bottjer, D.J. 2001. Taphonomy and environmental distribution of helicoplacoid echinoderms. *Palaios*, 16, 197-204.

Gaines, R.R., Briggs, D.E.G., Orr, P.J. and Van Roy, P. 2012. Preservation of giant anomalocaridids in silica-chlorite concretions from the Early Ordovician of Morocco. *Palaios*, 27, 317-325.

Gorzelak, P. and Salamon, M.A. 2013. Experimental tumbling of echinoderms - taphonomic patterns and implications. *Palaeogeography, Palaeoclimatology, Palaeoecology*, 386, 569-574.

Gutiérrez-Marco, J.M., Destombes, J., Rábano, I., Aceñolaza, G.F., Sarmiento, G.N. and San José, M.A. 2003. The Middle Ordovician of the Moroccan Anti-Atlas: paleobiodiversity, biostratigraphic review and correlation. *Geobios*, 36, 151-177.

Havliček, V. 1971. Brachiopodes de l'Ordovicien du Maroc. *Notes et Mémoires du Service géologique du Maroc*, 230, 1-135.

Kerr, T.J.V. and Twitchett, R.J. 2004. Experimental decay and disarticulation of *Ophiura texturata*: implications for the fossil record of ophiuroids. In Heinzeller T. and Nebelsick J.H. (Eds.), *Echinoderms: München*. Balkema, Rotterdam, 439-446.

Lefebvre, B. 2003. Functional morphology of stylophoran echinoderms. *Palaeontology*, 46, 511-555.

Lefebvre, B. 2007. Early Palaeozoic palaeobiogeography and palaeoecology of stylophoran echinoderms. *Palaeogeography, Palaeoclimatology, Palaeoecology*, 245, 156-199.

Lefebvre, B. and Botting, J.P. 2007. First report of the mitrate *Peltocystis cornuta* Thoral (Echinodermata, Stylophora) in the Lower Ordovician of central Anti-Atlas (Morocco). *Annales de Paléontologie*, 93, 183-198.

Martin, E., Pittet, B., Gutiérrez-Marco, J.C., Vannier, J., El Hariri, K., Lerosey-Aubril, R., Masrour, M., Nowak, H., Servais, T., Vandenbroucke, T., Van Roy, P., Vaucher, R. and Lefebvre, B. in press. The Lower Ordovician Fezouata Konservat-Lagerstätte from Morocco: age, environment and evolutionary perspectives. *Gondwana Research*.

Noailles, F., Lefebvre, B., Guensburg, T.E., Hunter, A.W., Nardin, E., Sumrall, C.D. and Zamora S. 2010. New echinoderm-Lagerstätten from the Lower Ordovician of central Anti-Atlas (Zagora area, Morocco): a Gondwanan perspective of the Great Ordovician Biodiversification Event. In Reich M., Reitner J., Roden V. and Thuy B. (Eds.), *Echinoderm Research 2010*. Universitätsverlag Göttingen, Göttingen, 77-78.

Parsley, R.L. 1988. Feeding and respiratory strategies in Stylophora. In Paul C.R.C. and Smith A.B. (Eds.), *Echinoderm Phylogeny and Evolutionary Biology*. Clarendon Press, Oxford, 347-361.

Parsley, R.L. and Gutiérrez-Marco, J.C. 2005. Stylophorans in middle Arenig shallow water siliciclastics: *Vizcainocarpus* from the Imfout syncline in Morocco's western Meseta. *Bulletin of Geosciences*, 80, 185-192.

Schäfer, W. 1972. *Ecology and Palaeoecology of Marine Environments*. Oliver and Boyd, Edinburgh, 568 pp.

Ubaghs, G. 1968. Stylophora. In Moore R.C. (Ed.), *Treatise on Invertebrate Paleontology. Part S: Echinodermata 1(2).* Geological Society of America and the University of Kansas Press, Lawrence, S495-S565.

Van Roy, P., Orr, P.J., Botting, J.P., Muir, L.A., Vinther, J., Lefebvre, B., El Hariri, K. and Briggs, D.E.G. 2010. Ordovician faunas of Burgess Shale type. *Nature*, 465, 215-218

Vidal, M. 1998. Le modèle des biofaciès à trilobites: un test dans l'Ordovicien inférieur de l'Anti-Atlas, Maroc. *Comptes-Rendus de l'Académie des Sciences, Paris, Sciences de la Terre et des planètes*, 327, 327-333.

Ware, D. and Lefebvre, B. 2007. Abnormalities in the Lower Ordovician cornute *Phyllocystis* Thoral, 1935 (Echinodermata, Stylophora) from Montagne Noire (southern France): implications for plate homology and phylogeny. *Journal of Paleontology*, 81, 779-787.

Zatoń, M., Salamon, M.A., Boczarowski, A. and Sitek, S. 2008. Taphonomy of dense ophiuroid accumulations from the Middle Triassic of Poland. *Lethaia*, 41, 47-58.